Master's thesis

NTNU
Norwegian University of Science and Technology
Faculty of Natural Sciences
Department of Chemistry

Thomas Nordbø Solvi

Studies on Au(III) complexes and reactions

Master's thesis in Chemistry
Supervisor: Anne Fiksdahl
May 2020

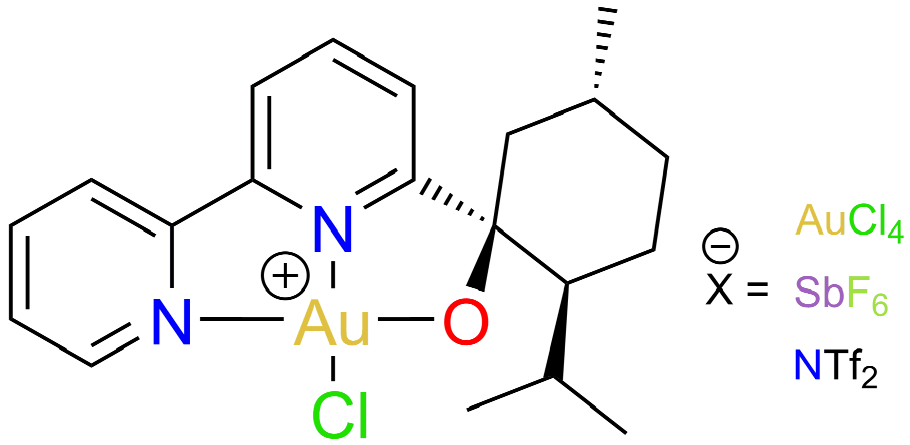

NTNU
Norwegian University of
Science and Technology

Thomas Nordbø Solvi

Studies on Au(III) complexes and reactions

Master's thesis in Chemistry
Supervisor: Anne Fiksdahl
May 2020

Norwegian University of Science and Technology
Faculty of Natural Sciences
Department of Chemistry

NTNU
Norwegian University of
Science and Technology

Declaration

I hereby declare that the work presented in this master's thesis has been conducted individually. The work was conducted in accordance with the rules and regulations of the master's degree programme in chemistry at the Norwegian University of Science and technology (NTNU). The work presented herein was conducted from August 2018 to May 2020.

Trondheim, 15th of May 2020.

Thomas Nordbø Solvi

Preface

The work presented herein was performed at the Department of Chemistry, Norwegian University of Science and Technology (NTNU) from August 2018 to May 2020.

During the time period from 12th of March to 26th of April 2020, the university was shut down for all students due to the COVID-19 pandemic. This had quite severe consequences for this master's thesis, as laboratory work ceased in less than a day's notice. Under strict protocols, work could be resumed from the 27th of April, but the time restriction this enforced inevitably had impacts on my work; for instance, it was decided that IR and m.p. analysis of some compounds was not a priority as long as NMR and HRMS were in agreement. I ask for understanding that some things had to be prioritised over others. Furthermore, XRD crystals that had been acquired – or indeed would have been acquired within the time lost – could not be analysed, as XRD labs were also shut down. I say this with a heavy heart, as XRD analysis would be greatly desired for this thesis to unambiguously confirm proposed structures. Hopefully, analysis will be performed at some point, and I apologise for any potential wrong results presented as a result of these difficulties.

With that sombre remark out of the way, let's thank those who deserve it:

I am very grateful to my supervisor Anne Fiksdahl, for the golden opportunity to work in her research group. Her enthusiasm for the work, the persistent smile and the door that always stood open is all that one could ever hope for. Thank you!

I would then like to thank the rest of the research group, Ann Christin, Melanie, Helgi and Jostein. An extra thanks goes to my co-supervisor Ann Christin for her help and guidance.

I would like to thank Roger Aarvik for always being ready to conjure forth solvents, chemicals and equipment, even though cinnamon buns were never received despite multiple orders. Thank you to Julie Asmussen for help with HPLC and HRMS, Susana Villa Gonzalez for HRMS results, and Torun Margareta Melø for keeping the NMR instruments in shape. Thanks to my friend Tor Strømsem Haugland for help with setting up DFT calculations.

Finally, a big thanks to my mom and dad, my friends, and my girlfriend Idunn for their loving support, especially during the last, stressful months of the project.

Abstract

The initial purpose of this master's project was to investigate the capability of derivatives of 1,4,8,11-tetraazacyclotetradecane (cyclam, **6**) to act as chiral polydentate ligands in Au(III)-complexes. Due to unpromising results of the aforementioned study, investigations of polydentate 2,6-disubstiuted pyridine-systems (**15**) as sources of chiral ligands for Au(III) was initiated. In addition, study of a recently reported gold catalysed test-reaction was undertaken.

With the aim to synthesise new chiral organo-Au(III)-complexes, derivatives of the cyclam framework were propsed as ligands. After preparation of tetraamide **7b** from diamine **8b** and dimethyl malonyl chloride, attempts of reduction using $LiAlH_4$ to cyclam **6b** were unsuccessful. Consequently, an alternative strategy was formulated: mono-Boc-protection of the diamine precursor **8b** to **8b-Boc** allowed for the preparation of chiral 'open cyclam' derivatives **21** and **22**. Unfortunately, these 'open cyclam' systems were incapable of incorporating Au(III).

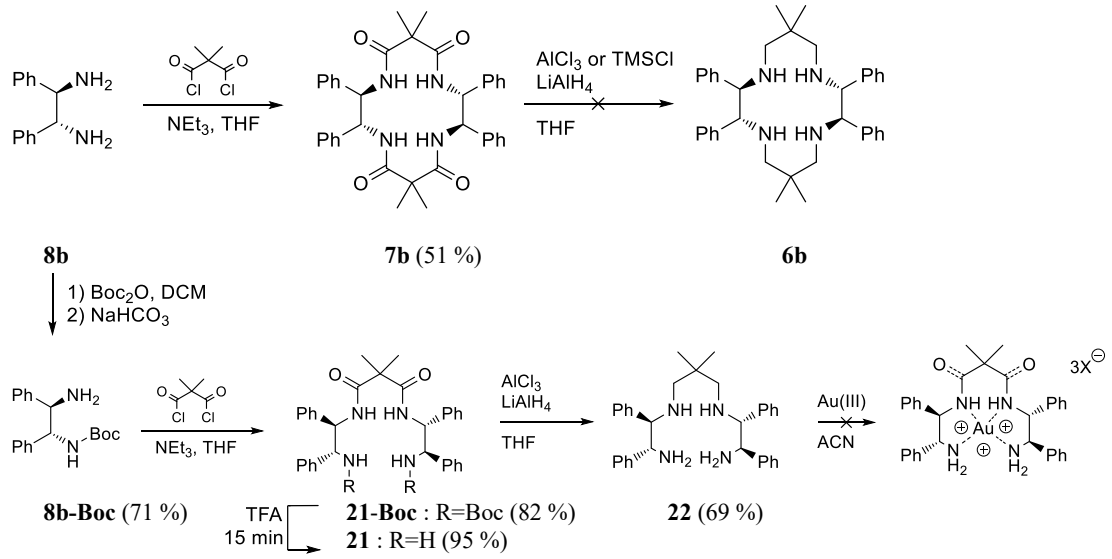

Synthesis and attempted Au(III)-coordination of various chiral cyclam derivatives.

Chiral 2-bromo-6-alkylpyridine alcohols **12a-b** were synthesised from 2,6-dibromopyridine (**13**) by treatment with BuLi and stereoselective addition to the chiral ketones (-)-menthone **14a** and (+)-camphor **14b**. A bipyridine analogue **15h** was synthesised in similar fashion. Subsequent Suzuki cross-couplings of **12a-b** with various commercially available boronic acids gave chiral 2-aryl-6-alkylpyridine alcohols **15a-g** in 41% to quantitative yields. Several of these compounds were novel and as such characterised.

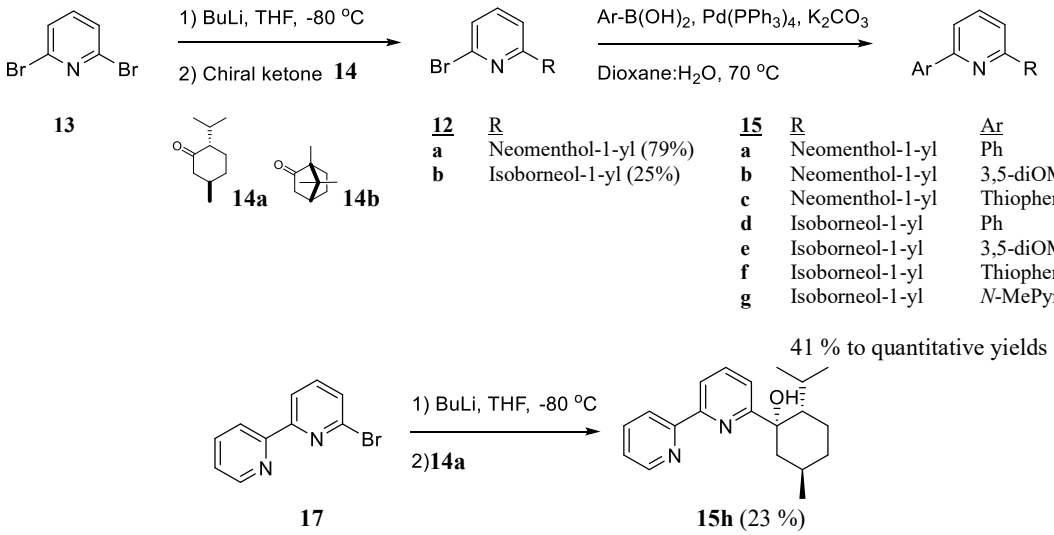

*Synthesis of chiral 2-aryl-6-alkylpyridine alcohols **15a-h**.*

Selected pyridine alcohols were also synthesised as the corresponding methyl ether by treatment with NaH and reaction with MeI. All methylated compounds were novel and therefore characterised.

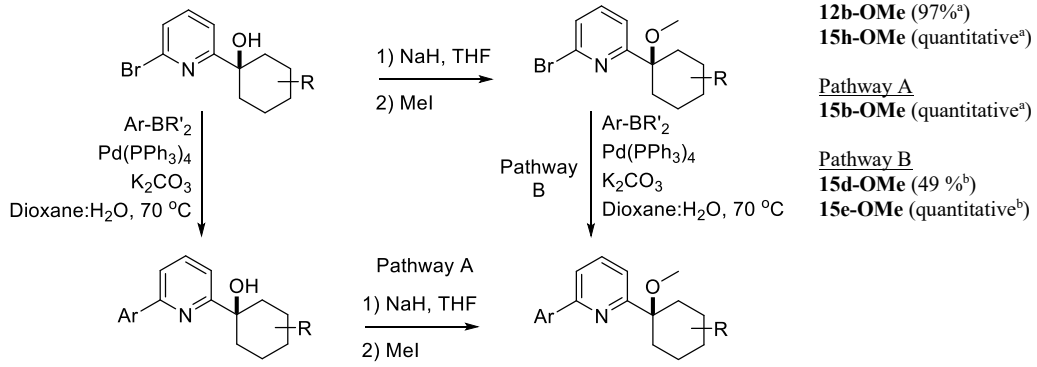

Synthesis of chiral pyridine methyl ethers. [a] Yield for methylation step. [b] Yield for Suzuki cross coupling.

Attempted coordinations of pyridine based ligands to gold(III) showed variable results, greatly depending on the pyridine substituents, as well as the reaction conditions. A series of coordination conditions were tested, but using an ACN:H_2O mixture as the solvent with inclusion of acetate and a silver-salt was found to be the optimal conditions for formation of Au(III)-complexes. Application of the present coordination protocol allowed for isolation and characterisation of the N,N,O-tridentate complexes Au(III)-**15h**-X (X = $AuCl_4$, NTf_2, SbF_6). While other N,N-bidentate and X,N,O-tridentate (X=N or S) Au(III) complexes are believed to have been prepared and crystals for XRD analysis acquired, their structures have not presently been confirmed. Efforts to achieve C-H activation for C,N,O-tridentate coordination by modification of substituent or altered reaction conditions were unsuccessful.

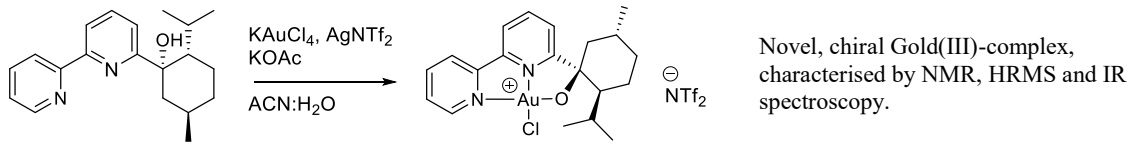

15h Au(III)-**15h**-NTf_2

Preparation of chiral Au(III) complex.

The novel bipyridine complex Au(III)-**15h**-NTf_2 was catalytically active in a [1+2]-cycloaddition reaction between propargyl acetate **11** and styrene. The resulting cyclopropane **20** was formed as a 76:24 *trans*:*cis* mixture, with no enantiomeric excess of either diastereomer. Analysis of the complex' NMR coupling constants gave important information on the conformation of the chiral auxilliary.

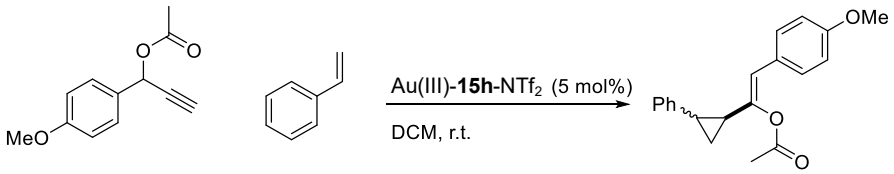

11 **20**

*Use of chiral Au(III)-**15h**-NTf_2 catalyst in a cyclopropanation test-reaction.*

Furthermore, a recently reported Au catalysed reaction between propargyl alcohols **1** and aryl nucleophiles was investigated with the aim to achieve asymmetric synthesis of the product allenes **3** and indenes **4**. The reaction was scoped with regards to solvent, Au-source, electronic, and steric effects of both the propargyl alcohol **1** and aryl nucleophile.

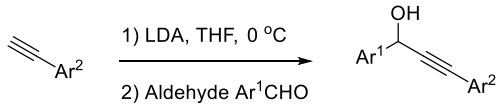

1	Ar^1	Ar^2
a	Ph	Ph
b	Ph	Mes
c	Ph	4-OMePh
d	Ph	4-CF_3Ph
e	Mes	Ph
f	Mes	4-CF_3Ph
g	2,6-diMePh	Ph
h	4-OMePh	Ph
i	4-CF_3Ph	Ph

18-67 % yields

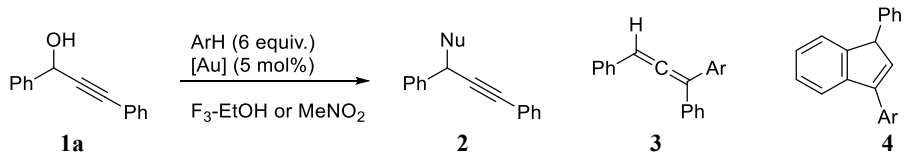

1a **2** **3** **4**

Gold catalysed reactions of propargyl alcohols.

Polar, non-nucleophilic solvents such as $MeNO_2$ or CF_3CH_2OH (F_3-EtOH) were most suited to avoid formation of undesired side products **2** (Nu = Ar or solvent). EtOH was found to be a better nucleophile than the included aryls, and an unexpected side reaction took place leading to dimer α,β-unsaturated ketone **19**. A mechanism for its formation is suggested.

Au(III) salts were generally more effective than Au(I) for these reactions. Electronic effects greatly governed the outcome of the reactions, and, in general, anything other than electronically neutral propargyl alcohols **1** and aryl nucleophiles gave undesired side products

2. Sterically encumbering the propargylic position by choice of aldehyde precursor resulted in great reduction of undesired propargylic substitution product **2** and primarily yielded the allene **3**.

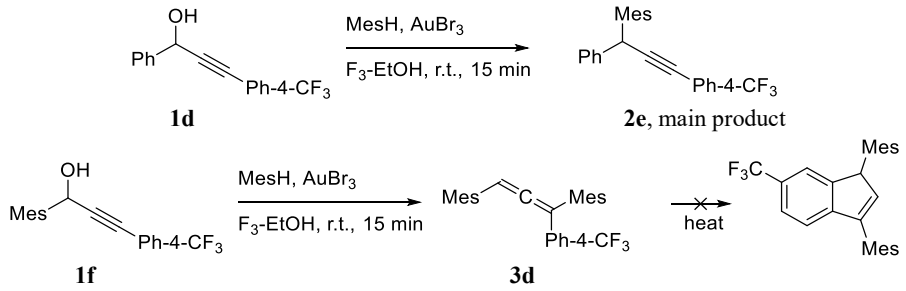

Different behaviour of sterically encumbering propargylic position.

Separation of the products was labour intensive due to their non-polar nature. Baseline separation of enantiomers by chiral HPLC was unsuccessful with various compounds, columns, and eluents, rendering these test-reactions unsuitable for new chiral Au-complexes.

Sammendrag

Det tiltenkte målet med denne masteroppgave var å undersøke mulighetene for bruk av derivater av 1,4,8,11-tetraazasyklotetradecan (cyclam, **6**) som ligander for Au(III)-komplekser. Grunnet lite givende resultater i det ovenfornevnte studiet, begynte utforskning av polidentate 2,6-disubstituerte pyridinsystemer (**15**) som kilde for kirale ligander for Au(III). I tillegg ble et studie av en nylig rapportert gullkatalysert testreaksjon utført.

Med sikte på å syntetisere nye kirale organo-Au(III)-komplekser ble cyclamderivater foreslått som ligander. Etter fremstilling av tetraamid **7b** fra diamin **8b** og dimetylmalonylklorid, var forsøk på reduksjon ved bruk av $LiAlH_4$ til cyclam **6b** ikke vellykkede. Følgelig ble en alternativ strategi formulert: mono-Boc-beskyttelse av diaminforløperen **8b** til **8b-Boc** muliggjorde fremstilling av kirale 'åpen cyclam' derivater **21** og **22**. Dessverre var ikke disse 'åpen cyclam' systemene i stand til å innlemme Au(III).

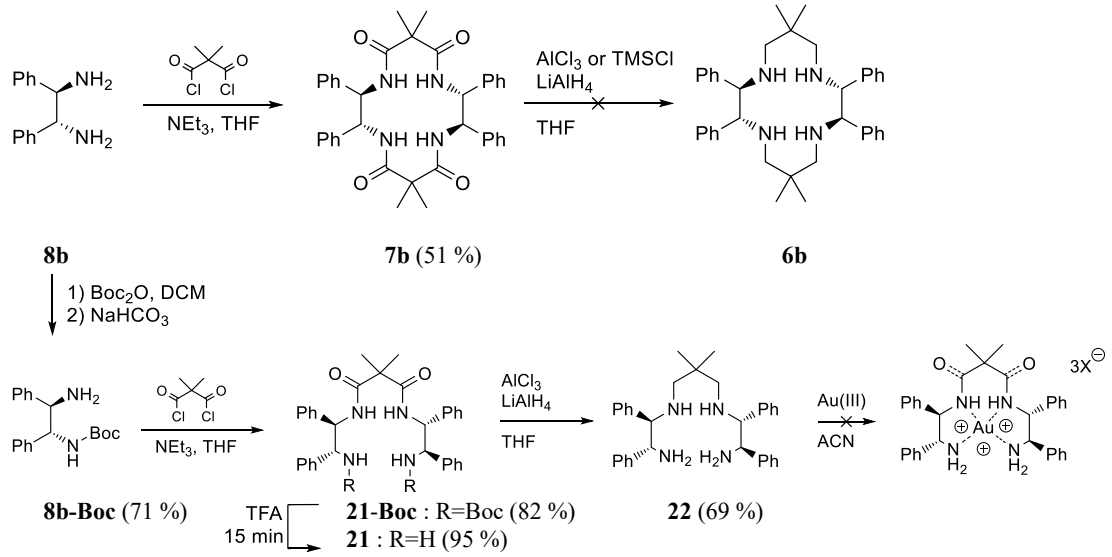

Syntese og forsøkt Au(III)-koordinering av forskjellige kirale cyclam derivater.

Kirale 2-brom-6-alkylpyridinalkoholer **12a-b** ble syntetisert fra 2,6-dibromopyridin (**13**) ved tilsats av BuLi og stereoselektiv tilnærming til de kirale ketonene (-)-menton **14a** og (+)-kamfer **14b**. En bipyridinanalog **15h** ble syntetisert på lignende måte. Etterfølgende Suzuki krysskoblinger av **12a-b** med forskjellige kommersielt tilgjengelige boronsyrer ga kirale 2-aryl-6-alkylpyridinalkoholer **15a-g** i 41% til kvantitative utbytter. Flere av disse forbindelsene var nye og som sådan karakteriserte.

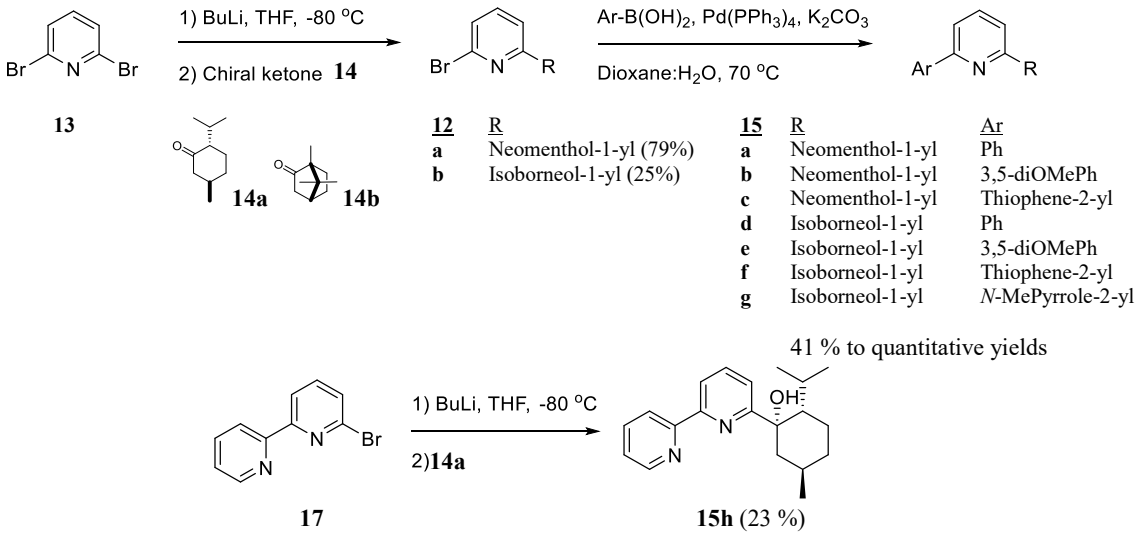

*Syntese av kirale 2-aryl-6-alkylpyridinealksohyoler **15a-h**.*

Utvalgte pyridinalkoholer ble også syntetisert som den tilsvarende metyleteren ved behandling med NaH og reaksjon med MeI. Alle metylerte forbindelser var nye og derfor karakteriserte.

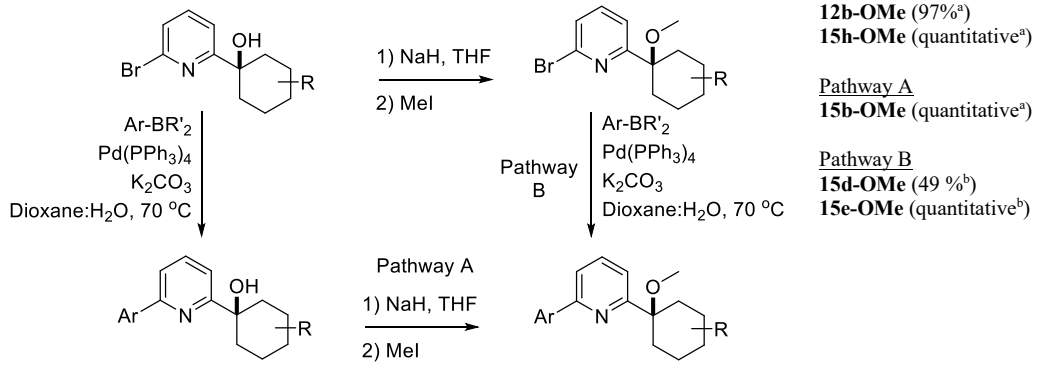

Syntese av kirale pyridin metyl etere. [a] Ubytte for metyleringssteg. [b] Utbytte for Suzuki krysskobling.

Forsøkte koordineringer av pyridinbaserte ligander til gull(III) ga varierende resultater, sterkt avhengig av pyridinsubstituentene, så vel som reaksjonsbetingelsene. En rekke koordinasjonsbetingelser ble testet, men bruk av en ACN:H_2O-blanding som løsningsmiddel med tilsats acetat og et sølvsalt ble det bestemt til å være de optimale betingelser for dannelse av Au(III)-komplekser. Anvendelse av den presenterte koordineringsprotokollen tillot isolering og karakterisering av N,N,O-tridentate komplekser Au(III)-**15h**-X (X = $AuCl_4$, NTf_2, SbF_6). Andre N,N-bidentate og X,N,O-tridentate (X = N eller S) Au(III)-komplekser antas å ha blitt fremstilt, og krystaller for XRD-analyse anskaffet, men deres strukturer foreløpig ikke bekreftet. Forsøk på å oppnå C-H-aktivering for C,N,O-tridentat-koordinering ved modifisering av substituenter eller endrede reaksjonsbetingelser var ikke vellykkede.

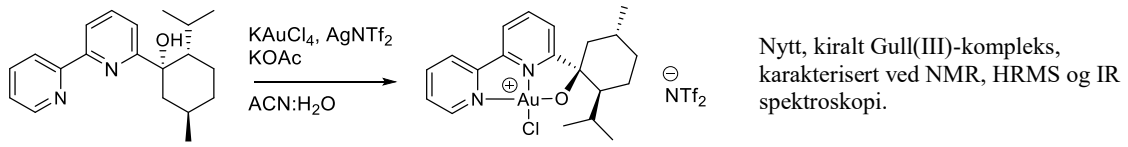

Fremstilling av kiralt Au(III) kompleks.

Det nye bipyridinkomplekset Au(III)-**15h**-NTf_2 var katalytisk aktivt i en [1+2]-sykloaddisjonsreaksjon mellom propargylacetat **11** og styren. Den resulterende cyklopropanen **20** ble dannet som en 76:24 *trans*:*cis*-blanding, uten noe enantiomert overskudd av noen diastereomerene. Analyse av kompleksets NMR-koblingskonstanter ga viktig informasjon om konformasjonen av det kirale neomentholsystemet.

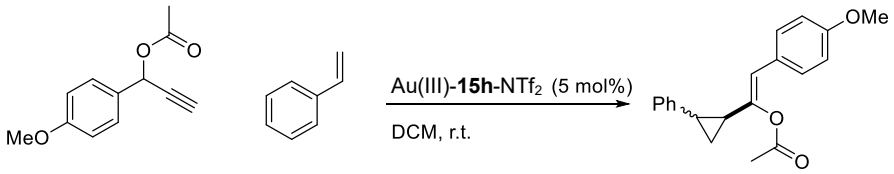

*Bruk av den kirale Au(III)-**15h**-NTf_2 katalysatoren i en syklopropanerings testreaksjon.*

Videre ble en nylig rapportert Au-katalysert reaksjon mellom propargylalkoholer **1** og arylnukleofiler undersøkt med sikte på å oppnå asymmetrisk syntese av allener **3** og indener **4**. Reaksjonen ble testet med hensyn på løsningsmiddel, Au-kilde, elektronisk og sterisk effekter av både propargylalkohol **1** og arylnukleofil.

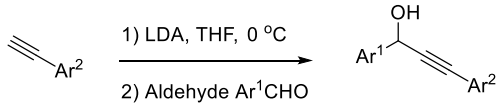

1	Ar^1	Ar^2
a	Ph	Ph
b	Ph	Mes
c	Ph	4-OMePh
d	Ph	4-CF_3Ph
e	Mes	Ph
f	Mes	4-CF_3Ph
g	2,6-diMePh	Ph
h	4-OMePh	Ph
i	4-CF_3Ph	Ph

18-67 % yields

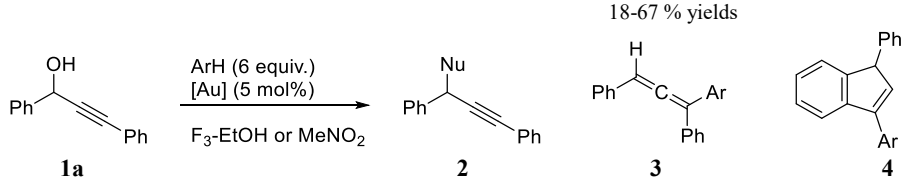

Gullkatalysert reaksjon av propargylalkoholer.

Polare, ikke-nukleofile løsningsmidler som $MeNO_2$ eller CF_3CH_2OH (F_3-EtOH) var mest egnet for å unngå dannelse av uønskede biprodukter **2** (Nu = Ar eller løsningsmiddel). EtOH ble vist til å være en bedre nukleofil enn de inkluderte arenene, og en uventet sidereaksjon fant sted som førte til et dimerisk α,β-umettet keton **19**. En mekanisme for dens dannelse er foreslått.

Au(III)-salter var generelt mer effektive enn Au(I) for disse reaksjonene. Elektroniske effekter styrte resultatet av reaksjonene i stor grad, og generelt, alt annet enn elektronisk nøytrale propargylalkoholer **1** og arylnukleofiler ga uønskede biprodukter. Sterisk begrensning

av propargylposisjonen ved valg av aldehyd-forløper resulterte i stor reduksjon av uønsket propargylsubstitusjon produkt **2** og ga primært allen **3**.

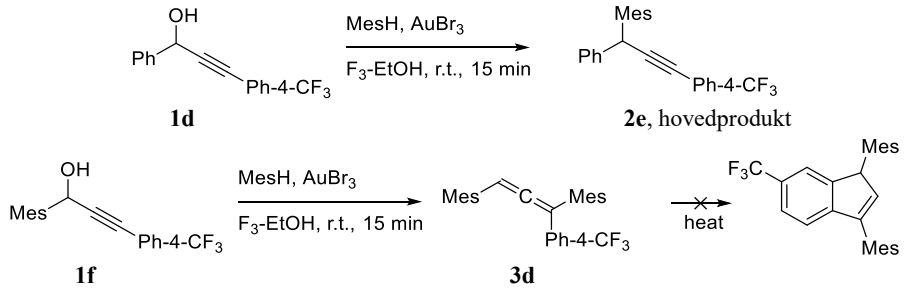

Forskjellige oppførsel av sterisk begrensede propargylalkohol.

Separasjonen av produktene var arbeidskrevende siden de var sammenlignbart upolare. Basislinjeseparasjon av enantiomerer ved kiral HPLC var ikke vellykket med forskjellige forbindelser, kolonner og elueringsmidler, noe som gjorde disse testreaksjonene uegnet for nye kirale Au-komplekser.

Symbols and abbreviations

Ac	Acetyl
ACN	Acetonitrile
AcOH	Acetic acid
Ar	Aromatic / Aryl
ax	Axial
cm^{-1}	Wave number
COSY	^{1}H-^{1}H Correlation spectroscopy
δ	Chemical shift (ppm)
DCM	Dichloromethane
DCE	1,2-Dichloroethane
DEE	Diethylether
d	Doublet, or Deuterated
dd	Doublet of doublets
E	Electrophile
ee	Enantiomeric excess
equiv.	Equivalent(s)
eq	Equatorial
Et	Ethyl
HMBC	Heteronuclear multiple bond correlation
HRMS	High resolution mass spectrometry
HSQC	Heteronuclear single quantum correlation
Hz	Hertz
*i*Pr	*iso*-Propyl
IR	Infrared spectroscopy
J	Coupling constant
L	Ligand
LDA	Lithium di*iso*propyl amide
M^{+}	Molecular ion
m	Multiplet
Me	Methyl

MeOH	Methanol
Mes	Mesityl
MS	Molecular sieves
m/z	Mass-per-charge ratio
NMR	Nuclear magnetic resonance
n.o.	Not observed
NOESY	^{1}H,^{1}H-Nuclear Overhauser effect spectroscopy
Nu	Nucleophile
obsd	Observed
o.n.	Over night
Ph	Phenyl
Piv	Pivaloyl
Py	Pyridyl
ppm	Parts per million
refl.	Reflux
R_f	Retention factor
r.t.	Room temperature
s	Singlet
TFA	2,2,2-trifluoroacetic acid
t	Triplet
*t*Bu	*tert*-Butyl
THF	Tetrahydrofuran
TLC	Thin layer chromatography
TOCSY	^{1}H,^{1}H-Total correlation spectroscopy

Contents

1 Introduction

Everyone is familiar with gold as a dark yellow metal, highly priced in most societies that we have historical records from. It was one of the first metals to be discovered, as it can be found in its metallic form in nature. While the universe has produced gold by supernova nucleosynthesis and through the collision of neutron stars,[1] alchemists thought they could create gold by mixing of various liquids and other lower metals. Such endeavours were of course unsuccessful, but their ideas and experiments started a way of thinking and working that we today know as chemistry.

Over the centuries, the table has indeed turned from chemists trying to transform other materials into gold, to using gold to transform other materials. In the recent decades, the use of gold as a catalyst in organic reactions has seen a pique in interest as the field of organometallic chemistry is well established and one of the largest areas of current research. The chemical transformations that gold enables allow for new synthetic routes to valuable compounds.

1.1 Aim of Project

The original aim of this project was to synthesise polydentate ligands based on the structure of 1,4,8,11-tetraazacyclotetradecane (cyclam, **6**), followed by their attempted coordination to Au(III).

Furthermore, a study was undertaken of a recently reported Au(III)-catalysed reaction between propargyl alcohols (**1**) and aryl nucleophiles, producing either allenes **3** or indenes **4** (Scheme 1).[2] The Fiksdahl research-group is continuously involved in the synthesis of novel organometallic Au(I) and Au(III) complexes. Thus, achieving asymmetric formation of either allenes (**3**) or indenes (**4**) through the present reaction would allow for another complimentary method to those already established in the research group to assess enantioselectivities of novel chiral Au-catalysts.

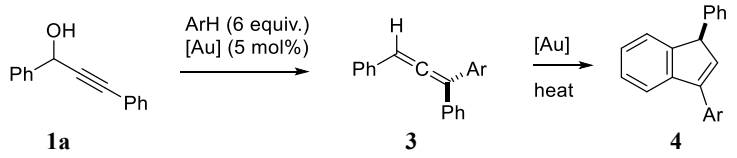

*Scheme 1 – Gold catalysed reaction between propargyl alcohols **1** and aryl nucleophiles.*

In addition, the synthesis of chiral pyridine based ligands and their attempted coordination to Au(III) was of interest for this master's project. If successful, these complexes would be fully characterized by HRMS, NMR-, IR-, and XRD spectroscopy, and applied in our available test-reactions for gauging catalytic activity and enantioselectivity.

2 Theory

This chapter will cover relevant theoretical concepts for this master's thesis. It will start with an introduction to the field of gold catalysis in organic chemistry. Some theory related to organogold ligands will then be presented. The relevant chemical motifs of allenes, indenes, and cyclams, which might not be familiar to every organic chemist, will be introduced. Finally, the Morita-Baylis-Hillman reaction for preparation of α-substituted α,β-unsaturated ketones will be briefly presented.

2.1 The Chemistry of Gold

Elemental gold has since the cradle of chemistry been known to be stable, which is one of the attributes that has made it so famous and timeless; while nitric acid is generally strong enough to oxidize most other transition metals, gold requires the addition of hydrochloric acid as well. This mixture is commonly known as *aqua regia* – royal water – named after its ability to dissolve the royal metals of group 11. Furthermore, gold can be oxidized by oxygen in aqueous cyanide, which is the most commonly employed process for leaching gold from ores.[3]

The field of gold catalysis for organic transformations was for many years notoriously neglected in favour of other transition metals. Whether this was due to the perceived high cost of the metal or the known stability of gold(0) is unclear. Still, other metals of higher market cost – such as Pd, Ir, and Rh – have received a lot of successful attention and are now incorporated into routine reactions known by any organic chemist.

In homogenous reactions, gold generally exists in the +1 or +3 oxidation states. Still, Au(0) can exist as nanoparticles which are catalytically active.[4,5] As a result, uncertainty to what the active species in solution is can arise. Over the past decades, Au(I) has received the most attention, and it has been argued that Au(III) catalysts are only precursors to Au(I) which is formed *in situ*. Such statements have in later time been proven wrong, and the present work also exemplifies this. Consequently, further research into Au(III) catalysts have started to catch on.

Gold is mostly considered a carbophilic Lewis acid, having a strong affinity towards carbon-carbon multiple bonds, especially alkynes, but also alkenes and allenes. It has also been argued that carbonyl compounds can show activation in presence of Au(III).[6] Since organogold complexes are generally stable towards air and moisture handling is straightforward. Gold complexes have also in the last couple of decades been investigated for biological activity.[7,8] Since Au is considered a Lewis acid it normally has quite different catalytic cycles compared to other transition metals; oxidation states are often omitted, instead simply varying between a free cation and a bound neutral species (or alternatively, a free neutral species and a bound anionic species). Because of this, note that the positive charge of $[AuL]^+$ does not say anything about gold's oxidation state, but only signifies a catalytically active species. A catalytic cycle for a nucleophilic attack to a triple bond is depicted in Scheme 2.

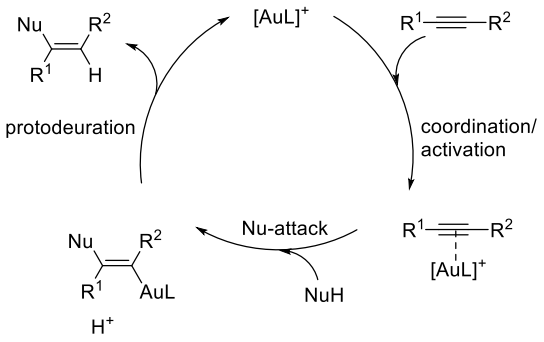

Scheme 2 – Catalytic cycle of Au facilitating nucleophilic attack on an alkyne.

Coordination of Au to the alkyne makes the triple bond electron deficient, activating for nucleophilic attack in the subsequent step. If the nucleophilic atom bears a hydrogen, liberation of gold in a process known as protodeauration follows, which regenerates the catalyst and releases the alkene product. Interesting cases exist, for example if the nucleophile is water, as the following tautomerization will yield a ketone,[9] allowing for mild and selective hydration of alkynes.

In addition to acting as an electron deficient Lewis acid, gold is also able to act as an electron donor. Relativistic effects are invoked to explain this, by the contraction of the *6s* orbital. The closer packing of the inner orbitals causes a heightened shielding effect for the valence *5d* orbital, thereby expanding and delocalizing it. The delocalization allows for facile backbonding from gold to stabilize cationic intermediates through carbenoid species.[3] The effect is shown schematically with an alkene nucleophile in Scheme 3a, and an example of a Au(I)-catalysed intramolecular tandem cyclopropanation given in Scheme 3b.[10]

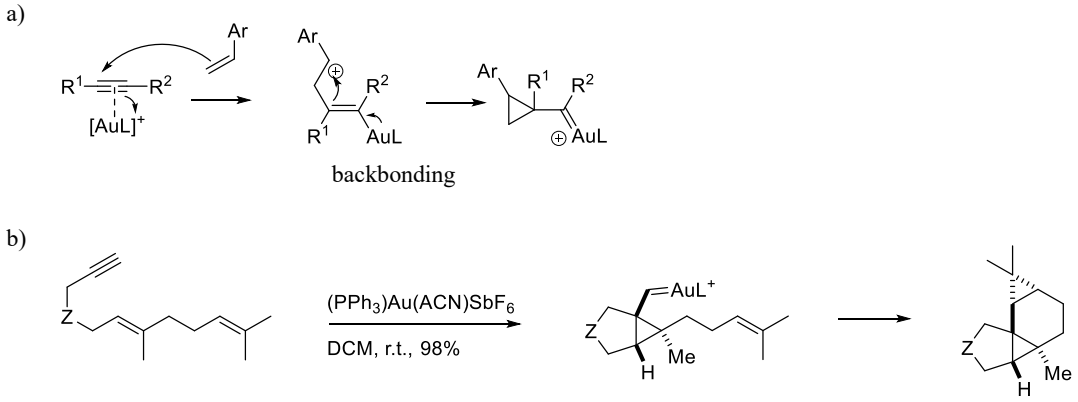

Scheme 3 – Gold backbonding to form carbenoid species, stabilizing the intermediate cation ($Z=C(CO_2Me)_2$).

2.2 Ligands of Homogenous Gold Catalysts

Ligands for commercial Au(I) and Au(III) catalysts vary due to the different electronic configurations of the two oxidation states. Au(I) complexes are linear with two coordination points, while Au(III) are square planar with four coordination points. Au(I) forms stable bonds to chloride, phosphines, thioethers and nitriles as ligands, and NHC complexes are also readily

available. Au(III) is most commonly commercially available as either a trihalide or tetrahalide salt (Figure 1).

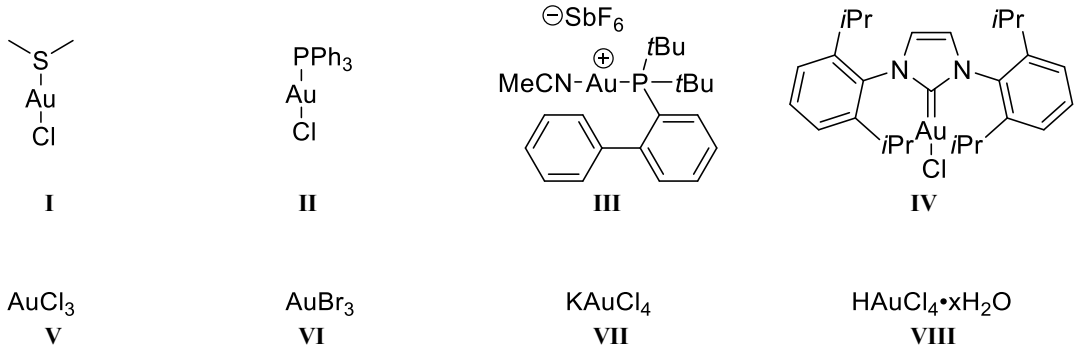

*Figure 1 – Various commercially available gold(I) (**I-IV**) and gold(III) (**V-VIII**) complexes and salts.*

Gold(I) salts such as **III** are active catalysts by dissociation of ACN in solution. All the illustrated gold(III) salts **V-VIII** are also active without the need for further activation. For some other catalysts, however, more forceful removal of a ligand is necessary to open up an active site at the metal. Conveniently, this can be done by addition of a silver salt AgX to act as a halide abstraction agent. X is generally a spherical, weakly coordinating anion such as SbF_6^- or BF_4^-, though more strongly coordinating alternatives such as NTf_2^- are also common. Moreover, the choice of counterion can have a significant effect on the catalysts action;[11] an achiral gold ligand with a chiral ferrocene counterion has been shown to produce great %ee.[12]

The gold catalysts become more interesting when attaching organic ligands, as this enables tailoring their reactivity. What follows is one of the currently most attractive facets of Au(III)-chemistry; the linearity of Au(I) complexes naturally holds the ligand at the opposite side of the metal from the substrate binding-site, and chemoselectivity is achieved by having bulky ligands that wrap around to the other side of gold, as can be seen in **IV**. Au(III), on the other hand, has in theory a greater potential to achieve chemo- and enantioselectivity by being able to bring the ligand(s) closer to the substrate through its square planar geometry.

Several heteroatoms have been shown to coordinate to gold, but its fastidious oxidation state[13] plays a crucial role; while phosphor ligands readily coordinates to Au(I),[14] P-Au(III) bonds do not form spontaneously and are acquired by oxidation of their analoguous Au(I) complexes.[15] Nitrogen is recognized as the heteroatom which most readily coordinates Au(III), though the functional group in which it is situated affects the strength of the resulting Au-N bond. For example, amines normally form strong, irreversible tethers to Au(III), whilst coordination through an amide-N seems to require the carbonyl to have further stabilization, such as in derivatives of benzamide and picolinamide.[16-19] Gold(III) complexes not involving the coordination to a nitrogen are mostly restricted to NHCs[20] (and even then, nitrogen has a pivotal role).

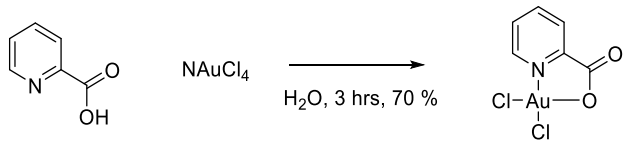

IX

Scheme 4 – N,O-bidentate Au(III) complex.

N,O-bidentate Au(III) complexes, such as **IX** (Scheme 4) have previously been synthesised by various groups and shown to be catalytically active.[21-23] Carboxylic acids allow for unaided coordination, whilst alcohols require further motivation. One reported method for achieving a Au-alkoxide σ-bond consists of mixing the ligand and Au(III)-salt precursor in an alkaline mixture of ACN:H_2O.[22] The 'required' N-Au(III) bond forms naturally, and the O-Au(III) forms by deprotonation of an alcohol by base ($^-$OH or $^-$OAc). In such a case, Au(III) is coordinated to the two heteroatoms from the ligand, and two halogens from the salt precursor (typically chloride). Normally, halides do not passively dissociate from the metal centre to allow for catalytic activity. Such behaviour is however possible for coordinative heteroatoms of organoligands. The 16-electron pyridine-oxazoline complex **X** was by ^{1}H,^{15}N-HMBC shown to dissociate pyridine, forming **X**' *in situ*, which creates an active site at gold without the need for added silver-salts (Scheme 5).[24] This was observed by a downfield shift of the pyridine-N and a corresponding upfield shift of the oxazoline-N, indicating a weakened/broken Au-pyridine bond and a strengthened Au-oxazoline bond as the positive charge becomes distributed over fewer atoms.

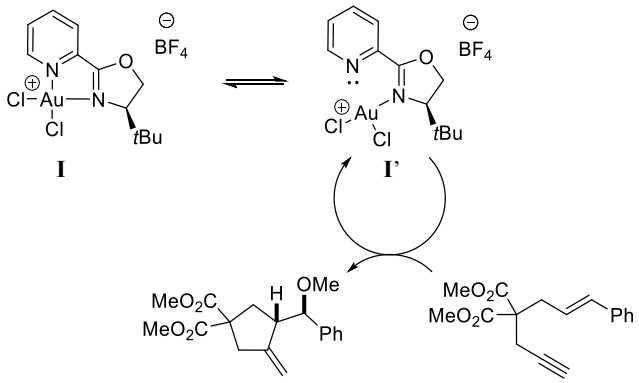

Scheme 5 – Catalytic activity achieved by temporary ligand dissociation.

2.3 Propargyl Esters and -Alcohols

Propargylic esters have earned an exceptional amount of attention within the field of gold catalysis, with several documented inter- and intramolecular transformations available from the same class of starting materials. The acyl group has the interesting ability to either perform a 1,2- or 1,3-shift, leading to carbenoid or allene species, respectively, both of which are prone for further transformations (Scheme 6a).[25-31] The 1,2-acyl shift also exemplifies the aforementioned backbonding ability of gold. Propargyl acetals have also been shown to be able

to undergo similar 1,2-alkoxy shifts.[32] Also, in the presence of water and gold, propargyl esters are also readily hydrated.[33,34] A reaction developed and utilised in our group for investigation of stereoselectivity of newly synthesised gold-complexes is the cyclopropanation of propargyl acetate **11** with styrene (Scheme 6b).[21,35] The resulting cyclopropane **20** has been theorised to preferentially form the *cis* diastereomer by proceeding through the most stable intermediate, but can – again by gold catalysis – isomerise to the *trans* diastereomer, often concomitant with loss of any enantiomeric excess the *cis* product might have achieved.[21]

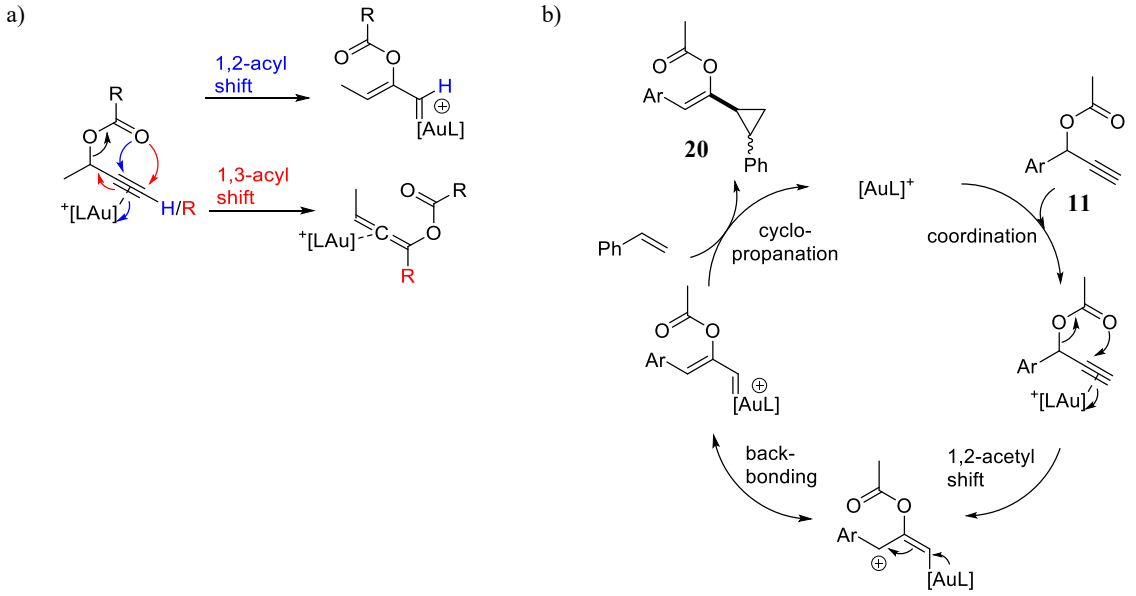

*Scheme 6 – a) Two reactivity patterns of propargyl esters. b) Gold-catalysed cyclopropanation of propargyl acetate **11** (Ar = 4-OMePh).*

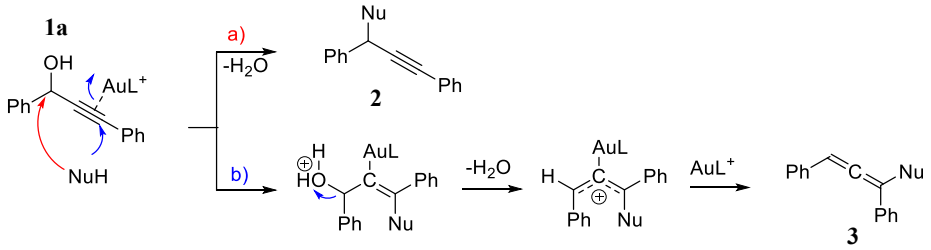

*Scheme 7 – Propargyl alcohol **1a** either yielding a 1,1,3-trisubstituted alkyne **2** (path a) or an allene **3** (path b).*

Another way of interpreting the 1,3-acyl shift for propargyl esters is by a nucleophilic attack on the terminal position of the alkyne accompanied by a leaving group in the propargylic position; it just so happens that the nucleophile and the leaving group are one and the same for the case of esters. However, substituting the ester for another leaving group and inclusion of an external protic nucleophile NuH should allow for similar reactivity, but with access to new compounds. An example of such a leaving group is an alcohol, releasing as water, shown in Scheme 7, path b. Xu and co-workers showed that from an enantiomerically enriched propargyl alcohol, only minor enantiomeric excess of the allene was formed under the catalytic activity

of **IX**,[36] indicative of an intermediate which loses the chiral information of the starting material.

Propargyl alcohols have also been thoroughly investigated for direct propargylic substitution, forming 1,1,3-trisubstituted prop-2-yns (**2**) from a variety of nucleophiles (Scheme 7a). Such reactions can be gold-catalysed,[37-39] though a variety of other transition metals and Lewis acids have also been used for this purpose.[40-44]

2.4 Allenes

An allene, or cumulene, is a functional group with the motif C=C=C. Despite their resemblance to a conjugated diene, allenes show no conjugative throughput. This is due to the p-orbitals on the central sp-hybridised carbon being orthogonal, thereby resulting in no orbital overlap and a twisted structure (se Figure 2). Followingly, allenes can form stereoisomers, as was suggested as early as in 1875 by van't Hoff. It wasn't until 60 years later that this was verified, when Maitland and Mills were the first to successfully synthesise two optically active allenes.[45]

The significance of broken conjugation becomes apparent when considering the addition reaction of HX to propadiene; one would expect protonation to occur at the central carbon as this would create a more stable allylic cation intermediate. However, since such a cation wouldn't be stabilised without bond-rotation, protonation occurs on a terminal position instead.[46-48] This seems to only be the case for propadiene though, as adding substituents yields products originating from protonation of the sp-carbon, maybe due to inductive effects.[49,50] These observations are shown in Scheme 8.

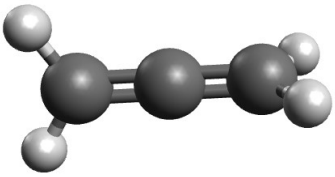

Figure 2 – Structure of propadiene.

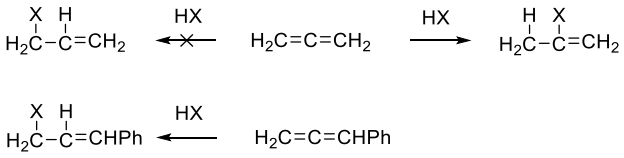

Scheme 8 – Addition of HX to propadiene and phenylallene.

Allenes are normally synthesised by prototropic rearrangement, from the corresponding propyne,[51-53] or by [2,3]- or [3,3]-sigmatropic rearrangments.[54-56] A gold(I)-catalysed Claisen-rearrangement forming an allene is shown in Scheme 9. Other synthetic routes for allene formation also exist, such as Cu(II)-catalysed coupling, additions to enynes, 1,2-eliminations, Wittig-type reaction, and more.[57-59]

2.5 Indenes

Synthetically, allenes are very useful in cyclisation reactions by various means. For example, vinyl allenes readily participate in Diels-Alder reactions as the product is inherently conjugated.[60] Homoallenic alcohols can form 2,5-dihydrofurans by gold(III)-catalysis.[13] Au is known to interact well with allenes, even forming stable, isolable complexes such as **XI** (Figure 3).[61] Such complexes can fluctuate between η^1 and η^2 coordination modes, which causes what is known as π-face exchange. This allows gold to dynamically 'twist' around the allene, thereby changing which C=C bond of the allene it is coordinated to. This is illustrated in Scheme 10.

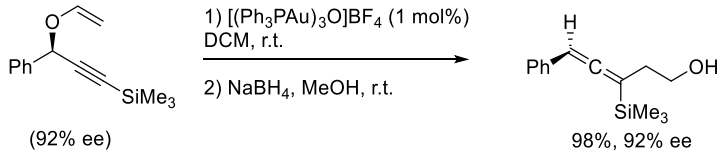

Scheme 9 – Gold(I)-catalysed Claisen rearrangement of a propargyl vinyl ether to an allene.[62]

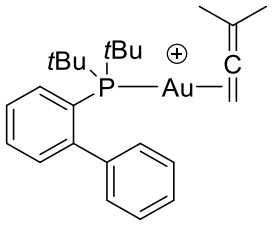

XI

Figure 3 – A stable, isolable Au(I)-allene complex.[61]

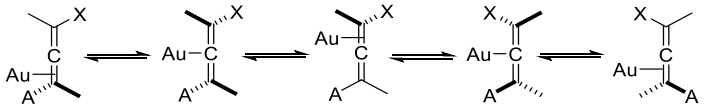

Scheme 10 – Au undergoing π-face exchange of an allene.

2.5 Indenes

An indene (**4**) is an attractive scaffold due to its biological activities, as exemplified by Sulindac (**5**) which is used as a non-steroidal anti-inflammatory drug (NSAID) in its racemic form (Figure 4a).[63] Two different isomers exist, 1*H*-indene and 2*H*-indene, the former being the most common due to increased stability of its aromatic system (Figure 4b and c). 'Indene' will from here on assume the 1*H*-isomer. Indene is a remarkably stable structures, resisting oxidation of the cyclopentene-ring even in harsh conditions.[64] Several metal-catalysed reactions have been reported for the synthesis of substituted indenes such as by Fe,[65] Zr,[66] Rh,[67], Pt,[30] and Co.[68] Au(I) has also been shown to facilitate such reactions from propargyl acetates,[31] and also being able to form the saturated derivative 2,3-dihydro-1*H*-indene in a dimeric reaction of vinyl phenyls.[69]

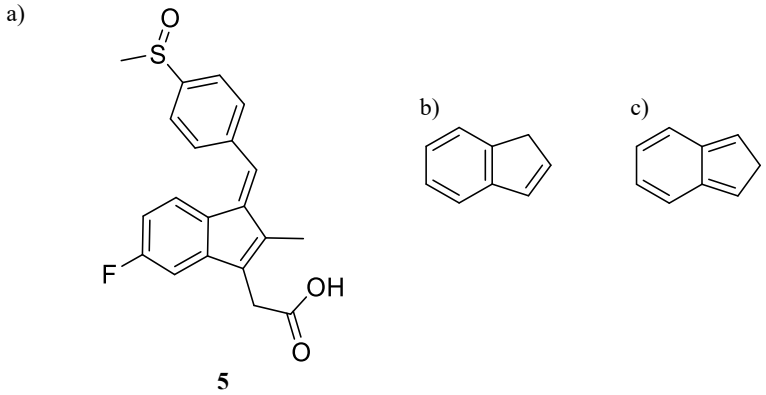

*Figure 4 – a) The structure of sulindac (**5**), and the two forms of indene, b) 1*H*-indene and c) 2*H*-indene.*

The Au-catalysed cyclisation of allenes to indenes was observed in 2006 by Marion and co-workers, and picked up in 2016 by Morita and co-workers, though their mechanistic explanations of the reaction differed.[2,31] Marion investigated propargyl acetates in the presence of Au(I) species, and found that the resulting indenes could give various regioisomers. The varying products were explained the acetyl group undergoing a 1,2-shift, 1,3-shift, or no shift at all, and the final cyclisation simply explained by a general hydroarylation.[70] Morita investigated propargyl alcohols in the presence of Au(III) species, with an added aryl nucleophile. They found substrate **1a** to initially form an allene **3a**, and formulated a subsequent Nazarov cyclisation-like step[71,72] that required heating, forming the indene product **4a** (Scheme 11). Whether heating assists the Au-allene interaction or the Nazarov cyclisation is unknown. The cyclisation could also be performed by either of the two phenyl rings of **3a**, one being sterically favoured (as shown) while the other being electronically favoured as the intermediate positive charge would be predominant on a doubly benzylic carbon. Gauging by the isolated products, steric effects were dominant for these reactions.

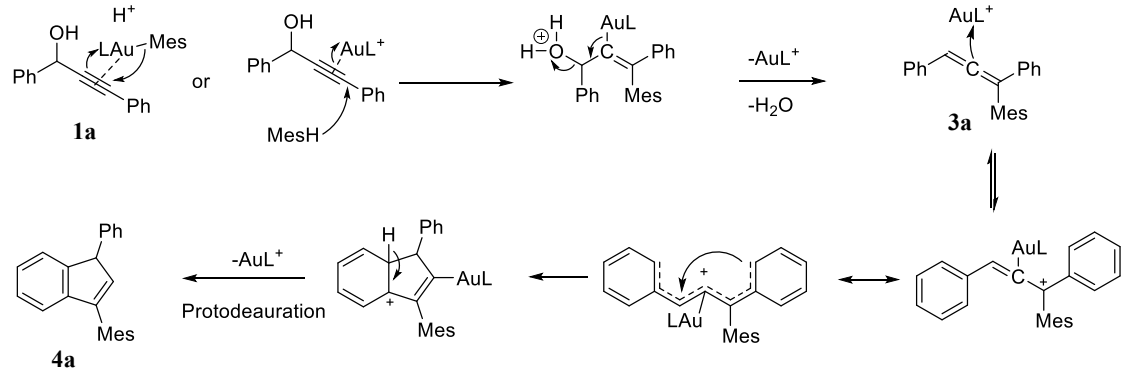

Scheme 11 – Suggested mechanism by Morita et al.[2] for the Au-catalysed formation of allenes and indenes from propargyl alcohols.

2.6 Cyclams

1,4,8,11-Tetraazacyclotetradecanes (cyclams, **6**, Figure 5) are macrocyclic compounds, known as strongly chelating ligands.[73] The four nitrogens create an electron rich cavity in the interior of the ring-system which well accommodates a cationic metal in a square-planar

configuration. Cyclam-systems have also found useful applications in biological studies.[74,75] Ni(II)(cyclam)-complexes have been quite thoroughly investigated.[76] Other metals have also been incorporated into the cyclam-scaffold,[77] even as η^1- and η^2-coordinated species to elemental oxygen.[78]

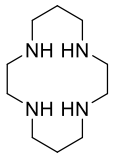

6

*Figure 5 – Structure of cyclam, **6**.*

A few Au(III)-cyclam complexes have been synthesised, but the related work focused on selective uptake of Au-particles.[16] Chiral, enantiopure cyclams were synthesised for the first time in 1988 by Wagler and Burrows by the use of L-phenylalanine.[79] Recently, synthesis of some chiral amide-cyclam derivatives, such as **7a**, were reported in low yields by condensation reactions between a malonyl chlorides and chiral 1,2-diamines (**8**).[80] An example is given in Scheme 12.

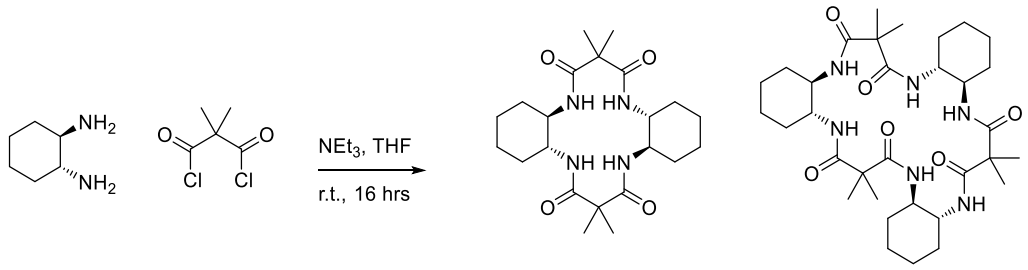

8a **7a** (36 %) **7a'** (14 %)

*Scheme 12 – Condensation of (1R, 2R)-cyclohexane-1,2-diamine (**8a**) with dimethyl malonyl chloride, forming chiral cyclam **7a** along with the trimer side product **7a'**.[80]*

2.7 Morita-Baylis-Hillman (MBH) Reaction

In the MBH reaction (sometimes only called a Baylis-Hillman reaction), a conjugatively activated vinyl system and a suitable electrophile add to form α-substituted α,β-unsaturated compounds, catalysed by a mild base such as NEt_3.[81] The reaction is schematically shown in Scheme 13, where an aldehyde acts as the electrophile. The activated vinyl system (for example an α,β-unsaturated ester) is attacked by the base, forming a zwitterion with a stabilised negative charge. The resulting enolate nucleophilic carbon attacks the aldehyde in the C-C bond forming step, and an additional equivalent of base then assists release of the product. These reactions allow for a versatile method for C-C bond formation to densely functionalised compounds.

2.7 Morita-Baylis-Hillman (MBH) Reaction

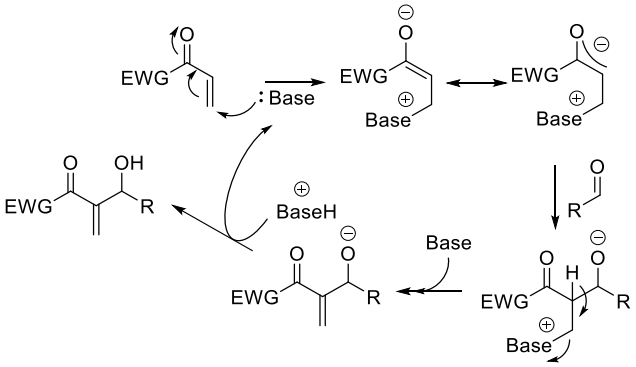

Scheme 13 – A base catalysed MBH reaction. EWG = Electron withdrawing group.

Several modifications exist, such as aza-MBH reactions where an imine acts as the electrophile,[82] or the use of phosphines[83] or carbenes[84,85] as the catalyst. Systems using a TMS-ether substituted allene as the activated vinyl-species have also been reported.[86]

3 Results and Discussion

This section will be split into 4 parts. The first section will cover synthesis of relevant starting materials for later sections, namely propargyl alcohols, substituted pyridines and their related compounds. The second section covers the gold catalysed reactions of propargyl alcohols **1** with aryl nucleophiles, and related studies. Next, coordination studies of pyridine based ligands, forming chiral organogold(III)-complexes, will be presented, along with investigation of catalytic activity in a [1+2]-cycloaddition reaction. Finally, synthesis of cyclam ligands and related coordination to Au(III) will be presented.

3.1 Synthesis of Starting Materials

This section covers the synthesis propargyl alcohols (**1a-i**), chiral pyridine derivatives (**12a-b**, **15a-h**, **12b-OMe** and **15b,d,e,h-OMe**), and other related compounds.

3.1.1 Synthesis of Propargyl Alcohols, 1a-i

For the investigation of the reaction of propargyl alcohols **1** with aryl nucleophiles in the presence of a Au-catalyst, a range of propargyl alcohols needed to be prepared. Therefore, the propargyl alcohols **1a-i** were synthesised according to literature procedure from aldehydes **9a-e** and arylacetylenes **10a-d**, shown in Scheme 14.[87]

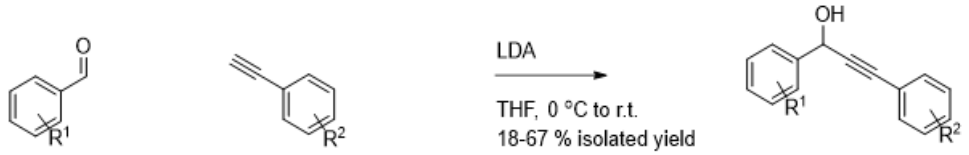

9	R^1
a	H
b	2,4,6-triMe
c	2,6-diMe
d	4-OMe
e	4-CF_3

10	R^2
a	H
b	2,4,6-triMe
c	4-OMe
d	4-CF_3

1	R^1	R^2
a	H	H
b	H	2,4,6-triMe
c	H	4-OMe
d	H	4-CF_3
e	2,4,6-triMe	H
f	2,4,6-triMe	4-CF_3
g	2,6-diMe	H
h	4-OMe	H
i	4-CF_3	H

*Scheme 14 – Synthesis of propargyl alcohols **1a-i**.*

Arylacetylenes **10** were deprotonated by LDA to give the corresponding lithium alkynyl anion. Upon addition of the aldehyde, the acetylide anion acts as a nucleophile towards the carbonyl, forming racemic propargyl lithium alkoxides. Protonation by aqueous workup formed the desired propargyl alcohol products **1a-i** in fair isolated yields (41-67 %) with the exception of **1c** which was isolated in only 18 % yield. Similar reactions have been reported in good to excellent yields,[88] only differing by the use of *n*-BuLi instead of LDA and performing the deprotonation at -78 °C instead of 0 °C. A combination of these factors can have contributed the decreased yields. The poor yield of **1c** is due to extensive overlap with an unknown side-product during flash chromatography.

3.1 Synthesis of Starting Materials

Propargyl alcohols **1a**, **1c-d** and **1g-i** have been previously reported, and ^{1}H NMR spectra were in accordance with the reported values.[83,89,90] Products **1b**, **e** and **f** have not been reported, and were consequently fully characterized by NMR and HRMS. The assigned ^{1}H and ^{13}C NMR shifts of the novel propargyl alcohols are presented in Figure 6.

The propargyl alcohols **1e-f** originating from mesitaldehyde (**9b**), displayed the curious behaviour of changing colour from yellow to green upon standing without any signs of degradation by ^{1}H NMR. A second flash column of **1f** returned the product to the original yellow coloured oil, which once again turned back to green even when protected from light in the freezer. Regardless, the green colour did not seem to hinder the reactivity of the compounds in further reactions.

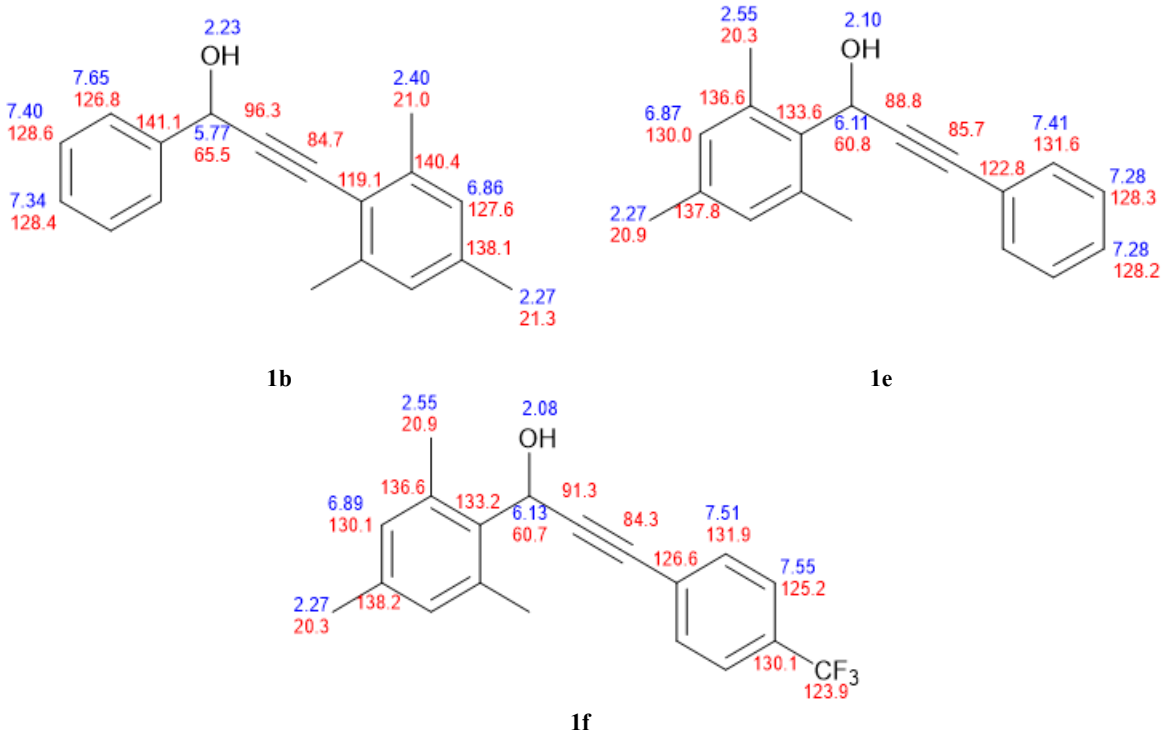

*Figure 6 – Assigned ^{1}H and ^{13}C shifts of previously unreported propargyl alcohols **1b**, **1e** and **1f**.*

3.1.2 Synthesis of Propargyl Acetate, 11

Propargyl acetate **11** was synthesised based on a previously reported strategy.[41] The reaction is shown in Scheme 15.

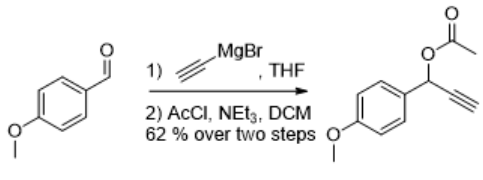

9d **11**

*Scheme 15 – Synthesis of propargyl acetate **11**.*

The commercially available ethynyl Grignard reagent was added slowly to a stirred solution of aldehyde **9d** at r.t., forming the corresponding propargyl alkoxide in 1 hr. Addition of NH_4Cl (sat.) simultaneously quenched the slight excess of the Grignard and protonated the alkoxide. Extraction gave the intermediate propargyl alcohol. Without further purification, this intermediate alcohol was reacted with an excess of acetyl chloride at r.t. overnight to give the desired product **11** in 62% yield over 2 steps. ^{1}H NMR of both the intermediate propargyl alcohol and the product propargyl acetate **11** were in accordance with previously reported data.[41,42]

3.1.3 Synthesis of Chiral 2-bromo-6-alkylpyridines Alcohols, 12a-c

Organogold(III)-complexes in literature greatly revolve around coordination to nitrogens, situated in various functional groups. The N,O-bidentate 2-(neomenthol-1'-yl)pyridine Au(III) complex **XII** was recently synthesised in our group, and further investigation into such hetero-polydentate complexes was desired.[21] The features of the Au-O bond are of particular interest.

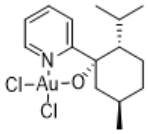

XII

*Figure 7 – Structure of previously synthesised Au(III) complex **XII**.*

The 2-bromo-6-alkylpyridines **12a-c** were synthesised based on previously reported procedures from 2,6-dibromopyridine (**13**) and chiral ketones from natural ketones (**14**).[91,92] The chiral ketones used were chosen based on availability: (-)-menthone (**14a**), (+)-camphor (**14b**) and (-)-fenchone (**14c**). These reactions are summarised in Scheme 16.

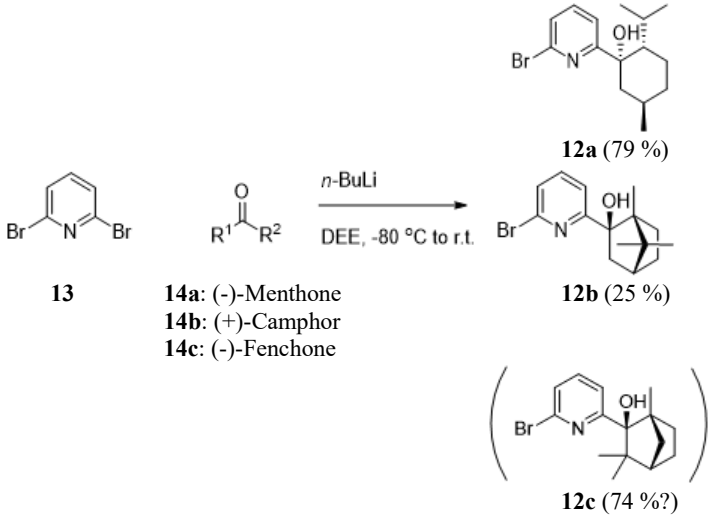

*Scheme 16 – Synthesis of chiral 2-bromo-6-alkylpyridines **12a-c.***

Treatment of 2,6-dibromopyridine (**13**) with 1.05 equiv. *n*-BuLi in dry DEE at -80 °C results in halogen-lithium exchange forming the reactive species 2-bromo-6-lithiopyrdine *in*

situ. Organolithium compounds are strongly nucleophilic, and addition of an electrophilic ketone gives the adduct. Aqueous workup protonates the formed lithium alkoxides to yield the products **12a-c**. Due to the chirality of the ketones, attack by the lithiopyridine to the carbonyl will preferentially take place from one face. Consequently, the stereochemistry of the hydroxyl-bearing carbon will be determined by the innate stereochemistry of the substrate. The resulting reduced forms of the menthone, camphor, and fenchone systems are called neomenthol, isoborneol and β-fenchol, respectively.

The products **12a** and **12b** were isolated in 79% and 25% yield. Purification by flash chromatography was sufficient for the neomenthol derivative **12a**, but the isoborneol derivative **12b** also required further purification by sublimating unreacted camphor at 70 °C under vacuum. The considerably lower yield of **12b** is attributed to increased steric constraints around the carbonyl of camphor (**14b**), hindering the attack by the lithiopyridine. In repeated attempts, the reaction mixture was kept at -80 °C for a longer period before warming to r.t., but did not result in discernible increased yield. Since literature preparations of **12b** report noticeably higher yield (42%[91]), the quality of our camphor was checked by ^{1}H NMR, showing no sign of contamination. The β-fenchol compound **12c** was initially believed to have been isolated in 74% yield, but NMR spectra were not in accordance with literature data.[91] Thus, it was decided to disregard the β-fenchol derivative **12c**.

It has been argued that menthone and camphor have enolizable hydrogens, which could set up for competing deprotonation of the equilibrating enol.[93] Ma *et al.* used this argument to reason for their high yield of **12c** (90%) compared to **12a** and **12b** (68% and 42%, respectively). This argument does not seem to be applicable to my findings, and it is unknown why our yields show different trends and why NMR spectra for **12c** were incorrect.

3.1.4 Synthesis of Chiral 2-aryl-6-alkylpyridine Alcohols 15a-h

With 2-bromo-6-alkylpyridines **12a** and **12b** in hand, various chiral 2-aryl-6-alkylpyridines **15a-g** were synthesised by Suzuki cross couplings with available arylboronic acids **16a-d**. The arylboronic acids used were chosen by either having a potentially coordinating heteroatom in the 2-position or based on phenyl. These reactions are shown in Scheme 17.

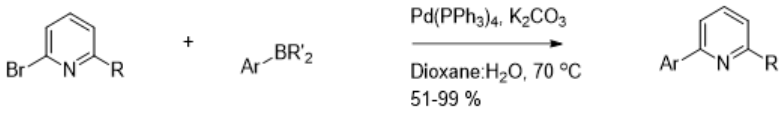

12	R
a	Menthol
b	Isoborneol

16	Ar
a	Ph
b	3,5-diOMePh
c	Thiophene-2-yl
d	*N*-methylpyrrole-2-yl

15	R	Ar
a	Menthol	Ph
b	Menthol	3,5-diOMePh
c	Menthol	Thiophene-2-yl
d	Isoborneol	Ph
e	Isoborneol	3,5-diOMePh
f	Isoborneol	Thiophene-2-yl
g	Isoborneol	*N*-methylpyrrole-2-yl

*Scheme 17 – Synthesis of chiral 2-aryl-6-alkylpyridines **15a-g** by Suzuki cross coupling reactions.*

Under a N_2-atmosphere, the 2-bromo-6-alkylpyridine alcohol (**12**) and boronic acid/pinacol ester (**16**) were dissolved in dioxane (1 mL) and mixed with the potassium carbonate in H_2O

(0.5 mL). The Pd-catalyst dissolved in dioxane (1 mL) was then introduced either directly from the preformed complex as commercially available, or formed *in situ* from $Pd(OAc)_2$ and PPh_3 with a small amount of NEt_3 as a reducing agent. The mixture was heated to 70 °C and stirred o.n. or until no remaining pyridine bromide remained (as determined by either TLC or ^1H NMR).

For the Pd-catalyst, 5 mol% was sufficient in most cases. If, however, black palladium particles were visible without complete consumption of starting material, more catalyst was added as necessary.

These reactions were generally very pleasant to work with. The boronic acid mostly used in stoichiometric amounts, and no unwanted homo-coupling of starting material was ever observed. After purification by flash column chromatography, the pure products **15a**-**g** were isolated in 54-99 % yield. The thiophene **15f** was more difficult to remove from unreacted bromide starting materials than the others. A 1:15 mixture of acetone:pentane was found to be somewhat effective but did still not give satisfactory purity. As such, the reaction was re-attempted with 2 equiv. of the boronic acid to ensure full consumption of starting material. This allowed for isolation in 51% yield of **15f** after purification by flash column chromatography (1:30 EtOAc:pentane).

Compounds **15b**-**c** and **15e**-**g** have previously not been reported in literature, and were fully characterised by NMR and HRMS. Through NOESY experiments, assignment of the two bridged methyl groups of isoborneol rings was possible. By analysis of coupling constants, all menthol rings had the conformations with the hydroxyl group in an axial position. The orientation of the *i*Pr-moieties could not be determined by the NMR spectra acquired. The assigned ^1H and ^{13}C chemical shifts of the novel compounds are shown in Figure 8.

Attempted reaction of 2-pyridyl boronic acid (**16e**) with substrate **12a** gave no conversion to the desired chiral 2,2'-bipyridine alcohol **15h**, attributed to the pyridine boronic acid being more electron deficient – thereby less nucleophilic for the transmetallation step – than the other utilized aryl boronic compounds. Luckily, 6-bromo-2,2'-bipyridine (**17**) was commercially available, so halogen-lithium exchange and addition of (-)-menthone (**14a**) gave the desired chiral bipyridine **15h** in 23% yield (Scheme 18). The ^1H NMR spectrum was in accordance with previously reported values.[92] The bipyridine-isoborneol derivative was not synthesised due to time limitations.

3.1 Synthesis of Starting Materials

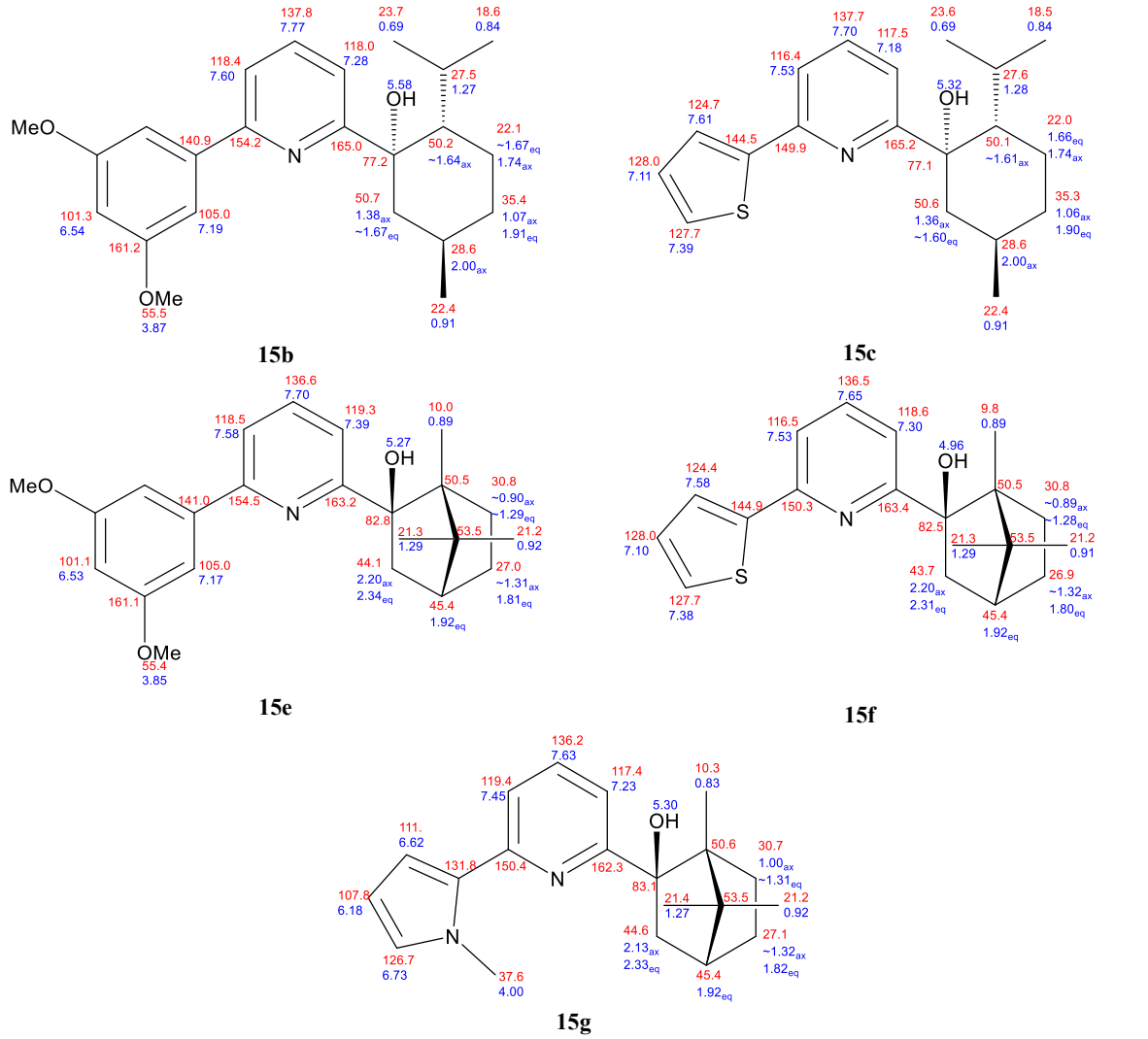

*Figure 8 – Assigned ^{1}H and ^{13}C shifts of novel 2-aryl-6-alkylpyridine alcohols **15b-c** and **15e-g**.*

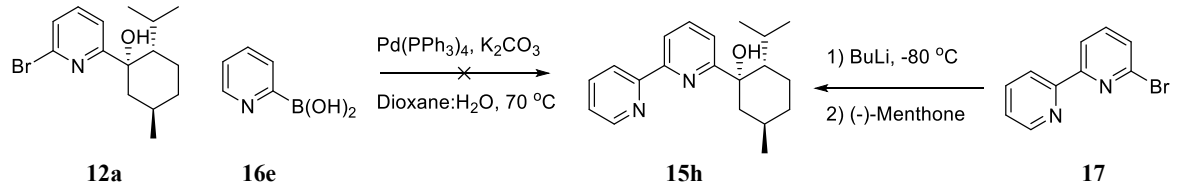

*Scheme 18 – Synthesis of chiral bipyridine alcohol **15h**.*

3.1.5 Methylation of Pyridine Alcohols

With several 2-aryl-6-alkylpyridines **15a-h** in hand, we also wanted to study effect of the hydroxyl group in Au-coordination; a weaker O-Au bond could allow for temporary dissociation of the oxygen, creating an active site at Au. As a result, the substrate would be brought as close as possible to the chiral group of the ligand, potentially increasing the effect of the chirality and increasing enantioselectivity in Au-catalysed reactions. Therefore, some methoxy analogues **15b**,**d**,**e**,**h-OMe** were synthesised.

3.1 Synthesis of Starting Materials

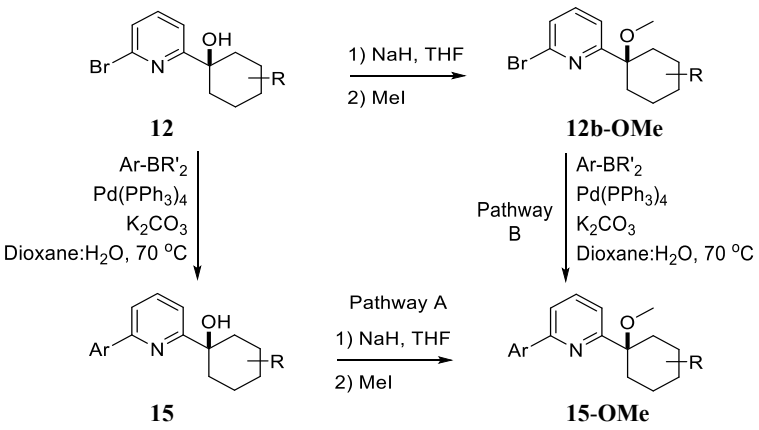

*Scheme 19 – Synthesis of methoxy derivatives **15-OMe** through two different pathways.*

The bromopyridine alcohol **12b** or the selected 2-aryl-6-alkylpyridine alcohols **15b**,**h** were dissolved in THF and the alcohol deprotonated by reaction with NaH. Subsequent S_N2 reaction with MeI yielded the corresponding methyl ether pyridines **12b-OMe**, **15b-OMe** and **15h-OMe** in excellent yields (≥97 %) after extraction into DCM. Suzuki cross coupling of **12b-OMe** yielded **15d-OMe** in 49 % yield and **15e-OMe** in quantitative yield. All synthesised methoxy derivatives were unreported in literature, and accordingly fully characterised. Chemical shifts of the novel compounds are presented in Figure 9.

Curiously, reactions in dry DEE instead of THF gave no conversion, but quantitative recovery of starting materials even if heated for several days. The large excess of NaH used (10 equiv.) was due to suspected degradation and slow initial rate of the reaction. As NaH is known to be able to act as a base, a reducing agent, and a nucleophile,[94] 12 equiv. of MeI was used to avoid formation of methane gas. Though such drastic excesses are not very economic, reactions sometimes required up to 24 hrs to reach full conversion and were therefore deemed necessary. No further optimization was explored.

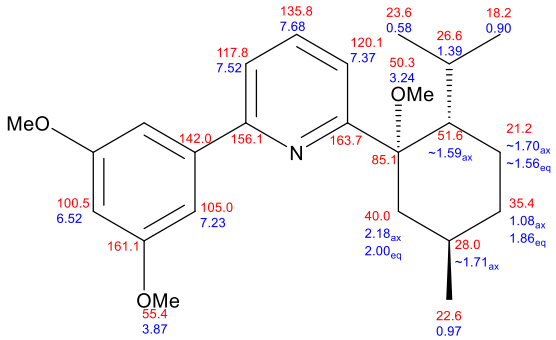

15b-OMe [a]

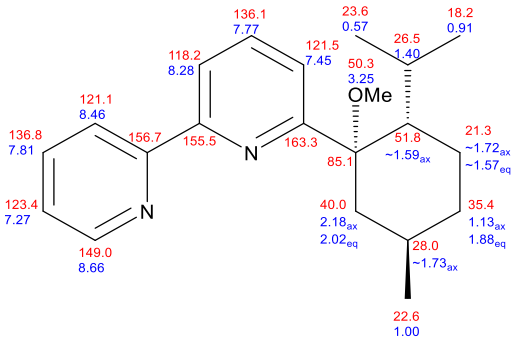

15h-OMe [a]

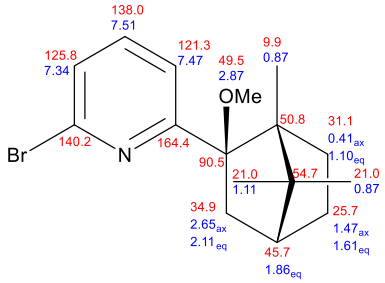

12b-OMe

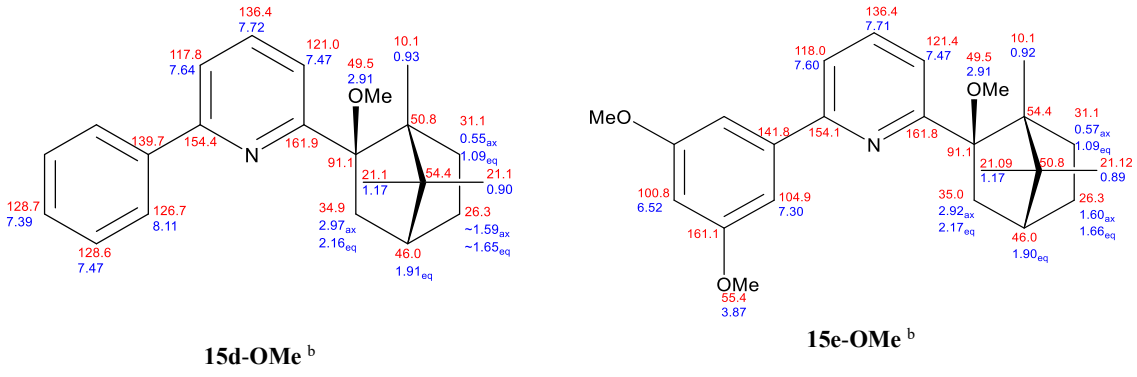

Figure 9 – Assigned [1]H and [13]C shifts of four novel 2-aryl-6-alkylpyridines methyl ethers and one novel 2-bromo-6-alkylpyridine methyl ether. [a] Synthesised through Pathway A. [b] Synthesised through Pathway B.

3.1.6 Synthesis of Chiral BOX-Au(III) complex XIII

The chiral bis-oxazoline (BOX) Au(III) complex **XIII** was synthesised from the commercially available ligand **18**, according to the procedure reported by our group.[21]

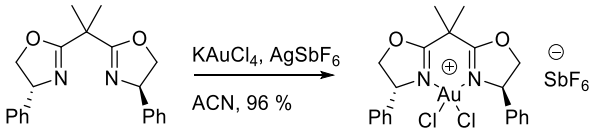

18 **XIII**

*Scheme 20 – Synthesis of BOX-Au(III) complex **XIII**.*

Mixing the ligand **18** with $KAuCl_4$ (**VII**, 1.1 equiv.) and $AgSbF_6$ (1.2 equiv.) in ACN for 1 hr gave the pure Au(III) complex **XIII** in 96 % yield as an orange powder after filtration through celite. The ^{1}H NMR spectrum was in accordance with reported data.[21]

3.2 Au-catalysed Reactions of Propargyl Alcohols and Aryl Nucleophiles

The Au(III)-catalysed reaction between propargyl alcohols (**1**) and aryl nucleophiles forming indenes **4** was recently reported by Morita *et al.*[2] The reaction is redrawn in Scheme 21. For mechanistic details, see Chapter 2.5, Scheme 11. These transformations sparked interest in our research-group due to propargyl alcohols **1** not being commonly reported in the field of Au-chemistry (propargyl esters have that honour). Moreover, due to the chirality of the products, asymmetric catalysis was envisioned. The product of the reaction could be conveniently tuned by simple time and temperature control to either stop at an intermediate allene **3**, or further proceed to a 1,3-diaryl-1*H*-indene **4**. Consequently, this project was initiated to investigate the scope of these reactions in regard to Au-source, propargyl alcohol substituents (**1**), aryl nucleophile and solvent (based on already reported findings by Morita *et al.*), and to finally investigate their potential for use in asymmetric catalysis.

3.2 Au-catalysed Reactions of Propargyl Alcohols and Aryl Nucleophiles

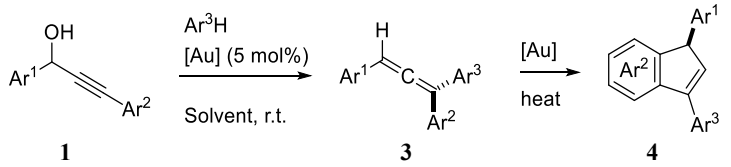

1 **3** **4**

*Scheme 21 – Reaction between propargyl alcohol **1** and an aryl nucleophile, producing either allene **3** or indene **4**.*

For use as a test-reaction of newly synthesised Au-complexes, the following reaction criteria should be satisfied: 1) easy to perform, 2) easy to workup, and 3) easy to analyse the product mixture. These three factors will be focused on in the following testing.

3.2.1 Effect of Au-source

Our group's interest in the transformations mentioned above is the capability to work with different chiral Au-catalysts in asymmetric catalysis. Therefore, it seemed reasonable to start by investigating how simple commercially available Au-salts affect the outcome of the reactions. Morita *et al*. had undertaken some investigation on how different Au(I)- and Au(III)-salts affect the obtained yield of indene **4a** by reaction of propargyl alcohol **1a** with mesitylene. Nevertheless, we found their choices to not be representative of the commonly employed Au-salts in the field. Also, no reasoning was given for their increased catalytic loading of Au(I)-salts (15 mol%) compared to Au(III)-salts (5 mol%).[2] Furthermore, no comment was made on the ratios of the other competing products of the reaction, but only the obtained yield of indene **4a**. Consequently, we decided that more investigation into the effect of the Au-source was needed.

Besides incomplete consumption of starting material, three primary products can be formed by the reaction of **1** (see Scheme 22): 1) nucleophile attacking C-1 of the substrate, substituting the hydroxyl group in an $S_N1/2$ fashion, yielding products akin to alkyne **2a**, 2) nucleophilic attack at C-3 of the substrate, forming the allene **3a** in an S_N2' fashion, or, 3) Nazarov cyclisation of the aforementioned allene to indene **4a**. Furthermore, there is a possibility for the solvent to act as the nucleophile, resulting in exchange of the hydroxyl group yielding alkynes of type **2b**.

With the different potential products in mind, the reaction was attempted with a selection of different Au(I)- and Au(III)-catalysts. For the time being, the reported recommended conditions were used: CF_3CH_2OH (F_3-EtOH) as solvent, 5 mol% catalyst and 6 equiv. of MesH. For allene (**3**) formation, solutions were stirred at r.t. for 15 mins, and for indene (**4**) formation, at 80 °C for 1.5 hrs. The only modification from the reported procedure was addition of NEt_3 in the workup to inoculate the catalyst. The relative abundance of the various compounds formed was determined by integration of characteristic signals of the ^{1}H NMR spectrum of the crude mixture (Scheme 22). The results can be seen in Table 1.

3.2 Au-catalysed Reactions of Propargyl Alcohols and Aryl Nucleophiles

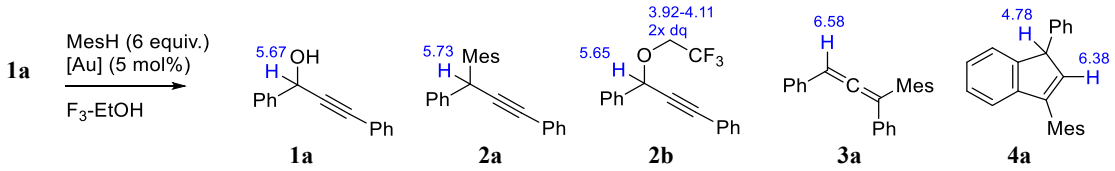

*Scheme 22 – Characteristic chemical shifts of the substrate **1a** and different potential products.*

Table 1 – Effect of Au-source [a]

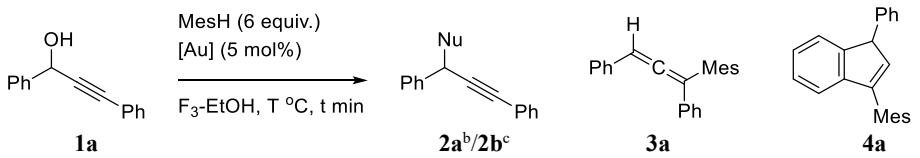

Entry		[Au]	T = r.t., t = 15				T = 80 °C, t = 90			
			1a	**2**	**3a**	**4a**	**1a**	**2**	**3a**	**4a**
1	Au(III)	$AuCl_3$ (**V**)	0	10[b]	86	4	0	8[b]	2	90
2		$AuBr_3$ (**VI**)	0	10[b]	85	5	0	7[b]	0	93
3		$KAuCl_4$ (**VII**)	0	9[b]	91	0	0	8[b]	2	90
4	Au(I)	(JohnPhos)Au(ACN)SbF_6 (**III**)	74	3[b],4[c]	19	0	0	8[b],2[c]	0	90
5		Me_2SAuCl (**I**)	74	3[b],4[c]	19	0	0	5[b]	0	95[d]

[a] Standard procedure: Au-catalyst (5 mol%) with propargyl alcohol **1a** (1 equiv.) and MesH (6 equiv.) in F_3-EtOH (1 mL). Mixture stirred at T °C for t mins before addition of water, a few drops of NEt_3 and extraction into DEE followed by removal of solvent *in vacuo*. Ratios are based on integration of the resulting ^{1}H NMR spectra.
[b] Nu = Mes, (**2a**). [c] Nu = F_3-EtO (**2b**). [d] Observed signals of unidentified compounds.

The tested Au(III)-salts (entries 1-3) show similar behaviour and form the desired allene **3a** and indene **4a**. Most notable is the ability of $KAuCl_4$ to form the allene intermediate **3a** more selectively without any traces of indene **4a**, and the ability of $AuBr_3$ to convert all the formed allene more selectively to indene when heated (see Scheme 21). The differences in the formed amount of 1,1,3-triarylpropyn **2a** are negligible within the precision of NMR-integration. The persistence of undesired alkyne **2a** after heating indicates a dead-end for the reaction, or alternatively that a transformation of **2a** to **4a** proceeds exceedingly slowly.

The two tested Au(I)-salts (entries 4-5) show drastic difference from the Au(III)-salts when attempting to form the allene **3a**; only 19% conversion can be seen after stirring for 15 mins, with a much higher relative ratio of the undesired alkyne **2a**. Marion *et al*. also observed the difficulty of Au(I) to form allenes in their similar study using propargyl acetates.[31] Heating and further stirring showed very promising conversion into the indene **4a**, with comparable results to the Au(III)-salts. Some reactions also showed formation of small amounts of propargyl ether **2b**; this is, however, not expected to have significantly impacted the formation of indene **4a**, as it will later be showed that these propargyl ethers are still capable of undergoing both conversion to allene and indene. Using catalyst **I** also showed aromatic signals not previously seen with other catalysts, possibly indicating a different competing reaction taking place. The reduced ability of Au(I)-salts to form allenes compared to the Au(III)-salts is clear evidence that these catalytic species are indeed different, and Au(III) is not simply a precursor to Au(I).

In conclusion, most Au-catalysts are capable of converting 1,3-diarylpropargyl alcohols **1** into indenes **4**, but Au(I)-sources are less effective at forming the intermediate allenes **3**.

3.2.2 **Effect of Solvent**

The proposed solvent of F_3-EtOH was seen as unusual, and when only compared towards toluene, THF and DCE, some further options should be explored in attempt to avoid the use of a fluorinated solvent. As such, some other solvents commonly used in organogold chemistry were attempted in indene formation using the other standard conditions recommended by Morita *et al*. The results are shown in Table 2.

Table 2 – Effect of solvent [a]

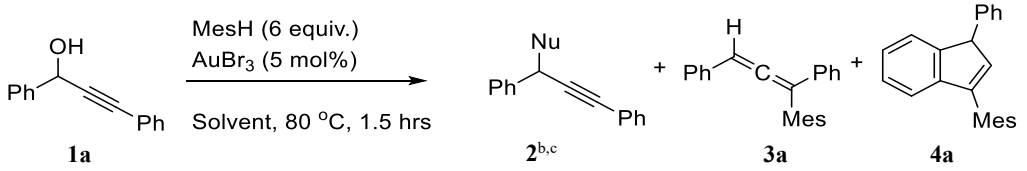

1a **2**[b,c] **3a** **4a**

Entry	Solvent	**1a**	**2**	**3a**	**4a**	Comment
1	EtOH	0	**c**:76[b]	0	0	Isolated products **2c** : **19**, 76 : 24[d]
2	F_3-EtOH	0	7[c]	0	93	
3	AcOH	?	77[c]	?	23	Complex mix of several products
4	ACN	0	72[c]	0	28	
5	DCM	35	3[c]	57	5	60 °C
6	$MeNO_2$	0	10[c]	5	85	

[a] Standard procedure: $AuBr_3$ (5 mol%) with propargyl alcohol **1a** (1 equiv.) and MesH (6 equiv.) in solvent (1 mL). Mixture stirred at 80 °C for 1.5 hrs before addition of water, a few drops of NEt_3 and extraction into DEE followed by removal of solvent *in vacuo*. Ratios are based on integration of the resulting ^{1}H NMR spectra.
[b] Nu = solvent. [c] Nu = Mes, (**2a**). [d] Due to overlapping ^{1}H NMR signals, ratio based on isolated yields after flash column chromatography.

As F_3-EtOH had been successful in these reactions, simple EtOH was first attempted (entry 1). By inspection of the crude ^{1}H NMR spectrum, none of the desired products could be observed, but instead the corresponding propargyl ether **2c** from nucleophilic attack by ethanol on the substrate **1a**, as well as some other unknown compound. Purification of the crude mixture by flash chromatography (1:20 EtOAc:pentane) gave the pure propargyl ether **2c** and also an unexpected, not previously reported, α,β-unsaturated ketone **19** containing three phenyls and no mesitylene. Its structure was elucidated by a combination of NMR spectroscopy and HRMS. For discussion about **19**, see section 3.2.2.1 below.

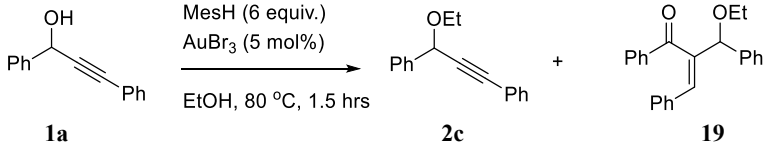

1a **2c** **19**

*Scheme 23 – Reaction of **1a** with EtOH, forming alkyne **2c** and α,β-unsaturated ketone **19**.*

Using AcOH as the solvent (entry 3) created a complex mix of products from which only the 1,1,3-triarylpropargyl **2a** and indene **4a** were recognizable in a relative ratio of 77:23. It is possible that replacement of OH by OAc could have taken place, forming the analogous propargyl acetate, which could react in very different manners from the starting alcohol (see section 2.3). Attempts were made to look for the corresponding propargyl acetate in the crude

^{1}H NMR spectrum, but, due to overlapping signals, its presence could not be confirmed.[40] Regardless, it was clear that AcOH was not an appropriate solvent for these reactions.

ACN is known to be a good solvent for Au(III)-salts and -complexes in terms of both solubility and stability (see section 2.2). It would therefore be convenient to use ACN in these reactions (entry 4). Unfortunately, efficiencient formation of the undesired alkyne **2a** compared to the indene **4a** was observed. Despite this, the crude reaction-mixture was surprisingly clean, not showing traces of any other compounds than these two, where the other solvents always showed slight formation of other minor side products.

Along with ACN, DCM is a common solvent in Au-catalysis, but showed poor conversion to indene **4a**, with the allene **3a** as the major product and discernible amounts of starting material left (entry 5). Due to the lower boiling point of DCM, the solution was only heated to 60 °C which is believed to have affected the conversion.

Eventually, $MeNO_2$ was attempted (entry 6). $MeNO_2$ showed comparable selectivity as F_3-EtOH, but some formation of alkyne **2a** (5%) could also be observed. Still, F_3-EtOH was more selective in the indene-formation. As it is unknown if Au-complexes are compatible with F_3-EtOH, $MeNO_2$ could serve as an alternative should instability or solubility problems develop.

In conclusion from solvent-screening, F_3-EtOH was indeed the most suitable solvent. It has been argued that F_3-EtOH is exceptionally good at stabilising cationic species, which might be the reason for this.[95] $MeNO_2$ gives lower selectivity but avoids the use a fluorinated solvent and can serve as an alternative if compatibility problems arise. The other solvents either created complex mixtures of products, or an increased amount of the undesired alkyne **2a**, and are as such unsuitable.

3.2.2.1. α,β-Unsaturated Ketone Dimer **19**

Using EtOH as the solvent for the reaction between 1,3-diphenylpropynol (**1a**) and MesH in the presence of catalytic $AuBr_3$ (**VI**) gave a mixture of the propargyl ether **2c** and the unexpected α,β-unsaturated ketone **19**. Its structure was determined by a combination of HRMS and NMR spectroscopy. A NOESY experiment was used to determine the orientation of the alkene. According to literature search, compound **19** is novel, but similar structural motifs are generated through the Morita-Baylis-Hillman (MBH) reaction (see section 2.6, page 9). MBH reactions have previously been reported to proceed best in polar protic solvents such as MeOH, without the incorporation of the solvent,[82] which is not in line with the structure of **19** which has the solvent ethoxy-group incorporated.

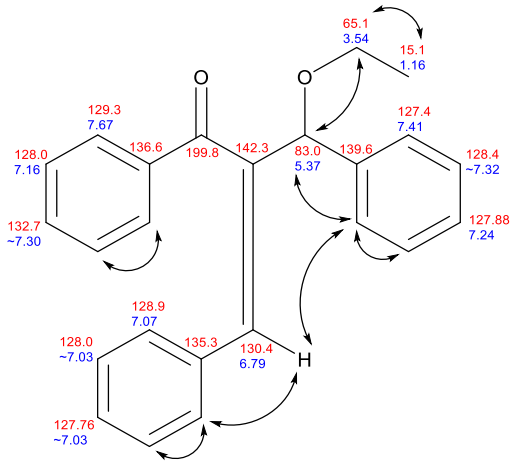

19

*Figure 10 – Assigned ^{1}H and ^{13}C shifts (relative to TMS in $CDCl_3$) the α,β-unsaturated ketone **19**. Arrows indicate $^{1}H,^{1}H$-NOESY correlations.*

From similar starting materials, Wadhwa *et al*. observed MBH side-products when they generated TMS-protected propargyl alcohols in a phosphor-catalysed reaction.[83] However, their proposed mechanism involves the reaction of an allene (formed *in situ*) with an electron-deficient aldehyde, whereas no aldehyde was present in my reactions; ^{1}H NMR confirmed no benzaldehyde-contaminant remained in the propargyl alcohol substrate.

Despite the striking structural similarity of **19** and MBH-products, we could not reason its formation through the standard MBH mechanism. A wide range of catalysts have been effective in MBH reactions such as amines,[81] phosphor compounds,[83] *t*BuOK,[86] and NHCs[84,85]. Yet, to the best of our knowledge, no reports exist for Au-catalysis. Attempted reaction between propargyl alcohol **1a** and anisole – a good aromatic nucleophile – still only showed EtOH as the acting nucleophile. Using F_3-EtOH as solvent gave no formation of the fluorinated derivative of **19**. This is attributed to the electron withdrawing effect of the CF_3 group, making this solvent less nucleophilic.

Our suggested mechanism for the formation of **19** is shown in Scheme 24. Nucleophilic attack by the solvent at C-1 of substrate **1a** (possibly aided by Au^{+} in solution) forms the propargyl ether **2c** (isolated from the reaction mixture). By Au-activation, the water released can give hydration of the alkyne, followed by protodeauration, keto-enol tautomerization and finally elimination of EtOH, which would yield 1,3-diphenylpropenone (Chalcone). Chalcone could possibly also form directly from **1a** without proceeding through the intermediate of **2c**. From the crude ^{1}H NMR mixture, weak signals possibly corresponding to (*E*)-Chalcone could be observed, but this is inconclusive due to low relative intensity and overlapping signals. Because of the elevated temperature, this 4-electron π-system could undergo a hetero-[4+2] cycloaddition with propargyl ether **2c** in solution, and a further hetero-[4+2] cycloreversion would give **19**. In the process, volatile phenylacetylene (**10a**) would be eliminated which would be removed by evaporation, and could therefore not be observed by ^{1}H NMR.

3.2 Au-catalysed Reactions of Propargyl Alcohols and Aryl Nucleophiles

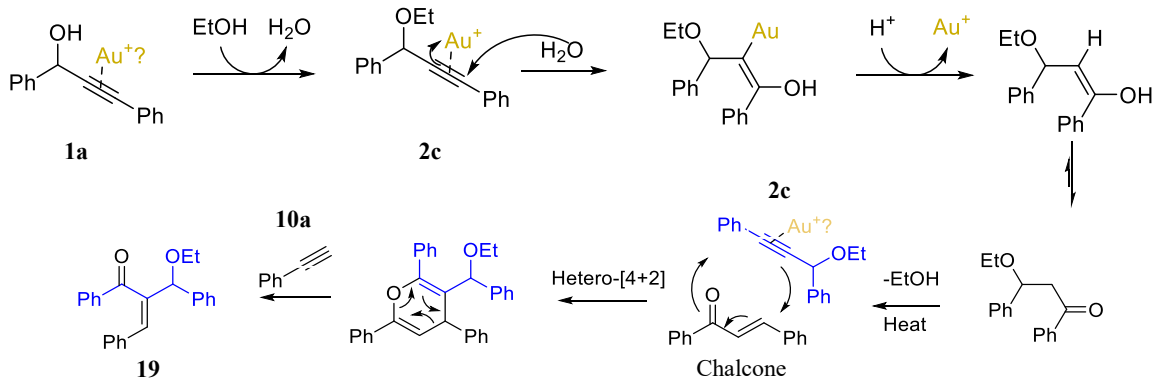

*Scheme 24 – Suggested mechanism for generation of α,β-unsaturated ketone **19**.*

Further work on this reaction is encouraged, as two stereocenters are incorporated. Assuming the mechanism shown in Scheme 24, control of the OEt-stereocenter would require an S_N1 substitution with a chiral Au-complex coordinated to the neighbouring alkyne. Stereocontrol of the alkene would depend on the approaching orientations of (*E*)-Chalcone and **2c** in the hetero-[4+2] cycloaddition step. It would be interesting to investigate the extent to which Au can affect this reaction. It was, however, decided that this reaction was outside the scope of the planned project, and, as such, no further investigation was undertaken.

3.2.3 Effect of Propargyl Alcohol Substituents

Varying the electronic- or steric characteristics of the substituents of propargyl-systems are known to impact Au-catalysed reactions.[31] The effect of different phenyl substituents on either side of the propargyl alcohol **1** was thus investigated. Several of the compounds produced from these reactions have not previously been reported, but due to the difficult purifications – often requiring flash column chromatography with ~1:200 EtOAc:pentane to achieve any form of separation – not all proposed compounds could be isolated in adequate quantities for structural confirmation by NMR and HRMS. However, based on various isolated derivatives of each compound class, characteristic structural fragments that makes up each product can be determined with feasible ease based on ^{1}H NMR spectra alone. If a novel compound was not isolated in adequate amounts for structural confirmation, it will not be listed in the experimental section, but its ^{1}H NMR spectrum can be found in the Appendices.

*Table 3 – Effect of propargyl alcohol (**1**) substituents* [a]

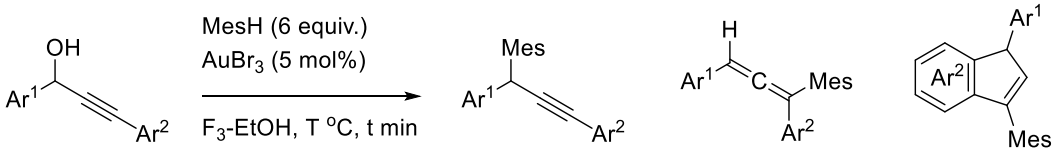

1 **2** **3** **4**

Entry	Ar^1	Ar^2	Propargyl alcohol	T = r.t., t = 15				T = 80 °C, t = 90			
				1	**2**	**3**	**4**	**1**	**2**	**3**	**4**
1	Ph	Ph	**1a**	0	**a**:10	**a**:85	**a**:5	0	**a**:7	0	**a**:93
2	4-OMePh	Ph	**1h**	0[b]	-	-	-				
3	4-CF_3Ph	Ph	**1i**	4	**d**:53	**b**:43	0	0	**d**:56	0	**b**:44
4	Ph	4-OMePh	**1c**	100 -[b,c]	0 -	0 -	0 -				
5	Ph	4-CF_3Ph	**1d**	2[b]	**e**:65	**c**:26	0				
6	Mes	4-CF_3Ph	**1f**	5[b]	0	**d**:95	0	5[b]	0	**d**:95	0
7	Mes	Ph	**1e**	0	0	**e**:100	0	0	0	0	**c**:100
8	2,6-diMePh	Ph	**1g**	0	0	**f**:98	**d**:2	0	0	0	**d**:100
9	Ph	Mes	**1b**	Observed[b]		-	-	Observed[b]		-	-

[a] Standard procedure: $AuBr_3$ (5 mol%) with propargyl alcohol **1** (1 equiv.) and MesH (6 equiv.) in F_3-EtOH (1 mL). Mixture stirred at T °C for t min before addition of water, a few drops of NEt_3 and extraction into DEE followed by removal of solvent *in vacuo*. Ratios are based on integration of the resulting ^{1}H NMR spectra.
[b] Complex mixture / polymerization makes integration unreliable/impossible. [c] Stirred o.n.

Exchanging to an electron rich phenyl at Ar^1 (entry 2) gave a complex mixture of various polymerization products after stirring at r.t. for 15 mins. The lack of formation of desired products is attributed to anisole being a better nucleophile than mesitylene. Through flash chromatography, a compound containing two equivalents of the starting propargyl alcohol and one mesityl fragment could be isolated. NMR indicates a mixed indene-alkyne compound, but their connectivity could not be elucidated due to the complexity and proximity of ^{1}H and ^{13}C signals; a TOCSY experiment was attempted to differentiate the different aromatic systems without success. Furthermore, the propargyl ether **2f**, resulting from nucleophilic attack by the solvent at C-1, could be isolated.

The electron deficient 4-CF_3-phenyl (entry 3) allowed for preferential formation of the corresponding undesired alkyne **2d**. Still, the novel corresponding allene **3b** was formed, isolated, and fully characterized. This allene was also able to complete the cyclization to the indene **4b** when heated. In an attempt to decrease the amount of the alkyne **2d** that was formed, a separate attempt at 0 °C was done, but resulted in no consumption of the starting material.

Next, varying the electronic nature of Ar^2 was investigated. The electron rich anisole (entry 4) showed no conversion after stirring at r.t. for 15 mins. Allowing further stirring o.n. revealed a complex mixture, assumed to be polymerization products. An electron deficient Ar^2 derivative (entry 5) also opened for preferential propargylic substitution forming **2e**, analogues to Ar^1 (entry 3). The corresponding allene **3c** was also be observed, but could not be isolated by flash column chromatography, but only as a mixture with alkyne **2e**. In addition, what is assumed to be a dimer of the propargylic alcohol was isolated after flash column chromatography; from ^{13}C NMR, two sets of alkynes can be seen, and ^{1}H NMR shows no incorporation of mesitylene. The structure of this compound could however not be elucidated

due to high degree of equivalent signals. Mixing the reagents at 0 °C and allowing to heat slowly to r.t. gave the same mixture of products, indicating that propargylic substitution is not controllable by temperature.

In an attempt to block the propargylic position for substitution, mesitylene was introduced as Ar^1 (entry 6). It was hoped that the steric factor imposed by the *ortho* methyl groups could prevent attack by the nucleophile on C1. Indeed, promising reduction in the formation of the undesired 1,1,3-triarylpropyn in favour for the desired allene **3d** was observed, however still with impurities assumed to be caused by partial polymerisation. Contrary to previously synthesised allenes, allene **3d** decomposed on storing and also showed a surprising broadening of some ^{1}H NMR signals belonging to the nucleophile mesitylene. Unsurprisingly, cyclization to the corresponding indene **4e** could not be accomplished due to Ar^2 being too electron deficient for the intermediate Au-**3d**' to perform a Nazarov cyclisation (Scheme 25).

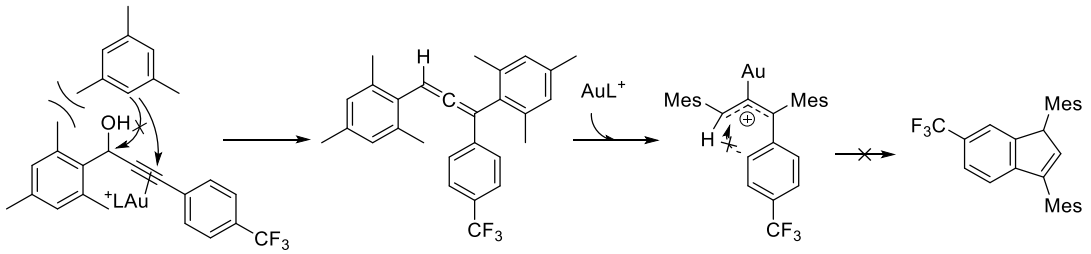

1f **3d** Au-**3d'** **4e**

Scheme 25 – Sterically encumbered Ar^1 prevents propargyl substitution, but electron deficient Ar^2 prevents indene formation.

Keeping the steric mesityl as Ar^1 but returning to Ar^2 = Ph, which we knew could cyclize to an indene (entry 7), pleasingly awarded complete consumption of starting material to the corresponding allene **3e**, with no recognizable amount of propargylic substitution, though still with the broadened ^{1}H NMR signals of the nucleophile. Furthermore, this allene could cyclize to 1,3-dimesitylindene (**4c**) after heating. For the sake of incorporating three distinctly different aromatic systems, the nucleophilic mesitylene was attempted replaced with 1,3,5-triisopropylbenzene, but this yielded only a complex mixture. Therefore, the 2,6-dimethylphenyl derivative was introduced as Ar^1 to maintain the desired steric encumbrance of the propargylic position, while still being NMR-distinguishable from the nucleophilic mesitylene (entry 8). This too showed great ability to form both the desired allene **3f** and indene **4d**, with no recognizable trace of propargylic substitution, also in $MeNO_2$ as solvent. Again, this allene also showed broadening of signals, and it was decided some further investigation was in place (see Section 3.2.3.1).

Finally, as a curiosity, mesitylene was also introduced as Ar^2 (entry 9), but surprisingly did not give pure propargylic substitution, but rather a complex mixture of compounds, indicating polymerization.

In conclusion, the propargyl alcohol system is sensitive to electronic factors in both of its aromatic rings. Electron rich rings favour dimerization/polymerization due to being better nucleophiles than mesitylene, while electron poor rings increase the relative amount of propargylic substitution that takes place. Electron neutral phenyl derivatives are preferred for

Ar^1 and required for Ar^2; only Ar^2 = Ph were able to form the corresponding indenes. Sterically encumbering the propargylic position by choice of aldehyde precursor eliminates the formation of undesired propargylic substitution.

3.2.3.1. NMR- and DFT Studies on Novel Allenes and Indenes

Some curious artefacts were observed in the NMR spectra of some of the synthesised allenes and indenes. The ^{1}H NMR spectra of allenes **3d-f** showed two broad peaks at δ^1H ~2.13ppm, and one broad peak at δ^1H~6.95 ppm (varying slightly between the compounds). This was seen as an indication of fluctuating conformations in solution (or some other dynamic process). Such broad peaks had not been seen for any of the other allenes isolated. These broad peaks integrated correctly as two methyls and two aromatic hydrogens, respectively, and were persistent even after purification by flash chromatography. Therefore, they were not the result of interaction with residual Au-particles in solution. Characterisation by NMR revealed the broad signals belonged to the nucleophile, Ar^3, and as the common trait of these systems was the methyl groups introduced on Ar^1, an interaction between these two ring systems was assumed to cause the broadening of signals. Closer inspection of the ^{13}C NMR spectra also showed broadening of signals at ~δ^{13}C 137 ppm. Albeit broadening of ^{13}C NMR signals is known, it is less common than for ^{1}H NMR.

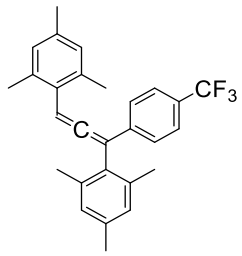

3d

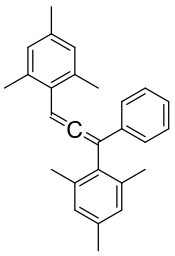

3e

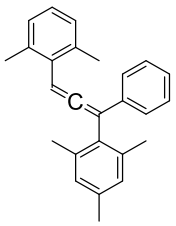

3f

*Figure 11 – Allenes **3d-f** that exhibit broadening of signals in ^{1}H and ^{13}C NMR.*

To verify presence of fluctuating conformers, ^{1}H NMR spectra of **3d** were collected at different temperatures (Figure 12). Cooling to 263 K gave clear sharpening of the signals into four distinct peaks, as a result of slower dynamic processes. Furthermore, heating of the sample to 313 K gave coalescence of signals; the most upfield methyls showed one broad peak, whilst the downfield aromatics were shown as one peak, only slightly broader than other aromatic hydrogens. Other spectra at intermediate temperatures (collected at intervals of 10 K) showed smooth transitioning between the two edge-cases. Heating of the sample beyond 313 K is expected to cause further coalescence to sharp peaks, as the rate of dynamic processes continue to increase, but such spectra could not be acquired due to spectrometer limitations.

Due to the 90 ° twist of allenes (see section 2.4, page 7), the *ortho*-methyls of Ar^1 and Ar^2 can be in close proximity given correct dihedral angles. In an attempt to identify the fluctuating conformations, DFT calculations of **3f** were performed with different dihedral angles about each aryl, as well as for the phenyl derivative **3a** for reference. **3f** was chosen instead of the other options due to it having the least number of atoms, and therefore cheaper to calculate. Indeed, calculations support observations of a hindered rotation of Ar^3 in **3f** for certain dihedral angles. Energy barrier for rotation of Ar^1 is also greater in **3f**, but still low enough to allow for

free rotation at ambient temperature, in agreement with the NMR observations. Selected structures, calculated energies, further detailed discussion and other relevant data regarding DFT calculations can be found in Appendix A.

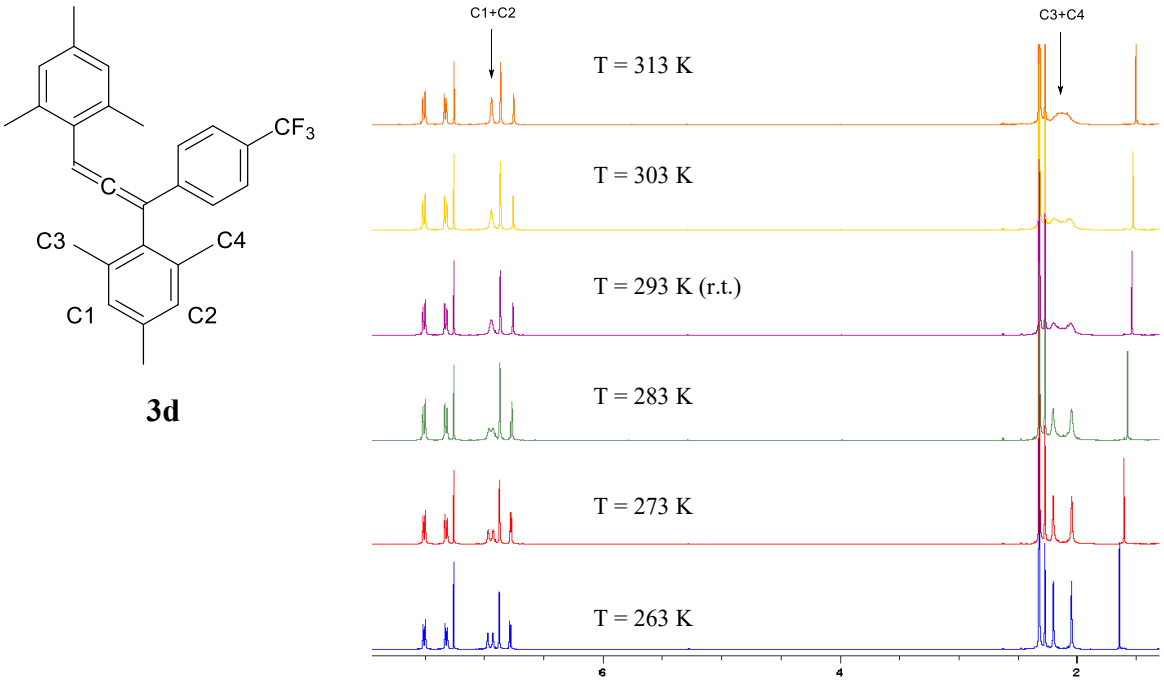

*Figure 12 – ^{1}H NMR spectra of allene **3d** at varying temperatures, showing presence of a dynamic process in solution ($CDCl_3$, 400 MHz).*

The complete NMR characterisation of indenes **4** was a challenging task, indeed, due to several factors: 1) the high degree of aromaticity meant overlapping signals in both ^{1}H and ^{13}C spectra, 2) the various other sideproducts produced from the related reactions were equally unpolar, which made their chromatographic separation labour intensive, and 3) the small scale of the reactions (10-20 mg of the propargyl alcohol) meant the isolation of sufficient amount of compound for NMR characterisation could be difficult, especially for insensitive quaternary carbons. To make matters worse, due to the presence of a stereo centre and hindered ring-rotations, no symmetry was observed for any ring-system, meaning every hydrogen and carbon would have their own individual NMR signal; this further complicates the NMR spectra and meant that extraction of peak-data from 1D experiments alone was unfeasible. Overlapping signals also meant that COSY spectra were of only limited help in isolating each ring-system from each other.

In order to be able to perform reliable assignments of ^{1}H signals, the use of TOCSY experiments were found to be very helpful. By this, overlapping signals of different spin-systems, i.e. the different aryls, could be distinguished from each other, and their ordering determined by combination with COSY. In some cases where HSQC and/or HMBC spectra had closely overlapping ^{13}C signals that needed to be distinguished, selective experiments were performed to achieve increased resolution of the spectral windows of interest. Finally, to

identify the relative syn/anti configurations of the twisted indene substituents, NOESY experiments were used.

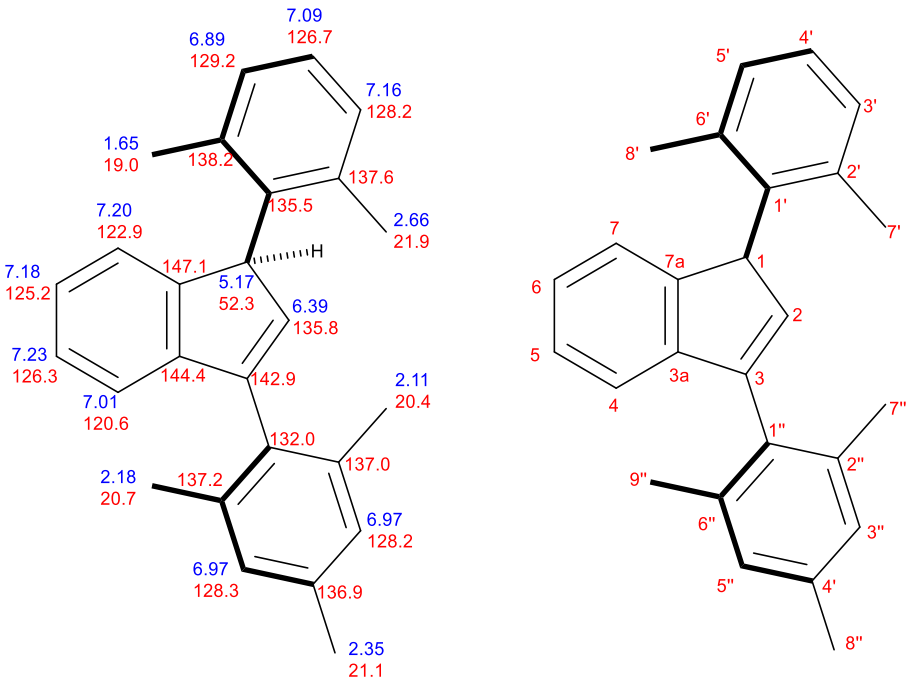

*Figure 13 – Assigned ^{1}H and ^{13}C NMR shifts of indene **4d** (left) and reference labelling (right).*

As an example of such assignment, the novel indene **4d** will be used and is shown in Figure 13. Due to the purity and quantity isolated of novel indene **4d** (12.8 mg) the compound was fully characterized by NMR and HRMS. The twisted/non-planar orientation of each mesityl substituent is attributed to steric hindrance between H8' and H7 as well as H9'' and H4. This would explain why the analogue **4a** only shows the same asymmetric behaviour for the mesityl moiety whereas the phenyl shows symmetry due to permitted rotation.

The characteristic benzylic and vinylic hydrogens (H1 and H2, respectively) were essential to determining the position and orientation of substituents. 2D-NOESY experiment shows clear correlation of the benzylic H1 to methyls H7' and H7'' indicating these are *syn* to one another. No signals were observed for methyls H8' nor H9'' to H1, but there is however correlation of H8' to H7 as well as H9'' to H4. HMBC correlations of carbon signals in close proximity to each other were distinguishable by a acquiring a selective HMBC spectrum, which utilizes a specific pulse for excitation of ^{13}C nuclei only within the range of interest ($\delta^{13}C$ 119-149 ppm). This, for example, unambiguously reveals that C3' and C3'' have overlapping signals at $\delta^{13}C$ 128.2 ppm, and are indeed distinguishable from C5'' at $\delta^{13}C$ 128.3 ppm, which is not possible to determine from a standard HMBC due to the much broader signals (see Appendix F.4-Appendix F.11).

3.2.4 Effect of Nucleophile

The final aspect to investigate was the effect of the aromatic nucleophile (Ar^3). The original article by Morita *et al.* showed the use of different nucleophiles, such as 1,3,5-

triisopropylbenzene, pentamethylbenzene, hydroxymesitylene and bromomesitylene to successfully generate indenes in varying yields.[2] The two latter systems generated a mixture of two diastereomers in lower yields. Moreover, combined with the knowledge that varying the electron-density of the aryl in the propargyl alcohol **1** negatively impacted the studied reactions, it was decided to mainly focus on aryls without heteroatoms. Still, some further investigation into the impacts of electron rich and -poor nucleophiles was done. These experiments were conducted simultaneously as the other screening experiments presented above, so the beneficial effects of *ortho*-blocking Ar^1 had not been discovered yet. The unsubstituted propargyl alcohol **1a** was therefore used. The results are summarized in Table 4.

Using the quite sterically hindered 1,3,5-triisopropylbenzene (entry 2) revealed a complex mix containing the propargyl ether resulting from attack by solvent (**2b**) after stirring at r.t. from 15 min. Surprisingly, heating for 1.5 hrs still yielded the corresponding indene **4f** with no traces of **2b** remaining. As the corresponding allene was never isolated, and it is not reported in literature, no reference could be used to integrate the correct allenic hydrogen if any traces remained. A small NMR peak at δ^1H 6.71 ppm could be seen in both crude NMR spectra, and assumed to be the allene, but this has not been confirmed. The results from this experiment also confirms that F_3-EtOH as the solvent might not only have the effect of stabilizing the positive charges of transition states, but also be incorporated in the intermediate structure **2b** which can still undergo further transformations. This was also confirmed by reacting pure, isolated propargyl ether **2b** with mesitylene to form the indene **4a**.This is contrasted to the corresponding non-fluorinated propargyl ethoxide **2c** which was shown to undergo a very different reaction (see section 3.2.2.1). During purification, removal of unreacted, high-boiling triisopropylbenzene was more troublesome than the parallel runs of mesitylene, and was also mostly UV inactive.

Table 4 – Investigation of the effect of aromatic nucleophiles on Au-catalysed formation of allenes and indenes[a]

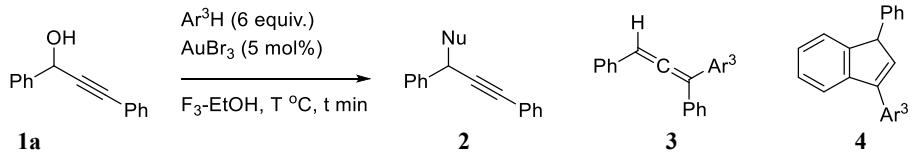

1a **2** **3** **4**

Entry	Ar^3H	T = r.t., t = 15				T = 80 °C, t = 90			
		1a	**2**	**3**	**4**	**1a**	**2**	**3**	**4**
1	Mesitylene	0	10	85	5	0	7	0	93
2	1,3,5-triisopropylbenzene	0	main[b,d]	-	0	0	0	-	**f**:100
3	Pentamethylbenzene	0	-	**g**:100	0	0	-	0	**g**:main[b]
4	Anisole	0	**g**:100[c]	-	-	0	**g**:100[c]	-	-
5	1,3,5-trimethoxybenzene	0	**h**:main[b,c]	-	-	0	**h**:main[b,c]	-	-
6	Nitrobenzene	0	100[d]	-	-	0[b]	-	-	-
7	1,3-bis(trifluoromethyl)benzene	0	100[d]	-	-	0[b]	-	-	-

[a] Standard procedure: $AuBr_3$ (5 mol%) with propargyl alcohol **1a** (1 equiv.) and aryl nucleophile Ar^3H (6 equiv.) in F_3-EtOH (1 mL). Mixture stirred at T °C for t min before addition of water, a few drops of NEt_3 and extraction into DEE followed by removal of solvent *in vacuo*. Ratios are based on integration of the resulting ^{1}H NMR spectra.
[b] Complex mixture / polymerization. [c] Nu = Ar. [d] Nu = F_3-EtO (**2b**)

Pentamethylbenzene (entry 3) showed clean conversion to allene **3g** and good conversion to indene **4g**, though formation of other unidentified materials could also be observed by ^{1}H NMR after heating. No formation of neither 1,3-diphenyl-1-pentamethylphenylprop-2-yn nor propargyl ether **2b** could be observed. However, likewise to entry 2, removal of unreacted Ar^{3}H was difficult as it was only vaguely visible under UV light. Even after three flash columns, a substantial amount or pentamethylbenzene still remained. Attempts with different eluent systems were not successful, despite often being separable by TLC. As a result, to get a pure NMR sample of indene **4g**, 1.5 mg of the mixture of **4g** and pentamethylbenzene was applied to a TLC-plate, eluted with pentane, and the silica of the indene-band scraped off and washed with EtOAc. By this, preparative TLC seems to be a better method for purification of **3g** and **4g** than flash column chromatography.

Tests with the electron rich aryls of anisole and 1,3,5-trimethoxybenzene (entries 4-5) only yielded propargylic substitution as the recognizable and isolable products (**2g** and **2h**, respectively). Changing to the more sterically encumbered propargyl alcohol **1e** did still not enable formation of allene. Electron deficient aryls (entries 6-7) were weaker nucleophiles than the solvent, and so only the propargyl ether **2b** was isolated. For both electron rich and deficient phenyls, heating of the solutions gave complex mixtures, assumed to be due to polymerization.

It can from this, once again, be seen that electronic neutrality seems to be a requirement for these reactions. While some other aryl nucleophiles are also compatible with this reaction, they are generally more difficult to remove from the products due to being high-boiling and UV-inactive. This means they are incompatible with HPLC analysis.

3.2.5 **Analysis of Enantiomers by Chiral HPLC**

With the caveats of the reactions scoped out, attempts to separate enantiomers of racemic mixtures by chiral HPLC followed. As our group continues to develop new chiral gold catalysts, their catalytic activity and selectivity must be monitored in various test-reactions. For routine incorporation of the reaction of propargyl alcohols **1** with aryl nucleophiles, purification of product allenes (**3**) and/or indenes (**4**) must be quick, and analysis of their isomers by chiral HPLC must be straightforward. By the various techniques attempted for formation of allenes and indenes in the present work, only the reactions of the three propargyl alcohols **1a**, **1e** and **1g** with mesitylene formed the desired products with sufficient control and ease. As such, their corresponding allene **3** and indene **4** products (see Figure 14) were analysed by chiral HPLC.

3.2 Au-catalysed Reactions of Propargyl Alcohols and Aryl Nucleophiles

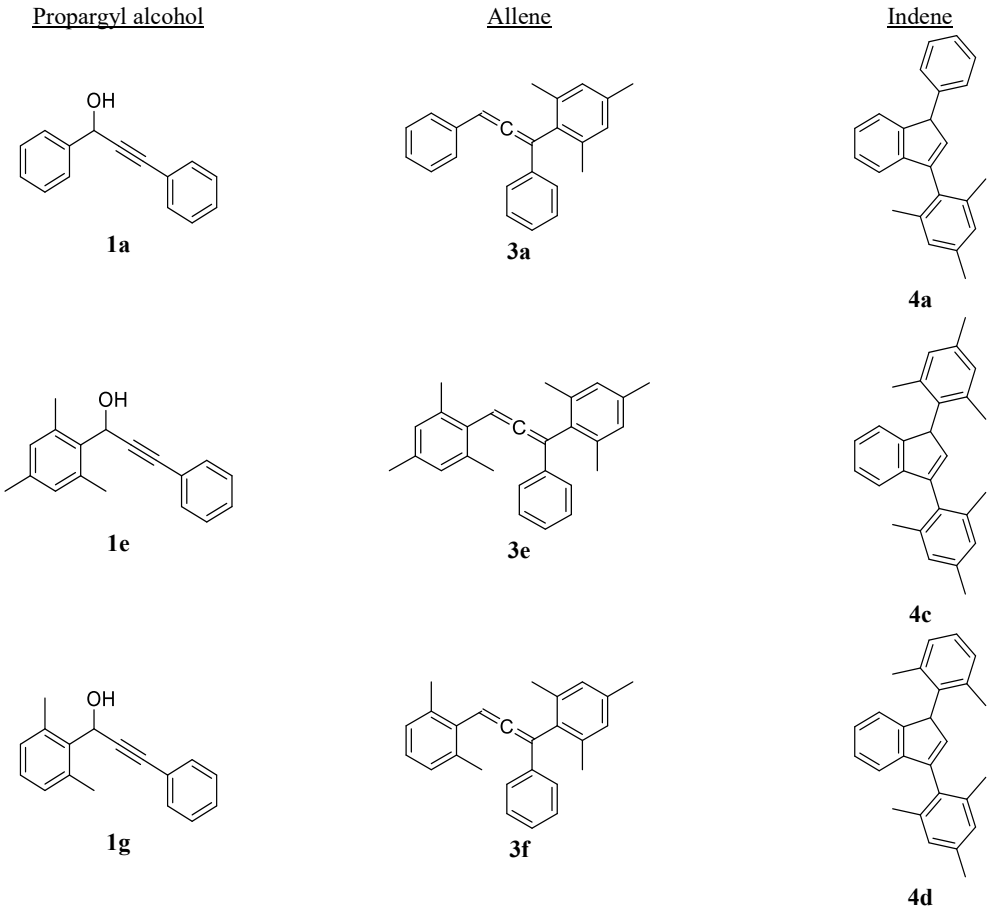

*Figure 14 – Structures of allenes **3** and indenes **4** (along with their corresponding propargyl alcohols **1**) that were chosen for analysis by chiral HPLC.*

First, allenes **3e**-**f** and indenes **4c**-**d** formed from the sterically encumbered propargyl alcohols **1e** and **1g** were tested; the reaction mixtures were the easiest to purify due to prevented propargylic substitution, and therefore the more attractive alternatives for routine operation.

A Chiralpak® AD-H 5 µm 4.6 mm x 250 mm NP-column was used with isocratic *n*-hexane:*i*PrOH as the eluent (0.8 mL/min) at r.t. and detected using a DAD. A racemic sample of allene **3e** showed no sign of separation of enantiomers with various eluent compositions ranging from 100:0 to 90:10. The same was seen for the corresponding racemic indene **4c**. The presence of two mesityl moieties can have caused the compounds to be too spherically unpolar, thereby resulting in no separation. Unfortunately, the allene **3f** and indene **4d** displayed the same behaviour. Brief attempts using a Lux® Cellulose-1 5 µm 4.6 mm x 150 mm NP-column with similar eluent compositions were also unsuccessful in separating the enantiomers.

Unencouraged by these results, the simpler allene **3a** was attempted, despite its purification being slightly more labour intensive. With an isocratic eluent of 95:5 *n*-hexane:*i*PrOH, separation was finally achieved, however without baseline separation. Therefore, despite the sample being racemic, integration of the chromatogram did not reproducibly yield a 1:1 ratio of enantiomers; different runs of the same sample resulted in the 'enantiomeric excess' varying by up to 5 % due ambiguous integration ranges. Attempts with the indene **4a** showed the exact same trends.

The present results indicate that chiral analysis cannot be reliably performed with our available HPLC systems. Still, attempts were made to see if any stereocontrol could be achieved by application of two chiral Au(III) catalysts developed in our group, shown in Figure 15. Both complexes **XIII** and **XIV** were catalytically active in the reaction between propargyl alcohol **1a** with mesitylene producing the allene **3a**. Alas, subsequent HPLC analysis of the purified products indicated potential low %ee. Due to the racemic control-sample generating integrals concordant with 5 %ee, these studies cannot confirm whether the tested chiral catalysts display enantioselectivity in the synthesis of allene **3a**.

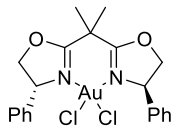

XIII

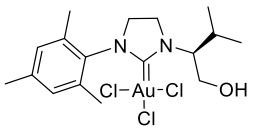

XIV

*Figure 15 – Chiral Au(III) complexes used as catalyst in the reaction of propargyl alcohol **1a** with mesitylene.*

In conclusion, analysis of various allenes **3** and indenes **4** – synthesised by the Au(III) catalysed reaction of propargyl alcohols **1** and mesitylene – by chiral HPLC was not able to adequately separate the product enantiomers. Subsequently, with the HPLC systems investigated, a routine methodology for evaluation of new chiral gold complexes' enantioselectivity could not be established. It is possible that other HPLC columns or eluent systems would be successful for this endeavour, but could not be explored due to time limitations.

3.3 Coordination of Au(III) to Chiral Pyridine Based Ligands

2-Substituted pyridines have previously been used as ligands for Au(III) in our group,[96] and further derivatisation of such compounds to novel Au(III)-complexes was highly attractive. Having synthesised a range of 2-aryl-6-alkylpyridins **15a-h** along with some methylated derivatives **15-OMe** (see sections 3.1.3-3.1.5), coordination studies followed. The chiral 2-aryl-6-alkylpyridine compounds **15a-h** were attempted coordinated to Au(III) following various minor modifications of the strategy by Cinellu *et al*.[22]

3.3.1 2-Aryl-6-Neomenthol Pyridine Alcohols 15a-c and 15h

The present pyridine based ligands were all potentially N,O-bidentate through the pyridine nitrogen and the alcohol oxygen. Furthermore, the aryl group in the 2-position of the pyridine could also be used as an additional bonding-site generating X,N,O-tridentate ligands (X=C, N, S); the bipyridine **15h**, for example, has clear potential to act as a N,N,O-tridentate ligand, while the 3,5-dimethoxybenzene derivative **15b** could through C-H activation act as a C,N,O-tridentate ligand. Attempted coordinations of various neomenthol derivatives (**15a-c**,**h**, prepared in section 3.1.4, page 15) are summarized in Table 5.

Table 5 – Attempted coordinations of 2-aryl-6-neomentholpyridines to Au. [a]

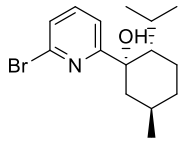

12a

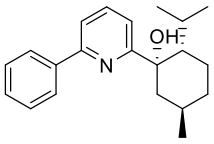

15a

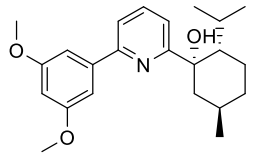

15b

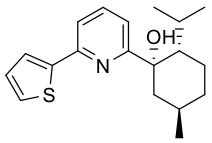

15c

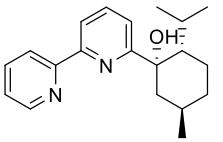

15h

Me_2SAuCl (**I**) $AuCl_3$ (**V**) $KAuCl_4$ (**VII**)

Entry	Ligand	Au	AgX, X=	Base	Solvent, condition	Result [b]
1	**12a**	**V** (1.2)		NaOAc (1.1)	ACN:H_2O	Ligand recovered
2	**12a**	**I** (1.1)			d_2-DCM	Ligand recovered
3	**15a**	**V** (1.2)			ACN:H_2O	PyH^+
4	**15a**	**VII** (1.3)		KOAc (3)	ACN:H_2O	Ligand recovered
5	**15a**	**VII** (1.3)	SbF_6 (1.3)	KOAc (3)	ACN:	Decomposition
6	**15b**	**V** (1.2)		KOAc (3)	ACN:H_2O	Free ligand + unknown compound
7	**15b**	**VII** (1.3)	SbF_6 (1.3)	KOAc (3)	ACN:H_2O, (70 °C)	Ligand recovered
8	**15b**	**VII** (1.2)	SbF_6 (1.2)		ACN, (70 °C)	PyH^+
9	**15c**	**V** (1.1)			d_3-ACN	Black particles + PyH^+
10	**15c**	**V** (1.1)		KOAc (3)	ACN	Ligand recovered
11	**15c**	**V** (1.3)	BF_4 (1.3)	KOAc (3)	ACN:H_2O	Black particles, ligand recovered
12	**15h**	**V** (2.5)		KOAc (6)	ACN:H_2O	Au(III)-**15h**-$AuCl_4$
13	**15h**	**V** (1.2)	NTf_2 (1.2)		d_3-ACN	PyH^+ + Au(III)-**15h**-NTf_2
14	**15h**	**VII** (1.3)	NTf_2 (1.3)	KOAc (3)	ACN:H_2O	Au(III)-**15h**-NTf_2

[a] Equivalents used, relative to ligand (5-10 mg), are given in parentheses after the reagent. Solutions (0.2-1 mL) stirred for at least 1 hr, often o.n.
[b] Black particles assumed to be reduced Au^0; PyH^+ = Protonated pyridine

As a diagnostic test for Au-coordination, the downfield shift of the characteristic triplet of the aromatic hydrogen in the 4-position of the pyridine will be used and is reported as $\Delta\delta^1H = \delta^1H_{complex} - \delta^1H_{ligand}$. All NMRs related to Au-coordinations are performed in d_3-ACN, unless otherwise specified. $^1H,^{15}N$-HMBC was also used to determine the upfield shift of ^{15}N due to complexation and will likewise be reported as $\Delta\delta^{15}N = \delta^{15}N_{complex} - \delta^{15}N_{ligand}$.[97]

The simple bromide **12a** was tested since it was available, but was unsurprisingly unable to coordinate to neither Au(I) nor Au(III) (entries 1 and 2). A derivative of **12a** with a hydrogen in the place of the bromide has previously been shown to successfully coordinate Au(III) in our group (**XII**, Figure 7, page 14). As such, the lack of coordination of the **12a** is assumed to be due to the bromide being too electron withdrawing, leading to a decreased electron density on the nitrogen. The solution of **12a**, $AuCl_3$ and NaOAc changed colour on stirring from yellow to deep orange, assumed to be caused by anion exchange of chloride for acetate at Au. A pink solution appeared by mixing of the ligand with Me_2SAuCl in DCM, normally indicative of decomposition to Au^0 nanoparticles.

The 2-phenyl derivative **15a** was first stirred with $AuCl_3$ in a mixture of ACN and H_2O (entry 3) and after extracting into DCM and drying, a golden oil remained. The resulting NMR

showed promising downfield shift of $\Delta\delta^1$H = 0.60 ppm. However, a combination of broad aromatic signals, only slightly shifted alkyl signals, and lacking crystallinity indicates that this is not a desired Au(III)-complex but instead a pyridinium salt, possibly with an anionic gold species as the counter ion. As such, a new attempt with inclusion of mild base (entry 4) was done. However, this only revealed the free ligand, which consolidates the hypothesis of protonation of pyridine. Attempted activation of the gold salt by addition of $AgSbF_6$ (entry 5) initially gave a pale yellow solution, which rapidly decomposed to a rusty-red solid when dried, which was insoluble in both DCM and ACN.

As there appeared to be some incompatibility problems with ligand **15a**, the ligand was modified in an attempt to better accommodate gold(III). Thermal C-H activation of aryls have been reported to be successful for C-Au bond formation. It is suggested that such reactions takes place by S_EAr-type mechanism by Au^+, forming a carbocationic intermediate.[98] Therefore, the electron rich 3,5-dimethoxyphenyl derivative **15b** was synthesised, aiming to facilitate such an S_EAr mechanism and thereby formation of C,N,O-tridentate gold(III)-complexes. Initial tests of **15b** with gold(III) and mild base at r.t. gave the free ligand with traces of conversion to an unknown compound with a diminutive downfield shift of $\Delta\delta^1$H = 0.25 ppm (entry 6), which is too small to indicate a desired Au-N coordination. Stirring at 70 °C for 2.5 hrs and extraction into DCM was also unsuccessful. Attempted activation of Au by removal of a halogen (entry 7), even when heated at 70 °C for 2.5 hrs, was also ineffectual. Speculations were arising of either the water or base impacting the reaction negatively. Therefore, another attempt was done in which only the ligand **15b**, $KAuCl_4$ and $AgSbF_6$ were mixed in ACN at 70 °C (entry 8). The resulting ^{1}H NMR spectrum showed a mixture of two compounds with a more promising downfield shifts of $\Delta\delta^1$H = 0.72 and 0.77 ppm, respectively. One of these compounds could be observed by ^{1}H,^{15}N-HMBC, and its corresponding pyridine-nitrogen showed a drastic shift of $\Delta\delta^{15}$N = -103.6 ppm. However, NMR signals corresponding to the aromatic 2,6-hydrogens of the phenyl-ring still integrated to 2H, meaning no C-Au bond had formed. Moreover, broad signals at δ^1H ~12.5 ppm were reminiscent with protonation of the pyridine. Crystallization attempts using ACN:DEE or DCM:pentane all proved unsuccessful, only yielding a brown oil which turned to an orange powder when dried, still with impurities present. Decomposition was observed after storing for two weeks. The above results indicate C-H activation of **15b** might require higher temperatures or heating by microwaves irradiation, but, due to time limitations, this could not be tested.

Owing to the variable oxidation state of sulphur, it is sometimes argued to be poisonous to metals for catalytic activity.[99] Notwithstanding, sulphur has been incorporated into ligands in organometallic reactions,[41,100] and due to its compatibility with Au(I) – for example in the precursor **I** – it would be interesting to see if coordination of sulphur to Au(III) was possible. Consequently, thiophene ligand **15c** was synthesised. Incorporation of the sulphur in thiophene – rather than as a simple alkyl thiol or thioether – was done as the related Suzuki cross coupling had proven useful for similar reactions, and since oxidation of thiophene compared to non-aromatic analogues generally requires peracids.[101] Sulphur in normal thiophene has a +2 oxidation state; even though the +4 and +6 oxidised forms thiophene-1-oxide and thiophene-1,1-dioxide are known, they are thermally unstable and non-aromatic.[101] Theoretical

calculations and experiments have also investigated the σ-hole of 1,4-N···S systems and showed there to be a preference for the two heteroatoms being conformationally syn,[102] which is promising for forming S,N-bidentate or S,N,O-tridentate Au(III)-complexes. An initial attempt of stirring ligand **15c** with $AuCl_3$ showed a promising shift of $\Delta\delta^1H$ = 0.48 ppm (entry 9). Nevertheless, appearance of black particles was concerning. Filtering off the particles and addition of DCM gave further precipitation of black particles. Precipitation from DCM by addition of pentane gave a brown powder, which, surprisingly, displayed a ^1H NMR spectrum with sharper signals and a further downfield shift of 0.20 ppm of the characteristic pyridine hydrogen in the 4-position (for a total $\Delta\delta^1H$ = 0.68 ppm). Still, the substantial amount of Au^0 particles that had been removed clearly meant the isolated compound was not a desired Au(III)-complex, but instead a pyridinium salt. Attempts were made with inclusion of KOAc, but only led to recovery of the free ligand (entry 10). Formation of a more assertive Au-species by addition of silver, and a small amount of water to ensure adequate solubility of the base, again gave black particles and only the free ligand was observed by ^1H NMR (entry 11). Unfortunately, these results indicate that the thiophene ligand **15c** is unsuitable for coordination to Au(III) with this strategy.

Lastly, the bipyridine **15h** was attempted. As bipyridine was one of the earliest ligands used in organogold chemistry,[103] we were optimistic that this could yield successful coordinations for the chiral neomenthol derivative. Stirring of ligand **15h** with $AuCl_3$ (1.2 equiv.) and base overnight gave a 1:1 mixture of a new compound ($\Delta\delta^1H$ = 0.58 ppm) and the free ligand (entry 12). Adding more gold (1.3 equiv.) and base to the same solution and stirring for an additional 3 hrs gave complete conversion to the new compound (see ^1H NMR in Figure 16). This new compound exhibited clear and pronounced downfield shift of the *ortho* and *para* hydrogens of each pyridine, indicative of a strongly electron withdrawing species coordinated to each/both nitrogens. Furthermore, one of the *meta* hydrogens on the central pyridine shows an upfield shift of $\Delta\delta^1H_{meta}$ = -0.11 ppm, which is unprecedented. In an attempt to form crystals by slow evaporation of pentane into DCM, a single red oil drop of the pure complex was collected. NMR spectra of this compound could not confirm whether the hydroxyl group was coordinated or not; a broad peak could be observed in the ^1H NMR spectrum at δ^1H 2.13 ppm, which could correspond to either an uncoordinated OH-group or residual H_2O. HRMS could observe an ion corresponding to N,N,O-tridentate coordination to $[AuCl]^+$, as well as a weak signal corresponding to N,N-bidentate coordination to $[AuCl_2]^+$ (Figure 17). If the N,N-bidentate is in fact the main product, fragmentation of HCl during MS ionisation would lead to the observed N,N,O-tridentate complex. The present data were as such inconclusive in determining the coordination-mode of the ligand. IR would be able to differentiate by observation of the OH-group (or lack thereof), but due to a combination of the potentially oxidising nature of Au(III) and the complex being liquid, it was a concern the instrumentation would sustain damage. Furthermore, HRMS observed $AuCl_4^-$ as the counter anion. This explains why the initial 1.2 equivalents added gave a mixture of two complexes, as two gold atoms seem to be included in the complex, hereon named Au(III)-**15h**-$AuCl_4$.

3.3 Coordination of Au(III) to Chiral Pyridine Based Ligands

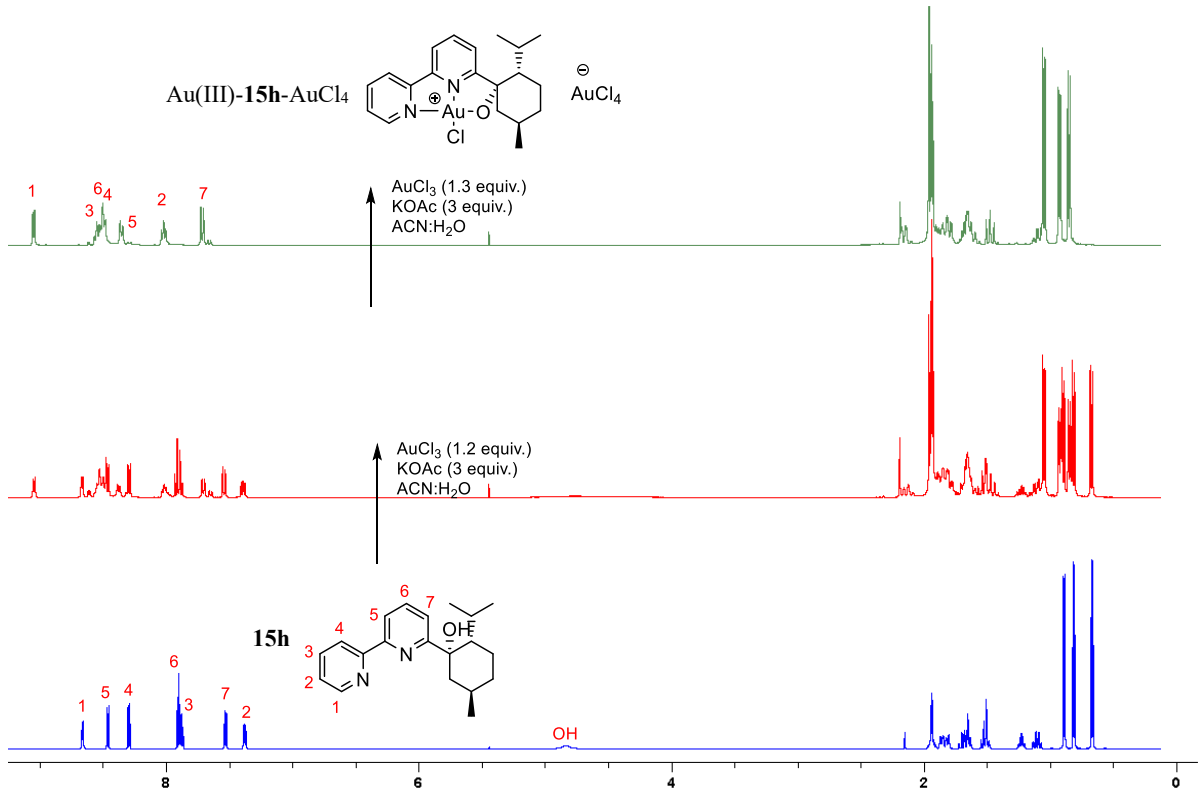

*Figure 16 – ^{1}H NMR spectra of formation of complex Au(III)-**15h**-AuCl$_4$, drawn in the N,N,O-tridentate coordination-mode (Table 5, entry 12).*

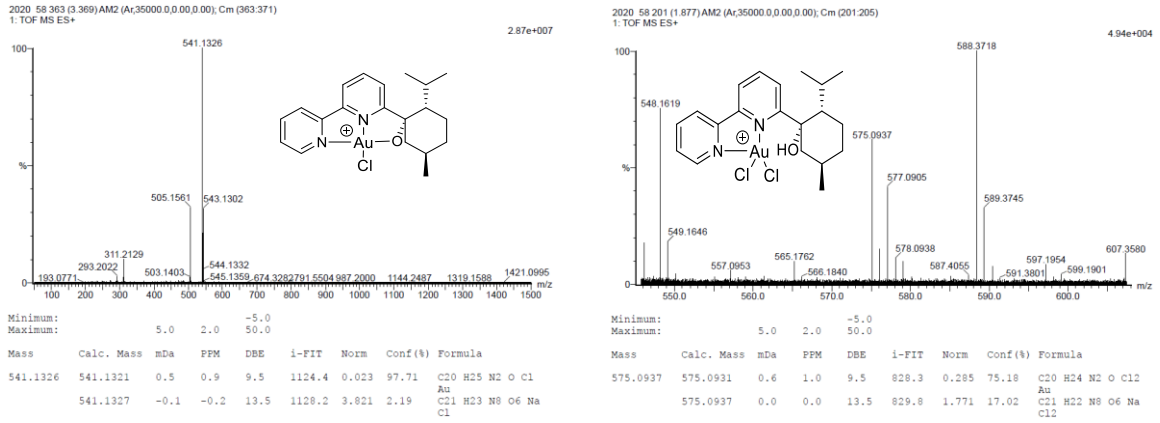

*Figure 17 – HRMS spectra of Au(III)-**15h**-AuCl$_4$, inconclusively showing both N,N-bidentate and N,N,O-tridentate coordination of the ligand.*

The formation of a new chiral Au(III)-complex was encouraging, but a non-auric counterion is needed as to not interfere with any catalytic stereo- or enantioselectivities. Therefore, a new attempt with $AuCl_3$ and $AgNTf_2$ was performed (entry 13), but this revealed a 1:1 mixture of the same set of signals as Au(III)-**15h**-AuCl$_4$ and a new compound that had not been previously observed. Further addition of gold- and silver salts showed no effect. However, addition of KOAc to the existing mixture gave conversion of the new compound to the free ligand, while the other set of signals persisted. This advances the claim that protonated pyridines are quite prevalent for these coordinations, as addition of base caused deprotonation of the pyridinium and regeneration of the free ligand. The same mixture of protonated pyridine

and Au(III)-complex was also observed with $AgSbF_6$ as the source of silver, and inclusion of base once again resulted in the free ligand **15h** and Au(III)-complex.

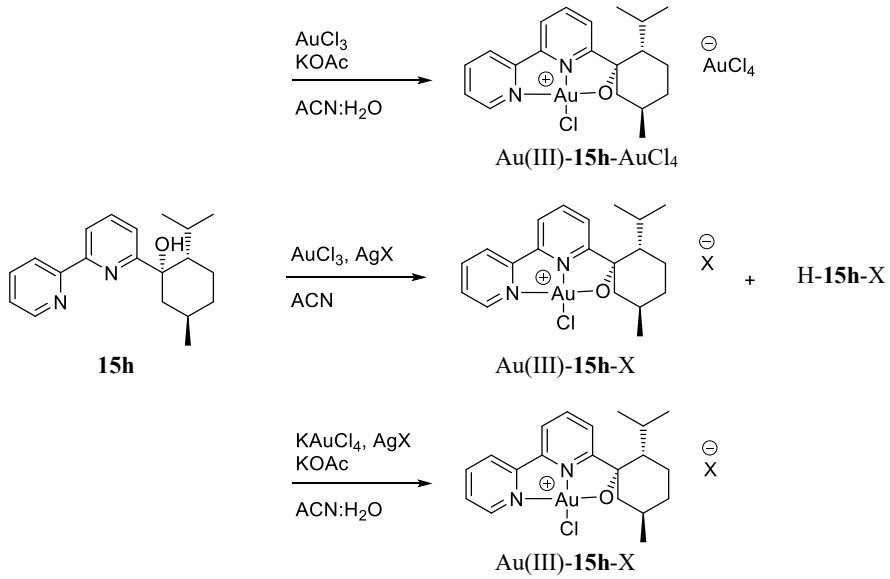

Scheme 26 – Synthesis of novel chiral bipyridine based Au(III) complexes. X=NTf_2, SbF_6.

Finally, a mixture of $KAuCl_4$, $AgNTf_2$ and mild base (entry 14) was attempted, as this should give the optimal conditions for formation of the desired N,N-bidentate/N,N,O-tridentate Au(III)-complex. Pleasingly, stirring over night gave quantitative conversion to the N,N,O-tridentate complex Au(III)-**15h**-NTf_2 as a deep orange powder after precipitation from DCM by addition of pentane (Scheme 26). The novel complex was fully characterised by HRMS, NMR, and IR spectroscopy, and its ^{1}H, ^{13}C and ^{15}N chemical shifts (in d_3-ACN) are displayed in Figure 18a. ^{19}F-NMR could also observe the NTf_2^- counterion, but without an internal fluorinated reference standard its chemical shift will not be reported here (but the NMR spectrum is available in Appendix N.4). IR spectroscopy revealed no OH-signals, verifying N,N,O tridentate mode of coordination (Appendix N.9). Tridentate coordination is also supported by the large difference in the chemical shift of the benzylic carbon on the neomenthol moiety, moving from $\delta^{13}C$ 77.3 ppm ($CDCl_3$) to $\delta^{13}C$ 105.5 ppm (CD_3CN). The two pyridines show an unsymmetric cooridination strength judging by the nitrogen shifts: the central pyridine shifts by $\Delta\delta^{15}N_{central}$ = -49.9 ppm, whilst the terminal pyridine shows a tigher binding by a larger shift $\Delta\delta^{15}N_{terminal}$ = -80.1 ppm, as shown in Figure 18b. Analysis of the coupling constants in the neomenthol moiety clearly shows the same coupling pattern as the free ligand for all hydrogens. Therefore, it can be concluded that the conformation of the cyclohexane ring has not changed by accommodating gold, and the oxygen remains axially oriented, presented in Figure 18c. The unique shifts of $H6_{eq}$ from $\delta^{1}H$ 1.51 to $\delta^{1}H$ 2.12 ppm as well as H7 from $\delta^{1}H$ 1.23 to $\delta^{1}H$ 1.67 ppm is indicative of their spatial proximity of the gold cation center. This demonstrates that the *i*Pr-group has oriented itself so that H7 is oriented towards – and the *i*Pr-methyls are pointing back and away from – the cationic gold center, minimising steric interactions.

3.3 Coordination of Au(III) to Chiral Pyridine Based Ligands

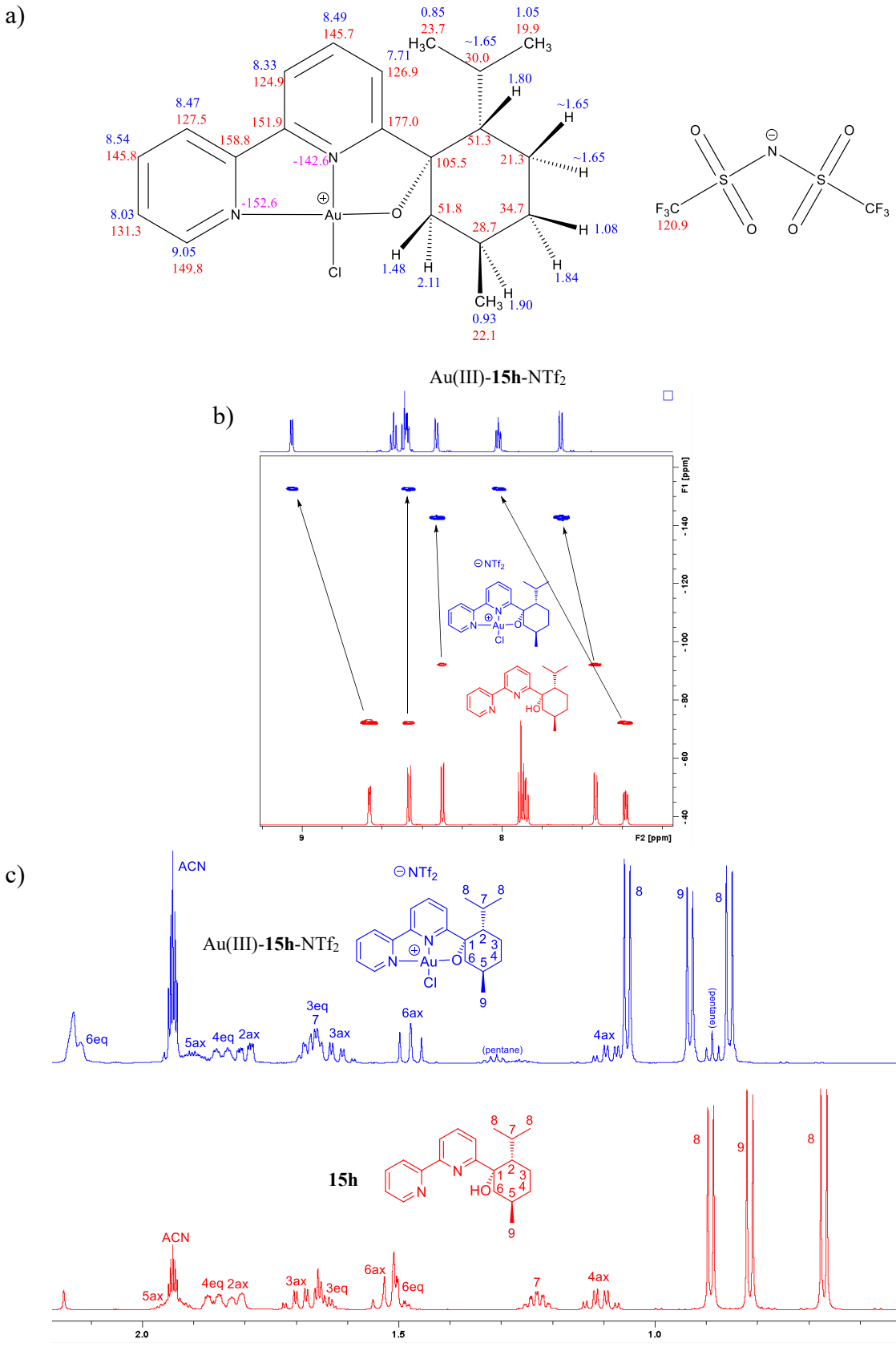

*Figure 18 – a) Chemical shifts of the novel complex Au(III)-**15h**-NTf$_2$. b) Excerpt of overlayed ^{1}H,^{15}N-HMBC spectra of ligand (red) and complex (blue). c) Exercpt of ^{1}H NMR spectra of ligand (red) and complex (blue).*

3.3 Coordination of Au(III) to Chiral Pyridine Based Ligands

Another attempt with $AgSbF_6$ as the source of silver gave 85% conversion to the Au(III)-**15h**-SbF_6 complex after 2 hrs, producing the same NMR spectra as Au(III)-**15h**-NTf_2, except for the quartet in the ^{13}C spectrum belonging to the CF_3-groups of the counterion that were absent. Efforts to acquire crystals for XRD analysis by slow diffusion of pentane into DCM mostly yielded oils, which turned to a powder when dried; it is assumed there is a substantial interaction between DCM and the Au(III)-complexes which prevents adequate mixing of pentane to cause crystallisation. Still, after several attempts, potentially usable crystals for XRD could be acquired, which would be attempted analysed in future work.

3.3.2 Isoborneol Pyridine Alcohols 15d-g

Similarly to the neomenthol-based compounds presented above, the derivatives containing isoborneol as the chiral auxiliary (**15d-g**, prepared in section 3.1.4, page 15) were attempted coordinated to Au(III), and the results are summarized in Table 6. Due to time limitations, less investigation was done with these derivatives compared to the neomenthol analogues.

Table 6 – Attempted coordinations of 2-aryl-6-isoborneolpyridines to Au. [a]

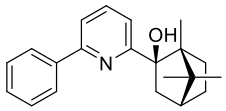

15d

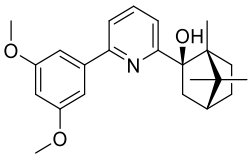

15e

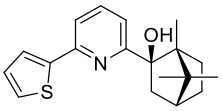

15f

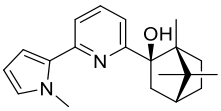

15g

$AuCl_3$ (**V**) $KAuCl_4$ (**VII**)

Entry	Ligand	Au	AgX, X=	Base	Solvent, condition	Result [b]
1	**15d**	**V** (1)		NaOAc (3)	ACN:H_2O	Ligand recovered
2	**15d**	**V** (1)		NaH (1)	ACN	New compound, decomposed o.n
3	**15d**	**VII** (1.3)	SbF_6 (1.3)	KOAc (3)	ACN:H_2O	Decomposed when dried
4	**15e**	**V** (1.1)		KOAc (2)	d_3-ACN	Ligand recovered
5	**15f**	**V** (1.1)			d_3-ACN	PyH^+, broad peaks
6	**15f**	**V** (1.1)		NaOAc (3)	ACN:H_2O	Ligand recovered or black particles, depending on workup
7	**15f**	**V** (1.1)	SbF_6 (2.2)	NaOAc (3)	ACN:H_2O	New compound, decomposes

[a] Equivalents used, relative to ligand (5-10 mg), are given in parentheses after the reagent. Solutions (0.2-1 mL) stirred for at least 1 hr, often o.n.
[b] Black particles assumed to be reduced Au^0; PyH^+ = Protonated pyridine

Starting from the phenyl substituted **15d**, simple attempts to stir the ligand with $AuCl_3$ overnight showed no conversion, with or without mild base (entry 1). As the isoborneol-OH group is more sterically enclosed than the neomenthol derivative, a smaller base (NaH) was attempted (entry 2). Since NaH is not assumed to be compatible with Au(III), only the ligand and base was first stirred for 30 minutes, before addition of $AuCl_3$, causing conversion to a new compound ($\Delta\delta$ ^1H = 0.24 ppm), which decomposed on standing. Repeated attempts to reproduce this method were unsuccessful. The low coordination-shift of the hydrogen in the 4-position of pyridine does not seem to indicate that a gold-complex was formed. Inclusion of silver initially gave a yellow solution which decomposed to a red, insoluble solid upon drying (entry 3).

3.3 Coordination of Au(III) to Chiral Pyridine Based Ligands

The 3,5-dimethoxyphenyl **15e** was only investigated by stirring with $AuCl_3$ and base in ACN, and resulted in recovery of the free ligand (entry 4). This is in line with previous observations that no change occurs if base is included without water, possibly due to deactivation of Au(III) by anionic ligand exchange.

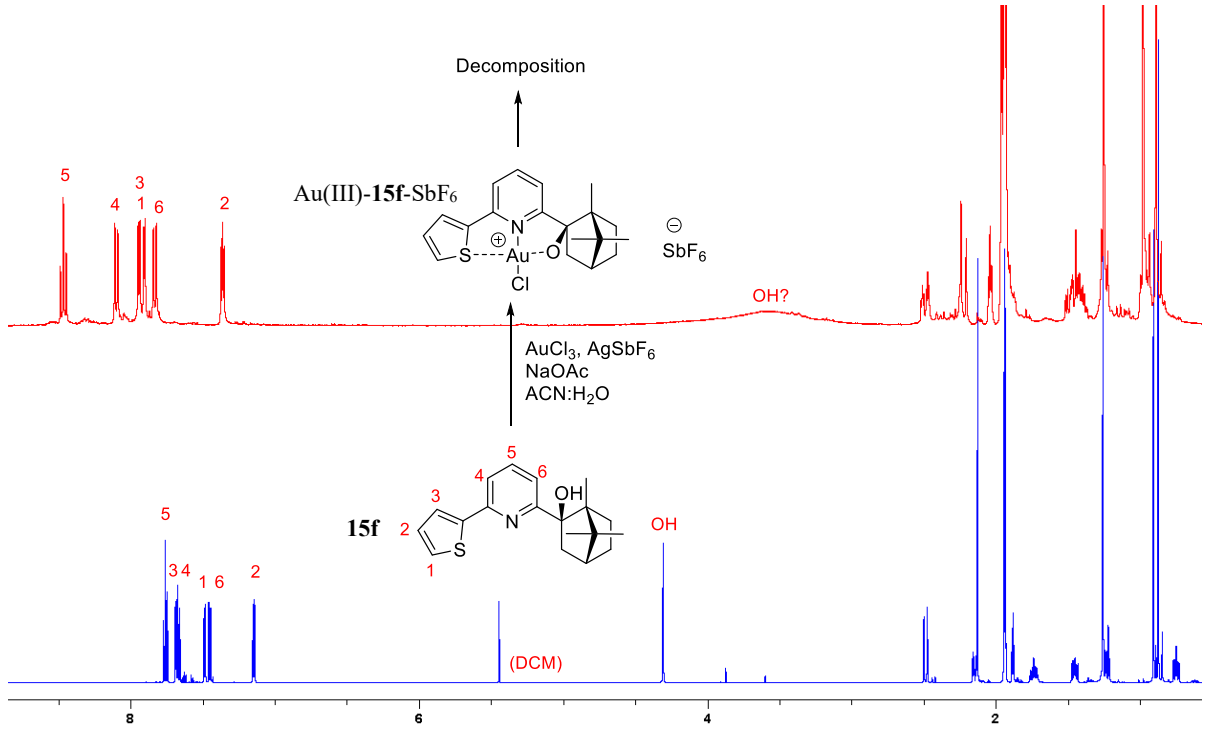

*Figure 19 – Synthesis and ^{1}H NMR spectrum of the assumed complex Au(III)-**15f**-SbF_6.*

The thiophene **15f** showed a downfield shift of $\Delta\delta^1$H = 0.42 ppm along with significant peak broadening when stirred with $AuCl_3$ (entry 5). Precipitation of an unknown yellow powder in the NMR tube is assumed to be the cause of the broadened signals, as this results in poor shimming of the sample. When acetate and water was included (entry 6), black particles appeared upon addition of DCM, and NMR showed only the free ligand. Assuming instability in DCM, a different workup was attempted consisting of addition of further 2 mL ACN and removal of water by drying over Na_2SO_4, and finally removal of ACN *in vacuo*. This workup gave no black particles, but also showed no coordination by NMR. Finally, silver was added (entry 7). Since decomposition was previously observed by adding DCM, the Na_2SO_4-strategy was attempted again, and NMR finally revealed a new compound with $\Delta\delta^1$H = 0.71 ppm, assumed to be the novel complex Au(III)-**15f**-SbF_6, Figure 19. It was not concluded whether an S,N,O-tridentate, N,O-bidentate, or S,N-bidentate complex formed, but appearance of a broad peak (spanning ~3 ppm in width) might indicate the OH-group has not coordinated. Attempts to form crystals for XRD analysis from ACN:THF of ACN:DEE were unsuccessful and caused decomposition. The reaction could not be re-attempted due to time limitations.

The *N*-methylpyrrole ligand **15g** was synthesised, but was not attempted in viable coordination reactions due to time limitations. Nonetheless, ligand **15g** was not expected to be able to form a Au(III)-complex due to the *N*-methyl hindering the approach of gold and

occupying the coordination site at pyrrole. Furthemore, the nitrogen lone pair of pyrrole is occupied in the aromatic system. To circumvent these limitations, synthesising an unmethylated pyrrole derivative by construction of the pyrrole ring from the appropriate 1,4-dicarbonyl and ammonia was debated (no corresponding boronic acid is commerically available), but never attempted.

Coordination of the bipyridine derivative of isborneol would have been interesting owing to the successful results of neomenthol **15h**. However, it is assumed synthesis of the bipyridine-isoborneol ligand would result in low yields, and given the time left of the project, it was not attempted. Synthesis of this bipyridine-isoborneol ligand would have allowed for a better comparison of the utilised chiral auxillaries.

3.3.3 Methyl Ether Derivatives of Chiral Pyridine Based Ligands

To increase the stereoselectivity a catalyst would have, the effects a chiral group has on the substrate should be maximised. Adapting the ligand, so as to bring a substrate closer to the chiral environment provided by the auxiliary, is one way of achieving such stereocontrol. We hypothesised that a weakened Au-O bond – such as by changing from a σ-bond to a π-bond – would enable temporary release of the chiral auxiliary, thereby opening an active site at gold as close to the chiral group as possible. Additionally, the effects a non-covalent Au-O bond would have on the stability of the Au(III)-complexes could be investigated. Hence, the methylated derivatives **15b,d,e,h-OMe** were synthesised (see section 3.1.5, page 17). Their attempted coordinations to Au(III) are summarised in Table 7.

*Table 7 – Attempted coordinations of methylated 2-aryl-6-alkylpyridines (**15-OMe**) to Au.* [a]

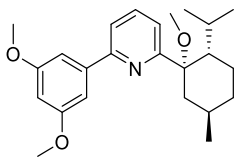

15b-OMe

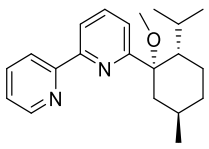

15h-OMe

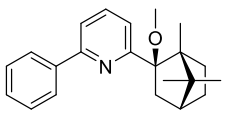

15d-OMe

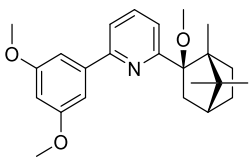

15e-OMe

$AuCl_3$ (**V**) $KAuCl_4$ (**VII**)

Entry	Ligand	Au	AgX, X=	Base	Solvent, condition	Result [b]
1	**15b-OMe**	**V** (1.1)			ACN	Broad peaks, slight downfield shift
2	**15h-OMe**	**V** (1.1)			d_3-ACN	PyH^+ + Au(III)-complex
3	**15h-OMe**	**V** (1.2)	BF_4 (1.2)		ACN:H_2O	PyH^+ + Au(III)-**15h-OMe**-BF_4, crystals acquired
4	**15h-OMe**	**VII** (1.3)	NTf_2 (1.3)	KOAc (3)	ACN:H_2O	Free ligand and Au(III)-**15h-OMe**-NTf_2
5	**15d-OMe**	**VII** (1)	SbF_6 (1)		d_3-ACN	Broad peaks
6	**15e-OMe**	**V** (1.1)			d_3-ACN	Broad peaks, downfield shift

[a] Equivalents used, relative to ligand (5-10 mg), are given in parentheses after the reagent. Solutions (0.2-1 mL) stirred for at least 1 hr, often o.n.
[b] Black particles assumed to be reduced Au^0; PyH^+ = Protonated pyridine

Stirring **15b-OMe** with $AuCl_3$ only gave broad aromatic peaks in ^1H NMR along with slight movement of the alkyl signals (entry 1). A separate attempt at 60 °C gave the same broad peaks and no C-H activation of the dimethoxyphenyl. Since there was no success with the hydroxyl derivative **15b**, no further attempts were made.

3.3 Coordination of Au(III) to Chiral Pyridine Based Ligands

The methylated bipyridine neomenthol **15h-OMe** was completely consumed, forming two different new compounds when stirred with $AuCl_3$ in ACN (entry 2), assumed to be protonated pyridine and the desired complex, or alternatively two different forms of protonated pyridine. Addition of further $AuCl_3$ had no effect. $^{1}H,^{15}N$-HMBC only showed one signal strong enough to confirm coordination to the terminal pyridine, whose nitrogen shifted $\Delta\delta^{15}N_{terminal}$ = -88.1 ppm. Comparing to the hydroxyl analogue **15h**, this N-shift is more drastic than for either pyridine in the isolated Au(III)-**15h** complexes (see Figure 18b). Therefore, it is reasonable to assume the ether oxygen of **15h-OMe** is not coordinating to gold, causing to the positive charge to be distributed over fewer atoms. Including $AgBF_4$ (entry 3) still gave the same mixture, but with a higher amount of the desired complex, Au(III)-**15h-OMe**-BF_4. Addition of DCM gave immediate white precipitation assumed to be AgCl, which when removed allowed for formation of crystals usable for XRD analysis (which presently have not been possible to analyse). Repeated attempts to acquire expendable catalyst for test-reaction screening could not be performed due to time limitations. Finally, inclusion of base and the tightly binding NTf_2^- anion again gave the free ligand and the corresponding Au(III)-complex Au(III)-**15h-OMe**-NTf_2 (entry 4). Unfortunately, including both silver and base was not able to give complete conversion to a complex, but still a discernible amount of free ligand.

Finally, the two methylated isoborneol derivatives **15d-OMe** and **15e-OMe** were briefly tested for coordination to Au(III) (entry 5-6), but did not show any promising results, in line with their corresponding hydroxyl versions **15d** and **15e** (see Table 6, entries 1-4).

3.3.4 Catalytic Testing of Chiral Au(III)-complex

The catalytic activity and enantioselectivity of the newly synthesised Au(III)-**15h**-NTf_2 complex was investigated. For this purpose, the complex' action was investigated in the [1+2]-cycloaddition of propargyl acetate (**11**) with styrene. The cyclopropane product can be formed as either the *cis* or *trans* diastereomers, while the alkene is produced only as the *Z*-isomer (Scheme 27). For mechanistic details of this reaction, see section 2.3, Scheme 6b, page 6.

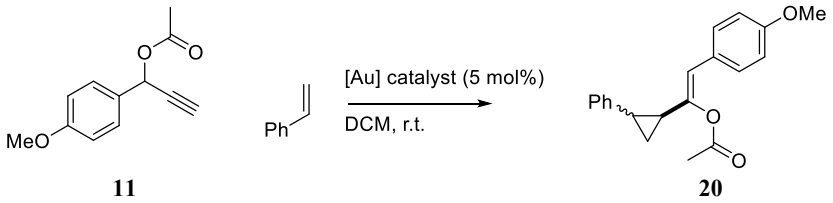

11 **20**

*Scheme 27 – Au-catalysed [1+2]-cycloaddition between propargyl acetate **11** and styrene.*

The novel complex Au(III)-**15h**-NTf_2 was highly active in the above reaction, causing complete consumption of substrate **11** after just 10 mins. Workup and purification by flash column chromatography yielded the cyclopropane product **20** in 71 % yield. Analysis by chiral HPLC showed the diastereomers to be formed in relative ratios *trans*:*cis* 76:24 (52 %de, see Appendix M.2). Elevated amounts of the *trans* diastereomer is however not surprising, as the model reaction has in our group been shown to undergo *cis*-to-*trans* isomerisation in the presence of catalytic gold.[21] Unfortunately, no discernible enantiomeric excess was formed for each diastereomer.

The other Au(III)-complexes that were synthesised were reserved for XRD analysis, and therefore not attempted in the above cycloaddition reaction. Further work would focus on their isolation, characterisation, and screening in the above reaction, along with other available test-reactions in our group.

3.4 Synthesis and Coordination of Cyclam Ligands

As part of a collaboration with PhD-candidate Ann Christin Reiersølmoen, various chiral cyclam ligands (**6**) were synthesised to be coordinated to Au(III). If successful, the resulting chiral Au(III)-complexes were then to be investigated as catalysts in asymmetric reactions. The data presented herein are the results of syntheses individually conducted for this master's thesis, and the combined results of the collaboration can be seen in our manuscript in preparation for a short communication in Appendix B.

3.4.1 Synthesis of Chiral Cyclam

Following the strategy reported by De *et al.*,[80] synthesis of chiral tetraphenyl substituted cyclam **6b** was planned according to Scheme 28. The phenyl derivative **8b** was chosen as it was commercially available, and can conveniently be visualised for TLC by UV light. For ease of discussion, the cyclam **7b** will be referred to the 'dimer' of the reaction, **7b'** as the 'trimer', etc.

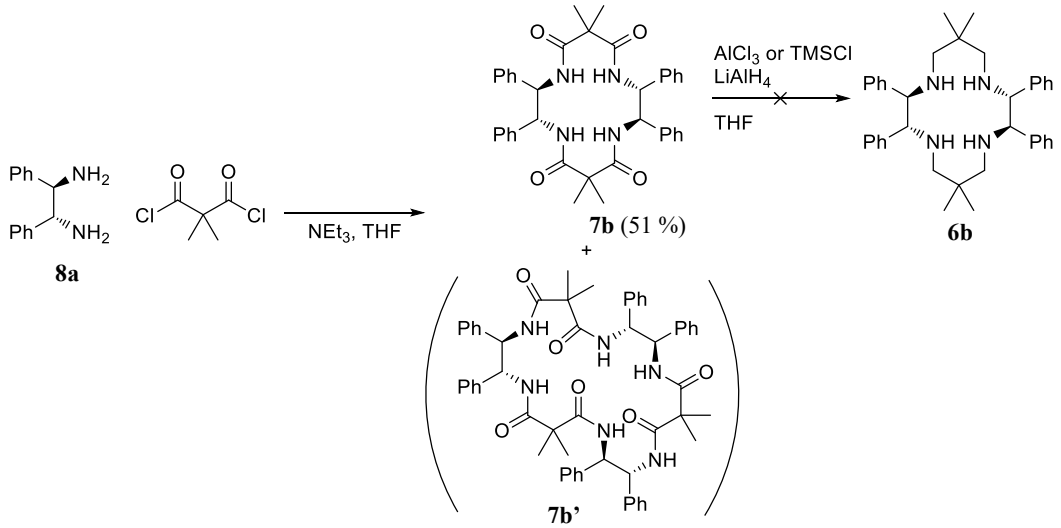

*Scheme 28 – Unsuccessful synthesis of chiral cyclam **6b**.*

Mixing dimethylmalonyl chloride and diamine **8b** in dry THF with NEt_3 at r.t. gave a complex mixture of the desired cyclam **7b** together with its analogue 21-membered cyclic trimer **7b'** and the 28-membered cyclic tetramer **7b''** (not depicted), as indicated by HRMS. Purification by flash column chromatography (5:1 EtOAc:pentane) gave the novel cyclam **7b** in 44 % yield. In an attempt to reduce the amount of undesired oligomers that formed, a repeated reaction with greater dilution was conducted. Indeed, increased formation of the desired cyclam **7b** was observed by NMR, and could be isolated in 51 % yield after three consecutive flash columns.

3.4 Synthesis and Coordination of Cyclam Ligands

With cyclam **7b** in hand, attempted reduction to the final product **6b** followed (Scheme 28). As four reductions on the same molecule were required for formation of **6b**, the reaction was modified by inclusion of a Lewis acid; binding to the amide carbonyls would polarise the bond, assisting the hydride attack. Consequently, a solution of tetraamide **7b** and $AlCl_3$ in THF were cooled to 0 °C before addition of excess $LiAlH_4$. After quenching with *i*PrOH, the following extraction proved problematic due to various Al-salts causing emulsions. Moreover, cyclams (**6**) can be water-soluble, making for an ineffective extraction. Attempted purification by flash column chromatography (2:13 MeOH:DCM) only yielded complex mixtures of various partially reduced cyclam compounds. Change of Lewis acid to TMSCl was also unsuccessful in achieving the fully reduced product **6b**.

Owing to the great difficulty of synthesising the fully reduced cyclam **6b**, an alternative method was suggested. Mono-*N*-protection of the diamine precursor **8b** using Boc_2O would form **8b-Boc**, from which the selective synthesis of the 'open cyclam' derivative **21-Boc** could be possible. Following deprotection of the terminal amines to give **21** leaves us with a scenario where only two amides need to be reduced, rather than the required four in **7b** (Scheme 29).

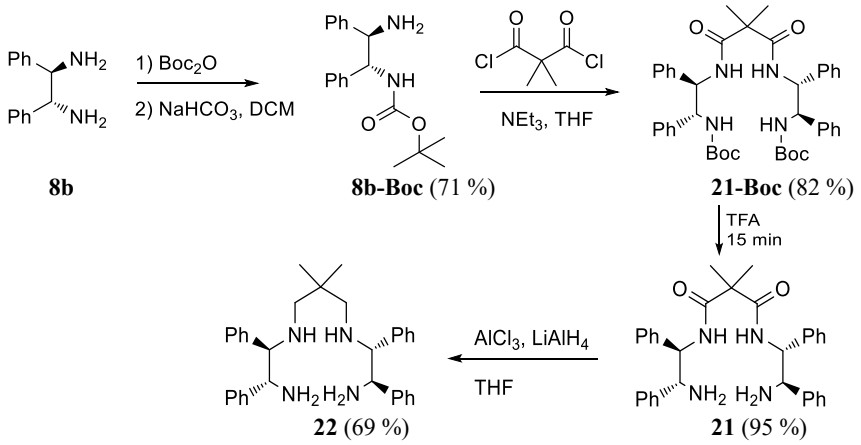

*Scheme 29 – Synthesis of chiral 'open cyclam' **22**.*

Methods for selective mono-protection of diamines have been reported, but require the use of dangerous HCl-gas.[104] As such, simple mixing of the diamine **8b** with less than one equivalent of Boc_2O was attempted. Purification by flash column chromatography (EtOAc) gave the pure mono-protected amine **8b-Boc** in 71 % yield. Subsequent reaction with dimethyl malonyl chloride precipitated the Boc-protected 'open cyclam' product **21-Boc** in 82 % yield from the reaction mixture. Derivative **21-Boc** was insoluble in several tested polar and nonpolar organic solvents, making the succeeding removal of the Boc-groups troublesome. Deprotection of **21-Boc** was planned to be performed in an EtOH/HCl solution, but stirring for 2 days resulted in quantitative recovery of the protected starting material. Various attempts with other solvent-acid combinations were also unsuccessful. Finally, addition of neat TFA was found to successfully dissolve and deprotect **21-Boc** to give the novel 'open cyclam' tetraamine **21** in just 15 mins. The following reduction using the aforementioned $AlCl_3$-$LiAlH_4$ strategy lead to the previously unreported target 'open cyclam' **22** in 69 % yield.

Some of the compounds synthesised above were insoluble in $CDCl_3$ and were characterised in d_6-DMSO.

3.4.2 Coordination of Chiral 'Open Cyclams' 21 and 22 to Au(III)

The two 'open cyclam' ligands **21** and **22** were briefly attempted coordinated to Au(III) without any success. In the field of organogold(III)-chemistry, coordinations are commonly performed in ACN due to good solubility and stability of Au(III)-salts (see Section 2.2). However, due to the poor solubility of the ligands in ACN, resulting ^{1}H NMR spectra showed broad and inconclusive signals. Coordinations were attempted from both $AuCl_3$ and $KAuCl_4$ salts without any clear signs of successful incorporation of Au(III) to the 'open cyclam' core. Activation of the gold-species by abstraction of a halide through addition of a silver-salt was also unsuccessful, as shown in Scheme 30.

It is unknown why coordinations of ligands **21** and **22** to Au(III) failed. Additional coordination attempts of ligands **21** and **22** by Ann Christin Reiersølmoen were also unsuccessful. Even though insufficient solubility of the ligands might be the cause, we have theorised that the strongly chelating effects of the cyclam systems can also have resulted in trapping of aluminium from previous synthetic steps (see Scheme 29). Chelation of other metals in the cyclams could be the cause of failed the insertion of Au(III).

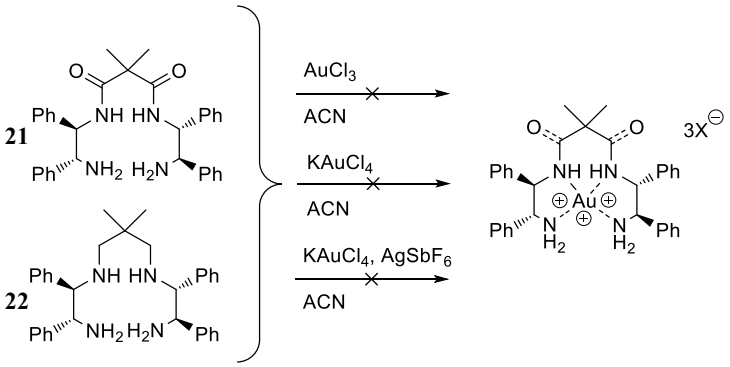

*Scheme 30 – Unsuccessful coordinations of 'open cyclams' **21** and **22** to Au(III).*

4 Conclusion

In this master's thesis, several novel compounds have been presented for the first time.

As the Fiksdahl research group is continuously interested in the preparation of novel, chiral Au-complexes, there is a pressing need for standardised Au-catalysed test-reactions to gauge their enantioselectivities. Consequently, the study of the recently reported reaction between propargyl alcohols **1** and aryl nucleophiles, forming allenes (**3**) and indenes (**4**) in the presence of Au-catalysts has been presented. The reactions were shown to be highly sensitive to several reaction conditions. Au(I) and Au(III) catalysts were both successful in forming indene products **4** by thermal activation, but Au(III) catalysts were superior for forming the intermediate allene products **3**. This demonstrates a crucial difference in reactivity of Au(I) and Au(III) catalysts, which have sometimes been argued to be equivalent and interchangeable. Several solvent systems were tested, and few were shown to be applicable. Varying electronic- and steric substituents on both the propargyl alcohol **1** substituents and aryl nucleophile demonstrated the fastidious nature of the reactions, often forming mixtures of several products. Chiral HPLC was unsuccessful in the enantiomeric separation of various allenes **3** and indenes **4**.

Ligands based on *ortho*-substituted pyridines have previously been successful at coordinating to Au(III) in our group, and consequently, further derivatisation of such systems was attractive. Synthesis of several chiral 2-aryl-6-alkyl pyridine alcohols **15a**-**h** and methyl ether derivatives **15b**,**d**,**e**,**h**-**OMe** have been presented, either containing neomenthol or isoborneol as the chiral auxiliaries. Several of the prepared pyridine derivatives have never been reported in literature and were as such fully characterised. Numerous attempted coordinations of these potential pyridine based ligands to Au(III) were conducted, mostly resulting in decomposition of the formed complexes or protonation of the pyridine instead of incorporation of gold. Still, through several attempts, the novel complexes Au(III)-**15h**-X (X=$AuCl_4$, NTf_2, SbF_6) were prepared and isolated, and characterised by HRMS, NMR and IR spectroscopy. The Au(III)-complexes Au(III)-**15f**-SbF_6 and Au(III)-**15h**-**OMe**-X (X=BF_4, NTf_2) were also synthesised, but their structures not conclusively determined, pending XRD analysis. The complex Au(III)-**15h**-NTf_2 was used in a model [1+2]-cycloaddition reaction between propargyl acetate **11** and styrene, forming the product cyclopropane in 71 % yield in 10 mins with 52 %de (*trans*:*cis* 76:24).

Preparation of cyclam derivatives, to act as chiral polydentate ligands for square planer Au(III), was performed. Unsuccessful synthesis of the chiral cyclam **6b** by reduction of the corresponding tetraamide **7b** prompted the alternative synthesis 'open cyclams' **21** and **22**, neither of which could be successfully coordinated to Au(III). The low solubility of the ligands, along with the possibility of the cyclam-core already being occupied by another metal, are believed to be the main causes that prevented incorporation of Au(III).

5 Further work

On allene/indene test-reaction: The test-reactions of 1,3-diarylpropargyl alcohols (**1**) with aryl nucleophiles have been extensively discussed in this thesis, but were only limited to 1,3-diaryls. How these reactions would be affected by non-aromatic substituents on C-1 has not been discussed herein. Expanding the investigation of the mild nucleophiles to non-aromatic systems would allow for the synthesis of new indene derivatives, which indeed could be useful in the field of medicinal chemistry. Additionally, development of a suitable chiral HPLC system that allows for the routine analysis of allene and/or indene products would be highly attractive. In doing so, one would permit a more in depth investigation of asymmetric synthesis of the aforementioned allenes and indenes through chiral Au-catalysts.

On chiral pyridine based ligands: Further trials for forming chiral Au(III)-catalysts from the numerous pyridine based ligands **15a-h** synthesised in this thesis is encouraged, possibly by a different strategy than the one focused on herein. Re-preparation of the Au(III)-complexes propsed herein, and their catalytic testing, is high interest. Adaptions of these systems by use of pyrrole as the central nitrogen-bearing heterocycle would be fascinating, as such Au(III)-complexes are – to the best of our knowledge – not reported. Since pyrrole is more electron rich than pyridine, tighter binding and facile complex-formation can be expected. Finally, XRD analysis of the acquired crystalline Au(III)-complexes must be finalised.

On chiral cyclam based ligands: Coordination of the chiral 'open cyclams' **21** and **22** to Au were only briefly investigated due to the poor solubility of the ligands in ACN. These ligands should be excellent for the incorporation of square planar Au(III). Therefore, further experiments for their coordination would be interesting to investigate. Furthermore, different synthetic strategies for the formation of cyclams that do not involve the use of metals (such as Al) would be desirable, to prevent chelation to the products.

6 Experimental

All reactions, except the synthesis of gold complexes, were performed under inert N_2-atmosphere. Commercial grade reagents were used without any additional purification. Dry solvents were collected from a MB SPS-800 solvent purification system. All reactions were monitored by NMR and/or thin-layer chromatography (TLC) using silica gel 60 F254 (0.25 mm thickness). TLC plates were developed using UV-light, *p*-anisaldehyde stain, or I_2 stain. Flash chromatography was performed with Merck silica gel 60 (0.040- 0.063 mm). ^{1}H and ^{13}C NMR spectra were recorded either a Bruker Avance DPX 400 MHz or a Bruker Avance III 600 MHz spectrometer. Chemical shifts are reported in ppm (δ) downfield from tetramethylsilane (TMS) as an internal standard when using $CDCl_3$ as the solvent, or relative to d_2-ACN when using d_3-ACN as the solvent, calibrated to δ^1H 1.94 ppm, δ^{13}C 1.32 ppm and δ^{15}N -135.5 ppm.[105] Peak multiplicity is given by the apparent splitting pattern. Coupling constants (*J*) are given in Hz. Assignment of NMR signals to their corresponding atom is done only when possible from the spectra acquired, and if not, only characteristic spectral data is listed. Accurate mass determination in positive and negative mode was performed on a "Synapt G2-S" Q-TOF instrument from Water TM. Samples were ionized by the use of ASAP probe (APCI) or ESI probe. No chromatographic separation was used prior to mass analysis. Calculated exact mass and spectra processing was done by Waters TM Software Masslynx V4.1 SCN871. IR spectra were recorded with a Bruker Alpha FT-IR spectrometer using OPUS V7 software to analyse the spectra.

6.1 Synthesis of propargyl alcohols, 1a-i

General procedure A

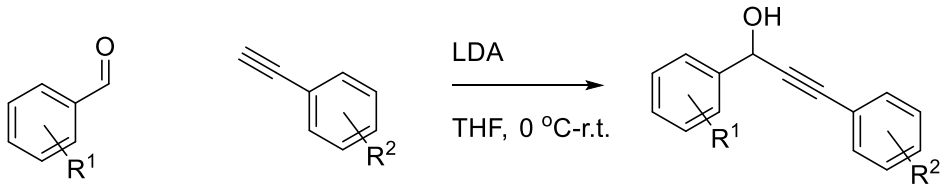

9	R^1
a	H
b	2,4,6-triMe
c	2,6-diMe
d	4-OMe
e	4-CF_3

10	R^2
a	H
b	2,4,6-triMe
c	4-OMe
d	4-CF_3

1	R^1	R^2
a	H	H
b	H	2,4,6-triMe
c	H	4-OMe
d	H	4-CF_3
e	2,4,6-triMe	H
f	2,4,6-triMe	4-CF_3
g	2,6-diMe	H
h	4-OMe	H
i	4-CF_3	H

A solution of arylacetylene **10a-d** (1-1.1 equiv.) in dry THF was cooled to 0 °C and LDA (1.5 equiv., 2M in THF) was added slowly under a N_2-atmosphere. The solution was stirred for 30 mins before aldehyde **9a-e** (1 equiv.) was added. The solution was stirred for 2 hrs and allowed to warm to r.t. before being quenched with aqueous NH_4Cl (sat., 10 mL). The layers were separated, and the aqueous phase was extracted with EtOAc (3x15 mL). The combined organic layers were washed with brine, dried over Na_2SO_4, and the solvent removed *in vacuo*.

Purification by flash column chromatography (EtOAc:pentane) yielded pure propargyl alcohol **1a-i**.

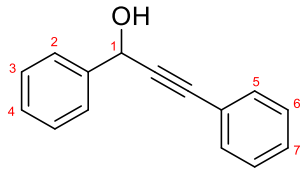

1a

1,3-Diphenylprop-2-yn-1-ol (**1a**): Following general procedure A, acetylene **10a** (580 μL, 5.28 mmol) in THF (10 mL) was reacted with LDA (3.6 mL, 2M, 7.20 mmol). Addition of aldehyde **9a** (490 μL, 4.80 mmol) yielded propargyl alcohol **1a** (647 mg, 65 %) as a pale yellow oil after flash column chromatography (1:10 EtOAc:pentane).

^{1}H NMR (600 MHz, $CDCl_3$) δ (ppm): 7.61 (d, J = 7.1, 2H, H2), 7.46 (m, 2H, H5), 7.39 (t, J = 7.1, 2H, H3), 7.36-7.25 (m, 4H, H4, H6 and H7), 5.67 (d, J = 6.1, 1H, H1), 2.45 (d, 1H, OH).

^{1}H NMR was in accordance with literature data.[89]

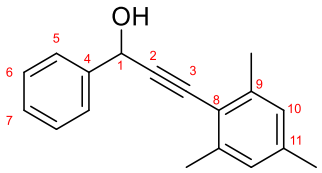

1b

3-Mesityl-1-phenylprop-2-yn-1-ol (**1b**): Following general procedure A, acetylene **10b** (510 μL, 3.26 mmol) in THF (5 mL) was reacted with LDA (2.2 mL, 2M, 4.34 mmol). Addition of aldehyde **9a** (221 μL, 2.17 mmol) yielded propargyl alcohol **1b** (329 mg, 61 %) as a light brown powder after flash column chromatography (1:13 EtOAc:pentane).

^{1}H NMR (600 MHz, $CDCl_3$) δ (ppm): 7.65 (d, J = 7.3, 2H, H5), 7.40 (t, J = 7.5, 2H, H6), 7.34 (t, J = 7.3, 1H, H7), 6.86 (s, 2H, H10), 5.77 (d, J = 6.3, 1H, H1), 2.40 (s, 6H, Me9), 2.27 (s, 3H, Me11), 2.23 (d, J = 6.3, 1H, OH).

^{13}C NMR (150 MHz, $CDCl_3$) δ (ppm): 141.1 (C4), 140.4 (C9), 138.1 (C11), 128.6 (C6), 128.4 (C7), 127.6 (C10), 126.8 (C5), 119.1 (C8), 96.3 (C2), 84.7 (C3), 65.5 (C1), 21.30 (C13), 21.03 (C12).

HRMS (ASAP) calcd for $C_{18}H_{17}$ $[M\text{-}OH]^+$ 233.1330, obsd 233.1328.

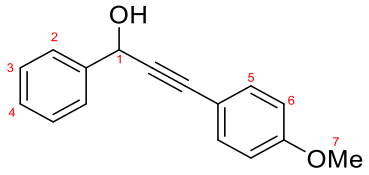

1c

3-(4-Methoxyphenyl)-1-phenylprop-2-yn-1-ol (**1c**): Following general procedure A, acetylene **10c** (599 μL, 4.61 mmol) in THF (10 mL) was reacted with LDA (3.5 mL, 2M, 7.0 mmol). Addition of aldehyde **9a** (427 μL, 4.20 mmol) yielded propargyl alcohol **1c** (183mg, 18%) as a yellow solid after flash column chromatography (1:5 EtOAc:pentane).

^{1}H NMR (400 MHz, $CDCl_3$) δ (ppm): 7.62 (dm, J = 7.3, 2H, H2), 7.39-7.42 (m, 4H, H3 and H5), 7.34 (tt, J = 8.2, 2.0, 1H, H4), 6.84 (d, J = 8.8, 2H, H6), 5.68 (d, J = 6.1, 1H, H1), 3.81 (s, 3H, H7), 2.26 (d, J = 6.1, 1H, OH).

^{1}H NMR was in accordance with literature data.[90]

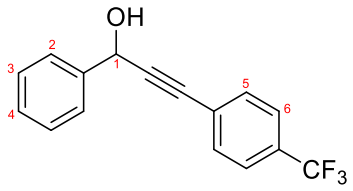

1d

1-Phenyl-3-(4-(trifluoromethyl)phenyl)prop-2-yn-1-ol (**1d**): Following general procedure A, acetylene **10d** (580 μL, 3.556 mmol) in THF (5 mL) was reacted with LDA (2.5 mL, 2M, 5.0 mmol). Addition of aldehyde **9a** (330 μL, 3.25 mmol) yielded propargyl alcohol **1d** (367.4 mg, 41 %) as a white powder after flash column chromatography (1:10 EtOAc:pentane).

^{1}H NMR (600 MHz, $CDCl_3$) δ (ppm): 7.61 (m, 2H, H2), 7.58 (s, 4H, H5 and H6), 7.43 (m, 2H, H3), 7.37 (m, 1H, H4), 5.71 (d, J = 6.1, H1), 2.27 (d, J = 6.2, OH).

^{1}H NMR was in accordance with literature data.[90]

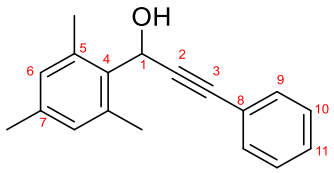

1e

1-Mesityl-3-phenylprop-2-yn-1-ol (**1e**): Following general procedure A, acetylene **10a** (658 μL, 5.99 mmol) in THF (3 mL) was reacted with LDA (4.0 mL, 2M, 8.0 mmol). Addition of aldehyde **9b** (589 μL, 3.99 mmol) yielded propargyl alcohol **1e** as a yellow oil after flash column chromatography (1:9 EtOAC:pentane).

^{1}H NMR (600 MHz, $CDCl_3$) δ (ppm): 7.38-7.44 (m, 2H, H9), 7.25-7.32 (m, 3H, H10 and H11), 6.87 (s, 2H, H6), 6.11 (s, 1H, H1), 2.55 (s, 6H, Me5), 2.27 (s, 3H, Me7), 2.10 (bs, 1H, OH).

^{13}C NMR (150 MHz, $CDCl_3$) δ (ppm): 137.8 (C7), 136. (C5), 133.6 (C4), 131.6 (C9), 130.0 (C6), 128.3 (C10), 128.2 (C11), 122.8 (C8), 88.8 (C2), 85.7 (C3), 60.8 (C1), 20.9 (Me7), 20.3 (Me5).

HRMS (ASAP) calcd for $C_{18}H_{17}$ $[M\text{-}OH]^+$ 233.1330, obsd 233.1330.

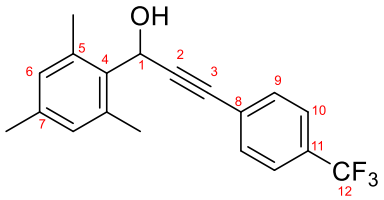

1f

1-Mesityl-3-(4-(trifluoromethyl)phenyl)prop-2-yn-1-ol (**1f**): Following general procedure A, acetylene **10d** (564 μL, 3.46 mmol) in THF (3 mL) was reacted with LDA (3.00 mL, 2M, 6.00 mmol). Addition of aldehyde **9b** (463 μL, 3.14 mmol) yielded propargyl alcohol **1f** (528 mg, 53 %) as a green solid after flash column chromatography (1:10 EtOAc:pentane).

^{1}H NMR (600 MHz, $CDCl_3$) δ (ppm): 7.55 (d, J = 8.4, 2H, H10), 7.51 (d, J = 8.3, 2H, H9), 6.89 (s, 2H, H6), 6.13 (d, J = 3.3, 1H, H1), 2.55 (s, 6H, Me5), 2.27 (s, 3H, Me7), 2.08 (bs, 1H, OH).

^{13}C NMR (150 MHz, CDCl3) δ (ppm): 138.2 (C7), 136.6 (C5), 133.2 (C4), 131.9 (C9), 130.12 (C6), 130.11 (q, J = 32.6, C11), 126.6 (C8), 125.2 (q, J = 3.7, C10), 123.9 (q, J = 272.5, C12), 91.3 (C2), 84.3 (C3), 60.7 (C1), 20.9 (Me5), 20.3 (Me7).

HRMS (ASAP) calcd for $C_{19}H_{17}OF_3$ $[M^*]^+$ 318.1231, obsd 318.1229.

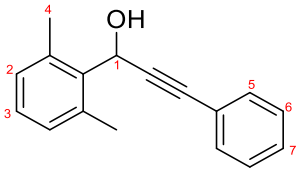

1g

1-(2,6-Dimethylphenyl)-3-phenylprop-2-yn-1-ol (**1g**): Following general procedure A, acetylene **10a** (511 μL, 4.65 mmol) in THF (3 mL) was reacted with LDA (3.17 mL, 2M, 6.34 mmol). Addition of aldehyde **9c** (565 mg, 4.23 mmol) yielded propargyl alcohol **1g** (666 mg, 67 %) as a green solid after flash column chromatography (1:9 EtOAc:pentane).

^{1}H NMR (400 MHz, $CDCl_3$) δ (ppm): 7.38-7.45 (m, 2H, H5), 7.27-7.33 (m, 3H, H3 and H7), 7.12 (dd, J = 8.4, 6.5, 1H, H2), 7.05 (m, 2H, H6), 6.16 (d, J = 3.6, 1H, H1), 2.60 (s, 6H, H4), 2.10 (d, J = 3.9, 1H, OH).

^{1}H NMR was in accordance with literature data.[83]

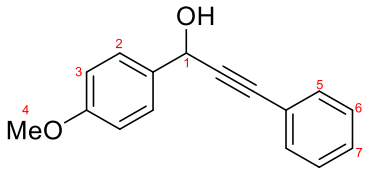

1h

1-(4-Methoxyphenyl)-3-phenylprop-2-yn-1-ol (**1h**): Following general procedure A, acetylene **10a** (507 μL, 4.62 mmol) in THF (10 mL) was reacted with LDA (3.2 mL, 2M, 6.4 mmol). Addition of aldehyde **9d** (571 μL, 4.69 mmol) yielded propargyl alcohol **1h** (702 mg, 64 %) as a yellow solid after flash column chromatography (1:7 EtOAc:pentane).

^{1}H NMR (600 MHz, $CDCl_3$) δ (ppm): 7.54 (d, J = 8.5, 2H, H2), 7.47 (m, 2H, H5), 7.28-7.35 (m, 3H, H6 and H7), 6.93 (d, J = 8.8, 2H, H3), 5.65 (d, J = 6.1, 1H, H1), 3.82 (s, 3H, H4), 2.20 (d, J = 6.1, 1H, OH).

^{1}H NMR was in accordance with literature data.[90]

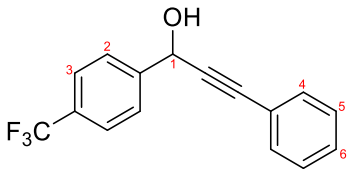

1i

3-Phenyl-1-(4-(trifluoromethyl)phenyl)prop-2-yn-1-ol (**1i**): Following general procedure A, acetylene **10a** (437 μL, 3.98 mmol) in THF (5 mL) was reacted with LDA (2.8 mL, 2M, 5.6 mmol). Addition of aldehyde **9e** (494 μL, 3.62 mmol) yielded propargyl alcohol **1i** (652 mg, 65 %) as an orange oil after flash chromatography (1:9 EtOAc:pentane).

^{1}H NMR (400 MHz, $CDCl_3$) δ (ppm): 7.72 (d, J = 8.0, 2H, H3), 7.64 (d, J = 8.3, 2H, H2), 7.48 (m, 2H, H4), 7.30-7.40 (m, 3H, H5 and H6), 5.75 (s, 1H, H1), 3.37 (s, 1H, OH).

^{1}H NMR was in accordance with literature data.[90]

6.2 Gold-catalysed reactions

6.2.1 Synthesis of 1,1,3-trisubstituted prop-2-yns, 2a-h

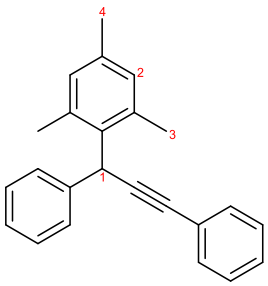

2a

(3-Mesitylprop-1-yne-1,3-diyl)dibenzene (**2a**): Propargyl alcohol **1a** (42.2 mg, 0.203 mmol), mesitylene (169 μL, 1.216 mmol) and $AuBr_3$ (5.8 mg, 0.013 mmol) were stirred in ACN (3 mL) at 85 °C for 1.5 hrs. Water (10 mL) was added, and the solution extracted into DEE (3x10 mL), dried over Na_2SO_4 and the solvent removed *in vacuo*. Purification by flash column chromatography (1:100 EtOAc:pentane) gave a 1:3 mixture of alkyne **2a** and indene **4a** (51.3 mg total).

^{1}H NMR values are extracted from a 1:3 mixture with indene **4a**. See Appendix D.1 for their combined ^{1}H NMR spectrum.

^{1}H NMR (400 MHz, $CDCl_3$) δ (ppm): 7.46 (m, 2H, Ph), 7.38 (d, J = 7.7, 2H, Ph), 7.25-7.31 (m, 4H, Ph), 7.20 (m, 2H, Ph), 6.88 (s, 2H, H2), 5.72 (s, 1H, H1), 2.29 (bs, 6H, H3), 2.28 (bs, 3H, H4).

^{1}H NMR was in accordance with previously reported data.[43]

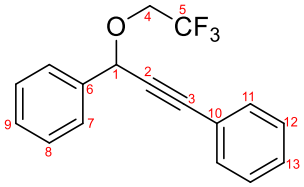

2b

(3-(2,2,2-Trifluoroethoxy)prop-1-yne-1,3-diyl)dibenzene (**2b**): Propargyl alcohol **1a** (23.9 mg, 0.115 mmol) was stirred with 1,3,5-triisopropylbenzene (166.2 μL, 0.687 mmol) and $AuBr_3$ (2.5 mg, 0.006 mmol) in F_3-EtOH (1 mL). The solution was stirred at r.t. for 15 mins before addition of water (5 mL), extraction into DEE (3x10 mL) and drying over Na_2SO_4. Removal of solvent *in vacuo* and purification by flash column chromatography (1:25 EtOAc:pentane) yielded alkyne **2b** (7.7 mg, 23 %).

^{1}H NMR (600 MHz, $CDCl_3$) δ (ppm): 7.60 (m, 2H, H7), 7.50 (m, 2H, H11), 7.42 (m, 2H, H8), 7.38 (m, 1H, H9), 7.36 (m, 1H, H13), 7.34 (m, 2H, H12), 5.65 (s, 1H, H1), 4.06 (dq, J = 12.0, 8.6, 1H, H4), 3.98 (dq, J = 12.0, 8.8, 1H, H4).

^{13}C NMR (150 MHz, CDCl3) δ (ppm): 137.0 (C6), 131.9 (C11), 128.98-128.99 (C9 and C13), 128.7 (C8), 128.4 (C12), 127.6 (C7), 124.05 (q, *J* = 279.0, C5), 121.9 (C10), 89.2 (C3), 84.7 (C2), 72.8 (C1), 64.6 (q, *J* = 34.6, C4).

HRMS (ASAP) calcd for $C_{17}H_{13}OF_3$ $[M^*]^+$ 290.0918, obsd 290.0920.

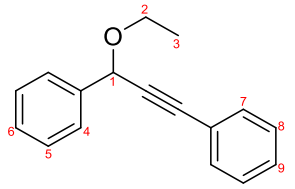

2c

(3-Ethoxyprop-1-yne-1,3-diyl)dibenzene (**2c**): Propargyl alcohol **1a** (39.5 mg, 0.190 mmol) was stirred with anisole (120 μL, 1.104 mmol) in EtOH (4 mL) and $AuBr_3$ (4.0 mg, 0.009 mmol) was added. The solution was heated to 60 °C and stirred for 1.5 hrs. Water (5 mL) was added and the solution extracted into DEE (3x10 mL) and dried over Na_2SO_4. Removal of solvent *in vacuo* and purification by flash column chromatography (1:20 EtOAc:pentane) yielded alkyne **2c** (25.5 mg, 57 %) as a faint yellow oil.

^{1}H NMR (400 MHz, $CDCl_3$) δ (ppm): 7.58 (d, *J* = 7.6, 2H, H4), 7.47 (m, 2H, H7), 7.39 (t, *J* = 7.6, 2H, H5), 7.27-7.36 (m, 4H, H6, H8 and H9), 5.39 (s, 1H, H1), 3.80 (dq, *J* = 8.8, 7.1, 1H, H2), 3.63 (dq, *J* = 8.9, 7.1, 1H, H2), 1.29 (t, *J* = 7.0, 3H, H3).

^{1}H NMR was in accordance with previously reported data.[44]

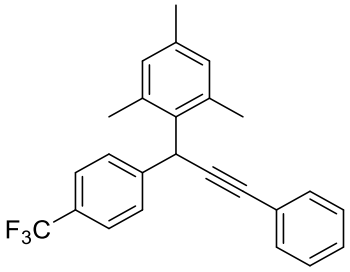

2d

1,3,5-Trimethyl-2-(3-phenyl-1-(4-(trifluoromethyl)phenyl)prop-2-yn-1-yl)benzene (**2d**): Propargyl alcohol **1i** (19.0 mg, 0.069 mmol), mesitylene (57 μL, 0.4122 mmol) and $AuBr_3$ (1.5 mg, 0.003 mmol) were stirred in F_3-EtOH at r.t. for 15 mins. H_2O (5 mL) was added and the solution extracted into DEE (3x10 mL), dried over Na_2SO_4 and solvent removed *in vacuo*. Through flash column chromatography (1:100 EtOAc:pentane) alkyne **2d** was isolated as a minor product (1.2 mg, 5 %).

^{1}H NMR (600 MHz, $CDCl_3$) δ (ppm): 7.54 (m, 2H), 7.49 (m, 2H), 7.47 (m, 2H), 7.31 (m, 3H), 6.90 (s, 2H), 5.73 (s, 1H), 2.25-2.32 (m, 6H).

Not enough compound was collected for ^{13}C NMR or HRMS.

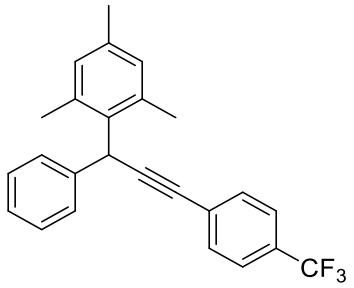

2e

1,3,5-Trimethyl-2-(1-phenyl-3-(4-(trifluoromethyl)phenyl)prop-2-yn-1-yl)benzene (**2e**): Propargyl alcohol **1d** (20 mg, 0.072 mmol), mesitylene (15 μL, 0.109 mmol) and $AuBr_3$ (1.6 mg, 0.004 mmol) were stirred in $MeNO_2$ at r.t. for 15 mins. H_2O (5 mL) was added and the solution extracted into DEE (3x10 mL), dried over Na_2SO_4 and solvent removed *in vacuo*. Through flash column chromatography (petroleum ether) a mixture of alkyne **2e** and allene **3c** were collected (total 11.7 mg). See Appendix D.10 for their combined ^{1}H NMR spectrum.

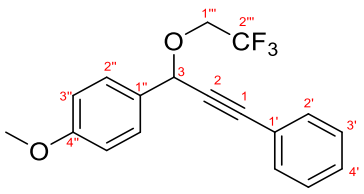

2f

1-Methoxy-4-(3-phenyl-1-(2,2,2-trifluoroethoxy)prop-2-yn-1-yl)benzene (**2f**): Propargyl alcohol **1h** (16.5 mg, 0.069 mmol) was stirred with mesitylene (57.3 μL, 0.412 mmol) in F_3-EtOH. $AuBr_3$ (1.5 mg, 0.003 mmol) was added and the mixture stirred at r.t. for 15 mins before H_2O (5 mL) was added. The solution was extracted with DEE (3x10 mL) and dried over Na_2SO_4. Removal of the solvent *in vacuo* and purification by flash column chromatography (1:100 EtOAc:pentane) gave alkyne **2f** (6.2 mg, 28 %) as a yellow oil.

^{1}H NMR (600 MHz, $CDCl_3$) δ (ppm): 7.47-7.54 (m, 4H, H2' and H2''), 7.31-7.39 (m, 3H, H3' and H4'), 6.94 (d, J = 8.7, 2H, H3''), 5.61 (s, 1H, H3), 4.03 (dq, J = 12.0, 8.6, 1H, H1'''), 3.93 (dq, J =11.8, 8.9, 1H, H1'''), 3.83 (s, 3H, Me4'').

^{13}C NMR (150 MHz, $CDCl_3$) δ (ppm): 160.2 (C4''), 131.9 (C2'), 129.15 (C2''), 129.12 (C1''), 128.9 (C4'), 128.4 (C3'), 124.1 (q, J = 279.5, C2'''), 122.0 (C1'), 114.0 (C3''), 89.0 (C1), 84.9 (C2), 72.4 (C3), 64.4 (q, J = 34.4, C1'''), 55.4 (Me4'').

HRMS (ASAP) calcd for $C_{18}H_{15}O_2F_3$ $[M^*]^+$ 320.1024, obsd 320.1019.

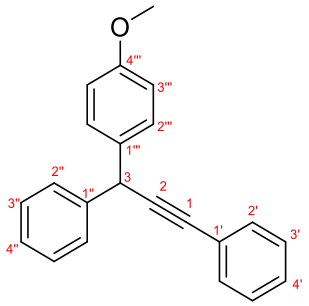

2g

(3-(4-Methoxyphenyl)prop-1-yne-1,3-diyl)dibenzene (**2g**): Propargyl alcohol **1a** (48.2 mg, 0.231 mmol) was stirred with anisole (147 μL, 1.353 mmol) in F_3-EtOH. $AuBr_3$ (4.8 mg, 0.011 mmol) was added and the mixture heated to 85 °C and stirred for 1.5 hrs before H_2O (5 mL) was added. The solution was extracted with DEE (3x10 mL) and dried over Na_2SO_4. Removal of the solvent *in vacuo* and purification by flash column chromatography (1:24 EtOAc:pentane) gave alkyne **2g** (53.1 mg, 77%) as a yellow oil.

^{1}H NMR (600 MHz, $CDCl_3$) δ (ppm): 7.44-7.48 (m, 2H, H2'), 7.40-7.44 (m, 2H, H2''), 7.25-7.36 (m, 7H, H3', H4', H3'' and H2'''), 7.18-7.24 (m, 2H, H4''), 6.82-6.87 (m, 2H, H3'''), 5.16 (s, 1H, H3), 3.75 (s, 3H, Me4''').

^{1}H NMR was in accordance with previously reported data.[106]

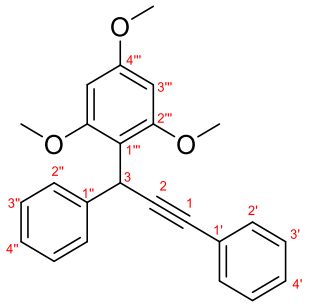

2h

(3-(2,4,6-Trimethoxyphenyl)prop-1-yne-1,3-diyl)dibenzene (**2h**): Propargyl alcohol **1a** (9.5 mg, 0.046 mmol) was stirred with 1,3,5-trimethoxybenzene (41.8 mg, 0.275 mmol) in F_3-EtOH. $AuBr_3$ (1.1 mg, 0.002 mmol) was added and the mixture stirred at r.t. for 15 mins before H_2O (5 mL) was added. The solution was extracted with DEE (3x10 mL) and dried over Na_2SO_4. Removal of the solvent *in vacuo* and purification by flash column chromatography (1:30 EtOAc:pentane) gave alkyne **2h** (8.5 mg, 52 %) as a yellow oil.

^{1}H NMR (600 MHz, $CDCl_3$) δ (ppm): 7.50 (d, J = 7.8, 2H, H2''), 7.43-7.48 (m, 2H, H2'), 7.22-7.48 (m, 5H, H3', H4' and H3''), 7.15 (t, J = 7.3, 1H, H4''), 6.15 (s, 2H, H3'''), 5.86 (s, 1H, H3), 3.80 (s, 6H, Me2'''), 3.78 (s, 3H, Me4''').

^{1}H NMR was in accordance with literature data.[107]

6.2.2 Synthesis of allenes, 3a-g

General procedure B

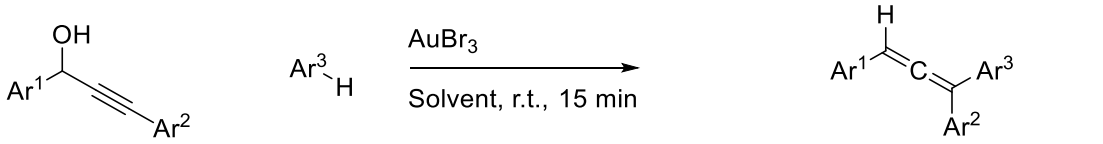

1	Ar^1	Ar^2
a	Ph	Ph
e	Mes	Ph
f	Mes	4-CF_3Ph
g	2,6-diMePh	Ph
i	4-CF_3Ph	Ph

3	Ar^1	Ar^2	Ar^3
a	Ph	Ph	Mes
b	4-CF_3Ph	Ph	Mes
c	Ph	4-CF_3Ph	Mes
d	Mes	4-CF_3Ph	Mes
e	Mes	Ph	Mes
f	2,6-diMePh	Ph	Mes
g	Ph	Ph	PentaMePh

Propargyl alcohol **1** (1 equiv.) and an aromatic nucleophile (1 - 6 equiv.) were dissolved in either F_3-EtOH or $MeNO_2$ (1 mL). A solution of $AuBr_3$ (0.05 equiv.) in the same solvent (1 mL) was added, and the solution stirred at r.t. for 15 mins. H_2O (5 mL), a few drops of NEt_3 and DEE (5 mL) were added and the layers separated. The aqueous layer was extracted with DEE (3x10 mL), the combined organic layers dried over Na_2SO_4, followed by removal of solvent *in vacuo*. Purification by flash column chromatography (1:200 EtOAc:pentane) yielded allenes **3a-g**.

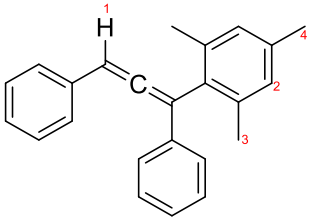

3a

(1-Mesitylpropa-1,2-diene-1,3-diyl)dibenzene (**3a**): Following general procedure B, propargyl alcohol **1a** (45.7 mg, 0.219 mmol) was reacted with mesitylene (140 μL, 1.006 mmol) in F_3-EtOH, with catalytic $AuBr_3$ (4.3 mg, 0.010 mmol). Workup and purification by crystallization from petroleum ether yielded allene **3a** (26.5 mg, 40 %) as a white solid.

^{1}H NMR (600 MHz, $CDCl_3$) δ (ppm): 7.38 (m, 2H), 7.16-7.34 (m, 8H), 6.94 (s, 2H, H2), 6.59 (s, 1H, H1), 2.31 (s, 3H, H4), 2.25 (s, 6H, H3).

^{1}H NMR was in accordance with literature data.[2]

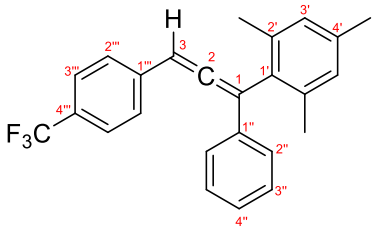

3b

1,3,5-Trimethyl-2-(1-phenyl-3-(4-(trifluoromethyl)phenyl)propa-1,2-dien-1-yl)benzene (**3b**): Following general procedure B, propargyl alcohol **1i** (19.2 mg, 0.069 mmol) was reacted with mesitylene (57.3 μL, 0.412 mmol) in the presence of $AuBr_3$ (1.5 mg, 0.003 mmol) in F_3-EtOH. Workup and purification gave pure allene **3b** (4.9 mg, 19 %).

^{1}H NMR (600 MHz, $CDCl_3$) δ (ppm): 7.55 (d, J = 8.2, 2H, H3’’’), 7.46 (d, J = 8.1, 2H, H2’’’), 7.29 (m, 2H, H3’’), 7.20-7.25 (m, 3H, H2’’ and H4’’), 6.95 (s, 2H, H3’), 6.61 (s, 1H, H3), 2.32 (s, 3H, Me4’), 2.25 (s, 6H, Me2’).

^{13}C NMR (150 MHz, $CDCl_3$) δ (ppm): 206.8 (C2), 138.2 (C1’’’), 137.4 (C4’), 136.8 (C2’), 134.9 (C1’’), 131.1 (C1’), 126.0 (q, J = 32.2, C4’’’), 128.8 (C3’’), 128.6 (C3’), 127.5 (C4’’), 127.2 (C2’’’), 126.3 (C2’’), 125.7 (q, J = 3.7, C3’’’), 124.2 (q, J = 271.8, $CF_3$4’’’), 110.2 (C1), 96.1 (C3), 21.1 (Me4’), 20.5 (Me2’).

HRMS (ESI) calcd for $C_{25}H_{22}F_3$ $[M+H]^+$ 379.1674, obsd 379.1667.

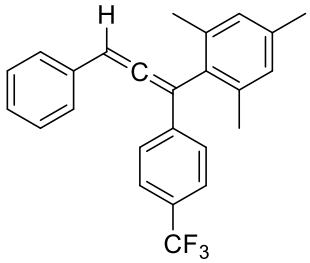

3c

1,3,5-Trimethyl-2-(3-phenyl-1-(4-(trifluoromethyl)phenyl)propa-1,2-dien-1-yl)benzene (**3c**): Following general procedure B, propargyl alcohol **1d** (20.1 mg, 0.072 mmol) was reacted with mesitylene (15 μL, 0.109 mmol) in the presence of $AuBr_3$ (1.7 mg, 0.004 mmol) in $MeNO_2$. Workup and flash column chromatography gave a mixture of allene **3c** and alkyne **2e** as a 1:4 mixture (8.7 mg total). See Appendix E.8 for their combined ^{1}H NMR spectrum.

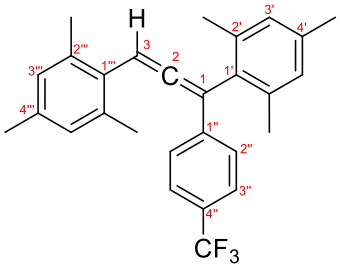

3d

2,2'-(1-(4-(Trifluoromethyl)phenyl)propa-1,2-diene-1,3-diyl)bis(1,3,5-trimethylbenzene) (**3d**): Following general procedure B, propargyl alcohol **1f** (15.0 mg, 0.047 mmol) was reacted with mesitylene (10 μL, 0.071 mmol) in the presence of catalytic $AuBr_3$ (1.1 mg, 0.002 mmol) in $MeNO_2$. Workup and purification gave pure allene **3d** (8.0 mg, 40 %) as an orange oil.

^{1}H NMR (600 MHz, $CDCl_3$) δ (ppm): 7.51 (d, J = 8.2, 2H, H3''), 7.32 (d, J = 8.2, 2H, H2''), 6.94 (bs, 2H, H3'), 6.86 (s, 2H, H3'''), 6.76 (s, 1H, H3), 2.32 (s, 3H, Me4'), 2.31 (s, 6H, Me2'''), 2.27 (s, 3H, Me4'''), 2.20 (bs, 3H, Me2'), 2.04 (bs, 3H, Me2').

^{13}C NMR (150 MHz, $CDCl_3$) δ (ppm): 206.5 (C2), 140.5 (C1''), 137.4 (C4'), 137.3 (broad, C2'), 136.9 (broad, C2'), 136.7 (C4'''), 136.5 (C2'''), 131.1 (C1'), 129.1 (C3'''), 128.7 (C3'), 128.6 (J = 32.3, C4''), 127.7 (C1'''), 126.4 (C2''), 125.4 (J = 3.7, C3''), 124.3 (J = 271.8, $CF_3$4''), 105.6 (C1), 92.5 (C3), 21.2 (Me2'''), 21.1 (Me4'), 20.9 (Me4'''), 20.3 (Me2').

HRMS (ASAP) calcd for $C_{28}H_{28}F_3$ $[M+H]^+$ 421.2143, obsd 421.2137.

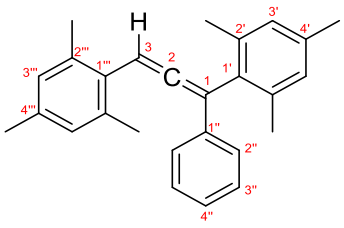

3e

2,2'-(1-Phenylpropa-1,2-diene-1,3-diyl)bis(1,3,5-trimethylbenzene) (**3e**): Following general procedure B, propargyl alcohol **1e** (20.2 mg, 0.080 mmol) was reacted with mesitylene (17 μL, 0.120 mmol) in the presence of catalytic $AuBr_3$ (1.7 mg, 0.004 mmol) in $MeNO_2$. Workup and purification gave allene **3e** (10.5 mg, 37 %).

^{1}H NMR (600 MHz, $CDCl_3$) δ (ppm): 7.27 (dd, J = 7.5, 7.5. 2H, H3''), 7.22 (d, J = 7.2, 2H, H2''), 7.18 (dd, J = 7.1, 7.1, 1H, H4''), 6.92 (bs, 2H, H3'), 6.85 (s, 2H, H3'''), 6.70 (s, 1H, H3), 2.32 (s, 6H, Me2'''), 2.31 (s, 3H, Me4'), 2.26 (s, 3H, Me4'''), 2.21 (bs, 3H, Me2'), 2.07 (bs, 3H, Me2').

^{13}C NMR (150 MHz, $CDCl_3$) δ (ppm): 205.8 (C2), 137.2 (broad, C2'), 137.0 (broad, C2'), 136.9 (C4'), 136.5 (C2''' and C4'''), 136.3 (C1''), 131.9 (C1'), 129.0 (C3'''), 128.49 (C3'),

128.45 (C3''), 128.3 (C1'''), 126.6 (C4''), 126.3 (C2''), 106.2 (C1), 92.1 (C3), 21.2 (Me2'''), 21.1 (Me4'), 20.9 (Me4'''), 20.3 (Me2').

HRMS (ASAP) calcd for $C_{27}H_{29}$ $[M+H]^+$ 353.2269, obsd 353.2263.

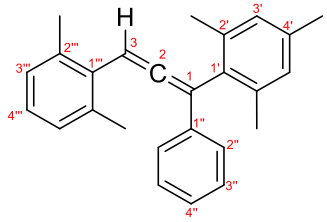

3f

2-(3-(2,6-Dimethylphenyl)-1-phenylpropa-1,2-dien-1-yl)-1,3,5-trimethylbenzene (**3f**): Following general procedure B, propargyl alcohol **1g** (20.1 mg, 0.085 mmol) was reacted with mesitylene (17.7 μL, 0.127 mmol) in the presence of catalytic $AuBr_3$ (1.9 mg, 0.004 mmol) in $MeNO_2$. Workup and purification gave pure allene **3f** (9.9 mg, 34 %).

^{1}H NMR (600 MHz, $CDCl_3$) δ (ppm): 7.27 (dd, J = 7.6, 7.6, 2H, H3''), 7.23 (d, J = 8.3, 2H, H2''), 7.19 (t, J = 7.1, 1H, H4''), 6.99-7.06 (m, 3H, H3''' and H4'''), 6.92 (bs, 2H, H3'), 6.71 (s, 1H, H3), 2.35 (s, 6H, Me2'''), 2.31 (s, 3H, Me4'), 2.22 (bs, 3H, Me2'), 2.07 (bs, 3H, Me2').

^{13}C NMR (150 MHz, $CDCl_3$) δ (ppm): 205.8 (C2), 137.2 (broad, C2'), 137.1 (broad, C2'), 137.0 (C4'), 136.6 (C2'''), 136.3 (C1''), 131.7 (C1'), 131.4 (C1'''), 128.51 (C3'), 128.48 (C3''), 128.1 (C3'''), 126.74 (C4'''), 126.70 (C4''), 126.3 (C2''), 106.4 (C1), 92.2 (C3), 21.3 (Me2'''), 21.1 (Me4'), 20.3 (Me2').

HRMS (ASAP) calcd for $C_{26}H_{27}$ $[M+H]^+$ 339.2113, obsd 339.2108.

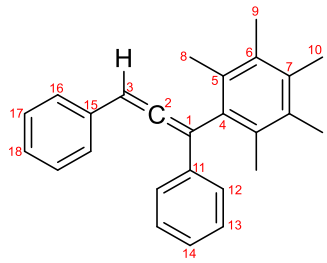

3g

(1-(2,3,4,5,6-Pentamethylphenyl)propa-1,2-diene-1,3-diyl)dibenzene (**3g**): Following general procedure B, propargyl alcohol **1a** (14.5 mg, 0.070 mmol) was reacted with pentamethylbenzene (15.6 mg, 0.105 mmol) using catalytic $AuBr_3$ (1.7 mg, 0.004 mmol) in F_3-EtOH. Extraction into DEE (3 x 10 mL) gave pure allene **3g** (23.3 mg, 99 %) without the need for further purification.

^{1}H NMR (400 MHz, $CDCl_3$) δ (ppm): 7.36 (d, *J* = 7.6, 2H, H16), 7.23-7.31 (m, 6H, H12, H13 and H17), 7.19 (m, 2H, H14 and H18), 6.56 (s, 1H, H3), 2.31 (s, 3H), 2.27 (s, 3H), 2.25 (s, 3H), 2.22 (s, 6H).

^{13}C NMR (150 MHz, $CDCl_3$) δ (ppm): 206.1 (C2), 136.1 (C15), 134.51, 134.45, 133.2, 132.75, 132.74, 132.5, 132.3, 132.2, 128.63, 128.60, 127.2 (C16), 127.1 and 127.0 (C14 and C18), 126.4, 111.2 (C1), 96.9 (C3), 18.8, 17.8, 16.8, 16.7, 16.6.

6.2.3 Synthesis of Indenes, 4a-d and 4f-g

General procedure C

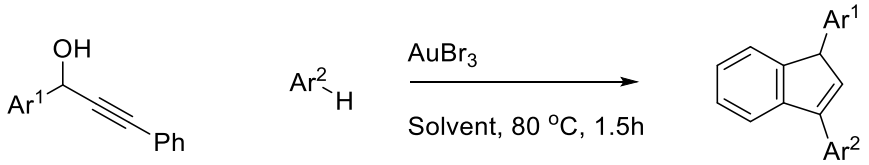

1	Ar^1
a	Ph
e	Mes
g	2,6-diMePh
i	4-CF_3Ph

4	Ar^1	Ar^2
a	Ph	Mes
b	4-CF_3Ph	Mes
c	Mes	Mes
d	2,6-diMePh	Mes
f	Ph	2,4,6-triisoPrPh
g	Ph	PentaMePh

Propargyl alcohol **1** (1 equiv.) and aromatic nucleophile (1 - 6 equiv.) were dissolved in either F_3-EtOH or $MeNO_2$ (1 mL). A solution of $AuBr_3$ (0.05 equiv.) in the same solvent (1 mL) was added, and the solution stirred at 80 °C for 1.5 hrs. H_2O (5 mL), a few drops of NEt_3 and DEE (5 mL) were added and the layers separated. The aqueous layer was extracted with DEE (3x5 mL), the combined organic layers dried over Na_2SO_4, followed by removal of solvent *in vacuo*. Purification by flash column chromatography (1:200 EtOAc:pentane) yielded indenes **4**.

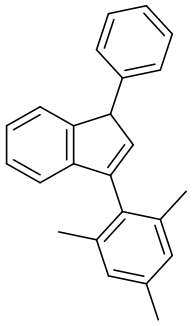

4a

3-Mesityl-1-phenyl-1H-indene (**4a**): Following general procedure C, propargyl alcohol **1a** (52.9 mg, 0.254 mmol) was reacted with mesitylene (103.8 μL, 1.524 mmol) in the presence of catalytic $AuBr_3$ (5.6 mg, 0.013 mmol) in F_3-EtOH. Workup and purification gave indene **4a** (72.7 mg, 92 %) as a colourless solid.

^{1}H NMR (600 MHz, $CDCl_3$) δ (ppm): 7.28-7.32 (m, 3H), 7.24 (m, 1H), 7.18-7.22 (m, 3H), 7.17 (m, 1H), 6.96-7.00 (m, 2H), 6.93 (d, *J* = 7.4, 1H), 6.37 (d, *J* = 2.0, 1H), 4.78 (d, *J* = 1.9, 1H), 2.35 (s, 3H), 2.21 (s, 3H), 2.13 (s, 3H).

^{1}H NMR was in accordance with previously reported data.[2]

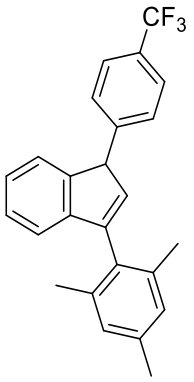

4b

3-Mesityl-1-(4-(trifluoromethyl)phenyl)-1H-indene (**4b**): Following general procedure C, propargyl alcohol **1i** (19.3 mg, 0.069 mmol) was reacted with mesitylene (57 μL, 0.412 mol) in the presence of $AuBr_3$ (1.8 mg, 0.004 mmol) in F_3-EtOH. Workup and flash column chromatography resulted in a mixture of indene **4b** and alkyne **2d**. See Appendix F.2 for their combined ^{1}H NMR spectrum.

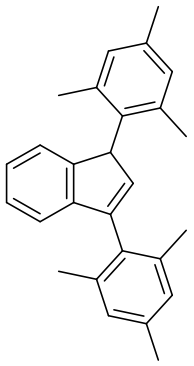

4c

1,3-Dimesityl-1H-indene (**4c**): Following general procedure C, propargyl alcohol **1e** (20.3 mg, 0.080 mmol) was reacted with mesitylene (17 μL, 0.120 mmol) in the presence of catalytic $AuBr_3$ (1.7 mg, 0.004 mmol) in $MeNO_2$. Workup and purification gave the pure indene **4c** (14.2 mg, 50 %) as a colourless solid.

^{1}H NMR (400 MHz, $CDCl_3$) δ (ppm): 7.12-7.24 (m, 3H), 6.94-7.03 (m, 4H), 6.73 (bs, 1H), 6.37 (d, *J* = 2.0, 1H), 5.13 (bs, 1H), 2.62 (s, 3H), 2.35 (s, 3H), 2.28 (s, 3H), 2.17 (s, 3H), 2.11 (s, 3H), 1.61 (s, 3H).

^{1}H NMR was in accordance with previously reported data.[64]

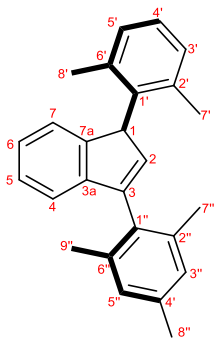

4d

1-(2,6-Dimethylphenyl)-3-mesityl-1H-indene (**4d**): Following general procedure C, propargyl alcohol **1g** (19.8 mg, 0.085 mmol) was reacted with mesitylene (17.7 μL, 0.127 mmo) in the presence of catalytic $AuBr_3$ (2.0 mg, 0.005 mmol) in $MeNO_2$. Workup and purification gave pure indene **4d** (12.8 mg, 45 %) as a colourless solid.

^{1}H NMR (600 MHz, $CDCl_3$) δ (ppm): 7.23 (t, J = 7.3, H5), 7.14-7.215 (m, 3H, H6, H7 and H3'), 7.09 (t, J = 7.5, 1H, H4'), 7.01 (d, J = 7.5, 1H, H4), 6.97 (bs, 2H, H3'' and H5''), 6.89 (d, J = 7.4, 1H, H5'), 6.39 (d, J = 2, 1H, H2), 5.17 (s, 1H, H1), 2.66 (s, 3H, H7'), 2.35 (s, 3H, H8''), 2.18 (s, 3H, H9''), 2.11 (s, 3H, H7''), 1.65 (s, 3H, H8').

^{13}C NMR (150 MHz, $CDCl_3$) δ (ppm): 147.1 (C7a), 144.4 (C3a), 142.9 (C3), 138.2 (C6'), 137.6 (C2'), 137.2 (C6''), 137.0 (C2''), 136.9 (C4''), 135.8 (C2), 135.5 (C1'), 132.0 (C1''), 129.2 (C5'), 128.3 (C3' and C3''), 128.2 (C5''), 126.7 (C4'), 126.3 (C5), 125.2 (C6), 122.9 (C7), 120.6 (C4), 52.3 (C1), 21.9 (C7'), 21.1 (C8''), 20.7 (C9''), 20.4 (C7''), 19.0 (C8').

HRMS (ASAP) calcd for $C_{26}H_{26}$ $[M^*]^+$ 338.2035, obsd 338.2034.

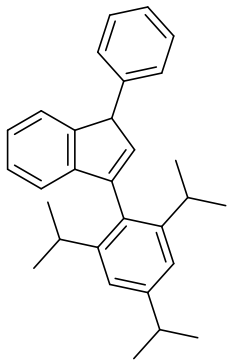

4f

1-Phenyl-3-(2,4,6-triisopropylphenyl)-1H-indene (**4f**): Following general procedure C, propargyl alcohol **1a** (23.9 mg, 0.115 mmol) was reacted with 1,3,5-triisopropylbenzene (166.2 μL, 0.687 mmol) in the presence of catalytic $AuBr_3$ (2.5 mg, 0.006 mmol) in F_3-EtOH. Workup and purification gave indene **4f** (6.8 mg, 15 %) as a colourless solid.

^{1}H NMR (600 MHz, $CDCl_3$) δ (ppm): 7.27-7.33 (m, 3H), 7.18-7.25 (m, 4H), 7.16 (ddd, J = 7.4, 7.4, 1.1, 1H), 7.10 (m, 2H), 6.96 (d, J = 7.3, 1H), 6.40 (d, J = 2.0, 1H), 4.78 (d, J = 1.5,

1H), 3.02 (hept, J = 6.9, 1H), 2.96 (hept, J = 6.9, 1H), 2.85 (hept, J = 6.9, 1H), 1.32 (d, J = 6.9, 6H), 1.15 (d, J = 6.8, 9H), 1.09 (d, J = 6.9, 3H).

^{1}H NMR was in accordance with previously reported data.[2]

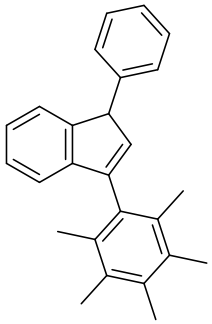

4g

3-(2,3,4,5,6-Pentamethylphenyl)-1-phenyl-1H-indene (**4g**): Following general procedure C, propargyl alcohol **1a** (14.3 mg, 0.069 mmol) was reacted with pentamethylbenzene (64.3 mg, 0.434 mmol) in the presence of catalytic $AuBr_3$ (1.5 mg, 0.003 mmol) in F_3-EtOH. Workup and purification by scraping product off from a TLC-plate and washing the silica with EtOAc gave indene **4g** (0.8 mg, 3 %).

^{1}H NMR (400 MHz, $CDCl_3$) δ (ppm): 7.13-7.35 (m, 8H), 6.92 (m, 1H), 6.34 (d, J = 2.1, 1H), 4.79 (d, J = 1.8, 1H), 2.32 (s, 3H), 2.28 (s, 3H), 2.27 (s, 3H), 2.18 (s, 3H), 2.09 (s, 3H).

^{1}H NMR was in accordance with previously reported data.[2]

6.2.4 Synthesis of α,β-unsaturated ketone, 19

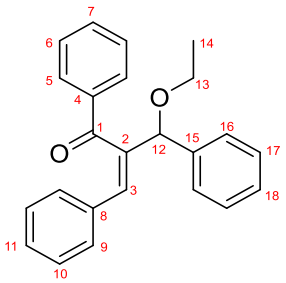

19

(Z)-2-(Ethoxy(phenyl)methyl)-1,3-diphenylprop-2-en-1-one (**19**): Propargyl alcohol **1a** (56.9 mg, 0.273 mmol), mesitylene (225 μL, 1.617 mmol) and $AuBr_3$ (5.9 mg, 0.014 mmol) were stirred in EtOH (2 mL) at 90 °C for 1.5 hrs. H_2O (10 mL) was added, the solution extracted into DEE (3x10 mL), dried over Na_2SO_4 and the solvent removed *in vacuo*. Flash column chromatography (1:20 EtOAc:pentane) gave α,β-unsaturated ketone **19** as a minor product (13.6 mg).

^{1}H NMR (600 MHz, $CDCl_3$) δ (ppm): 7.67 (m, 2H, H5), 7.41 (m, 2H, H16), 7.28-7.34 (m, 3H, H7 and H17), 7.24 (m, 1H, H18), 7.16 (m, 2H, H6), 7.07 (m, 2H, H9), 7.01-7.05 (m, 3H,

H10 and H11), 6.79 (d, *J* = 1.2, 1H, H3), 5.37 (d, *J* = 1.3, 1H, H12), 3.54 (q, *J* = 7.0, 2H, H13), 1.16 (t, *J* = 7.0, 3H, H14).

^{13}C NMR (150 MHz, $CDCl_3$) δ (ppm): 199.8 (C1), 142.3 (C2), 139.6 (C15), 136.6 (C4), 135.3 (C8), 132.7 (C7), 130.4 (C3), 129.3 (C5), 128.9 (C9), 128.4 (C17), 128.0 (C6 and C10), 127.88 (C18), 127.76 (C11), 127.4 (C16), 83.0 (C12), 65.1 (C13), 15.1 (C14).

HRMS (ESI) calcd for $C_{24}H_{22}O_2Na$ $[M+Na]^+$ 365.1517, obsd 365.1522.

6.2.5 Synthesis of Cyclopropane, 20

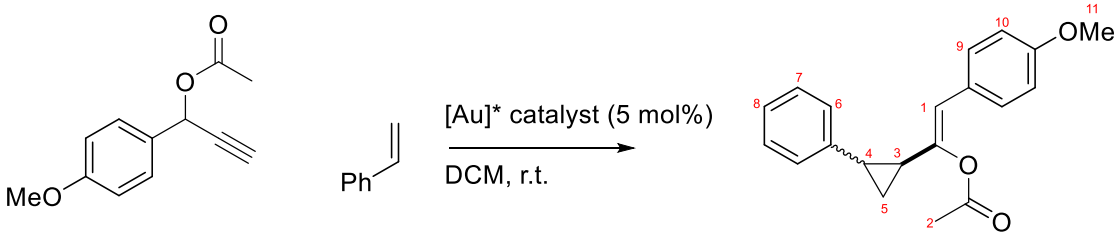

11 **20**

(Z)-2-(4-Methoxyphenyl)-1-(2-phenylcyclopropyl)vinyl acetate (**20**): Propargylacetate **11** (1 equiv.), styrene (4 equiv.), the appropriate Au-catalyst (0.05 equiv.) were stirred in DCM at r.t. until complete consumption of **11** as determined by TLC (EtOAc:pentane 1:8) or NMR. The solvent was removed under reduced pressure and flash column chromatography (EtOAc:pentane 1:15) yielded a mixture of stereoisomers of cyclopropane **20**.

Trans-**20**:

^{1}H NMR (600 MHz, $CDCl_3$) δ (ppm): 7.25-7.31 (m, 4H, H7 and H9), 7.18 (t, *J* = 7.4, 1H, H8), 7.11 (d, *J* = 7.2, 2H, H6), 6.83 (d, *J* = 8.8, 2H, H10), 6.03 (s, 1H, H1), 3.79 (s, 3H, H11), 2.21 (ddd, *J* = 9.1, 5.5, 5.2, 1H, H4), 2.19 (s, 3H, H2), 1.96 (ddd, *J* = 8.9, 5.3, 5.0, 1H, H3), 1.33 (ddd, *J* = 9.0, 5.6, 5.6, 1H, H5 syn to H4), 1.24 (ddd, *J* = 8.7, 5.6, 5.6, 1H, H5 syn to H3).

^{1}H NMR were in accordance with previously reported data.[21]

6.3 Synthesis of cyclam-related compounds

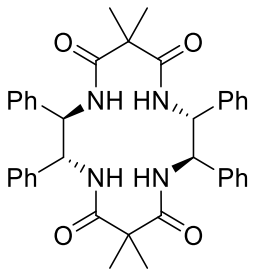

7b

(2R,3R,9R,10R)-6,6,13,13-Tetramethyl-2,3,9,10-tetraphenyl-1,4,8,11-tetraazacyclotetradecane-5,7,12,14-tetraone (**7b**): Under a N_2-atmosphere, (1R,2R)-1,2-

diphenylethane-1,2-diamine (**8b**) (126.0 mg, 0.594 mmol) was dissolved in THF (40 mL) and mixed with NEt_3 (0.19 mL, 1.36 mmol). Dimethyl malonyl chloride (78 μL, 0.595 mmol) was added and the solution stirred until no more diamine remained, as determined by TLC. H_2O (10 mL) was added, the solution extracted into DCM (3x20 mL), washed with brine (20 mL), and dried over Na_2SO_4. Removal of solvent *in vacuo* and purification by flash column chromatography (1:20 EtOAc:pentane) gave cyclic tetraamide **7b** (91.7 mg, 51 %) as a white solid.

^{1}H NMR (400 MHz, $CDCl_3$) δ (ppm): 7.74 (dd, *J* = 5.3, 2.6, 4H), 7.15-7.25 (m, 12H), 7.06-7.15 (m, 8H), 5.25 (dd, *J* = 5.6, 2.6, 4H), 1.43 (s, 12H).

HRMS (ASAP) calcd for $C_{38}H_{41}N_4O_4$ $[M+H]^+$ 617.3128. obsd 617.3124.

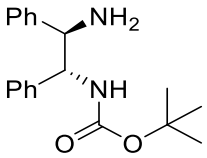

8b-Boc

Tert-butyl ((1R,2R)-2-amino-1,2-diphenylethyl)carbamate (**8b-Boc**): To a stirred solution of (1R,2R)-1,2-diphenylethane-1,2-diamine (**8b**) (365 mg, 1.72 mmol) in dry DCM (50 mL) di-*tert*-butyl decarbonate (340 mg, 1.56 mmol) dissolved in dry DCM (25 mL) was added dropwise over the course of 15 mins. After stirring for 2 days, $NaHCO_3$ (250 mg) was added and the mixture concentrated under reduced pressure. The solution was washed with aqueous NaOH (1M, 2x15 mL), dried over Na_2SO_4 and solvent removed *in vacuo*. Purification by flash column chromatography (EtOAc) gave pure product **8b-Boc** (347 mg, 71 %) as a white solid.

^{1}H NMR (400 MHz, $CDCl_3$) δ (ppm): 7.21-7.36 (m, 10H), 5.87 (m, 2H), 4.85 (s, 1H), 4.32 (s, 1H), 1.31 (s, 9H).

^{1}H NMR was in accordance with previously reported data.[108]

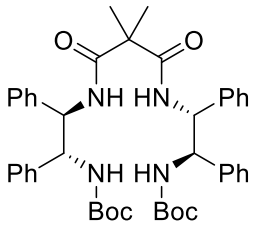

21b-Boc

Di-tert-butyl ((1R,1'R,2R,2'R)-((2,2-dimethylmalonyl)bis(azanediyl))bis(1,2-diphenylethane-2,1-diyl))dicarbamate (**21b-Boc**):): Mono-boc protected diamine **8b-Boc** (106 mg, 0.34 mmol) and NEt_3 (190 μL, 1.36 mmol) were mixed in THF (dry, 5 mL). Dimethyl malonyl chloride (23 μL, 0.17 mmol) was added and the solution stirred until no starting material remained, as determined by TLC. H_2O (5 mL) was added and product isolated by filtering the solution, leaving the product **21b-Boc** (102 mg, 82 %) as a white solid.

^{1}H NMR (600 MHz, d_6-DMSO) δ (ppm): 7.76 (d, J = 9.2, 2H), 7.66 (d, J = 9.5, 2H), 7.26 (d, J = 7.4, 4H), 7.22 (t, J = 7.4, 4H), 7.11-7.20 (m, 12H), 5.39 (dd, J = 8.8, 6.0, 2H), 5.10 (dd, J = 9.4, 6.0, 2H), 1.22 (s, 16H), 0.91 (s, 6H).

^{13}C NMR (150 MHz, d_6-DMSO) δ (ppm): 172.2, 155.2, 140.8, 140.2, 127.7, 127.6, 126.9, 126.6, 126.4, 77.9, 57.8, 56.9, 49.6, 28.1, 23.5.

HRMS (ESI) calcd for $C_{43}H_{52}N_4O_6Na$ $[M+Na]^+$ 743.3785, obsd 743.3782.

HRMS (ESI) calcd for $C_{38}H_{45}N_4O_4$ $[M\text{-}Boc+H]^+$ 621.3441, obsd 621.3446.

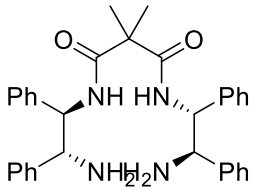

21b

N1,N3-Bis((1R,2R)-2-amino-1,2-diphenylethyl)-2,2-dimethylmalonamide (**21b**): Chiral dicarbamate **21b-Boc** (102 mg, 0.14 mmol) was dissolved in TFA (1 mL) at 0 °C, and the solution stirred for 20 mins. Aqueous NaOH (1M) was added dropwise until ~pH 10 and DCM (10 mL) was added. The layers were separated and the aqueous phase was extracted with DCM (3x10 mL), and the combined organic layers washed with H_2O (10 mL), dried over Na_2SO_4, and concentrated *in vacuo*, yielding pure product **21b** (71 mg, 95 %).

^{1}H NMR (600 MHz, $CDCl_3$) δ (ppm): 7.99 (d, J = 8.0, 2H), 7.16-7.35 (m, 20H), 5.10 (dd, J = 8.1, 3.3, 2H), 4.36 (d, J = 2.8, 2H), 1.29 (s, 6H), 1.22 (bs, 4H).

^{13}C NMR (150 MHz, CDCl3) δ (ppm): 173.1, 142.0, 140.3, 128.6, 128.3, 127.5, 127.2, 126.6, 126.2, 59.8, 58.8, 49.5, 23.9.

HRMS (ESI) calcd for $C_{33}H_{37}N_4O_2$ $[M+H]^+$ 521.2917, obsd 521.2926.

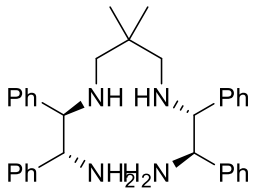

22b

(1R,1'R,2R,2'R)-N^1,N$^{1'}$-(2,2-Dimethylpropane-1,3-diyl)bis(1,2-diphenylethane-1,2-diamine) (**22b**): Chiral amidoamine **21b** (71 mg ,0.14 mmol) and $AlCl_3$ (73 mg, 0.54 mmol) were dissolved in dry THF (5 mL) and cooled to 0 °C. After stirring for 15 mins, $LiAlH_4$ (1M, 2.7 mL, 2.7 mmol) was added and the solution stirred o.n.. H_2O (20 mL) and NaOH were added until ~pH 14. The solution was filtered and extracted with DCM (3x10 mL), dried over Na_2SO_4 and concentrated *in vacuo* yielding product **22b** (19.5 mg, 30 %).

^{1}H NMR (400 MHz, $CDCl_3$) δ (ppm): 7.05-7.24 (m, 20H), 3.93 (d, *J* = 7.1, 2H), 3.59 (d, *J* = 7.1, 2H), 2.21 (d, *J* = 11.4, 2H), 2.14 (d, *J* = 11.4, 2H), 1.79 (bs, 6H), 0.79 (s, 6H).

^{13}C NMR (100 MHz, $CDCl_3$) *δ* (ppm): 143.9, 142.2, 128.13, 128.06, 127.9, 127.3, 126.94, 126.90, 70.8, 62.2, 57.2, 35.3, 24.8.

HRMS (ESI) calcd for $C_{33}H_{41}N_4$ $[M+H]^+$ 493.3331, obsd 493.3337.

6.4 Synthesis of propargyl acetate 11

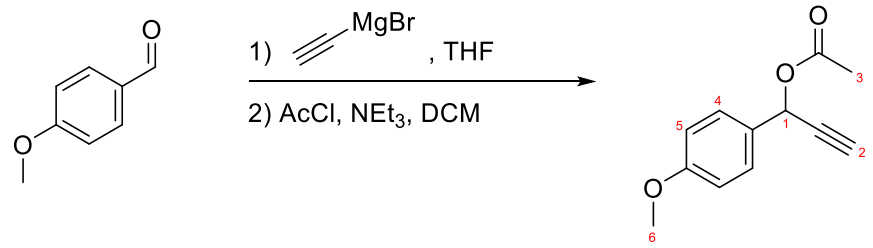

9d **11**

1-(4-Methoxyphenyl)prop-2-yn-1-yl acetate (**11**): Ethynyl magnesiumbromide in THF (9.5 mL, 0.5M, 4.77 mmol) was added dropwise to a solution of anisaldehyde (**9d**) (446.8 μL, 3.67 mmol) in dry THF (3 mL). After stirring for one hour, aqueous NH_4Cl (sat., 10 mL) was added and the layers separated. The aqueous layer was extracted with DCM (3x10 mL), the combined organic layers washed with brine (10 mL), dried over Na_2SO_4 and solvent removed *in vacuo*. Without further purification, the resulting orange oil was diluted in DCM (dry, 5 mL), and to it was added NEt_3 (2 mL, 14.43 mmol) and acetyl chloride (500 μL, 7.03 mmol) and the solution stirred for 1 hr. H_2O (10 mL) was added, and the same workup followed as for step one. Purification by flash column chromatography (1:7 EtOAc:pentane) yielded pure propargyl acetate **11** (466 mg, 62%) as a clear oil.

^{1}H NMR (400 MHz, $CDCl_3$) δ (ppm): 7.47 (d, *J* = 8.7, 2H, H4), 6.91 (d, *J* = 8.8, 2H, H5), 6.41 (d, *J* = 2.2, 1H, H1), 3.82 (s, 3H, H6), 2.64 (d, *J* = 2.3, 1H, H2), 2.09 (s, 3H, H3).

^{1}H NMR was in accordance with literature data.[41] ^{1}H NMR for intermediate propargyl alcohol was also in accordance with literature data.[42]

6.5 Synthesis of chiral 2-bromo-6-alkyl pyridine alcohols, 12a-b

General procedure D

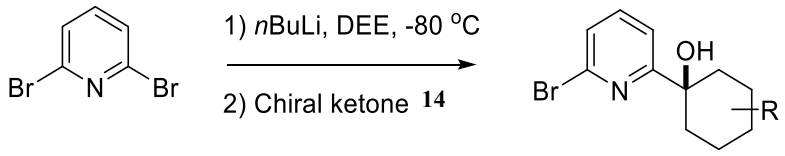

13

12a: Neomenthol
12b: Isoborneol

Under a N_2-atmosphere, 2,6-dibromopyridine (**13**) was dissolved in dry DEE and cooled to -80 °C. *n*BuLi (1.05 equiv., 2.5M in hexane) was added slowly and the solution stirred for 1 hr. The appropriate chiral ketone **14** (1.1 equiv.) was dissolved in DEE and added dropwise. The

solution was stirred at -80 °C for 2 hrs before allowing to warm to r.t. The reaction was quenched with NH_4Cl (sat.), extracted into DEE (3x20 mL), washed with brine (10 mL), and dried over Na_2SO_4. Removal of the solvent *in vacuo* and purification by flash column chromatography (DCM) gave the pure chiral 2-bromo-6-alkylpyridine alcohols **12**.

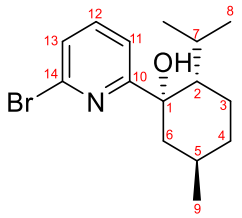

12a

(1S,2S,5R)-1-(6-Bromopyridin-2-yl)-2-isopropyl-5-methylcyclohexan-1-ol (**12a**): Following general procedure D, pyridine **13** (676.7 mg, 2.857 mmol) was treated with *n*BuLi (1.2 mL, 3.001 mmol) and reacted with (-)-menthone (**14a**) (543μL, 3.144 mmol). Workup and purification gave 2-bromo-6-alkylpyridine **12a** (702.3 mg, 79 %) as a white powder.

^{1}H NMR (400 MHz, $CDCl_3$) δ (ppm): 7.55 (t, J = 7.8, 1H, H12), 7.36 (d, J = 7.4, 1H, H11), 7.33 (d, J = 7.8, 1H, H13), 4.20 (bs ,1H, OH), 1.93 (m, 1H, $H5_{ax}$), 1.87 (m, 1H, $H4_{eq}$), 1.60-1.75 (m, 3H, $H3_{ax}$, $H5_{eq}$ and $H6_{eq}$), 1.56 (ddd, J = 13.1, 3.5, 2.4, $H6_{eq}$), 1.33 (dd, J = 12.5, 12.5, 1H, $H6_{ax}$), 1.26 (hept, J = 6.9, 1H, H7), 1.04 (m, 1H, $H4_{ax}$), 0.89 (d, J = 6.5, 3H, H9), 0.84 (d, J = 6.8, 3H, H8), 0.70 (d, J = 6.9, 3H, H8).

^{1}H NMR was in accordance with previously reported data.[92]

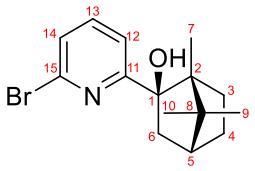

12b

(1R,2R,4R)-2-(6-Bromopyridin-2-yl)-1,7,7-trimethylbicyclo[2.2.1]heptan-2-ol (**12b**): Following general procedure D, pyridine **13** (764.9 mg, 3.229 mmol) was treated with *n*BuLi (1.5 mL, 3.546 mmol) and reacted with (1*R*)-(+)-camphor (**14b**) (491.6 mg, 3.223 mmol). Workup and purification gave 2-bromo-6-alkylpyridine **12b** (247.3 mg, 25 %) as a white powder.

^{1}H NMR (400 MHz, $CDCl_3$) δ (ppm): 7.51 (t, J = 7.7, 1H, H13), 7.40 (d, J = 7.5, 1H, H12), 7.36 (dd, J = 7.8, 0.6, 1H, H14), 4.31 (s, 1H, OH), 2.27 (ddd, J = 14.1, 3.7, 3.7, 1H, $H6_{eq}$), 2.15 (d, J = 14.0, 1H, $H6_{ax}$), 1.90 (t, J = 4.4, 1H, H5), 1.79 (m, 1H, $H4_{eq}$), 1.21-1.33 (m, 5H, $H3_{eq}$, $H4_{ax}$ and H10), 0.90 (s, 3H, H9), 0.85 (s, 3H, H7), 0.75 (m, 1H, $H3_{ax}$).

^{1}H NMR was in accordance with previously reported data.[92]

6.6 Synthesis of chiral 2-aryl-6-alkyl Pyridines, 15 and 15-OMe

6.6.1 Synthesis of 2,6-disubstituted pyridine alcohols, 15a-g

General procedure E

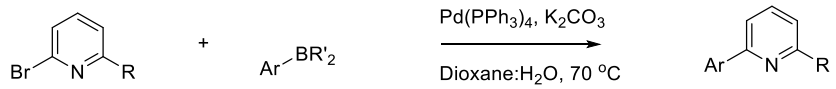

12	R
a	Menthol
b	Isoborneol

16	Ar
a	Ph
b	3,5-diOMePh
c	Thiophene-2-yl
d	*N*-methylpyrrole-2-yl

15	R	Ar
a	Menthol	Ph
b	Menthol	3,5-diOMePh
c	Menthol	Thiophene-2-yl
d	Isoborneol	Ph
e	Isoborneol	3,5-diOMePh
f	Isoborneol	Thiophene-2-yl
g	Isoborneol	*N*-methylpyrrole-2-yl

Under an N_2-atmosphere, chiral 2-bromopyridine **12a-b** (1 equiv.) and the appropriate aryl boronic acid or boron pinacol ester **16a-d** (1-2 equiv.) were dissolved in dioxane (1-2 mL) and K_2CO_3 (3 equiv.) dissolved in water (0.5 mL) was added. The solution was heated to 70 °C, and catalytic $Pd(PPh_3)_4$ (5-10 mol%) in dioxane (0.5 mL) was then added, either by formation *in situ* or by direct addition of preformed complex as commercially available. The solution was stirred over night or until full conversion as determined by TLC. Water (10 mL) was added, the product extracted into DCM, washed with brine (10 mL) and dried over Na_2SO_4. Removal of the solvent *in vacuo* and purification by flash column chromatography yielded the pure 2-aryl-6-alkylpyridines **15a-g**.

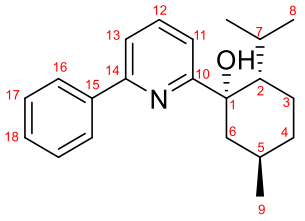

15a

(1S,2S,5R)-2-Isopropyl-5-methyl-1-(6-phenylpyridin-2-yl)cyclohexan-1-ol (**15a**): Following General Procedure E, 2-bromopyridine **12a** (50.2 mg, 0.160 mmol) was reacted with phenyl boronic acid (**16a**) (20.6 mg, 0.160 mmol) in the presence of catalytic $Pd(PPh_3)_4$ (9.6 mg, 0.009 mmol) and K_2CO_3 (64.1 mg, 0.480 mmol) to give 2,6-disubstituted pyridine **15a** (44.7 mg, 92 %) after workup and purification (1:25 EtOAc:pentane) as a white powder.

^{1}H NMR (400 MHz, $CDCl_3$) δ (ppm): 8.03 (m, 2H, H16), 7.78 (t, J = 7.8, 1H, H12), 7.64 (dd, J = 7.7, 0.5, 1H, H13), 7.49 (m, 2H, H17), 7.43 (m, 1H, H18), 7.27 (d, J = 8.1, 1H, H11), 5.62 (bs, 1H, OH), 2.01 (m, 1H, $H5_{ax}$), 1.91 (m, 1H, $H4_{eq}$), 1.58-1.83 (m, 4H, $H2_{ax}$, $H3_{ax}$, $H3_{eq}$ and $H6_{eq}$), 1.38 (dd, J = 12.5, 12.5, 1H, $H6_{ax}$), 1.28 (hept d, J = 7.0, 1.7, 1H, H7), 1.07 (dq, J = 12.5, 3.8, 1H, $H3_{ax}$), 0.91 (d, J = 6.6, 3H, H9), 0.85 (d, J = 6.8, 3H, H8), 0.69 (d, J = 7.0, 3H, H8).

^{1}H NMR was in accordance with previously reported data.[92]

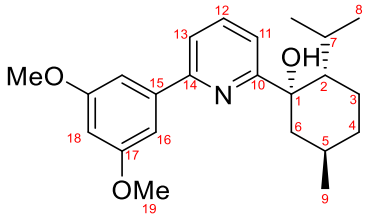

15b

(1S,2S,5R)-1-(6-(3,5-Dimethoxyphenyl)pyridin-2-yl)-2-isopropyl-5-methylcyclohexan-1-ol (**15b**): Following general procedure E, 2-bromopyridine **12a** (100.1 mg, 0.320 mmol) was reacted with (3,5-dimethoxyphenyl)boronic acid (**16b**) (115.4 mg, 0.640 mmol) in the presence of catalytic $Pd(PPh_3)_4$ (19.0 mg, 0.016 mmol) and K_2CO_3 (136.0 mg, 0.984 mmol) to give 2,6-disubstituted pyridine **15b** (103.1 mg, 87 %) after workup and purification (1:25 EtOAc:pentane) as a colourless oil.

^{1}H NMR (600 MHz, CDCl3) δ (ppm): 7.77 (t, J = 7.8, 1H, H12), 7.60 (d, J = 7.7, 1H, H13), 7.28 (d, J = 7.8, 1H, H11), 7.19 (d, J = 2.3, 2H, H16), 6.54 (t, J = 2.3, 1H, H18), 5.58 (bs, 1H, OH), 3.87 (s, 6H, H19), 2.00 (m, 1H, $H5_{ax}$), 1.91 (m, 1H, $H4_{eq}$), 1.74 (qd, J = 12.8, 3.4, 1H, $H3_{ax}$), 1.58-1.70 (m, 3H, $H2_{ax}$, $H3_{eq}$ and $H6_{eq}$), 1.38 (t, J = 12.6, 1H, $H6_{ax}$), 1.27 (hept d, J = 6.9, 1.9, 1H, H7), 1.07 (qd, J = 12.7, 3.7, 1, $H4_{ax}$), 0.91 (d, J = 6.6, 3H, H9), 0.84 (d, J = 6.8, 3H, H8), 0.69 (d, J = 7.0, 1H, H8).

^{13}C NMR (150 MHz, $CDCl_3$) δ (ppm): 165.0 (C10), 161.2 (C17), 154.2 (C14), 140.9 (C15), 137.8 (C12), 118.41 (C13), 118.04 (C11), 105.0 (C16), 101.3 (C18), 55.5 (C19), 50.71 (C6), 50.16 (C2), 35.4 (C4), 28.6 (C5), 27.5 (C7), 23.7 (C8), 22.43 (C9), 22.08 (C3), 18.6 (C8).

HRMS (ESI) calcd for $C_{23}H_{32}NO_3$ $[M+H]^+$ 370.2382, obsd 370.2387.

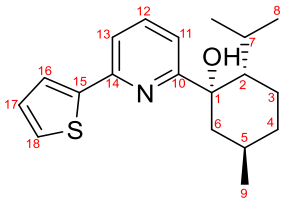

15c

(1S,2S,5R)-2-Isopropyl-5-methyl-1-(6-(thiophen-2-yl)pyridin-2-yl)cyclohexan-1-ol (**15c**): Following general procedure E, 2-bromopyridine **12a** (50.7 mg, 0.160 mmol) was reacted with (thiophene-2-yl)boronic acid (**16c**) (33.6 mg, 0.240 mmol) in the presence of catalytic $Pd(PPh_3)_4$ (18.6 mg, 0.016 mmol) and K_2CO_3 (68.6 mg, 0.480 mmol) to give 2,6-disubstituted pyridine **15c** (44.1 mg, 87 %) after workup and purification (1:30 EtOAc:pentane) as a white powder.

^{1}H NMR (600 MHz, $CDCl_3$) δ (ppm): 7.70 (t, J = 7.8,1H, H12), 7.61 (d, J = 3.5, 1H, H16), 7.53 (d, J = 7.7, 1H, H13), 7.39 (d, J = 5.0, 1H, H18), 7.18 (d, J = 7.8, 1, H11), 7.11 (dd, J =

4.9, 3.8, 1H, H17), 5.32 (bs, 1H, OH), 2.00 (m, 1H, H5), 1.90 (m, 1H, $H4_{eq}$), 1.74 (qd, J = 12.8, 3.4, 1H, $H3_{ax}$), 1.66 (dq, J = 13.0, 3.5, 1H, $H3_{eq}$), 1.58-1.63 (m, 2H, H2 and $H6_{eq}$), 1.36 (t, J = 12.6, 1H, $H6_{ax}$), 1.28 (hept d, J = 6.9, 1.7, 1H, H7), 1.06 (qd, J = 12.6, 3.8, 1H, $H4_{ax}$), 0.91 (d, J = 6.6, 3H, H9), 0.84 (d, J = 6.8, 3H, H8), 0.69 (d, J = 7.0, 3H, H8).

^{13}C NMR (150 MHz, $CDCl_3$) δ (ppm): 165.2 (C10), 149.9 (C14), 144.5 (c15), 137.7 (C12), 128.0 (C17), 127.7 (C18), 124.7 (C16), 117.5 (C11), 116.4 (C13), 77.1 (C1), 50.6 (C6), 50.1 (C2), 35.3 (C4), 28.6 (C5), 27.6 (C7), 23.6 (C8), 22.4 (C9), 22.0 (C3), 18.5 (C8).

HRMS (ASAP) calcd for $C_{23}H_{30}NO_3$ $[M+H]^+$ 368.2226, obsd 368.2223.

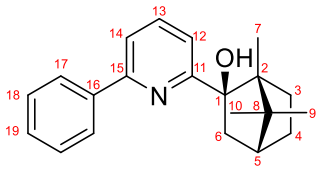

15d

(1R,2R,4R)-1,7,7-Trimethyl-2-(6-phenylpyridin-2-yl)bicyclo[2.2.1]heptan-2-ol (**15d**): Following general procedure E, 2-bromopyridine **12b** (100.0 mg, 0.322 mmol), was reacted with phenylboronic acid (**16a**) (43.2 mg, 0.355 mmol) in the presence of catalytic $Pd(PPh_3)_4$ formed *in situ* from $Pd(OAc)_2$ (3.6 mg, 0.016 mmol), PPh_3 (25.4 mg, 0.097 mmol) and NEt_3 (135 μL, 0.967 mmol) and K_2CO_3 (66.0 mg, 0.478 mmol) to give 2,6-disubstituted pyridine **15d** (95.8 mg, 97 %) after workup and purification (DCM) as a white oil.

^{1}H NMR (600 MHz, $CDCl_3$) δ (ppm): 8.00 (m, 2H, H17), 7.70 (t, J = 7.8, 1H, H13), 7.61 (d, J = 7.8, 1H, H14), 7.46 (m, 2H, H18), 7.61 (m, 1H, H19), 7.37 (d, J = 7.8, 1H, H12), 5.40 (s, 1H, OH), 2.35 (dt, J = 14.1, 3.7, 1H, $H6_{eq}$), 2.19 (d, J = 14.0, 1H, $H6_{ax}$), 1.92 (t, J = 4.4, 1H, H5), 1.82 (m, 1H, $H4_{eq}$), 1.25-1.38 (m, 5H, $H3_{eq}$, $H4_{ax}$ and H11), 0.86-0.96 (m, 7H, $H3_{ax}$, H8 and H10).

^{1}H NMR was in accordance with reported data.[92]

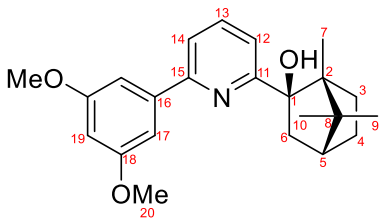

15e

(1R,2R,4R)-2-(6-(3,5-Dimethoxyphenyl)pyridin-2-yl)-1,7,7-trimethylbicyclo[2.2.1]heptan-2-ol (**15e**): Following general procedure E, 2-bromopyridine **12b** (50.1 mg, 0.161 mmol) was reacted with (3,5-dimethoxyphenyl)boronic acid (**16b**) (53.9 mg, 0.296 mmol) in the presence of catalytic $Pd(PPh_3)_4$ (9.9 mg, 0.009 mmol) and K_2CO_3 (66.0 mg, 0.478 mmol) to give 2,6-disubstituted pyridine **15e** (59.0 mg, 100 %) after workup and purification (1:10 EtOAc:pentane) as a colourless oil.

^{1}H NMR (600 MHz, $CDCl_3$) δ (ppm): 7.70 (t, *J* = 7.8, 1H, H13), 7.58 (d, *J* = 7.8, 1H, H14), 7.39 (d, *J* = 7.8, 1H, H12), 7.17 (d, *J* = 2.3, 2H, H17), 6.53 (t, *J* = 2.3, 1H, H19), 5.27 (s, 1H, OH), 3.85 (s, 6H, H20), 2.34 (dt, *J* = 14.1, 3.8, 1H, $H6_{eq}$), 2.20 (d, *J* = 14.0, 1H, H6ax), 1.92 (t, *J* = 4.4, 1H, H5), 1.81 (m, 1H, $H4_{eq}$), 1.24-1.37 (m, 5H, $H3_{eq}$, $H4_{ax}$ and H10), 0.85 (m, 7H, $H3_{ax}$, H7 and H9).

^{13}C NMR (150 MHz, $CDCl_3$) δ (ppm): 163.2 (C11), 161.1 (C18), 154.5 (C15), 141.0 (C16), 136.6 (C13), 119.3 (C12), 118.5 (C14), 105.0 (C17), 101.1 (C19), 82.8 (C1), 55.4 (C20), 53.5 (C8), 50.5 (C2), 45.4 (C5), 44.1 (C6), 30.8 (C3), 27.0 (C4), 21.3 (C10), 21.2 (C9), 10.0 (C7).

HRMS (ASAP) calcd for $C_{19}H_{26}NOS$ $[M+H]^+$ 316.1735, obsd 316.1742.

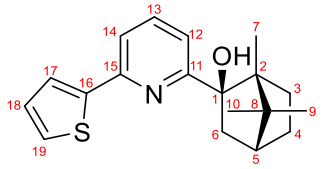

15f

(1R,2R,4R)-1,7,7-Trimethyl-2-(6-(thiophen-2-yl)pyridin-2-yl)bicyclo[2.2.1]heptan-2-ol (**15f**): Following general procedure E, 2-bromopyridine **12b** (50.0 mg, 0.161 mmol), was reacted with (thiophene-2-yl)boronic acid (**16c**) (22.7 mg, 0.177 mmol) in the presence of catalytic $Pd(PPh_3)_4$ formed *in situ* from $Pd(OAc)_2$ (1.8 mg, 0.008 mmol), PPh_3 (12.7 mg, 0.048 mmol) and NEt_3 (68 μL, 0.484 mmol), and K_2CO_3 (68.0 mg, 0.492 mmol) to give 2,6-disubstituted pyridine **15f** (25.6 mg, 51 %) after workup and purification (1:10 acetone:pentane) as a colourless oil.

^{1}H NMR (600 MHz, $CDCl_3$) δ (ppm): 7.65 (t, *J* = 7.8, 1H, H13), 7.58 (dd, *J* = 3.7, 1.0, 1H, H17), 7.53 (d, *J* = 7.8, 1H, H14), 7.38 (dd, *J* = 5.0, 1.0, 1H, H19), 7.30 (d, *J* = 7.8, 1H, H12), 7.10 (dd, *J* = 5.0, 3.7, 1H, H18), 4.96 (s, 1H, OH), 2.31 (dt, *J* = 14.1, 3.8, 1H, $H6_{eq}$), 2.20 (d, *J* = 14.0, 1H, $H6_{ax}$), 1.92 (t, *J* = 4.4, 1H, $H5_{eq}$), 1.80 (m, 1H, $H4_{eq}$), 1.23-1.35 (m, 7H, $H3_{eq}$, $H4_{ax}$ and H10), 0.91 (s, 3H, H9), 0.89 (s, 3H, H7), 0.86 (m, 1H, $H3_{ax}$).

^{13}C NMR (150 MHz, $CDCl_3$) δ (ppm): 163.4 (C11), 150.3 (C15), 144.9 (C16), 136.5 (C13), 128.0 (C18), 127.7 (C19), 124.4 (C17), 118.6 (C12), 116.5 (C14), 82.8 (C1), 53.5 (C8), 50.5 (C2), 45.4 (C5), 43.7 (C6), 30.8 (C3), 26.9 (C4), 21.3 (C10), 21.2 (C9), 9.8 (C7).

HRMS (ASAP) calcd for $C_{19}H_{24}NOS$ $[M+H]^+$ 314.1579, obsd 314.582.

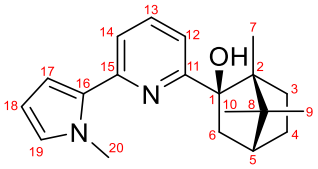

15g

(1R,2R,4R)-1,7,7-Trimethyl-2-(6-(1-methyl-1H-pyrrol-2-yl)pyridin-2-yl)bicyclo[2.2.1]heptan-2-ol (**15g**): Following general procedure E, 2-bromopyridine **12b** (50.0 mg, 0.161 mmol), was reacted with 1-Methyl-2-pyrroleboronic acid pinacol ester (**16d**) (72.4 mg, 0.350 mmol) in the presence of catalytic $Pd(PPh_3)_4$ formed *in situ* from $Pd(OAc)_2$ (3.8 mg, 0.0017 mmol), PPh_3 (25.9 mg, 0.099 mmol) and NEt_3 (68 μL, 0.484 mmol), and K_2CO_3 (136.5 mg, 0.988 mmol) to give 2,6-disubstituted pyridine **15g** (20.8 mg, 41 %) after workup and purification (1:1 DCM:pentane) as an orange oil.

^{1}H NMR (600 MHz, $CDCl_3$) δ (ppm): 7.63 (t, *J* = 7.9, 1H, H13), 7.45 (dd, *J* = 7.9, 0.6, 1H, H14), 7.23 (d, *J* = 7.8, 1H, H12), 6.73 (t, *J* = 2.2, 1H, H19), 6.62 (dd, *J* = 3.8, 1.8, 1H, H17), 6.18 (dd, *J* = 3.7, 2.6, 1H, H18), 5.30 (s, 1H, OH), 4.00 (s, 3H, H20), 2.33 (dt, *J* = 14.1, 3.8, 1H, $H6_{eq}$), 2.13 (d, *J* = 14.1, 1H, $H6_{ax}$), 1.92 (t, *J* = 4.4, 1H, H5), 1.82 (m, 1H, $H4_{eq}$), 1.28-1.36 (m, 2H, $H3_{eq}$ and $H4_{ax}$), 1.27 (s, 3H, H10), 1.00 (m, 1H, $H3_{ax}$), 0.92 (s, 3H, H9), 0.83 (s, 3H, H7).

^{13}C NMR (150 MHz, $CDCl_3$) δ (ppm): 162.3 (C11), 150.4 (C15), 136.2 (C13), 131.8 (C16), 126.7 (C19), 119.4 (C14), 117.4 (C12), 111.3 (C17), 107.8 (C18), 83.1 (C1), 53.5 (C8), 50.6 (C2), 45.4 (C5), 44.6 (C6), 37.6 (C20), 30.7 (C3), 27.1 (C4), 21.4 (C10), 21.2 (C9), 10.3 (C7).

HRMS (ASAP) calcd for $C_{20}H_{27}N_2O$ $[M+H]^+$ 311.2123, obsd 311.2127.

6.6.2 Synthesis of 2,6-disubstituted pyridine 15h

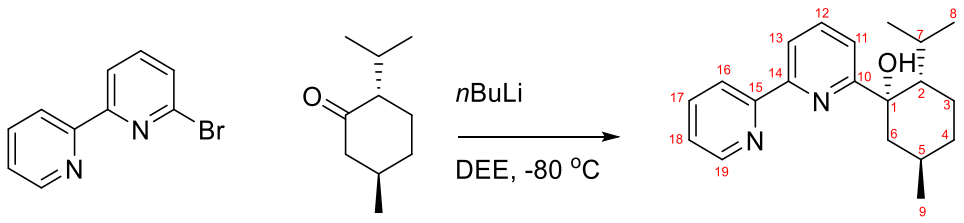

17 **14a** **15h**

(1S,2S,5R)-1-((2,2'-Bipyridin)-6-yl)-2-isopropyl-5-methylcyclohexan-1-ol (**15h**): 6-Bromo-2,2'-bipyridine (**17**) (497.2 mg, 2.115 mmol) was dissolved in dry DEE and cooled to -80 °C. *n*BuLi (850 μL, 2.5M in hexane, 2.125 mmol) was added dropwise and the solution stirred until it reached -40 °C before being cooled back to -80 °C. (-)-Menthone (**14a**) (367μL, 2.379 mmol) diluted in DEE (1 mL) was added dropwise, and the solution was stirred overnight and allowed to warm to r.t. The solution was quenched with sat. NH_4Cl (25 mL), extracted into DCM (3x20 mL), washed with brine (20 mL), dried over Na_2SO_4. Removal of the solvent *in vacuo* and purification by flash column chromatography (1:15 NEt_3:petroleum ether) and

product recrystallised from ACN by dropwise addition of water, yielding product **15h** (150.5 mg, 23 %) as white crystals.

^{1}H NMR (600 MHz, $CDCl_3$) δ (ppm): 8.69 (dm, J = 4.7, 1H, H19), 8.41 (d, J = 8.0, 1H, H16), 8.33 (d, J = 7.7, 1H, H13), 7.85 (t, J = 7.8, 1H, H12), 7.83 (td, J = 11.5, 1.8, 1H, H17), 7.37 (d, J = 7.8, 1H, H11), 7.32 (ddd, J = 7.4, 4.8, 0.9, 1H, H18), 5.42 (bs, 1H, OH), 2.01 (m, 1H, $H5_{ax}$), 1.92 (m, 1H, $H4_{eq}$), 1.76 (qd, J = 12.9, 3.4, 1H, $H3_{ax}$), 1.65-1.71 (m, 2H, $H2_{ax}$ and $H3_{eq}$), 1.62 (ddd, J = 13.1, 3.2, 2.5, 1H, $H6_{eq}$), 1.40 (t, J = 12.6, 1H, $H6_{ax}$), 1.28 (hept d, J = 6.9, 1.5, 1H, H7), 1.08 (qd, J = 12.6, 3.6, 1H, $H4_{ax}$), 0.92 (d, J = 6.8, 3H, H9), 0.84 (d, J = 6.8, 3H, H8), 0.69 (d, J = 7.0, 1H, H8).

^{15}N NMR (60.8 MHz, d_3-ACN) δ (ppm): -72.4 (between C15 and C19), -92.4 (between C10 and C14).

IR (thin film, cm^{-1}): 3369, 2946, 2915, 2840, 1563, 1429, 1387, 1048, 777, 496.

^{1}H NMR was in accordance with literature data.[92]

6.6.3 Synthesis of chiral 2,6-disubstituted pyridine methyl ethers, 12b-OMe and 15b,d,e,h-OMe

General procedure F

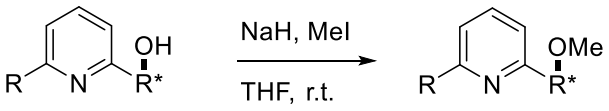

	R	R*	
12b	Br	Isoborneol	**12b-OMe**
15b	3,5-diOMePh	Neomenthol	**15b-OMe**
15h	Py	Neomenthol	**15h-OMe**

To a solution of pyridine alcohol **15** or **12b** (1 equiv.), in dry THF, under a N_2-atmosphere, was added NaH (10 equiv.) and the solution is stirred for 30 mins. MeI (12 equiv.) was added and the solution stirred until completion as determined by TLC (3 hrs – 2 dys). NaOH (1M, 10 mL) was added and the solution stirred for 30 mins. The solution was extracted into DCM, washed with NaOH (1M) and brine, and dried over Na_2SO_4. Removal of solvent *in vacuo* yielded the methylated derivatives **15-OMe** or **12b-OMe** without the need for further purification.

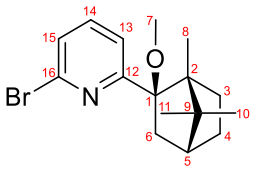

12b-OMe

2-Bromo-6-((1R,2R,4R)-2-methoxy-1,7,7-trimethylbicyclo[2.2.1]heptan-2-yl)pyridine (**12b-OMe**): Following general procedure F, pyridine alcohol **12b** (187.6 mg, 0.605 mmol)

was treated with NaH (145.4 mg, 6.047 mmol) and reacted with MeI (451.7 μL, 7.256 mmol), yielding pure **12b-OMe** (189.6 mg, 97%) as colourless oil after workup.

^{1}H NMR (600 MHz, $CDCl_3$) δ (ppm): 7.51 (t, J = 7.6, 1H, H14), 7.47 (dd, J = 7.7, 0.7, 1H, H13), 7.34 (dd, J = 7.6, 0.8, 1H, H15), 2.87 (s, 3H, H7), 2.65 (d, J = 13.1, 1H, $H6_{ax}$), 2.11 (ddd, J =13.1, 4.2, 3.2, 1H, $H6_{eq}$), 1.86 (t, J = 4.5, 1H, H5), 1.61 (ddddd, J = 12.1, 11.8, 4.5, 3.7, 3.2, 1H, $H4_{eq}$), 1.47 (ddd, J = 12.1, 9.1, 5.1, 1H, $H4_{ax}$), 1.11 (s, 3H, H11), 1.10 (ddd, J = 13.3, 11.8, 5.2, 1H, $H3_{eq}$), 0.87 (s, 6H, H8 and H10), 0.41 (ddd, J = 13.2, 9.4, 3.7, 1H, $H3_{ax}$).

^{13}C NMR (150 MHz, $CDCl_3$) δ (ppm): 164.4 (C12), 140.2 (C16), 138.0 (C14), 12.58 (C15), 121.3 (C13), 90.5 (C1), 54.7 (C9), 50.8 (C2), 49.5 (C7), 45.7 (C5), 34.9 (C6), 31.1 (C3), 25.7 (C4), 21.02 and 20.96 (C10 and C11), 9.9 (C8).

HRMS (ESI) calcd for $C_{15}H_{19}NBr$ $[M\text{-}OMe]^+$ 292.0701, obsd 292.0706.

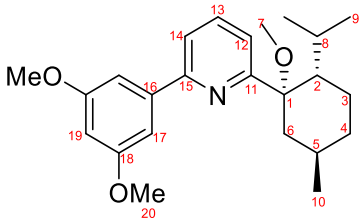

15b-OMe

2-(3,5-Dimethoxyphenyl)-6-((1S,2S,5R)-2-isopropyl-1-methoxy-5-methylcyclohexyl)pyridine (**15b-OMe**): Following general procedure F, pyridine alcohol **15b** (53.1 mg, 0.144 mmol) was treated with NaH (33.0 mg, 1.374 mmol) and reacted with MeI (101.1 μL, 1.624 mmol), yielding pure **15b-OMe** (55.5 mg, 100 %) as a yellow oil after workup.

^{1}H NMR (600 MHz, $CDCl_3$) δ (ppm): 7.68 (t, J = 7.8, 1H, H13), 7.52 (dd, J = 7.8, 0.7, 1H, H14), 7.37 (dd, J = 7.8, 0.7, 1H, H12), 7.23 (d, J = 2.3, 2H, H17), 6.52 (t, J = 2.3, 1H, H19), 3.87 (s, 6H, H20), 3.24 (s, 3H, H7), 2.18 (dd, J = 14.6, 12.7, 1H, $H6_{ax}$), 2.00 (dt, J = 14.6, 2.6, 1H, $H6_{eq}$), 1.86 (dm, J = 12.7, 1H, $H4_{eq}$), 1.65-1.76 (m, 2H, H5 and $H3_{ax}$), 1.52-1.62 (m, 2H, H2 and $H3_{eq}$), 1.39 (hept d, J = 13.8, 1.7, 1H, H8), 1.08 (qd, J = 12.7, 3.6, 1H, $H4_{ax}$), 0.97 (d, J = 6.6, 3H, H10), 0.90 (d, J = 6.8, 3H, H9), 0.58 (d, J = 7.0, 3H, H9).

^{13}C NMR (150 MHz, $CDCl_3$) δ (ppm): 163.7 (C11), 161.1 (C18), 156.1 (C15), 142.0 (C16), 135.8 (C13), 120.1 (C12), 117.8 (C14), 105.2 (C17), 100.5 (C19), 85.1 (C1), 55.4 (C20), 51.6 (C2), 50.3 (C7), 40.0 (C6), 35.4 (C4), 28.0 (C5), 26.6 (C8), 23.6 (C9), 22.6 (C10), 21.2 (C3), 18.2 (C9).

HRMS (ASAP) calcd for $C_{24}H_{33}NO_3$ $[M+H]^+$ 384.2539, obsd 384.2542.

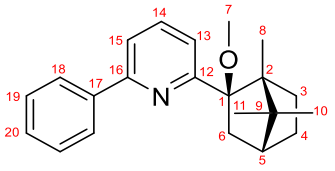

15d-OMe

2-((1R,2R,4R)-2-Methoxy-1,7,7-trimethylbicyclo[2.2.1]heptan-2-yl)-6-phenylpyridine (**15d-OMe**): Following general procedure E, 2-bromopyridine **12b-OMe** (50.0 mg, 0.154 mmol) was reacted with phenylboronic acid (**16a**) (19.2 mg, 0.157 mmol) in the presence of catalytic $Pd(PPh_3)_4$ (18.4 mg, 0.016 mmol) and K_2CO_3 (70.0 mg, 0.507 mmol). Workup and purification (1:24 EtOAc:pentane) yielded pure chiral 2,6-disubstituted pyridine methyl ether **15d-OMe** (24.1 mg, 49 %) as a pale yellow oil.

^{1}H NMR (600 MHz, $CDCl_3$) δ (ppm): 8.11 (m, 2H, H18), 7.72 (t, J = 7.8, 1H, H14), 7.64 (dd, J = 7.7, 0.8, 1H, H15), 7.44-7.50 (m, 3H, H19 and H13), 7.39 (m, 1H, H20), 2.97 (d, J = 13.0, 1H, $H6_{ax}$), 2.91 (s, 3H, H7), 2.16 (ddd, J = 13.0, 4.4, 2.9, 1H, $H6_{eq}$), 1.91 (t, J = 4.4, 1H, H5), 1.56-1.69 (m, 2H, $H4_{ax}$ and $H4_{eq}$), 1.17 (s, 3H, H11), 1.09 (ddd, J = 13.3, 11.6, 5.4, 1H, $H3_{eq}$), 0.93 (s, 3H, H8), 0.90 (s, 3H, H10), 0.55 (ddd, J = 13.1, 9.1, 3.9, 1H, $H3_{ax}$).

^{13}C NMR (150 MHz, $CDCl_3$) δ (ppm): 161.9 (C12), 154.4 (C16), 139.7 (C17), 136.4 (C14), 128.7 (C20), 128.6 (C19), 126.7 (C18), 121.0 (C13), 117.8 (C15), 91.1 (C1), 54.4 (C9), 50.8 (C2), 49.5 (C7), 46.0 (C5), 34.9 (C6), 31.1 (C3), 26.3 (C4), 21.13 and 21.09 (C10 and C11), 10.1 (C8).

HRMS (ESI) calcd for $C_{22}H_{28}NO$ $[M+H]^+$ 322.2171, obsd 322.2174.

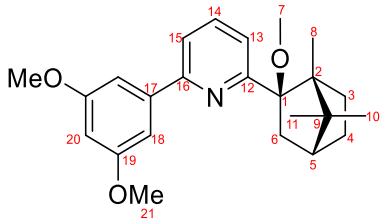

15e-OMe

2-(3,5-Dimethoxyphenyl)-6-((1R,2R,4R)-2-methoxy-1,7,7-trimethylbicyclo[2.2.1]heptan-2-yl)pyridine (**15e-OMe**): Following general procedure E, 2-bromopyridine **12b-OMe** (50.4 mg, 0.155 mmol) was reacted with (3,5-dimethoxyphenyl)boronic acid (**16b**) (55.8 mg, 0.308 mmol) in the presence of catalytic $Pd(PPh_3)_4$ (10.0 mg, 0.086 mmol) and K_2CO_3 (59.3 mg, 0.429 mmol). Workup and purification (1:30 EtOAc:pentane) yielded pure chiral 2,6-disubstituted pyridine methyl ether **15e-OMe** (59.0 mg, 100 %) as a pale colourless oil.

^{1}H NMR (600 MHz, $CDCl_3$) δ (ppm): 7.71 (t, J = 7.8, 1H, H14), 7.60 (dd, J = 7.7, 0.6, 1H, H15), 7.47 (dd, J = 7.8, 0.6, 1H, H13), 7.30 (d, J = 2.3, 2H, H18), 6.52 (t, J = 2.3, 1H, H20), 3.87 (s, 6H, H21), 2.92 (d, J = 12.9, 1H, $H6_{ax}$), 2.91 (s, 3H, H7), 2.17 (ddd, J = 13.0, 4.1, 3.0, 1H, $H6_{eq}$), 1.90 (t, J = 4.4, 1H, H5), 1.66 (m, 1H, $H4_{eq}$), 1.60 (m, 1H, $H4_{ax}$), 1.17 (s, 3H, H11),

1.09 (ddd, J = 13.1, 11.7, 5.2, 1H, $H3_{eq}$), 0.92 (s, 3H, H8), 0.89 (s, 3H, H10), 0.57 (ddd, J = 13.1, 9.2, 3.7, 1H, $H3_{ax}$).

^{13}C NMR (150 MHz, $CDCl_3$) δ (ppm): 161.8 (C12), 161.1 (C19), 154.1 (C16), 141.8 (C17), 136.4 (C14), 121.4 (C13), 118.0 (C15), 104.9 (C18), 100.8 (C20), 91.1 (C1), 55.4 (C21), 54.4 (C2), 50.8 (C9), 49.5 (C7), 46.0 (C5), 35.0 (C6), 31.1 (C3), 26.3 (C4), 21.12 (C10), 21.09 (C11), 10.1 (C8).

HRMS (ASAP) calcd for $C_{24}H_{32}NO_3$ M+H 382.2382, obsd 382.2387.

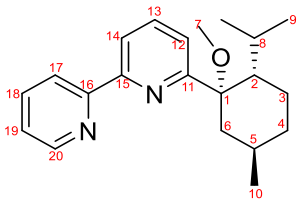

15h-OMe

6-((1S,2S,5R)-2-Isopropyl-1-methoxy-5-methylcyclohexyl)-2,2'-bipyridine (**15h-OMe**): Following general procedure F, pyridine alcohol **15h** (49.8 mg, 0.160 mmol) was treated with NaH (39.1 mg, 1.629 mmol) and reacted with MeI (120.3 μL, 1.933 mmol) yielding pure **15h-OMe** (52.1 mg, 100 %) as a yellow oil after workup.

^{1}H NMR (600 MHz, $CDCl_3$) δ (ppm): 8.66 (d, J = 4.7, 1H, H20), 8.46 (d, J = 8.0, 1H, H17), 8.25 (d, J = 7.8, 1H, H14), 7.81 (td, J = 7.7, 1.7, 1H, H18), 7.77 (t, J = 7.8, 1H, H13), 7.45 (d, J = 7.7, 1H, H12), 7.27 (dd, J = 6.6, 4.9, 1H, H19), 3.25 (s, 3H, H7), 2.18 (dd, J = 14.4, 12.8, 1H, $H6_{ax}$), 2.02 (dt, J = 14.6, 2.5, 1H, $H6_{eq}$), 1.88 (dt, J = 12.6, 2.5, 1H, $H4_{eq}$), 1.67-1.79 (m, 2H, H3 and H5), 1.53-1.61 (m, 2H, H2 and H3), 1.40 (hept d, J = 6.9, 1.0, 1H, H8), 1.13 (qd, J = 12.5, 3.6, 1H, $H4_{ax}$), 1.00 (d, J = 6.6, 3H, H10), 0.91 (d, J = 6.9, 3H, H9), 0.57 (d, J = 7.0, 3H, H9).

^{13}C NMR (150 MHz, $CDCl_3$) δ (ppm): 163.3 (C11), 156.7 (C16), 155.5 (C15), 149.0 (C20), 136.8 (C18), 136.1 (C13), 123.4 (C19), 121.5 (C12), 121.1 (C17), 118.2 (C14), 85.1 (C1), 51.8 (C2), 50.3 (C7), 40.0 (C6), 35.4 (C4), 28.0 (C5), 26.5 (C8), 23.6 (C9), 22.6 (C10), 21.3 (C3), 18.2 (C9).

HRMS (ASAP) calcd for $C_{21}H_{29}N_2O$ $[M+H]^+$ 325.2280, obsd 325.2286.

6.7 Synthesis of Au(III) complexes

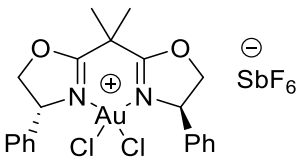

XIII

Box-Ph-Au(III)-SbF_6 (**XIII**): (4R,4'R)-2,2'-(propane-2,2-diyl)bis(4-phenyl-4,5-dihydrooxazole) (**18**) (21.0 mg, 0.063 mmol) was mixed with $KAuCl_4$ (**VII**) (24.9 mg, 0.066 mmol) and $AgSbF_6$ (45.0 mg, 0.132 mmol) in ACN (2 mL). After 1.5 hrs, the solution was filtered through celite and solvent removed *in vacuo*, yielding the product **XIII** (48.1 mg, 96 %) as a yellow powder.

^{1}H NMR (400 MHz, d_3-ACN) δ (ppm): 7.40-7.51 (m, 6H), 7.30-7.37 (m, 4H), 6.05 (dd, J = 10.0, 4.7, 2H), 5.18 (dd, J = 9.9, 9.4, 2H), 4.73 (dd, J = 9.3, 4.8, 2H), 2.03 (s, 6H).

^{1}H NMR was in accordance with previously reported data.[21]

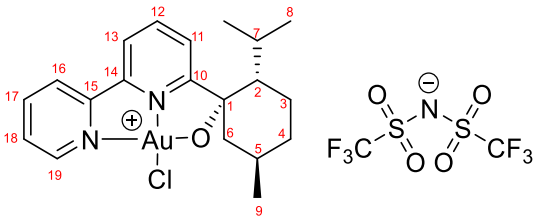

Au(III)-**15h**-NTf_2

Chiral bipyridine alcohol ligand **15h** (5.1 mg, 0.016 mmol) was stirred with $KAuCl_4$ (**VII**) (8.0 mg, 0.021 mmol) in ACN (0.5 mL) and KOAc (5.1 mg, 0.052 mmol) in H_2O (0.3 mL). $AgNTf_2$ (8.3 mg, 0.021 mmol) in ACN (0.4 mL) was added and the solution stirred for 1.5 hrs. H_2O (1 mL) was added and the solution extracted with DCM (3x1 mL) without inclusion of AgCl precipitate. Removal of solvent *in vacuo* yielded pure Au(III)-**15h**-NTf_2 (13.5 mg, 100 %).

^{1}H NMR (600 MHz, d_3-ACN) δ (ppm): 9.05 (d, J = 5.6, 1H, H19), 8.54 (td, J = 7.9, 1.4, 1H, H17), 8.49 (t, J = 8.1, 1H, H12), 8.47 (d, J = 8.1, 1H, H16), 8.33 (d, J = 8.1, 1H, H13), 8.02 (ddd, J = 7.9, 5.9, 1.6, 1H, H18), 7.71 (d, J = 8.2, 1H, H11), 2.11 (m, 1H, $H6_{eq}$), 1.90 (m, 1H, $H5_{ax}$), 1.84 (m, 1H, $H4_{eq}$), 1.80 (ddd, J = 12.4, 4.1, 1.8, 1H, $H2_{ax}$), 1.57-1.72 (m, 3H, $H3_{ax}$, $H3_{eq}$ and H7), 1.48 (dd, J = 12.7, 12.7, 1H, $H6_{ax}$), 1.08 (qd, J = 12.3, 4.1, 1H, $H4_{ax}$), 1.05 (d, J = 6.8, 3H, H8), 0.93 (d, J = 6.7, 3H, H9), 0.85 (d, J = 6.9, 3H, H8).

^{13}C NMR (150 MHz, d_3-ACN) δ (ppm): 177.0 (C10), 158.8 (C15), 151.9 (C14), 149.8 (C19), 145.8 (C17), 145.7 (C12), 131.3 (C18), 127.5 (C16), 126.9 (C11), 124.9 (C13), 120.9 (q, J = 320.6, CF_3), 105.5 (C1), 51.8 (C6), 51.3 (C2), 34.7 (C4), 30.0 (C7), 28.7 (C5), 23.7 (C8), 22.1 (C9), 21.3 (C3), 19.9 (C8).

^{15}N NMR (60.8 MHz, d_3-ACN) δ (ppm): -142.7 (between C10 and C14), -152.6 (between C15 and C19).

IR (thin film, cm^{-1}): 3086, 2954, 2870, 1602, 1492, 1347, 1180, 1131, 1053, 775, 614, 570.

HRMS (ESI) calcd for $C_{20}H_{25}N_2OClAu$ M^+ 541.1321, obsd 541.1326.

HRMS (ESI-) calcd for $C_2NO_4F_6S_2$ M^- 279.9173, obsd 279.9177.

References

[1] J. Knödlseder, *EAS Publications Series*, 2003, **7**, 177.

[2] N. Morita, M. Miyamoto, A. Yoda, *et al.*, *Tetrahedron Lett.*, 2016, **57**, 4460-4463.

[3] F. D. Toste and V. Michelet, *Gold Catalysis: An Homogenous Approach*, Imperial College Press, 1st edn., 2014.

[4] M.-C. Daniel and D. Astruc, *Chem. Rev.*, 2004, **104**, 293-346.

[5] G. L. Hallett-Tapley, C. D'Alfonso, N. L. Pacioni, *et al.*, *Chem. Commun.*, 2013, **49**, 10073-10075.

[6] A. W. Sromek, M. Rubina and V. Gevorgyan, *J. Am. Chem. Soc.*, 2005, **127**, 10500-10501.

[7] D. Fan, C.-T. Yang, J. D. Ranford and J. J. Vittal, *Dalton Trans.*, 2003, 4749-4753.

[8] M. Giordana, M. Luigi, O. Pierluigi, *et al.*, *Eur. J. Biochem.*, 2003, **270**, 4655-4661.

[9] E. Mizushima, K. Sato, T. Hayashi and M. Tanaka, *Angew. Chem. Int. Ed.*, 2002, **41**, 4563-4565.

[10] C. Nieto-Oberhuber, S. López, M. P. Muñoz, *et al.*, *Chem. Eur. J.*, 2006, **12**, 1694-1702.

[11] J. P. Reeds, A. C. Whitwood, M. P. Healy and I. J. S. Fairlamb, *Chem. Commun.*, 2010, **46**, 2046-2048.

[12] Y. Ito, M. Sawamura and T. Hayashi, *J. Am. Chem. Soc.*, 1986, **108**, 6405-6406.

[13] A. S. K. Hashmi, M. C. Blanco, D. Fischer and J. W. Bats, *Eur. J. Org. Chem.*, 2006, **2006**, 1387-1389.

[14] W. Zi and F. Dean Toste, *Chem. Soc. Rev.*, 2016, **45**, 4567-4589.

[15] J. Guenther, S. Mallet-Ladeira, L. Estevez, *et al.*, *J. Am. Chem. Soc.*, 2014, **136**, 1778-1781.

[16] E. Kimura, Y. Kurogi and T. Takahashi, *Inorg. Chem.*, 1991, **30**, 4117-4121.

[17] T.-C. Cheung, T.-F. Lai and C.-M. Che, *Polyhedron*, 1994, **13**, 2073-2077.

[18] D. T. Hill, K. Burns, D. D. Titus, *et al.*, *Inorg. Chim. Acta*, 2003, **346**, 1-6.

[19] K. J. Kilpin, W. Henderson and B. K. Nicholson, *Dalton Trans.*, 2008, 3899-3906.

[20] S. Gaillard, X. Bantreil, A. M. Z. Slawin and S. P. Nolan, *Dalton Trans.*, 2009, 6967-6971.

[21] A. C. Reiersølmoen, E. Østrem and A. Fiksdahl, *Eur. J. Org. Chem.*, 2018, **2018**, 3317-3325.

[22] M. A. Cinellu, L. Maiore, G. Minghetti, *et al.*, *Organometallics*, 2009, **28**, 7015-7024.

[23] Y. Zhang, B. Feng and C. Zhu, *Org. Biomol. Chem.*, 2012, **10**, 9137-9141.

[24] A. C. Reiersølmoen, D. Csókás, I. Pápai, *et al.*, *J. Am. Chem. Soc.*, 2019, **141**, 18221-18229.

[25] N. Marion and S. P. Nolan, *Angew. Chem. Int. Ed.*, 2007, **46**, 2750-2752.

[26] J. Marco-Contelles and E. Soriano, *Chem. Eur. J.*, 2007, **13**, 1350-1357.

[27] K. Miki, K. Ohe and S. Uemura, *Tetrahedron Lett.*, 2003, **44**, 2019-2022.

[28] K. Miki, K. Ohe and S. Uemura, *J. Org. Chem.*, 2003, **68**, 8505-8513.

[29] D. J. Gorin, I. D. G. Watson and F. D. Toste, *J. Am. Chem. Soc.*, 2008, **130**, 3736-3737.

[30] B. G. Pujanauski, B. A. Bhanu Prasad and R. Sarpong, *J. Am. Chem. Soc.*, 2006, **128**, 6786-6787.

[31] N. Marion, S. Díez-González, P. de Frémont, *et al.*, *Angew. Chem. Int. Ed.*, 2006, **45**, 3647-3650.

[32] H. F. Jónsson, S. Evjen and A. Fiksdahl, *Org. Lett.*, 2017, **19**, 2202-2205.

[33] Y. Fukuda and K. Utimoto, *Bull. Chem. Soc. Jpn.*, 1991, **64**, 2013-2015.

[34] Y. Fukuda and K. Utimoto, *J. Org. Chem.*, 1991, **56**, 3729-3731.

[35] M. J. Johansson, D. J. Gorin, S. T. Staben and F. D. Toste, *J. Am. Chem. Soc.*, 2005, **127**, 18002-18003.

References

[36] C.-F. Xu, M. Xu, L.-Q. Yang and C.-Y. Li, *J. Org. Chem.*, 2012, **77**, 3010-3016.

[37] M. Georgy, V. Boucard and J.-M. Campagne, *J. Am. Chem. Soc.*, 2005, **127**, 14180-14181.

[38] M. Georgy, V. Boucard, O. Debleds*, et al.*, *Tetrahedron*, 2009, **65**, 1758-1766.

[39] O. Debleds, E. Gayon, E. Vrancken and J.-M. Campagne, *Beilstein J. Org. Chem.*, 2011, **7**, 866-877.

[40] T. Schwier, M. Rubin and V. Gevorgyan, *Org. Lett.*, 2004, **6**, 1999-2001.

[41] R. J. Detz, Z. Abiri, R. le Griel*, et al.*, *Chem. Eur. J.*, 2011, **17**, 5921-5930.

[42] S. Kawanishi, S. Oki, D. Kundu and S. Akai, *Org. Lett.*, 2019, **21**, 2978-2982.

[43] G. Aridoss, V. D. Sarca, J. F. Ponder Jr*, et al.*, *Org. Biomol. Chem.*, 2011, **9**, 2518-2529.

[44] S.-S. Weng, K.-Y. Hsieh and Z.-J. Zeng, *Tetrahedron*, 2015, **71**, 2549-2554.

[45] P. Maitland and W. H. Mills, *Nature*, 1935, **135**, 994-994.

[46] P. Cramer and T. T. Tidwell, *J. Org. Chem.*, 1981, **46**, 2683-2686.

[47] S. Fornarini, M. Speranza, M. Attina*, et al.*, *J. Am. Chem. Soc.*, 1984, **106**, 2498-2501.

[48] K. Griesbaum, W. Naegele and G. G. Wanless, *J. Am. Chem. Soc.*, 1965, **87**, 3151-3158.

[49] T. Okuyama, K. Izawa and T. Fueno, *J. Am. Chem. Soc.*, 1973, **95**, 6749-6752.

[50] T. L. Jacobs and R. N. Johnson, *J. Am. Chem. Soc.*, 1960, **82**, 6397-6404.

[51] W. M. Braje, J. Frackenpohl, O. Schrake*, et al.*, *Helv. Chim. Acta*, 2000, **83**, 777-792.

[52] J. A. Marshall and X. J. Wang, *J. Org. Chem.*, 1991, **56**, 6264-6266.

[53] S. Doye, T. Hotopp, R. Wartchow and E. Winterfeldt, *Chem. Eur. J.*, 1998, **4**, 1480-1488.

[54] J. A. Marshall, E. D. Robinson and A. Zapata, *J. Org. Chem.*, 1989, **54**, 5854-5855.

[55] Z. Li, V. Boyarskikh, J. H. Hansen*, et al.*, *J. Am. Chem. Soc.*, 2012, **134**, 15497-15504.

[56] L. Barriault and I. Denissova, *Org. Lett.*, 2002, **4**, 1371-1374.

[57] M. Oestreich and D. Hoppe, *Tetrahedron Lett.*, 1999, **40**, 1881-1884.

[58] T. Shono, K. Ito, A. Tsubouchi and T. Takeda, *Org. Biomol. Chem.*, 2005, **3**, 2914-2916.

[59] A. Tsubouchi, T. Kira and T. Takeda, *Synlett*, 2006, **2006**, 2577-2580.

[60] M. Yang, N. Yokokawa, H. Ohmiya and M. Sawamura, *Org. Lett.*, 2012, **14**, 816-819.

[61] T. J. Brown, A. Sugie, M. G. D. Leed and R. A. Widenhoefer, *Chem. Eur. J.*, 2012, **18**, 6959-6971.

[62] B. D. Sherry and F. D. Toste, *J. Am. Chem. Soc.*, 2004, **126**, 15978-15979.

[63] A. Korte, J. Legros and C. Bolm, *Synlett*, 2004, **2004**, 2397-2399.

[64] D. W. Jones and A. Pomfret, *J. Chem. Soc., Perkin Trans. 1*, 1991, 249-253.

[65] J. Wang, L. Zhang, Y. Jing*, et al.*, *Tetrahedron Lett.*, 2009, **50**, 4978-4982.

[66] Z. Xi, R. Guo, S. Mito*, et al.*, *J. Org. Chem.*, 2003, **68**, 1252-1257.

[67] M. Lautens and T. Marquardt, *J. Org. Chem.*, 2004, **69**, 4607-4614.

[68] K.-J. Chang, D. K. Rayabarapu and C.-H. Cheng, *J. Org. Chem.*, 2004, **69**, 4781-4787.

[69] N. Morita, R. Mashiko, D. Hakuta*, et al.*, *Synthesis*, 2016, **48**, 1927-1933.

[70] D. R. Taylor, *Chem. Rev.*, 1967, **67**, 317-359.

[71] T. Vaidya, R. Cheng, P. N. Carlsen*, et al.*, *Org. Lett.*, 2014, **16**, 800-803.

[72] C. Shu, Y.-H. Wang, C.-H. Shen*, et al.*, *Org. Lett.*, 2016, **18**, 3254-3257.

[73] E. Kent Barefield, *Coord. Chem. Rev.*, 2010, **254**, 1607-1627.

[74] E. De Clercq, *Nature Reviews Drug Discovery*, 2003, **2**, 581-587.

[75] X. Liang and P. J. Sadler, *Chem. Soc. Rev.*, 2004, **33**, 246-266.

[76] I. Tasuku, K. Masako and I. Haruko, *Bull. Chem. Soc. Jpn.*, 1984, **57**, 2641-2649.

[77] A. S. Felten, N. Petry, B. Henry*, et al.*, *New J. Chem.*, 2016, **40**, 1507-1520.

[78] J. Cho, R. Sarangi and W. Nam, *Acc. Chem. Res.*, 2012, **45**, 1321-1330.

[79] T. R. Wagler and C. J. Burrows, *Tetrahedron Lett.*, 1988, **29**, 5091-5094.

[80] C. K. De, A. Paul, T. J. Emge and D. Seidel, *Supramol. Chem.*, 2016, **28**, 168-175.

[81] R. Innocenti, G. Menchi and A. Trabocchi, *Synlett*, 2018, **29**, 820-824.

[82] E. L. M. van Rozendaal, B. M. W. Voss and H. W. Scheeren, *Tetrahedron*, 1993, **49**, 6931-6936.

[83] K. Wadhwa, V. R. Chintareddy and J. G. Verkade, *J. Org. Chem.*, 2009, **74**, 6681-6690.

[84] P. Verma, P. Verma and R. B. Sunoj, *Org. Biomol. Chem.*, 2014, **12**, 2176-2179.

[85] X. Lu and U. Schneider, *Chem. Commun.*, 2016, **52**, 12980-12983.

[86] K. Yoshizawa and T. Shioiri, *Tetrahedron Lett.*, 2006, **47**, 757-761.

[87] X. Zhang, W. T. Teo, Sally and P. W. H. Chan, *J. Org. Chem.*, 2010, **75**, 6290-6293.

[88] I. Manjón-Mata, M. T. Quirós, E. Buñuel and D. J. Cárdenas, *Adv. Synth. Catal.*, 2020, **362**, 146-151.

[89] H. A. Stefani, R. Cella, F. A. Dörr*, et al.*, *Tetrahedron Lett.*, 2005, **46**, 2001-2003.

[90] E. E. Wilson, A. G. Oliver, R. P. Hughes and B. L. Ashfeld, *Organometallics*, 2011, **30**, 5214-5221.

[91] L. Ma, R.-Z. Jin, G.-H. Lü*, et al.*, *Synthesis*, 2007, **2007**, 2461-2470.

[92] H.-L. Kwong and W.-S. Lee, *Tetrahedron: Asymmetry*, 1999, **10**, 3791-3801.

[93] V. Lecomte, E. Stéphan, F. Le Bideau and G. Jaouen, *Tetrahedron*, 2003, **59**, 2169-2176.

[94] P. C. Too, G. H. Chan, Y. L. Tnay*, et al.*, *Angew. Chem. Int. Ed.*, 2016, **55**, 3719-3723.

[95] L. Eberson, M. P. Hartshorn, O. Persson and F. Radner, *Chem. Commun.*, 1996, 2105-2112.

[96] A. C. Reiersølmoen and A. Fiksdahl, *Eur. J. Org. Chem.*, 2020.

[97] R. Kleinmaier, S. Arenz, A. Karim*, et al.*, *Magn. Reson. Chem.*, 2013, **51**, 46-53.

[98] L. Rocchigiani, J. Fernandez-Cestau, P. H. M. Budzelaar and M. Bochmann, *Chem. Commun.*, 2017, **53**, 4358-4361.

[99] D. E. Grove, *Platinum Met. Rev.*, 2003, **47**, 44.

[100] Y. Grell, Y. Hong, X. Huang*, et al.*, *Organometallics*, 2019, **38**, 3948-3954.

[101] S. Gronowitz, *Thiophene and its derivatives : Part 1*, Wiley, New York, 1985.

[102] P. d. S. M. Pinheiro, D. A. Rodrigues, M. A. Alves*, et al.*, *New J. Chem.*, 2018, **42**, 497-505.

[103] B. P. Block and J. C. Bailar, *J. Am. Chem. Soc.*, 1951, **73**, 4722-4725.

[104] D. W. Lee, H. J. Ha and W. K. Lee, *Synth. Commun.*, 2007, **37**, 737-742.

[105] G. R. Fulmer, A. J. M. Miller, N. H. Sherden*, et al.*, *Organometallics*, 2010, **29**, 2176-2179.

[106] G. M. Martins, D. F. Back, T. S. Kaufman and C. C. Silveira, *J. Org. Chem.*, 2018, **83**, 3252-3264.

[107] R. Sanz, A. Martínez, J. M. Álvarez-Gutiérrez and F. Rodríguez, *Eur. J. Org. Chem.*, 2006, **2006**, 1383-1386.

[108] S. V. Kochetkov, A. S. Kucherenko and S. G. Zlotin, *Org. Biomol. Chem.*, 2018, **16**, 6423-6429.

References

[**109**] M. D. Hanwell, D. E. Curtis, D. C. Lonie*, et al.*, *J. Cheminformatics.*, 2012, **4**, 17.

[**110**] Q. Sun, T. C. Berkelbach, N. S. Blunt*, et al.*, *Wires. Comput. Mol. Sci.*, 2018, **8**, e1340.

Appendix A DFT Calculations for Different Conformations of Allenes 3a and 3f

A crude structure optimization of allene **3f** was performed in Avogadro[109] with UFF force field, before further refining the equilibrium structure with restricted Hartree-Fock (RHF) in the STO-3G basis set using the PySCF software package.[110] From this structure (Figure 20a), structures with rotated dihedral angles of the aryls were generated.

a) b)

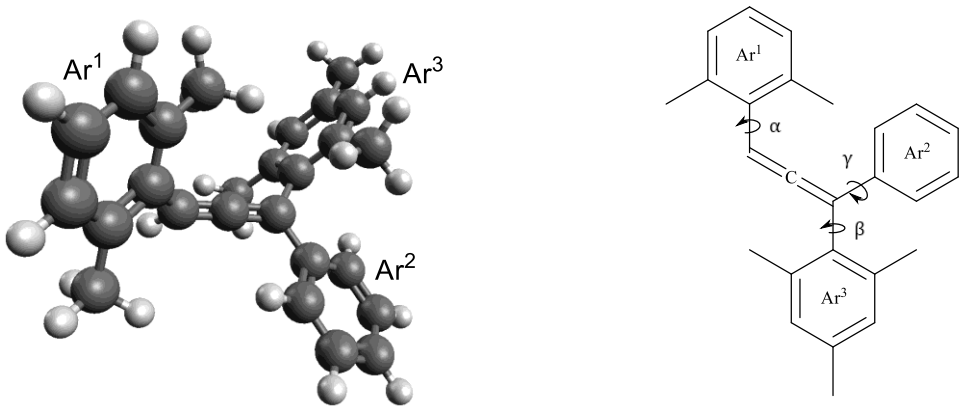

*Figure 20 – a) Optimized geometry of **3f** (RHF in the STO-3G basis set). b) Labels of aryls and dihedral angles.*

The three dihedral angels shown in Figure 20b were simplified by recognizing that Ar^2 and Ar^3 were close to perpendicular to each other (87.1 °) in the optimized structure for **3f**. It is reasonable to assume that this close-to-perpendicular relationship would hold for different angles of β. That is, changing β by a small amount, restricting rotation about that bond, and optimizing the geometry is assumed to enforce a similar rotation about γ such that the angle between Ar^2 and Ar^3 remains close to 90 °. This allows for reducing the number of free variables to only two by generating structures according to $\alpha = [0, 30, \dots, 150]$, $\beta = [0, 30, \dots, 150]$ and $\gamma = \beta + 90$, where (α,β) = (0,0) is defined as the optimized geometry. By setting Ar^2 to be perpendicular to Ar^3 in all cases, γ is no longer a free variable and can be omitted. Due to symmetry of each ring, an angle of 180 ° is equivalent to 0 ° and can also be disregarded. An interval of 30 ° can be too large to get a sufficient phase diagram, but was chosen as a compromise to computational time in this case. From the optimized geometry (α,β) = (0,0), Avogadro's Bond Centric Manipulation Tool allows for bond rotation by a set amount (here 30 °), and in this way all 36 structures were manually generated.

With all structures of **3f** in hand, a second set was generated by removing the methyl-groups of Ar^1, and thereby generating the exact equivalent 36 structures for the reference structure **3a**.

From the resulting 72 structures, the energy of each molecule was calculated in PySCF using (Kohn-Sham) Density Functional Theory (DFT) in the cc-pVDZ basis set and B3LYP as

the exchange correlation functional. No literature search was done to see if this was a good choice of basis set/exchange correlation functional for allenes. The resulting energies for **3a** and **3f** are shown in Table 8 and Table 9, respectively. The average time taken for each calculation was 388.1 and 554.6 seconds per conformation for **3a** and **3f**, respectively.

*Table 8 – Relative energies ($E_{\alpha,\beta} - E_{min}$, [Ha]) of different conformations of allene **3a**, colour-coded from green (low energy) to red (high energy).*

$\alpha\backslash\beta$	0	30	60	90	120	150	180
0	0.0031	0.0155	0.0592	0.0694	0.0317	0.0045	0.0031
30	0.0063	0.0186	0.0624	0.0609	0.0208	0.0068	0.0063
60	0.0058	0.0176	0.0591	0.0552	0.0152	0.0056	0.0058
90	0.0022	0.0146	0.0552	0.0508	0.0114	0.0020	0.0022
120	0.0000	0.0121	0.0532	0.0497	0.0118	0.0018	0.0000
150	0.0008	0.0128	0.0544	0.0602	0.0436	0.0183	0.0008
180	0.0031	0.0155	0.0592	0.0694	0.0317	0.0045	0.0031

*Table 9 – Relative energies ($E_{\alpha,\beta} - E_{min}$, [Ha]) of different conformations of allene **3f**, colour-coded from green (low energy) to red (high energy).*

$\alpha\backslash\beta$	0	30	60	90	120	150	180
0	0.0000	0.0126	0.1759	0.6712	0.4820	0.0438	0.0000
30	0.0055	0.3155	0.1059	0.1770	0.0404	0.0042	0.0055
60	0.0317	0.0331	0.0636	0.0573	0.0130	0.0066	0.0317
90	0.0300	0.0465	0.0671	0.0566	0.0167	0.0097	0.0300
120	0.0210	0.0350	0.0694	0.0701	0.0869	0.1244	0.0210
150	0.0137	0.0183	0.0716	0.7727	2.0917	0.2238	0.0137
180	0.0000	0.0126	0.1759	0.6712	0.4820	0.0438	0.0000

For allene **3a**, the calculations show that there is almost unhindered rotation of the Ar^1, as seen by minor variations (few m α is changed. Change of β, however, has a larger impact and shows a fluctuation of up to 66 mHa, almost independent of α. Since NMR signals are representations of the average structure in solution, free rotation about a dihedral angle means the symmetric (average) structure will be seen. Likewise, hindered rotation a about dihedral angle means it will occupy only a selection of substructures and not necessarily show symmetry. Since allene **3a** is NMR-symmetric for all aryls, this would mean that a barrier of 66 mHa is low enough to still allow for free rotation. It should however be noted that any solvent effects that might be present in solution are not accounted for in these calculations. The two structures of **3a**(α,β) = **3a**(0,0) and **3a**(0,90), which correspond to the largest difference in energy by change of β, are shown in Figure 21. For **3a**, only one local minimum was found, namely **3a**(120,0).

Allene **3f** indeed shows a difference in conformational energies. Most notable is the spike at **3f**(α,β) = **3f**(150,120), which corresponds to the greatest proximity of the *o*-methyls of Ar^1 and Ar^3. This energy-spike is exaggerated, as the structure corresponds to an atomic overlap of two hydrogens (see Figure 21); a lower energy should be found by rotation of the methyl groups so that hydrogens are intertwined rather than overlapping. Still, a significantly increased relative energy due to steric proximity is expected, and as these calculations aim to qualitatively investigate minima/maxima only, the results were left as is. Similar to **3a**, changing β has the largest impact on the energy. Moreover, change of α now has a larger impact than for **3a**, but still low enough to allow for free rotation (less than 66 mHa). Within the range of α = 60-90 there is little barrier of rotation of β, but any other value of α shows increased shows destabilisation. This indicates not all structures are equally likely to exist in solution, and can

be used as a plausible explanation for the observed broadening of signals in NMR spectra of **3f** (see Figure 12, section 3.2.3.1).

It is clear from this that the introduction of methyls in the ortho positions of Ar^1 creates steric restraints and elevated energy barriers of rotation of the ring(s). This energy barrier of rotation of Ar^1 is increased to the point where free rotation is no longer permitted for certain positions of Ar^3(/Ar^2), and its fluctuating orientation in solution can be seen by NMR spectroscopy. Change of temperature can control the rate of fluctuation by overcoming the increased energy barrier imposed by the extra methyls. That is, cooling of the solution to T < 270K freezes rotation of Ar^3 thereby causing desymmetrization and splitting of NMR signals. Heating to T > 310K allows for increased rotation of Ar^3 thereby coalescing the signals to one peak (the average structure). In the cases investigated here, Ar^1 shows sufficiently low energy barrier of rotation that cooling to T = 263K was not sufficiently cold to cause desymmetrization due to its lower energy barrier of rotation.

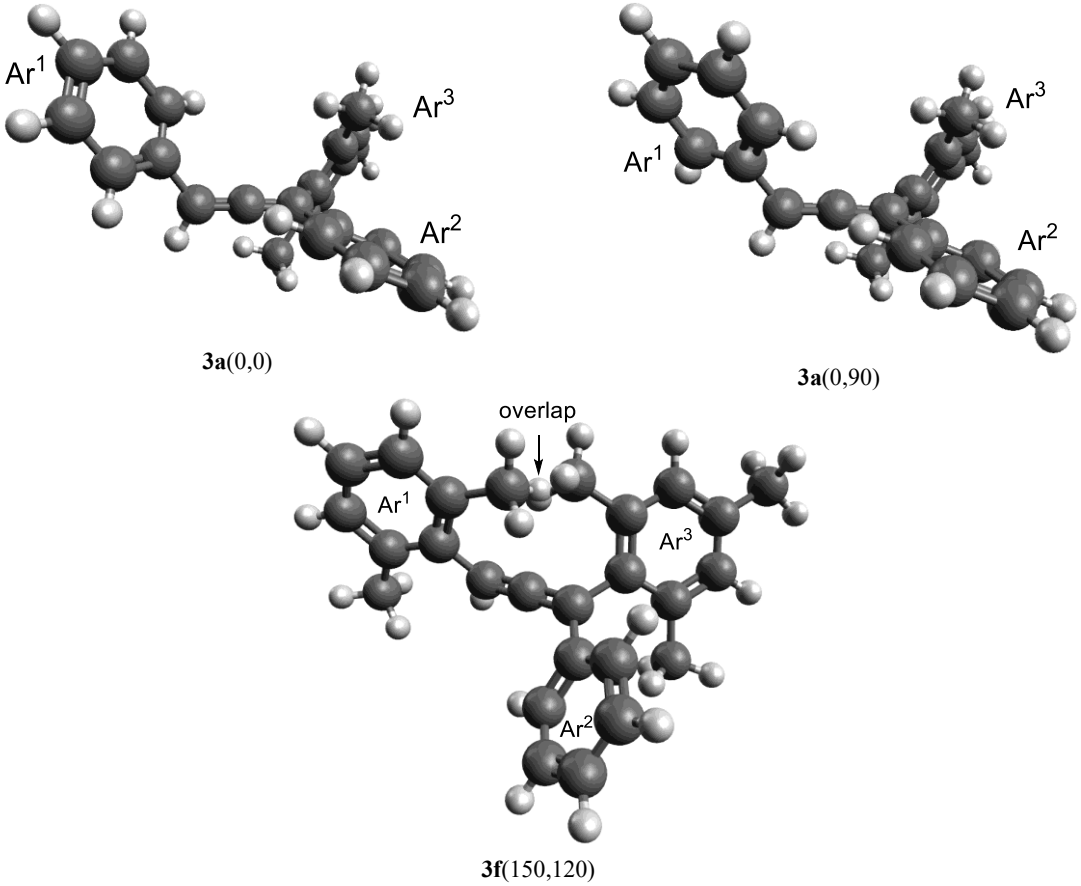

*Figure 21 – Selected conformations of **3a** and **3f***

Appendix B **Cyclam communication paper**

WILEY-VCH

MANUSCRIPT IN PREPARATION

N,N,N,N-Au(III) complexes with tetradentate cyclam based ligands.

Ann Christin Reiersølmoen, Thomas N. Solvi and Anne Fiksdahl*

Abstract: Chiral cyclam (1,4,8,11-tetraazacyclotetradecane) derivatives were synthesized stepwise from chiral mono-boc-1,2-diamines and (dialkyl)malonyl dichloride via the open diamide-di-(N-Boc-amino) intermediates (65-91%). Deprotection and ring closure with a second malonyl unit afforded the cyclam tetraamide precursors (80-95%). The new protocol allowed preparation of the target cyclam derivatives (53-59%) by a final optimized hydride reduction. Both the open tetraamine intermediates and the cyclam derivatives successfully coordinated with $AuCl_3$ to give moderate to excellent yields (50-96%) of the corresponding novel tetracoordinated N,N,N,N-Au(III) complexes with alternating five- and six-membered chelate rings. Testing of catalytic ability of the cyclam based N,N,N,N-Au(III) complexes demonstrated high catalytic activity of some complexes in selected test reactions (full conversion in 1-24h, 62-97% product yields).

Introduction

The importance of gold for humankind dates long back, and gold is linked to the evolution of many parts of the society. Contrary to the general fascination and importance of gold, the potential as homogenous catalyst has been neglected, compared to a range of other transition metals. The utilization of gold in synthetic organic chemistry has become a topic of interest during the last decades, as evidenced by the increasing number of review articles published in this period.[1] Whereas both gold(I) and gold(III) are proven to be catalytic active forms of gold, gold(I) has so far, received main attention, likely due to the higher stability, as demonstrated by development of a high number of gold(I) catalyzed transformation and ligated gold(I) complexes, along with improved mechanistic understanding.[2] In contrast, gold(III) catalysis were for a long time mostly based on inorganic salts, such as $AuCl_3$, $AuBr_3$, or pyridine-$AuCl_3$ and Pic-$AuCl_3$. However, Au(III) complexes with various coordinated ligands are about to become more explored. Different from the linear coordination mode of gold(I), gold(III) forms square planar complexes. This allows for greater steric control around the reaction center by using polydentate ligands. An interesting group of ligands which may coordinate to all the four coordination sites of gold(III), are represented by polyamine ligands, such as cyclam (1,4,8,11-tetraazacyclotetradecane), cyclen (1,4,7,10-tetraazacyclododecane)), ethylenediamine and triethylenetetramine derivatives. Such polyamine coordinated Au(III) complexes have mainly been prepared for studies on selective uptake of Au(III) from water[3] or of X-ray crystal structures,[4] or for investigation of biological properties.[5] Cyclam is known as a tetramino-macrocyclic ligand, which binds strongly to give complexes with many transition metal cations. While catalytic applications of square planar cyclam complexes are reported for metals, such as Ni,[6] Cu,[7] Fe[8], catalytic properties of cyclam coordinated gold(III) complexes are not known. Inspired by the tetracoordinated gold(III) complexes developed for biological purposes, we wanted to develop new chiral cyclam coordinated gold(III) complexes. We hereby present the synthesis of chiral cyclam ligands and related polyamino compounds, ligand coordination to Au(III), as well as testing of catalytic properties of the successfully obtained Au(III) complexes.

[a] A. C. Reiersølmoen, Thomas N. Solvi, Prof. Anne Fiksdahl
Department of Chemistry
Norwegian University of Science and Technology
Høgskoleringen 5, 7491, Trondheim, Norway

Supporting information for this article is given via a link at the end of the document.

Results and Discussion

Synthesis of potential ligands:

Chiral cyclam derivatives have previously been directly synthesized from (1R, 2R)-cyclohexane-1,2-diamine (**A**) and malonyl dichloride,[9] giving 36% yield of the wanted cyclam tetraamide product **2a** with dimethylmalonyl dichloride. Additionally, a macrocyclic by-product (14%) was formed by condensation of three units of diamine **A** and malonyl dichloride. To inhibit the formation of the trimer, we decided to prepare the cyclams in an indirect way. In fact, increased yields of cyclam derivative **2a** (68% yield over three steps) were obtained by malonyl reaction of the mono-boc-protected diamine (**A**-boc) followed by boc-deprotection with HCl, and final ring closure of diamide-diamine intermediate **1a** with one malonyl unit to give tetraamide product **2a** (Scheme 1a). The equivalent ethyl-substituted cyclam **4a** was prepared in comparable yield (63% over the three steps) by the same method with diethylmalonyl

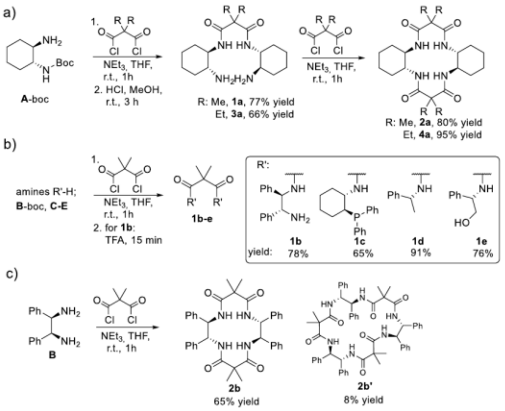

Scheme 1. Synthetic protocols for preparation of potential ligands **1-4**.

chloride. This method also allowed for isolation of the open diamide-diamine **1a** (77%). In addition, the similar potential ligands **1b-e** (65-91%, Scheme 1b) were likewise prepared from amines **B-E**. The phenyl-substituted cyclam tetramide derivative **2b** was prepared by the original direct method[9] (65%, Scheme 1c), as the mono-boc amine **B**-boc was less accessible.

As amide coordination to Au(III) in general, is challenging, and not successful in our hands, as discussed below, we wanted to prepare the reduced amine products (**5a-b**, **6a-b**) from amides **1a-b** and **2a-b**. Initially, by refluxing diamide-diamines **1a-b** and cyclam amide precursors **2a-b** in THF with $LiAlH_4$ for 3 days,[9] complex product mixtures of partly and fully reduces species were obtained for all besides **2a**. In order to activate the amides for reduction, improved reaction conditions were obtained by adding $AlCl_3$ to the reactions. Complete reduction of polyamides **1a-b** and **2a-b** yielded the open tetraamine products **5a-b** and the target cyclams **6a-b** with four secondary amine functions in moderate to high yields (30-88%, Scheme 2) within 1 - 2 days.

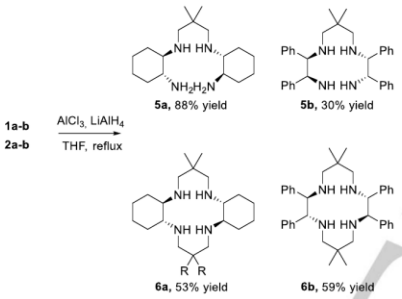

Scheme 2. Reduction of diamides **1a-b** and tetraamides **2a-b**.

Au(III) coordination studies:

Amide coordinated Au(III) complexes has so far scarcely been reported.[10] This is likely a result of the electron deficient character of the amide nitrogens. Coordination was initially tested with the cyclam tetraamide derivatives **2a-b** and **4a**. Judged from ^1H NMR, these ligands showed no interaction with Au(III), as expected. Similar resistance to coordinate was observed for the open diamide-diamines **1c-e**. The phosphorus containing ligand **1c** did undergo phosphor oxidation. No effect was obtained by refluxing or adding of additives, such as silver salts, NaOH or NH_4PF_6.

Given the previously reported coordinating studies of unsubstituted cyclam, [3a, 4b, 5h] the prepared new amine ligands **5a-b** and **6a-b** (Scheme 2) were used for Au(III) coordination. Both ligands **5a** and **6a** readily coordinated with $AuCl_3$ in methanol and gave moderate to excellent yields of tetracoordinated **5a**-Au(II) and **6a**-Au(III) N,N,N,N-complexes with alternating five- and six-membered chelate rings (50% and 96%, respectively, Scheme 3). NMR monitoring of the formation of complex **5a**-Au(III) clearly indicated a tetra-nitrogen-coordinated complex, as shown by the deshielding coordination effects $\Delta\delta^{15}N_{coord}$ 16.3 - 32.0 ppm for both primary and secondary amine nitrogens and $\Delta\delta^{1}H_{coord}$ 0.3-0.5 ppm for the neighboring N-C<u>H</u> and N-C<u>H</u>$_2$ protons. Comparable effects, $\Delta\delta^{1}H_{coord}$ 0.3-0.6 ppm, were also observed for the corresponding C<u>H</u> and C<u>H</u>$_2$ neighboring protons in complex **6a**-Au(III). Further on, cyclam **6b** readily coordinated to $AuCl_3$ in a mixture of dichloromethane and acetonitrile to obtain sufficient solubility of cyclam **6b**, allowing formation of **6b**-Au(III) in 64% yield (Scheme 3). The $\Delta\delta^{1}H$ coordination shifts of **6b**-Au(III) is similar to those discussed for **6a**-Au(III). Surprisingly, tetramine **5b** did not behave in a similar way as the other ligands, instead giving a complex mixture, as judged by ^1H NMR, when attempted coordinated to Au(III). Changing between the source of Au(III) and the solvents methanol, acetonitrile and dichloromethane did not improve the outcome.

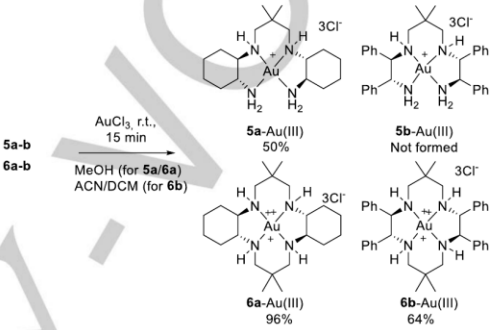

Scheme 3. Au(III) coordination conditions for ligands **5a-b** and **6a-b**. Coordination of **5b** was unsuccessful.

Catalytic activity:

The catalytic ability of the new Au(III) complexes were evaluated in two selected test reaction. High catalytic ability was shown for novel N,N,N,N-Au(III) complexes **5a** and **6a** in selected test reactions (full conversion in 1-24h, 62-97% product yields).

Conclusion

A new stepwise procedure was developed for improved preparation of chiral cyclam (1,4,8,11-tetraazacyclotetradecane) derivatives **6a-b** with cyclohexyl and a diphenyl-C2 bridge between the nitrogens, respectively. Reaction of chiral mono-boc-1,2-diamines and (dialkyl)malonyl dichloride gave the diamide-diamino intermediates **1a-b, 3a** (66-78%) after deprotection. Final ring closure with a second malonyl unit, afforded the cyclam tetraamides **2a ,4a** (80-95%), while the tetraamide cyclam **2b** was directly synthesized in from (dialkyl)malonyl dichloride and diamine **B** (65%). The fully reduced open tetraamine products **5a-b** (30-88%) as well as the target cyclam derivatives **6a-b** (53-59%) were obtained by optimized $LiAlH_4$ reduction by $AlCl_3$ activation of polyamides **1a-b** and **2a-b**, respectively. Successful $AuCl_3$ coordination of the open tetraamine ligand **5a** and the new cyclam derivatives **6a-b** gave the corresponding tetracoordinated N,N,N,N-Au(III) cyclam **5a** and **6a-b** complexes (50-96%) with alternating five- and six-membered chelate rings. High catalytic ability was shown for novel N,N,N,N-Au(III) complexes **5a** and **6a** in selected test reactions (full conversion in 1-24h, 62-97% product yields).

Appendix B Cyclam communication paper

Aknowledgements

This work was partly supported by the Research Council of Norway through the Norwegian NMR Platform, NNP (226244/F50).

Keywords: Gold • Au(III) • cyclam • catalysis • carboalkoxylation • cyclopropanation •

[1] a) A. Corma, A. Leyva-Pérez, M. J. Sabater, Chem. Rev. 2011, 111, 1657-1712; b) A. S. K. Hashmi, M. Buehrle, Aldrichimica Acta 2010, 43, 27-33; c) E. Jiménez-Núñez, A. M. Echavarren, Chem. Commun. 2007, 333-346; d) Z. Li, C. Brouwer, C. He, Chem. Rev. 2008, 108, 3239-3265; e) C. Nevado, CHIMIA International Journal for Chemistry 2010, 64, 247-251; f) S. Sengupta, X. Shi, ChemCatChem 2010, 2, 609-619; g) D. J. Gorin, B. D. Sherry, F. D. Toste, Chem. Rev. 2008, 108, 3351-3378; h) A. Arcadi, Chem. Rev. 2008, 108, 3266-3325.

[2] a) J. L. Mascareñas, I. Varela, F. López, Acc. Chem. Res. 2019, 52, 465-479; b) M. Mato, C. García-Morales, A. M. Echavarren, ChemCatChem 2019, 11, 53-72; c) C. García-Morales, A. M. Echavarren, Synlett 2018, 29, 2225-2237; d) Y.-M. Wang, A. D. Lackner, F. D. Toste, Acc. Chem. Res. 2014, 47, 889-901; e) C. Obradors, A. M. Echavarren, Chem. Commun. 2014, 50, 16-28; f) R. Dorel, A. M. Echavarren, Chem. Rev. 2015, 115, 9028-9072; g) W. Zi, F. Dean Toste, Chem. Soc. Rev. 2016, 45, 4567-4589.

[3] a) E. Kimura, Y. Kurogi, T. Takahashi, Inorg. Chem. 1991, 30, 4117-4121; b) C. Kavaklı, N. Özvatan, S. A. Tuncel, B. Salih, Anal.Chim. Acta 2002, 464, 313-322.

[4] a) J. Yau, D. M. P. Mingos, H. R. Powell, Polyhedron 1996, 15, 367-369; b) E. Kimura, Y. Kurogi, T. Koike, M. Shionoya, Y. Iitaka, J. Coord. Chem. 1993, 28, 33-49; c) G. Nardin, L. Randaccio, G. Annibale, G. Natile, B. Pitteri, J. Chem. Soc., Dalton Trans. 1980, 220-223; d) M. A. Cinellu, G. Minghetti, M. V. Pinna, S. Stoccoro, A. Zucca, M. Manassero, J. Chem. Soc., Dalton Trans. 2000, 1261-1265.

[5] a) S. Carotti, A. Guerri, T. Mazzei, L. Messori, E. Mini, P. Orioli, Inorg. Chim. Acta 1998, 281, 90-94; b) M. Navarro, Coord. Chem. Rev. 2009, 253, 1619-1626; c) C. Gabbiani, A. Casini, L. Messori, Gold Bull. 2007, 40, 73-81; d) L. Messori, P. Orioli, C. Tempi, G. Marcon, Biochem. Biophys. Res. Commun. 2001, 281, 352-360; e) A. Casini, C. Hartinger, C. Gabbiani, E. Mini, P. J. Dyson, B. K. Keppler, L. Messori, J. Inorg. Biochem. 2008, 102, 564-575; f) G. Marcon, L. Messori, P. Orioli, M. A. Cinellu, G. Minghetti, Eur. J. Biochem. 2003, 270, 4655-4661; g) R. W.-Y. Sun, C.-M. Che, Coord. Chem. Rev. 2009, 253, 1682-1691; h) L. Messori, F. Abbate, G. Marcon, P. Orioli, M. Fontani, E. Mini, T. Mazzei, S. Carotti, T. O'Connell, P. Zanello, J. Med. Chem. 2000, 43, 3541-3548.

[6] a) C. R. Schneider, L. C. Lewis, H. S. Shafaat, Dalton Trans. 2019, 48, 15810-15821; b) B. L. Mash, A. Raghavan, T. Ren, Eur. J. Inog. Chem. 2019, 2019, 2065-2070; c) E. M. Nichols, C. J. Chang, Organometallics 2019, 38, 1213-1218; d) C. J. Burrows, J. Muller, G. Poulter, S. Rokita, Acta Chem. Scand. 1996, 50, 337-344.

[7] M. Boiocchi, C. Ciarrocchi, L. Fabbrizzi, M. Licchelli, C. Mangano, A. Poggi, M. Vázquez López, Inorg. Chem 2015, 54, 10197-10207.

[8] A. D. Shircliff, K. R. Wilson, D. J. Cannon-Smith, D. G. Jones, Z. Zhang, Z. Chen, G. Yin, T. J. Prior, T. J. Hubin, Inorg. Chem. Commun. 2015, 59, 71-75.

[9] C. K. De, A. Paul, T. J. Emge, D. Seidel, Supramol. Chem. 2016, 28, 168-175.

[10] a) A. Dogan, B. Schwederski, T. Schleid, F. Lissner, J. Fiedler, W. Kaim, Inorg. Chem. Commun. 2004, 7, 220-223; b) T. Yang, C. Tu, J. Zhang, L. Lin, X. Zhang, Q. Liu, J. Ding, Q. Xu, Z. Guo, Dalton Trans. 2003, 3419-3424; c) D. Fan, C.-T. Yang, J. D. Ranford, J. J. Vittal, Dalton Trans. 2003, 4749-4753; d) K. J. Kilpin, W. Henderson, B. K. Nicholson, Dalton Trans. 2008, 3899-3906; e) D. T. Hill, K. Burns, D. D. Titus, G. R. Girard, W. M. Reiff, L. M. Mascavage, Inorg. Chim. Acta 2003, 346, 1-6; f) T.-C. Cheung, T.-F. Lai, C.-M. Che, Polyhedron 1994, 13, 2073-2077; g) A. C. Reiersølmoen, D. n. Csókás, I. Pápai, A. Fiksdahl, M. Erdélyi, J. Am. Chem. Soc. 2019, 141, 18221-18229.

[11] a) P. Dubé, F. D. Toste, J. Am. Chem. Soc. 2006, 128, 12062-12063; b) W. Zi, F. D. Toste, J. Am. Chem. Soc. 2013, 135, 12600-12603.

[12] a) C. A. Sperger, J. E. Tungen, A. Fiksdahl, Eur. J. Org. Chem. 2011, 2011, 3719-3722; b) N. Iqbal, C. A. Sperger, A. Fiksdahl, Eur. J. Org. Chem. 2013, 2013, 907-914; c) A. C. Reiersølmoen, E. Østrem, A. Fiksdahl, Eur. J. Org. Chem. 2018, 2018, 3317-3325; d) M. J. Johansson, D. J. Gorin, S. T. Staben, F. D. Toste, J. Am. Chem. Soc. 2005, 127, 18002-18003.

Appendix C **Spectra of Propargyl Alcohols, 1a-i**

Appendix C.1 **^{1}H NMR spectrum of Propargyl Alcohol 1a**

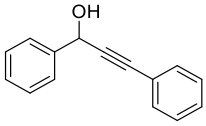

1a

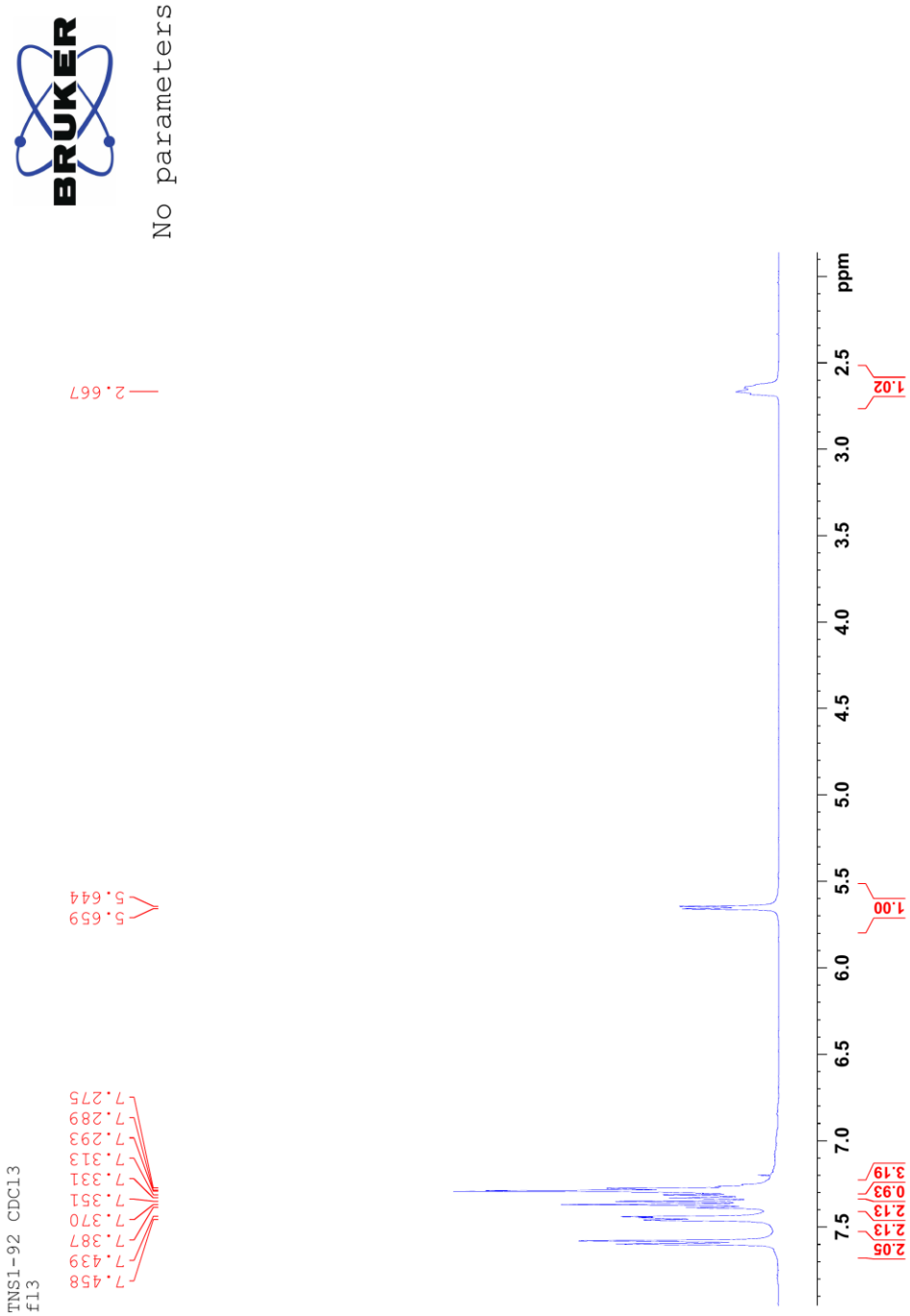

Appendix C Spectra of Propargyl Alcohols, 1a-i

Appendix C.2 **^{1}H NMR spectrum of Propargyl Alcohol 1b**

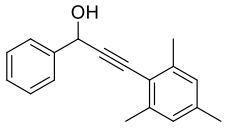

1b

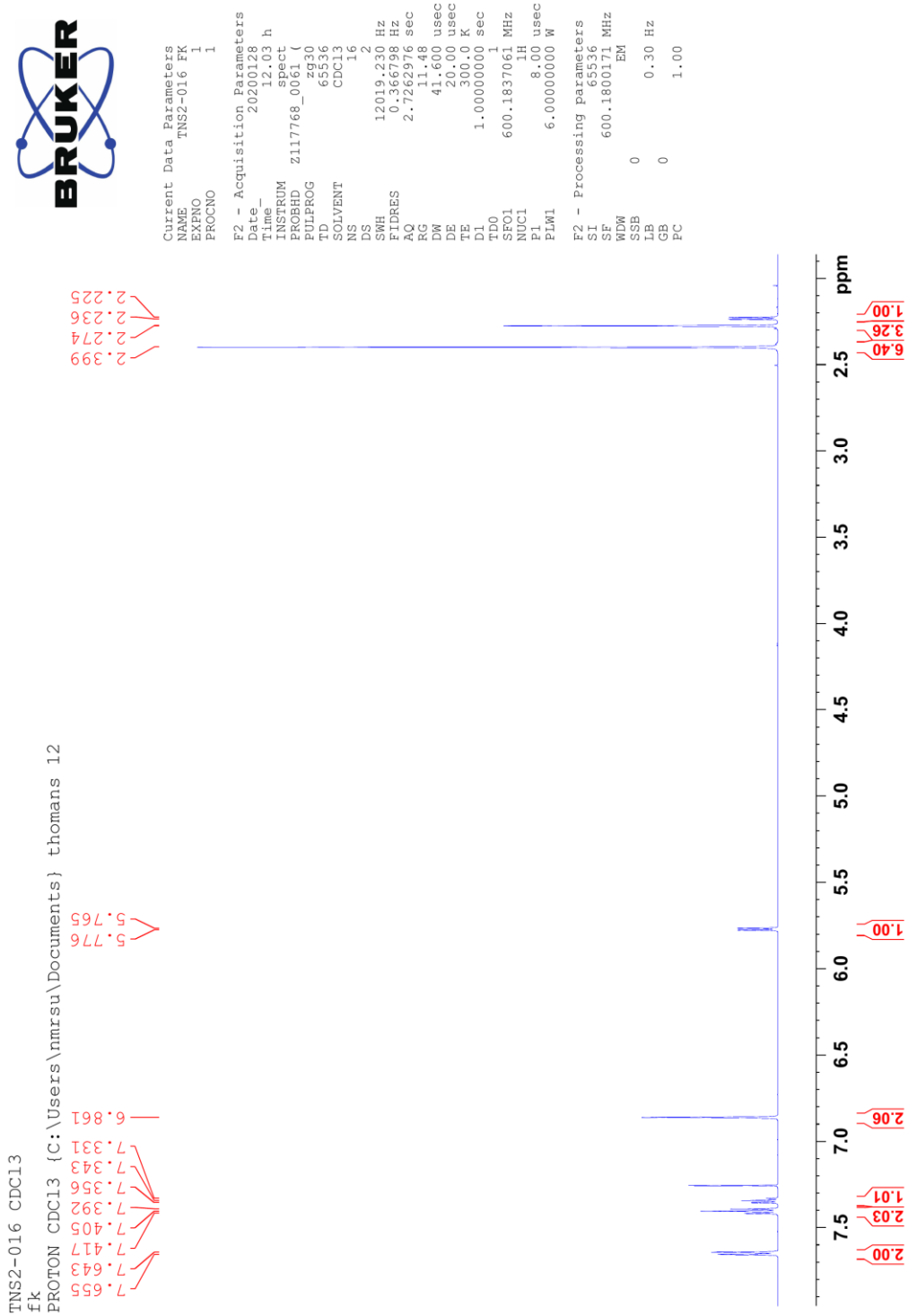

Appendix C Spectra of Propargyl Alcohols, 1a-i

Appendix C.3 **^{13}C NMR spectrum of Propargyl Alcohol 1b**

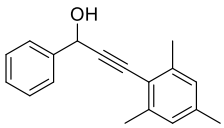

1b

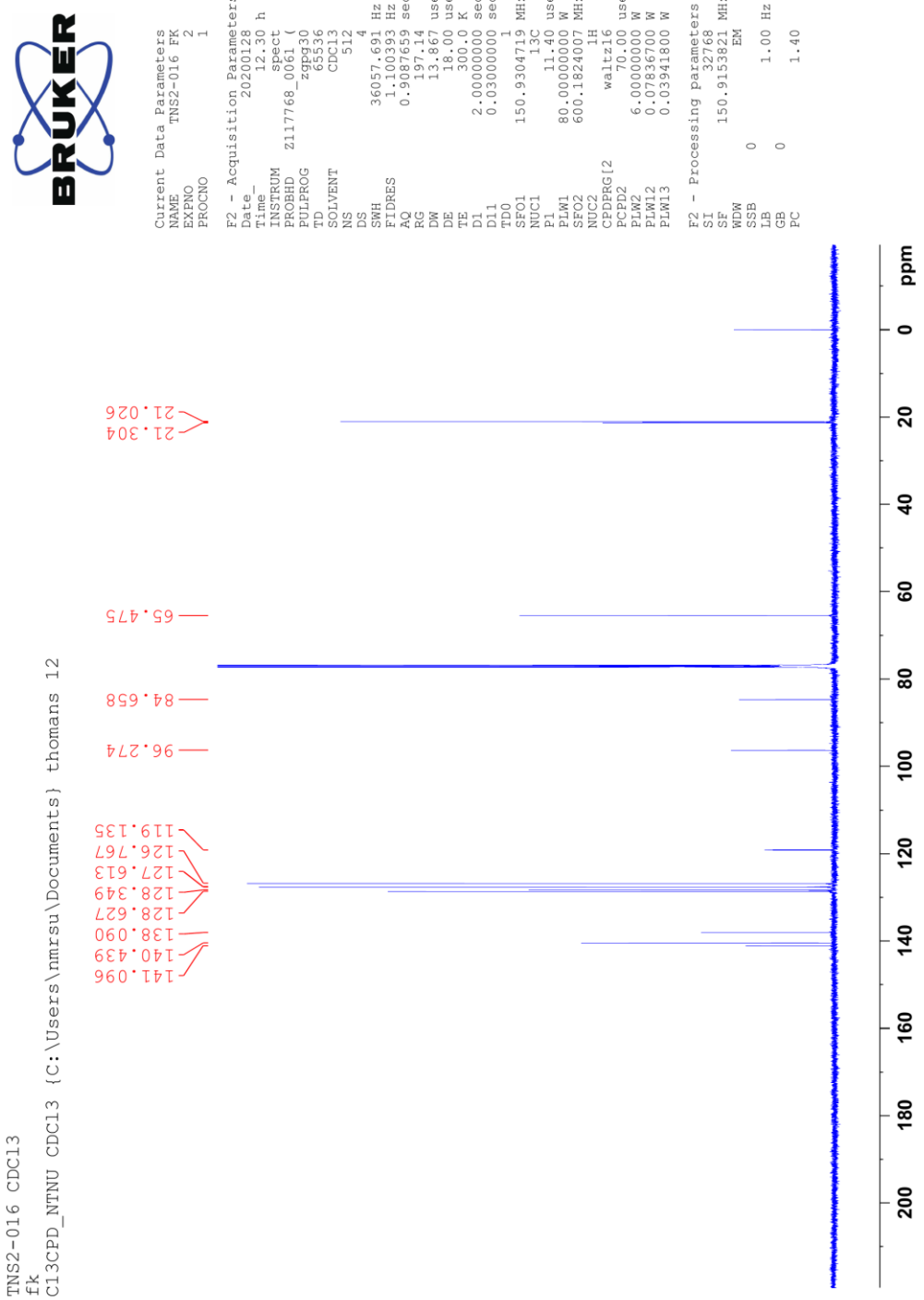

Appendix C Spectra of Propargyl Alcohols, 1a-i

Appendix C.4 **COSY NMR spectrum of Propargyl Alcohol 1b**

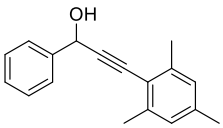

1b

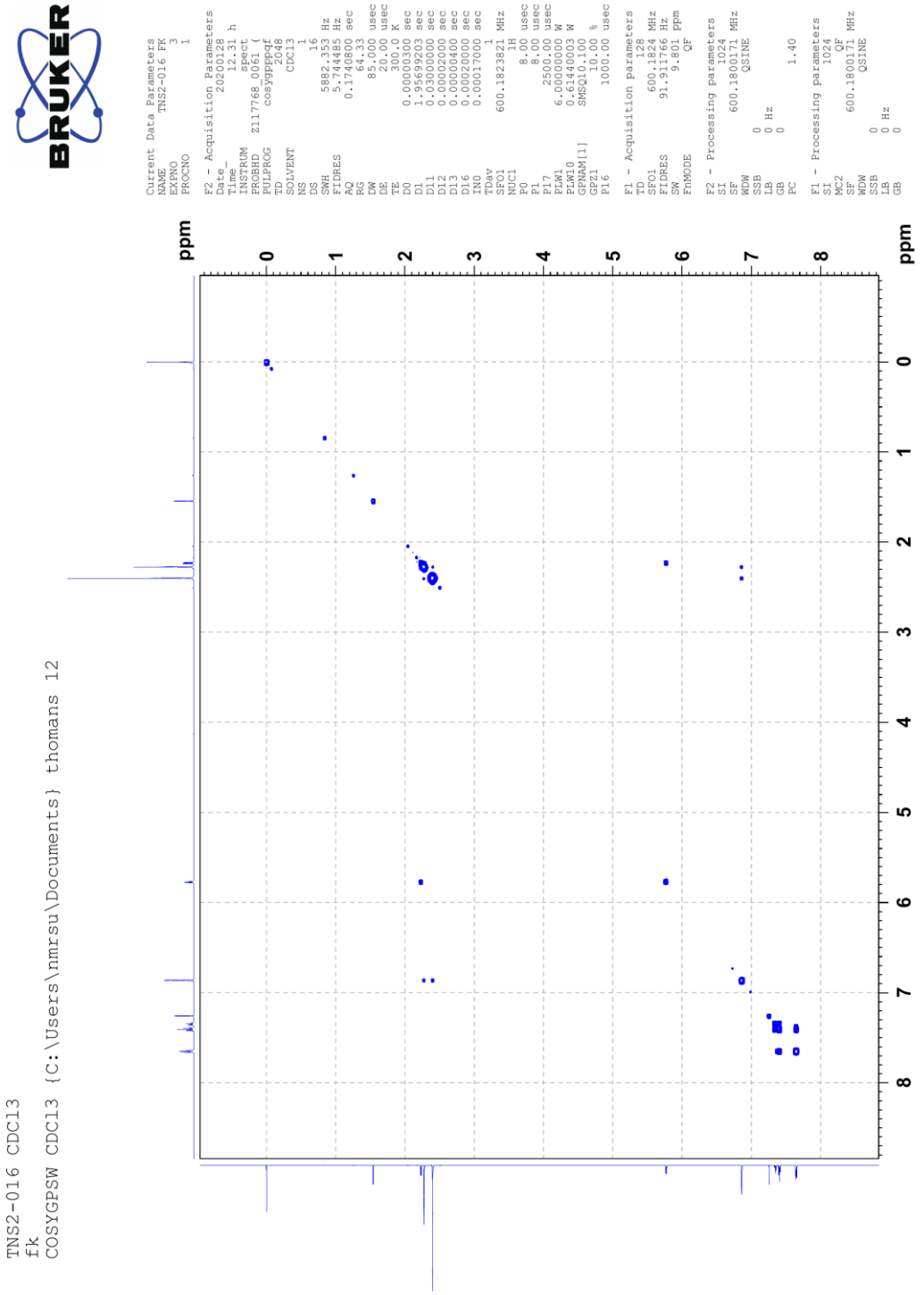

Appendix C Spectra of Propargyl Alcohols, 1a-i

Appendix C.5 **HSQC NMR spectrum of Propargyl Alcohol 1b**

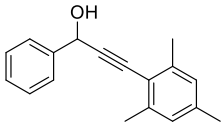

1b

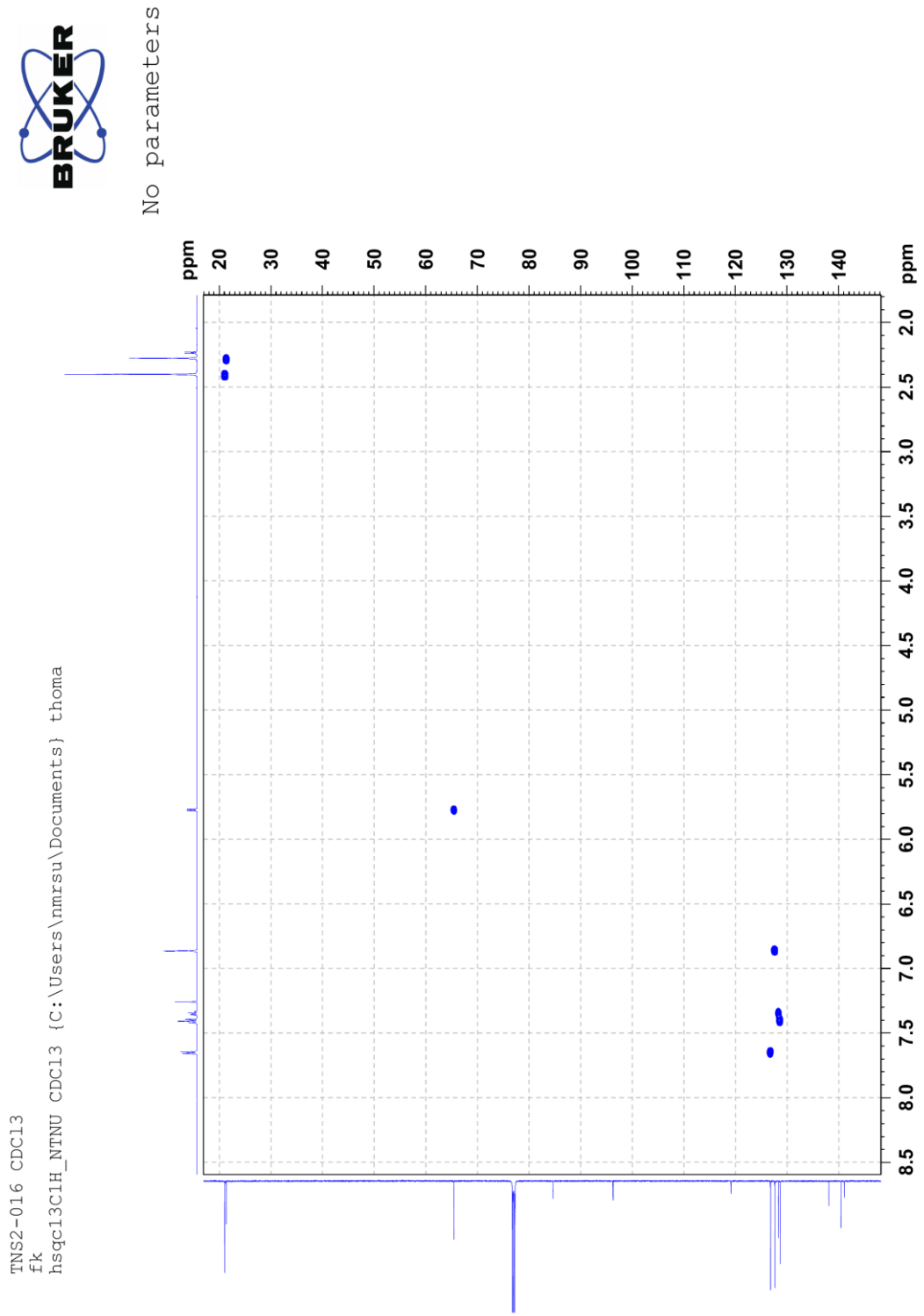

Appendix C Spectra of Propargyl Alcohols, 1a-i

Appendix C.6 **HMBC NMR spectrum of Propargyl Alcohol 1b**

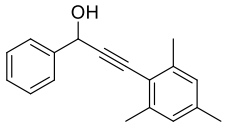

1b

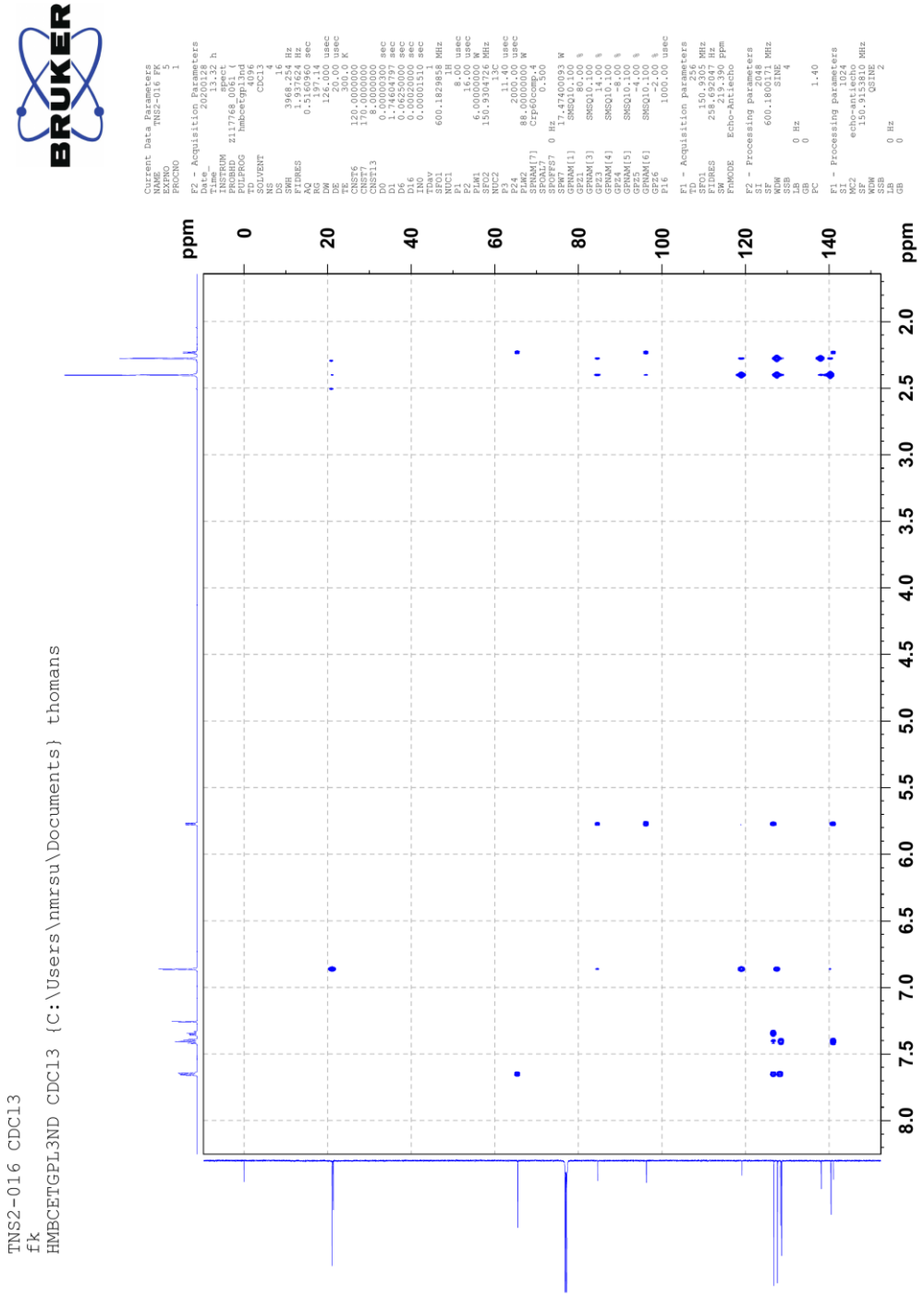

Appendix C Spectra of Propargyl Alcohols, 1a-i

Appendix C.7 **HRMS spectrum of Propargyl Alcohol 1b**

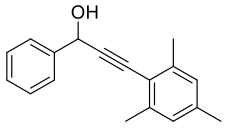

1b

Elemental Composition Report **Page 1**

Single Mass Analysis
Tolerance = 2.0 PPM / DBE: min = -50.0, max = 50.0
Element prediction: Off
Number of isotope peaks used for i-FIT = 3

Monoisotopic Mass, Even Electron Ions
401 formula(e) evaluated with 1 results within limits (all results (up to 1000) for each mass)
Elements Used:
C: 0-100 H: 0-150 10B: 0-3 O: 0-10
2019-677 18 (0.380) AM2 (Ar,35000.0,0.00,0.00); Cm (18:29)
1: TOF MS ASAP+

4.36e+007

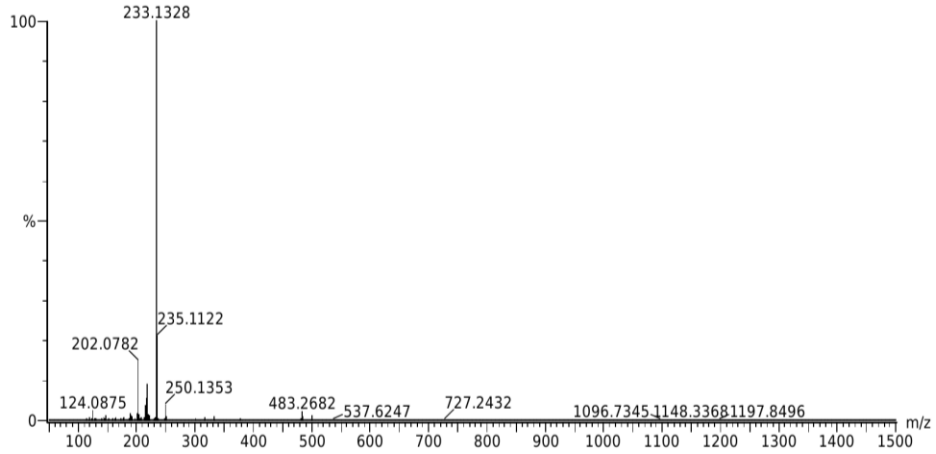

Minimum:				-50.0				
Maximum:		5.0	2.0	50.0				
Mass	Calc. Mass	mDa	PPM	DBE	i-FIT	Norm	Conf(%)	Formula
233.1328	233.1330	-0.2	-0.9	10.5	2182.6	n/a	n/a	C18 H17

Appendix C.8 **^{1}H NMR spectrum of Propargyl Alcohol 1c**

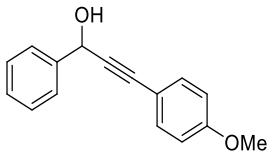

1c

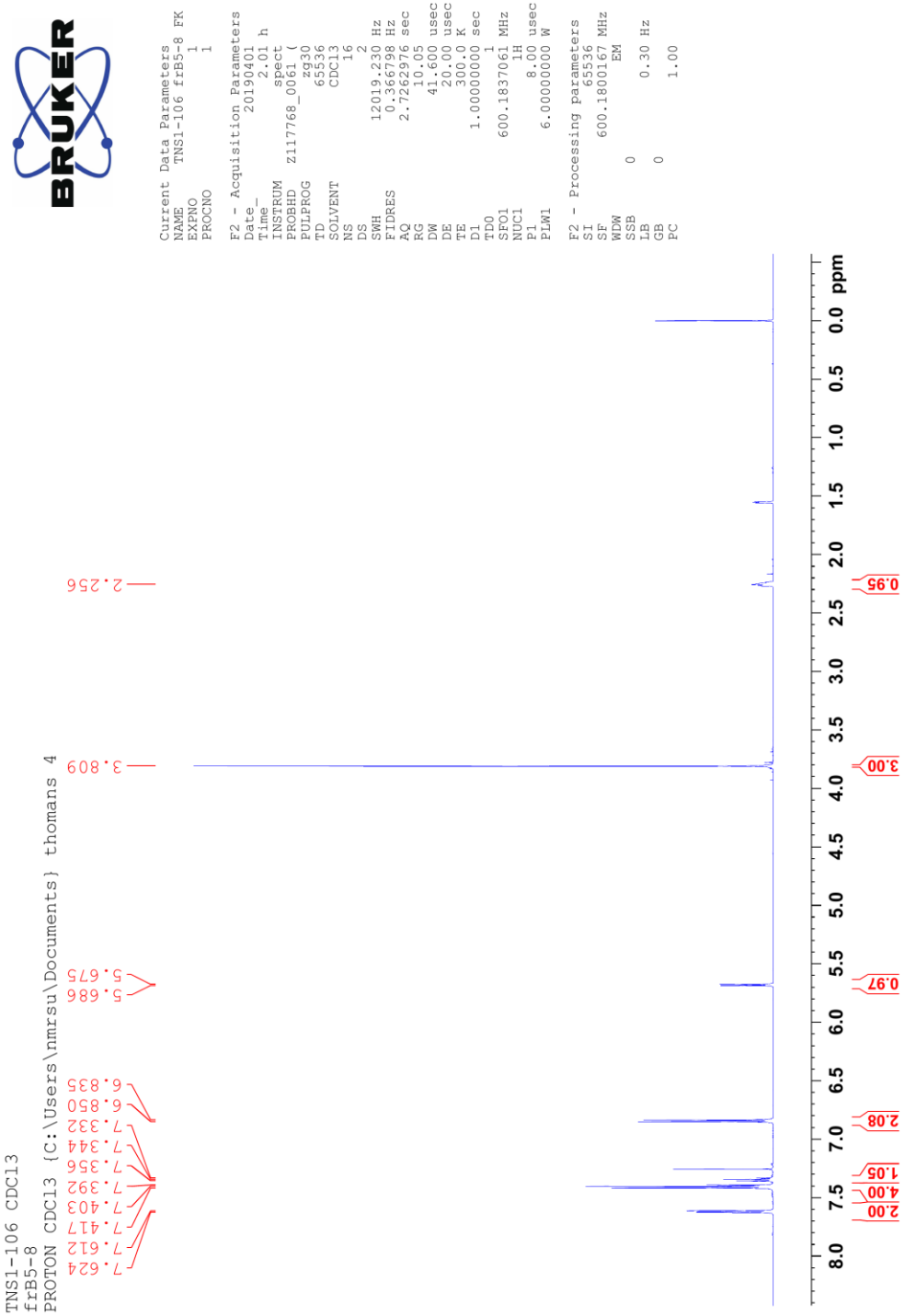

Appendix C Spectra of Propargyl Alcohols, 1a-i

Appendix C.9 **^{1}H NMR spectrum of Propargyl Alcohol 1d**

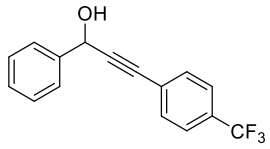

1d

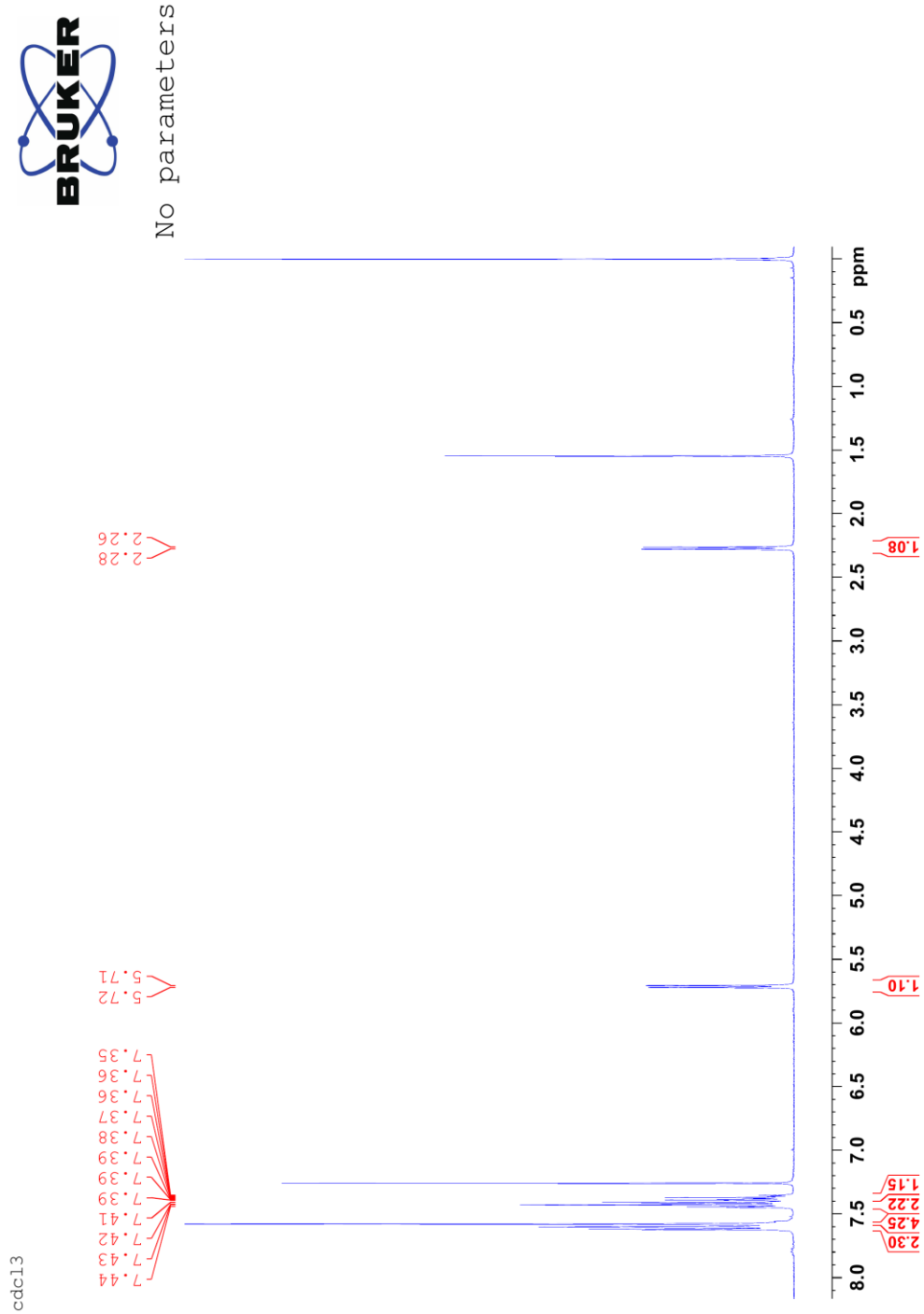

Appendix C Spectra of Propargyl Alcohols, 1a-i

Appendix C.10 **^{1}H NMR spectrum of Propargyl Alcohol 1e**

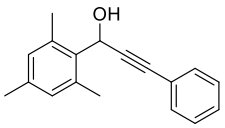

1e

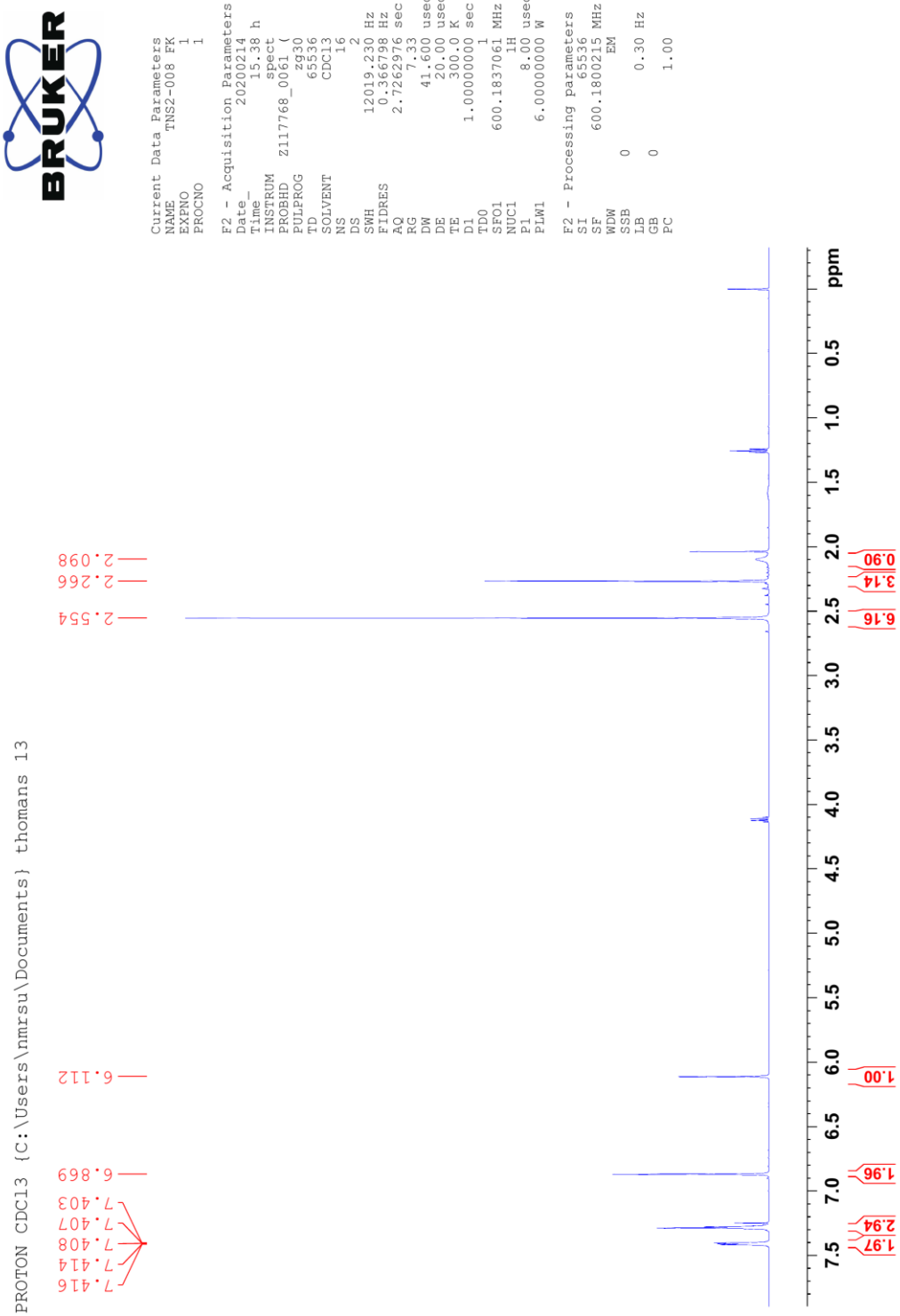

Appendix C Spectra of Propargyl Alcohols, 1a-i

Appendix C.11 **^{13}C NMR spectrum of Propargyl Alcohol 1e**

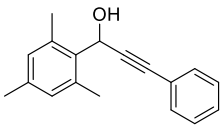

1e

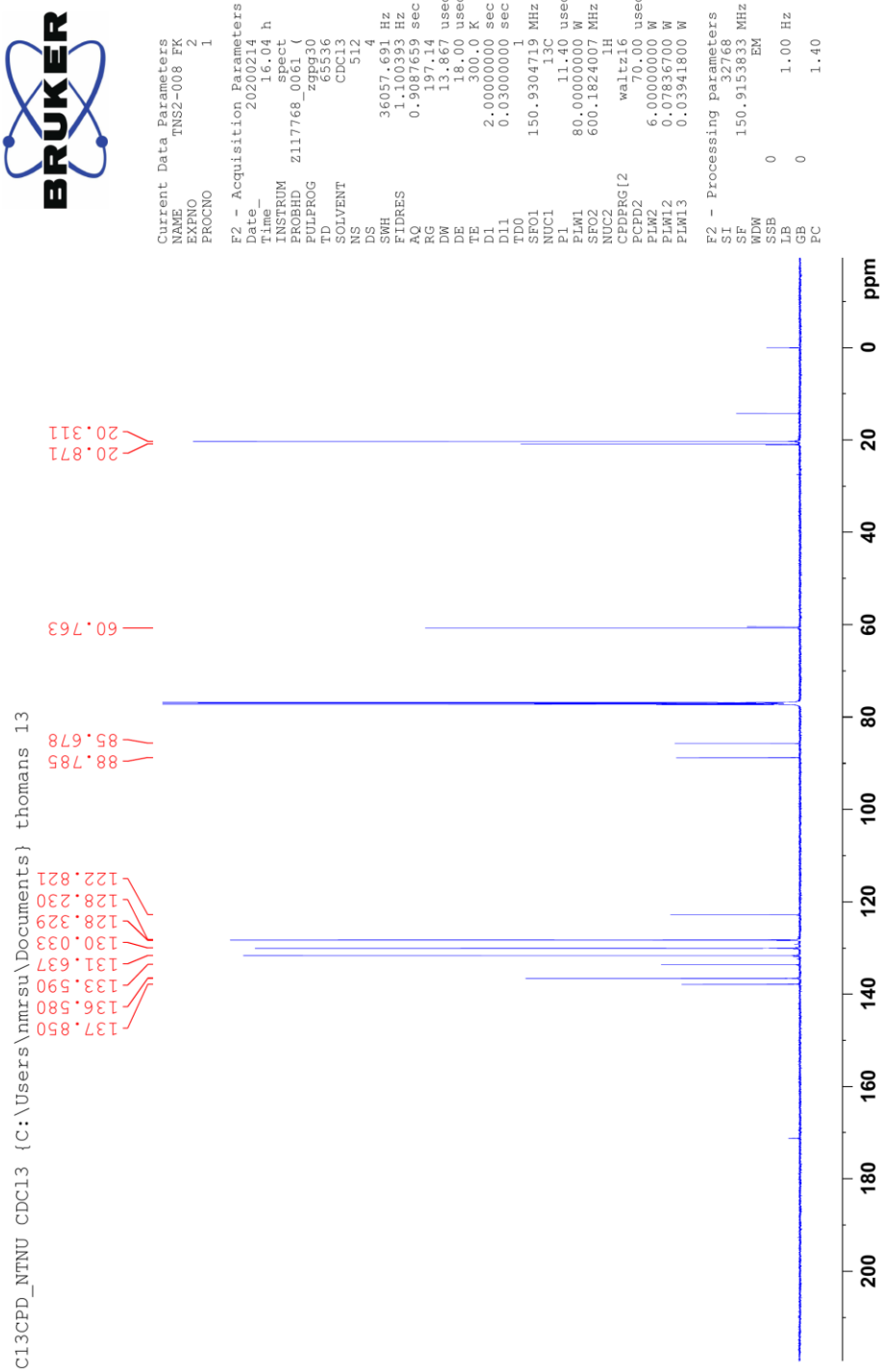

Appendix C Spectra of Propargyl Alcohols, 1a-i

Appendix C.12 **COSY NMR spectrum of Propargyl Alcohol 1e**

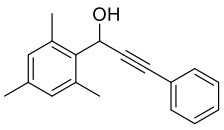

1e

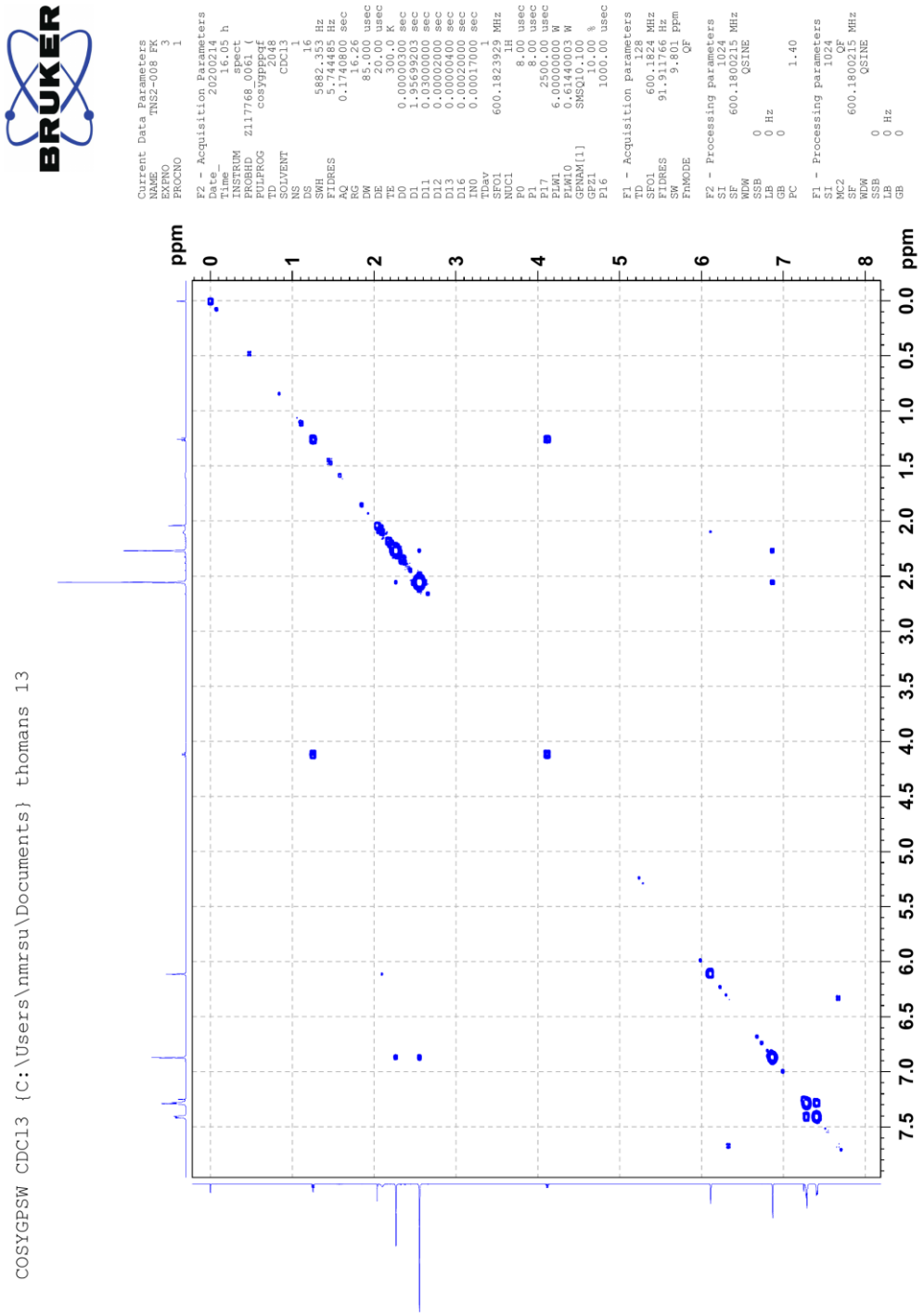

Appendix C Spectra of Propargyl Alcohols, 1a-i

Appendix C.13 **HSQC NMR spectrum of Propargyl Alcohol 1e**

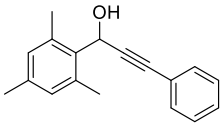

1e

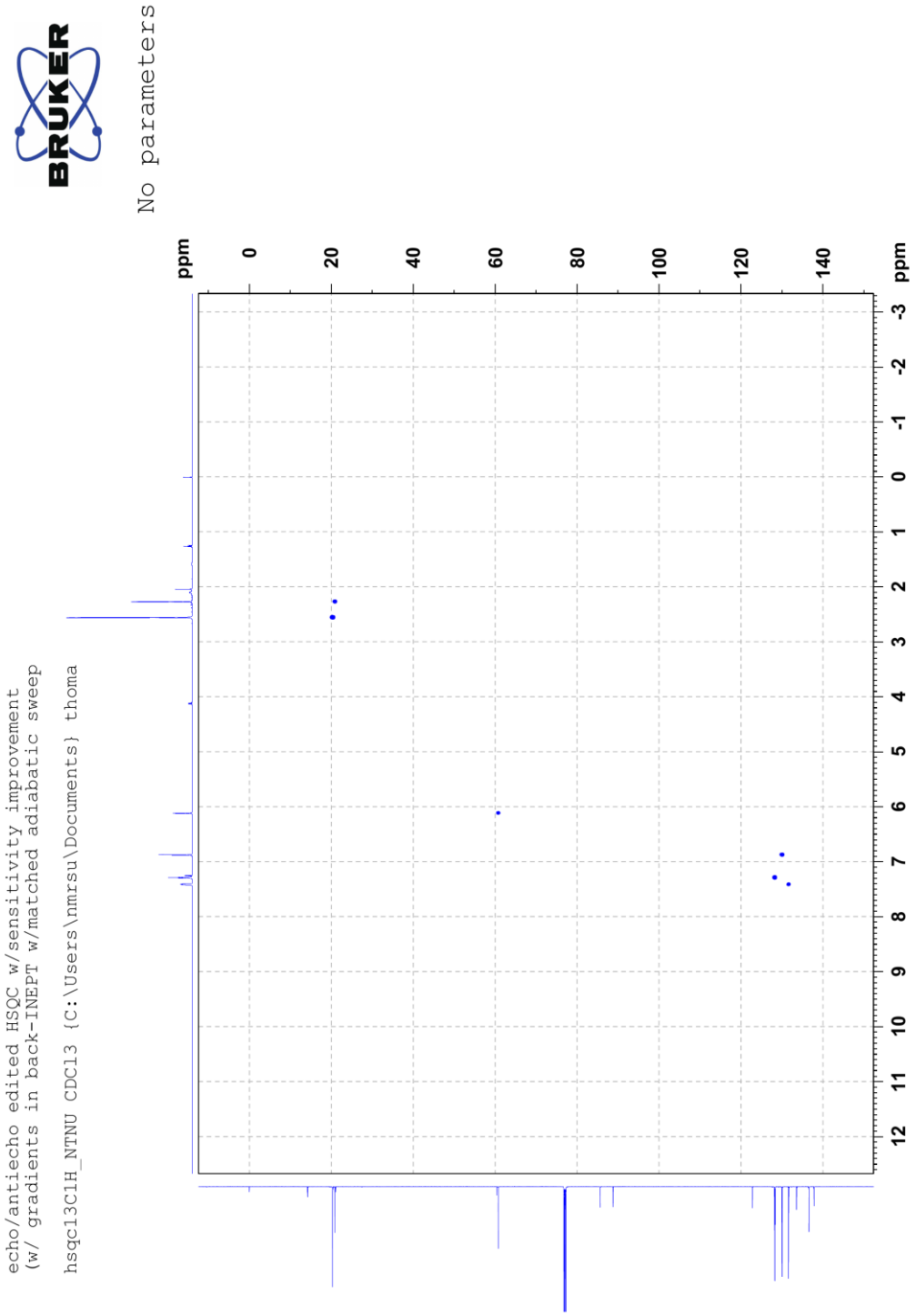

Appendix C Spectra of Propargyl Alcohols, 1a-i

Appendix C.14 **HMBC NMR spectrum of Propargyl Alcohol 1**e

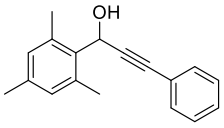

1e

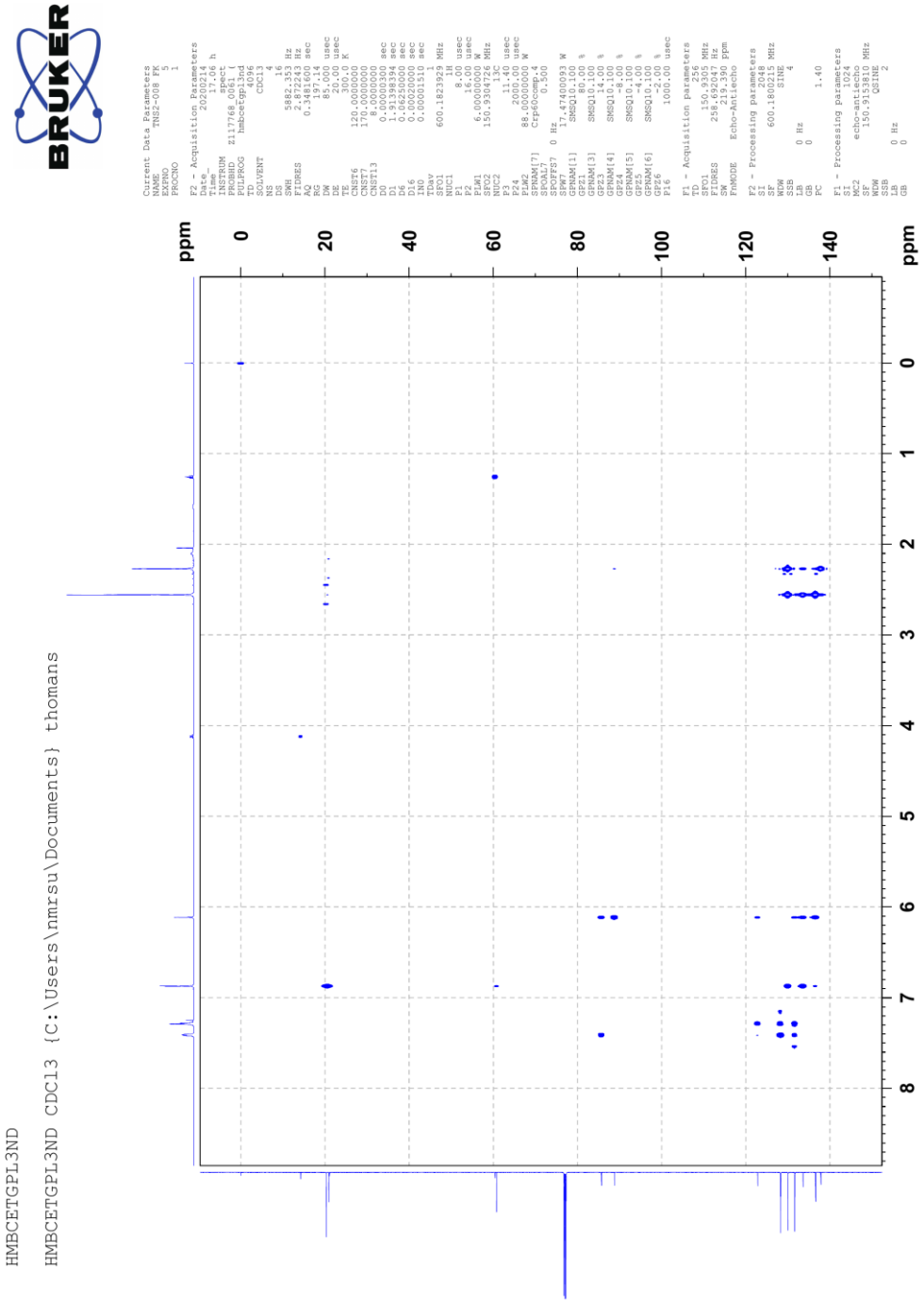

Appendix C Spectra of Propargyl Alcohols, 1a-i

Appendix C.15 **HRMS spectrum of Propargyl Alcohol 1e**

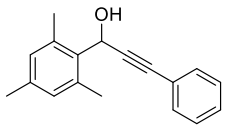

1e

Elemental Composition Report **Page 1**

Single Mass Analysis
Tolerance = 1.0 PPM / DBE: min = -50.0, max = 50.0
Element prediction: Off
Number of isotope peaks used for i-FIT = 3

Monoisotopic Mass, Even Electron Ions
401 formula(e) evaluated with 1 results within limits (all results (up to 1000) for each mass)
Elements Used:
C: 0-100 H: 0-150 10B: 0-3 O: 0-10
2019-676 40 (0.792) AM2 (Ar,35000.0,0.00,0.00); Cm (21:44)
1: TOF MS ASAP+

1.27e+008

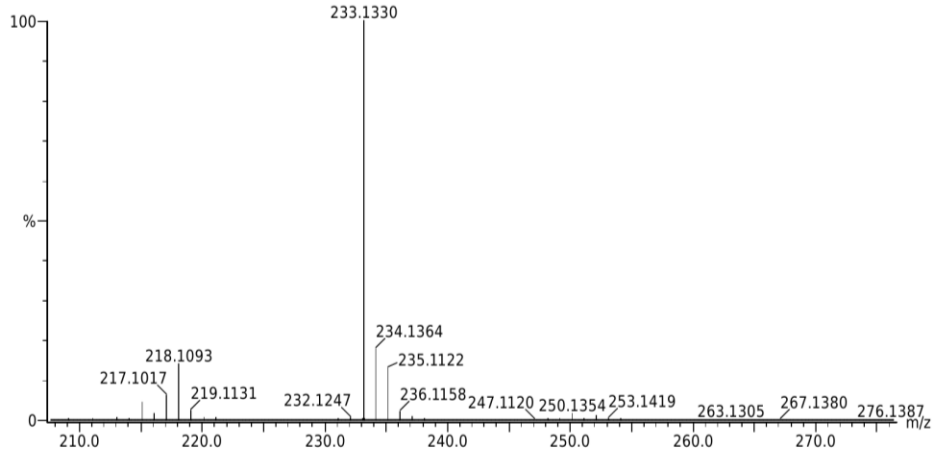

Minimum:				-50.0				
Maximum:		5.0	1.0	50.0				
Mass	Calc. Mass	mDa	PPM	DBE	i-FIT	Norm	Conf(%)	Formula
233.1330	233.1330	0.0	0.0	10.5	2328.1	n/a	n/a	C18 H17

Appendix C Spectra of Propargyl Alcohols, 1a-i

Appendix C.16 **^{1}H NMR spectrum of Propargyl Alcohol 1**f

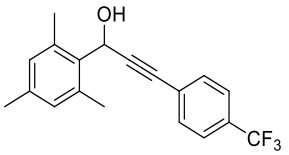

1f

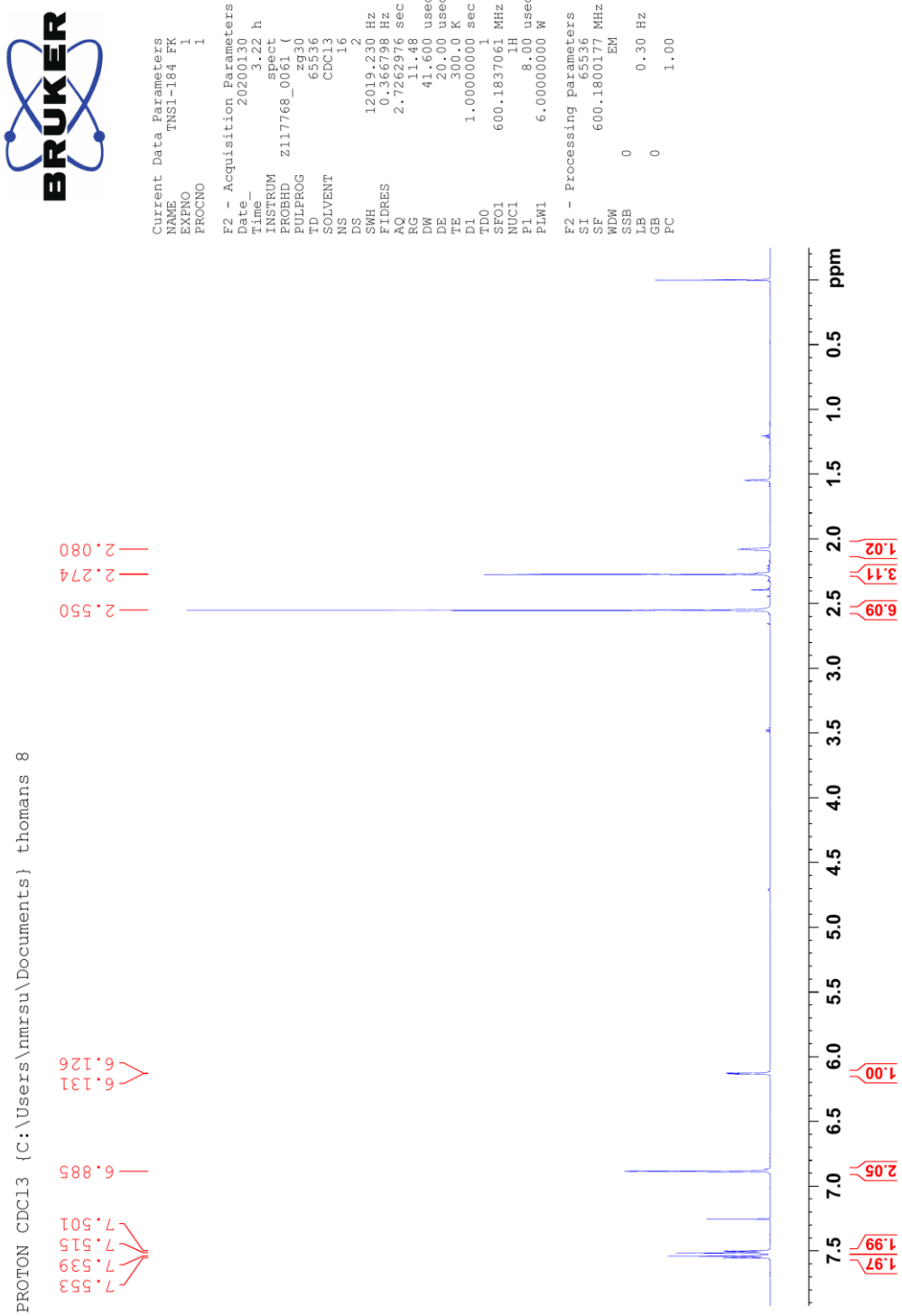

Appendix C Spectra of Propargyl Alcohols, 1a-i

Appendix C.17 **^{13}C NMR spectrum of Propargyl Alcohol 1f**

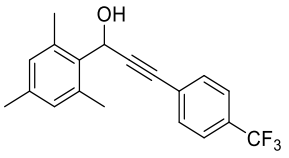

1f

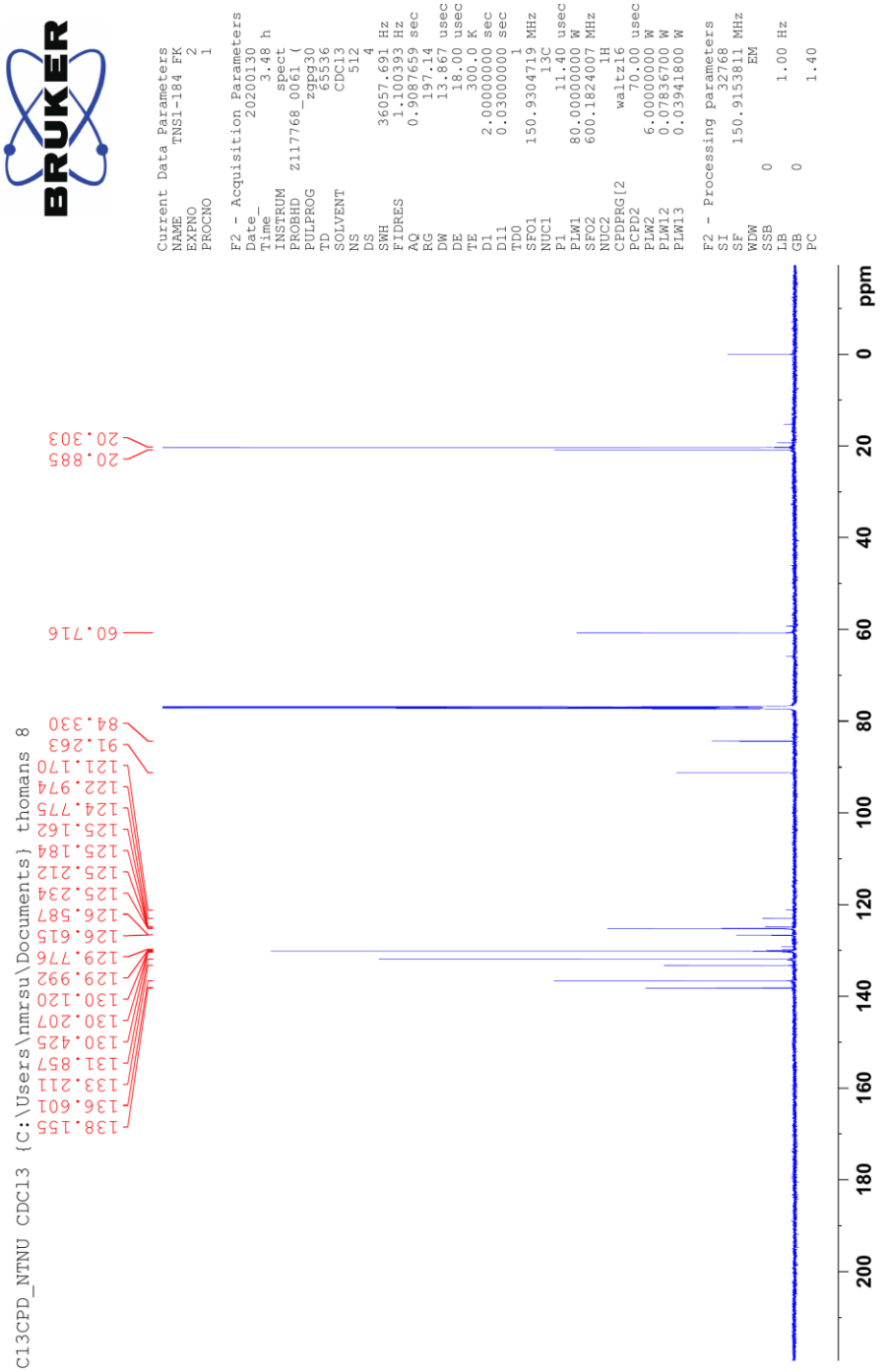

Appendix C Spectra of Propargyl Alcohols, 1a-i

Appendix C.18 **COSY NMR spectrum of Propargyl Alcohol 1**f

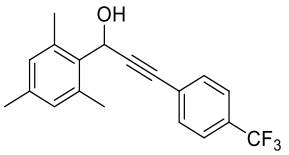

1f

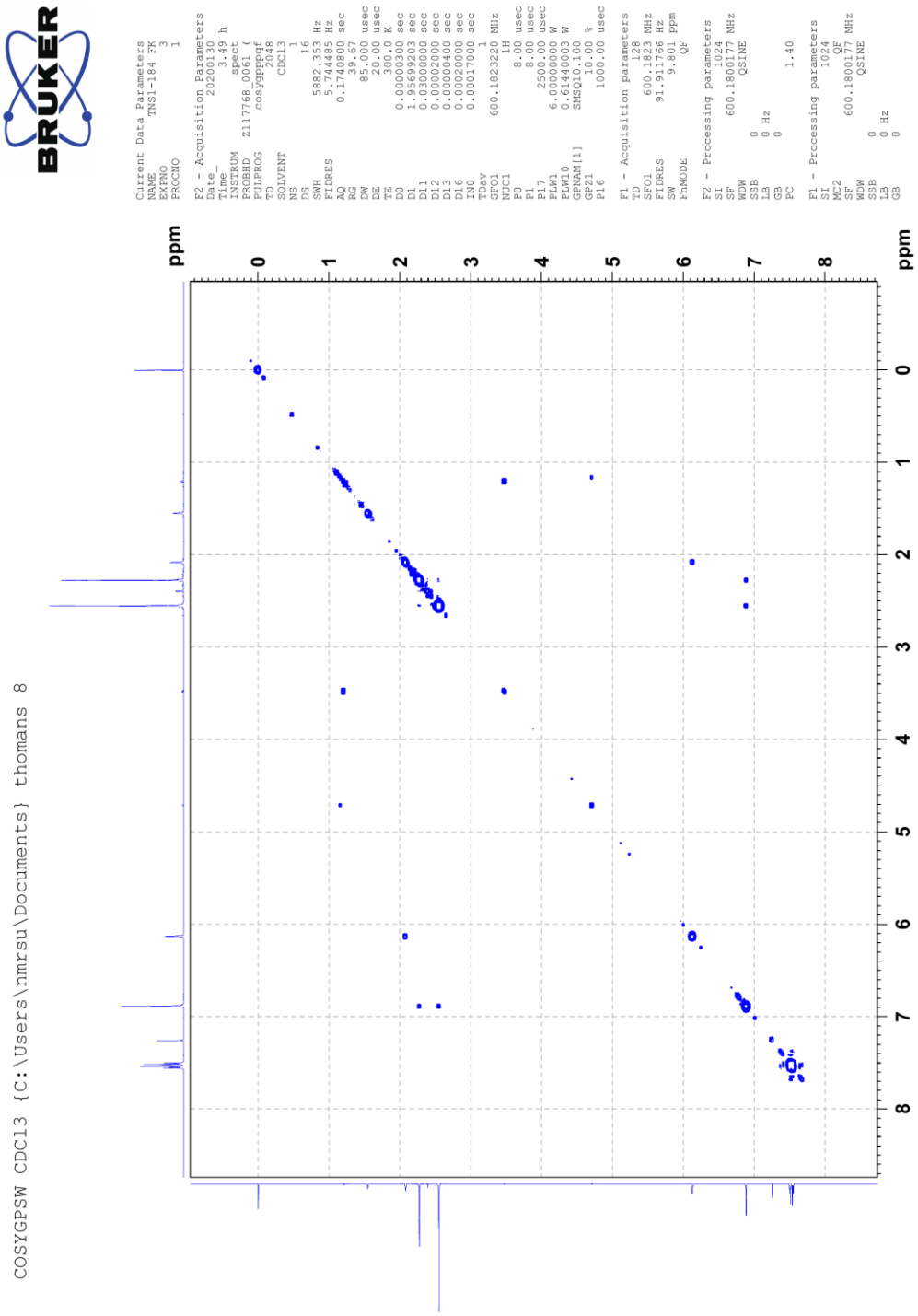

Appendix C Spectra of Propargyl Alcohols, 1a-i

Appendix C.19 **HSQC NMR spectrum of Propargyl Alcohol 1**f

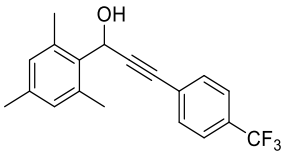

1f

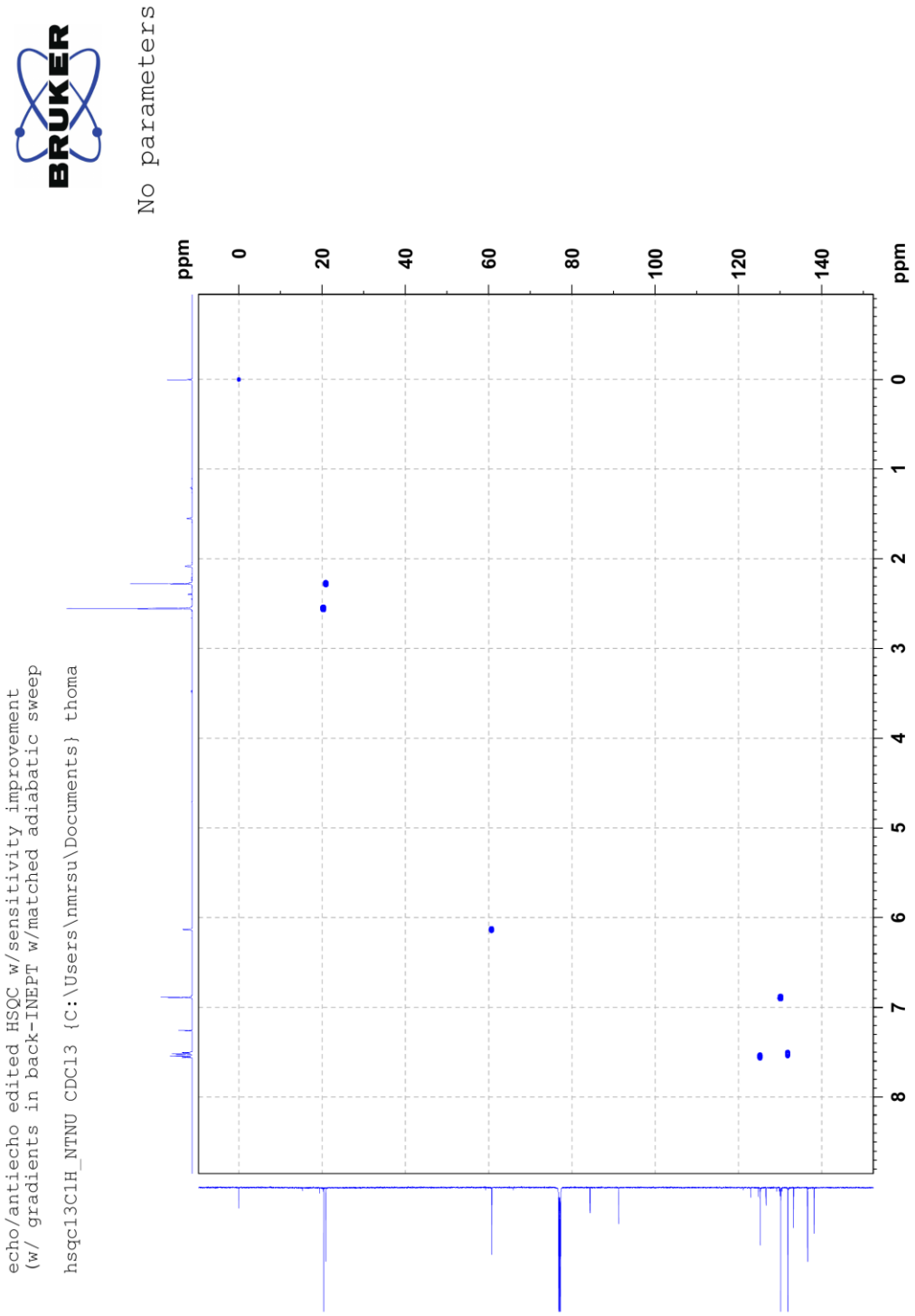

Appendix C Spectra of Propargyl Alcohols, 1a-i

Appendix C.20 **HMBC NMR spectrum of Propargyl Alcohol 1**f

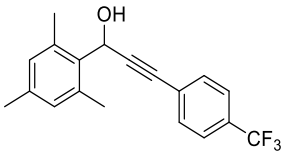

1f

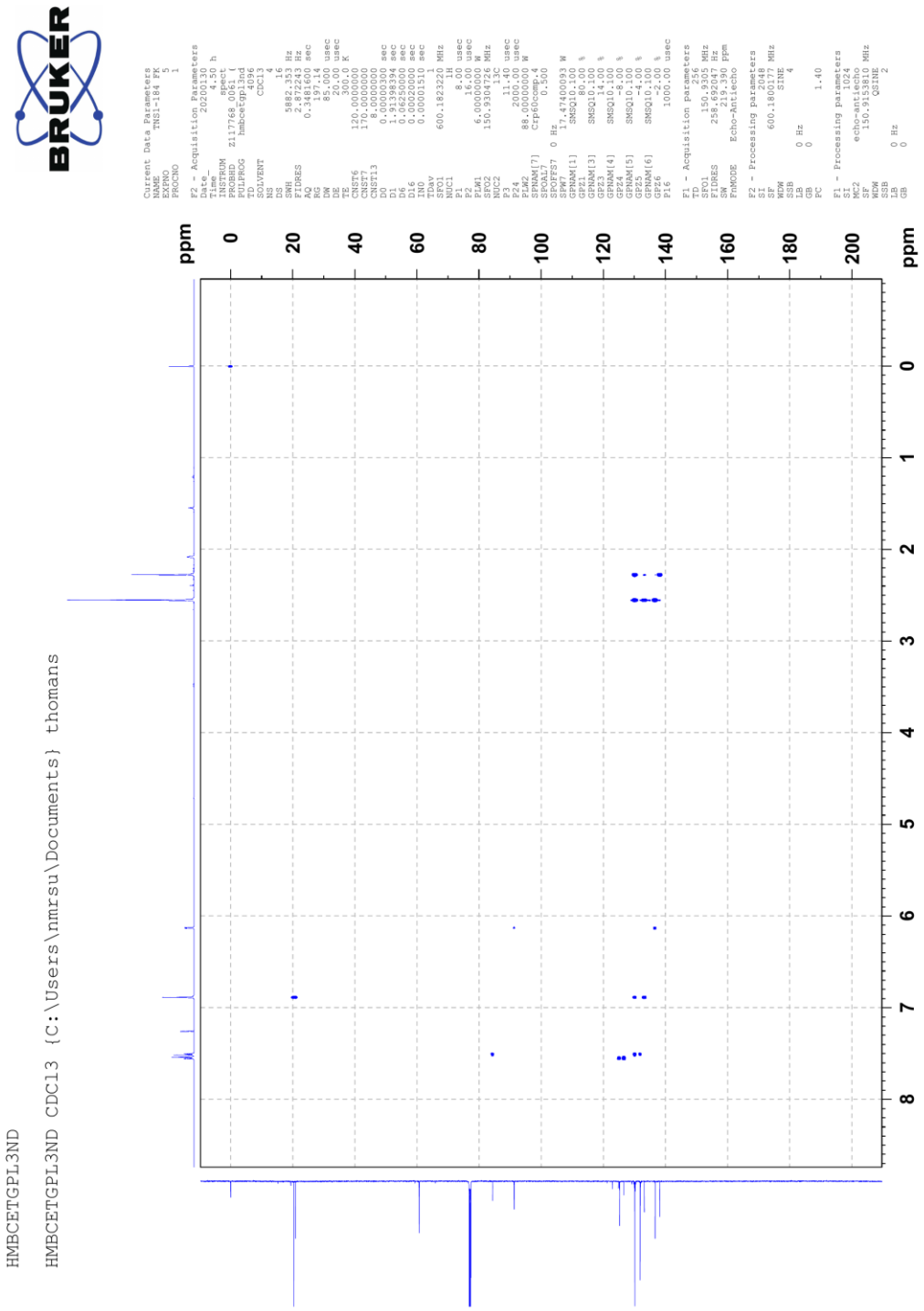

Appendix C Spectra of Propargyl Alcohols, 1a-i

Appendix C.21 **HRMS spectrum of Propargyl Alcohol 1f**

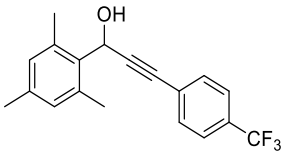

1f

Elemental Composition Report **Page 1**

Single Mass Analysis
Tolerance = 2.0 PPM / DBE: min = -50.0, max = 50.0
Element prediction: Off
Number of isotope peaks used for i-FIT = 3

Monoisotopic Mass, Odd Electron Ions
747 formula(e) evaluated with 1 results within limits (all results (up to 1000) for each mass)
Elements Used:
C: 0-100 H: 0-150 O: 0-10 F: 0-6
2019-645 36 (0.724) AM2 (Ar,35000.0,0.00,0.00); Cm (33:36)
1: TOF MS ASAP+

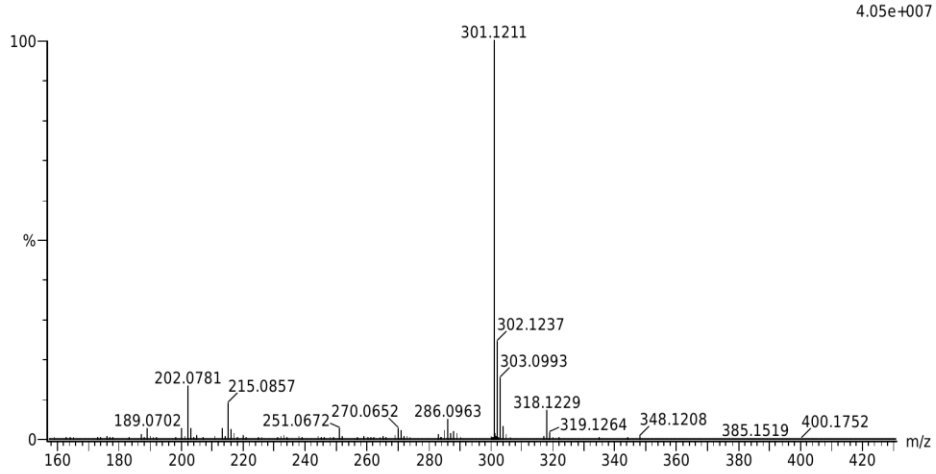

Minimum:				-50.0				
Maximum:		5.0	2.0	50.0				
Mass	Calc. Mass	mDa	PPM	DBE	i-FIT	Norm	Conf(%)	Formula
318.1229	318.1231	-0.2	-0.6	10.0	1595.5	n/a	n/a	C19 H17 O F3

Appendix C Spectra of Propargyl Alcohols, 1a-i

Appendix C.22 **^{1}H NMR spectrum of Propargyl Alcohol 1**g

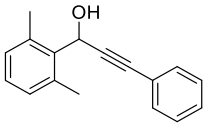

1g

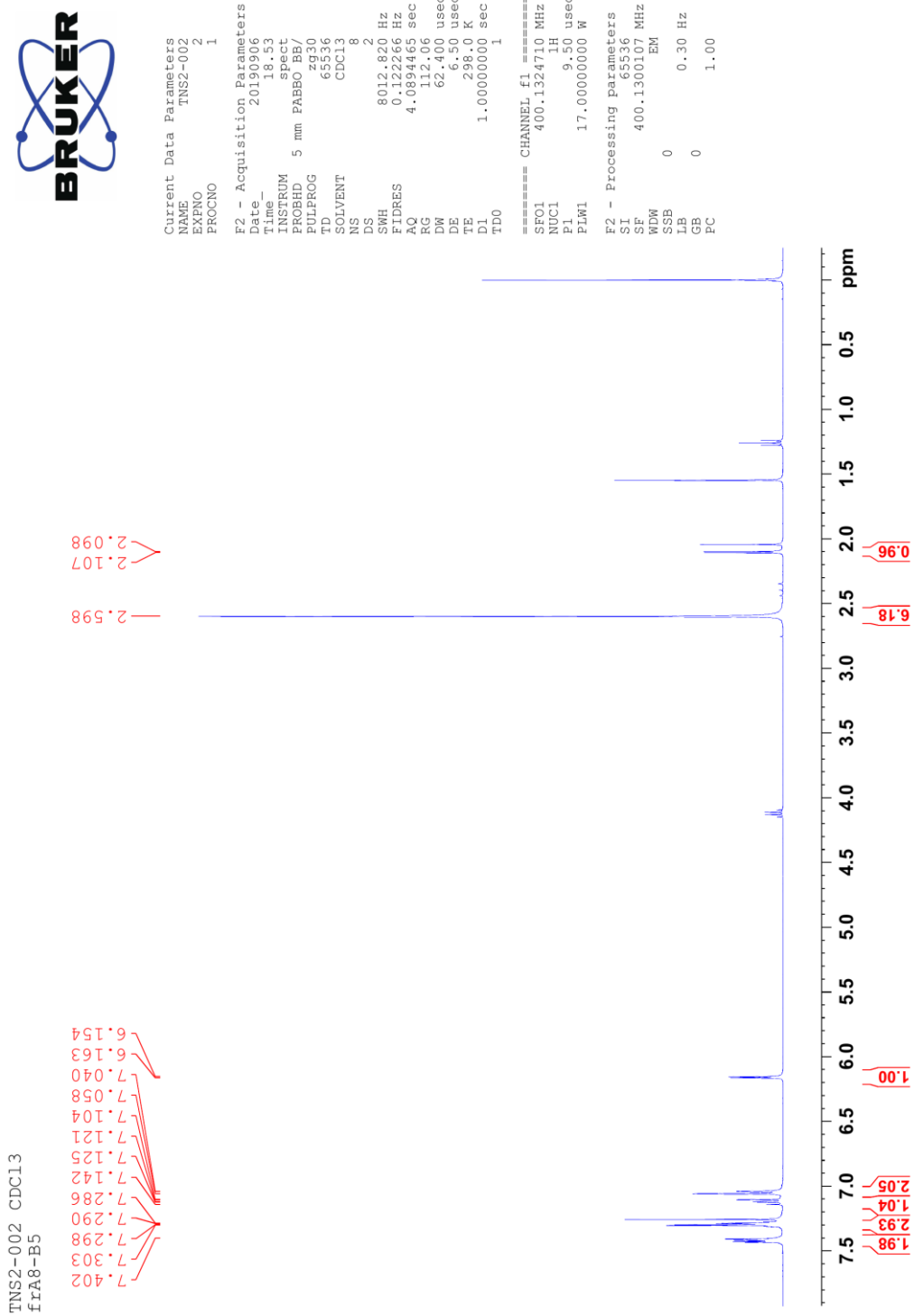

Appendix C Spectra of Propargyl Alcohols, 1a-i

Appendix C.23 **^{1}H NMR spectrum of Propargyl Alcohol 1h**

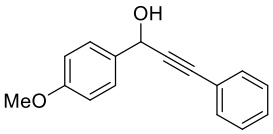

1h

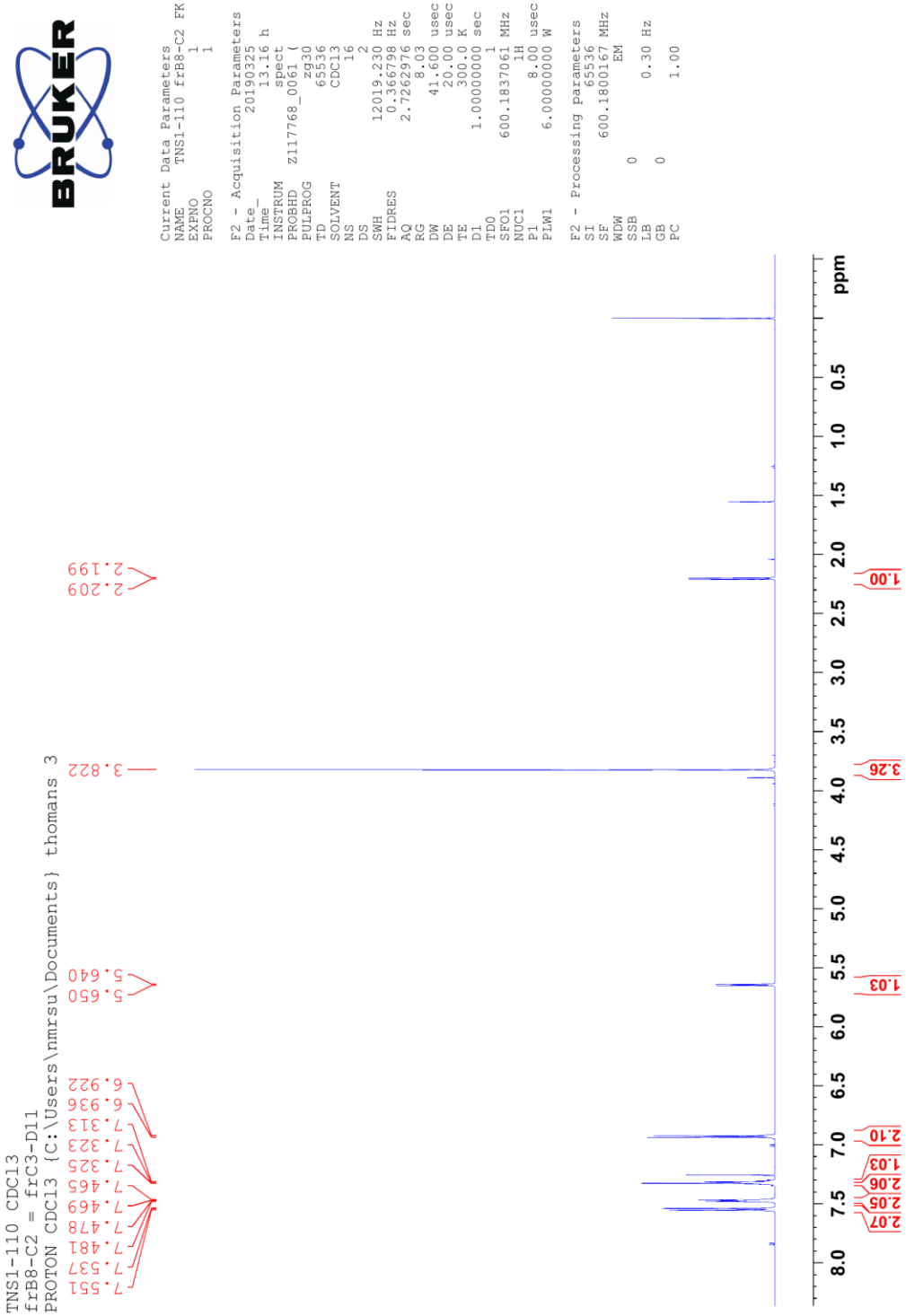

Appendix C Spectra of Propargyl Alcohols, 1a-i

Appendix C.24 **^{1}H NMR spectrum of Propargyl Alcohol 1**i

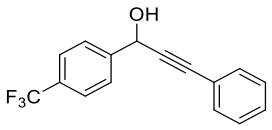

1i

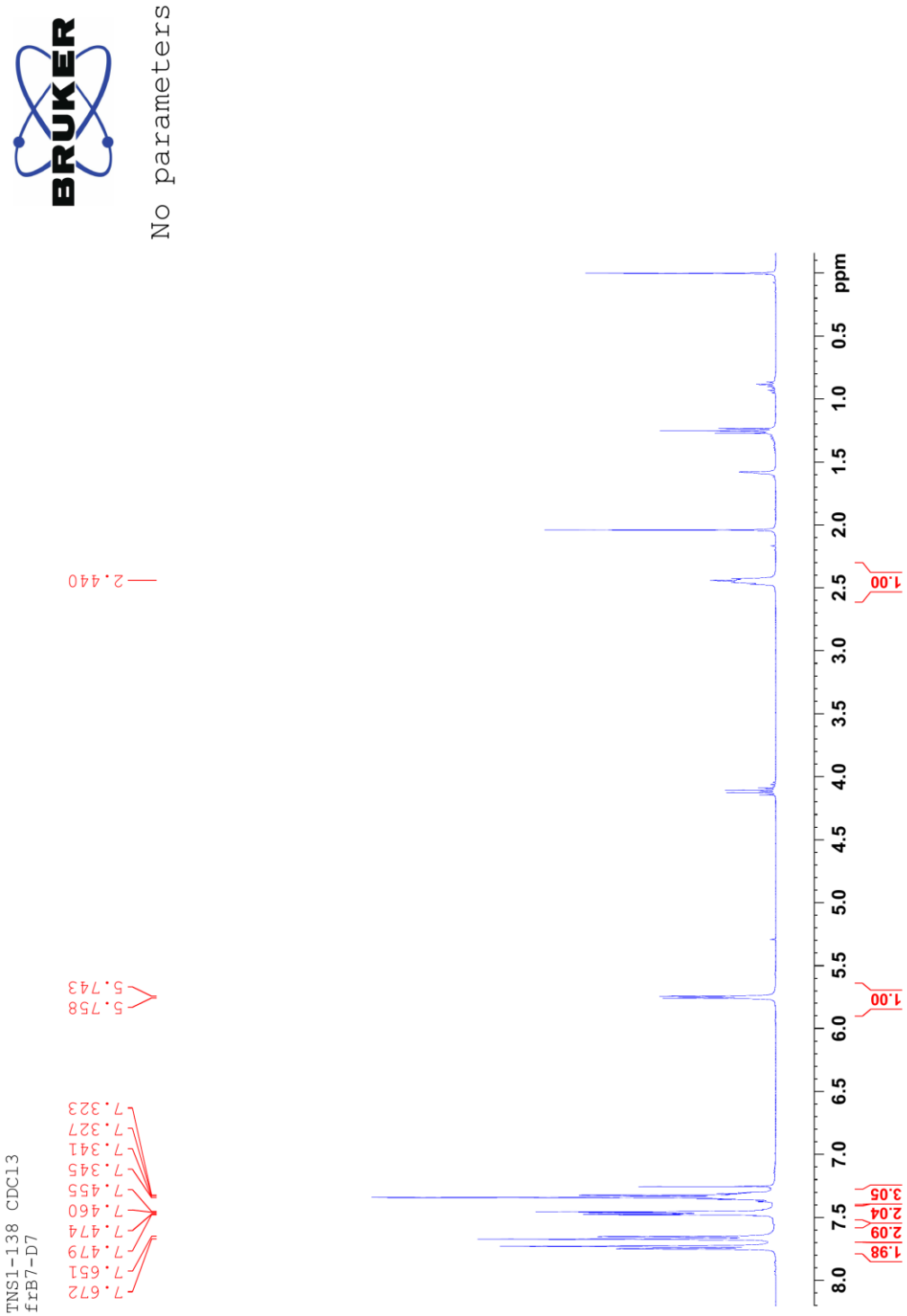

Appendix D **Spectra of 1,1,3-trisubstituted prop-2-yns, 2a-h**

Appendix D.1 **^{1}H NMR Spectrum of Mixture of Alkyne 2a and Indene 4a**

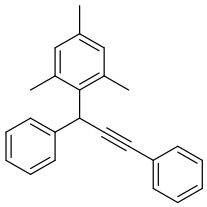

2a

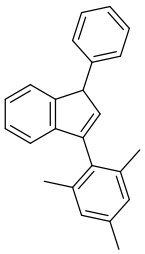

4a

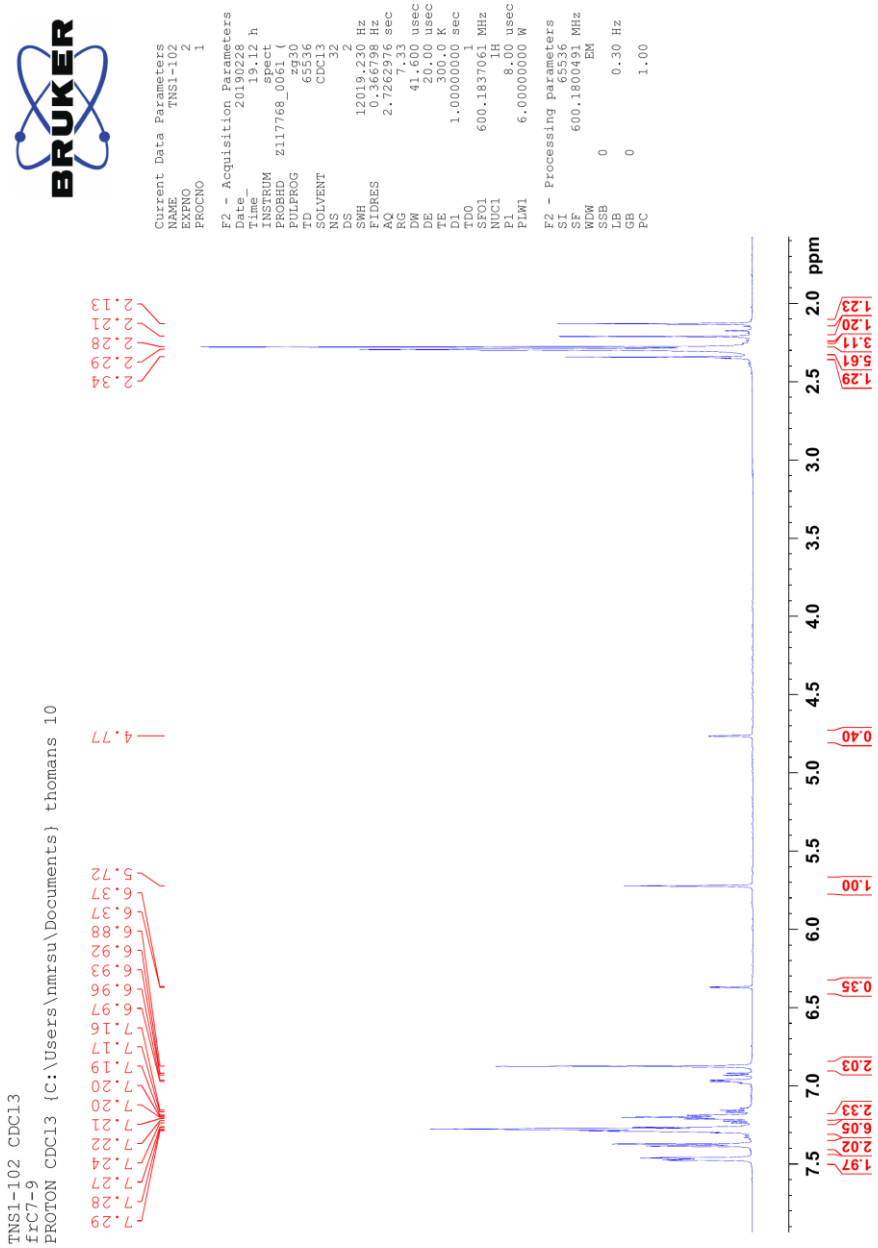

Appendix D Spectra of 1,1,3-trisubstituted prop-2-yns, 2a-h

Appendix D.2 **^{1}H NMR Spectrum of Alkyne 2b**

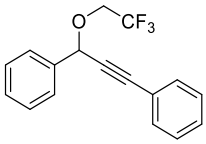

2b

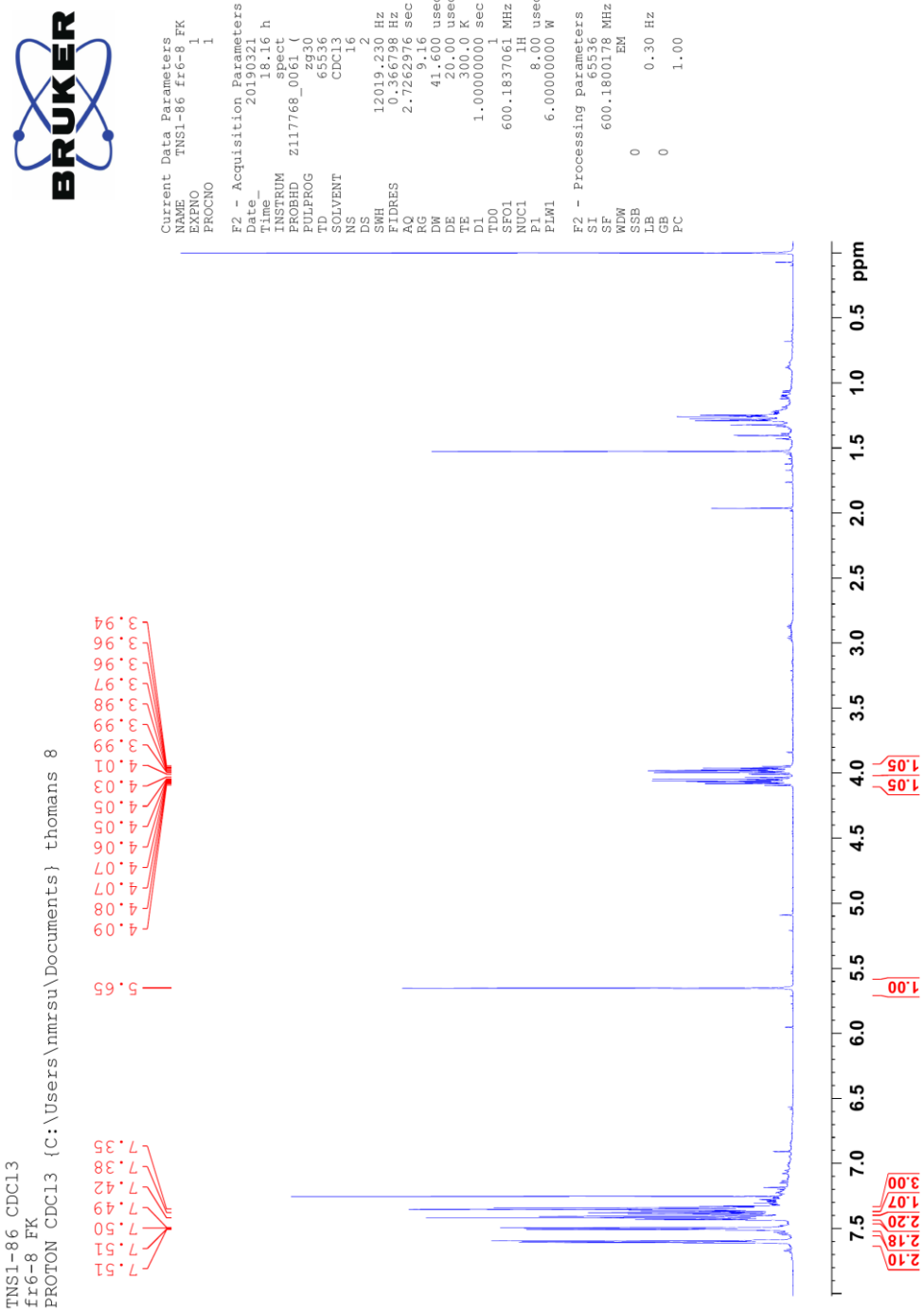

Appendix D Spectra of 1,1,3-trisubstituted prop-2-yns, 2a-h

Appendix D.3 **^{13}C NMR Spectrum of Alkyne 2b**

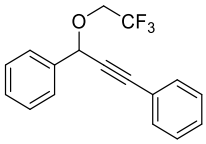

2b

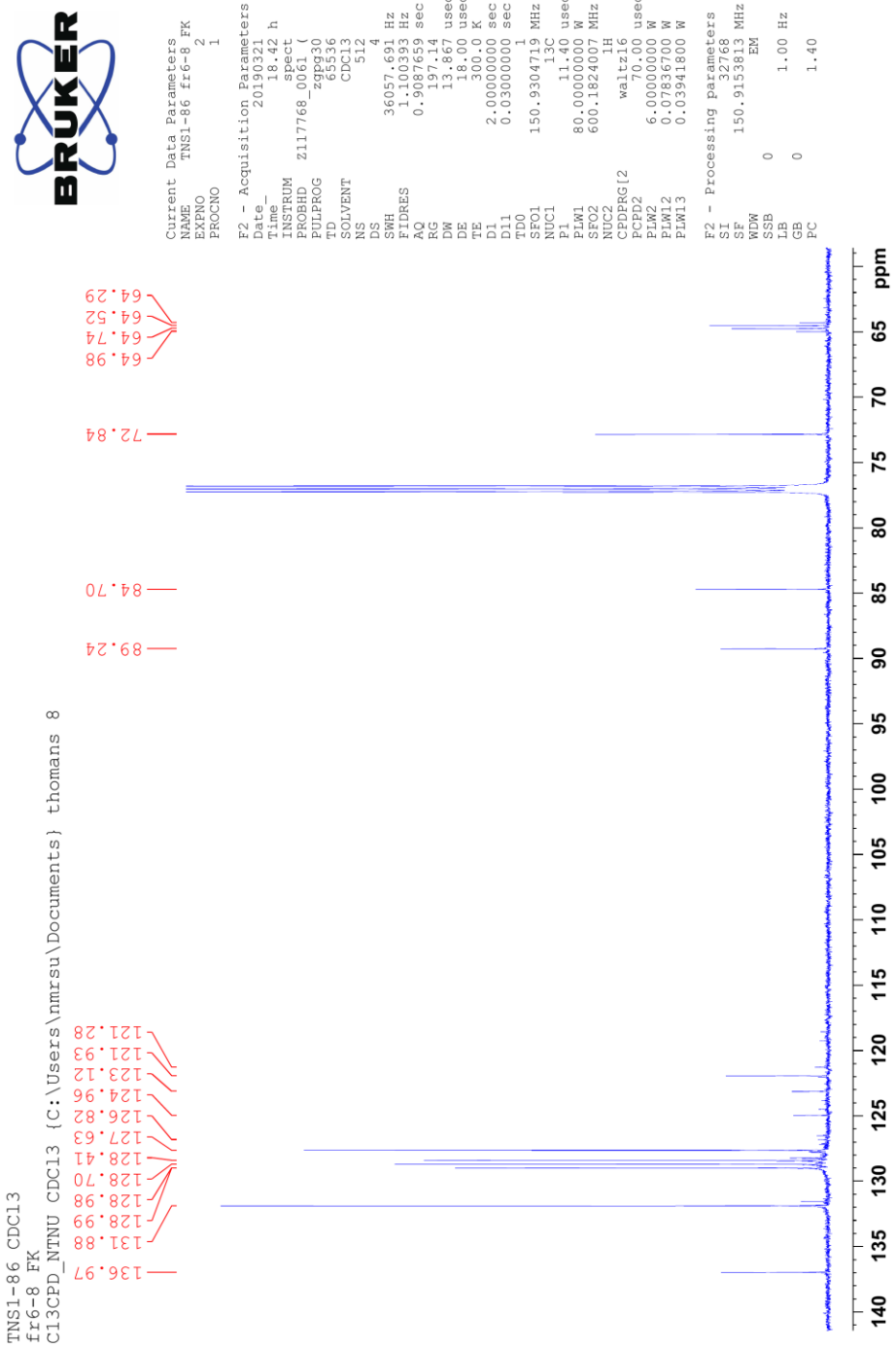

Appendix D Spectra of 1,1,3-trisubstituted prop-2-yns, 2a-h

Appendix D.4 **COSY NMR Spectrum of Alkyne 2b**

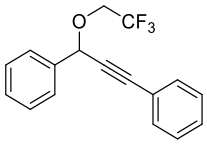

2b

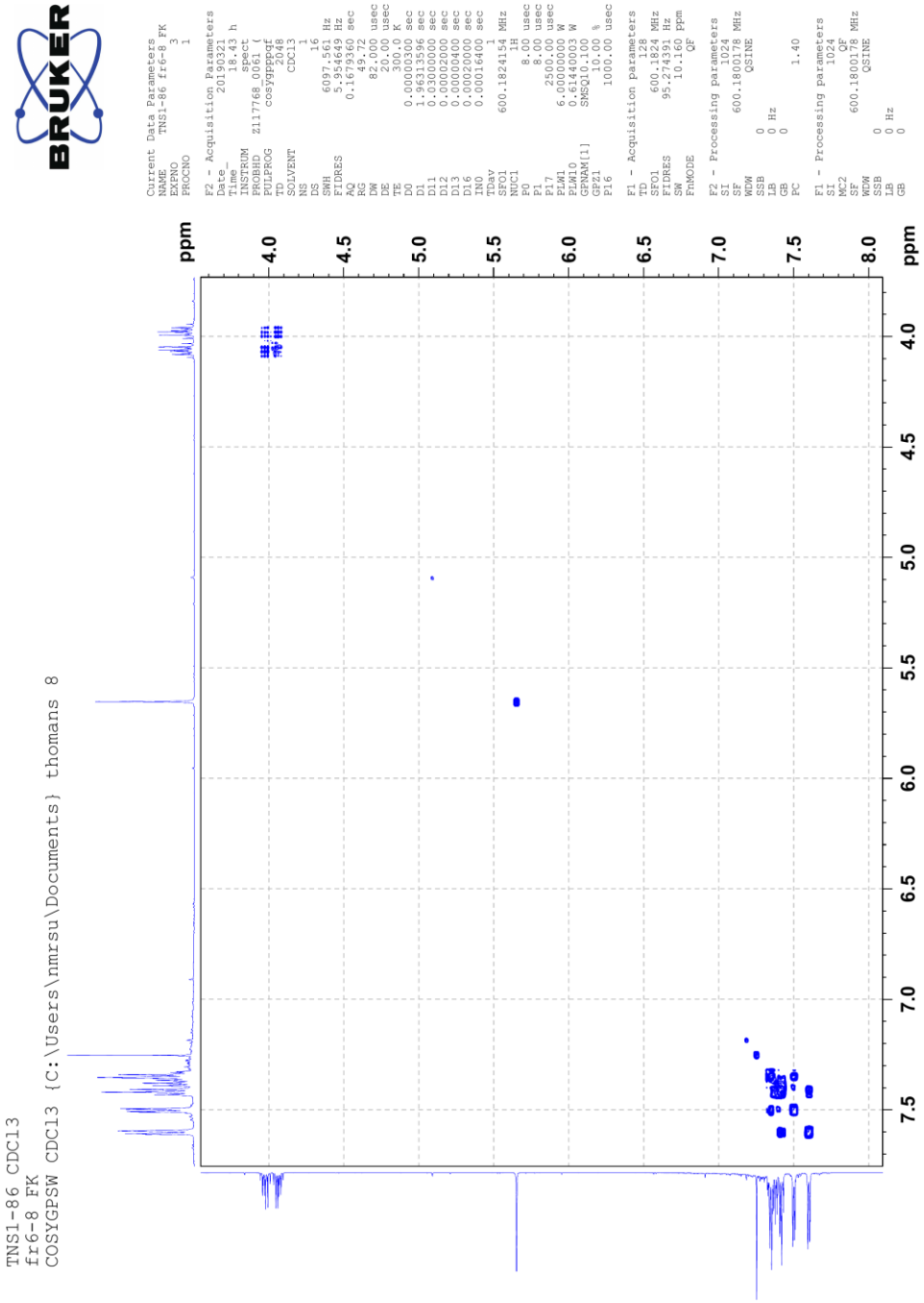

Appendix D Spectra of 1,1,3-trisubstituted prop-2-yns, 2a-h

Appendix D.5 **HSQC NMR Spectrum of Alkyne 2b**

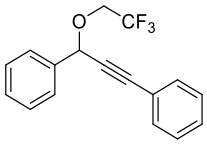

2b

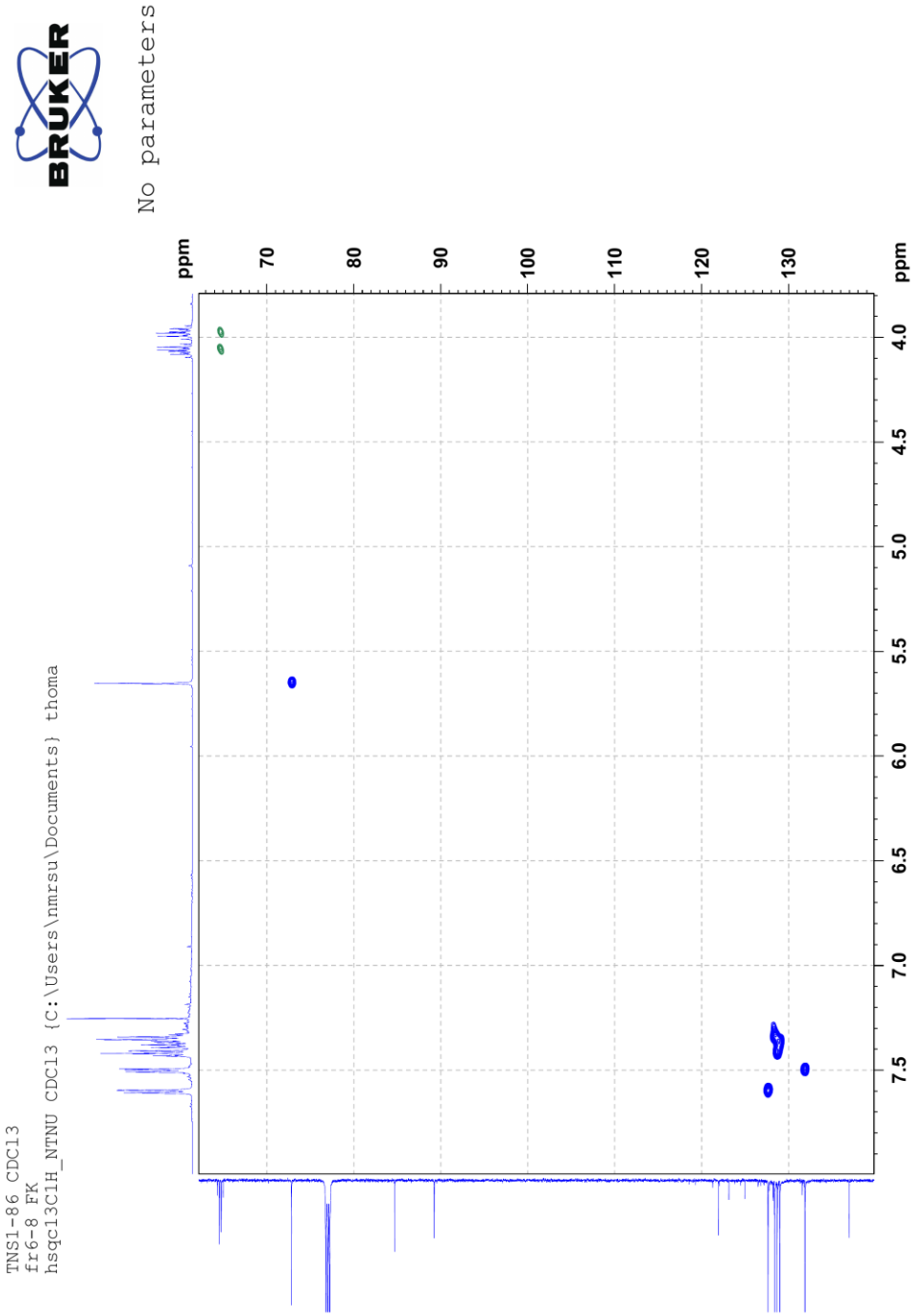

Appendix D Spectra of 1,1,3-trisubstituted prop-2-yns, 2a-h

Appendix D.6 **HMBC NMR Spectrum of Alkyne 2b**

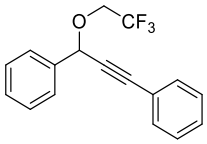

2b

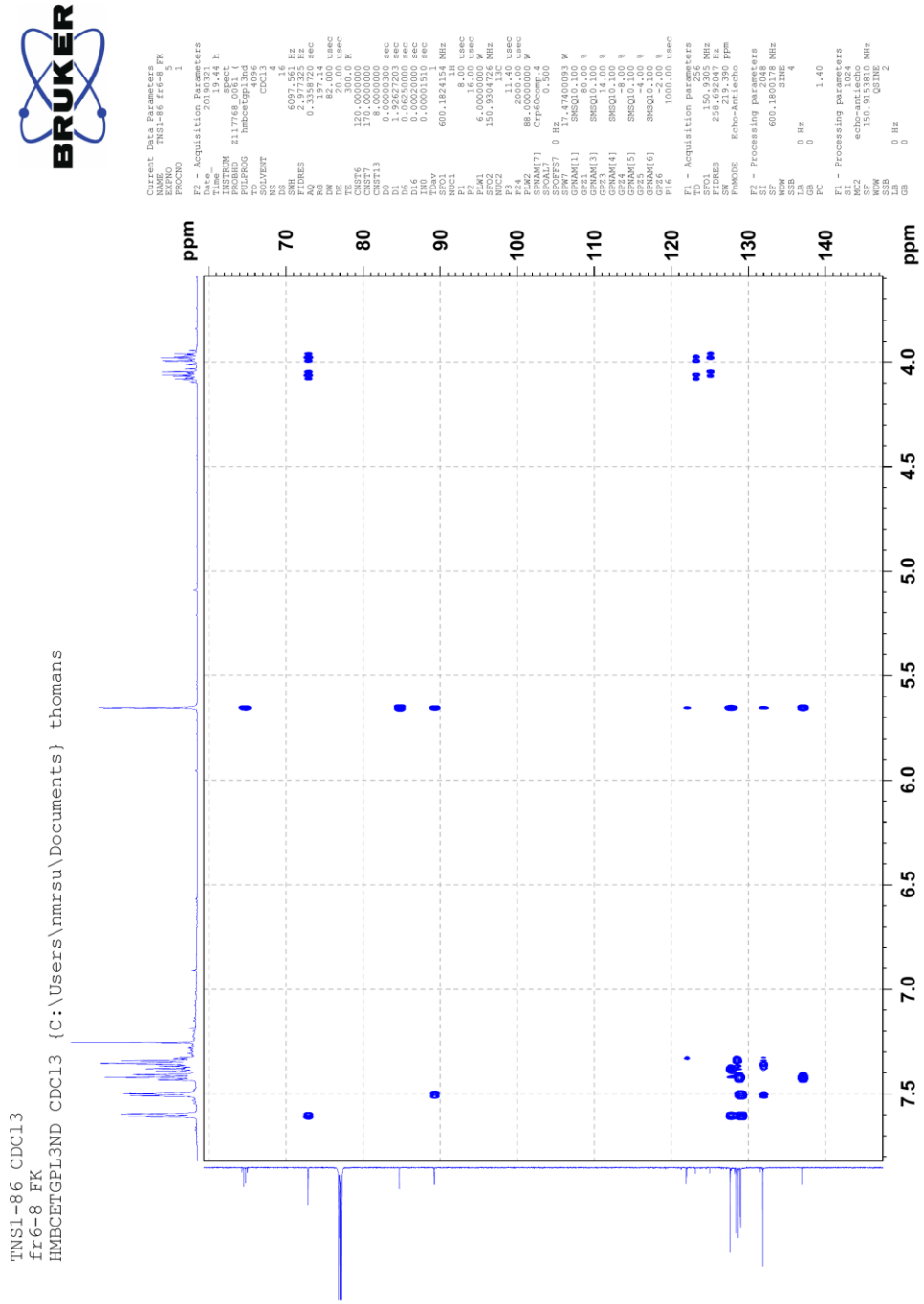

Appendix D Spectra of 1,1,3-trisubstituted prop-2-yns, 2a-h

Appendix D.7 **HRMS Spectrum of Alkyne 2b**

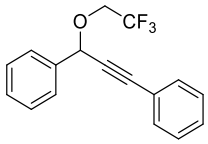

2b

Elemental Composition Report **Page 1**

Single Mass Analysis
Tolerance = 2.0 PPM / DBE: min = -50.0, max = 50.0
Element prediction: Off
Number of isotope peaks used for i-FIT = 3

Monoisotopic Mass, Odd Electron Ions
2399 formula(e) evaluated with 1 results within limits (all results (up to 1000) for each mass)
Elements Used:
C: 0-100 H: 0-150 N: 0-5 O: 0-5 F: 0-6
2019-294 52 (1.034) AM2 (Ar,35000.0,0.00,0.00); Cm (50:52)
1: TOF MS ASAP+

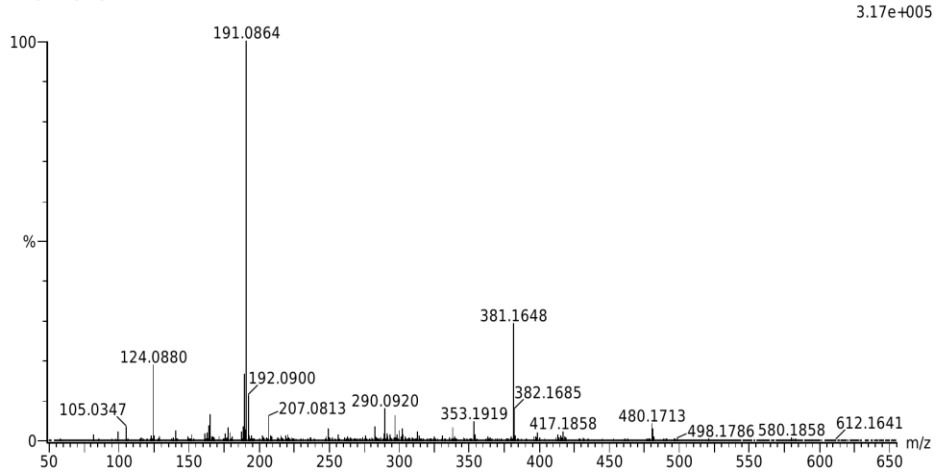

Minimum:				-50.0				
Maximum:		5.0	2.0	50.0				
Mass	Calc. Mass	mDa	PPM	DBE	i-FIT	Norm	Conf(%)	Formula
290.0920	290.0918	0.2	0.7	10.0	589.1	n/a	n/a	C17 H13 O F3

Appendix D Spectra of 1,1,3-trisubstituted prop-2-yns, 2a-h

Appendix D.8 **^{1}H NMR Spectrum of Alkyne 2c**

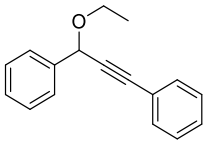

2c

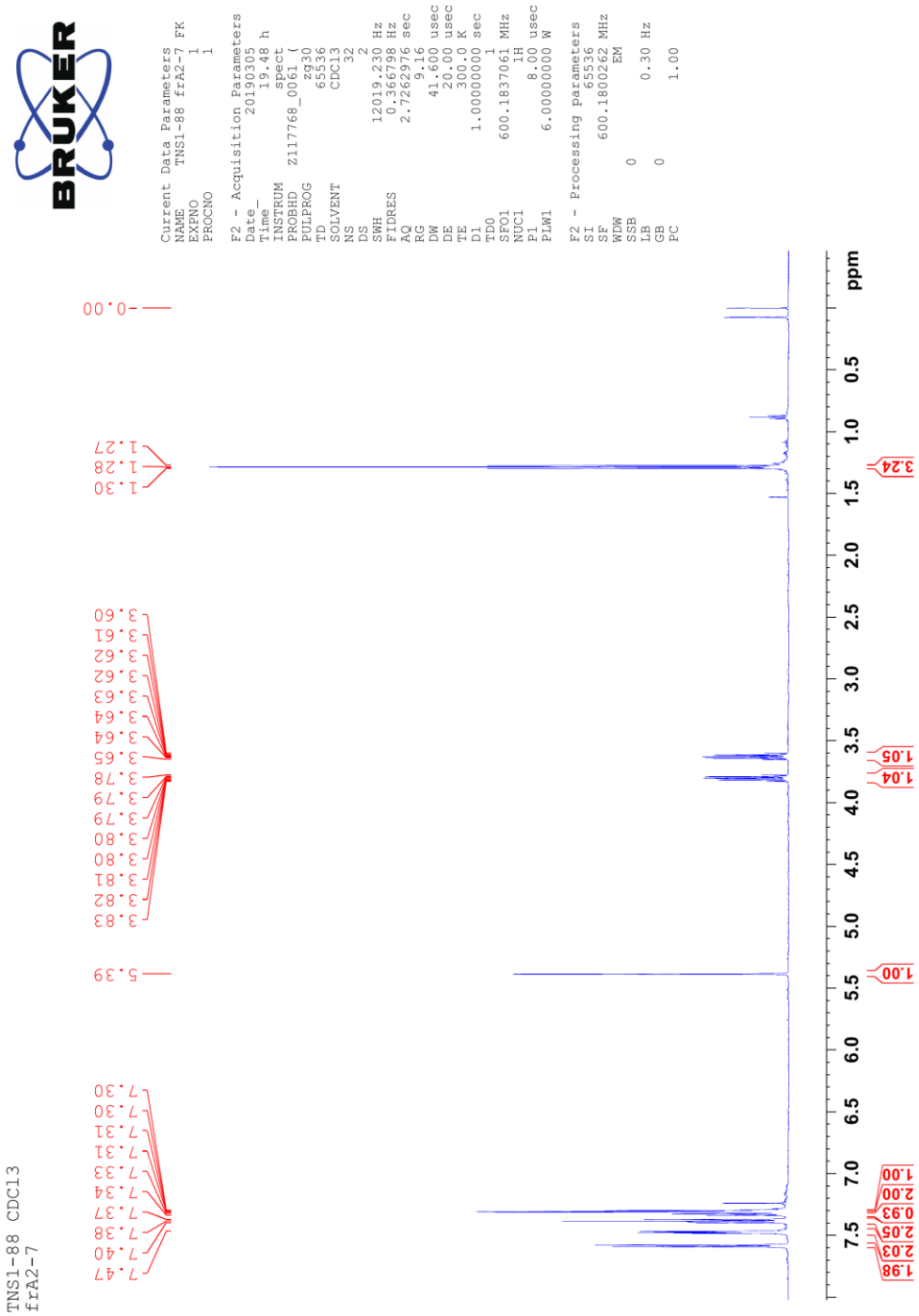

Appendix D Spectra of 1,1,3-trisubstituted prop-2-yns, 2a-h

Appendix D.9 **^{1}H NMR Spectrum of Alkyne 2d**

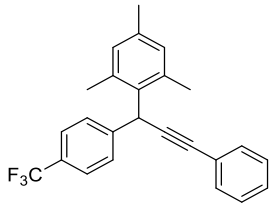

2d

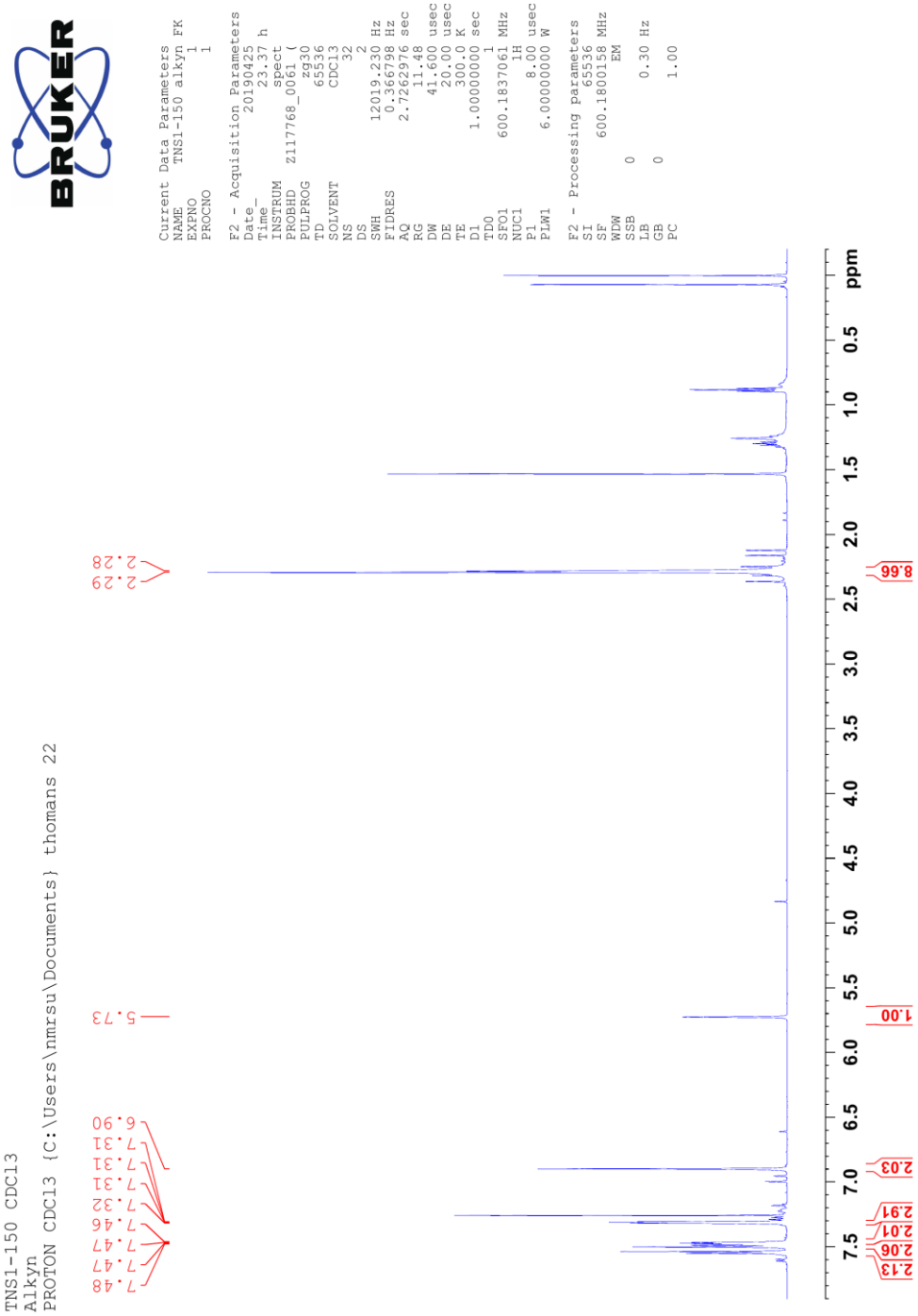

Appendix D Spectra of 1,1,3-trisubstituted prop-2-yns, 2a-h

Appendix D.10 **^{1}H NMR Spectrum of Mixture of Alkyne 2e and Allene 3c**

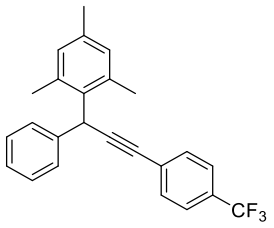

2e

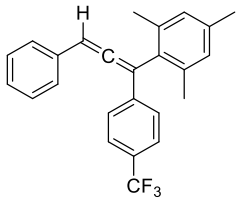

3c

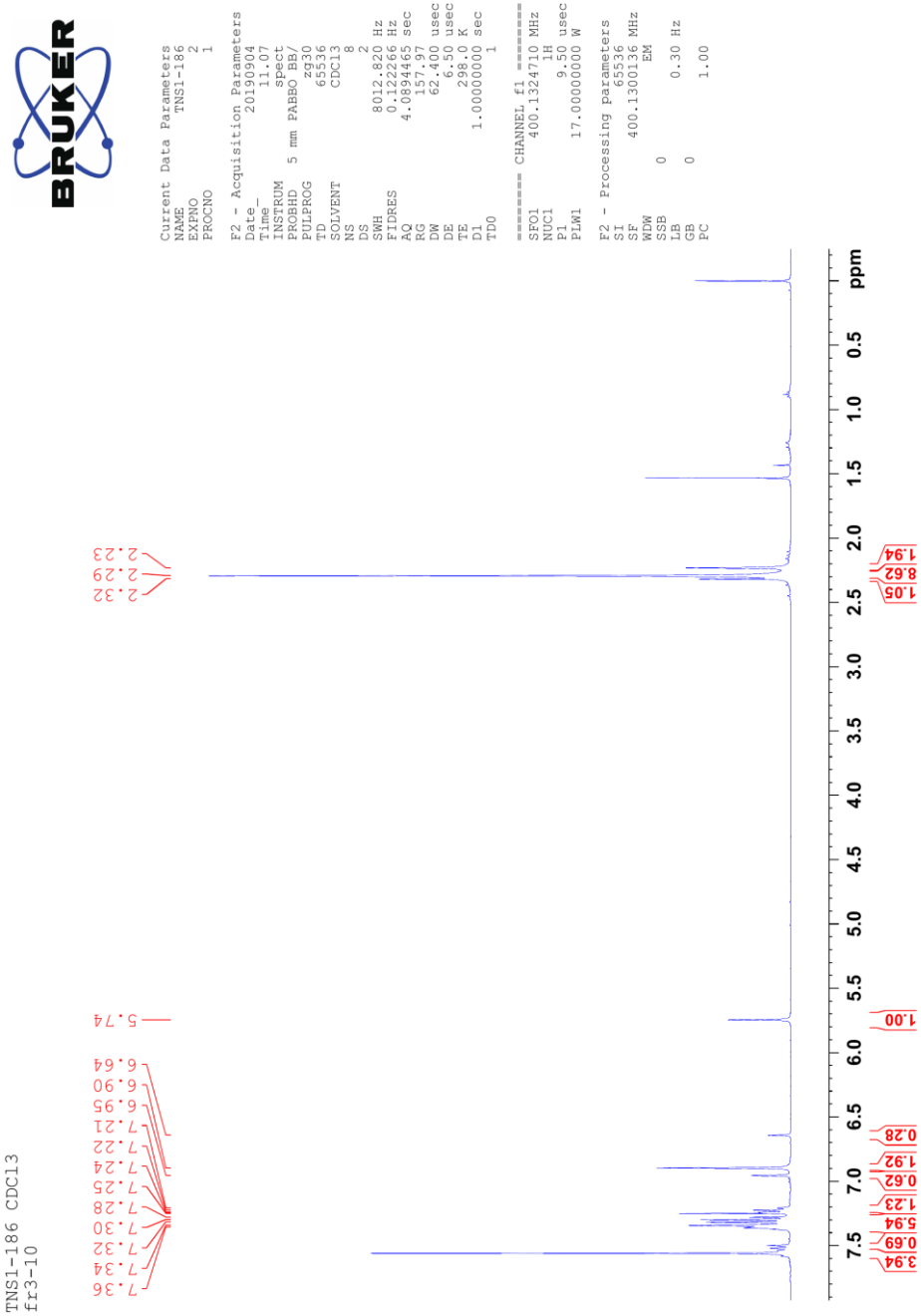

Appendix D Spectra of 1,1,3-trisubstituted prop-2-yns, 2a-h

Appendix D.11 **^{1}H NMR Spectrum of Alkyne 2f**

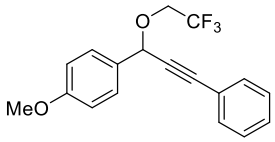

2f

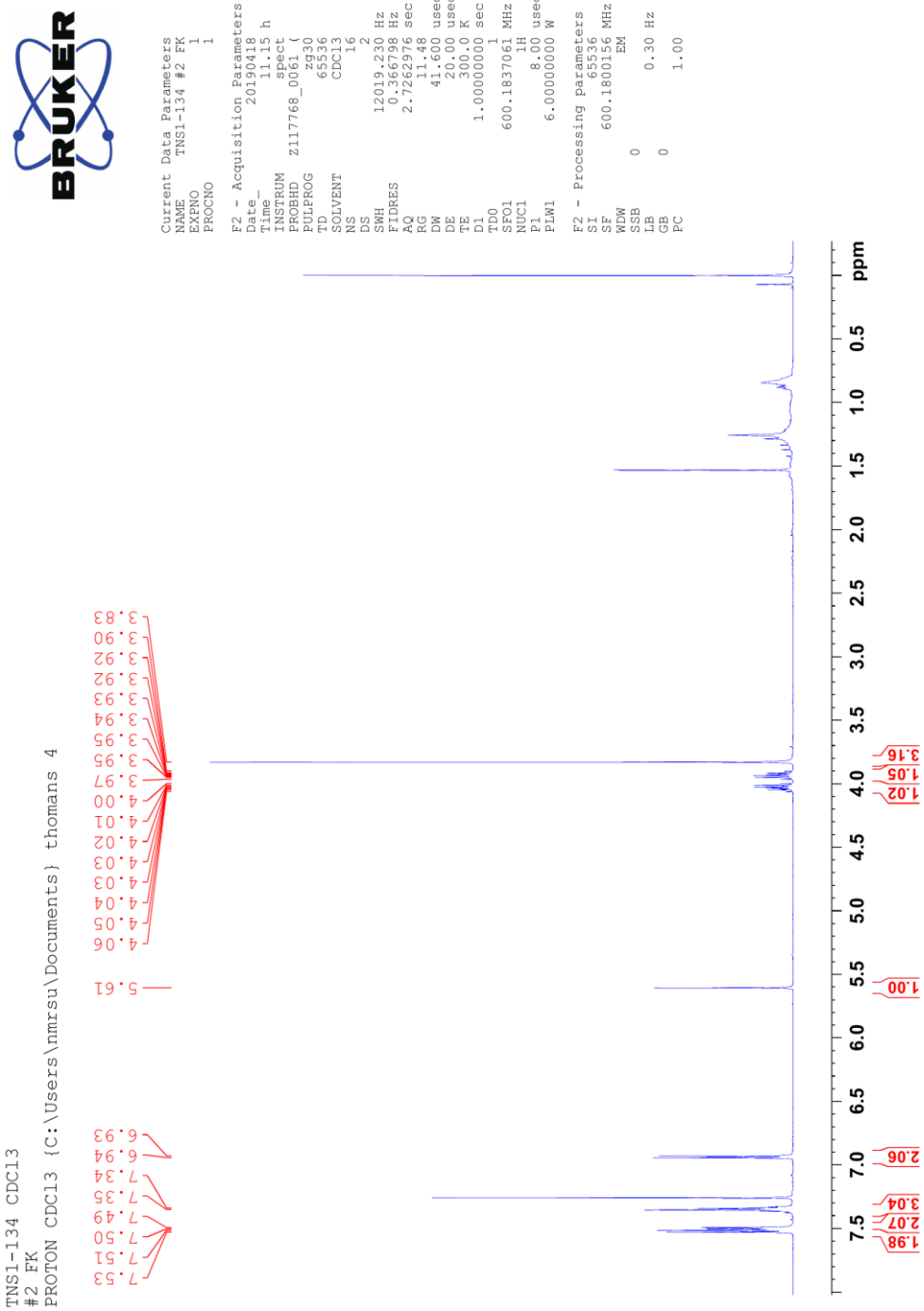

Appendix D Spectra of 1,1,3-trisubstituted prop-2-yns, 2a-h

Appendix D.12 **^{13}C NMR Spectrum of Alkyne 2f**

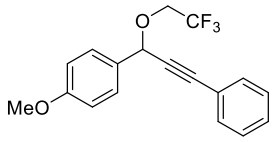

2f

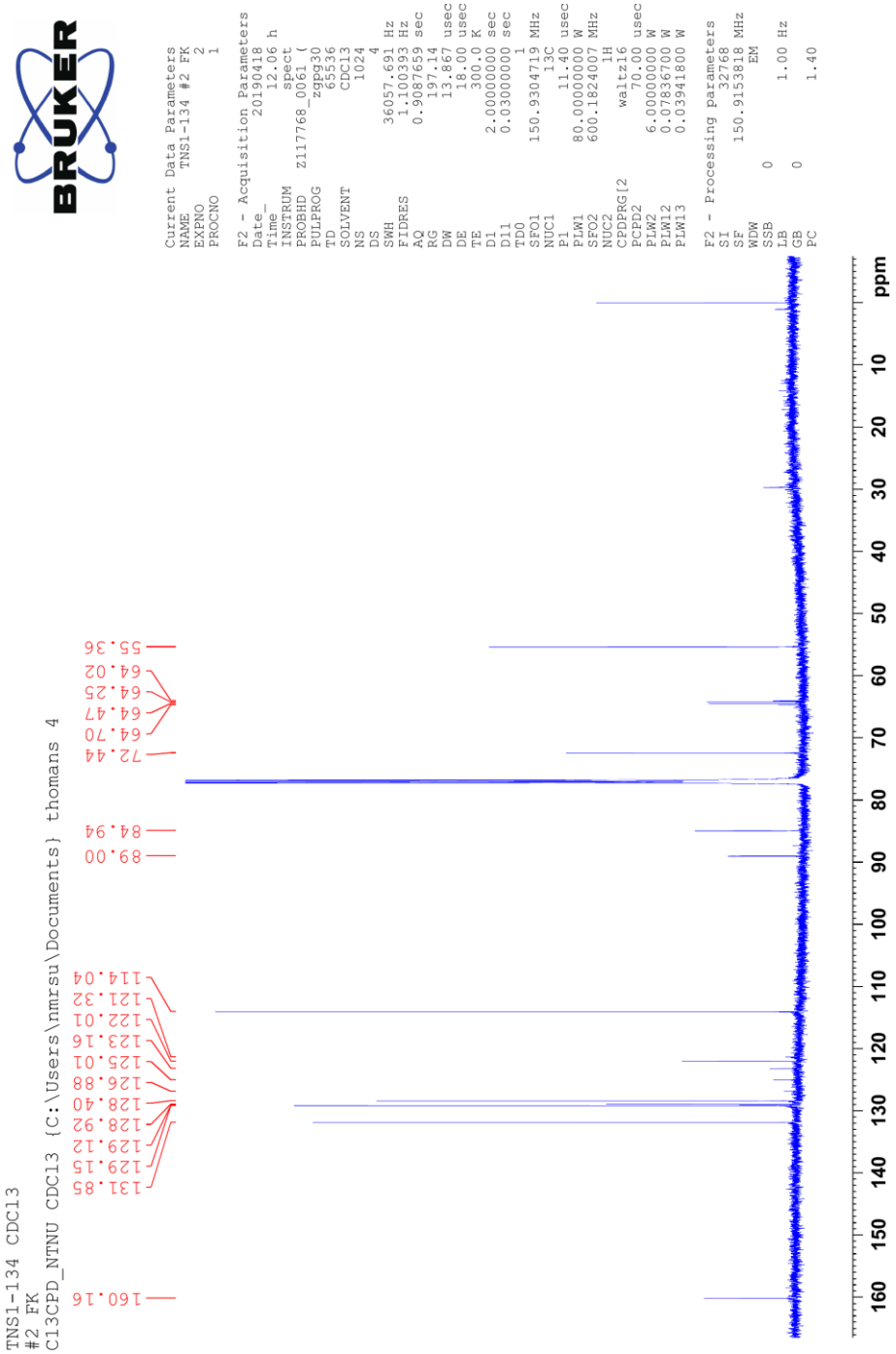

Appendix D Spectra of 1,1,3-trisubstituted prop-2-yns, 2a-h

Appendix D.13 **COSY NMR Spectrum of Alkyne 2f**

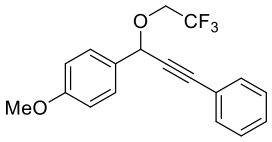

2f

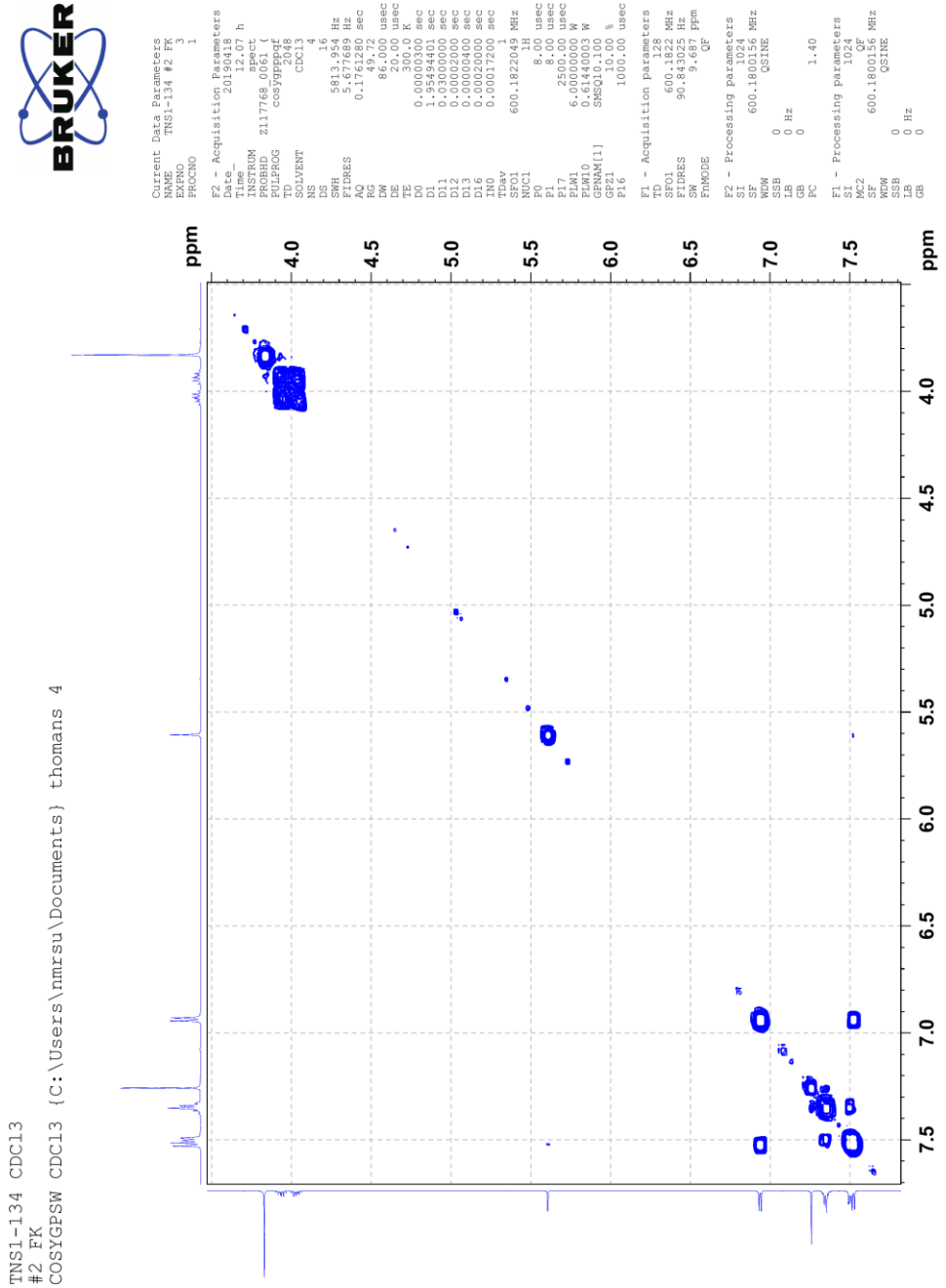

Appendix D Spectra of 1,1,3-trisubstituted prop-2-yns, 2a-h

Appendix D.14 **HSQC NMR Spectrum of Alkyne 2f**

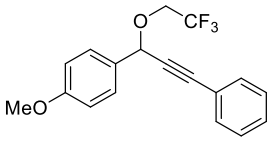

2f

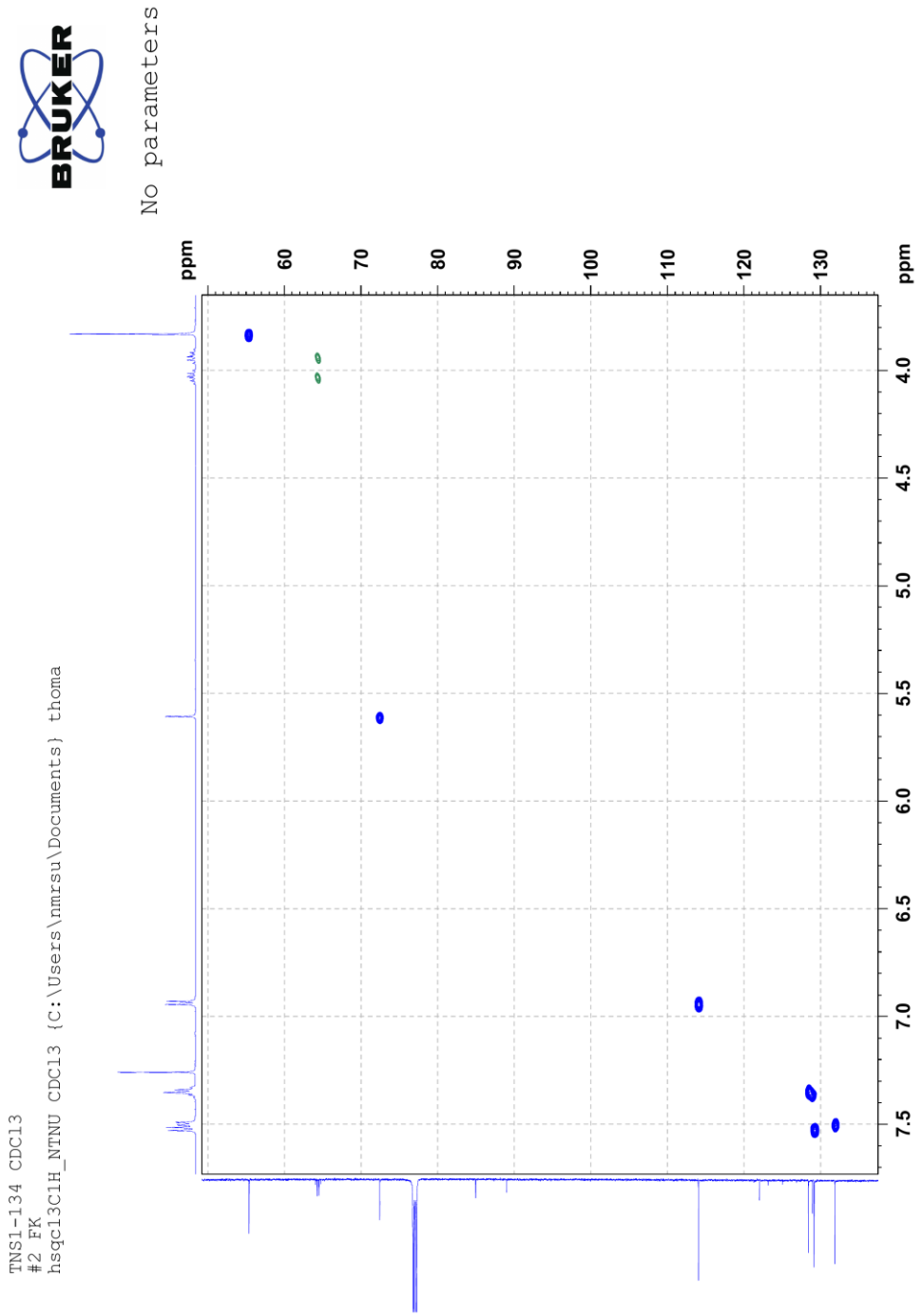

Appendix D Spectra of 1,1,3-trisubstituted prop-2-yns, 2a-h

Appendix D.15 **HMBC NMR Spectrum of Alkyne 2f**

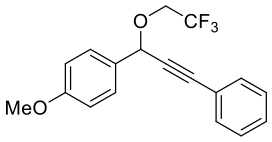

2f

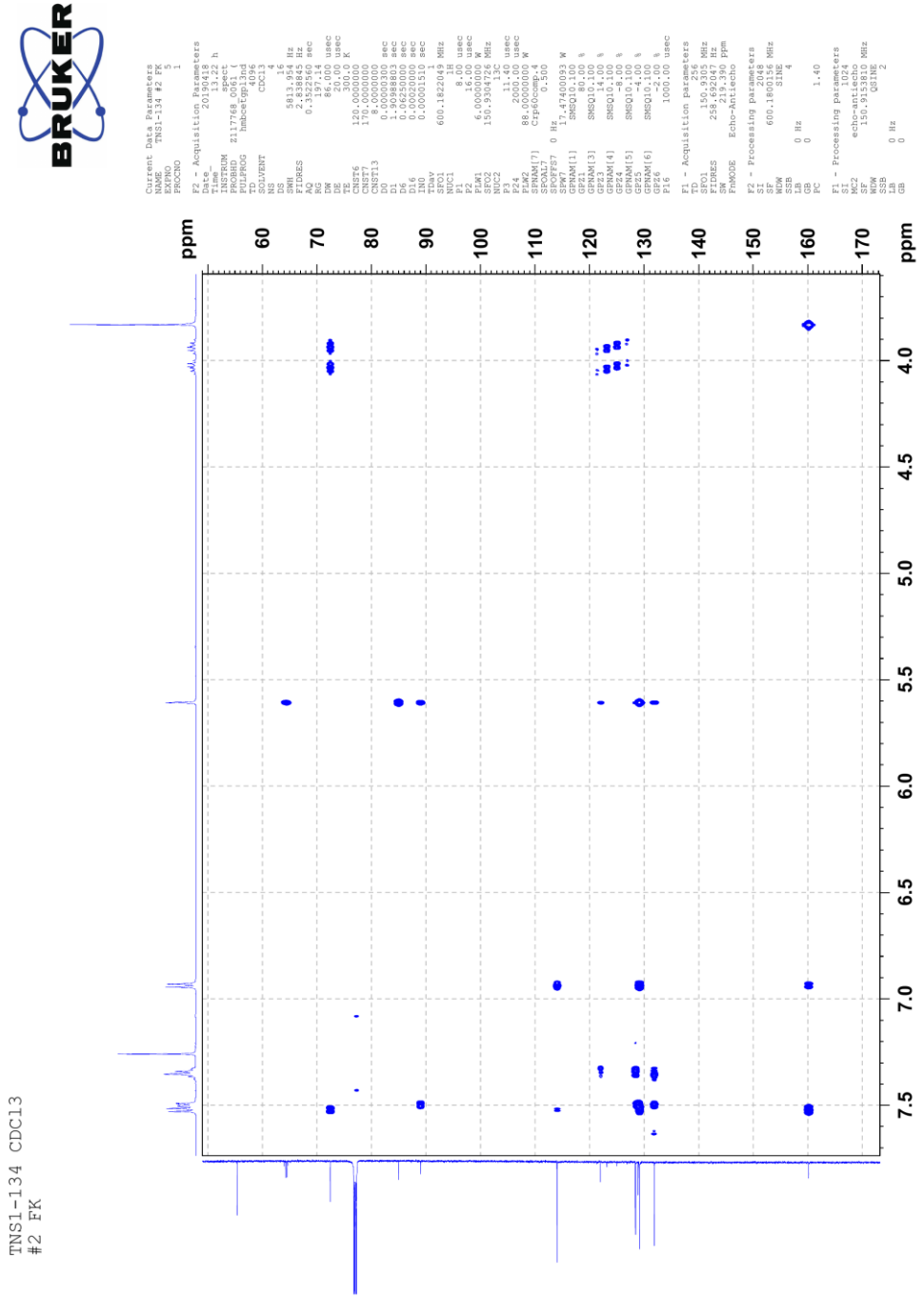

Appendix D Spectra of 1,1,3-trisubstituted prop-2-yns, 2a-h

Appendix D.16 **HRMS Spectrum of Alkyne 2f**

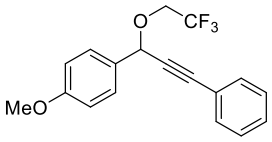

2f

Elemental Composition Report **Page 1**

Single Mass Analysis
Tolerance = 3.0 PPM / DBE: min = -50.0, max = 50.0
Element prediction: Off
Number of isotope peaks used for i-FIT = 3

Monoisotopic Mass, Odd Electron Ions
1016 formula(e) evaluated with 2 results within limits (all results (up to 1000) for each mass)
Elements Used:
C: 0-100 H: 0-150 N: 0-3 O: 0-3 F: 0-5
2019-356 23 (0.465) AM2 (Ar,35000.0,0.00,0.00); Cm (19:25)
1: TOF MS ASAP+

2.15e+007

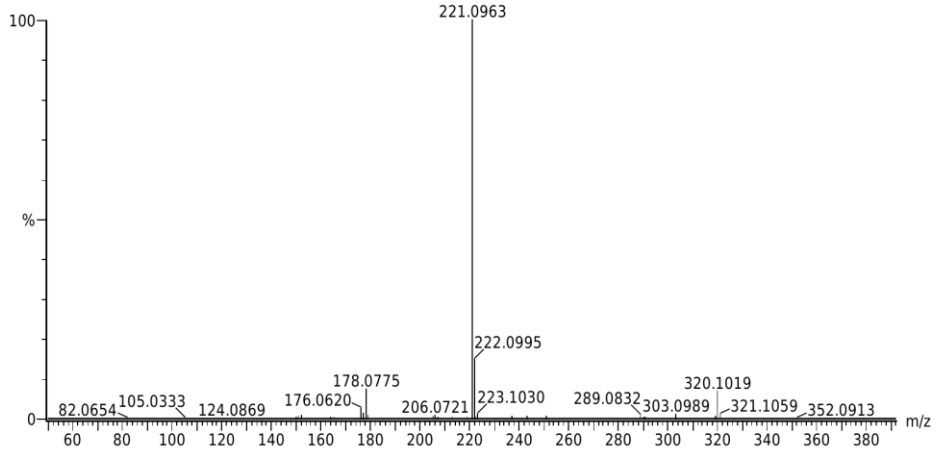

Minimum:				-50.0				
Maximum:		5.0	3.0	50.0				
Mass	Calc. Mass	mDa	PPM	DBE	i-FIT	Norm	Conf(%)	Formula
320.1019	320.1024	-0.5	-1.6	10.0	1182.1	0.045	95.56	C18 H15 O2 F3
	320.1013	0.6	1.9	14.0	1185.2	3.114	4.44	C21 H14 O F2

Appendix D Spectra of 1,1,3-trisubstituted prop-2-yns, 2a-h

Appendix D.17 **^{1}H NMR Spectrum of Alkyne 2g**

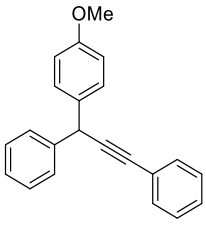

2g

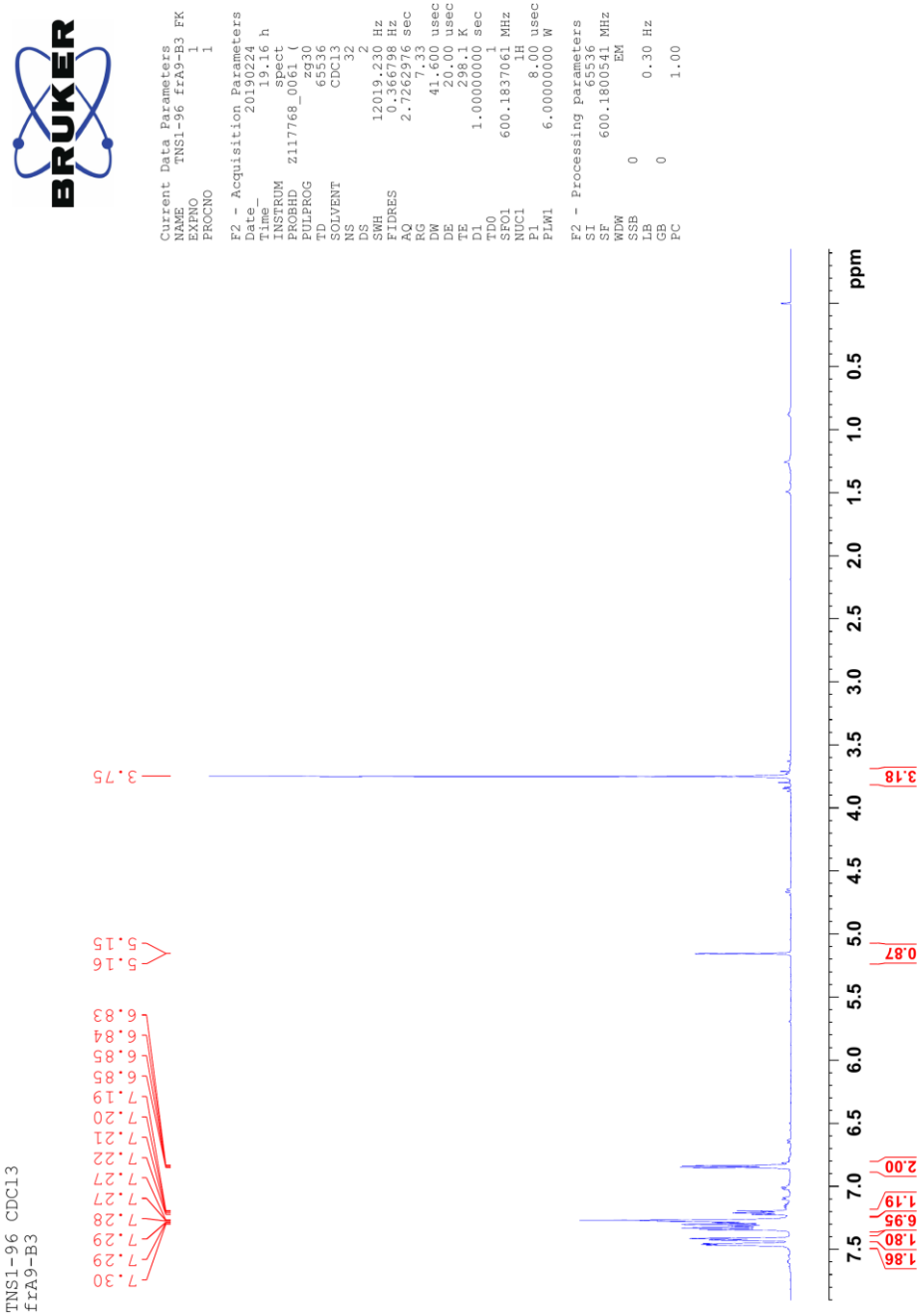

Appendix D Spectra of 1,1,3-trisubstituted prop-2-yns, 2a-h

Appendix D.18 **^{1}H NMR Spectrum of Alkyne 2h**

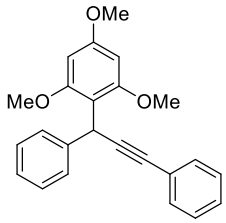

2h

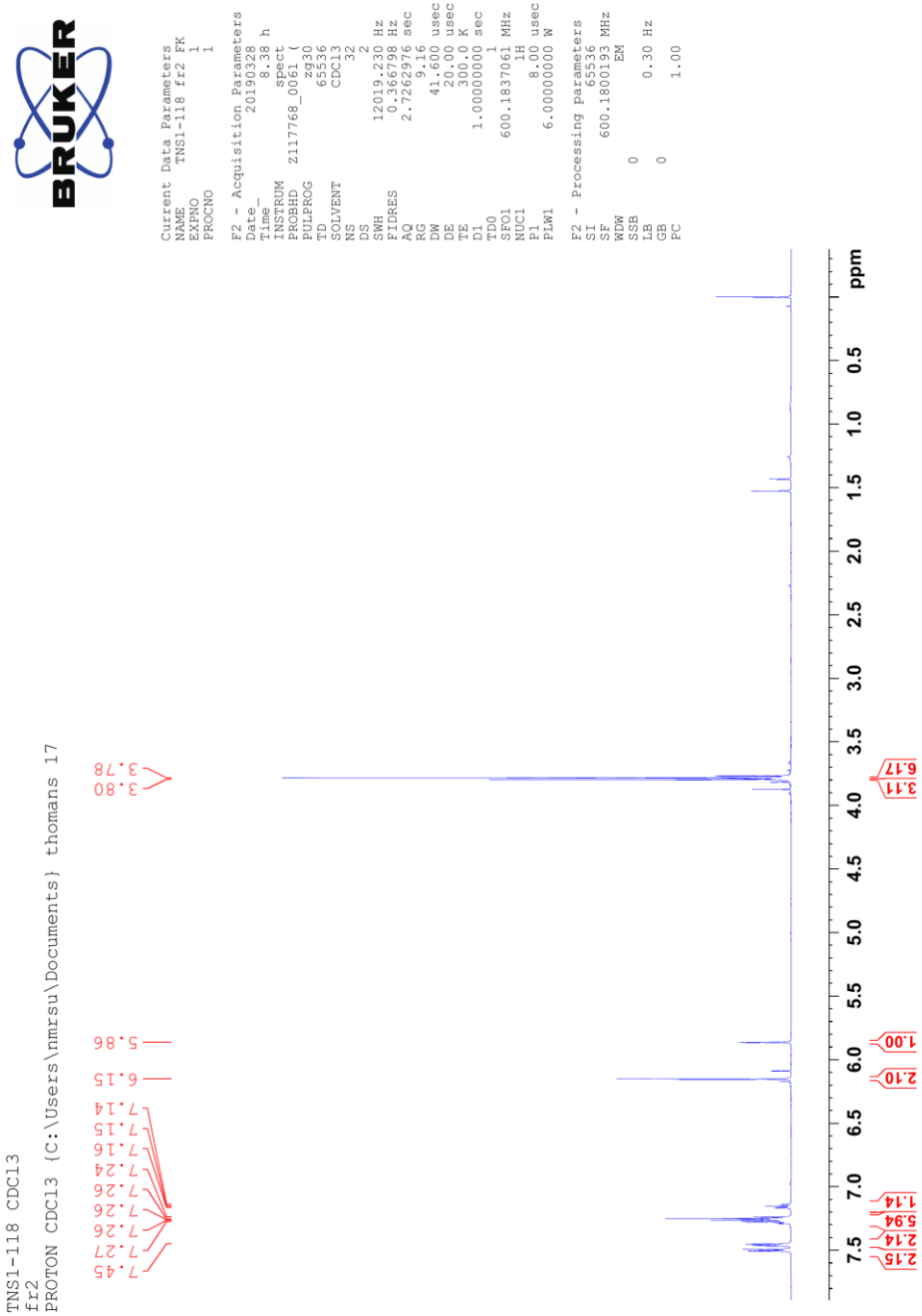

Appendix E **Spectra of Allenes, 3a-g**

Appendix E.1 **^{1}H NMR Spectrum of Allene 3a**

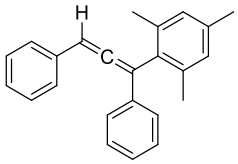

3a

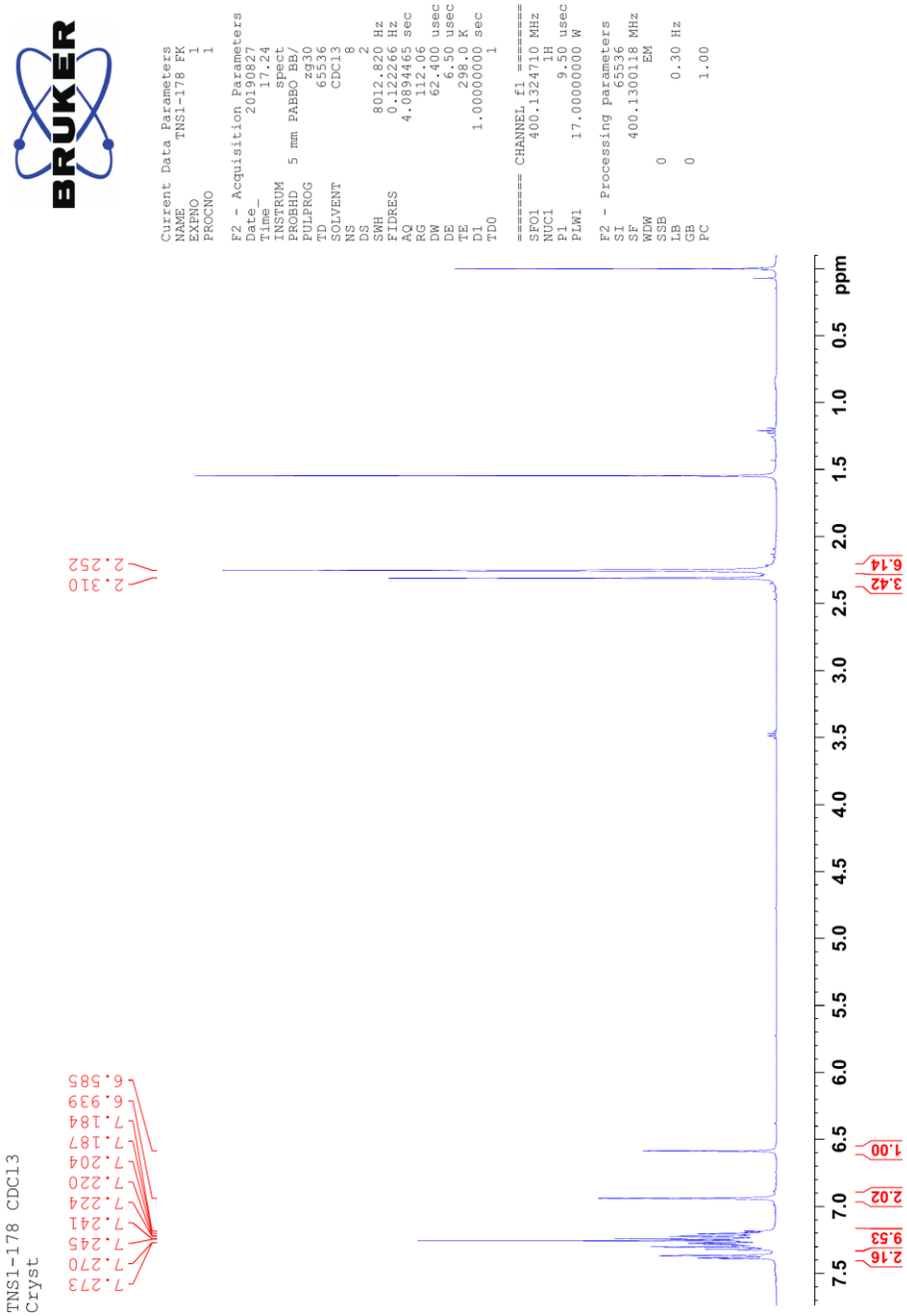

Appendix E Spectra of Allenes, 3a-g

Appendix E.2 **^{1}H NMR spectrum of Allene 3b**

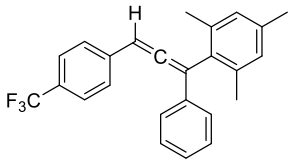

3b

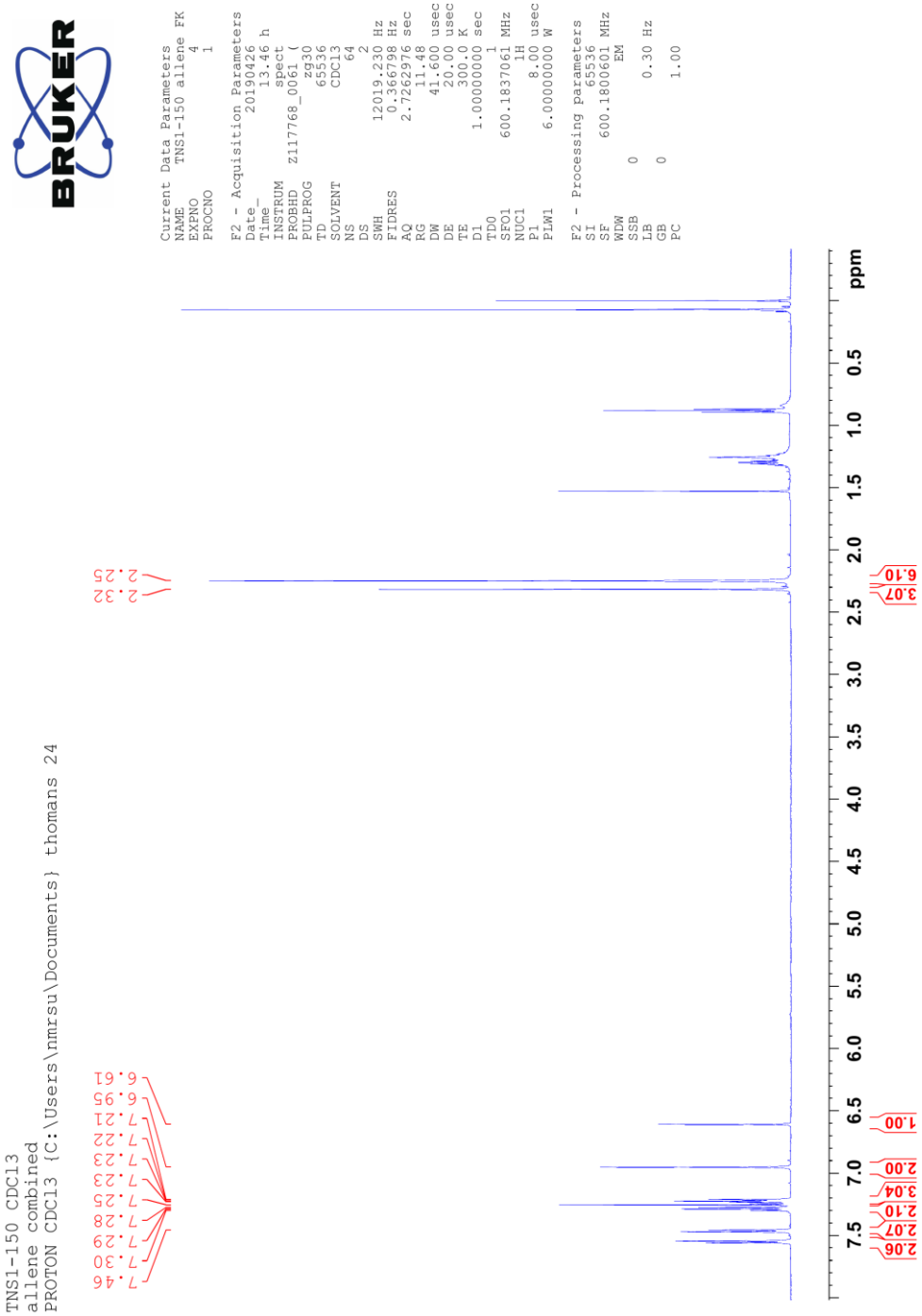

Appendix E Spectra of Allenes, 3a-g

Appendix E.3 **^{13}C NMR spectrum of Allene 3b**

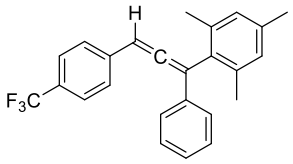

3b

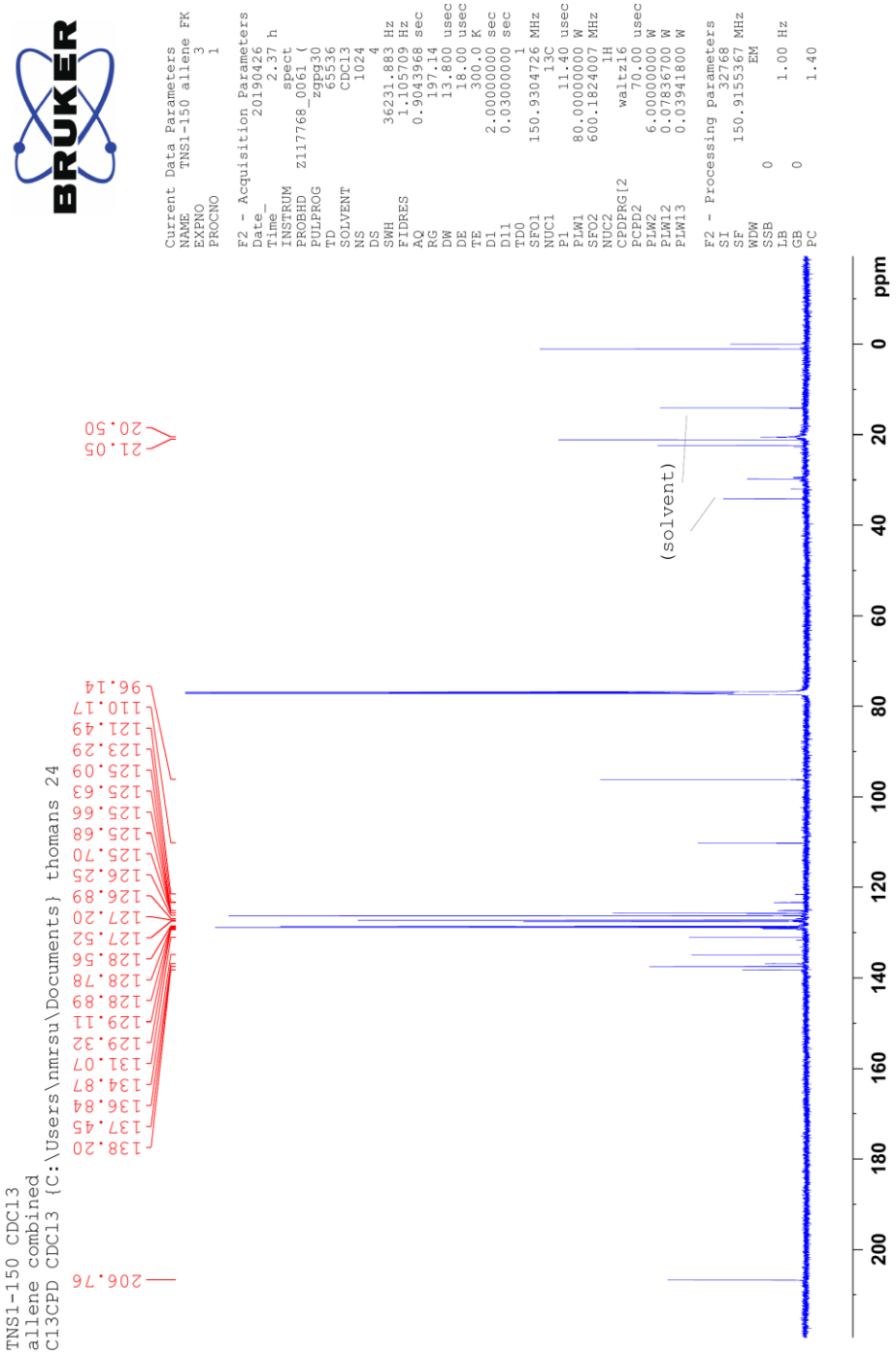

Appendix E Spectra of Allenes, 3a-g

Appendix E.4 **COSY NMR spectrum of Allene 3b**

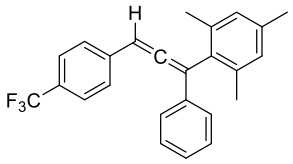

3b

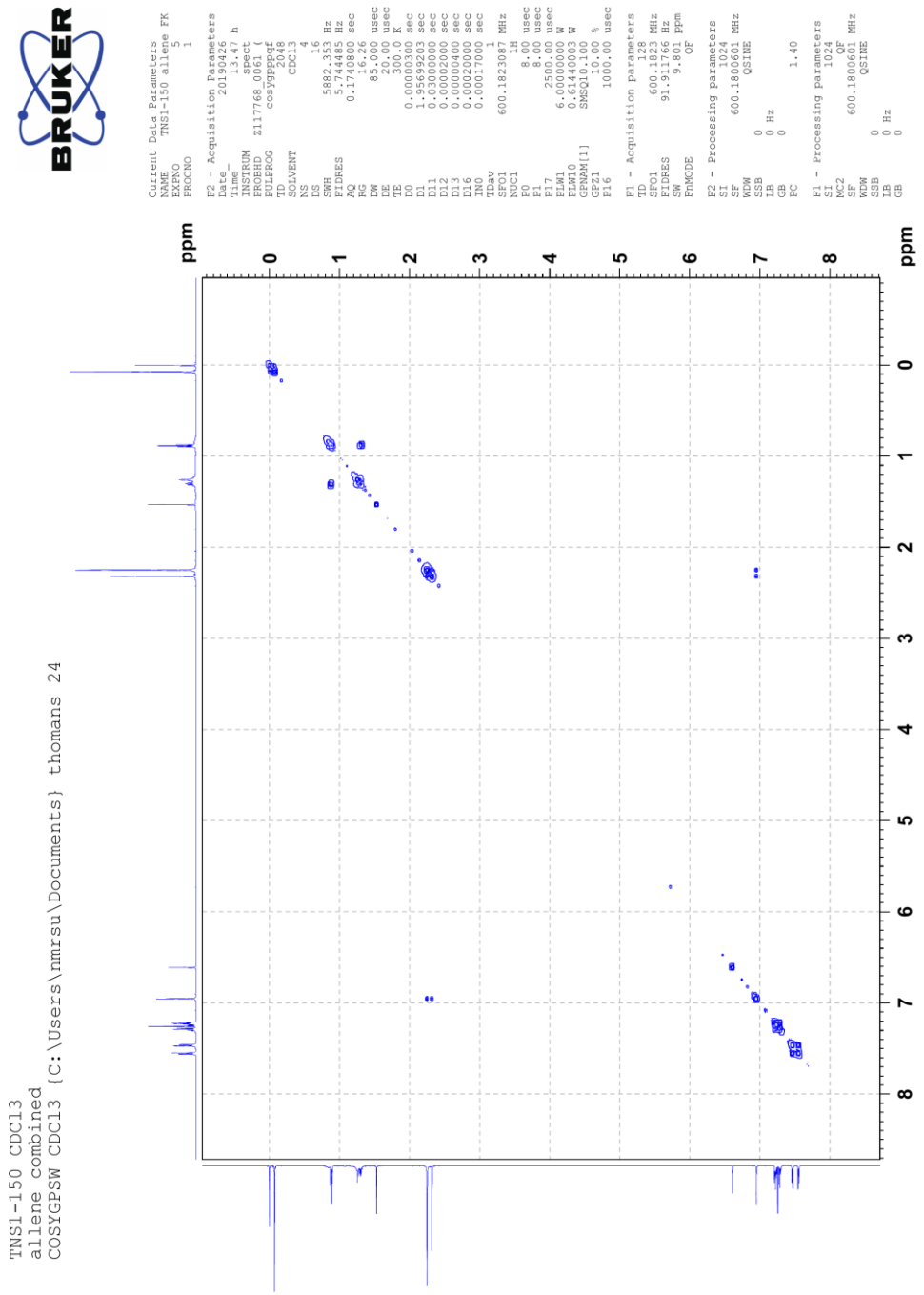

Appendix E Spectra of Allenes, 3a-g

Appendix E.5 **HSQC NMR spectrum of Allene 3b**

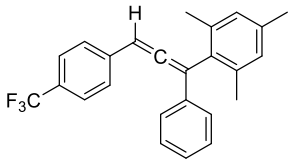

3b

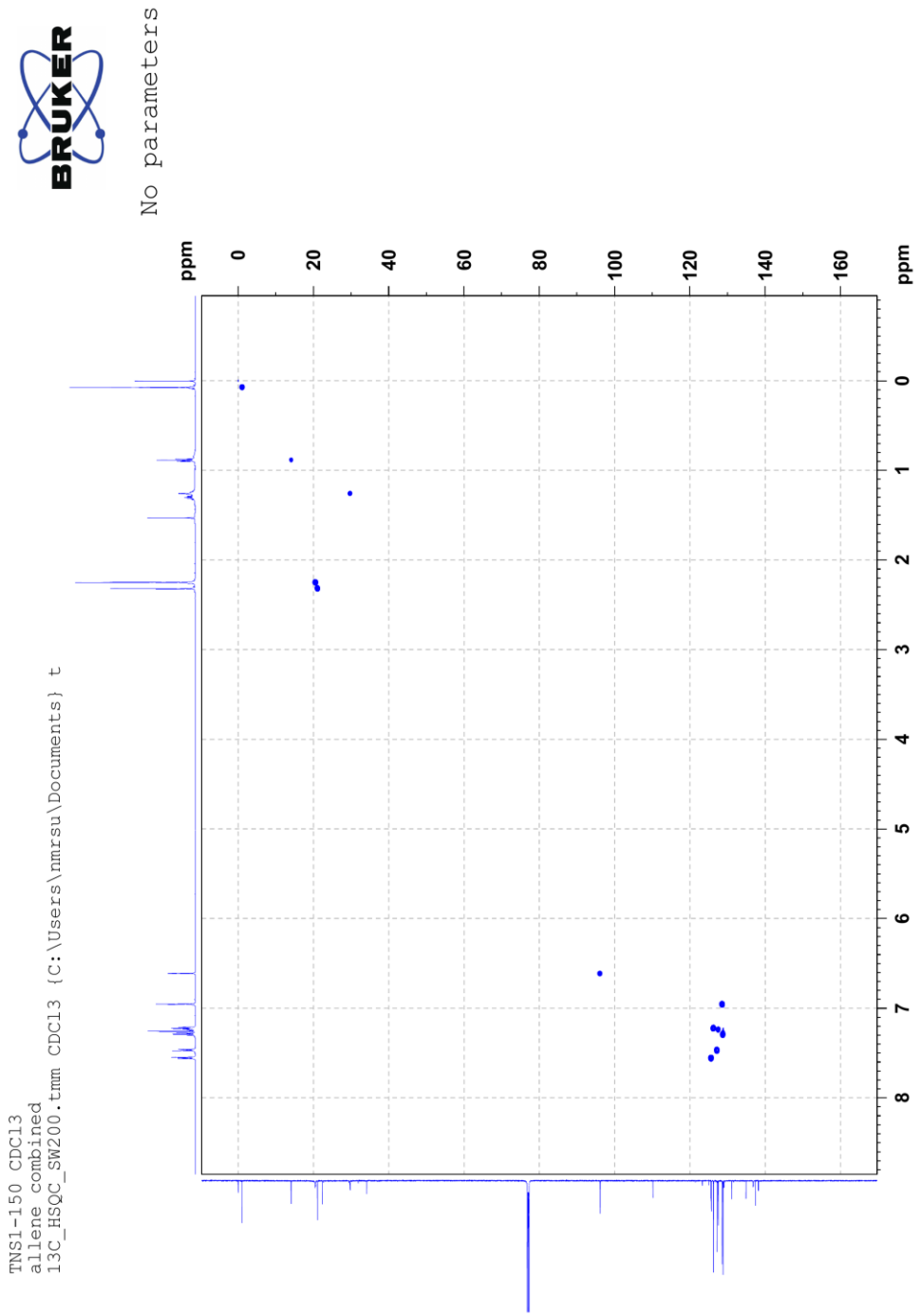

Appendix E Spectra of Allenes, 3a-g

Appendix E.6 **HMBC NMR spectrum of Allene 3b**

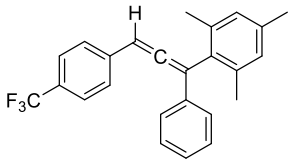

3b

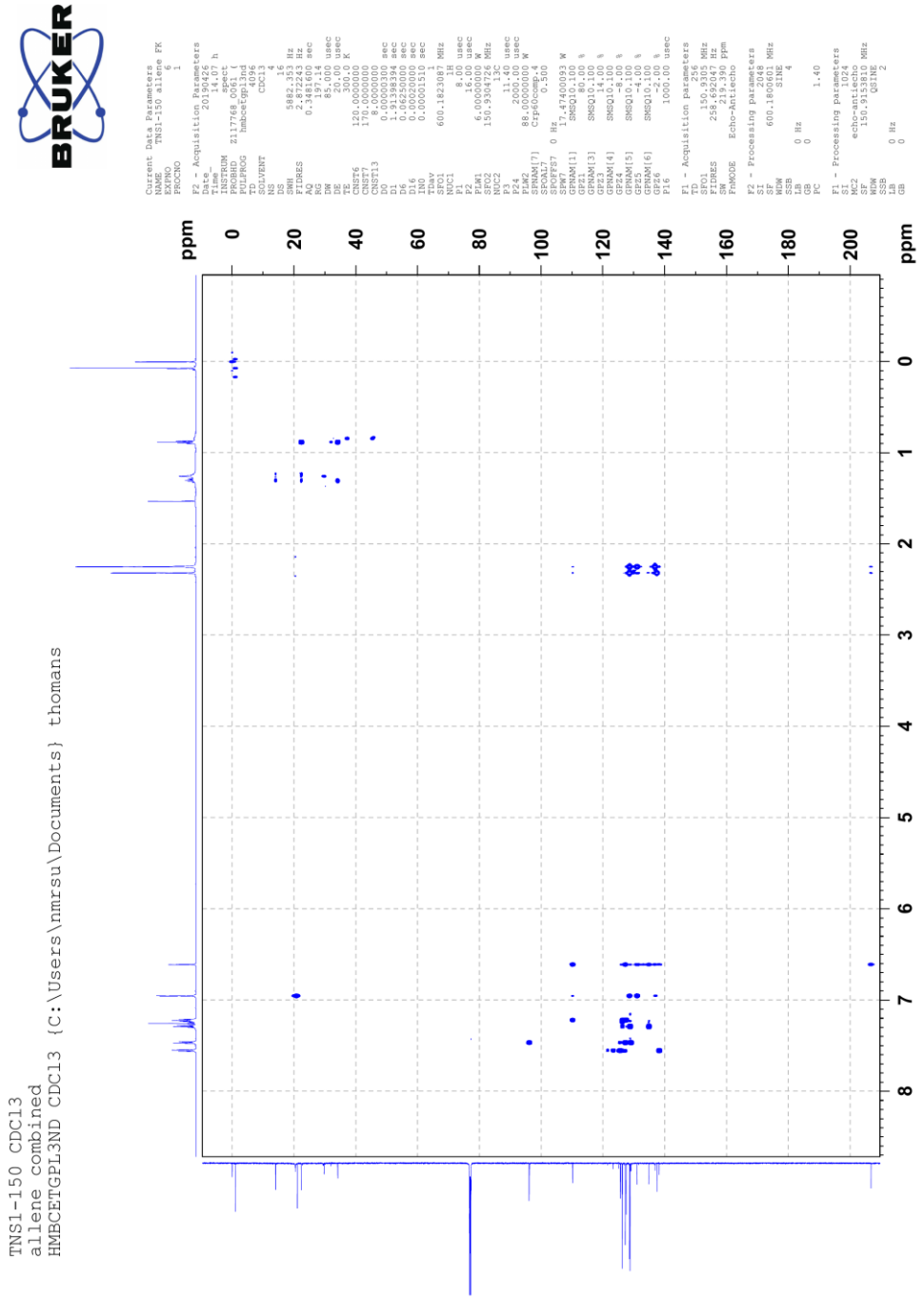

Appendix E Spectra of Allenes, 3a-g

Appendix E.7 **HRMS spectrum of Allene 3b**

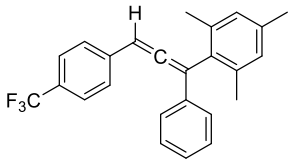

3b

Elemental Composition Report **Page 1**

Single Mass Analysis
Tolerance = 5.0 PPM / DBE: min = -5.0, max = 50.0
Element prediction: Off
Number of isotope peaks used for i-FIT = 3

Monoisotopic Mass, Even Electron Ions
40 formula(e) evaluated with 1 results within limits (all results (up to 1000) for each mass)
Elements Used:
C: 0-100 H: 0-100 F: 0-7

2020_153 66 (0.631) AM2 (Ar,35000.0,0.00,0.00); Cm (55:66)
1: TOF MS ES+

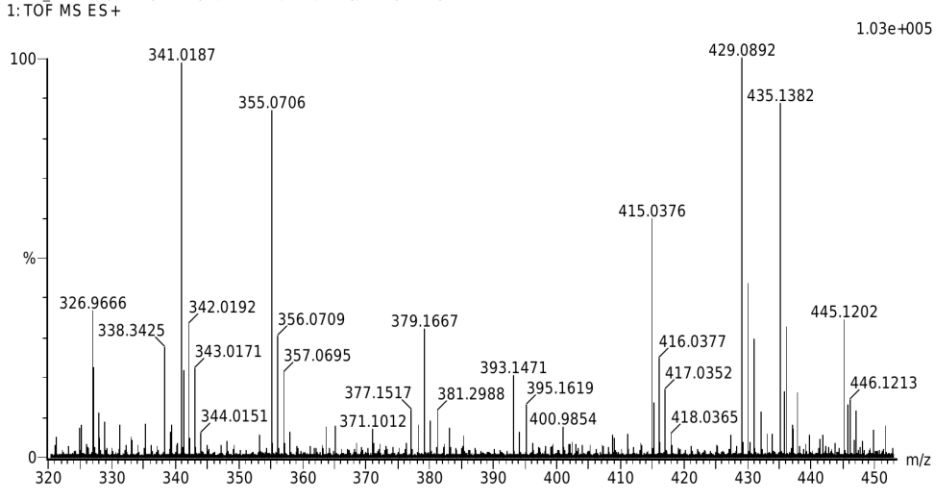

Minimum:				-5.0				
Maximum:		5.0	5.0	50.0				
Mass	Calc. Mass	mDa	PPM	DBE	i-FIT	Norm	Conf(%)	Formula
379.1667	379.1674	-0.7	-1.8	13.5	973.9	n/a	n/a	C25 H22 F3

Appendix E Spectra of Allenes, 3a-g

Appendix E.8 **^{1}H NMR Spectrum of Mixture of Allene 3c and Alkyne 2e**

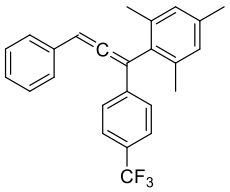

3c

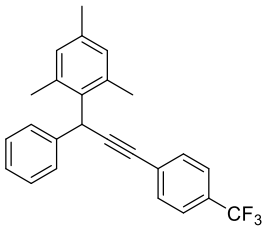

2e

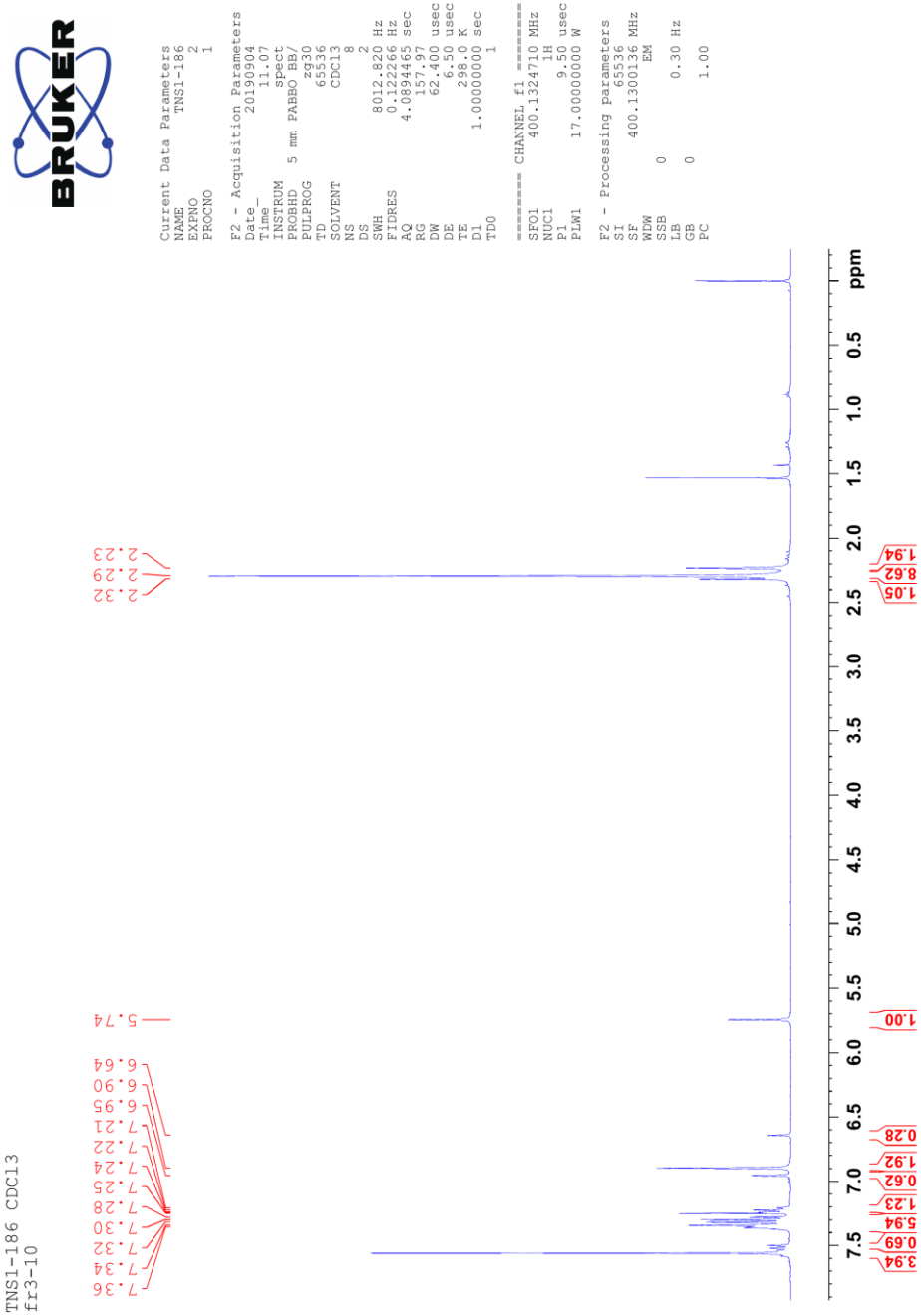

Appendix E Spectra of Allenes, 3a-g

Appendix E.9 **^{1}H NMR spectrum of Allene 3d**

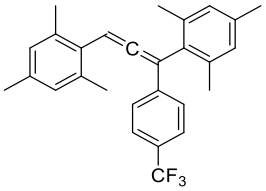

3d

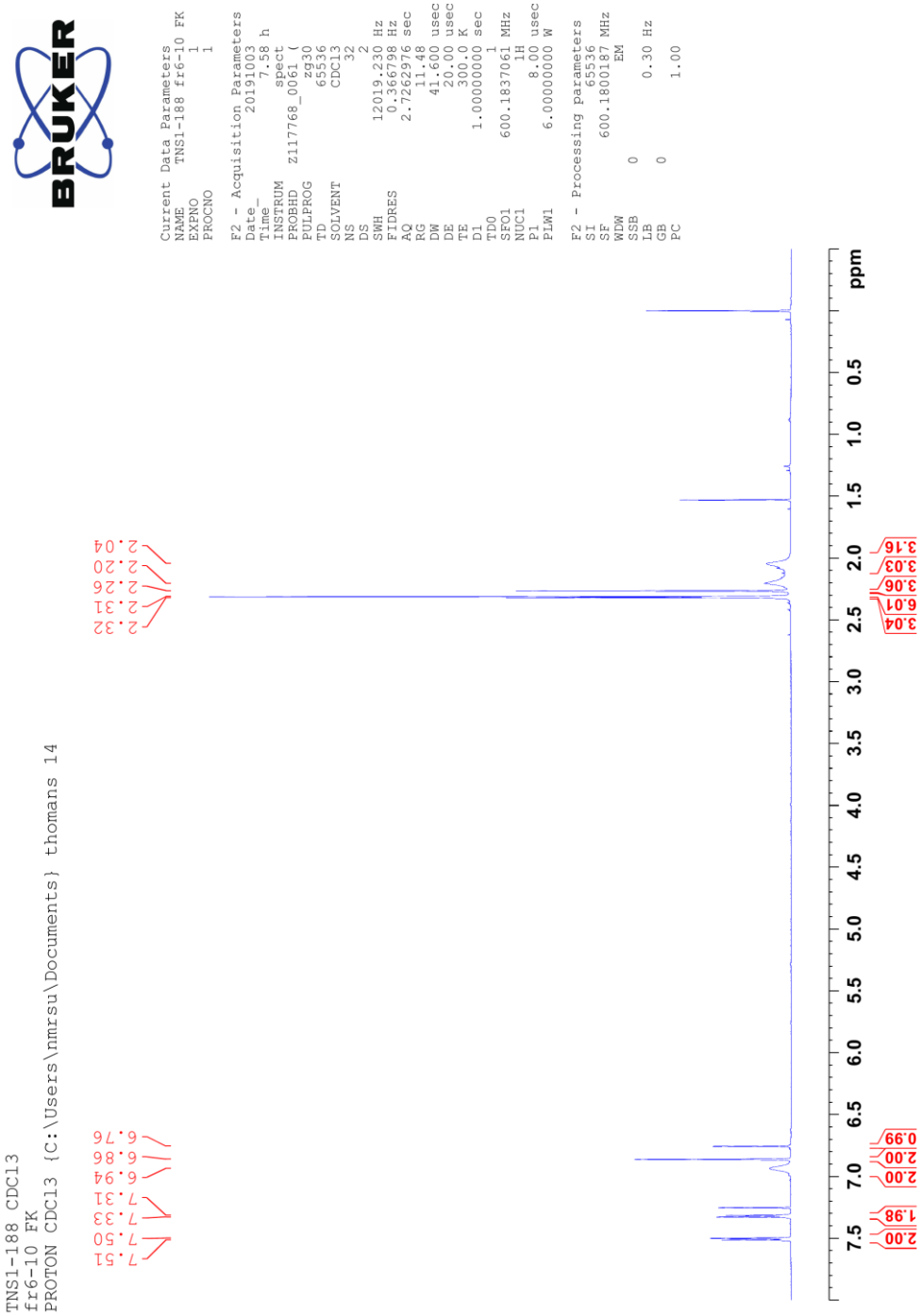

Appendix E Spectra of Allenes, 3a-g

Appendix E.10 **^{13}C NMR spectrum of Allene 3d**

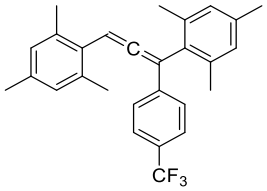

3d

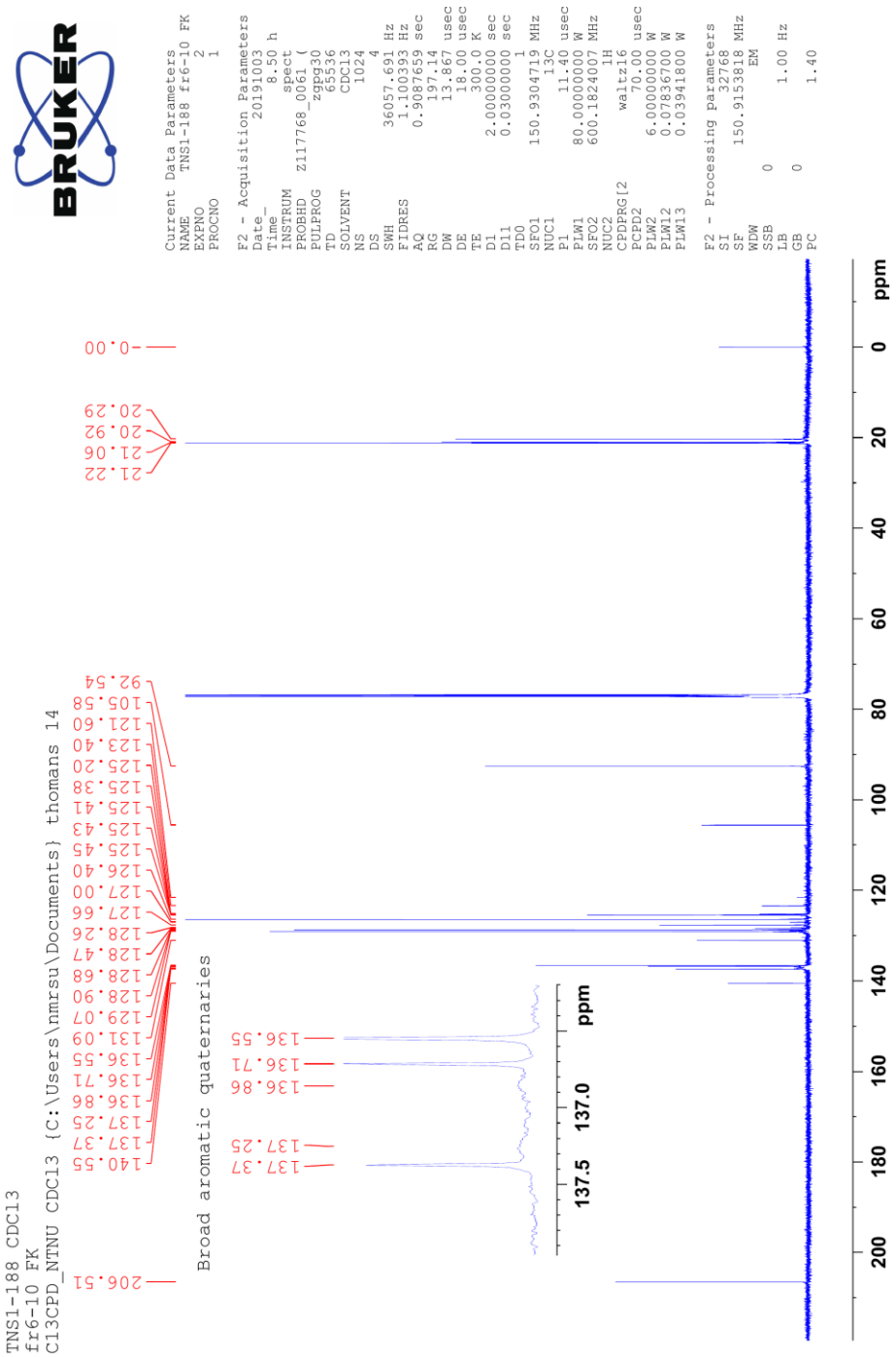

Appendix E Spectra of Allenes, 3a-g

Appendix E.11 **COSY NMR spectrum of Allene 3d**

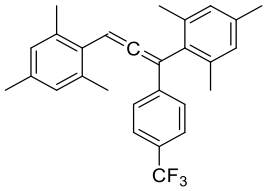

3d

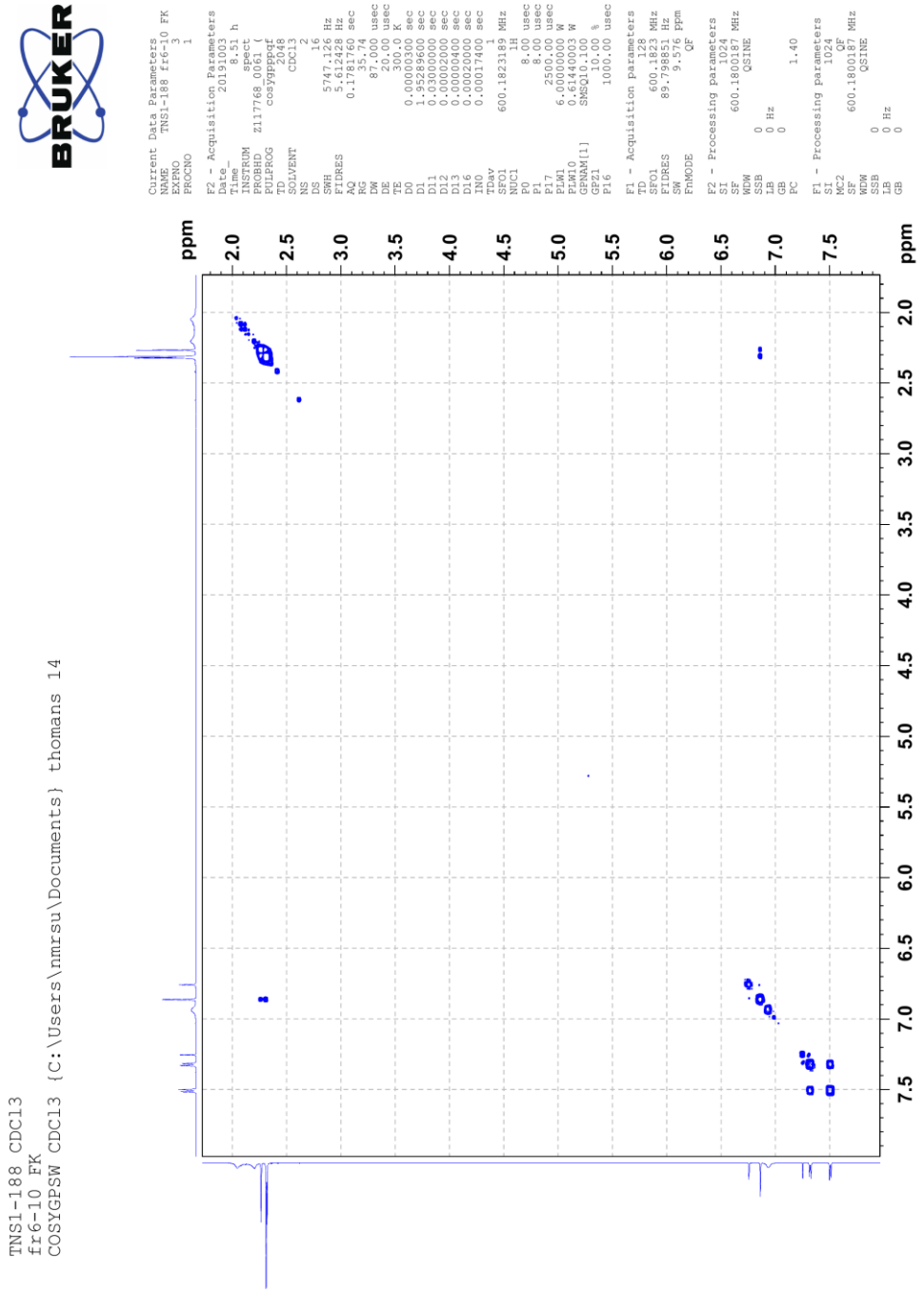

Appendix E Spectra of Allenes, 3a-g

Appendix E.12 **HSQC NMR spectrum of Allene 3d**

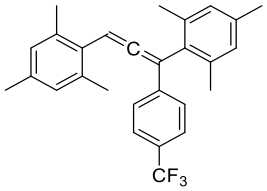

3d

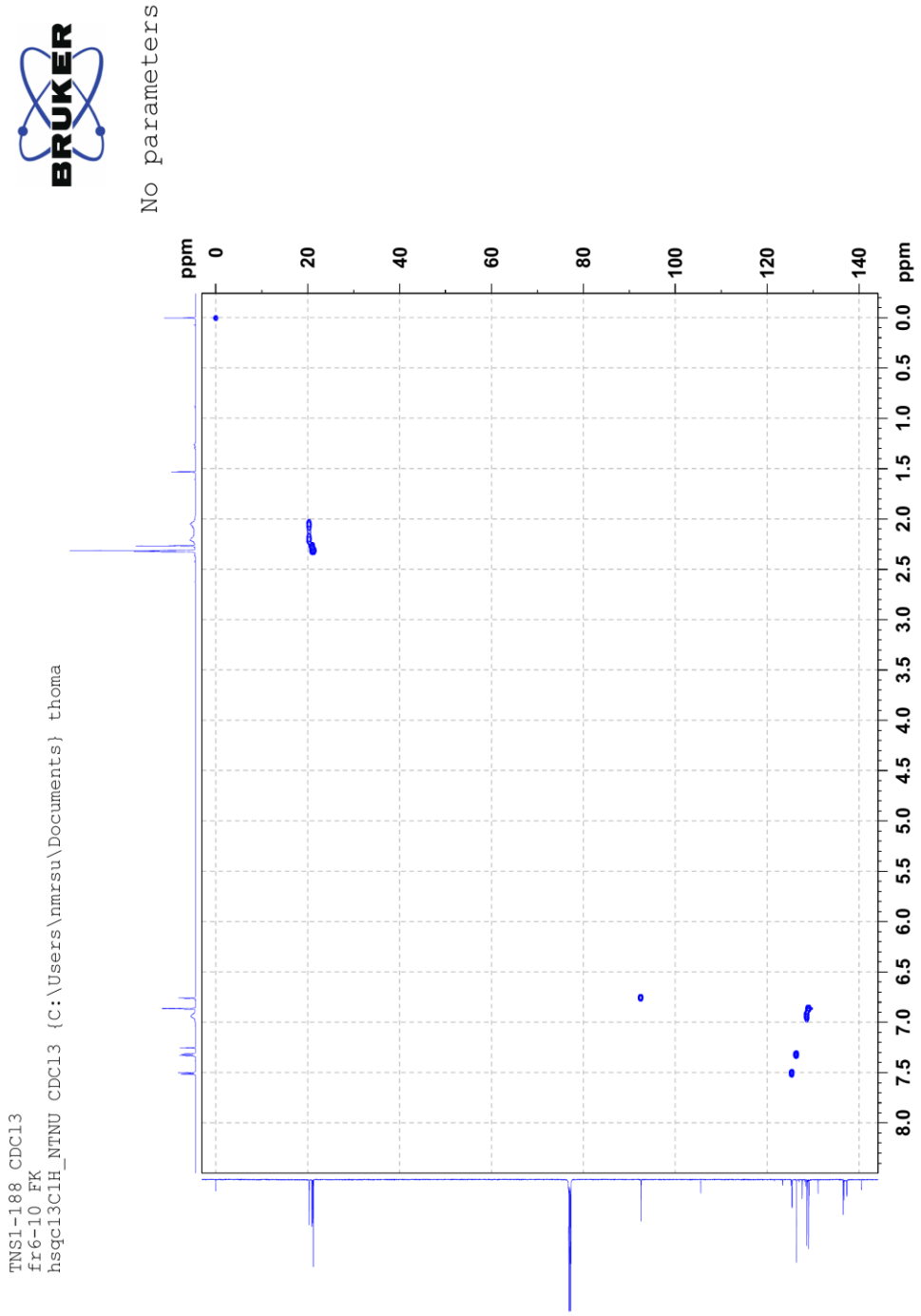

Appendix E Spectra of Allenes, 3a-g

Appendix E.13 **HMBC NMR spectrum of Allene 3d**

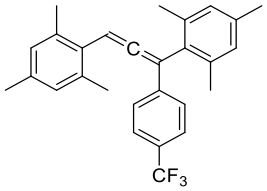

3d

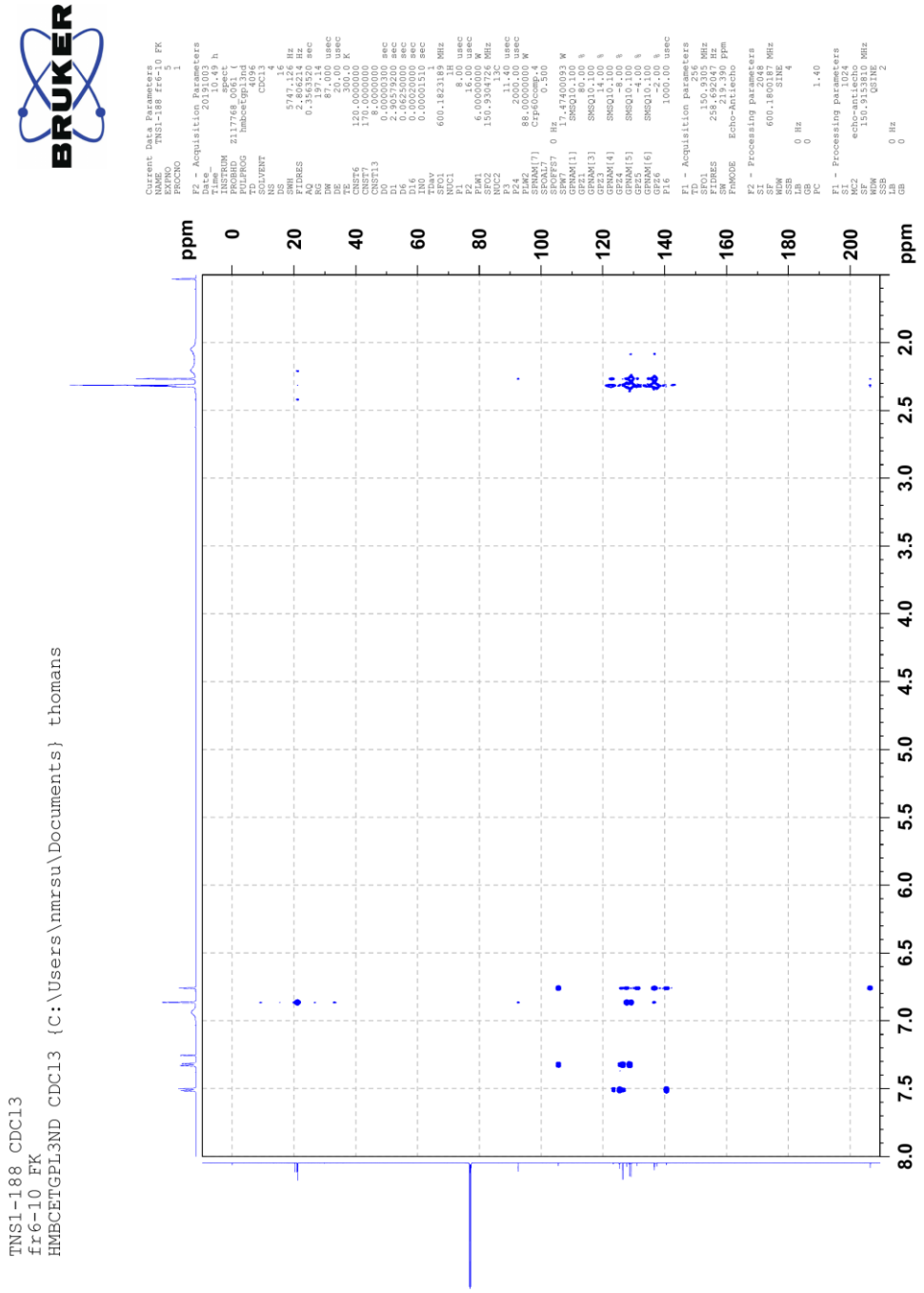

Appendix E Spectra of Allenes, 3a-g

Appendix E.14 **HRMS spectrum of Allene 3d**

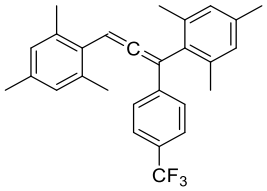

3d

Elemental Composition Report **Page 1**

Single Mass Analysis
Tolerance = 5.0 PPM / DBE: min = -5.0, max = 50.0
Element prediction: Off
Number of isotope peaks used for i-FIT = 3

Monoisotopic Mass, Even Electron Ions
30 formula(e) evaluated with 1 results within limits (all results (up to 1000) for each mass)
Elements Used:
C: 0-100 H: 0-100 F: 0-4

2020-117 93 (1.826) AM2 (Ar,35000.0,0.00,0.00); Cm (47:97)
1: TOF MS ASAP+

7.79e+007

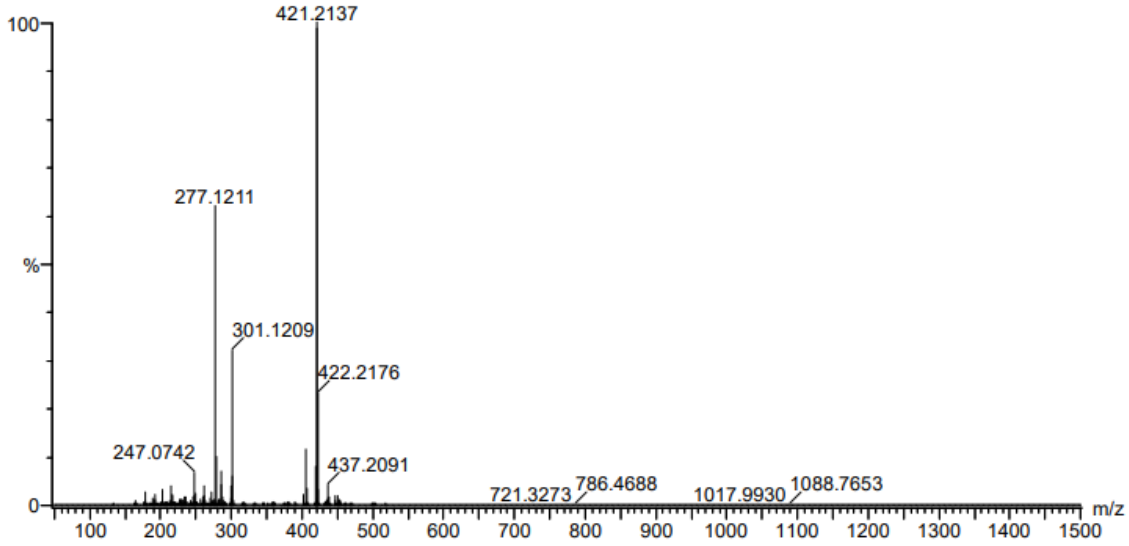

Minimum:				-5.0				
Maximum:		5.0	5.0	50.0				
Mass	Calc. Mass	mDa	PPM	DBE	i-FIT	Norm	Conf(%)	Formula
421.2137	421.2143	-0.6	-1.4	13.5	1597.9	n/a	n/a	C28 H28 F3

Appendix E Spectra of Allenes, 3a-g

Appendix E.15 **^{1}H NMR spectrum of Allene 3e**

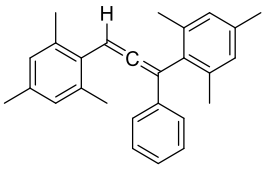

3e

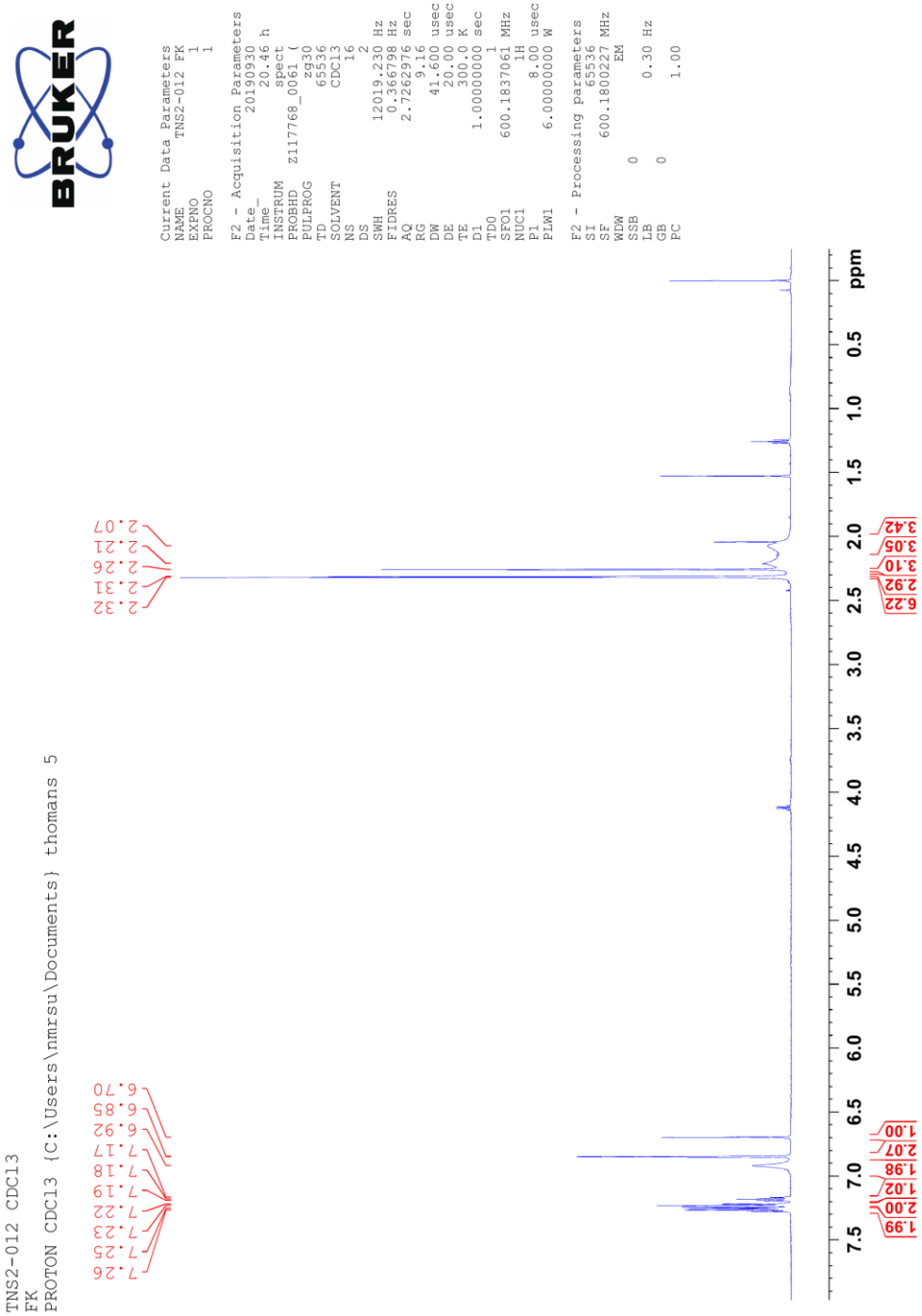

Appendix E Spectra of Allenes, 3a-g

Appendix E.16 **^{13}C NMR spectrum of Allene 3e**

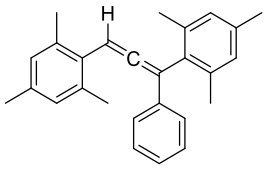

3e

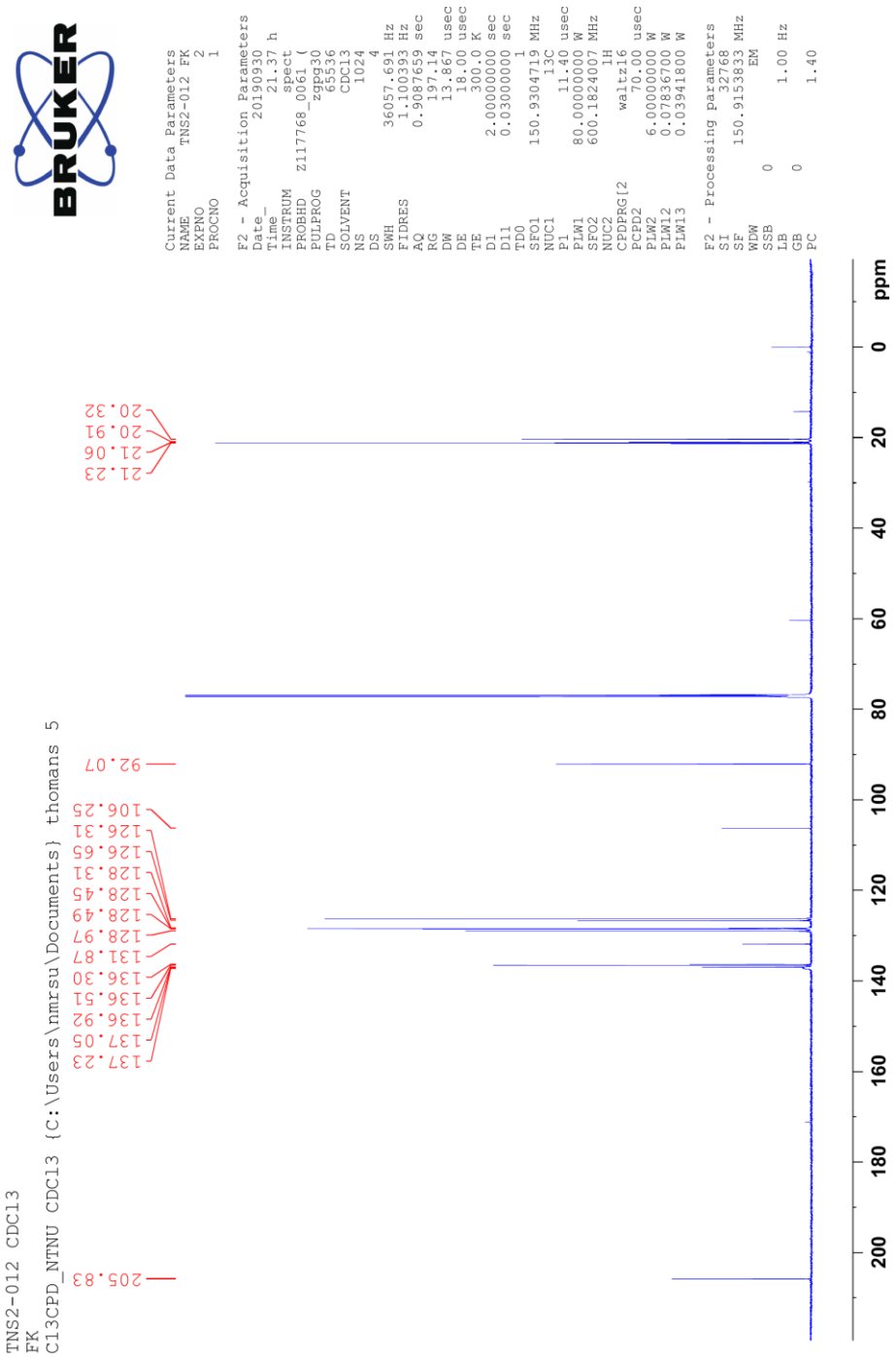

Appendix E Spectra of Allenes, 3a-g

Appendix E.17 **COSY NMR spectrum of Allene 3e**

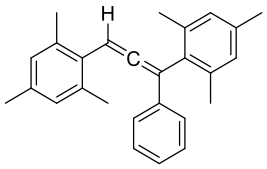

3e

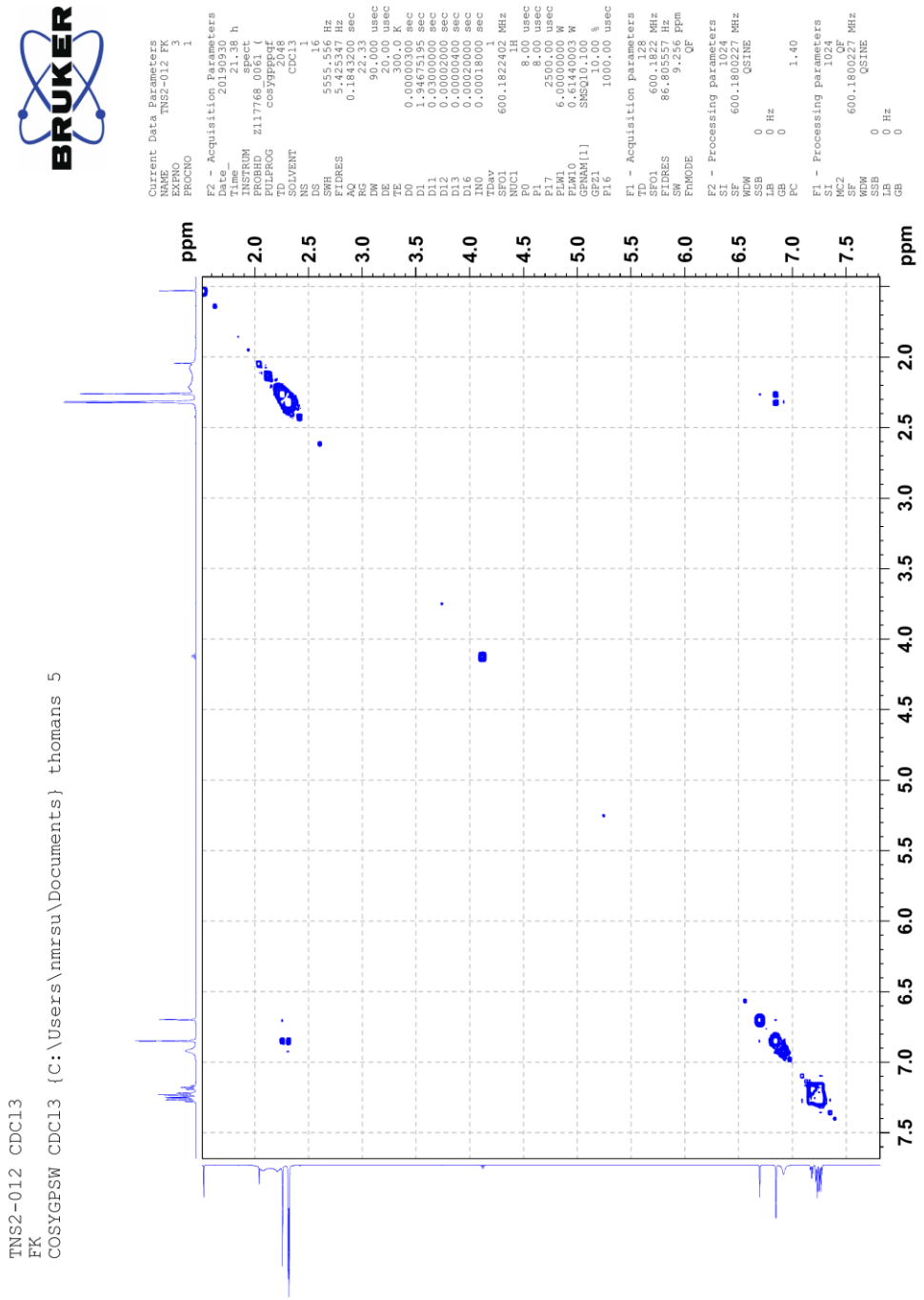

Appendix E Spectra of Allenes, 3a-g

Appendix E.18 **HSQC NMR spectrum of Allene 3e**

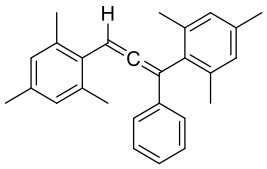

3e

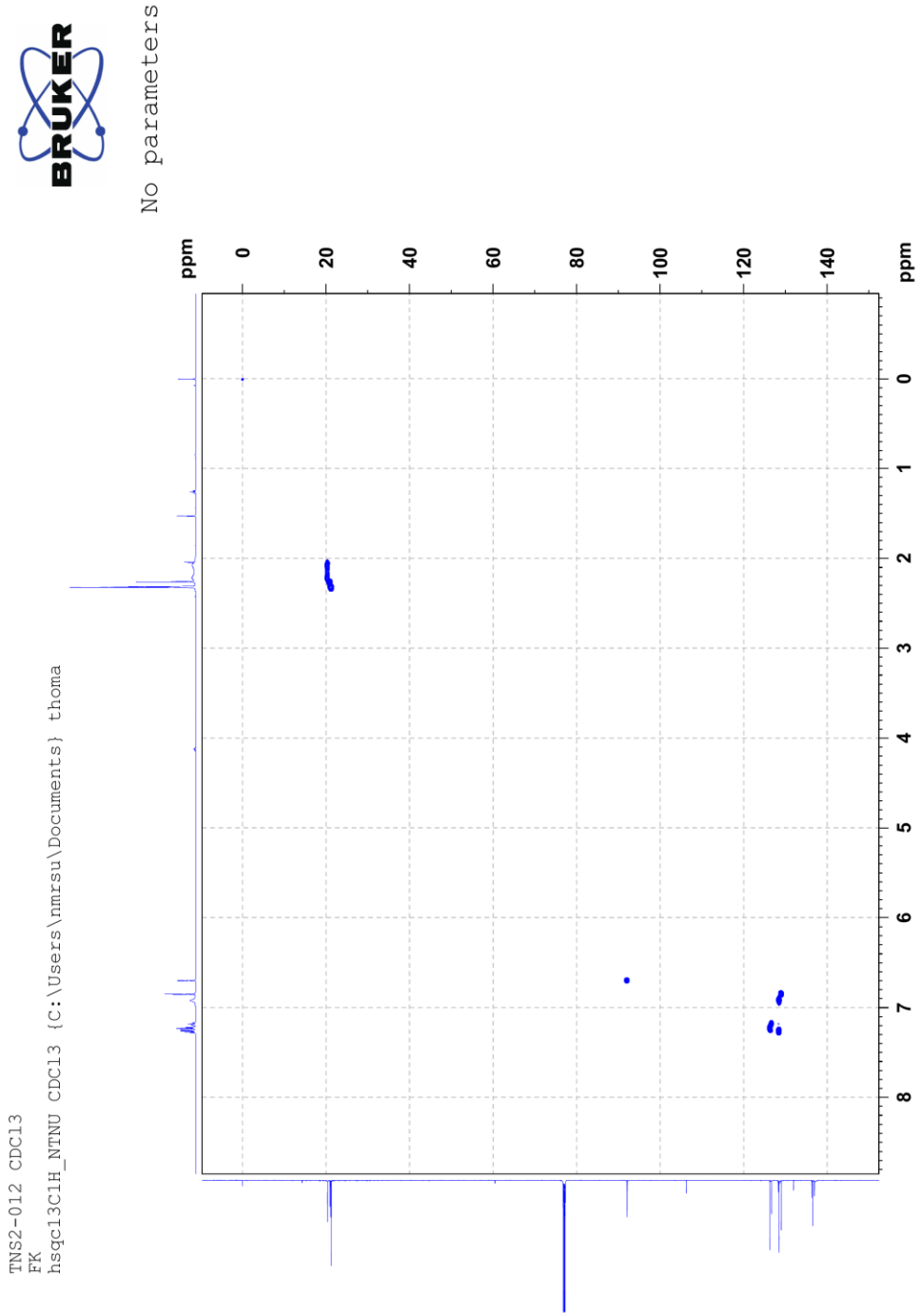

Appendix E Spectra of Allenes, 3a-g

Appendix E.19 **HMBC NMR spectrum of Allene 3e**

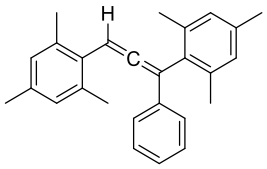

3e

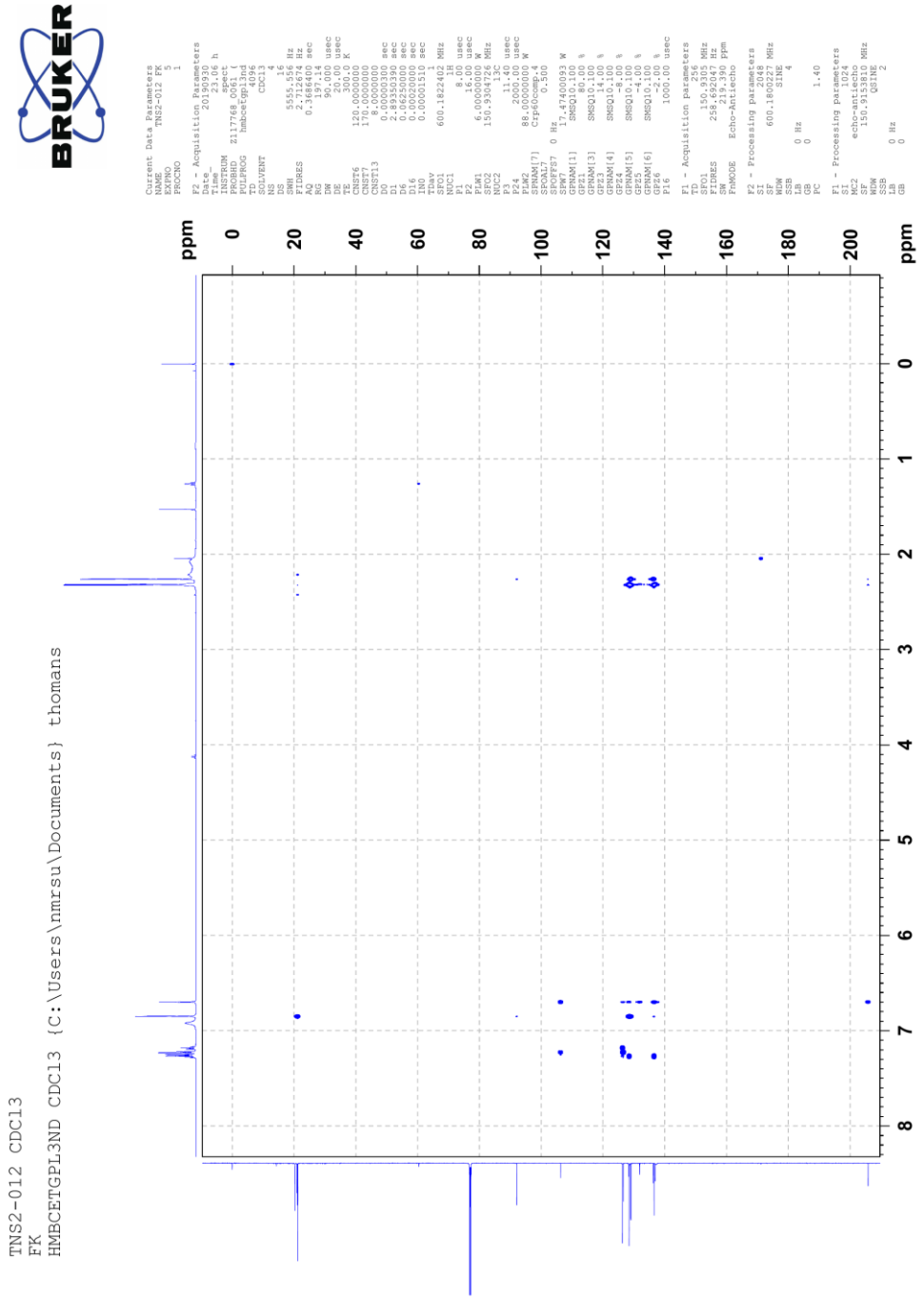

Appendix E Spectra of Allenes, 3a-g

Appendix E.20 **HRMS spectrum of Allene 3e**

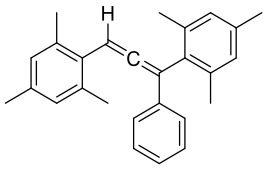

3e

Elemental Composition Report **Page 1**

Single Mass Analysis
Tolerance = 2.0 PPM / DBE: min = -50.0, max = 50.0
Element prediction: Off
Number of isotope peaks used for i-FIT = 3

Monoisotopic Mass, Even Electron Ions
491 formula(e) evaluated with 1 results within limits (all results (up to 1000) for each mass)
Elements Used:
C: 0-100 H: 0-150 10B: 0-3 O: 0-10
2019-679 63 (1.240) AM2 (Ar,35000.0,0.00,0.00); Cm (50:63)
1: TOF MS ASAP+

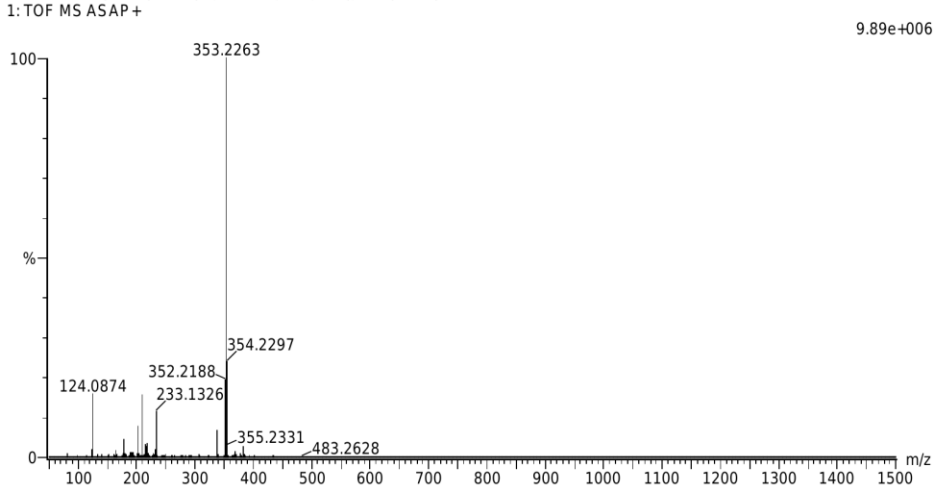

Minimum:				-50.0				
Maximum:		5.0	2.0	50.0				
Mass	Calc. Mass	mDa	PPM	DBE	i-FIT	Norm	Conf(%)	Formula
353.2263	353.2269	-0.6	-1.7	13.5	1259.8	n/a	n/a	C27 H29

Appendix E Spectra of Allenes, 3a-g

Appendix E.21 **^{1}H NMR spectrum for Allene 3f**

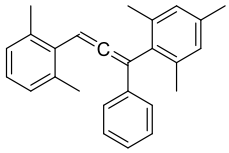

3f

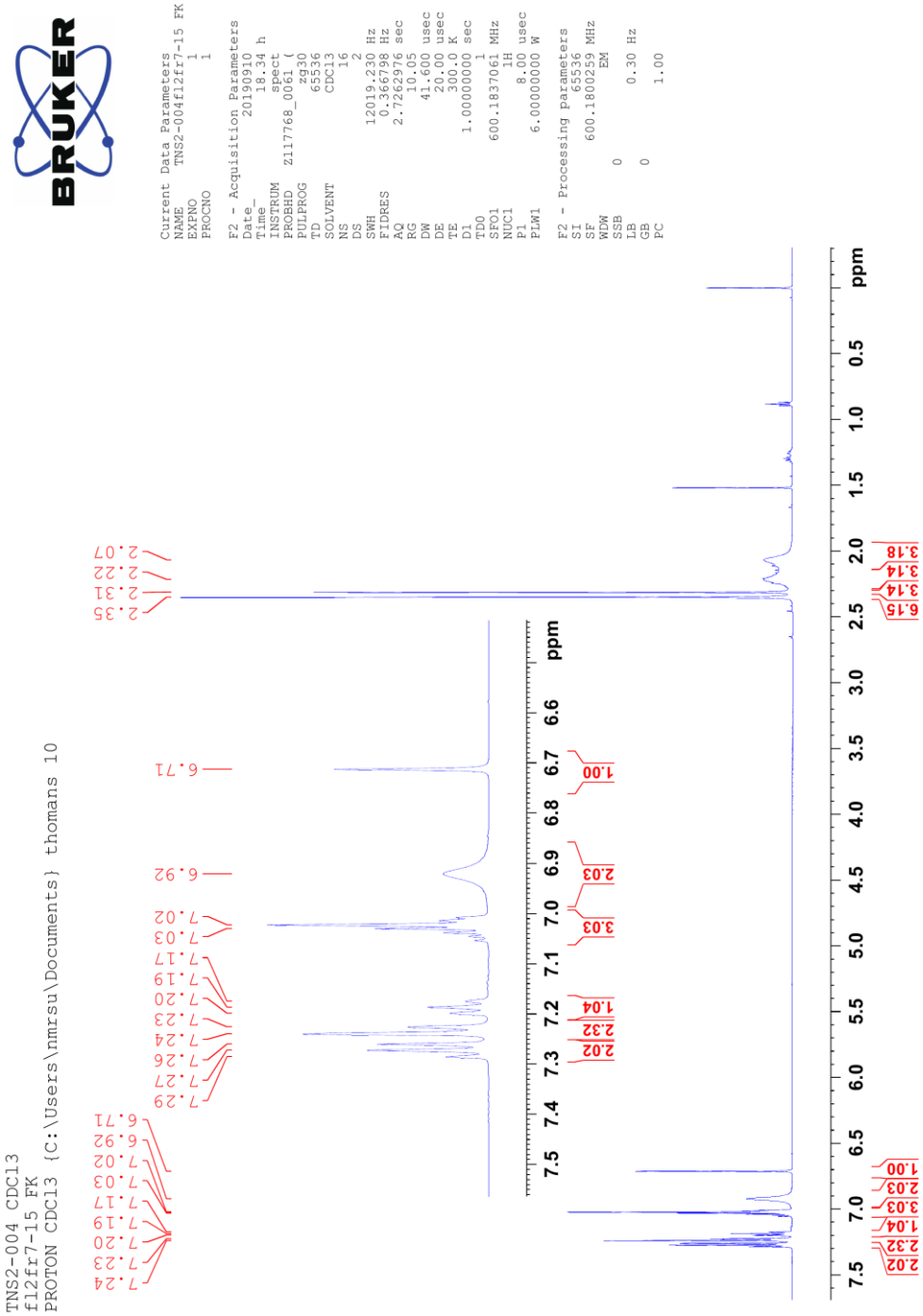

Appendix E Spectra of Allenes, 3a-g

Appendix E.22 **^{13}C NMR spectrum for Allene 3f**

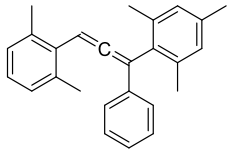

3f

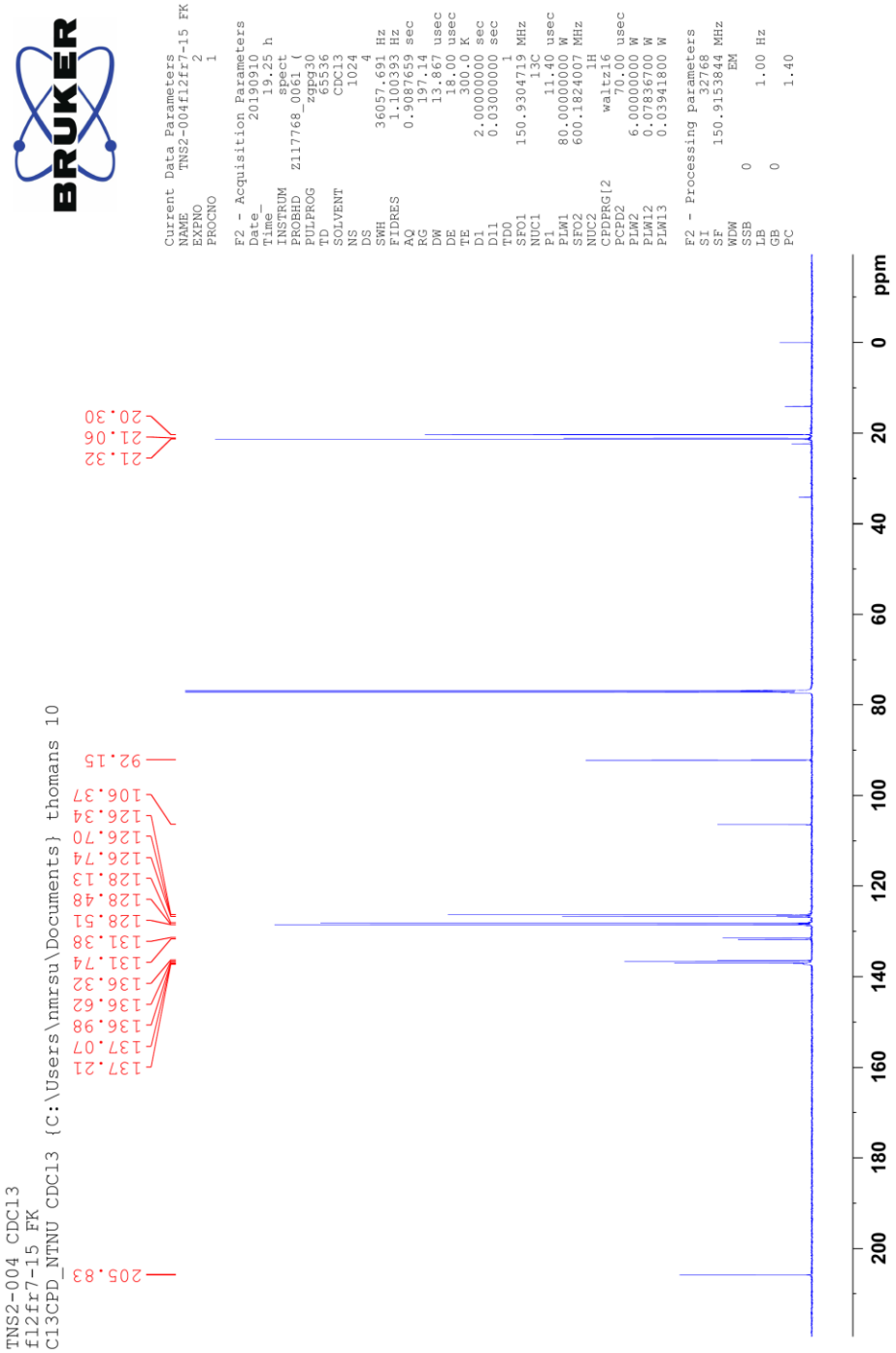

Appendix E Spectra of Allenes, 3a-g

Appendix E.23 **COSY NMR spectrum for Allene 3f**

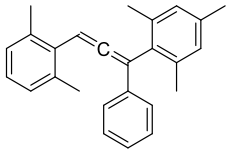

3f

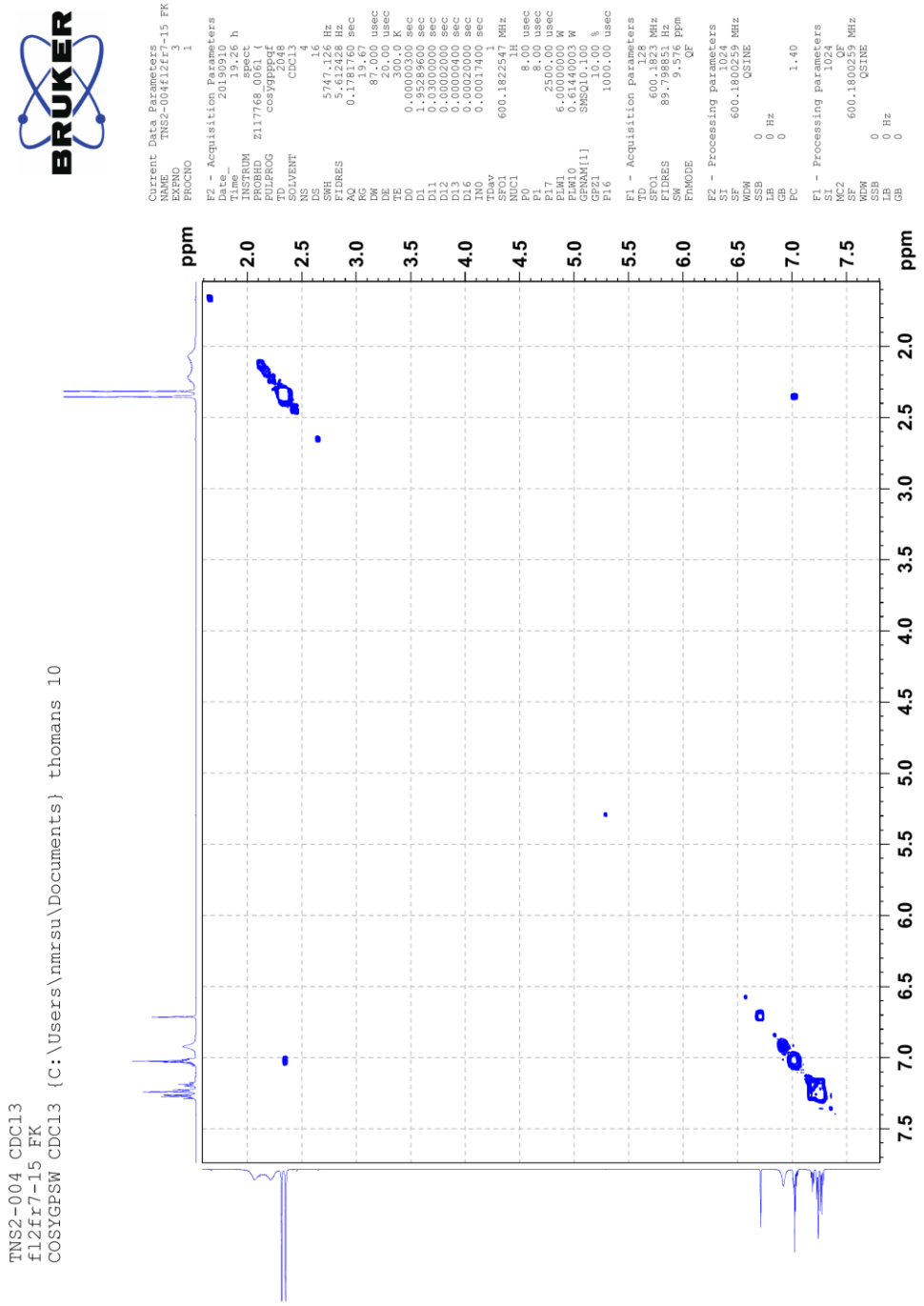

Appendix E Spectra of Allenes, 3a-g

Appendix E.24 **HSQC NMR spectrum for Allene 3f**

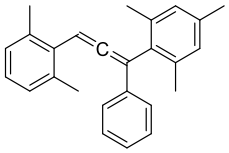

3f

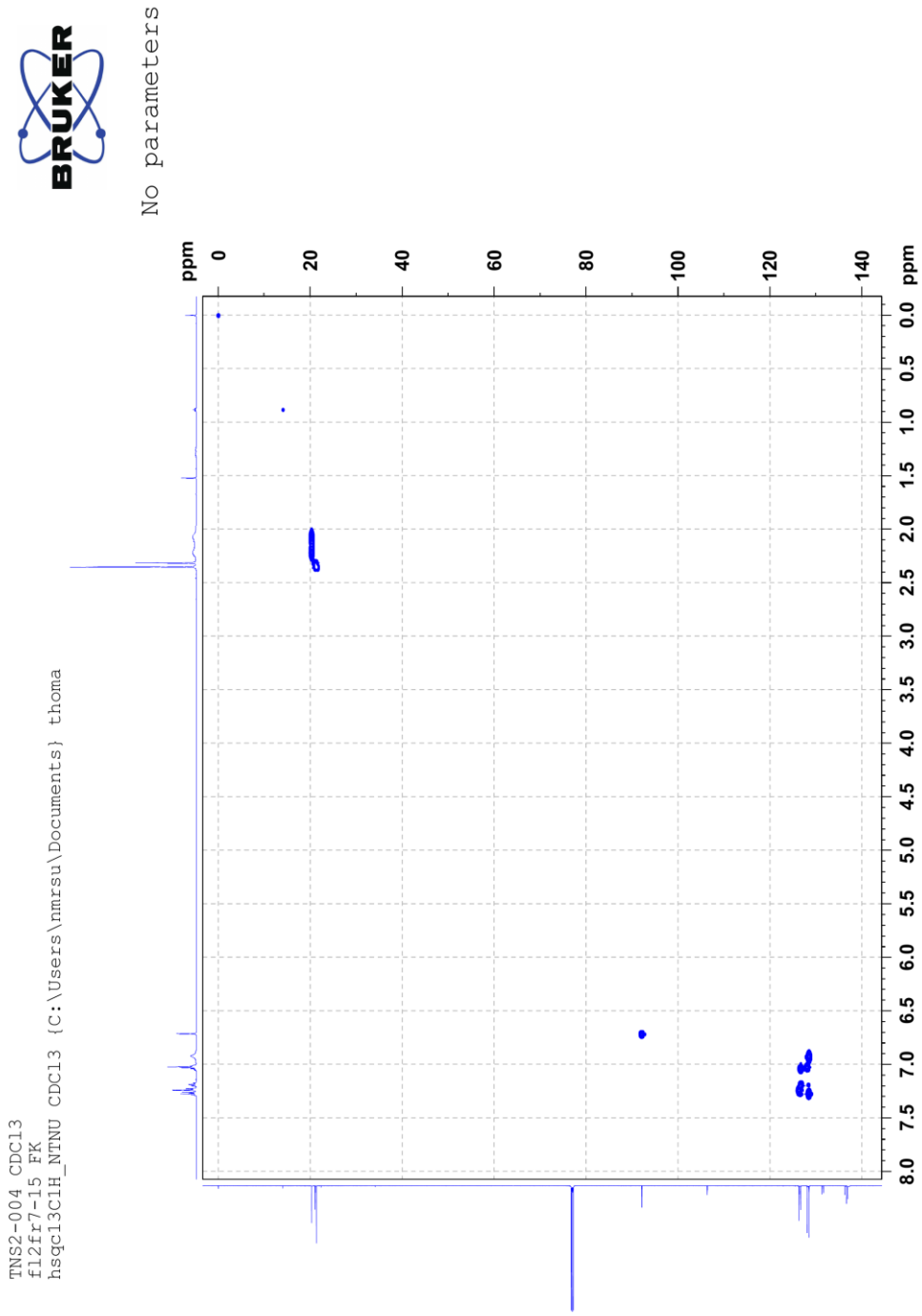

Appendix E Spectra of Allenes, 3a-g

Appendix E.25 **HMBC NMR spectrum for Allene 3f**

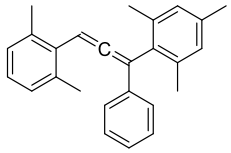

3f

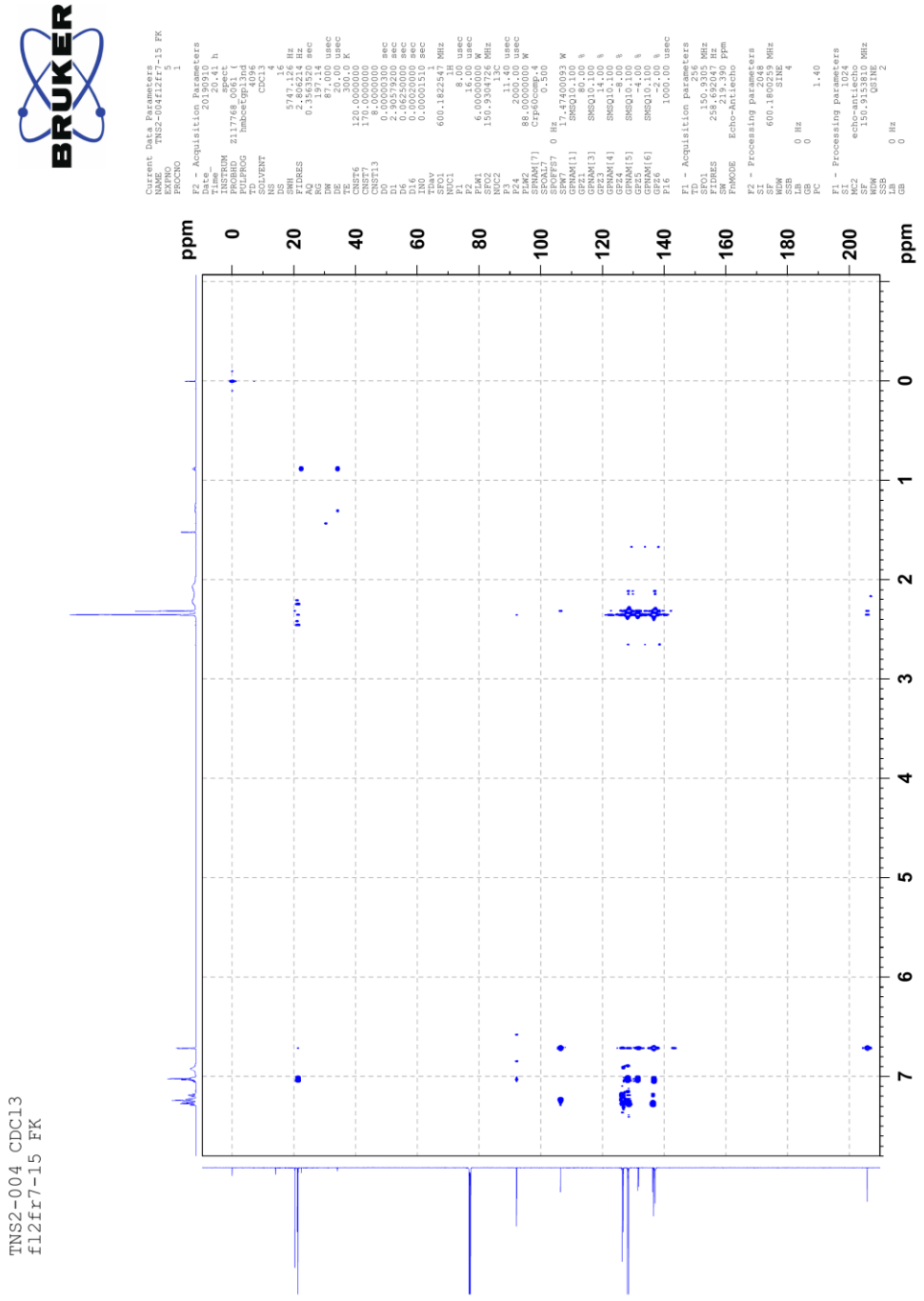

Appendix E Spectra of Allenes, 3a-g

Appendix E.26 **HRMS spectrum for Allene 3f**

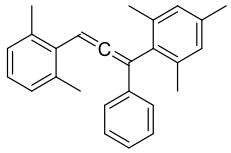

3f

Elemental Composition Report **Page 1**

Single Mass Analysis
Tolerance = 2.0 PPM / DBE: min = -50.0, max = 50.0
Element prediction: Off
Number of isotope peaks used for i-FIT = 3

Monoisotopic Mass, Even Electron Ions
484 formula(e) evaluated with 1 results within limits (all results (up to 1000) for each mass)
Elements Used:
C: 0-100 H: 0-150 10B: 0-3 O: 0-10
2019-678 68 (1.345) AM2 (Ar,35000.0,0.00,0.00); Cm (61:88)
1: TOF MS ASAP+

6.37e+006

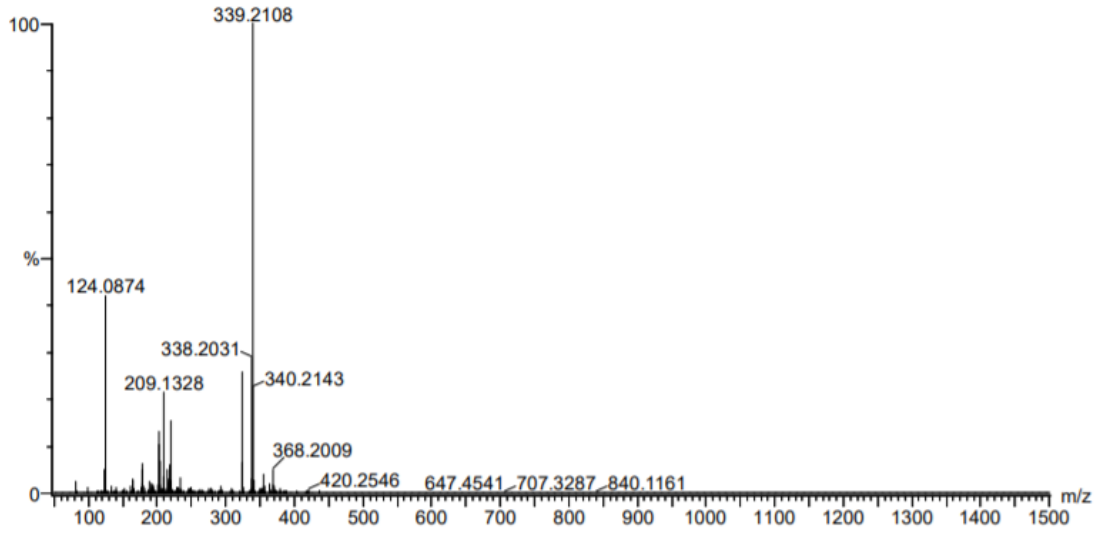

Minimum:				-50.0				
Maximum:		5.0	2.0	50.0				
Mass	Calc. Mass	mDa	PPM	DBE	i-FIT	Norm	Conf(%)	Formula
339.2108	339.2113	-0.5	-1.5	13.5	1336.0	n/a	n/a	C26 H27

Appendix E Spectra of Allenes, 3a-g

Appendix E.27 **^{1}H NMR Spectrum of Allene 3g**

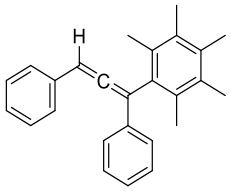

3g

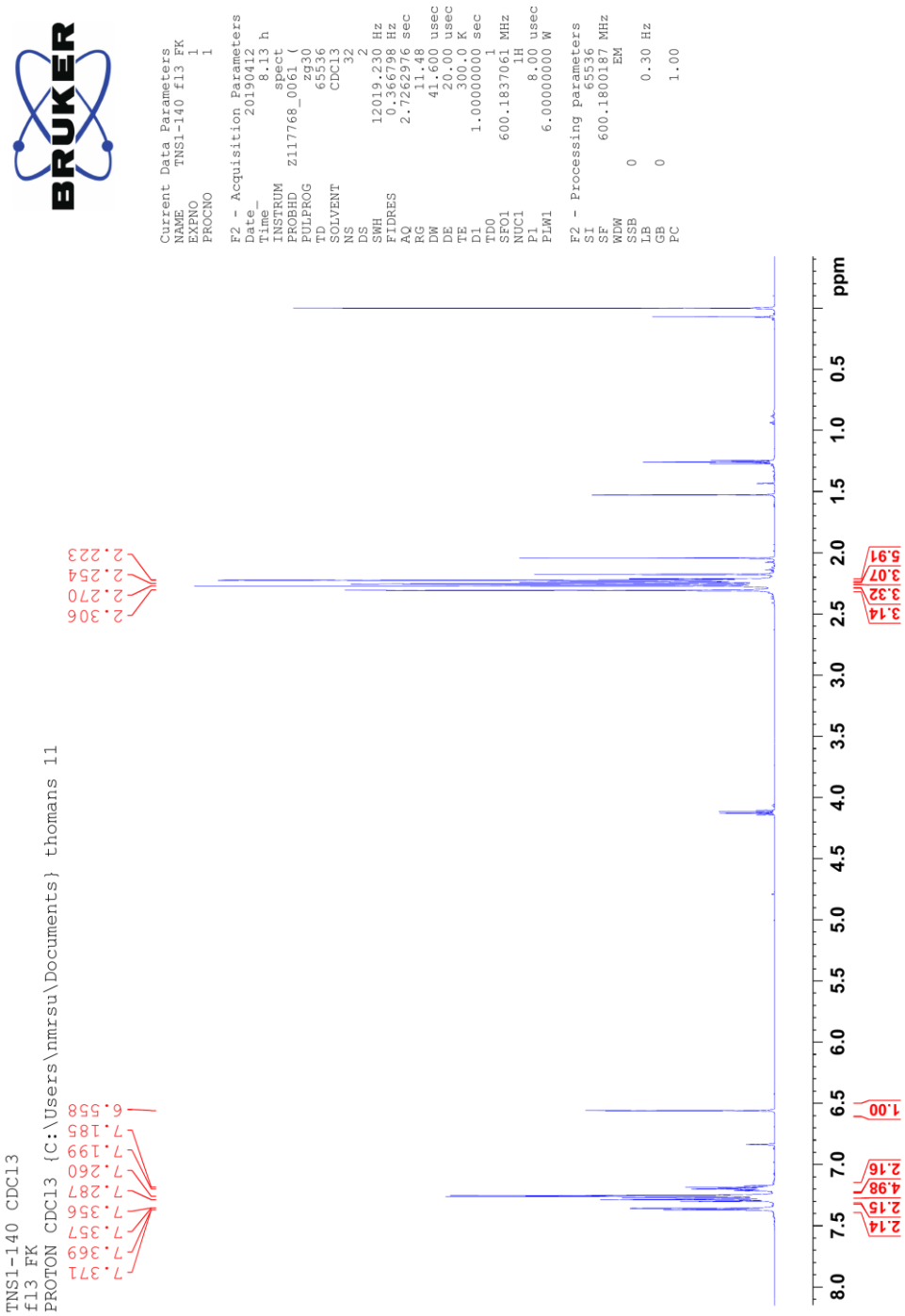

Appendix E Spectra of Allenes, 3a-g

Appendix E.28 **^{13}C NMR Spectrum of Allene 3g**

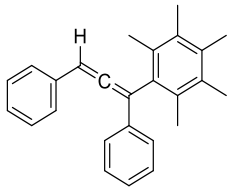

3g

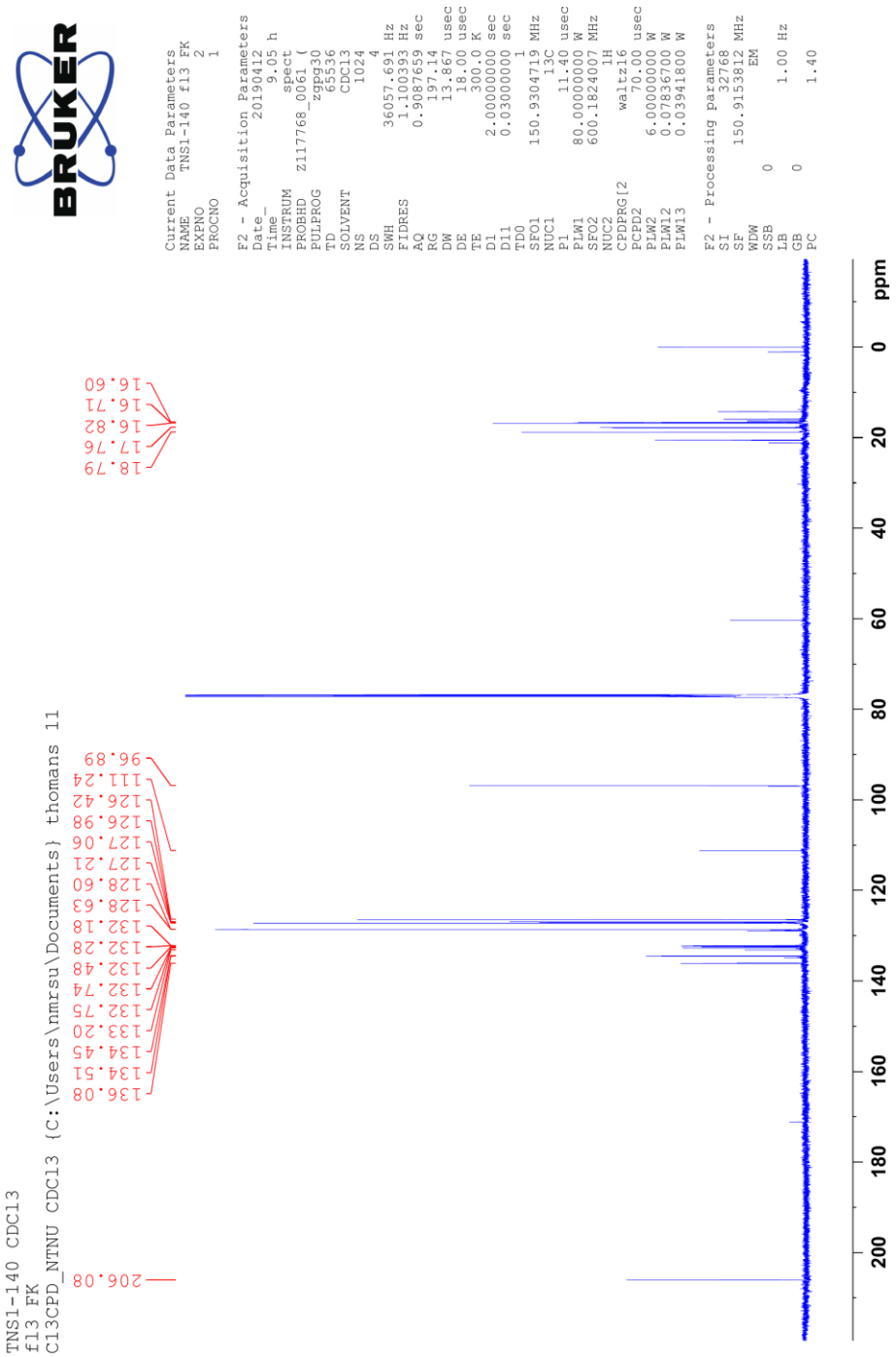

Appendix E Spectra of Allenes, 3a-g

Appendix E.29 **COSY NMR Spectrum of Allene 3g**

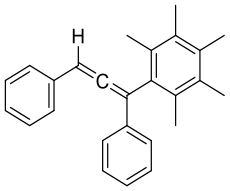

3g

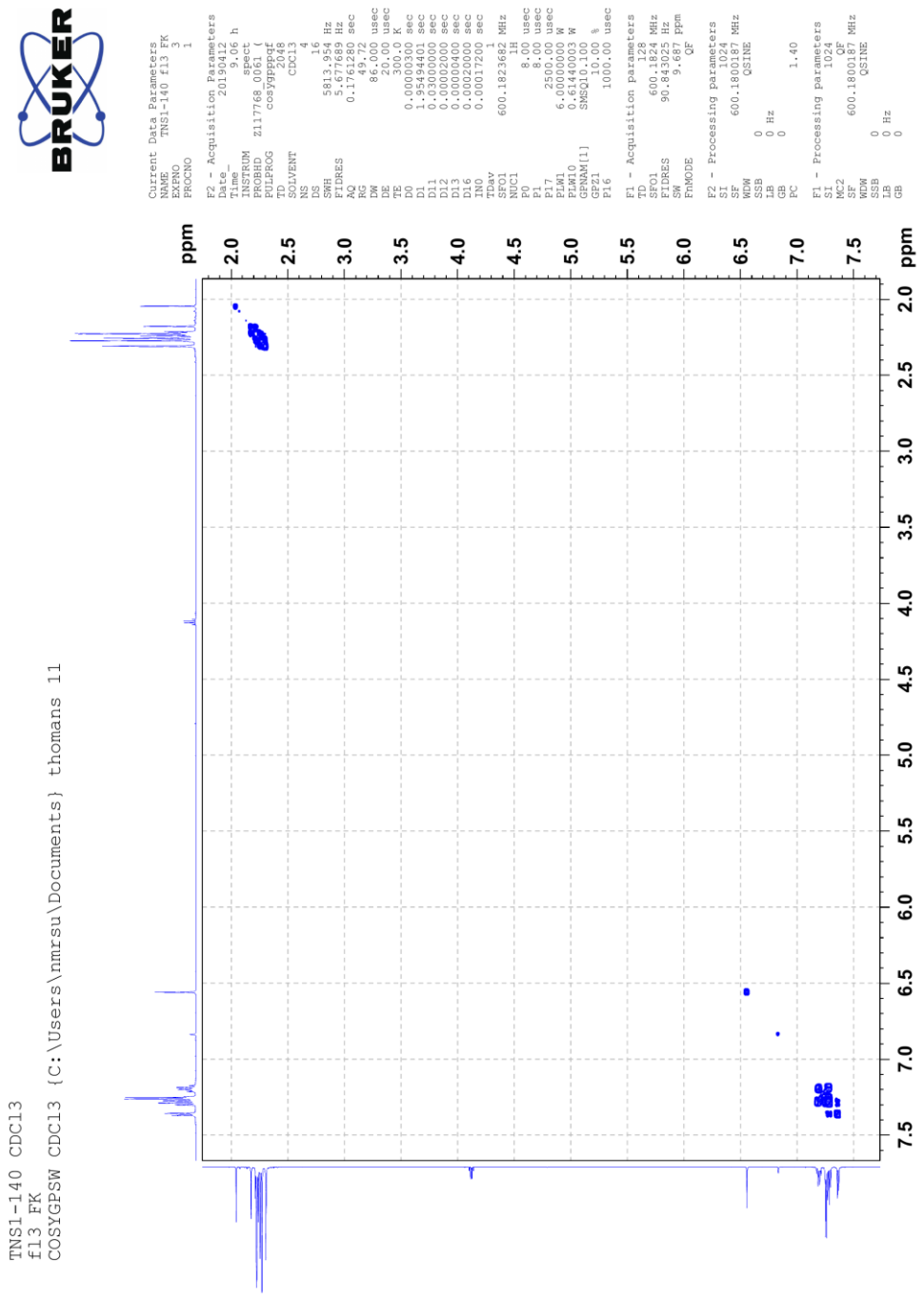

Appendix E Spectra of Allenes, 3a-g

Appendix E.30 **HSQC NMR Spectrum of Allene 3g**

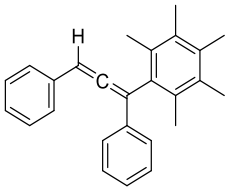

3g

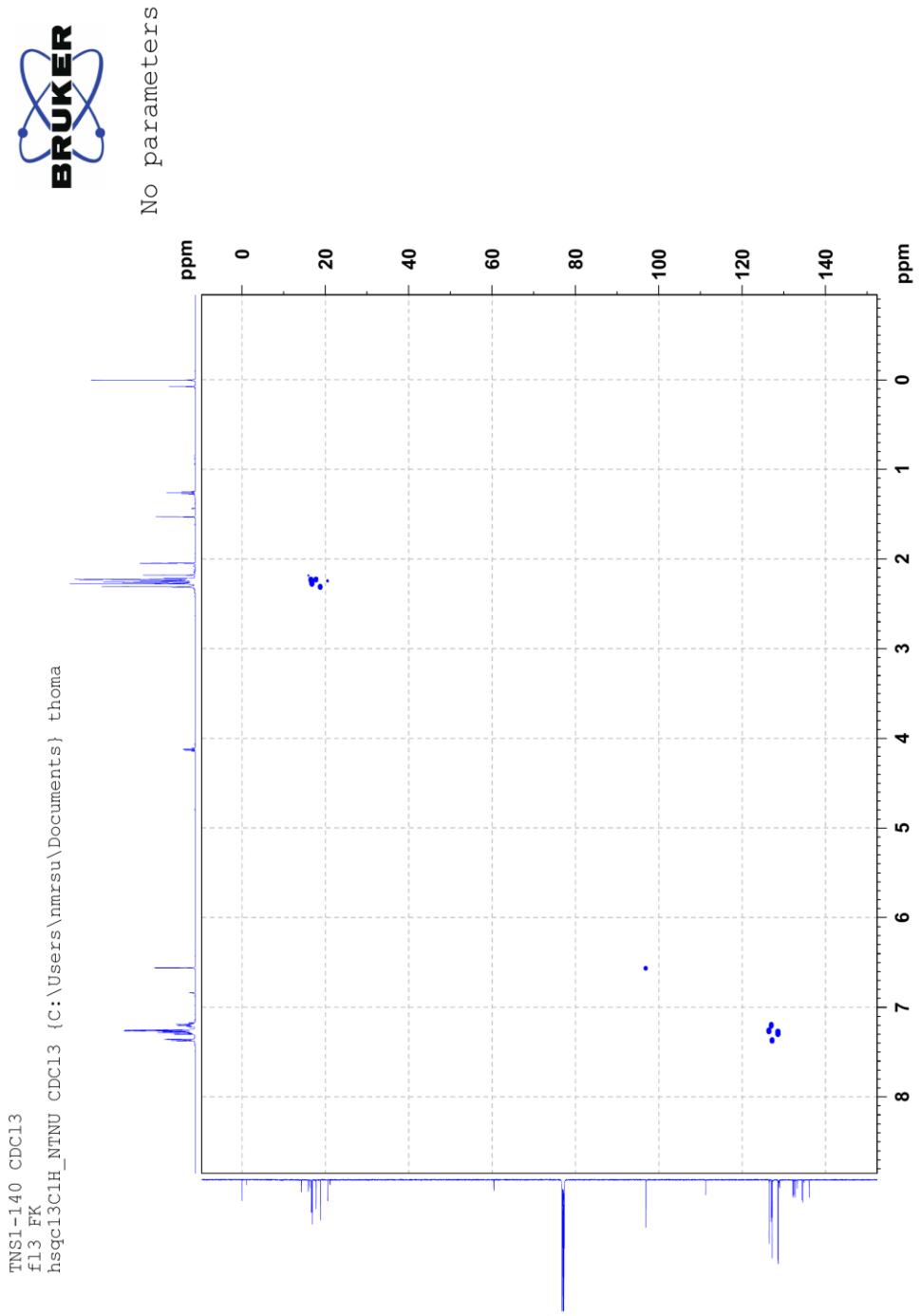

Appendix E Spectra of Allenes, 3a-g

Appendix E.31 **HMBC NMR Spectrum of Allene 3g**

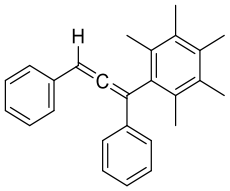

3g

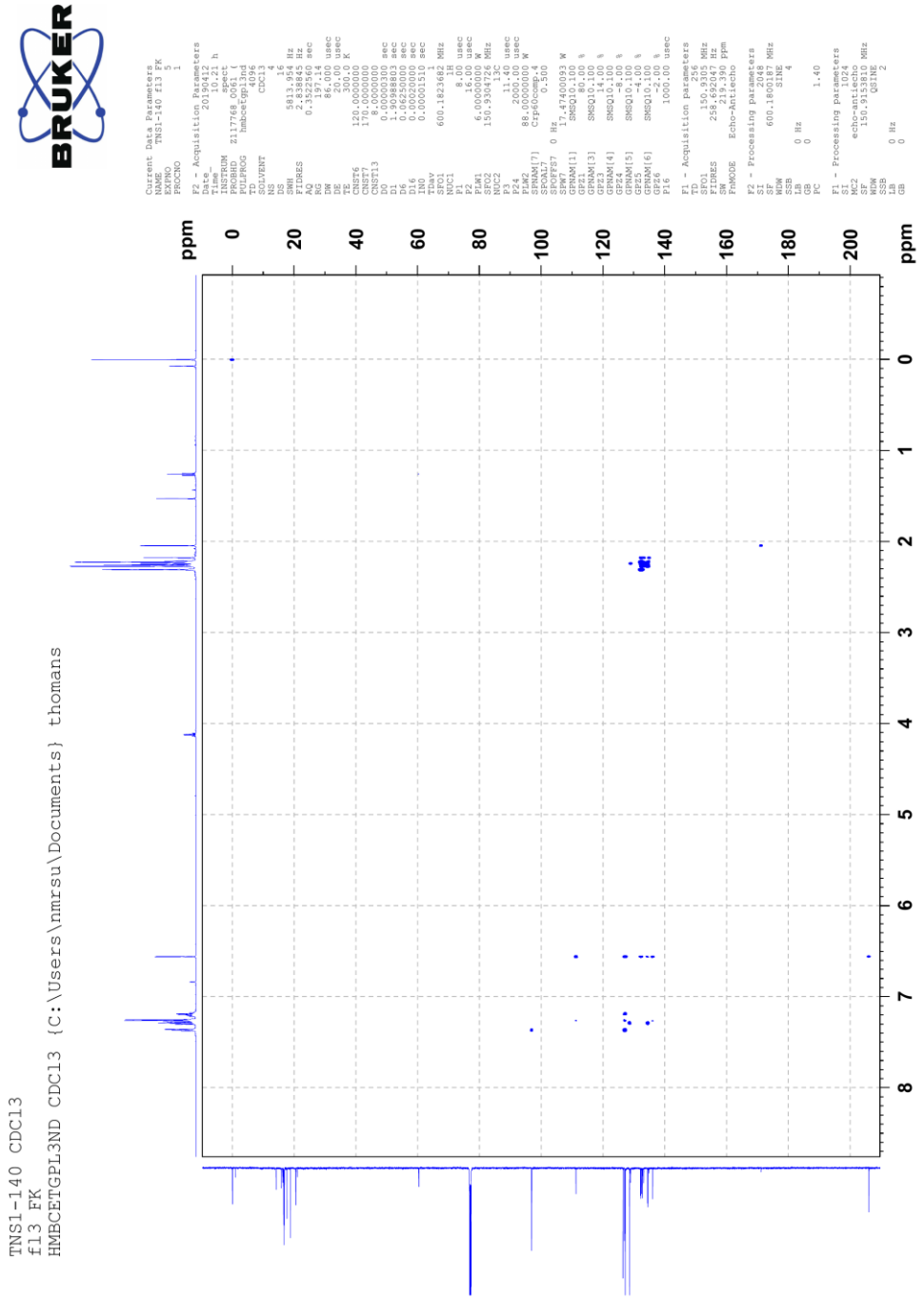

Appendix F **Spectra of Indenes, 4a-d and 4f-g**

Appendix F.1 **^{1}H NMR Spectrum of Indene 4a**

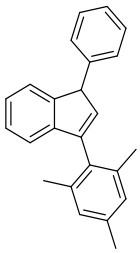

4a

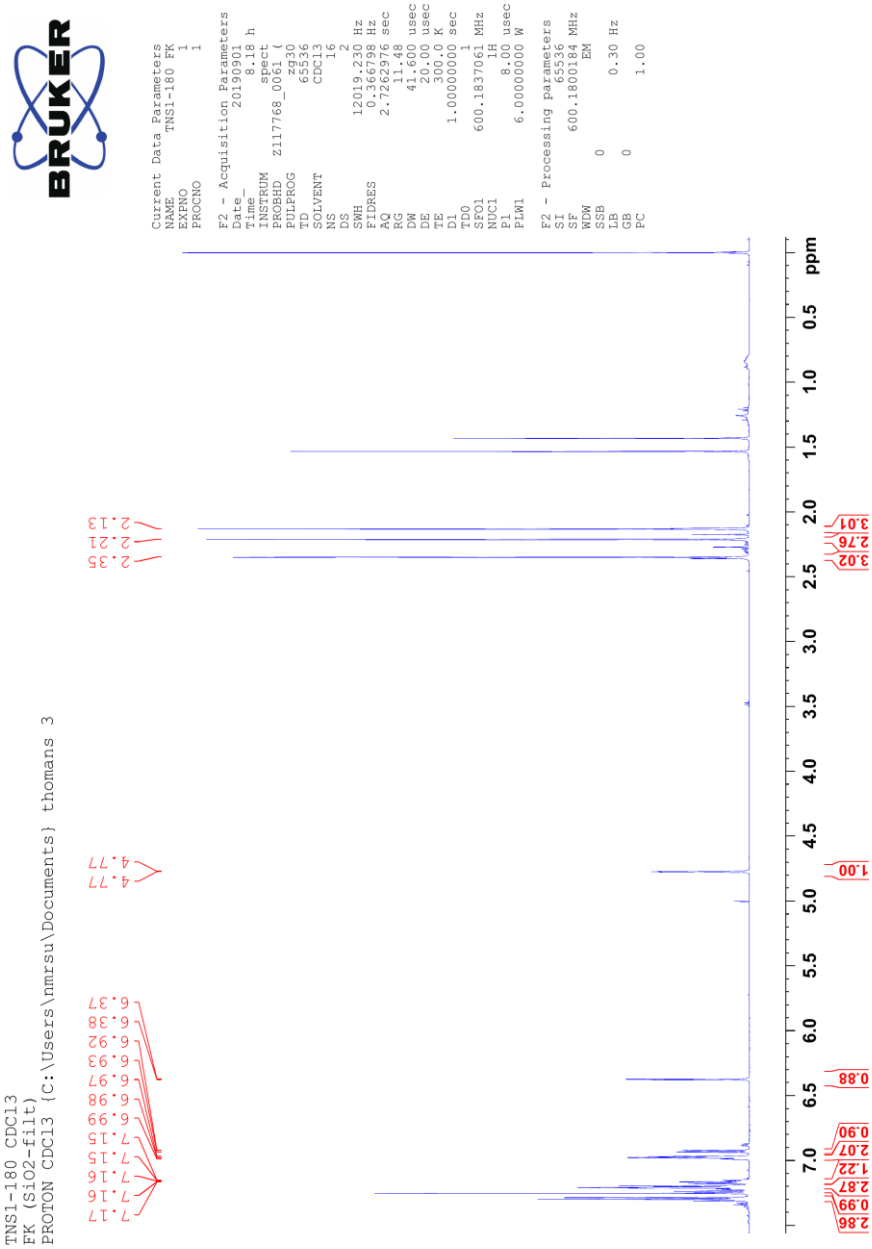

Appendix F Spectra of Indenes, 4a-d and 4f-g

Appendix F.2 **^{1}H NMR Spectrum of Indene 4b and Alkyne 2e**

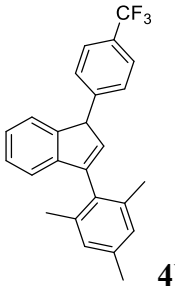

4b

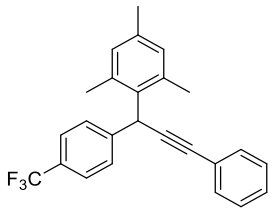

2e

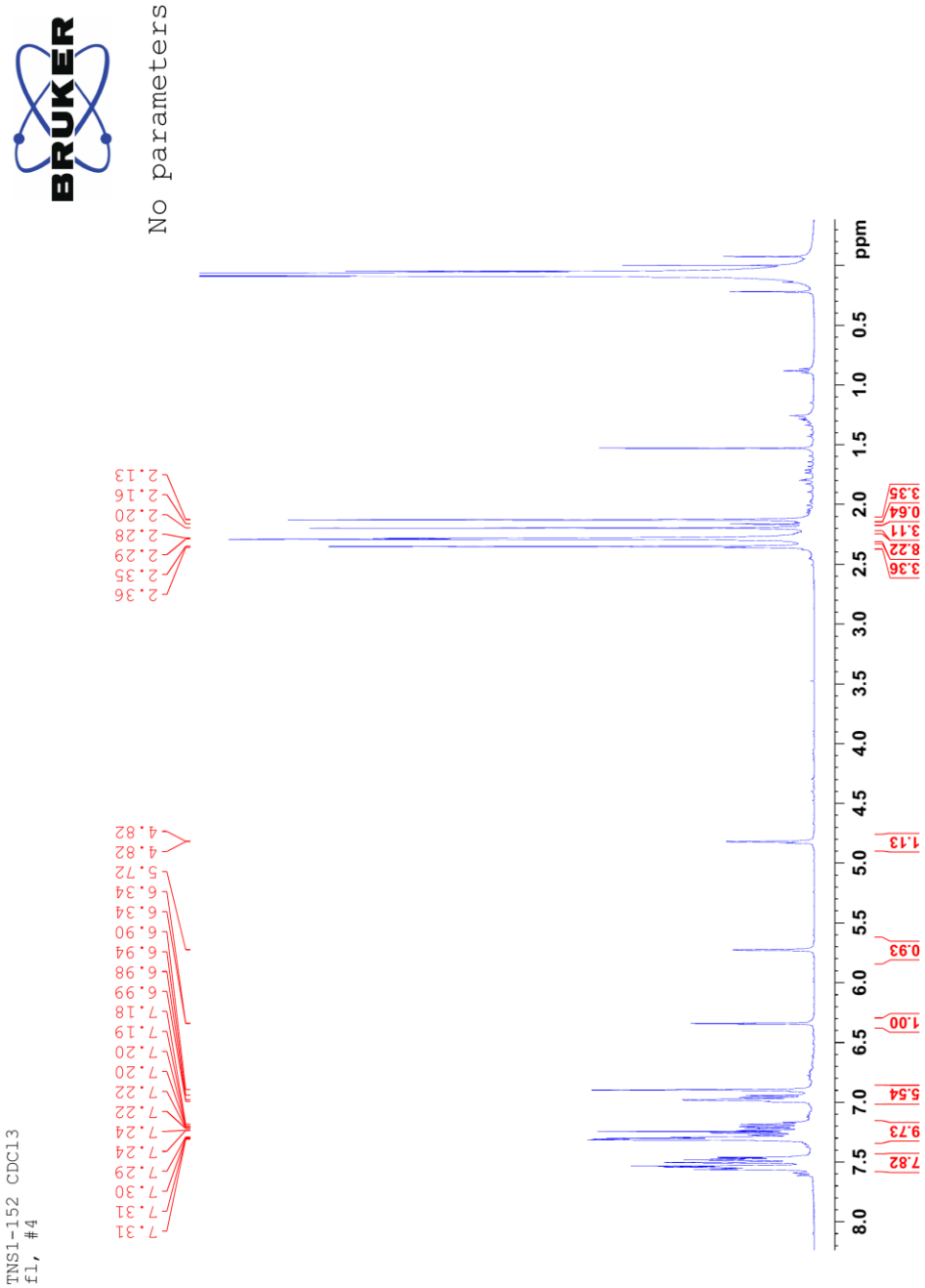

Appendix F Spectra of Indenes, 4a-d and 4f-g

Appendix F.3 **^{1}H NMR Spectrum of Indene 4c**

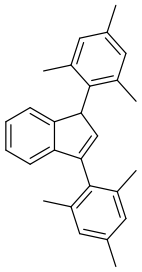

4c

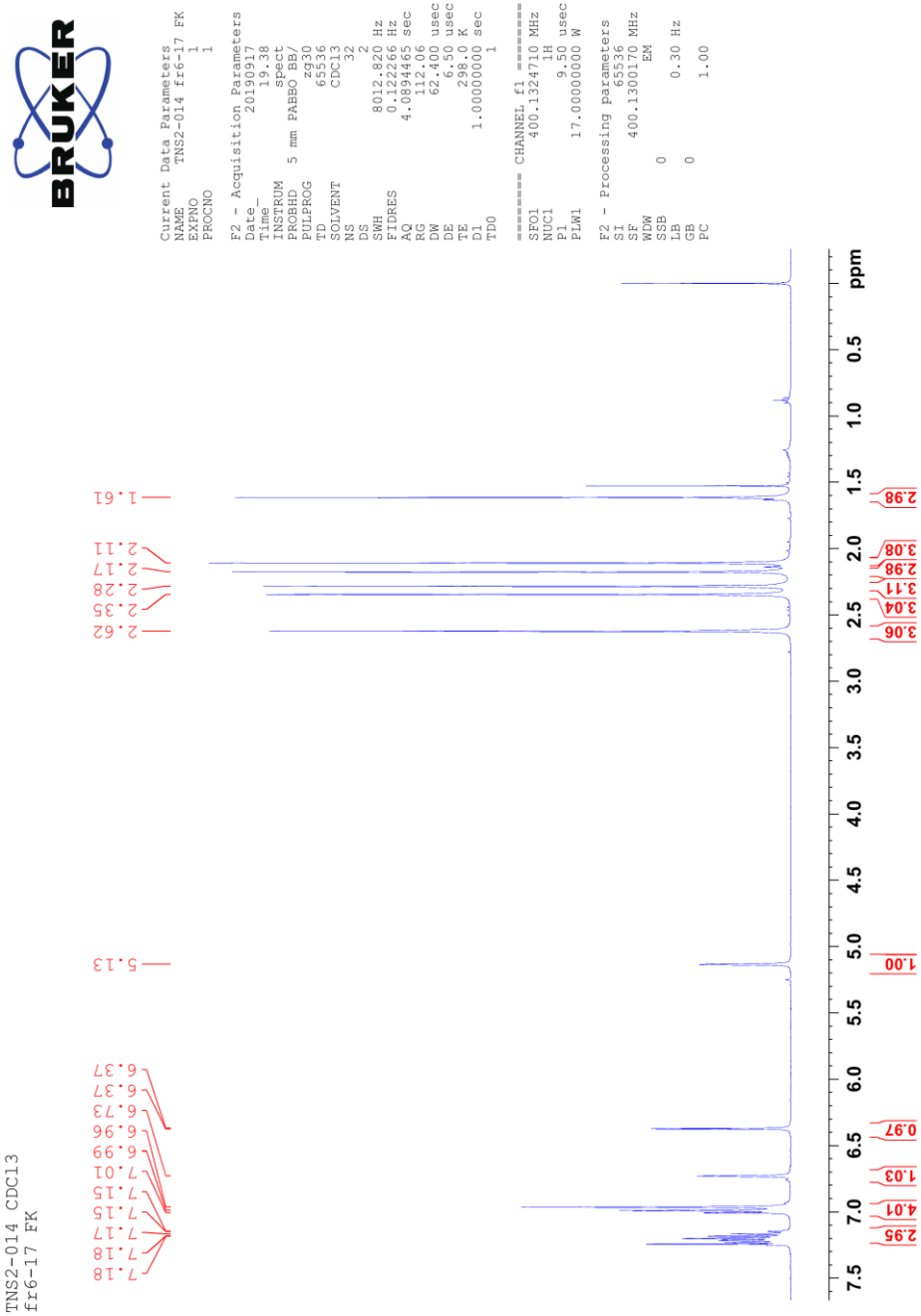

Appendix F Spectra of Indenes, 4a-d and 4f-g

Appendix F.4 **^{1}H NMR Spectrum of Indene 4d**

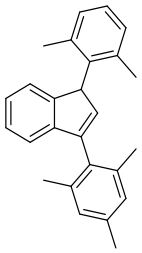

4d

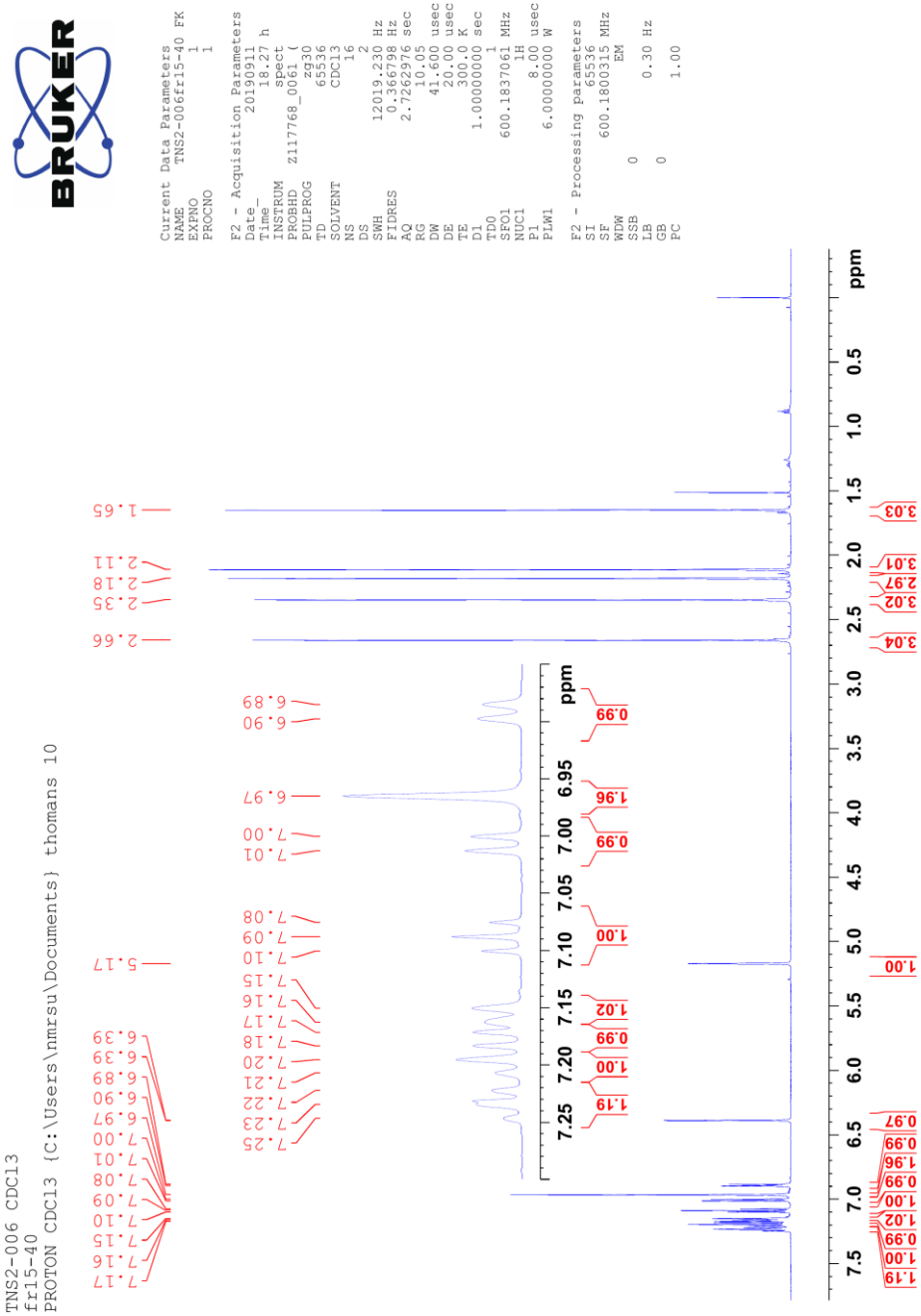

Appendix F Spectra of Indenes, 4a-d and 4f-g

Appendix F.5 **^{13}C NMR Spectrum of Indene 4d**

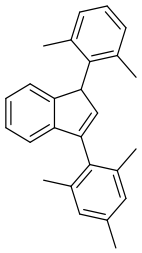

4d

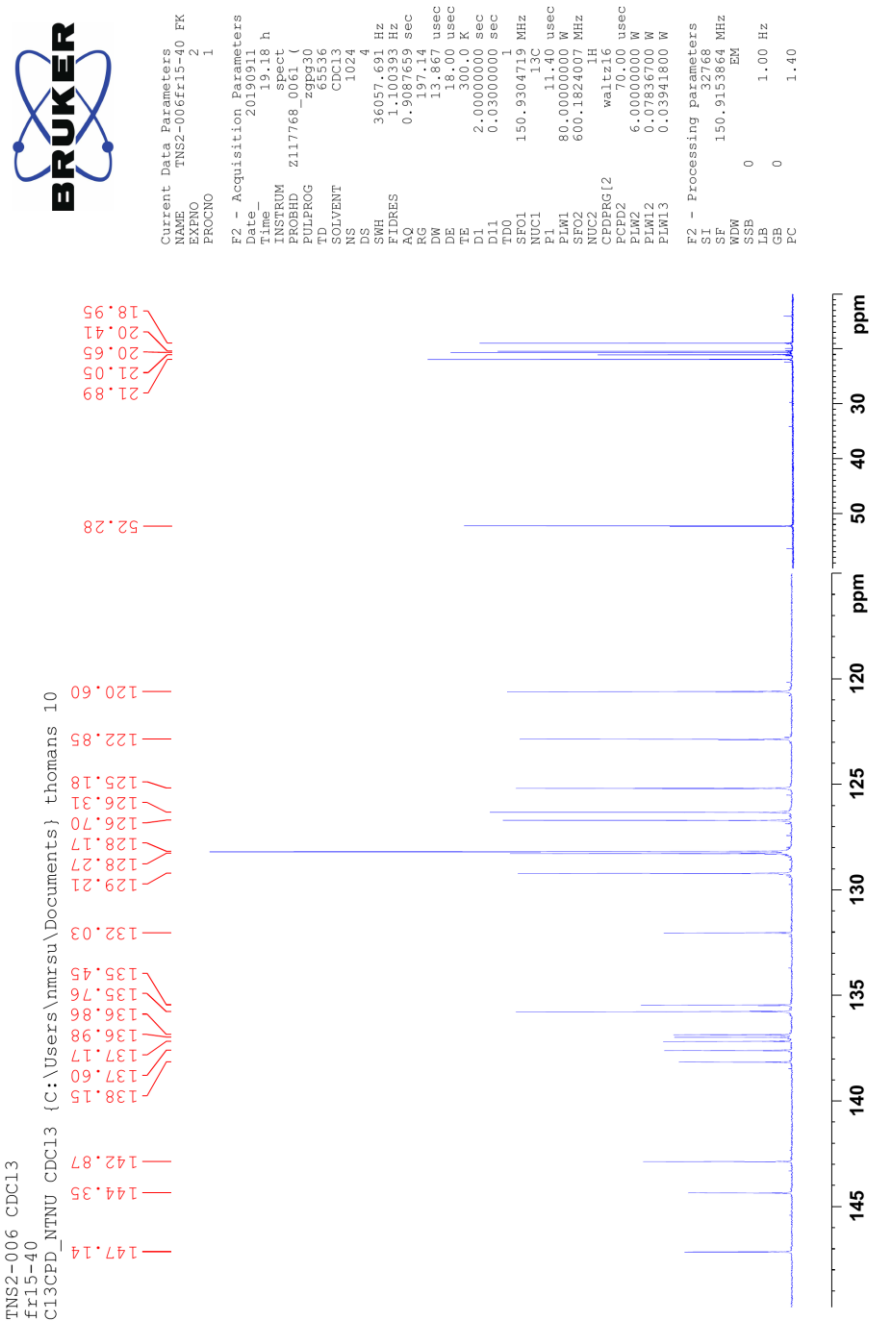

Appendix F Spectra of Indenes, 4a-d and 4f-g

Appendix F.6 **COSY NMR Spectrum of Indene 4d**

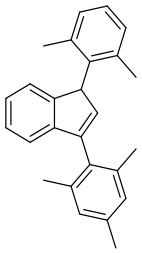

4d

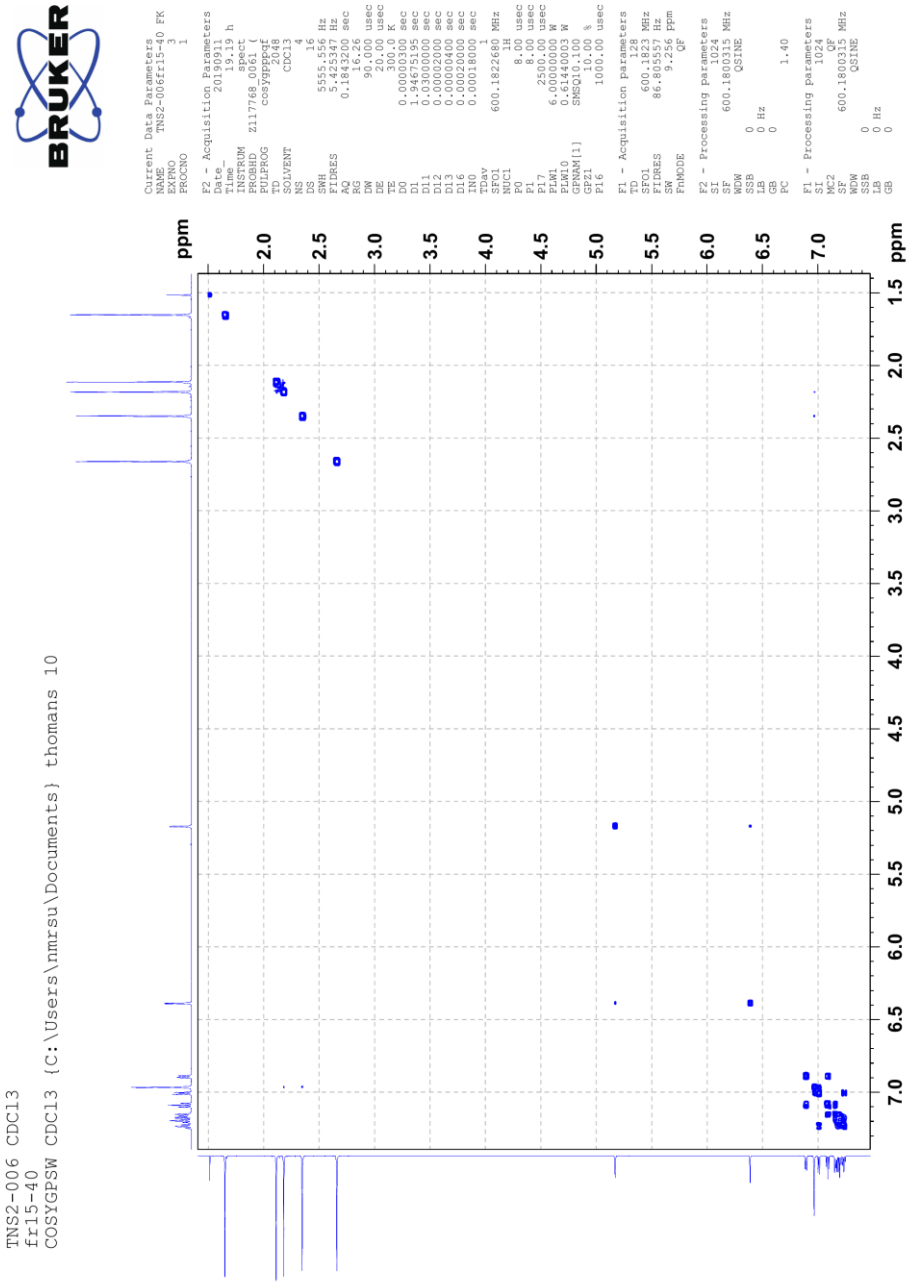

Appendix F Spectra of Indenes, 4a-d and 4f-g

Appendix F.7 **HSQC NMR Spectrum of Indene 4d**

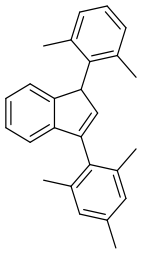

4d

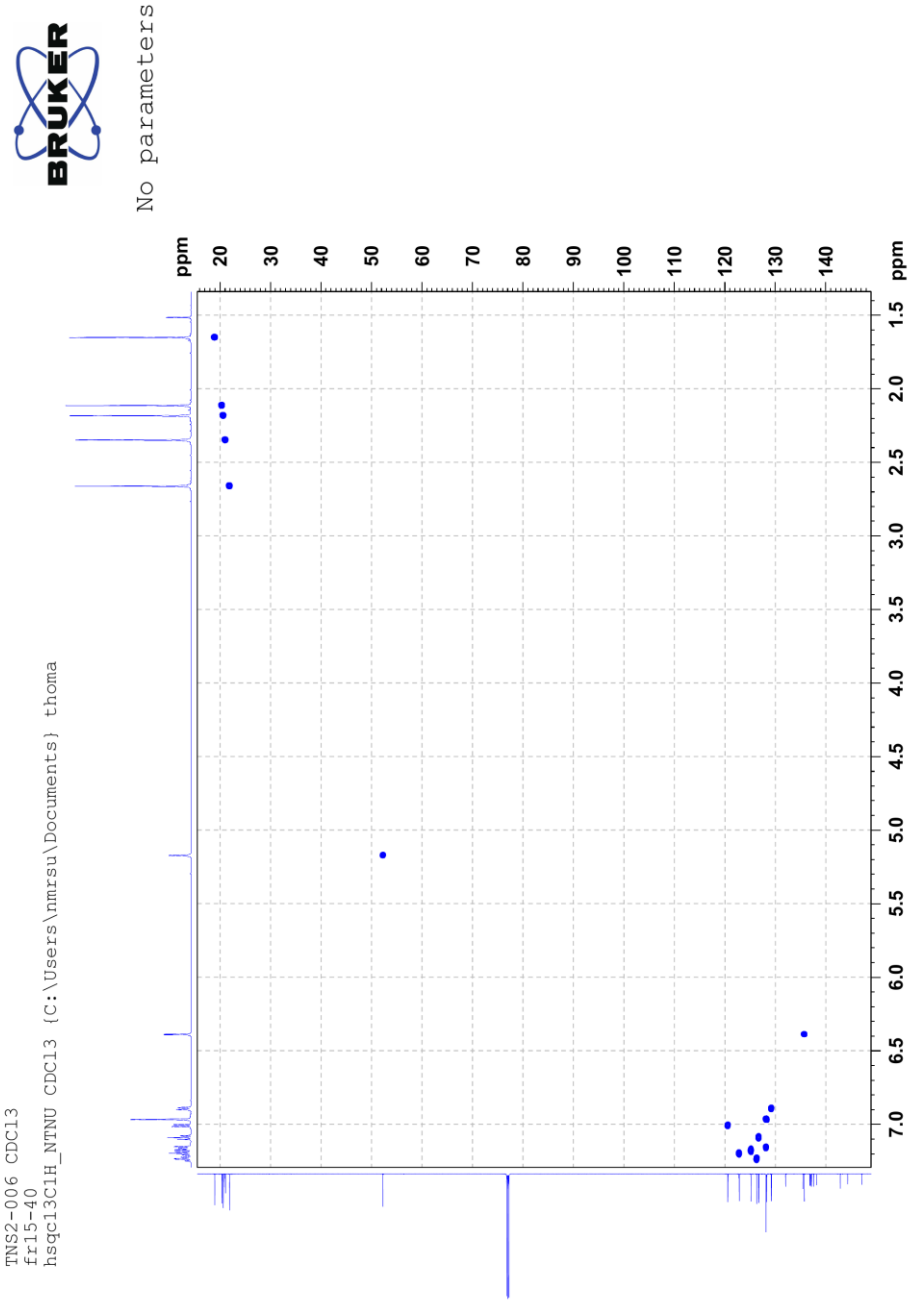

Appendix F Spectra of Indenes, 4a-d and 4f-g

Appendix F.8 **HMBC NMR Spectrum of Indene 4d**

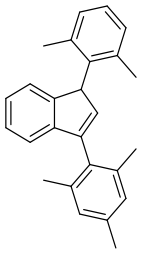

4d

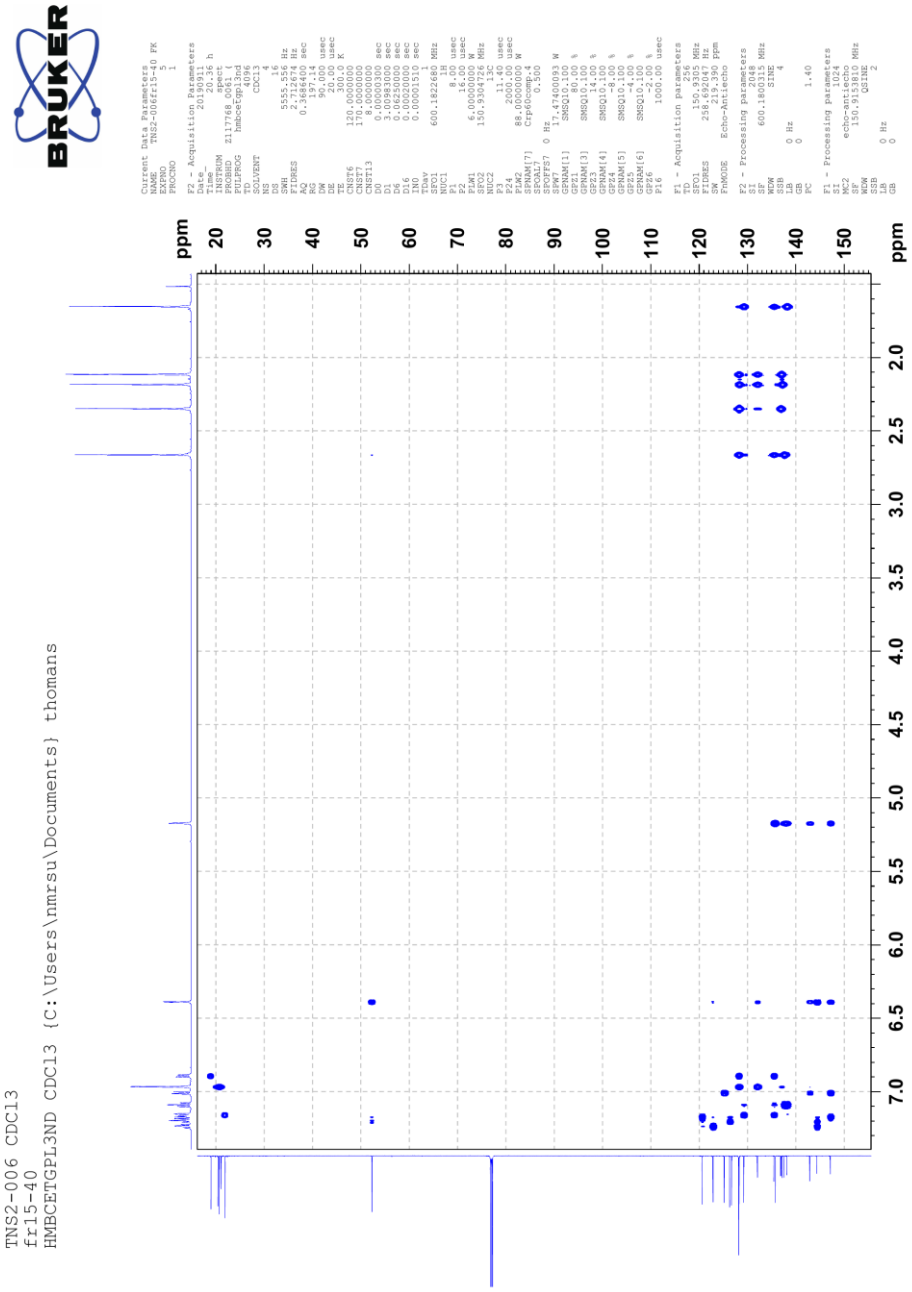

Appendix F Spectra of Indenes, 4a-d and 4f-g

Appendix F.9 **Selective HMBC NMR Spectrum of Indene 4d**

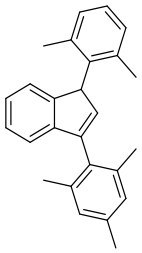

4d

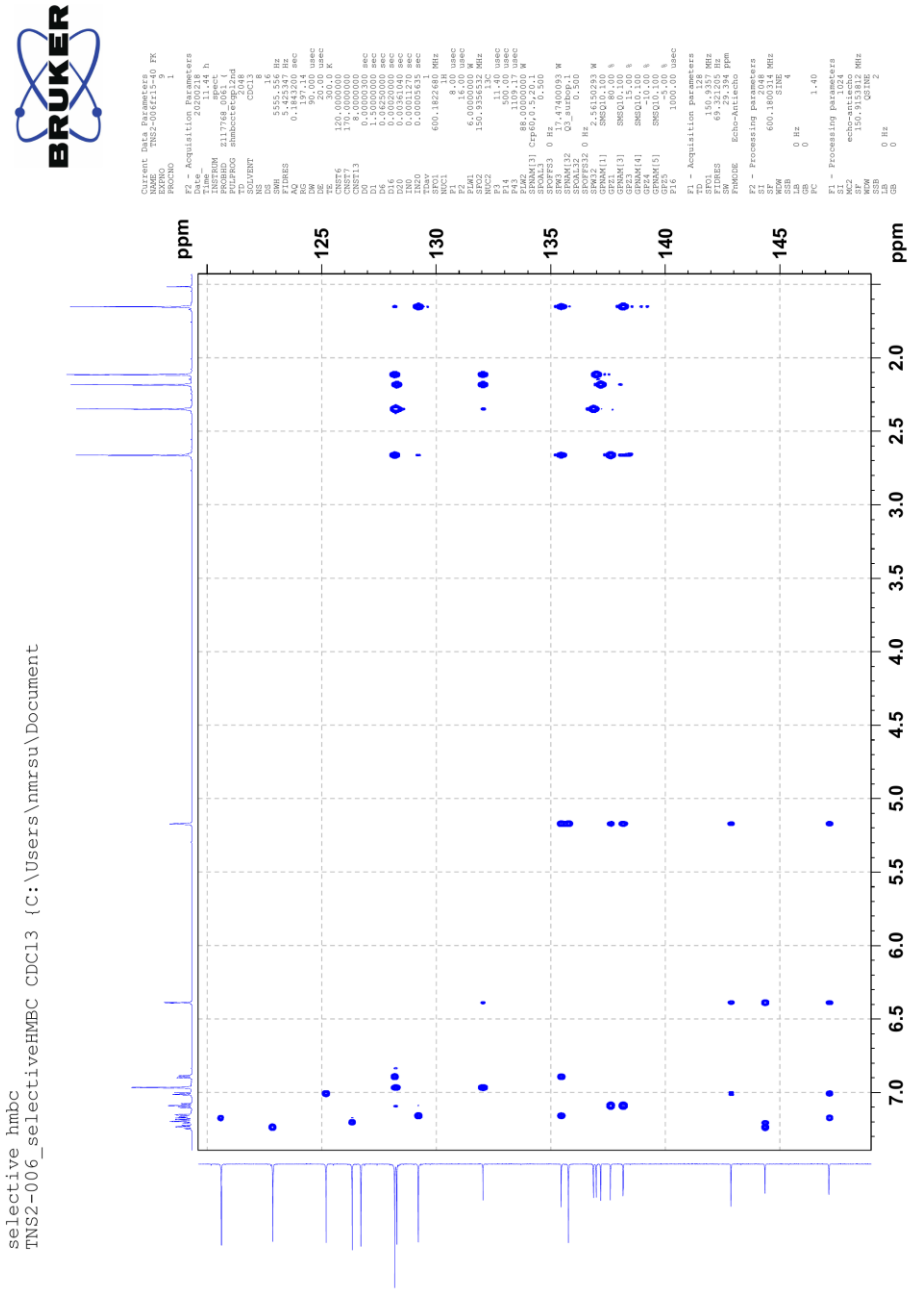

Appendix F Spectra of Indenes, 4a-d and 4f-g

Appendix F.10 **NOESY NMR Spectrum of Indene 4d**

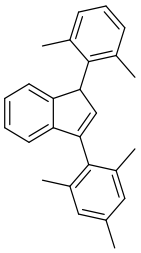

4d

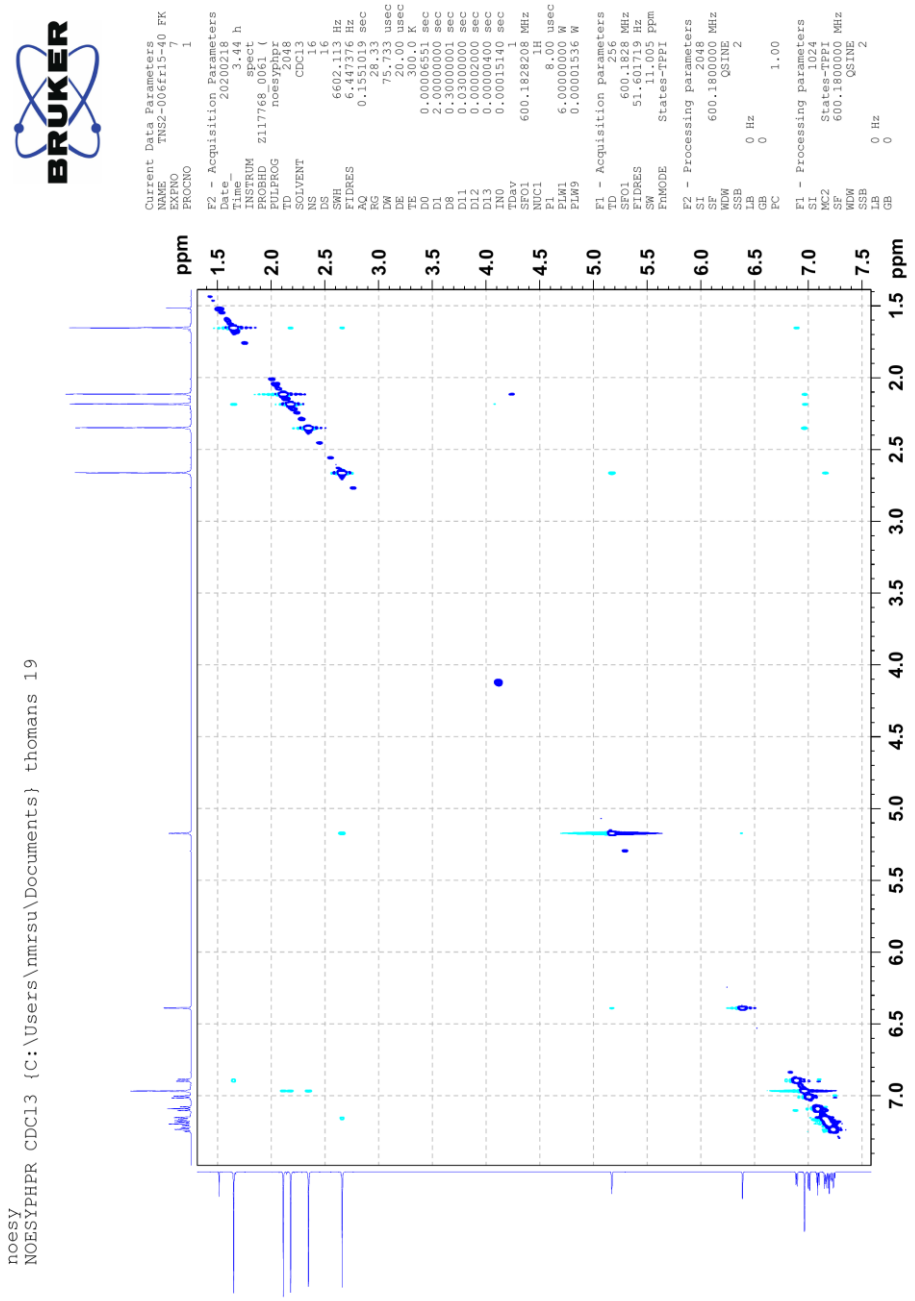

Appendix F Spectra of Indenes, 4a-d and 4f-g

Appendix F.11 **HRMS Spectrum of Indene 4d**

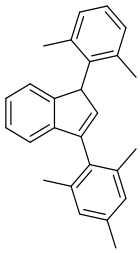

4d

Elemental Composition Report **Page 1**

Single Mass Analysis
Tolerance = 2.0 PPM / DBE: min = -50.0, max = 50.0
Element prediction: Off
Number of isotope peaks used for i-FIT = 3

Monoisotopic Mass, Odd Electron Ions
480 formula(e) evaluated with 1 results within limits (all results (up to 1000) for each mass)
Elements Used:
C: 0-100 H: 0-150 10B: 0-3 O: 0-10
2019-680 36 (0.724) AM2 (Ar,35000.0,0.00,0.00); Cm (27:38)
1: TOF MS ASAP+

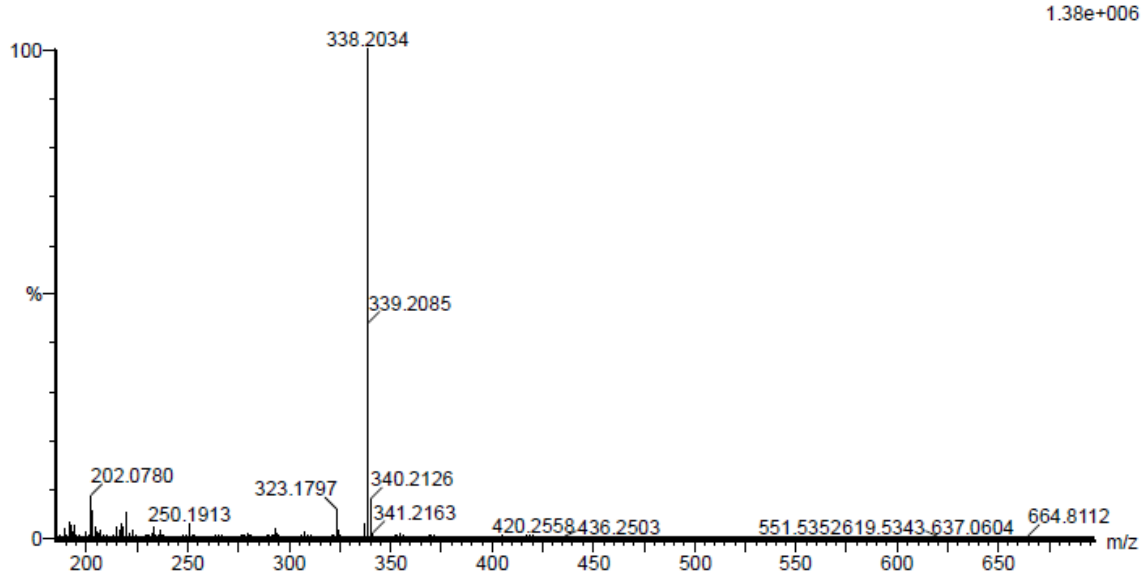

Minimum:				-50.0				
Maximum:		5.0	2.0	50.0				
Mass	Calc. Mass	mDa	PPM	DBE	i-FIT	Norm	Conf(%)	Formula
338.2034	338.2035	-0.1	-0.3	14.0	1116.7	n/a	n/a	C26 H26

Appendix F Spectra of Indenes, 4a-d and 4f-g

Appendix F.12 **^{1}H NMR Spectrum of Indene 4f**

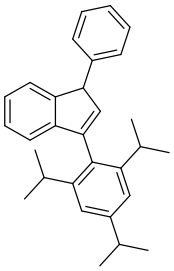

4f

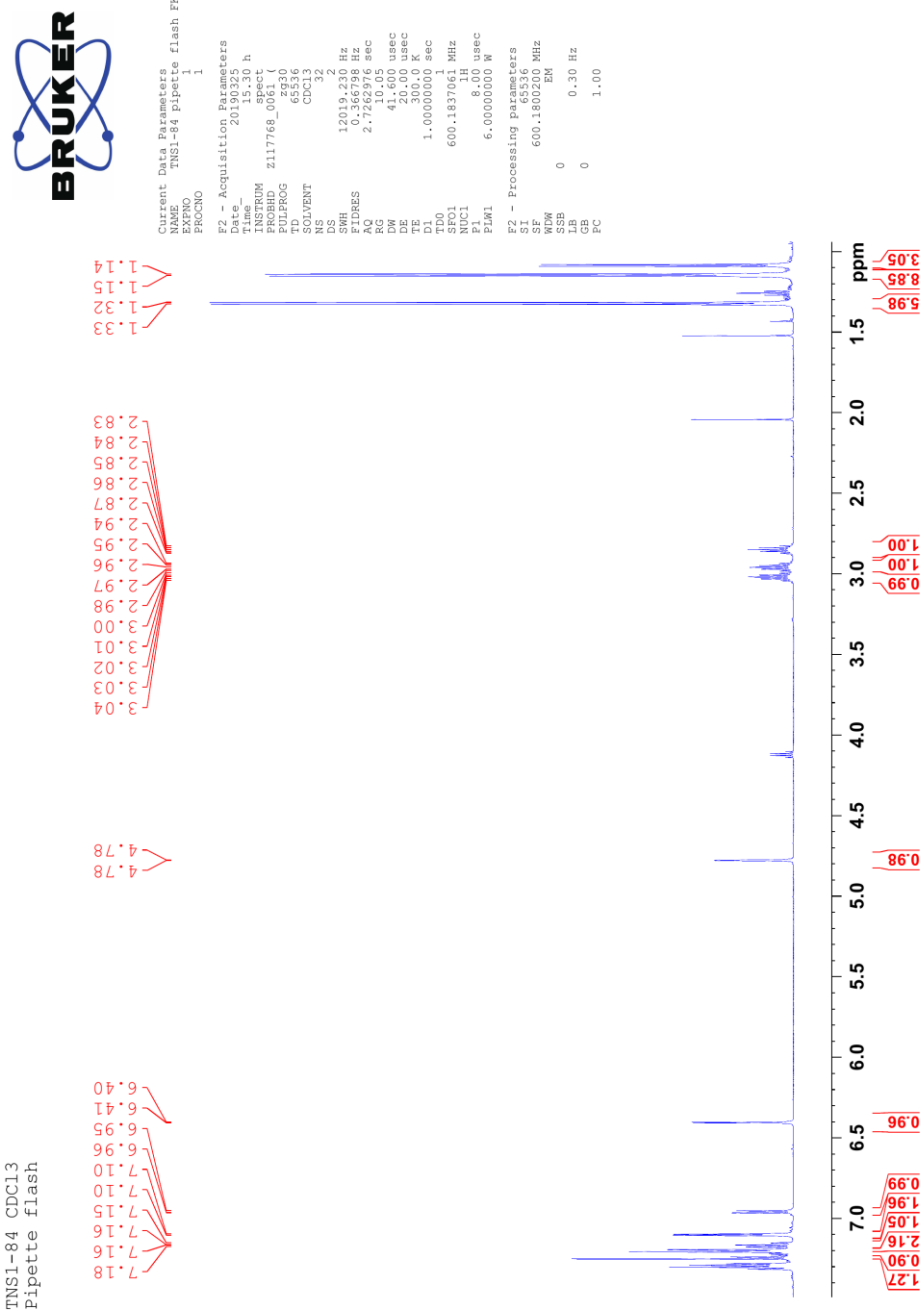

Appendix F Spectra of Indenes, 4a-d and 4f-g

Appendix F.13 **^{1}H NMR Spectrum of impure Indene 4g**

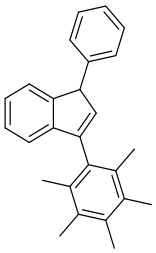

4g

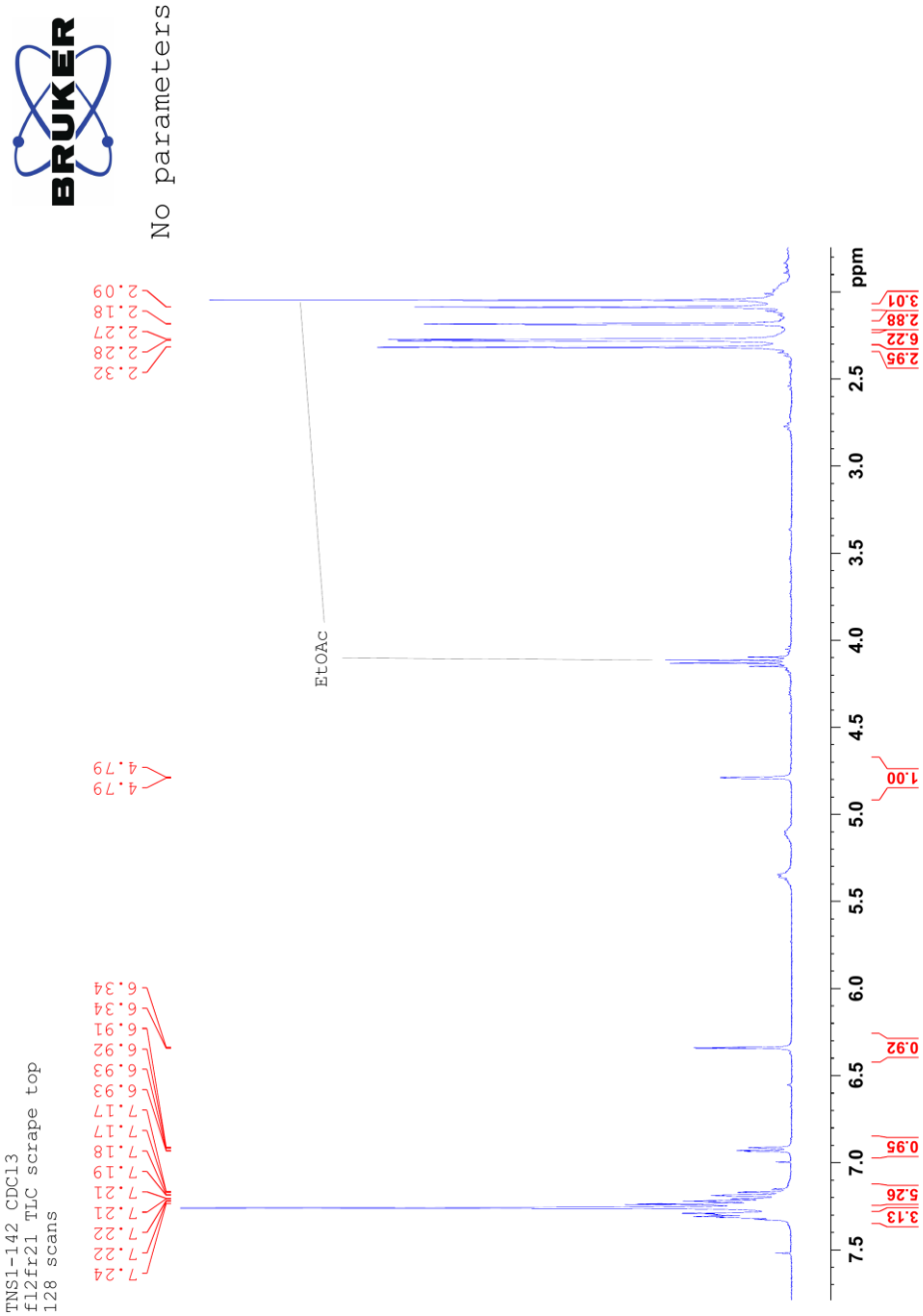

Appendix G Spectra of Cyclam-related compounds, 7, 8, 21 and 22

Appendix G.1 ^{1}H NMR Spectrum of cyclic tetraamide 7b

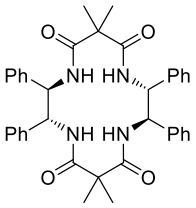

7b

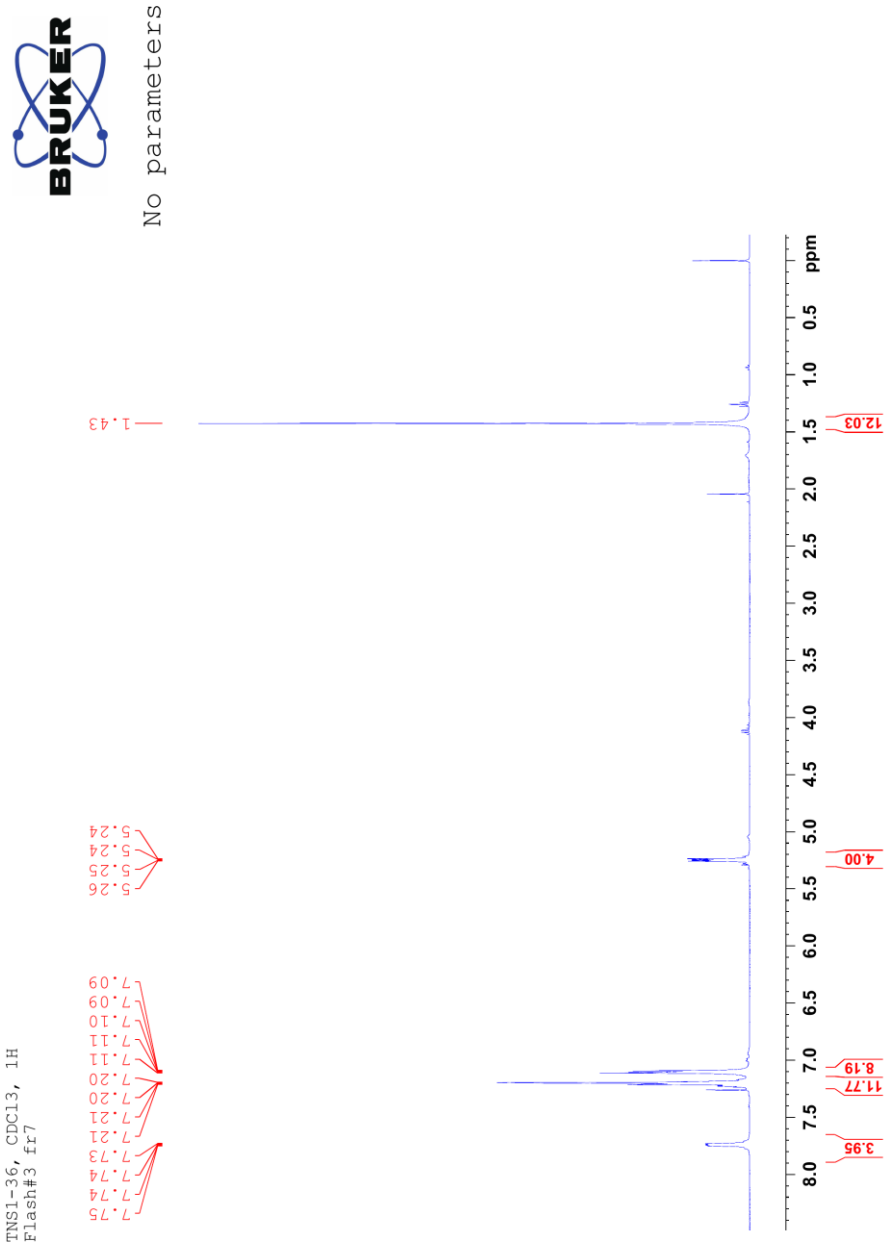

Appendix G Spectra of Cyclam-related compounds, 7, 8, 21 and 22

Appendix G.2 **HRMS Spectrum of cyclic tetraamide 7b**

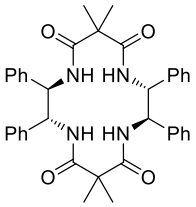

7b

Elemental Composition Report **Page 1**

Single Mass Analysis
Tolerance = 1.0 PPM / DBE: min = -2.0, max = 50.0
Element prediction: Off
Number of isotope peaks used for i-FIT = 2

Monoisotopic Mass, Even Electron Ions
1403 formula(e) evaluated with 1 results within limits (all results (up to 1000) for each mass)
Elements Used:
C: 0-100 H: 0-500 N: 0-10 O: 0-20
2018-517ny 148 (2.896) AM2 (Ar,35000.0,0.00,0.00); Cm (129:149)
1: TOF MS ASAP+

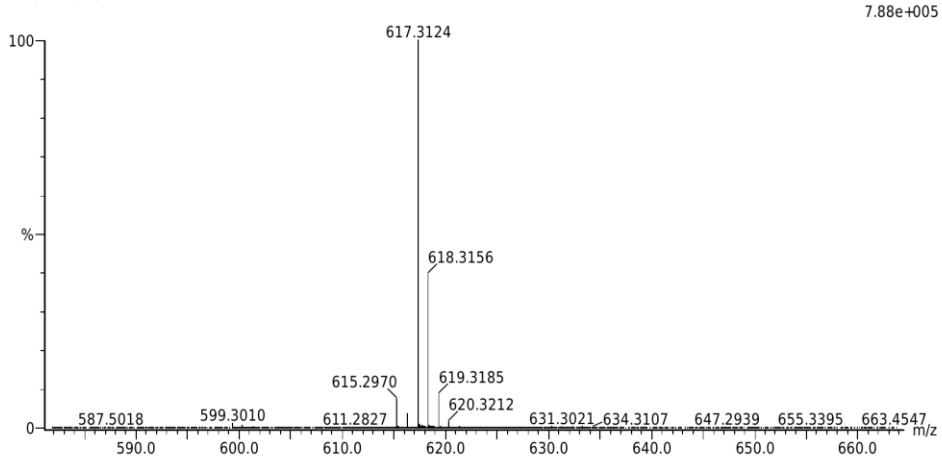

Minimum:				-2.0				
Maximum:		5.0	1.0	50.0				
Mass	Calc. Mass	mDa	PPM	DBE	i-FIT	Norm	Conf(%)	Formula
617.3124	617.3128	-0.4	-0.6	20.5	584.5	n/a	n/a	C38 H41 N4 O4

Appendix G Spectra of Cyclam-related compounds, 7, 8, 21 and 22

Appendix G.3 **^{1}H NMR Spectrum of mono-Boc-diamine 8b-Boc**

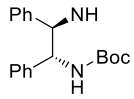

8b-Boc

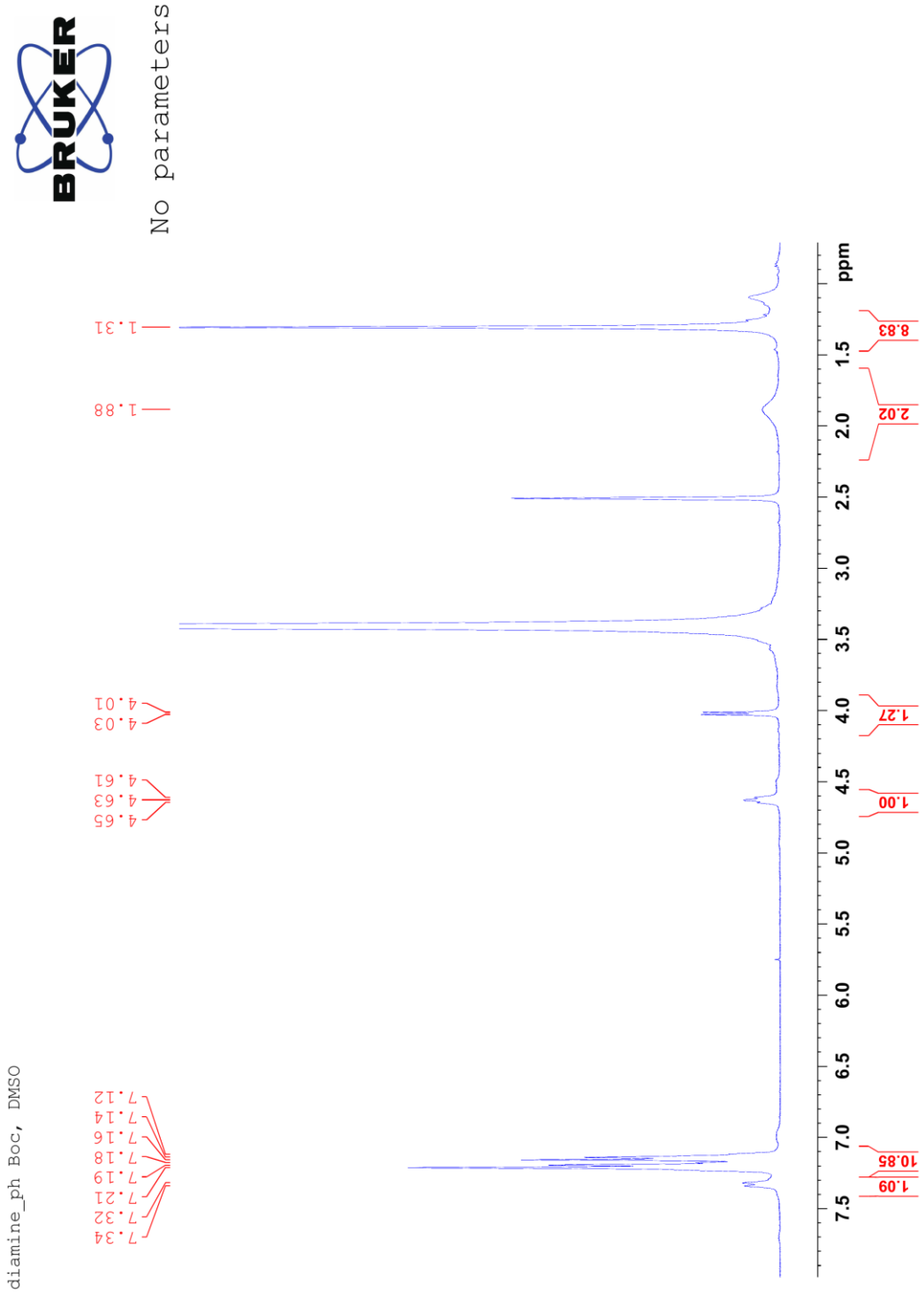

Appendix G Spectra of Cyclam-related compounds, 7, 8, 21 and 22

Appendix G.4 **^{1}H NMR Spectrum of di-Boc 'open cyclam' 21-Boc**

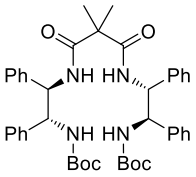

21-Boc

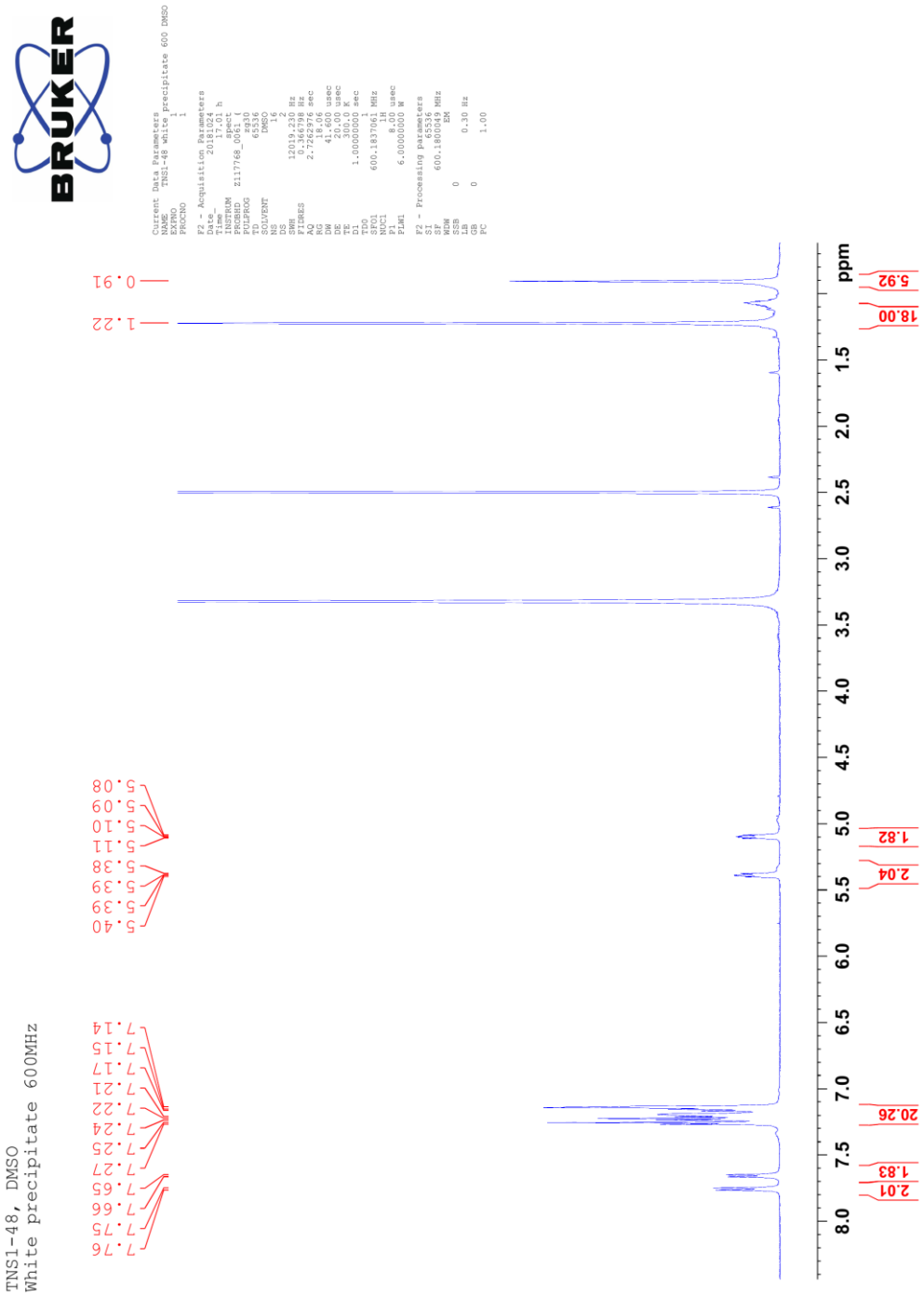

Appendix G Spectra of Cyclam-related compounds, 7, 8, 21 and 22

Appendix G.5 **^{13}C NMR Spectrum of di-Boc 'open cyclam' 21-Boc**

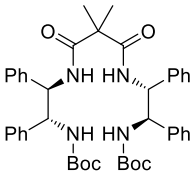

21-Boc

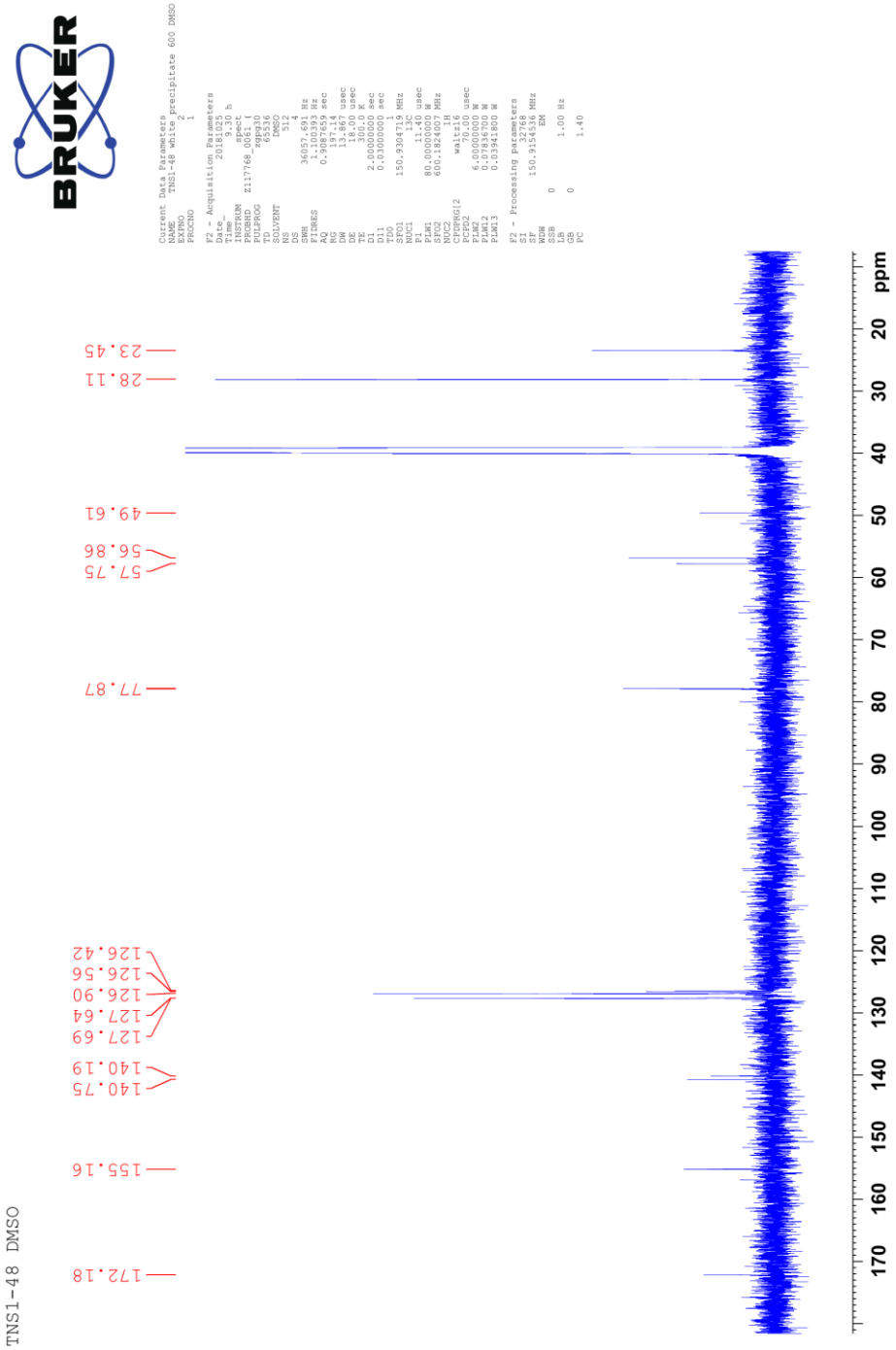

Appendix G Spectra of Cyclam-related compounds, 7, 8, 21 and 22

Appendix G.6 **COSY NMR Spectrum of di-Boc 'open cyclam' 21-Boc**

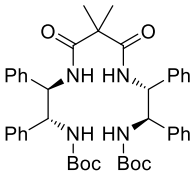

21-Boc

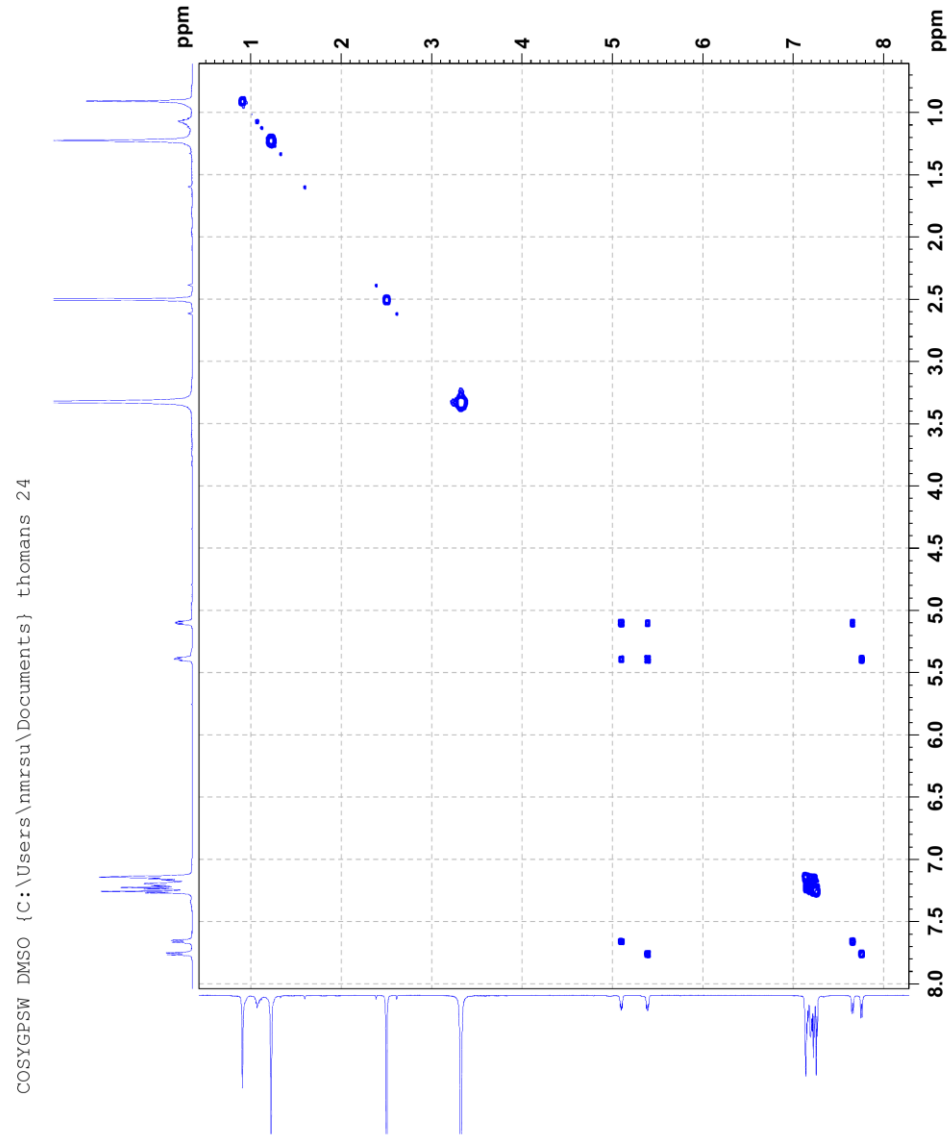

Appendix G Spectra of Cyclam-related compounds, 7, 8, 21 and 22

Appendix G.7 **HSQC NMR Spectrum of di-Boc 'open cyclam' 21-Boc**

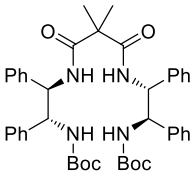

21-Boc

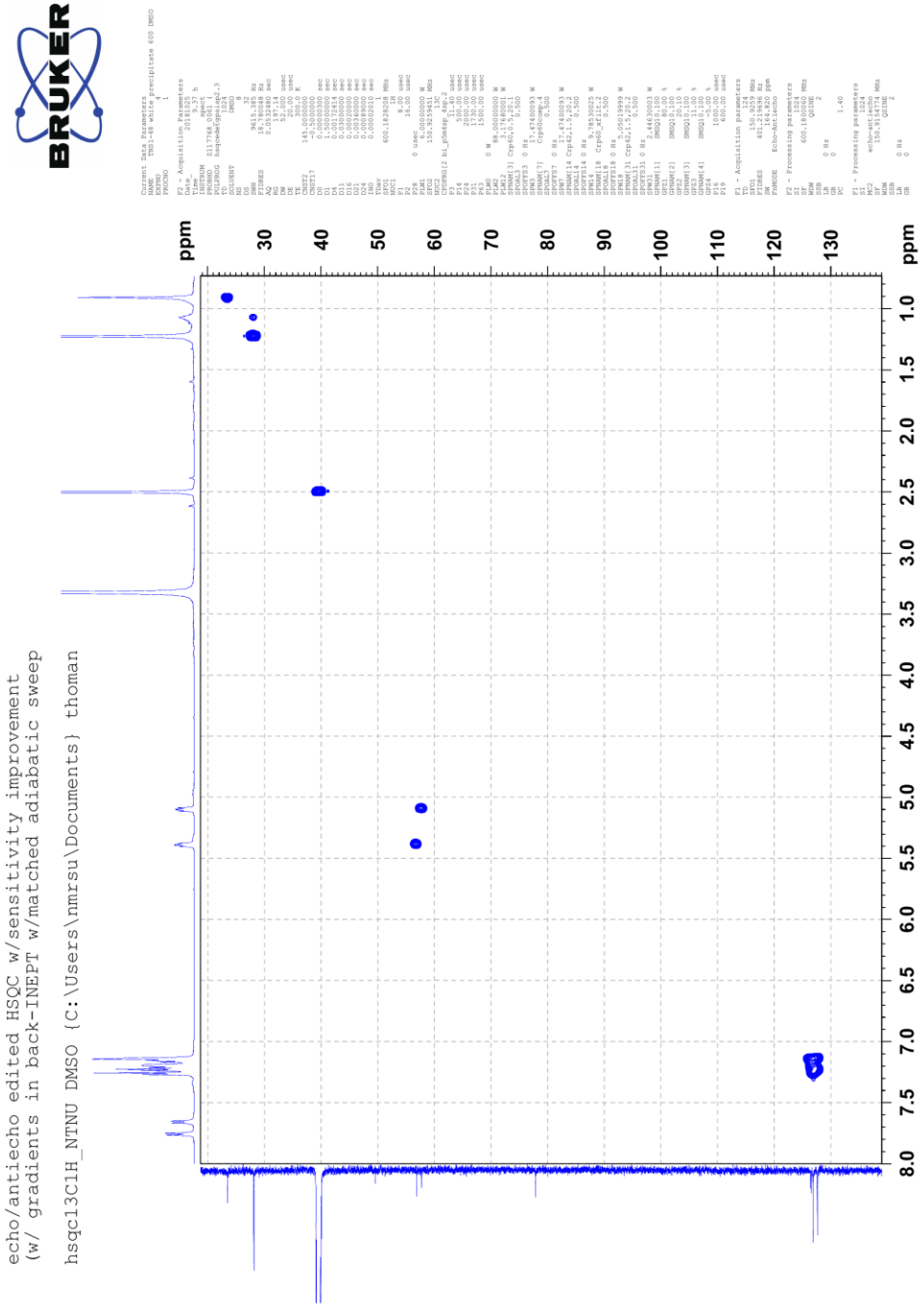

Appendix G Spectra of Cyclam-related compounds, 7, 8, 21 and 22

Appendix G.8 **HMBC NMR Spectrum of di-Boc 'open cyclam' 21-Boc**

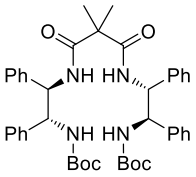

21-Boc

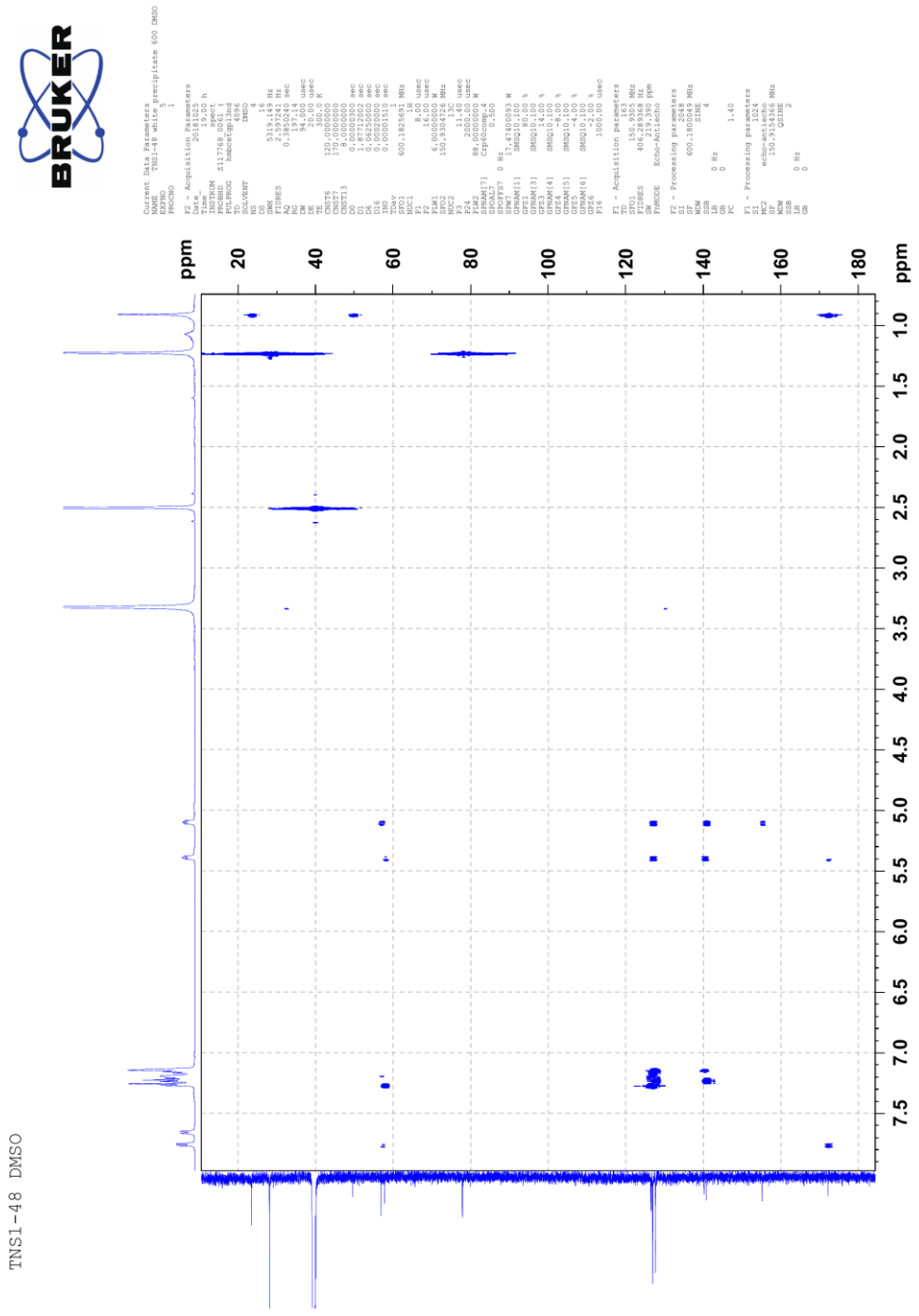

Appendix G Spectra of Cyclam-related compounds, 7, 8, 21 and 22

Appendix G.9 **HRMS Spectrum of di-Boc 'open cyclam' 21-Boc**

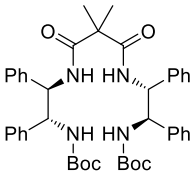

21-Boc

Elemental Composition Report **Page 1**

Multiple Mass Analysis: 2 mass(es) processed
Tolerance = 2.0 PPM / DBE: min = -2.0, max = 50.0
Element prediction: Off
Number of isotope peaks used for i-FIT = 2

Monoisotopic Mass, Even Electron Ions
6142 formula(e) evaluated with 14 results within limits (all results (up to 1000) for each mass)
Elements Used:
C: 0-100 H: 0-150 N: 0-10 O: 0-20 Na: 0-1
2018-610esi 119 (1.117) AM2 (Ar,35000.0,0.00,0.00); Cm (119:123)
1: TOF MS ES+

6.61e+006

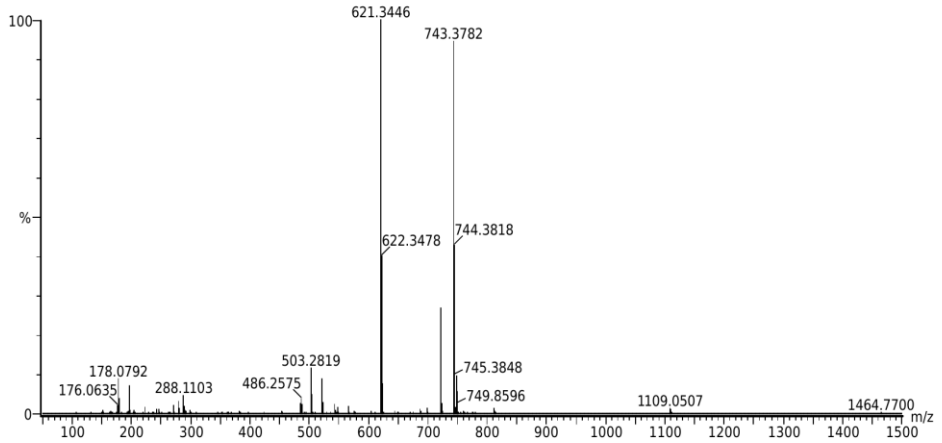

Minimum:	80.00				-2.0				
Maximum:	100.00		5.0	2.0	50.0				
Mass	RA	Calc. Mass	mDa	PPM	DBE	i-FIT	Norm	Conf(%)	Formula
621.3446	100.00	621.3446	0.0	0.0	0.5	631.8	3.943	1.94	C25 H53 N2 O15
		621.3449	-0.3	-0.5	7.5	631.1	3.319	3.62	C25 H46 N10 O7 Na
		621.3441	0.5	0.8	18.5	628.1	0.263	76.89	C38 H45 N4 O4
		621.3454	-0.8	-1.3	23.5	629.9	2.124	11.95	C39 H41 N8
		621.3457	-1.1	-1.8	19.5	630.8	2.971	5.12	C41 H46 N2 O2 Na
		621.3435	1.1	1.8	2.5	633.1	5.340	0.48	C24 H50 N6 O11 Na
743.3782	94.51	743.3782	0.0	0.0	23.5	531.6	3.099	4.51	C41 H47 N10 O4
		743.3785	-0.3	-0.4	19.5	531.5	2.940	5.29	C43 H52 N4 O6 Na
		743.3787	-0.5	-0.7	5.5	535.3	6.793	0.11	C28 H55 N8 O15
		743.3790	-0.8	-1.1	1.5	535.4	6.857	0.11	C30 H60 N2 O17 Na
		743.3774	0.8	1.1	0.5	536.6	8.084	0.03	C27 H59 N4 O19
		743.3771	1.1	1.5	14.5	529.2	0.619	53.84	C42 H56 O10 Na
		743.3795	-1.3	-1.7	17.5	532.4	3.830	2.17	C44 H55 O10
		743.3768	1.4	1.9	18.5	529.6	1.080	33.94	C40 H51 N6 O8

Appendix G Spectra of Cyclam-related compounds, 7, 8, 21 and 22

Appendix G.10 **^{1}H NMR Spectrum of diamidodiamine 'open cyclam' 21**

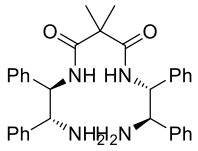

21

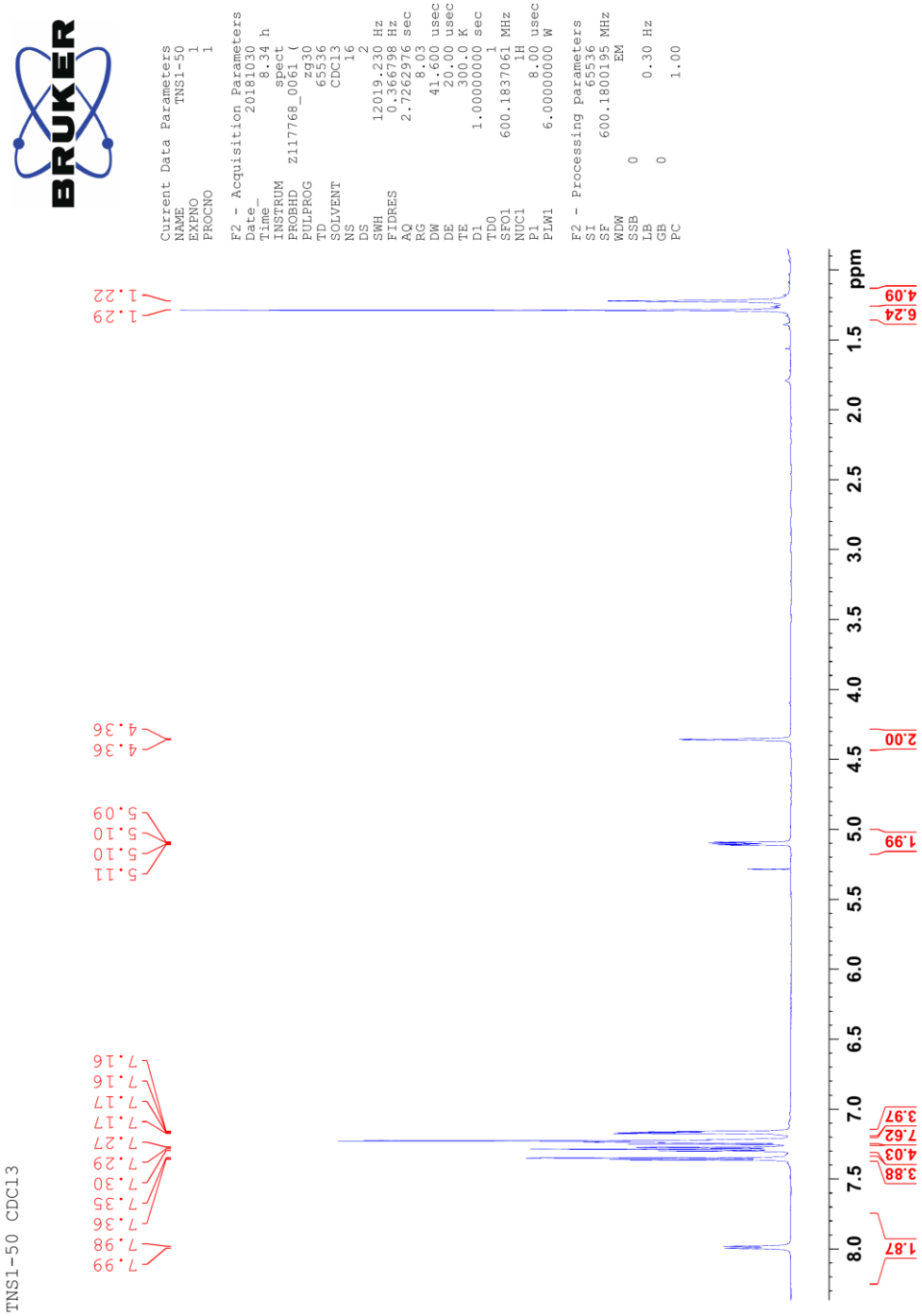

Appendix G Spectra of Cyclam-related compounds, 7, 8, 21 and 22

Appendix G.11 **^{13}C NMR Spectrum of diamidodiamine 'open cyclam' 21**

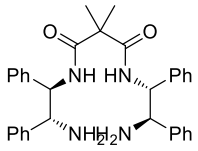

21

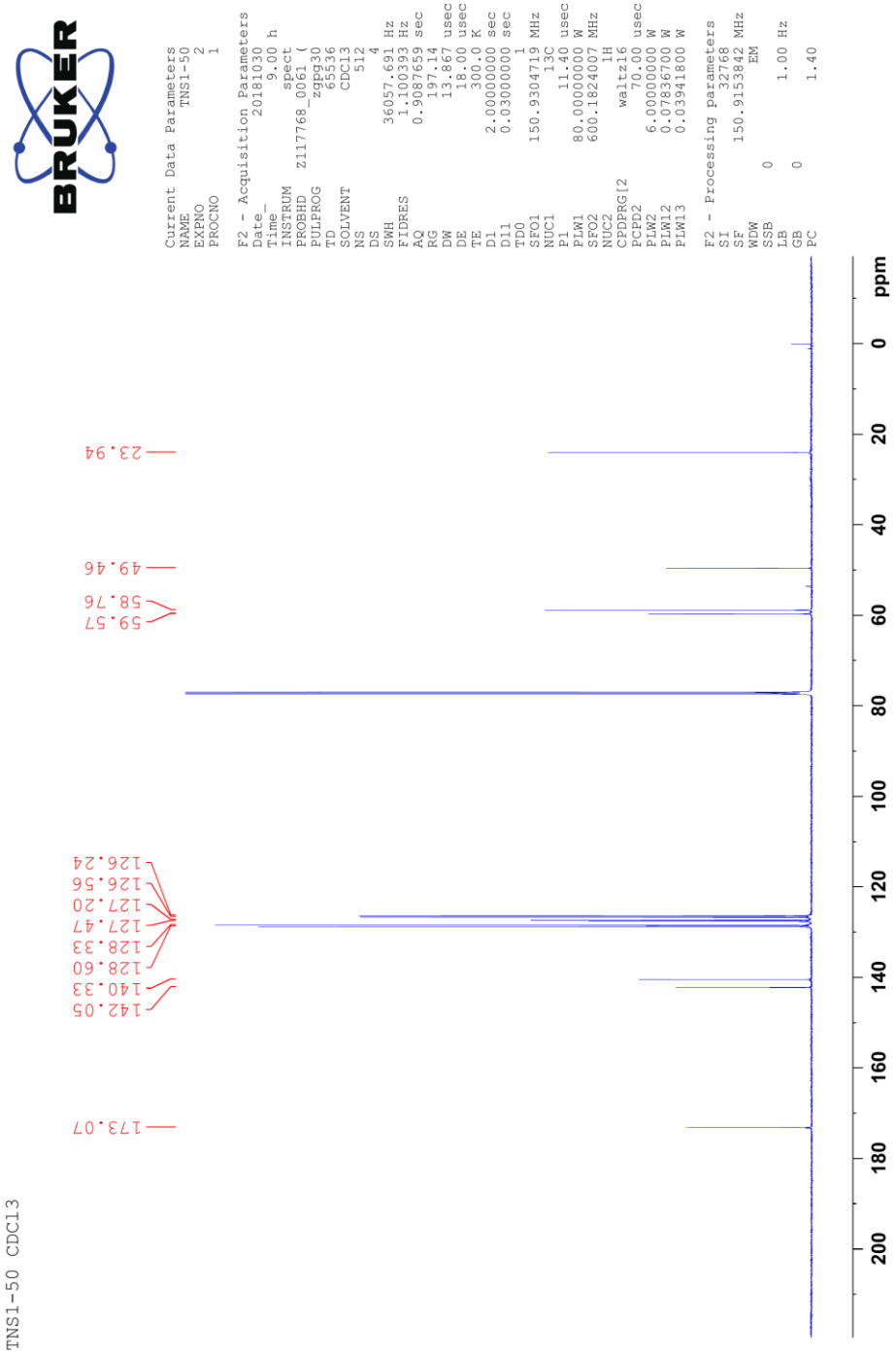

Appendix G Spectra of Cyclam-related compounds, 7, 8, 21 and 22

Appendix G.12 **COSY NMR Spectrum of diamidodiamine 'open cyclam' 21**

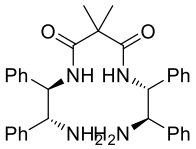

21

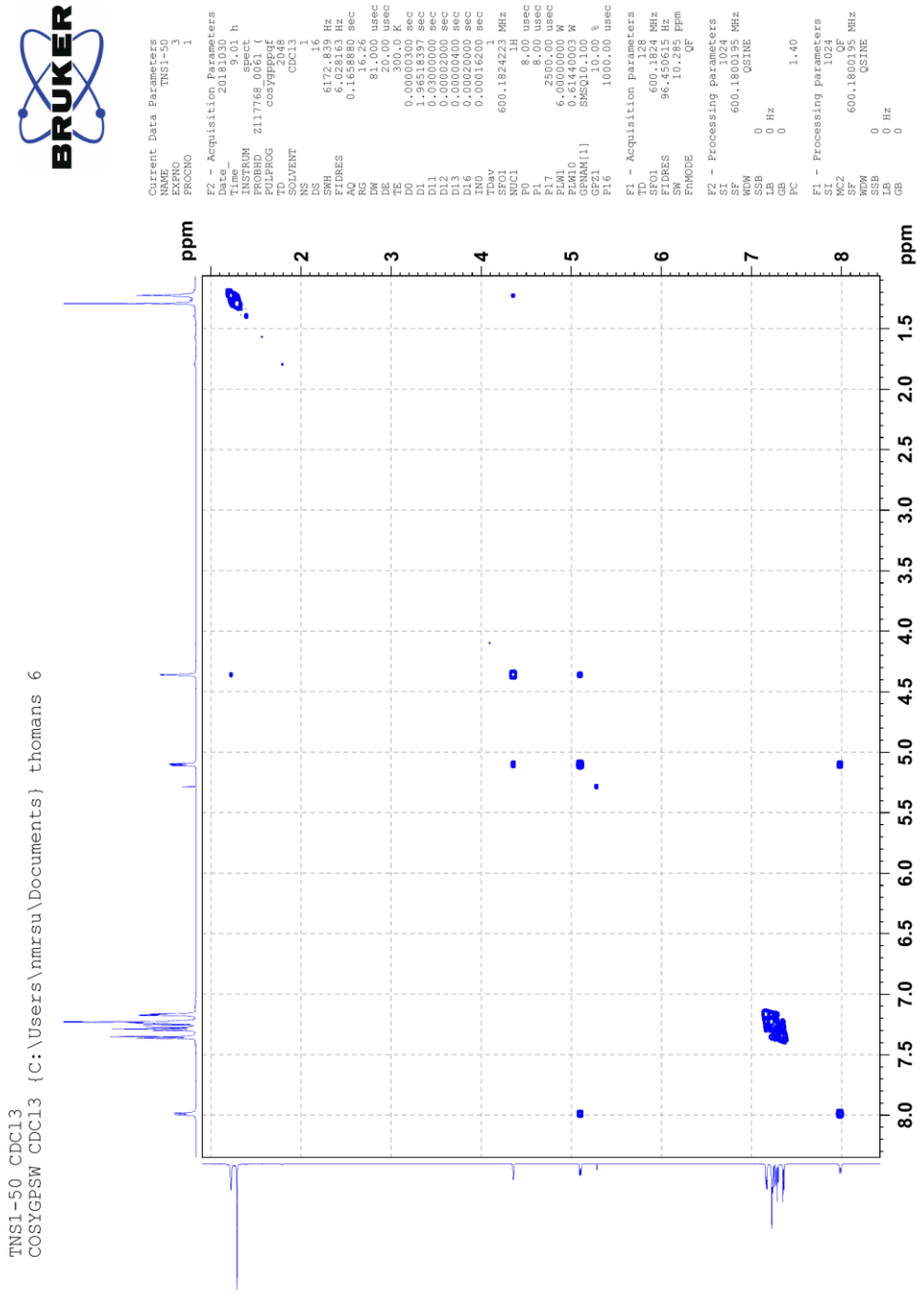

Appendix G Spectra of Cyclam-related compounds, 7, 8, 21 and 22

Appendix G.13 **HSQC NMR Spectrum of diamidodiamine 'open cyclam' 21**

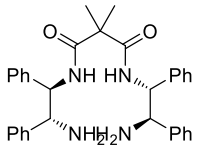

21

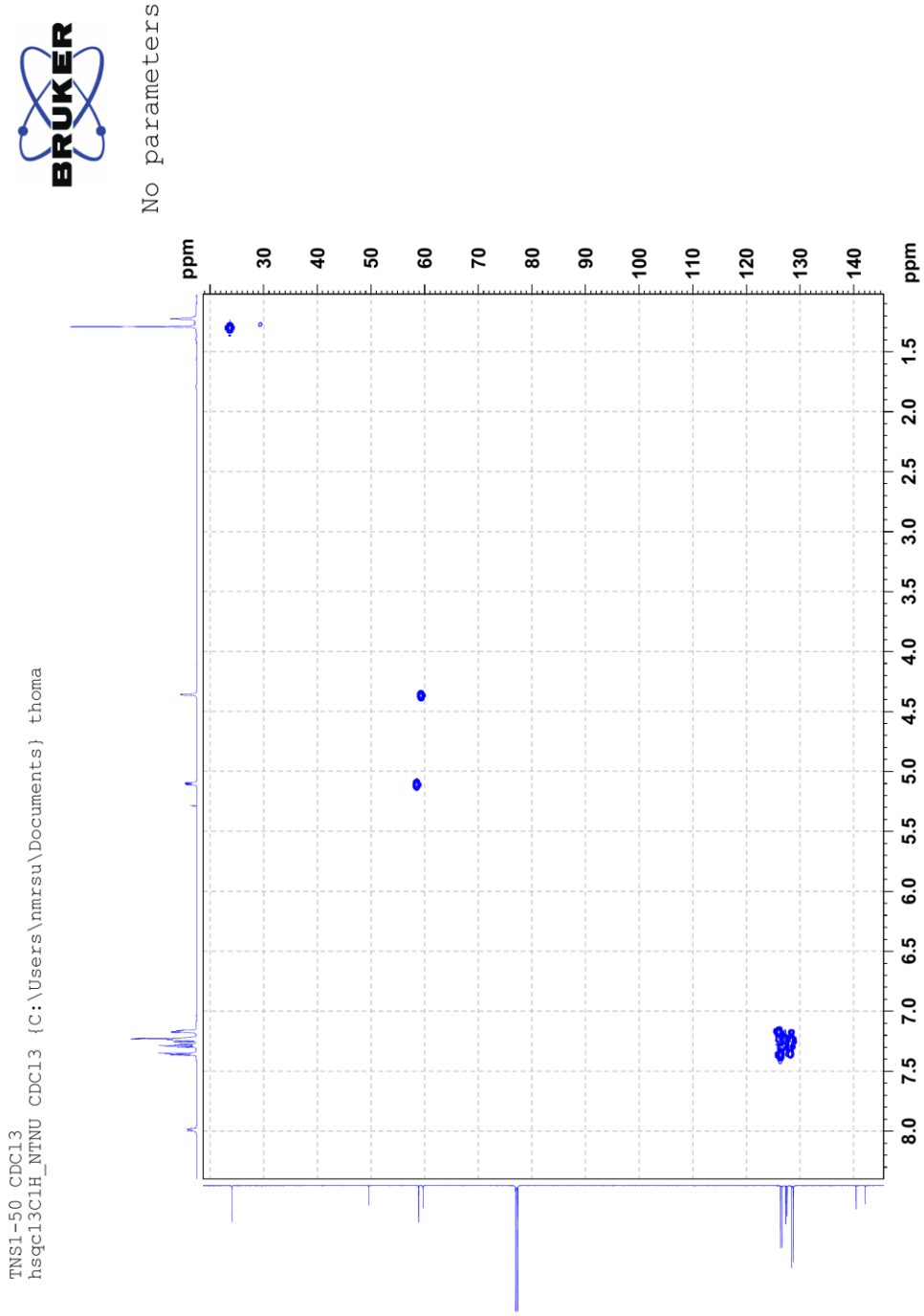

CV

Appendix G Spectra of Cyclam-related compounds, 7, 8, 21 and 22

Appendix G.14 **HMBC NMR Spectrum of diamidodiamine 'open cyclam' 21**

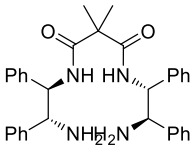

21

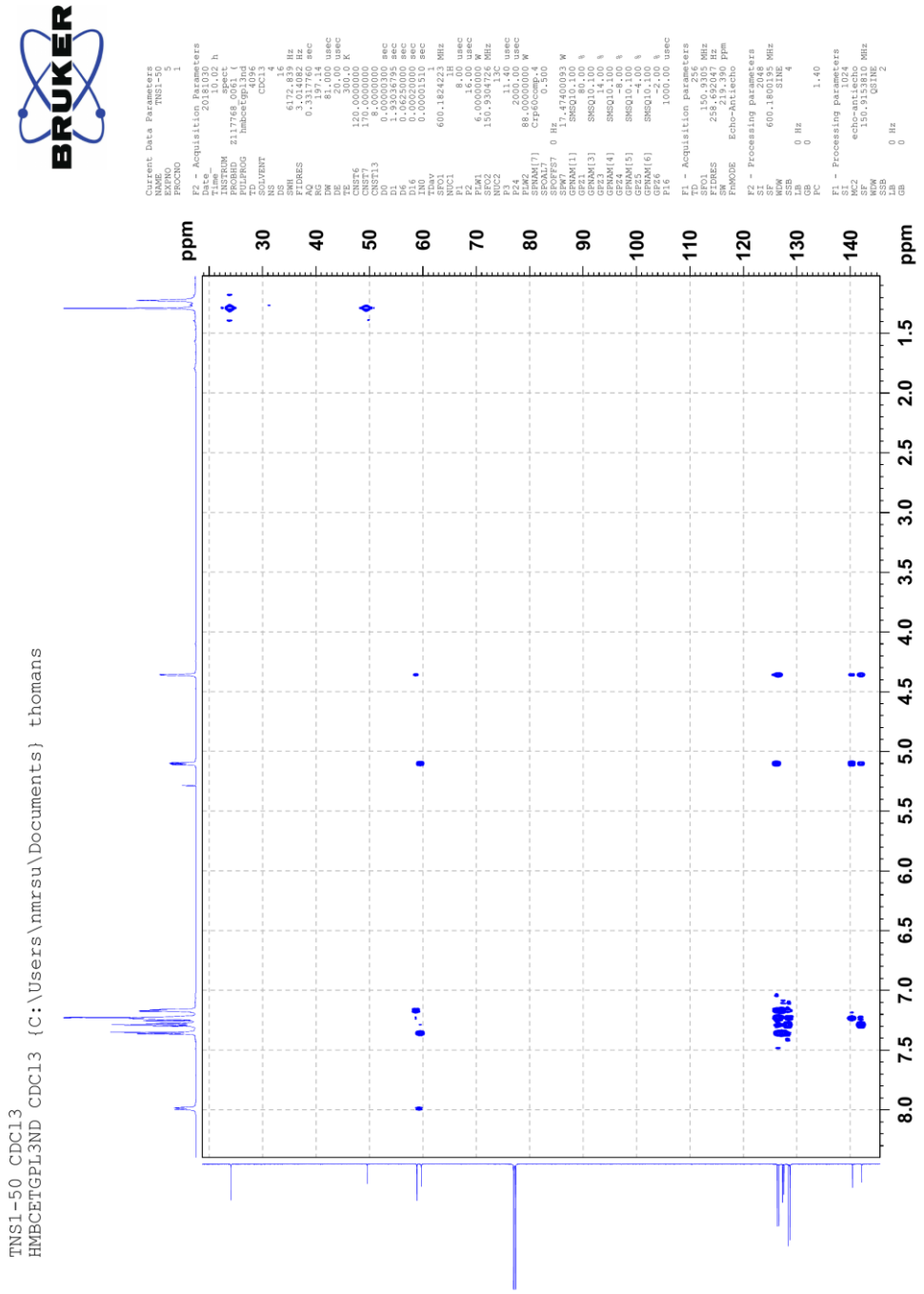

Appendix G Spectra of Cyclam-related compounds, 7, 8, 21 and 22

Appendix G.15 **HRMS Spectrum of diamidodiamine 'open cyclam' 21**

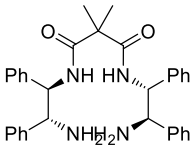

21

Elemental Composition Report **Page 1**

Single Mass Analysis
Tolerance = 2.0 PPM / DBE: min = -2.0, max = 50.0
Element prediction: Off
Number of isotope peaks used for i-FIT = 2

Monoisotopic Mass, Even Electron Ions
1814 formula(e) evaluated with 4 results within limits (all results (up to 1000) for each mass)
Elements Used:
C: 0-100 H: 0-150 N: 0-8 O: 0-20 Na: 0-1
2018-625esi 155 (1.448) AM2 (Ar,35000.0,0.00,0.00); Cm (154:166)
1: TOF MS ES+

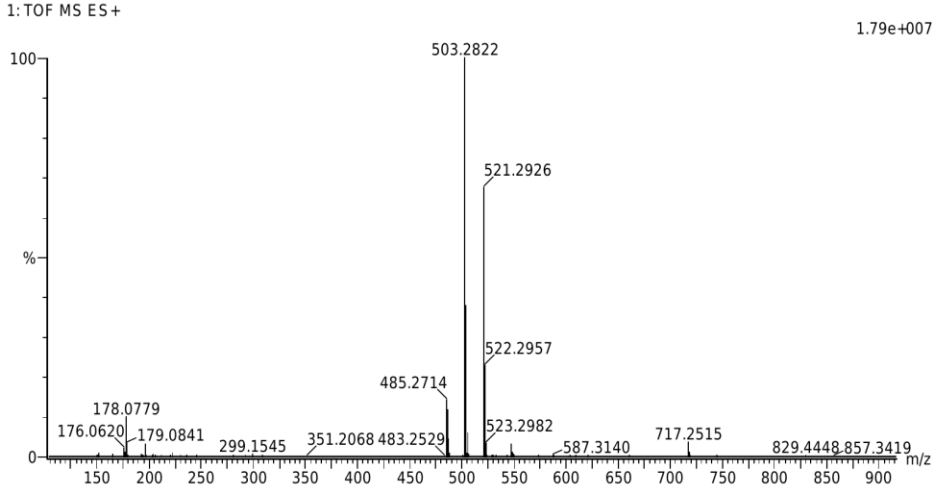

Minimum:				-2.0				
Maximum:		5.0	2.0	50.0				
Mass	Calc. Mass	mDa	PPM	DBE	i-FIT	Norm	Conf(%)	Formula
521.2926	521.2922	0.4	0.8	-0.5	757.2	2.587	7.52	C20 H45 N2 O13
	521.2933	-0.7	-1.3	18.5	756.1	1.488	22.58	C36 H38 N2 Na
	521.2917	0.9	1.7	17.5	755.0	0.476	62.14	C33 H37 N4 O2
	521.2935	-0.9	-1.7	4.5	757.1	2.556	7.76	C21 H41 N6 O9

Appendix G Spectra of Cyclam-related compounds, 7, 8, 21 and 22

Appendix G.16 **^{1}H NMR Spectrum of tetramine 'open cyclam' 22**

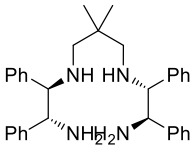

22

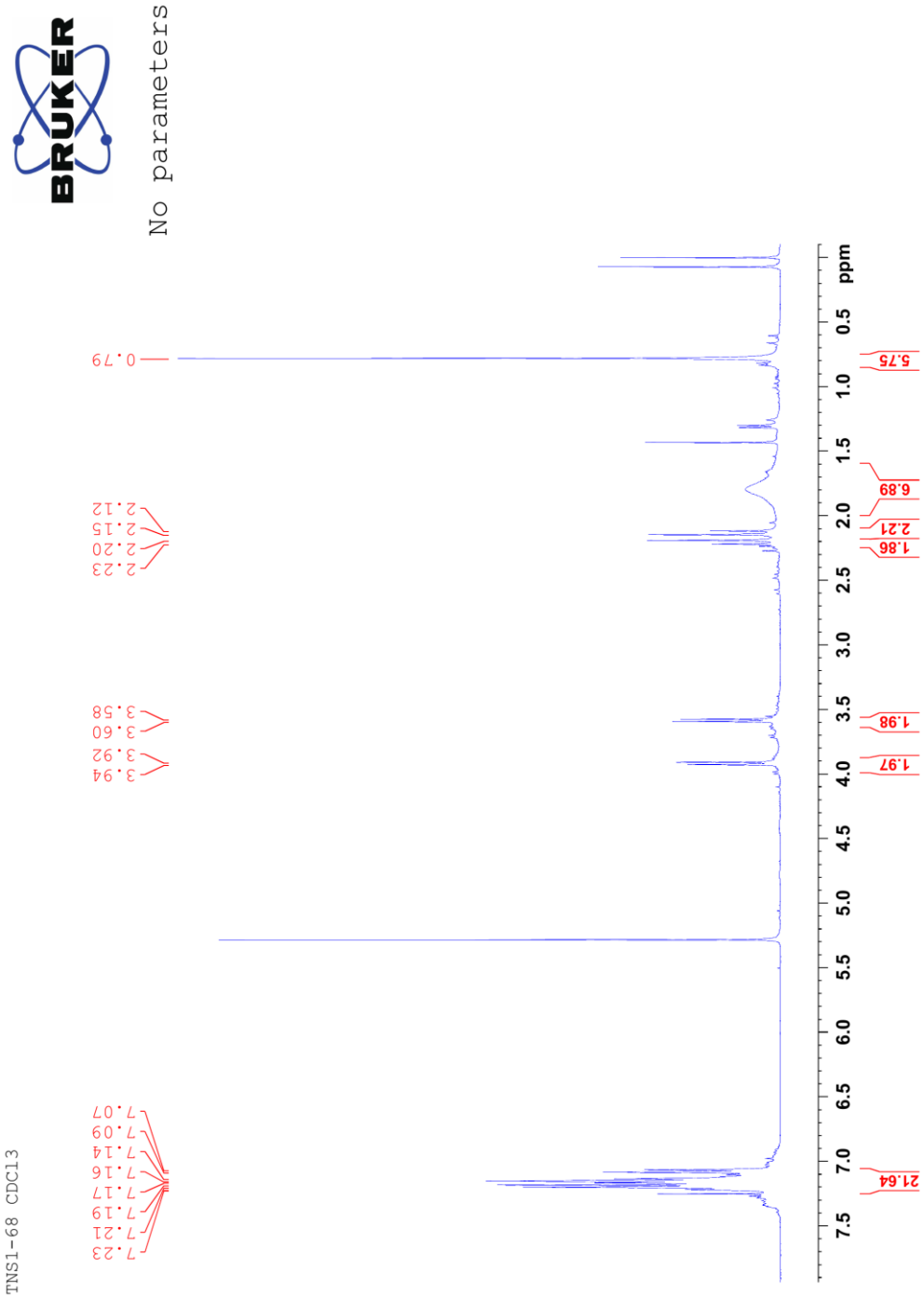

Appendix G Spectra of Cyclam-related compounds, 7, 8, 21 and 22

Appendix G.17 **^{13}C NMR Spectrum of tetramine 'open cyclam' 22**

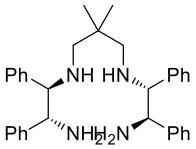

22

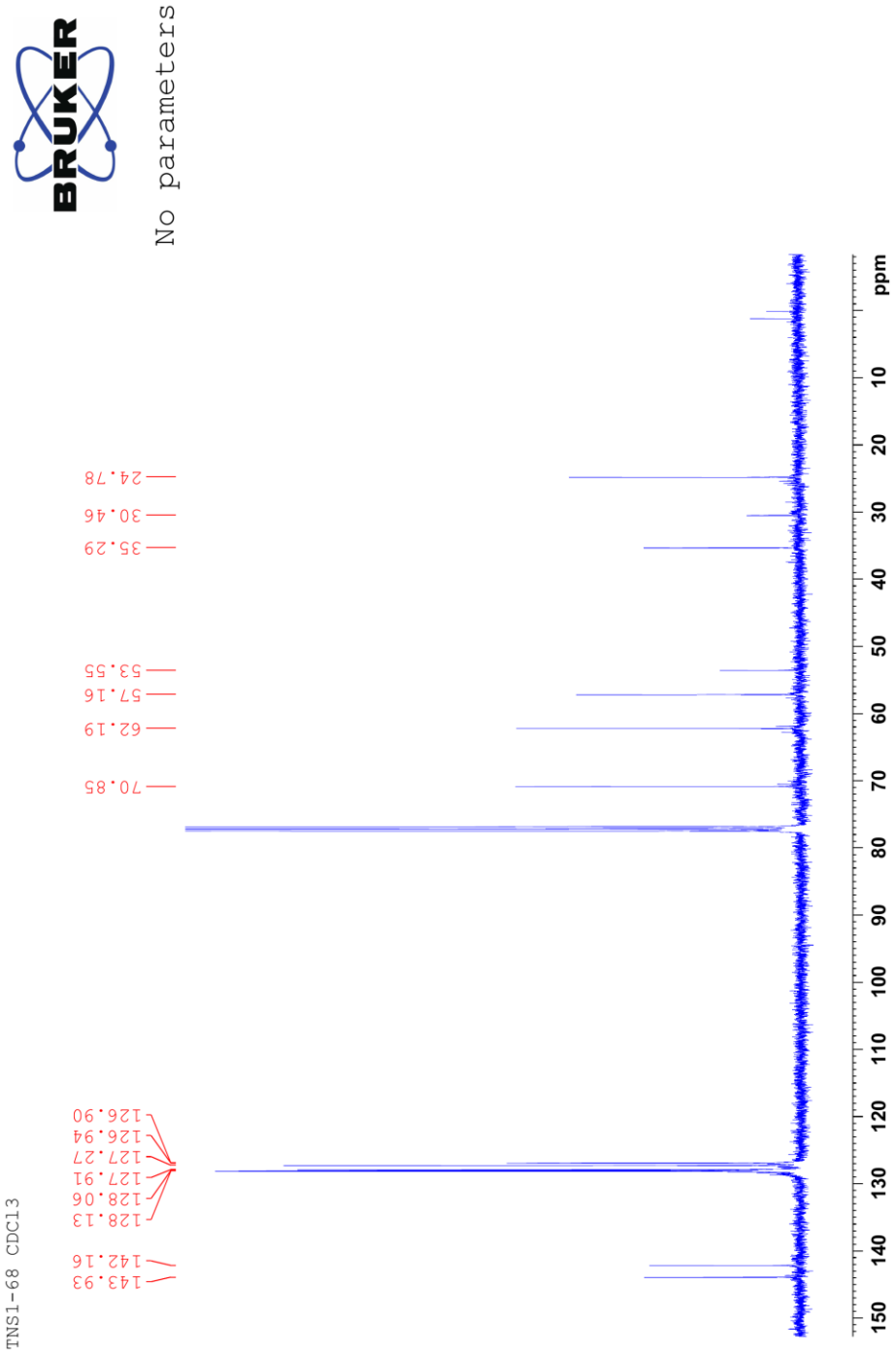

Appendix G Spectra of Cyclam-related compounds, 7, 8, 21 and 22

Appendix G.18 **COSY NMR Spectrum of tetramine 'open cyclam' 22**

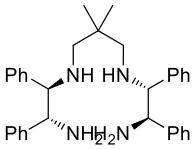

22

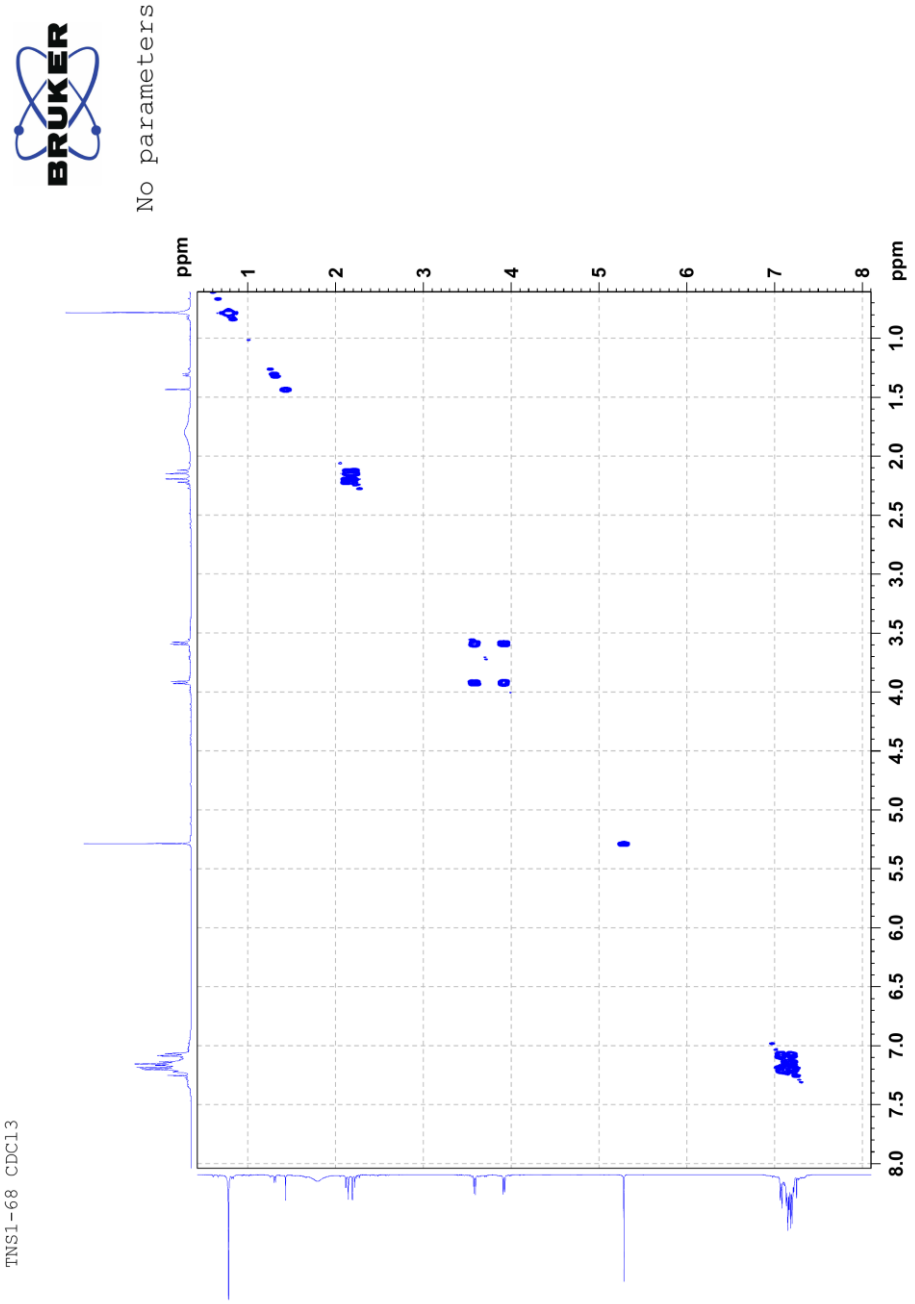

Appendix G Spectra of Cyclam-related compounds, 7, 8, 21 and 22

Appendix G.19 **HSQC NMR Spectrum of tetramine 'open cyclam' 22**

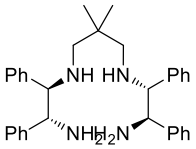

22

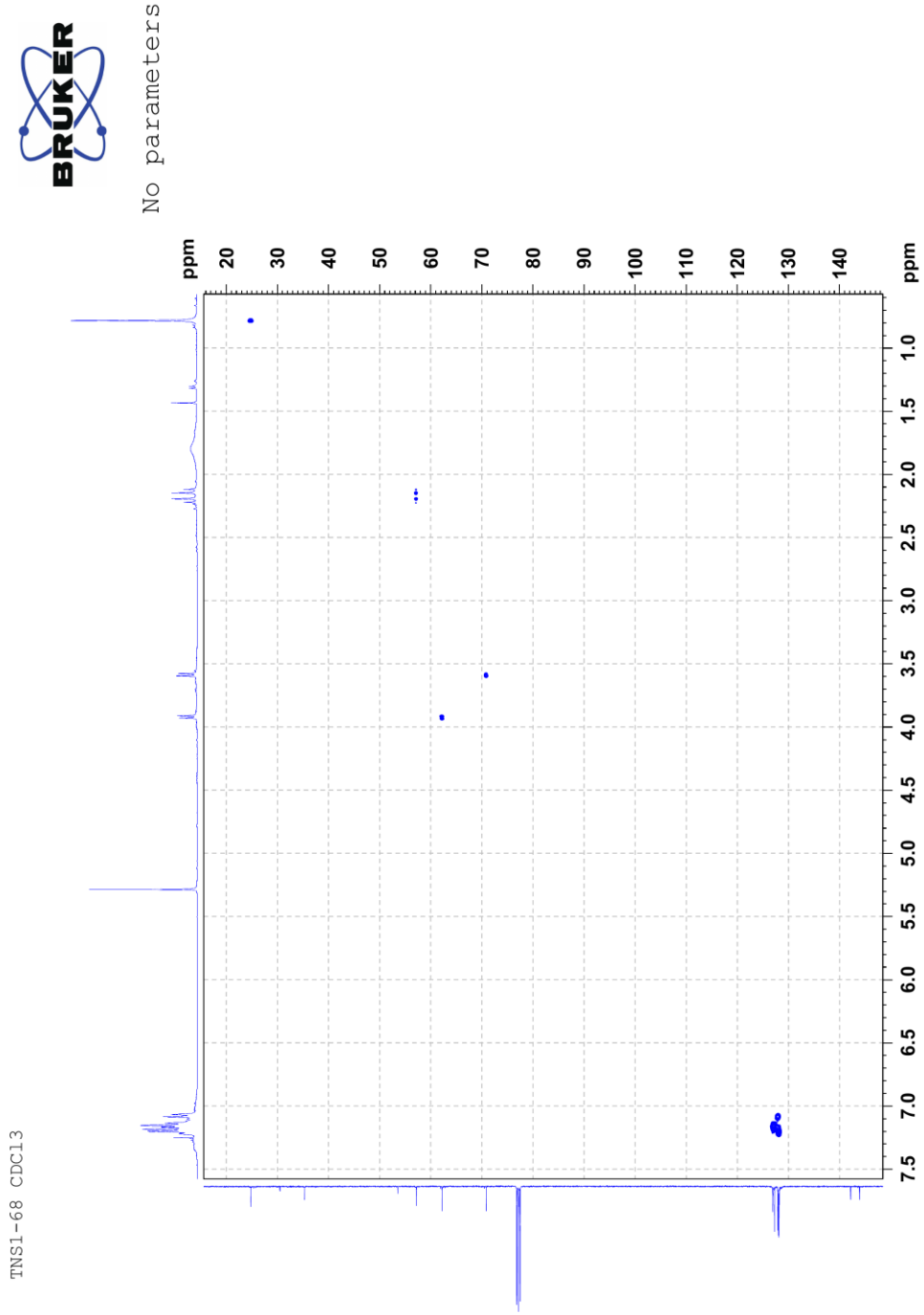

Appendix G Spectra of Cyclam-related compounds, 7, 8, 21 and 22

Appendix G.20 **HMBC NMR Spectrum of tetramine 'open cyclam' 22**

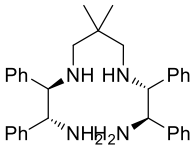

22

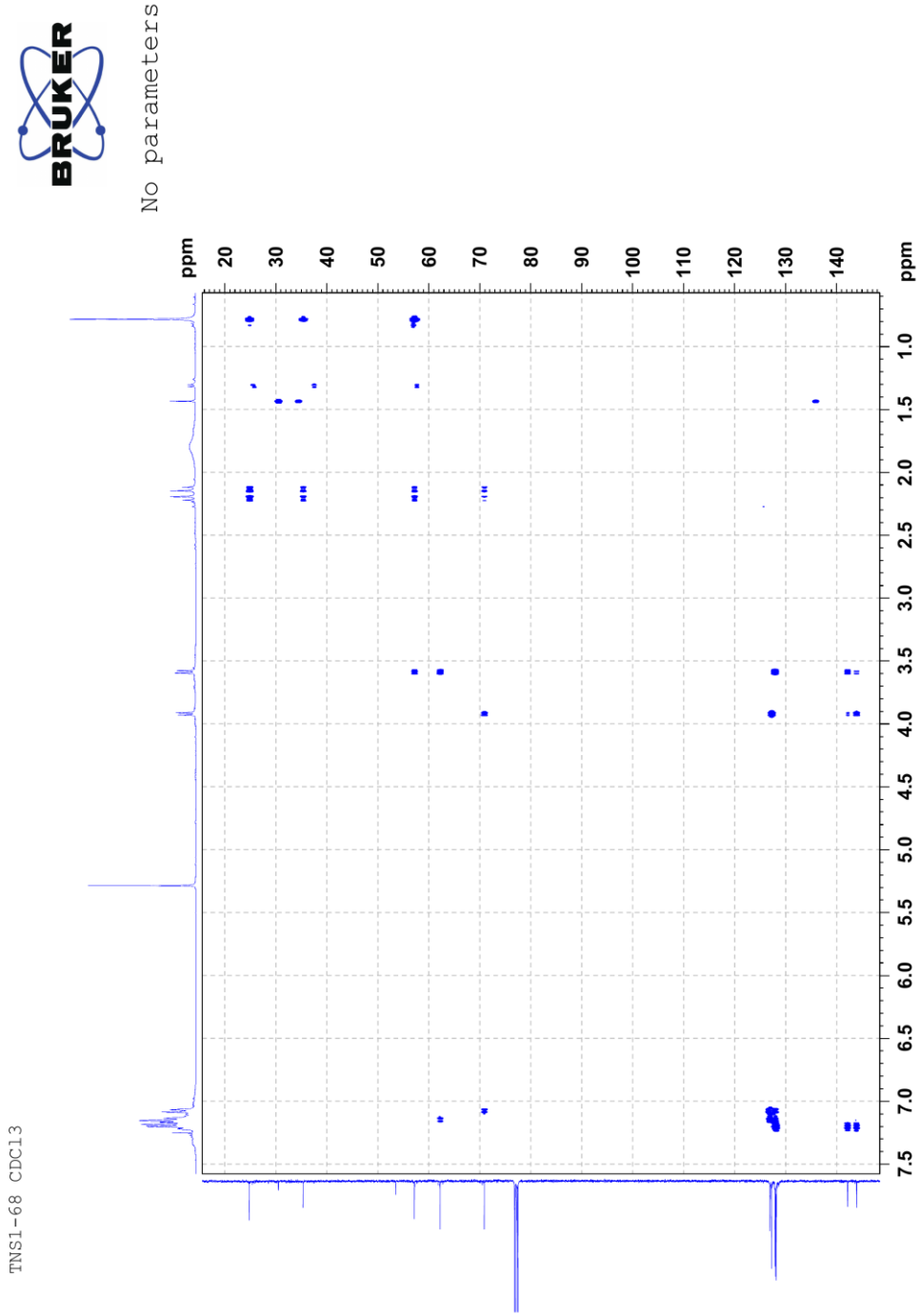

Appendix G Spectra of Cyclam-related compounds, 7, 8, 21 and 22

Appendix G.21 **HRMS Spectrum of tetramine 'open cyclam' 22**

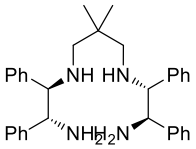

22

Elemental Composition Report **Page 1**

Single Mass Analysis
Tolerance = 2.0 PPM / DBE: min = -5.0, max = 50.0
Element prediction: Off
Number of isotope peaks used for i-FIT = 3

Monoisotopic Mass, Even Electron Ions
3255 formula(e) evaluated with 4 results within limits (all results (up to 1000) for each mass)
Elements Used:
C: 0-100 H: 0-100 N: 0-5 O: 0-5 P: 0-1 Cl: 0-4 Au: 0-3

2020_107_2 74 (0.708) AM2 (Ar,35000.0,0.00,0.00)
1: TOF MS ES+

1.69e+006

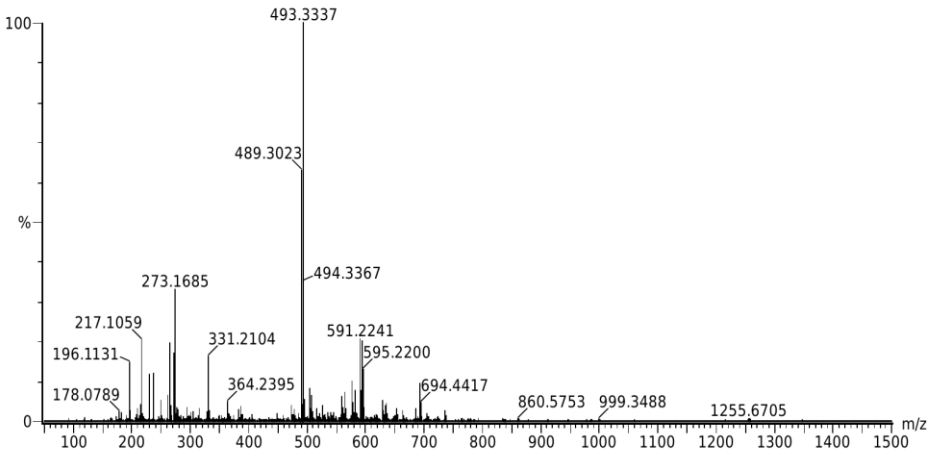

Minimum:				-5.0				
Maximum:		5.0	2.0	50.0				
Mass	Calc. Mass	mDa	PPM	DBE	i-FIT	Norm	Conf(%)	Formula
493.3337	493.3331	0.6	1.2	15.5	943.1	0.000	100.00	C33 H41 N4
	493.3344	-0.7	-1.4	-3.5	964.3	21.209	0.00	C24 H56 O3 P Cl2
	493.3346	-0.9	-1.8	-3.5	964.8	21.702	0.00	C25 H56 O2 Cl3
	493.3328	0.9	1.8	1.5	964.5	21.384	0.00	C26 H51 N2 O2 Cl2

Appendix H ^{1}H NMR Spectrum of Propargyl Acetate, 11

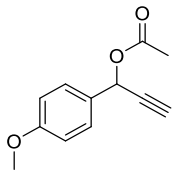

11

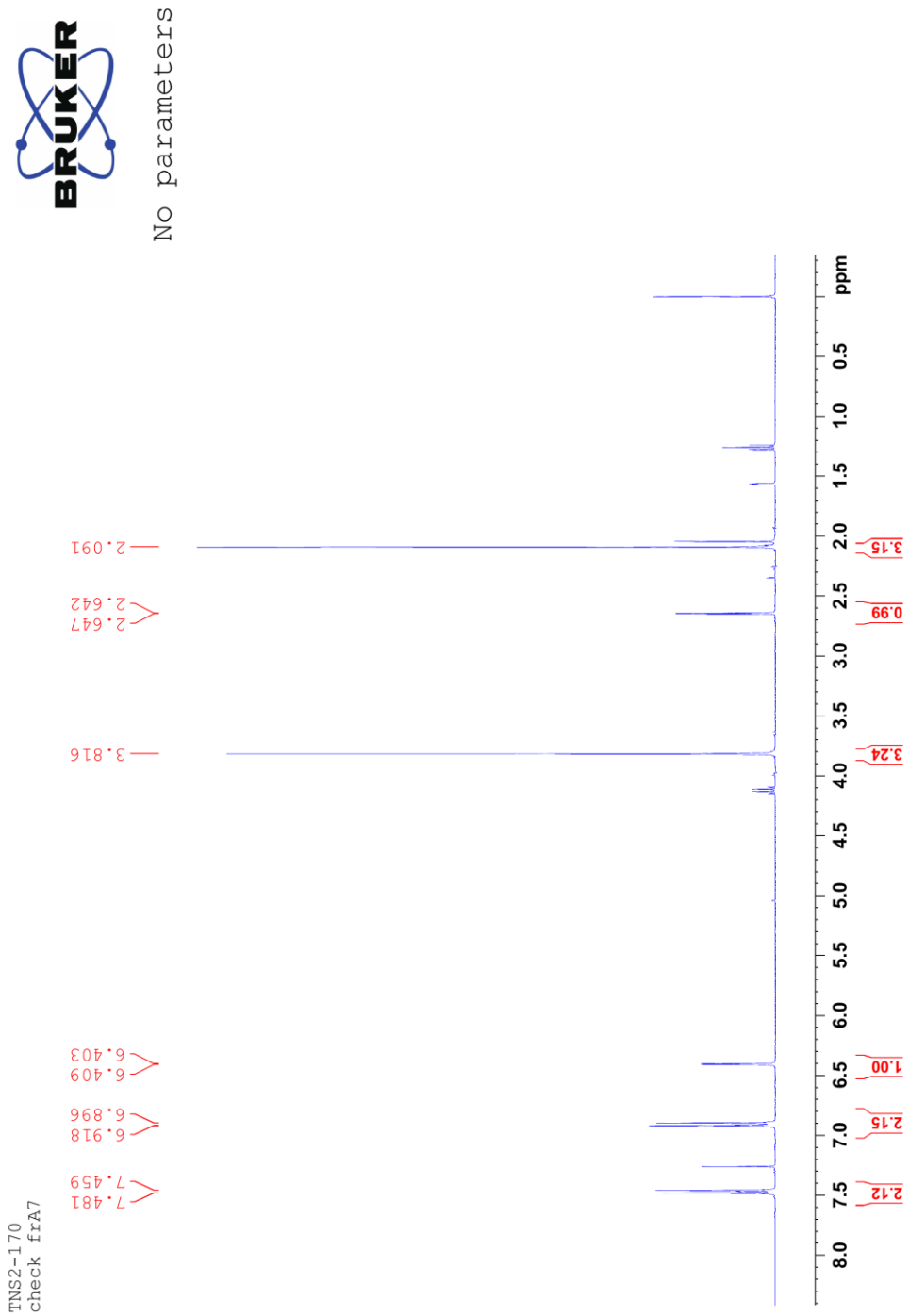

Appendix I **Spectra of 2-Bromo-6-Alkyl Pyridine Alcohols, 12a-c**

Appendix I.1 **^{1}H NMR spectrum of Pyridine alcohol 12a**

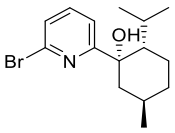

12a

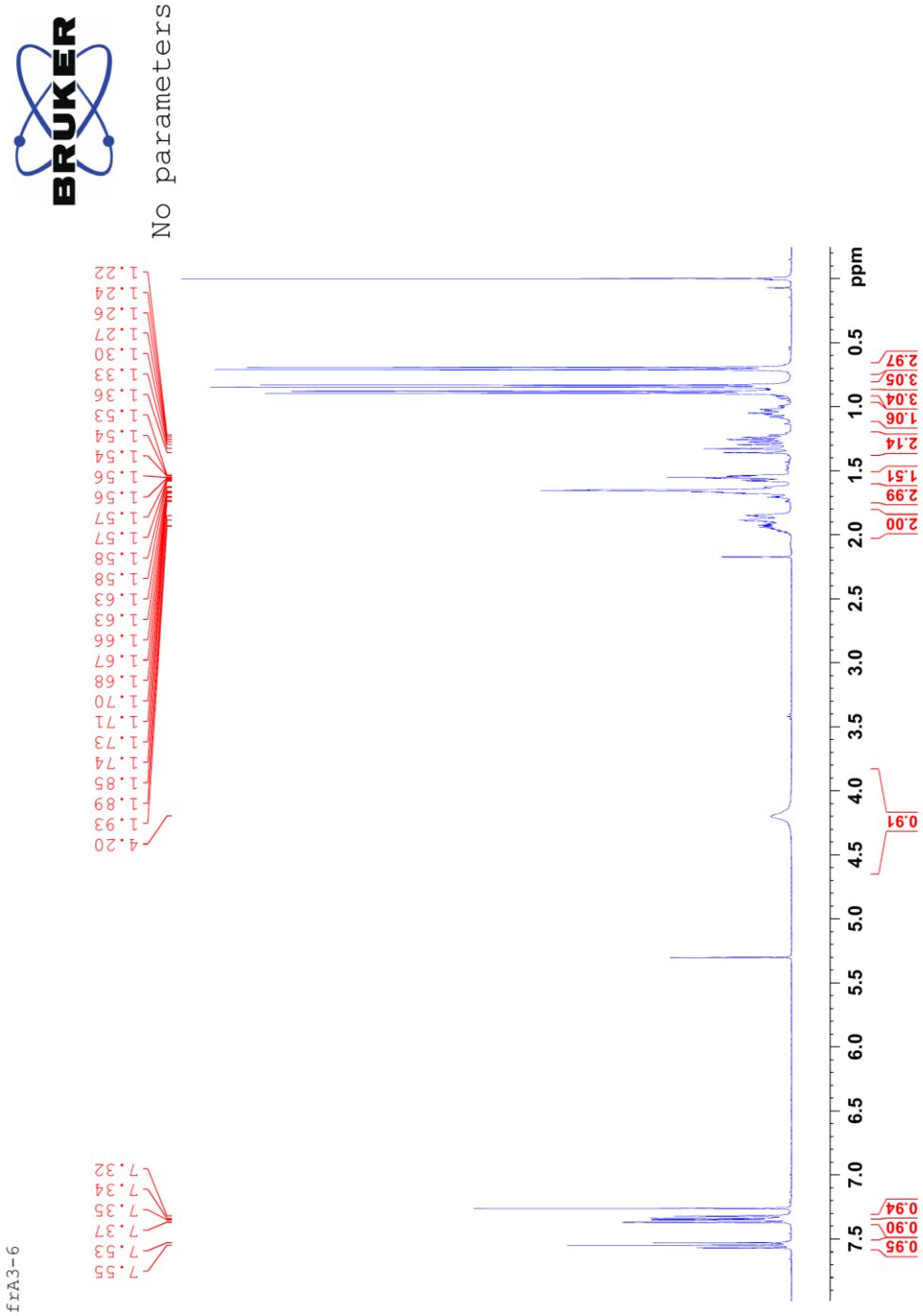

Appendix I Spectra of 2-Bromo-6-Alkyl Pyridine Alcohols, 12a-c

Appendix I.2 **^{1}H NMR spectrum of Pyridine alcohol 12b**

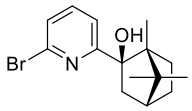

12b

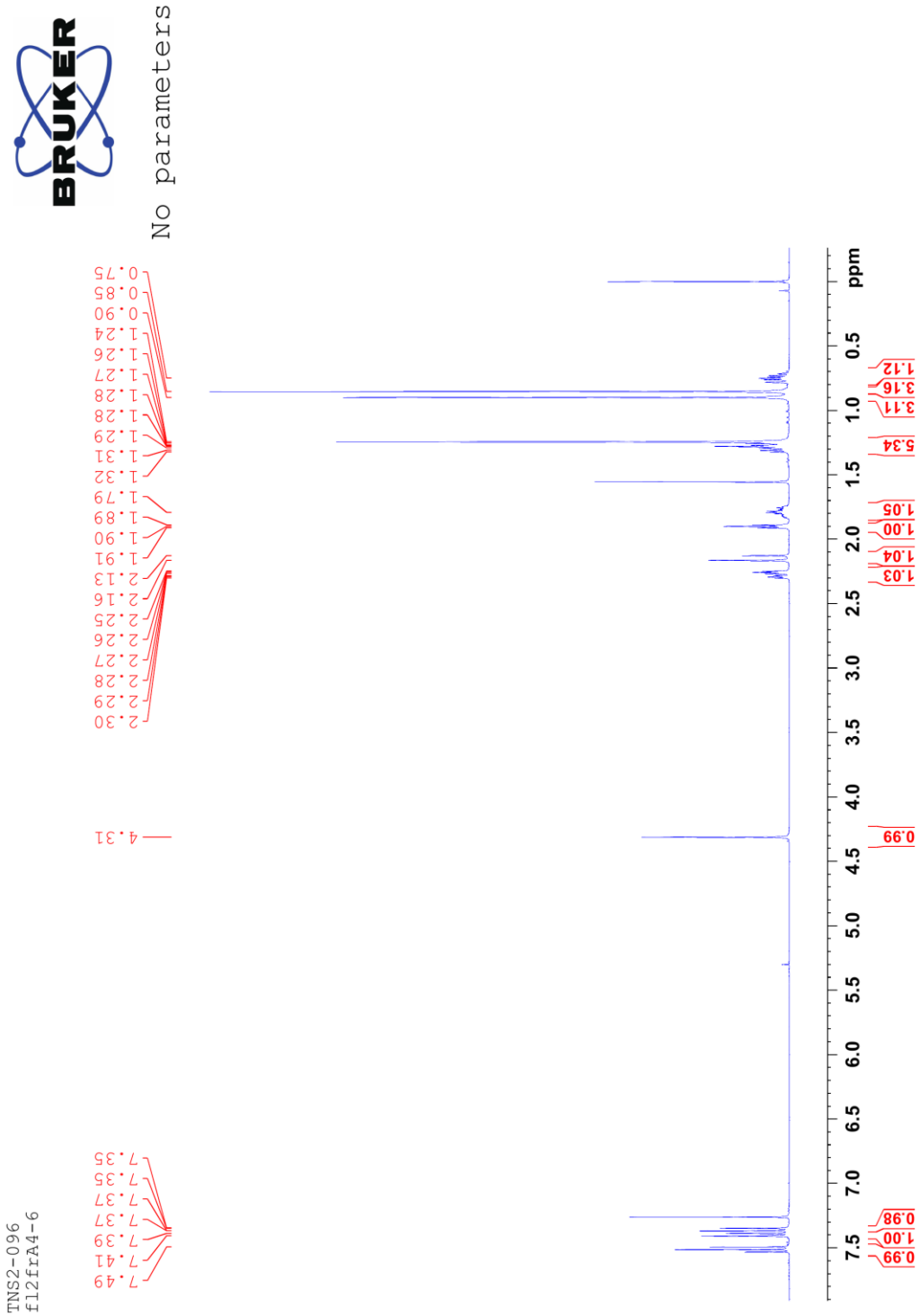

Appendix I Spectra of 2-Bromo-6-Alkyl Pyridine Alcohols, 12a-c

Appendix I.3 **^{1}H NMR spectrum of Pyridine alcohol 12c**

^{1}H NMR was not in accordance with previously reported data.[91] The structure of 12c is therefore uncertain. The acquired spectrum after flash column chromatography is included here for reference.

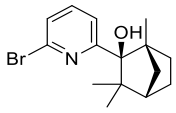

12c

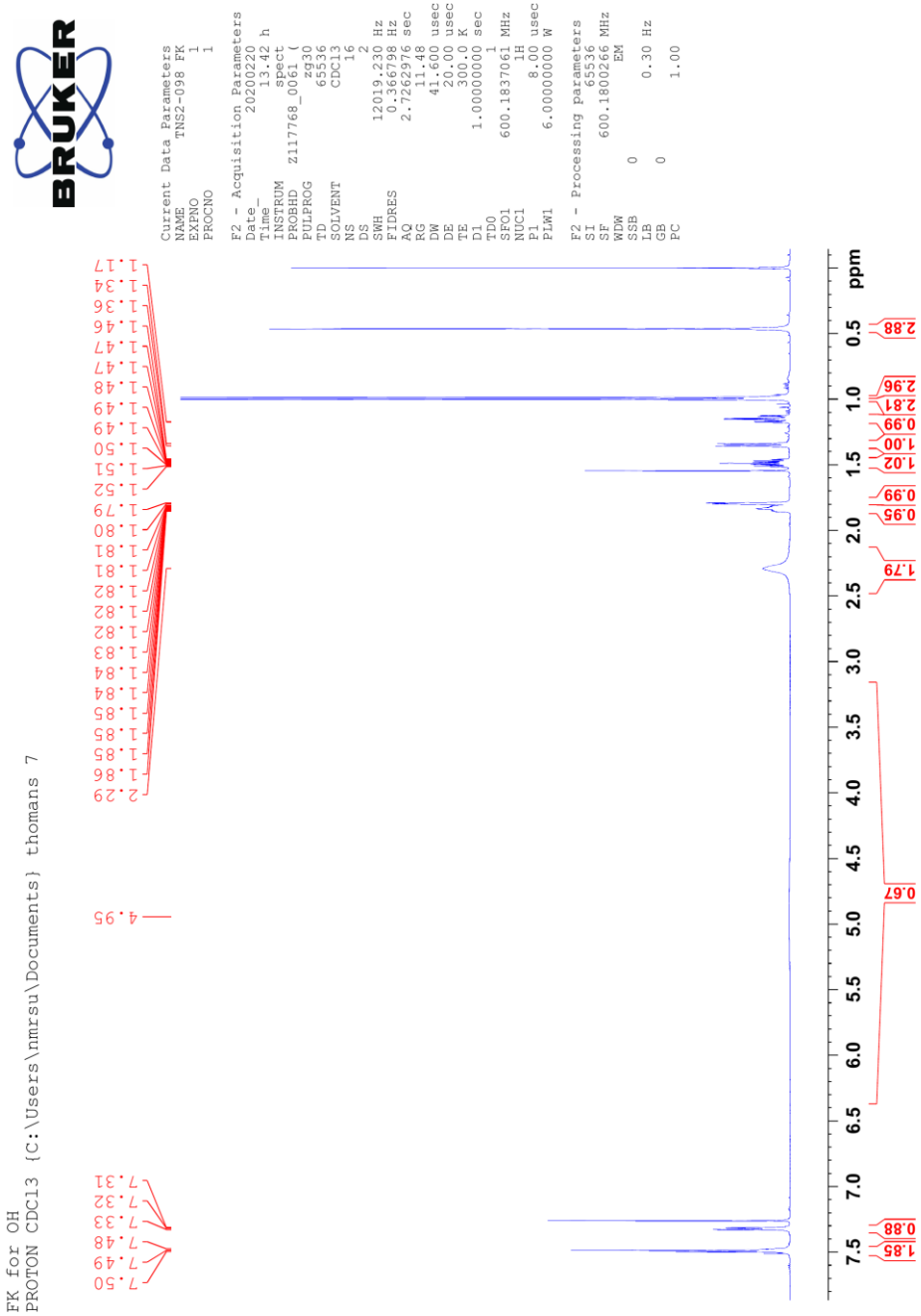

Appendix J **Spectra of 2-aryl-6-alkylpyridine Alcohols, 15a-g**

Appendix J.1 **^{1}H NMR spectra of Pyridine 15a**

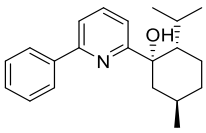

15a

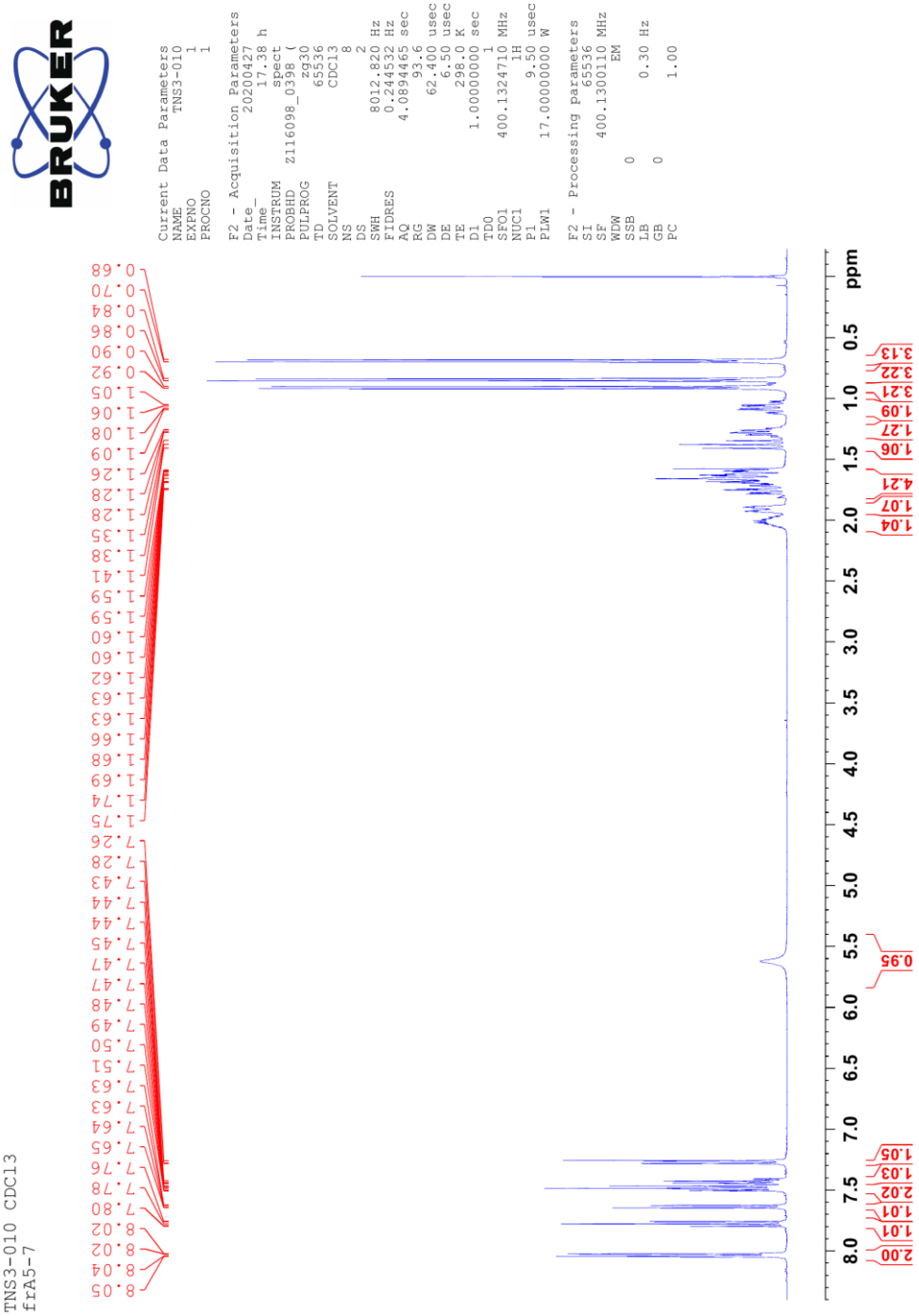

Appendix J Spectra of 2-aryl-6-alkylpyridine Alcohols, 15a-g

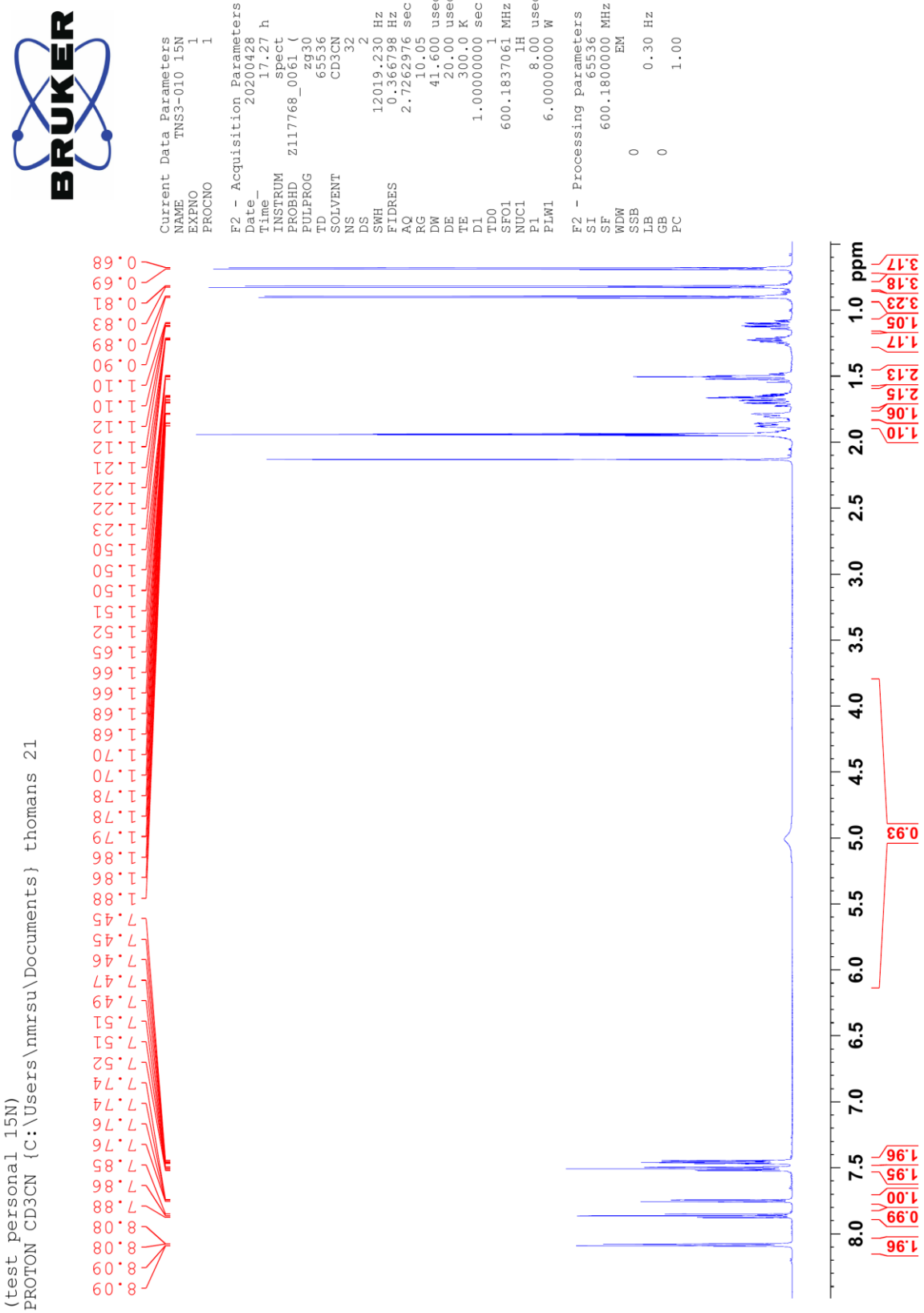

Appendix J Spectra of 2-aryl-6-alkylpyridine Alcohols, 15a-g

Appendix J.2 **^{1}H NMR Spectra of Pyridine 15b**

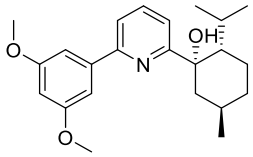

15b

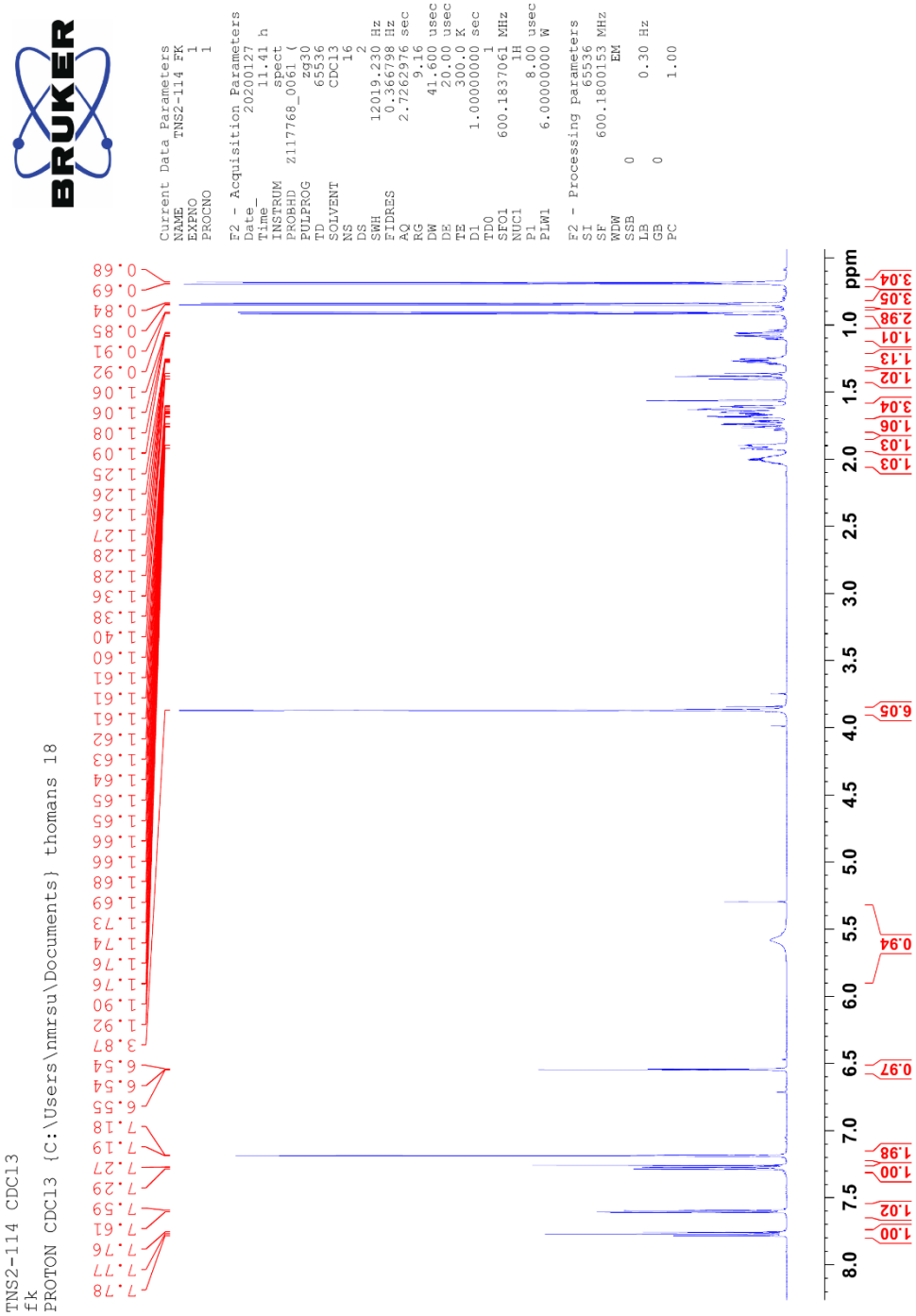

Appendix J Spectra of 2-aryl-6-alkylpyridine Alcohols, 15a-g

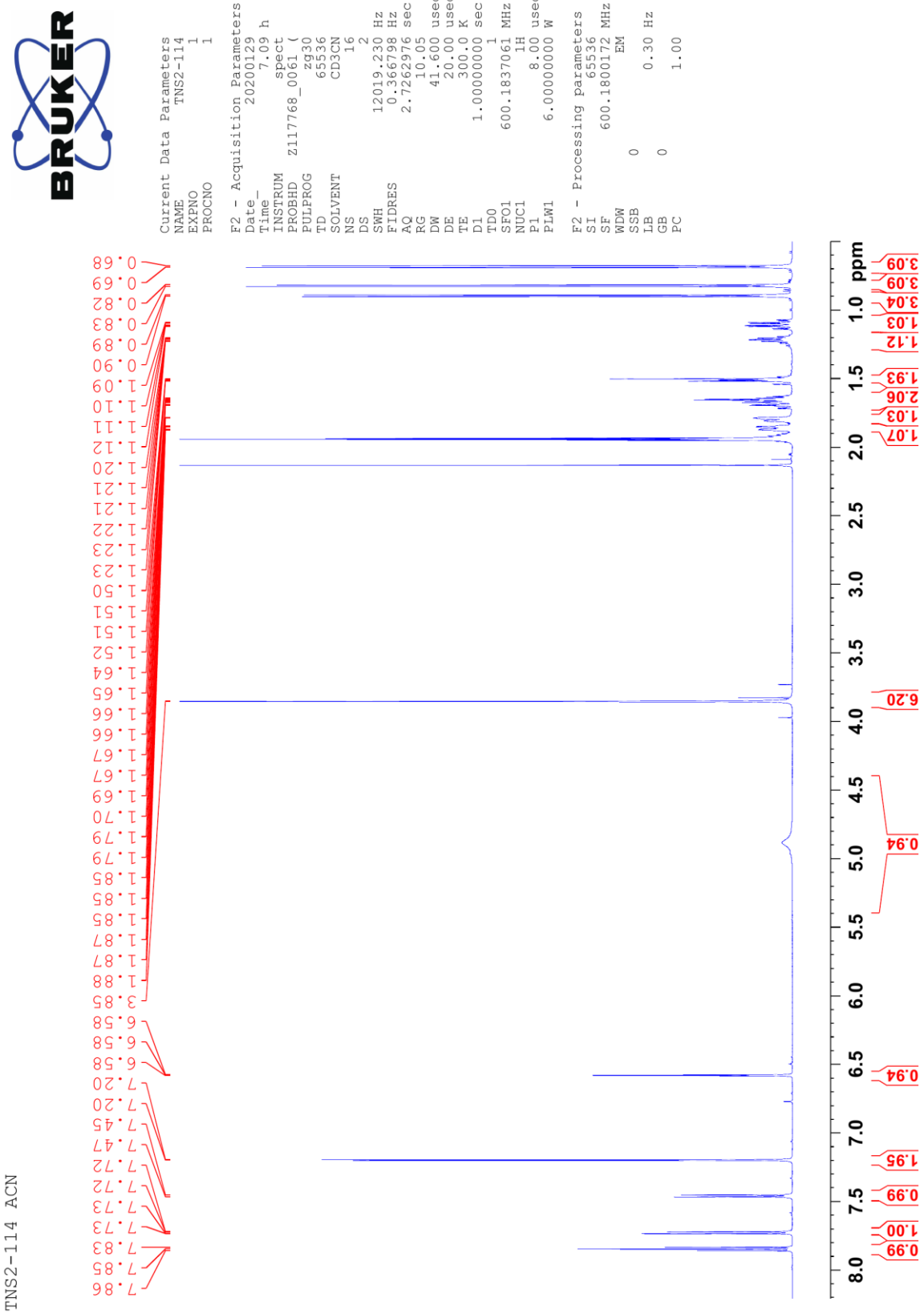

Appendix J Spectra of 2-aryl-6-alkylpyridine Alcohols, 15a-g

Appendix J.3 **^{13}C NMR Spectrum of Pyridine 15b**

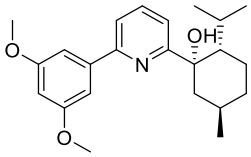

15b

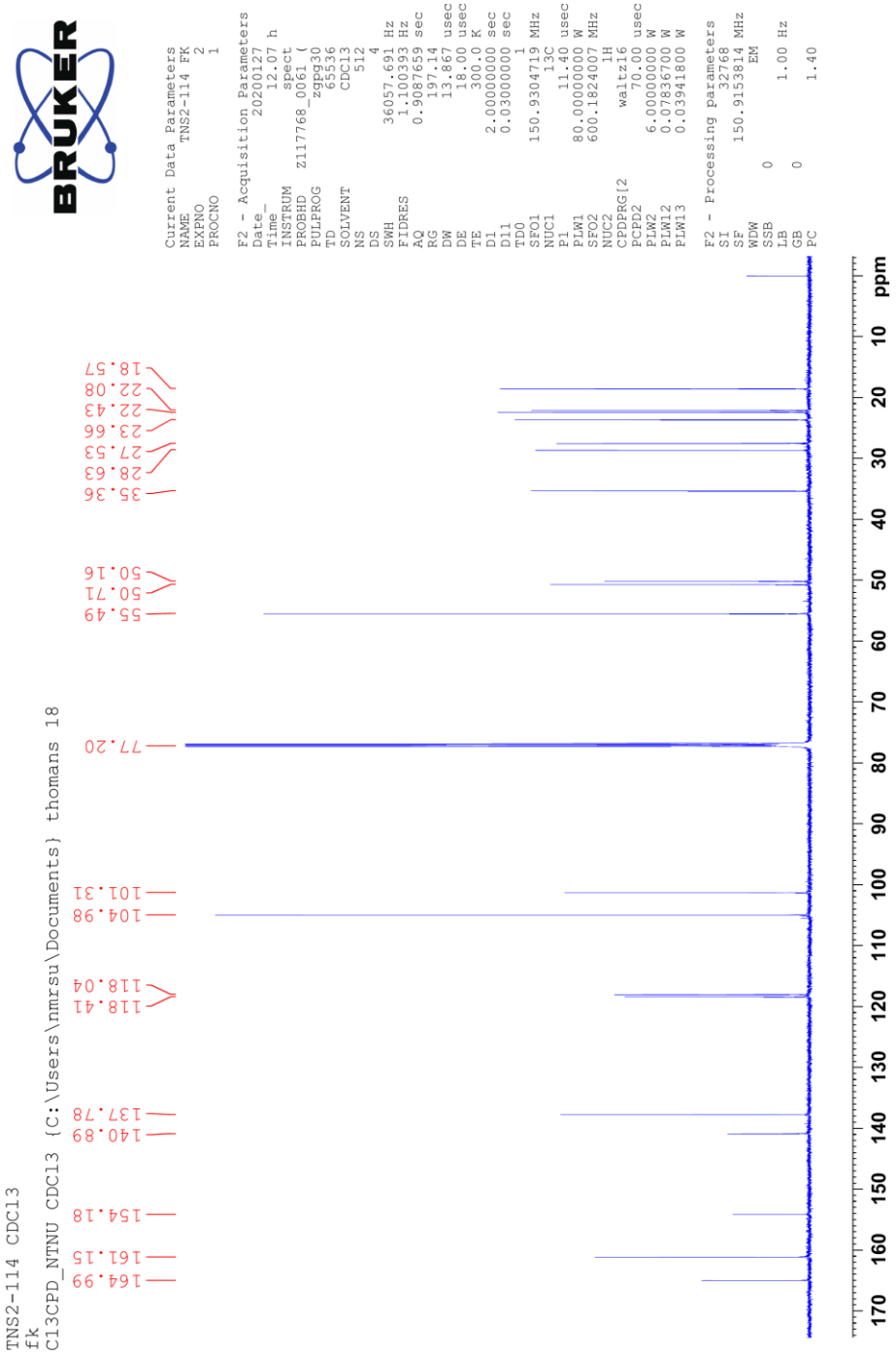

Appendix J.4 **COSY NMR Spectrum of Pyridine 15b**

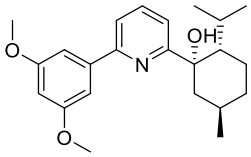

15b

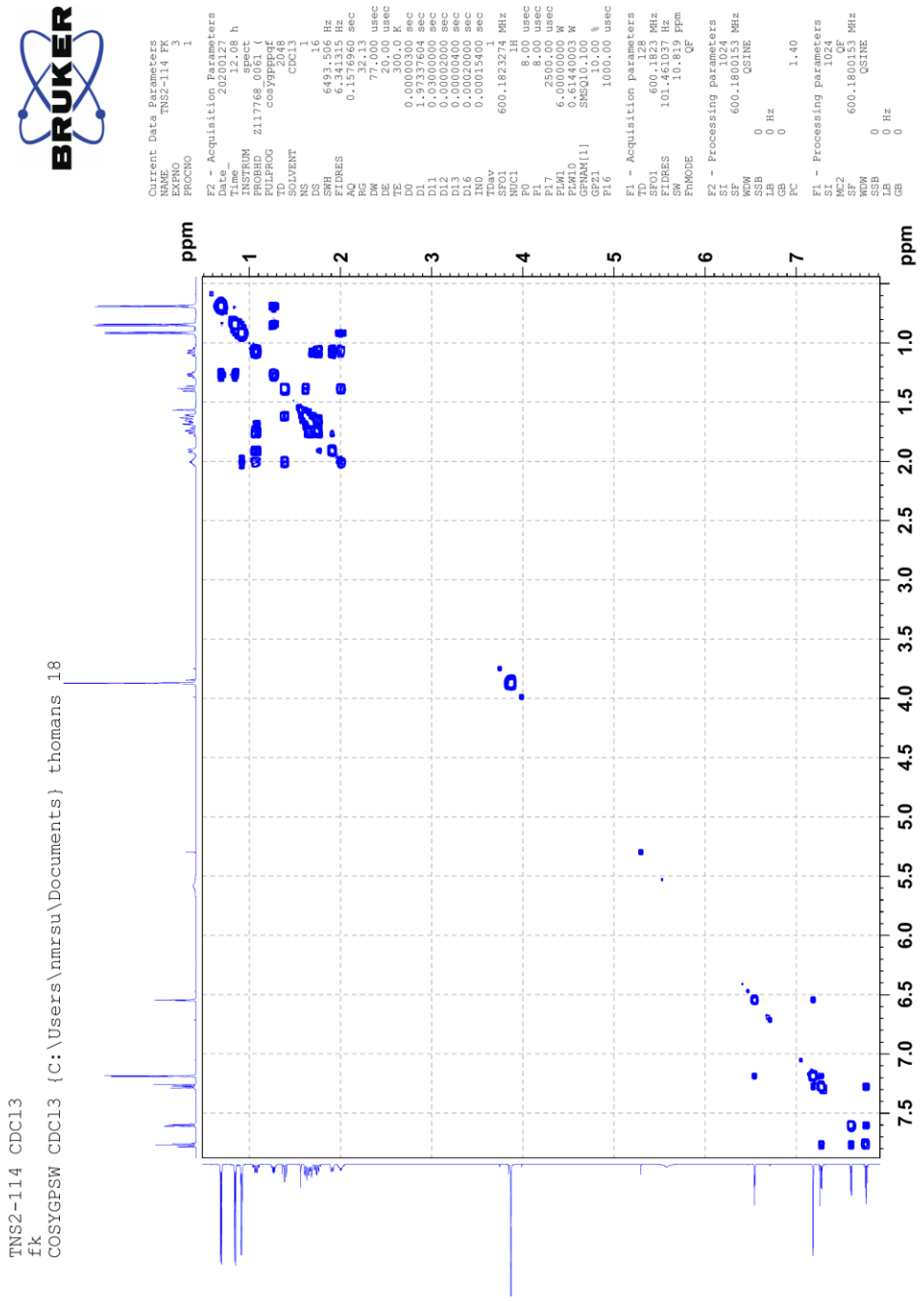

Appendix J.5 **HSQC NMR Spectrum of Pyridine 15b**

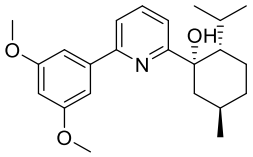

15b

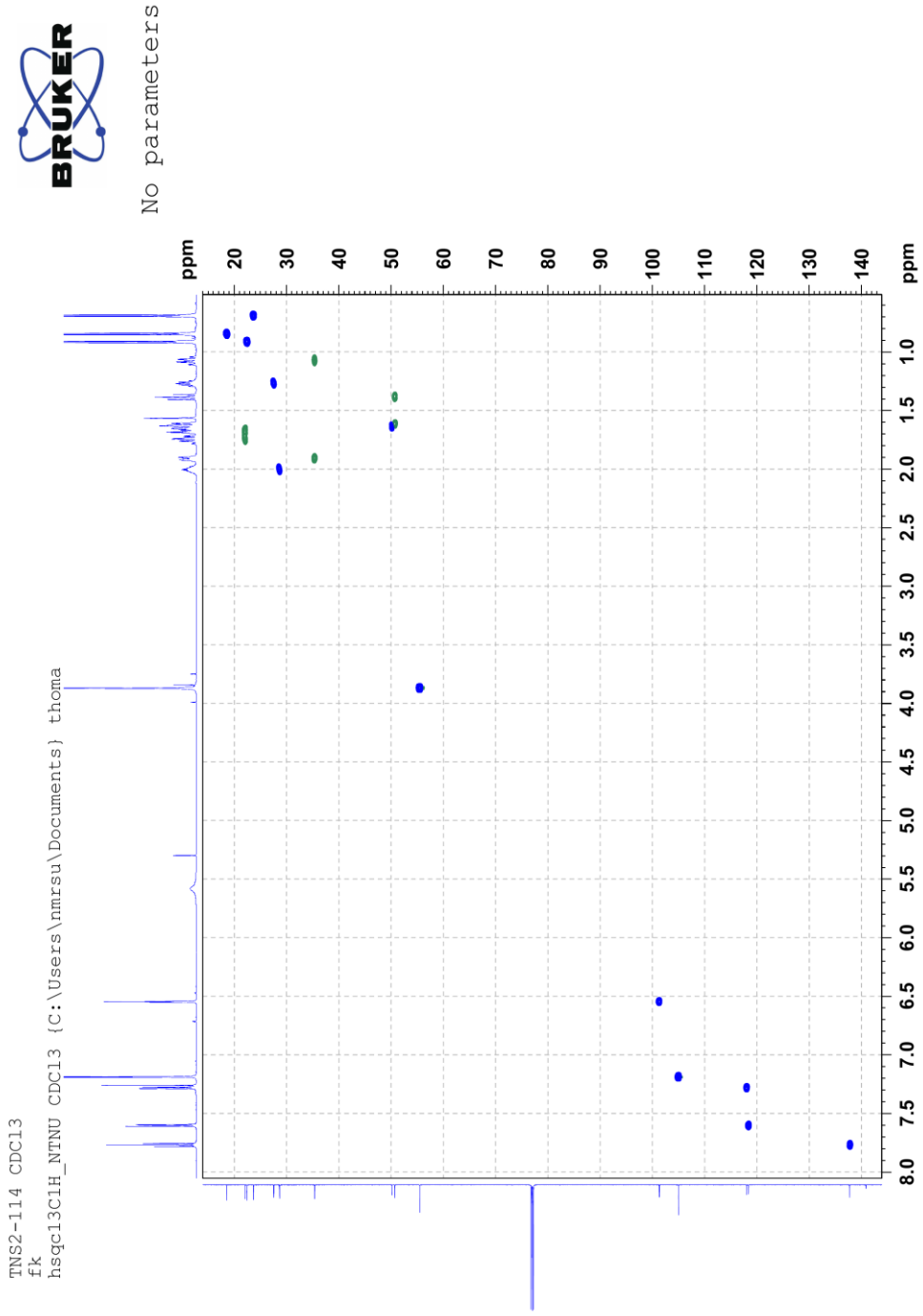

Appendix J Spectra of 2-aryl-6-alkylpyridine Alcohols, 15a-g

Appendix J.6 **^{1}H,^{13}C-HMBC NMR Spectrum of Pyridine 15b**

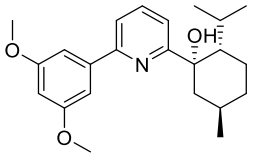

15b

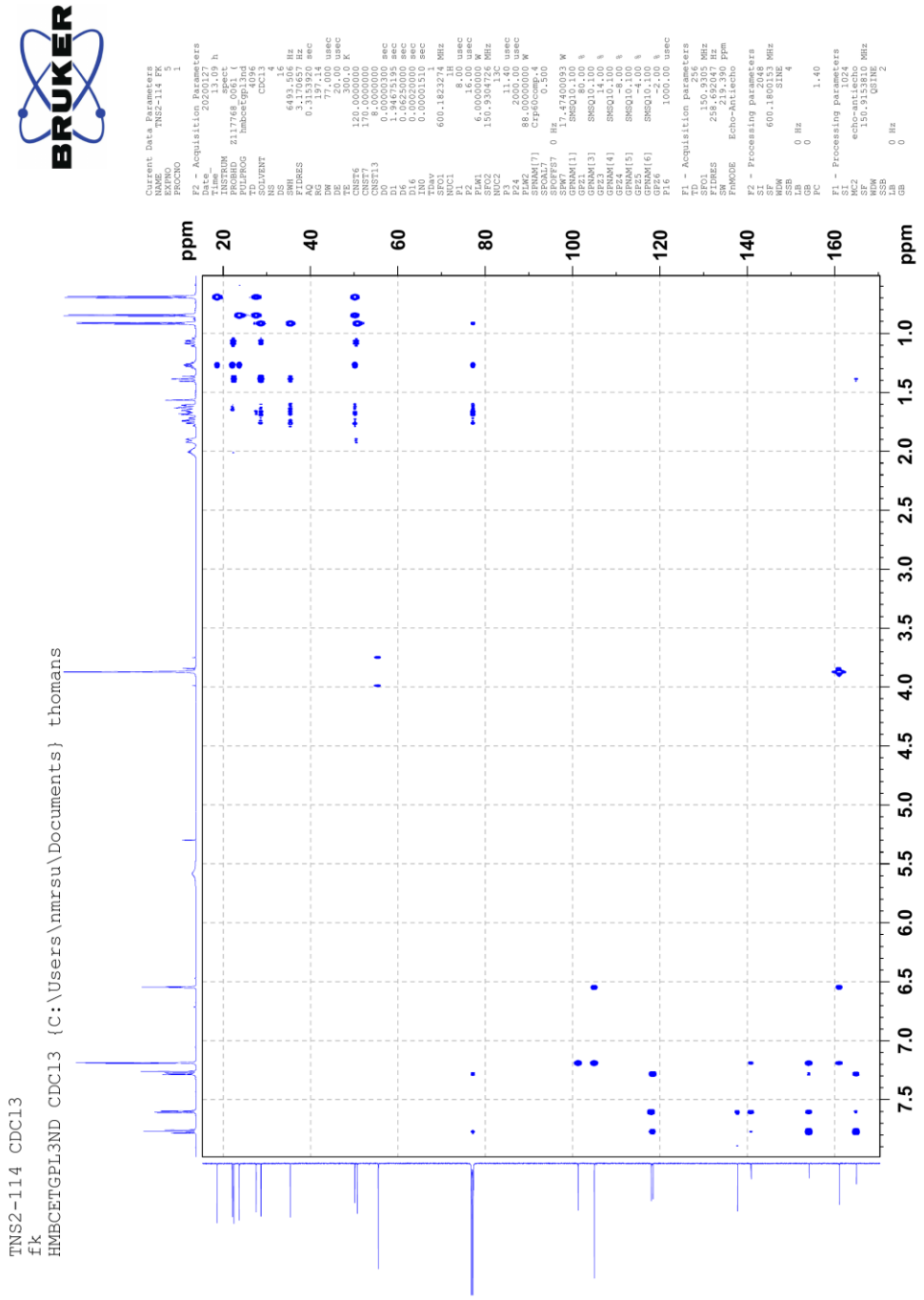

Appendix J Spectra of 2-aryl-6-alkylpyridine Alcohols, 15a-g

Appendix J.7 **$^{1}H,^{15}N$-HMBC NMR Spectrum of Pyridine 15b**

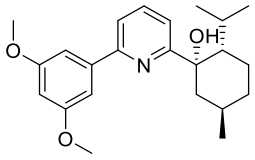

15b

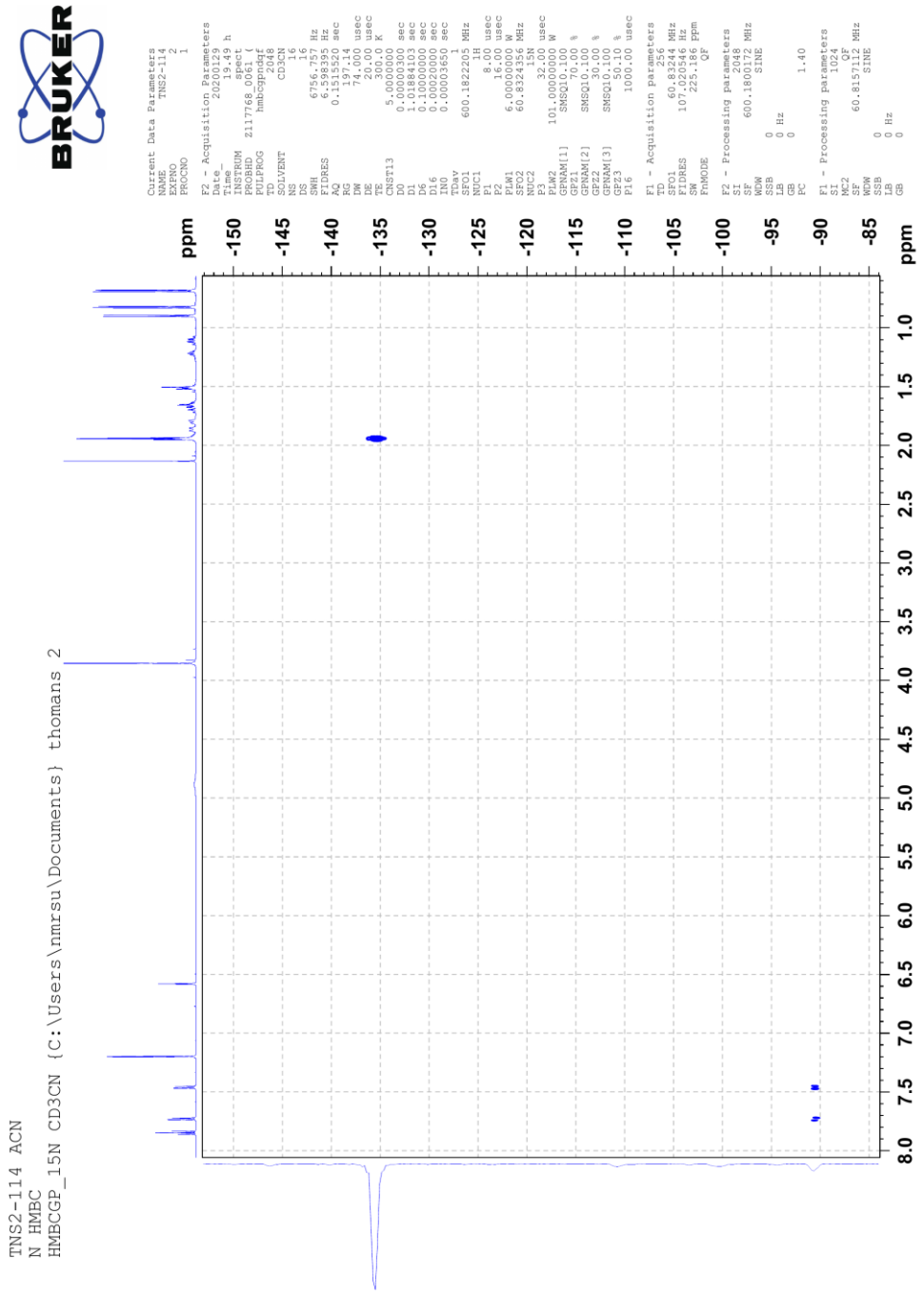

Appendix J Spectra of 2-aryl-6-alkylpyridine Alcohols, 15a-g

Appendix J.8 **HRMS Spectrum of Pyridine 15b**

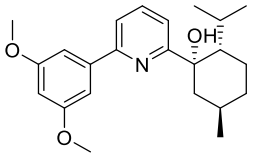

15b

Elemental Composition Report **Page 1**

Single Mass Analysis
Tolerance = 2.0 PPM / DBE: min = -5.0, max = 50.0
Element prediction: Off
Number of isotope peaks used for i-FIT = 3

Monoisotopic Mass, Even Electron Ions
2525 formula(e) evaluated with 3 results within limits (all results (up to 1000) for each mass)
Elements Used:
C: 0-100 H: 0-100 N: 0-10 O: 0-10 Si: 0-2 I: 0-2

2020_23 59 (0.568) AM2 (Ar,35000.0,0.00,0.00); Cm (58:61)
1: TOF MS ES+

1.58e+005

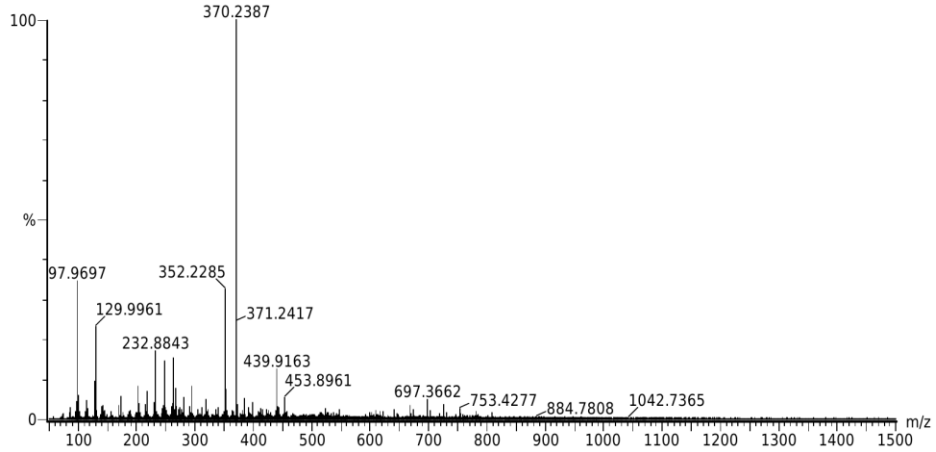

Minimum:				-5.0				
Maximum:		5.0	2.0	50.0				
Mass	Calc. Mass	mDa	PPM	DBE	i-FIT	Norm	Conf(%)	Formula
370.2387	370.2382	0.5	1.4	8.5	802.8	0.000	100.00	C23 H32 N O3
	370.2387	0.0	0.0	4.5	818.5	15.690	0.00	C15 H32 N7 O2 Si
	370.2386	0.1	0.3	7.5	822.5	19.769	0.00	C22 H36 N Si2

Appendix J Spectra of 2-aryl-6-alkylpyridine Alcohols, 15a-g

Appendix J.9 **^{1}H NMR Spectra of Pyridine 15c**

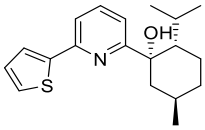

15c

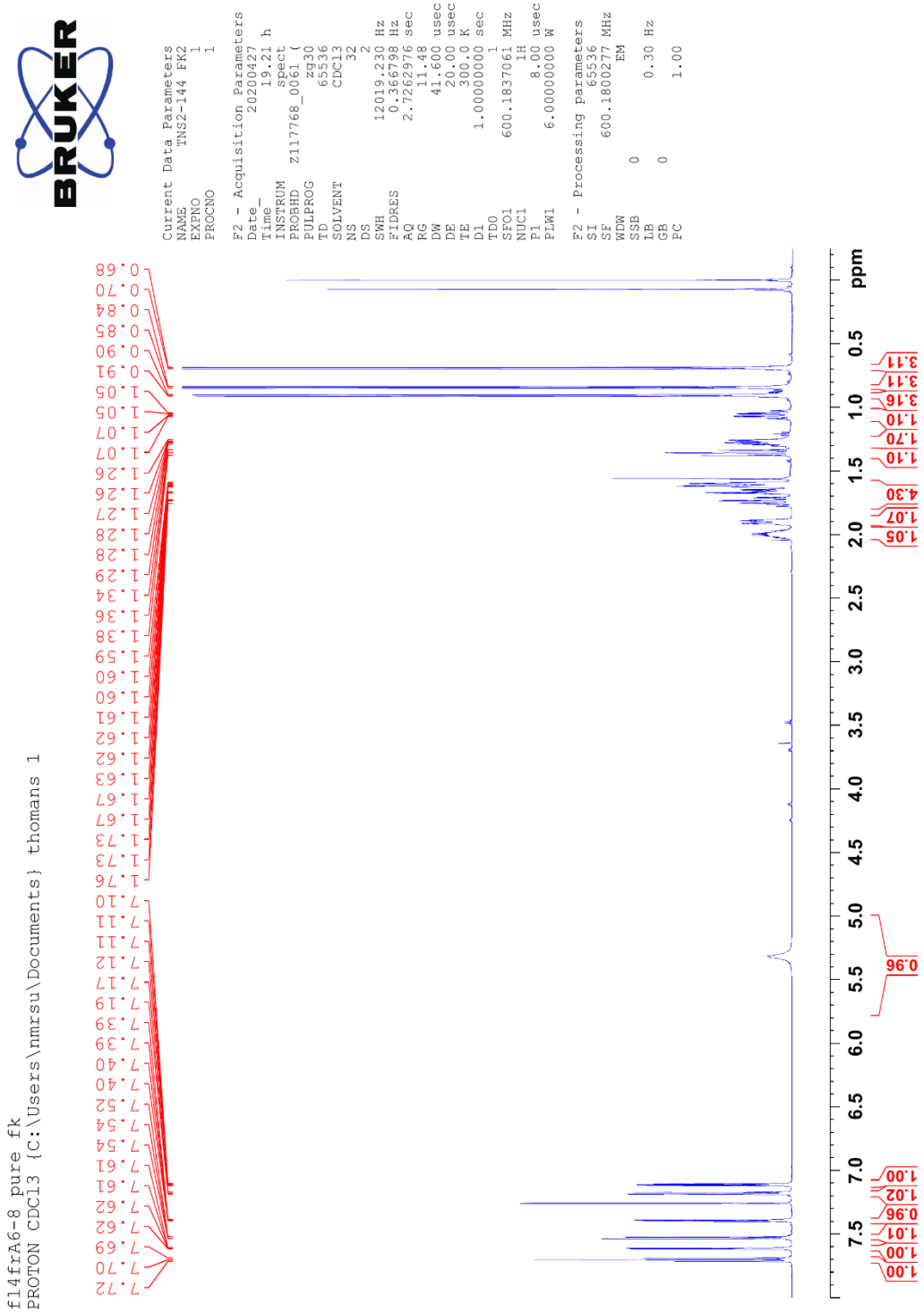

Appendix J Spectra of 2-aryl-6-alkylpyridine Alcohols, 15a-g

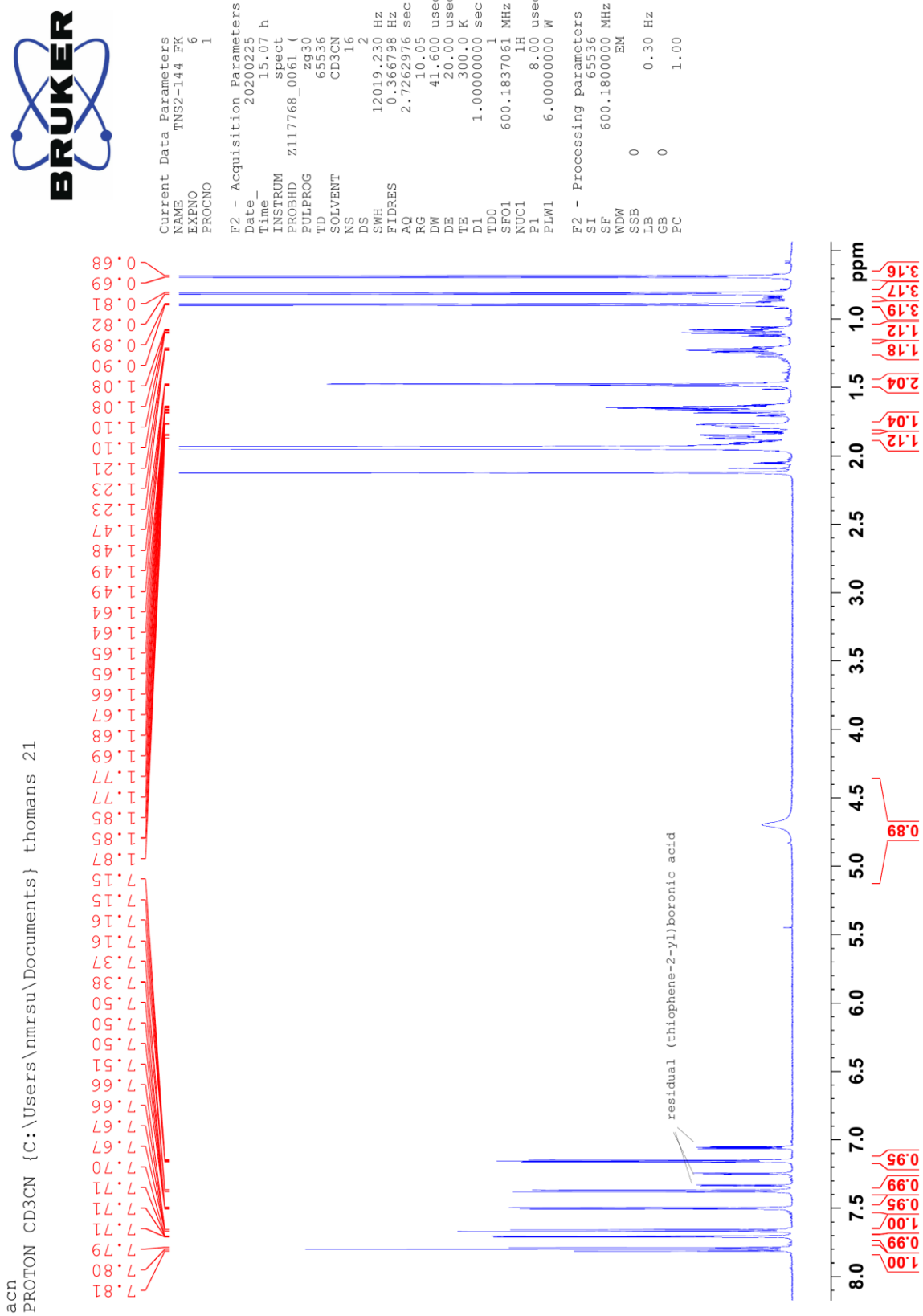

Appendix J Spectra of 2-aryl-6-alkylpyridine Alcohols, 15a-g

Appendix J.10 **^{13}C NMR Spectrum of Pyridine 15c**

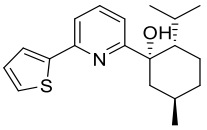

15c

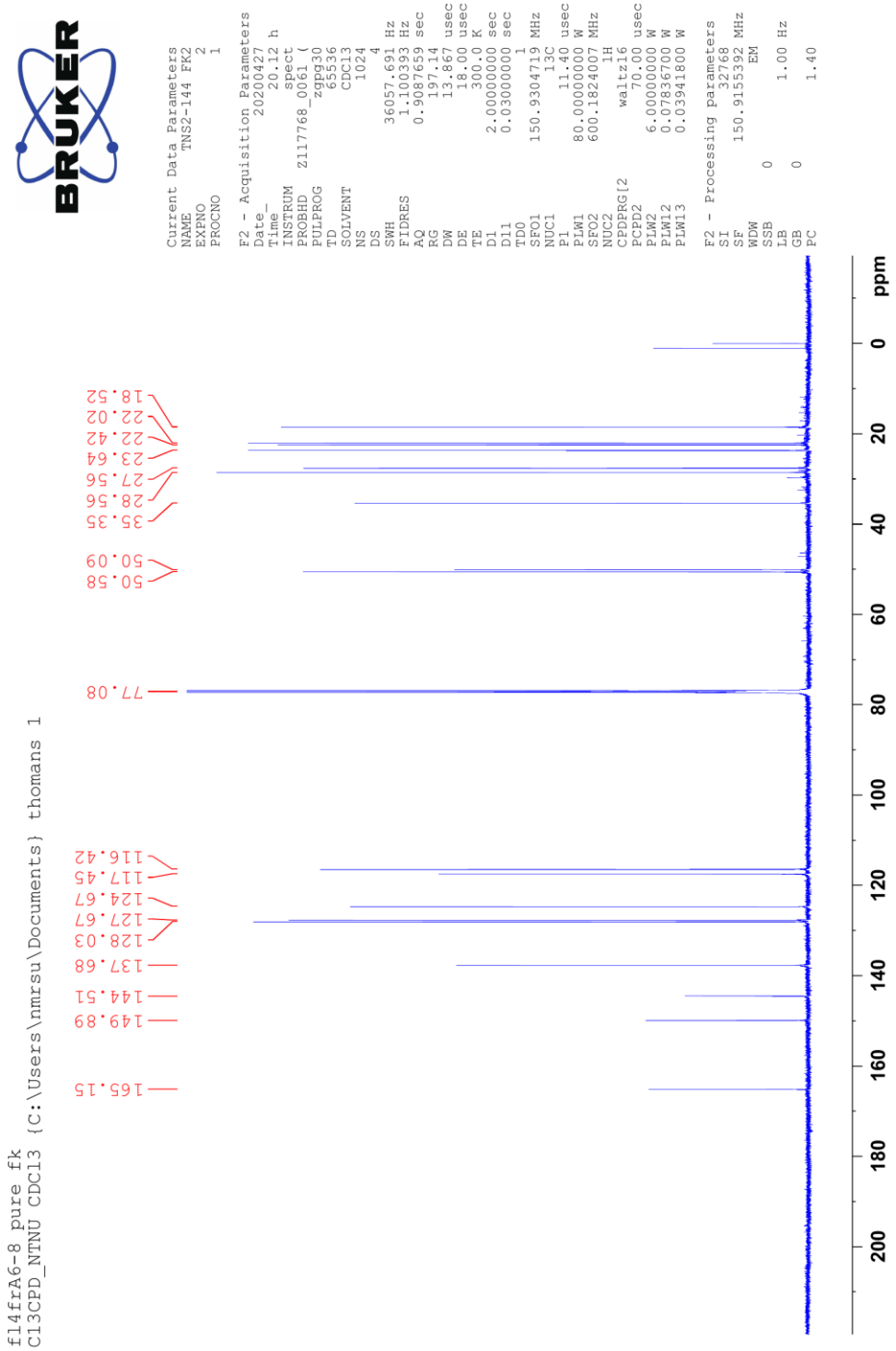

Appendix J Spectra of 2-aryl-6-alkylpyridine Alcohols, 15a-g

Appendix J.11 **COSY NMR Spectrum of Pyridine 15c**

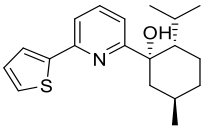

15c

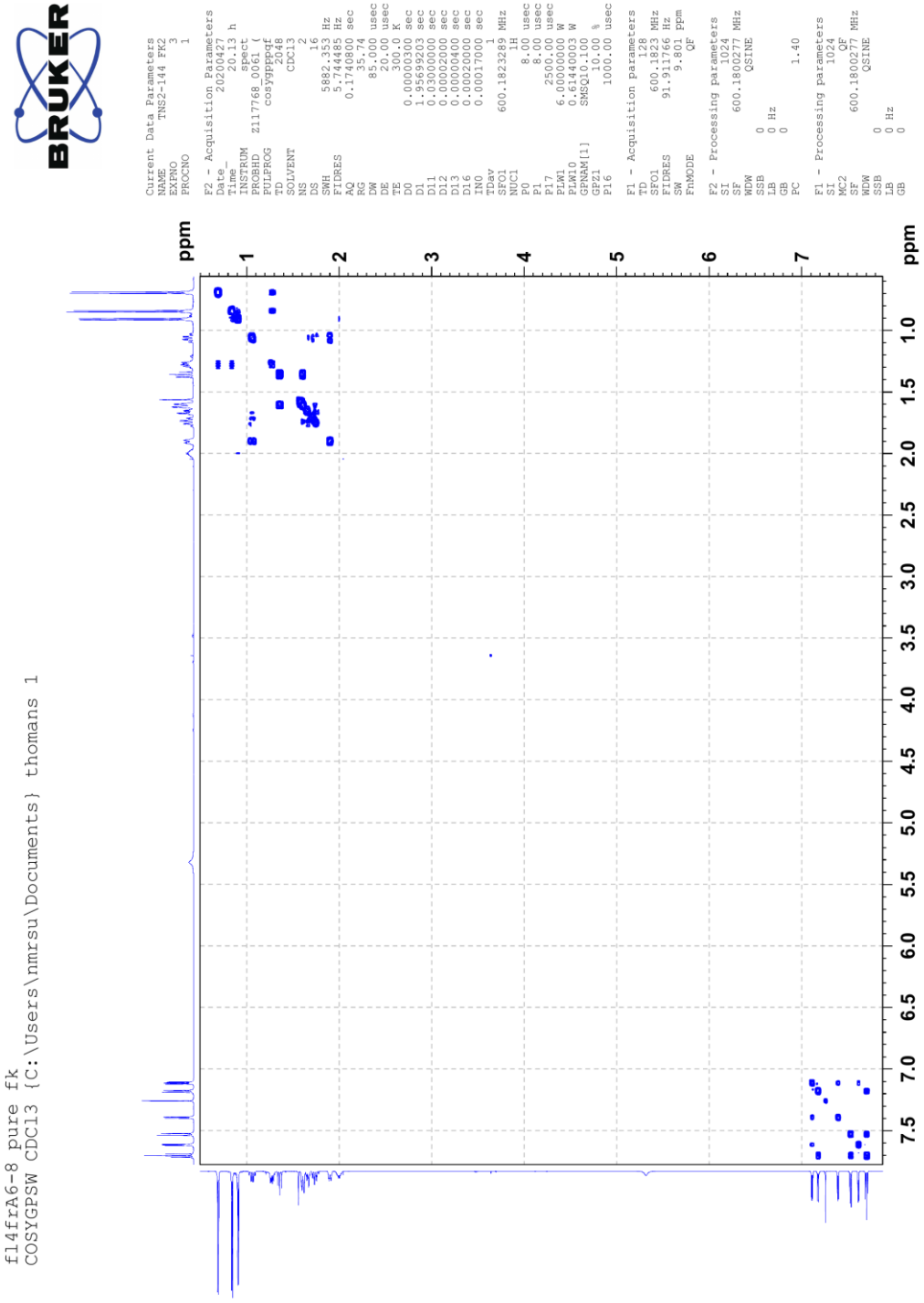

Appendix J Spectra of 2-aryl-6-alkylpyridine Alcohols, 15a-g

Appendix J.12 **HSQC NMR Spectrum of Pyridine 15c**

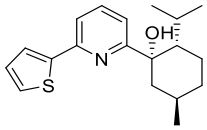

15c

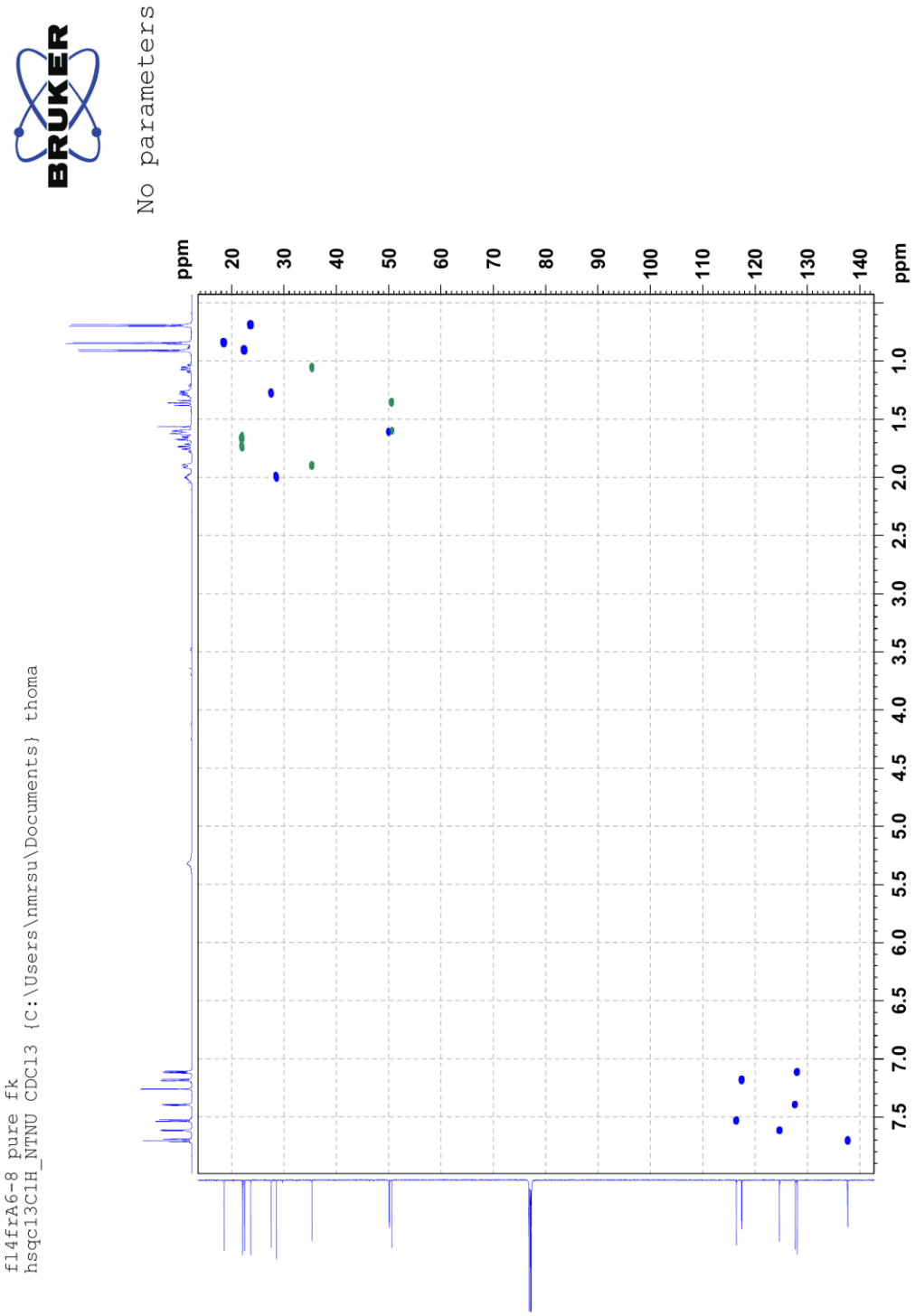

Appendix J Spectra of 2-aryl-6-alkylpyridine Alcohols, 15a-g

Appendix J.13 **^{1}H,^{13}C-HMBC NMR Spectrum of Pyridine 15c**

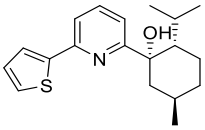

15c

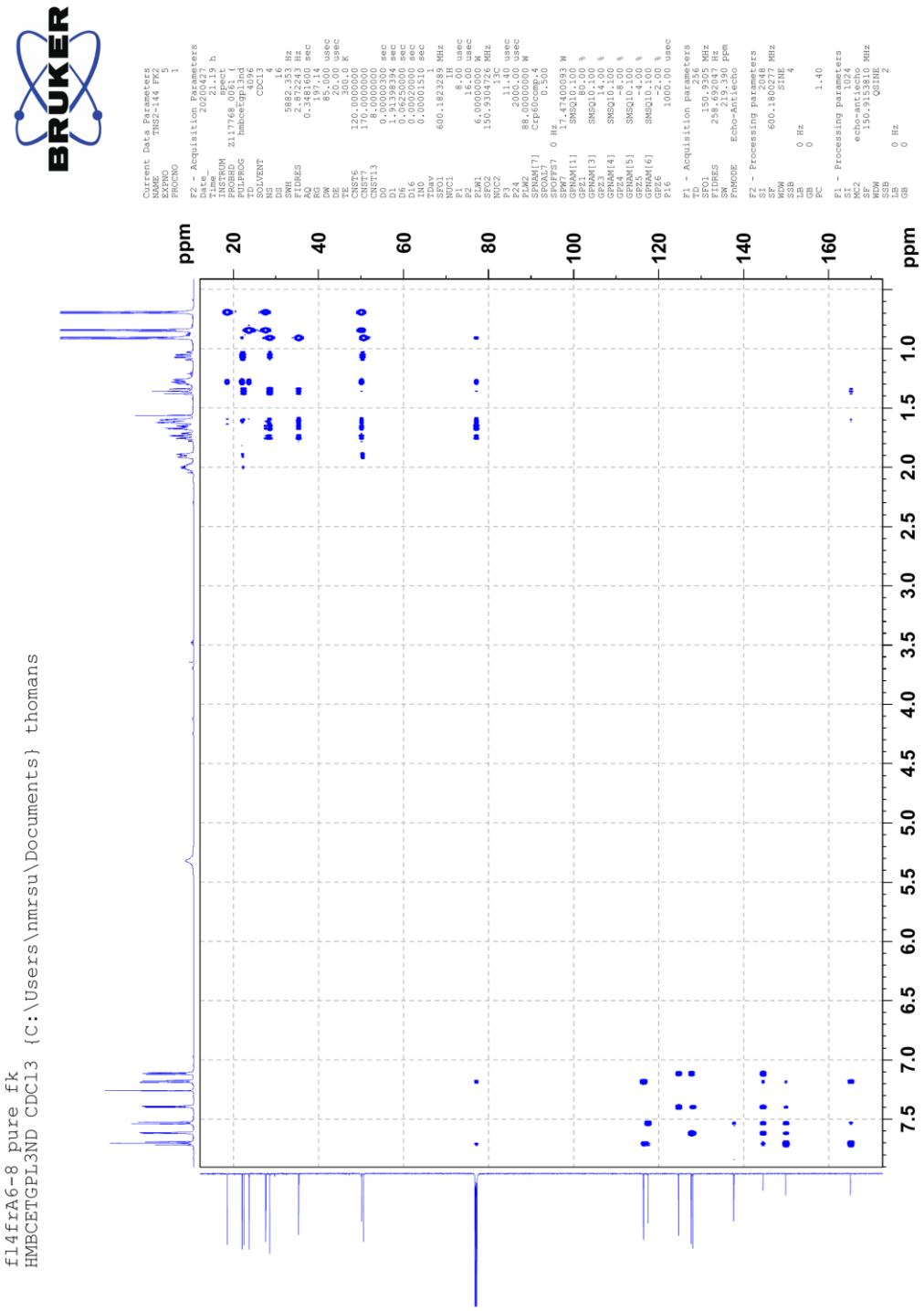

Appendix J Spectra of 2-aryl-6-alkylpyridine Alcohols, 15a-g

Appendix J.14 **HRMS Spectrum of Pyridine 15c**

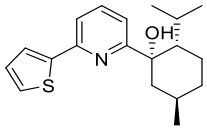

15c

Elemental Composition Report **Page 1**

Single Mass Analysis
Tolerance = 5.0 PPM / DBE: min = -5.0, max = 50.0
Element prediction: Off
Number of isotope peaks used for i-FIT = 3

Monoisotopic Mass, Even Electron Ions
1063 formula(e) evaluated with 2 results within limits (all results (up to 1000) for each mass)
Elements Used:
C: 0-100 H: 0-100 N: 0-5 O: 0-10 S: 0-4
2020_52 35 (0.707) AM2 (Ar,35000.0,0.00,0.00); Cm (34:48)
1: TOF MS ASAP+

8.76e+006

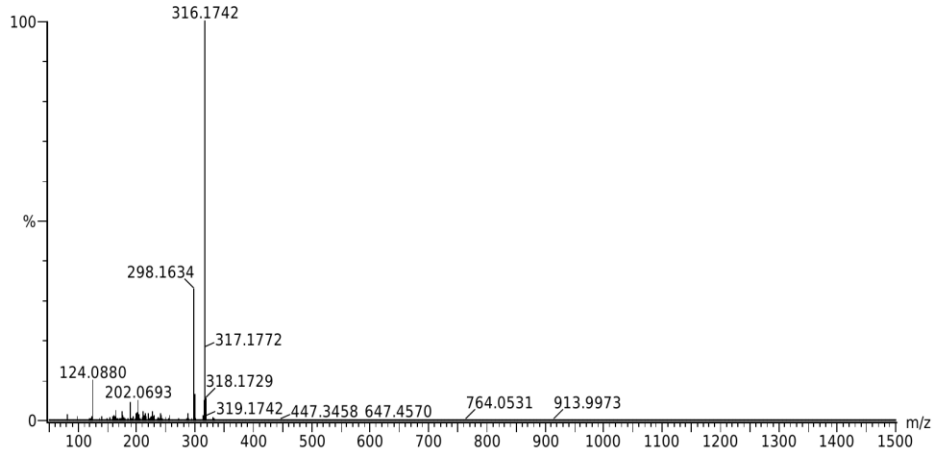

Minimum:				-5.0				
Maximum:		5.0	5.0	50.0				
Mass	Calc. Mass	mDa	PPM	DBE	i-FIT	Norm	Conf(%)	Formula
316.1742	316.1735	0.7	2.2	7.5	1491.8	0.001	99.87	C19 H26 N O S
	316.1729	1.3	4.1	-1.5	1498.5	6.666	0.13	C11 H30 N3 O3 S2

Appendix J Spectra of 2-aryl-6-alkylpyridine Alcohols, 15a-g

Appendix J.15 **^{1}H NMR Spectra of Pyridine 15d**

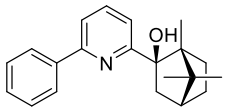

15d

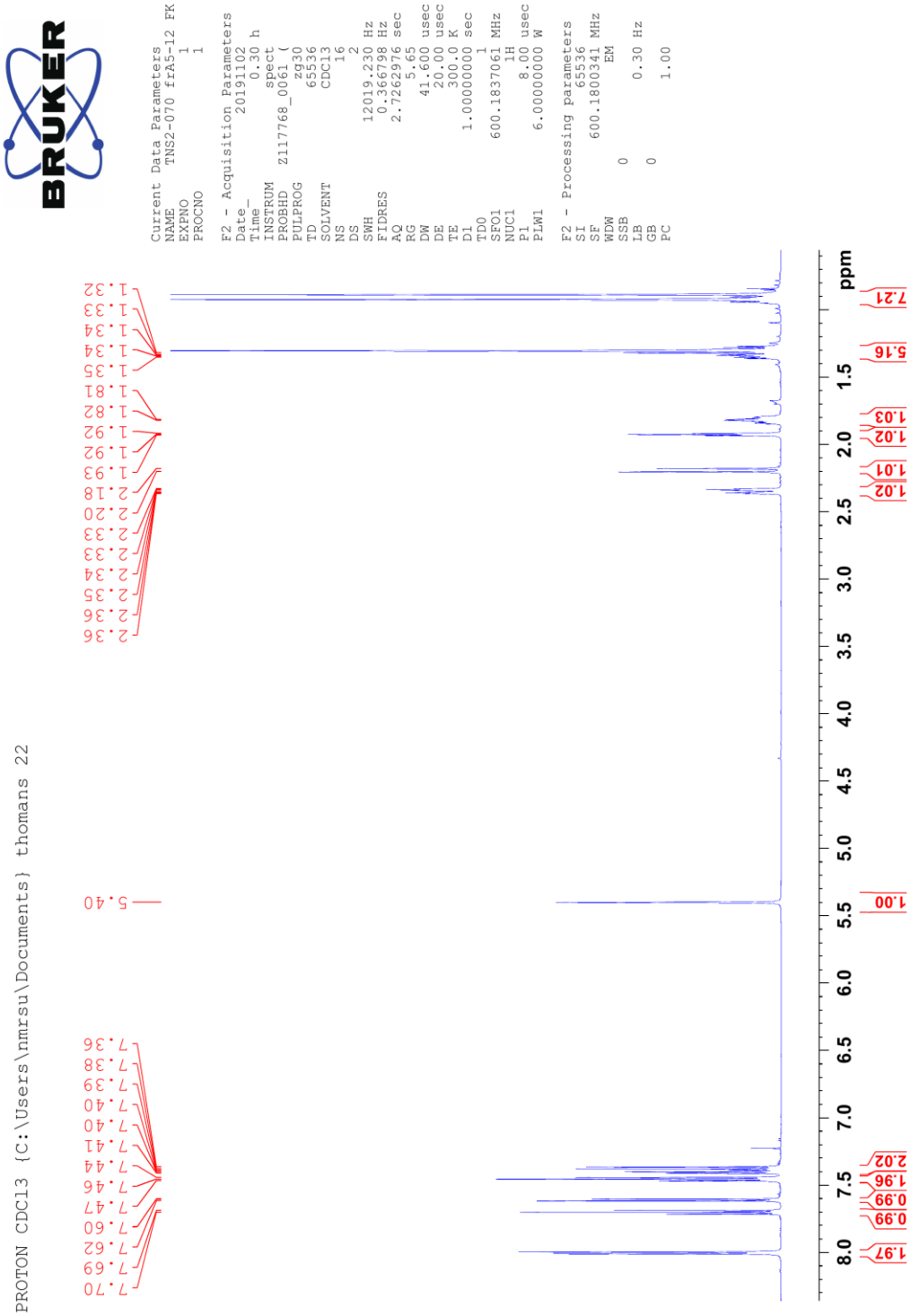

Appendix J Spectra of 2-aryl-6-alkylpyridine Alcohols, 15a-g

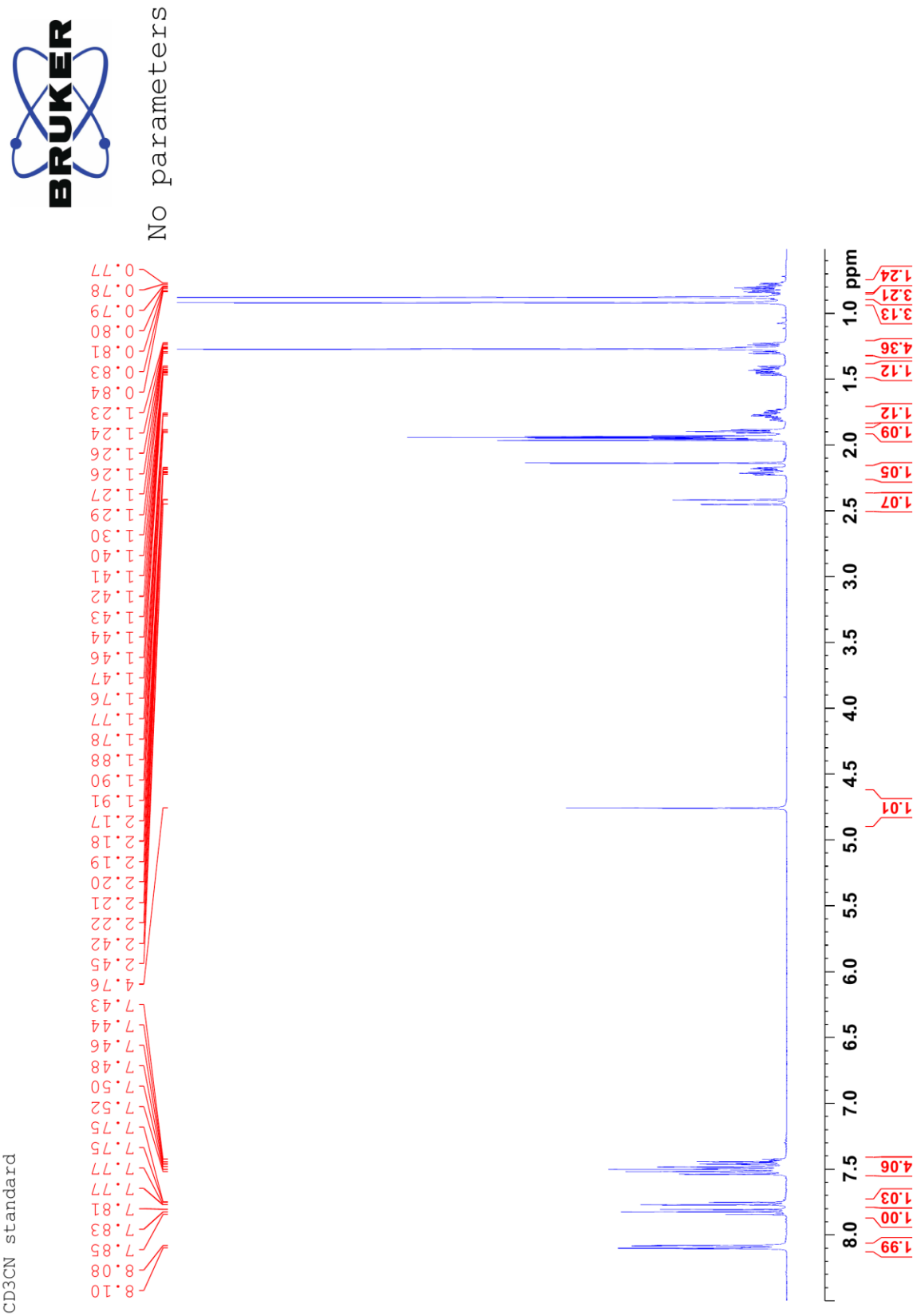

Appendix J Spectra of 2-aryl-6-alkylpyridine Alcohols, 15a-g

Appendix J.16 **^{1}H NMR Spectra of Pyridine 15e**

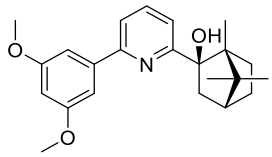

15e

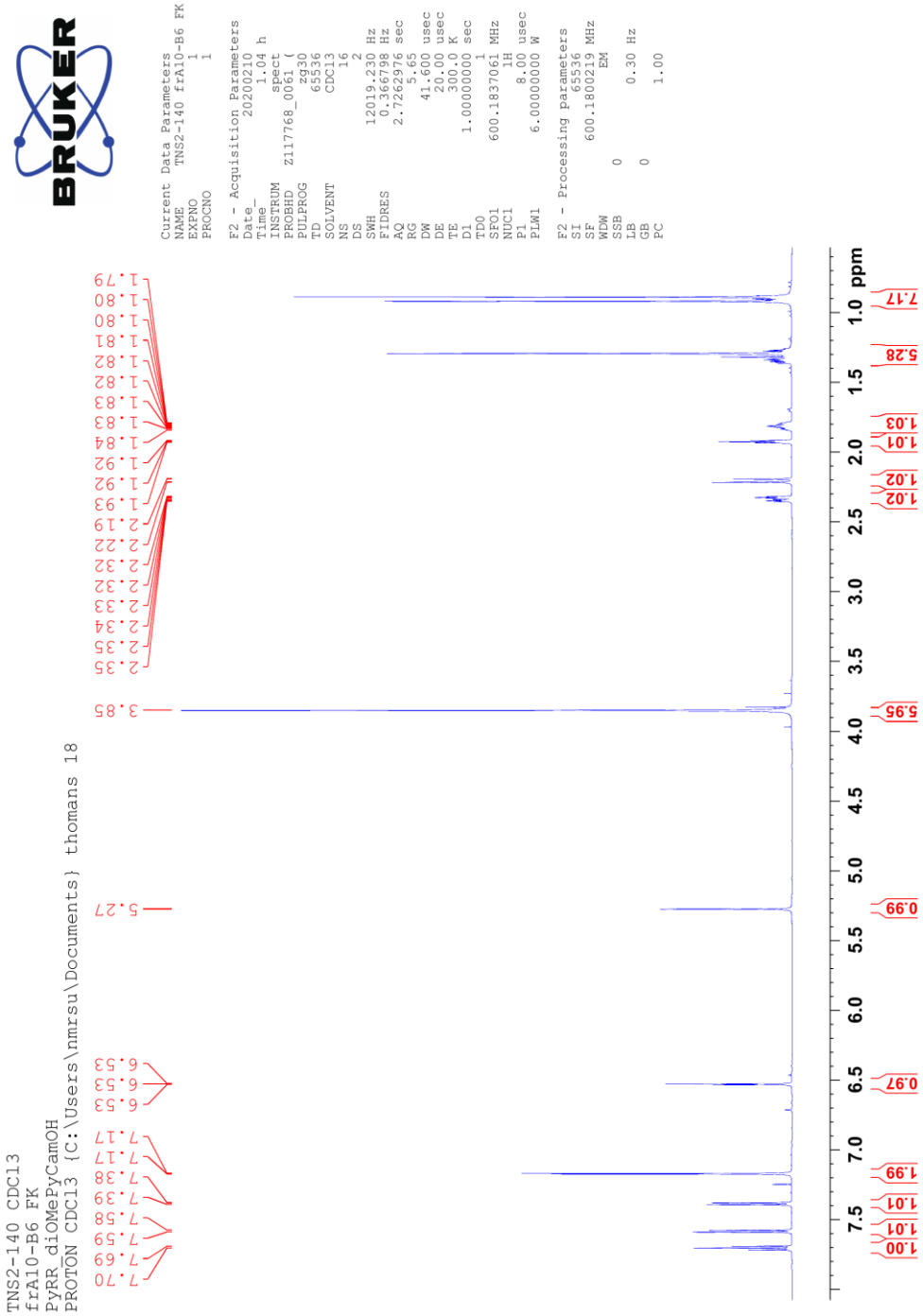

Appendix J Spectra of 2-aryl-6-alkylpyridine Alcohols, 15a-g

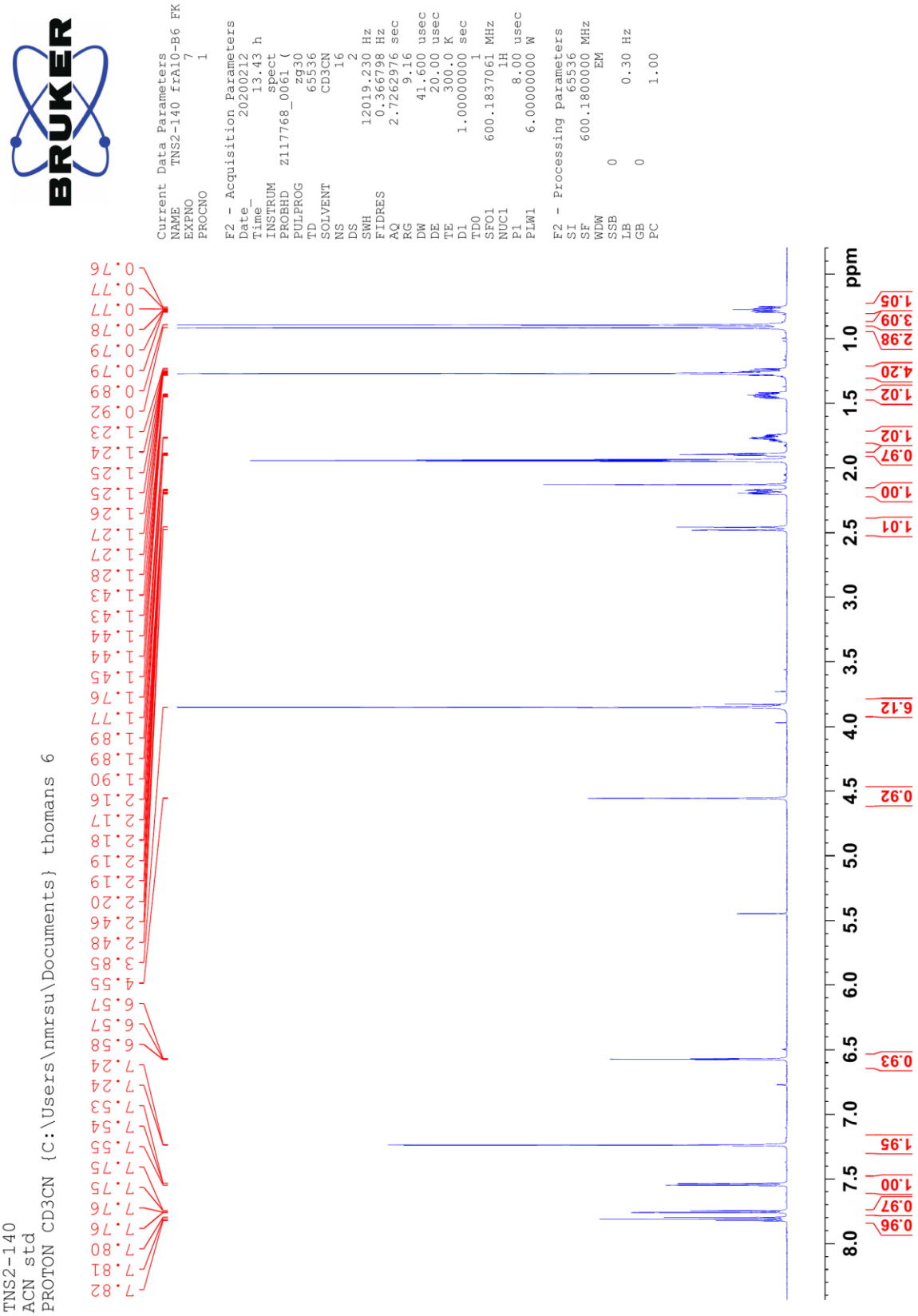

Appendix J Spectra of 2-aryl-6-alkylpyridine Alcohols, 15a-g

Appendix J.17 **^{13}C NMR Spectrum of Pyridine 15e**

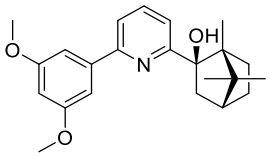

15e

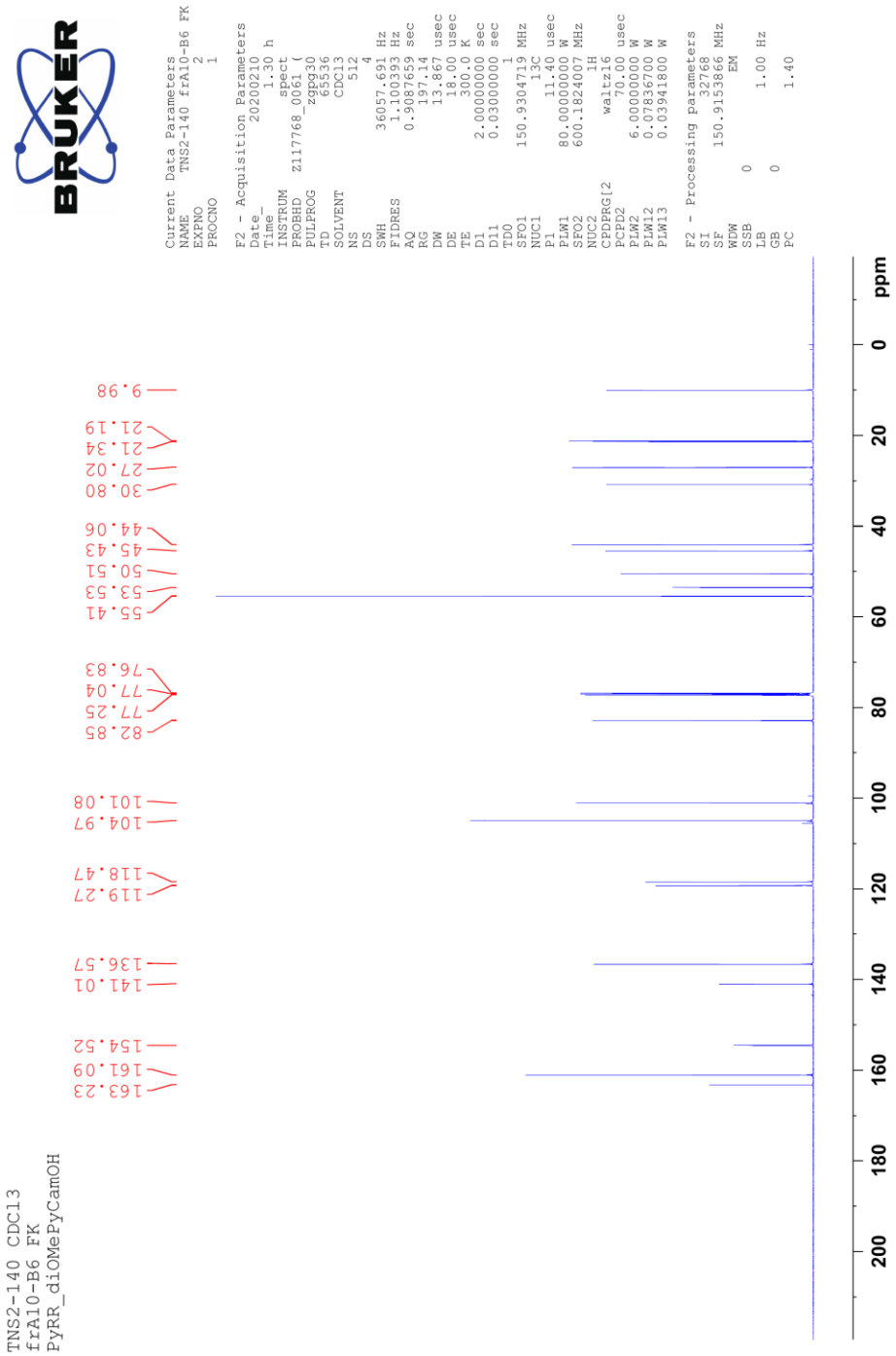

Appendix J.18 **COSY NMR Spectrum of Pyridine 15e**

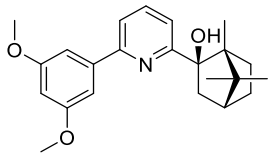

15e

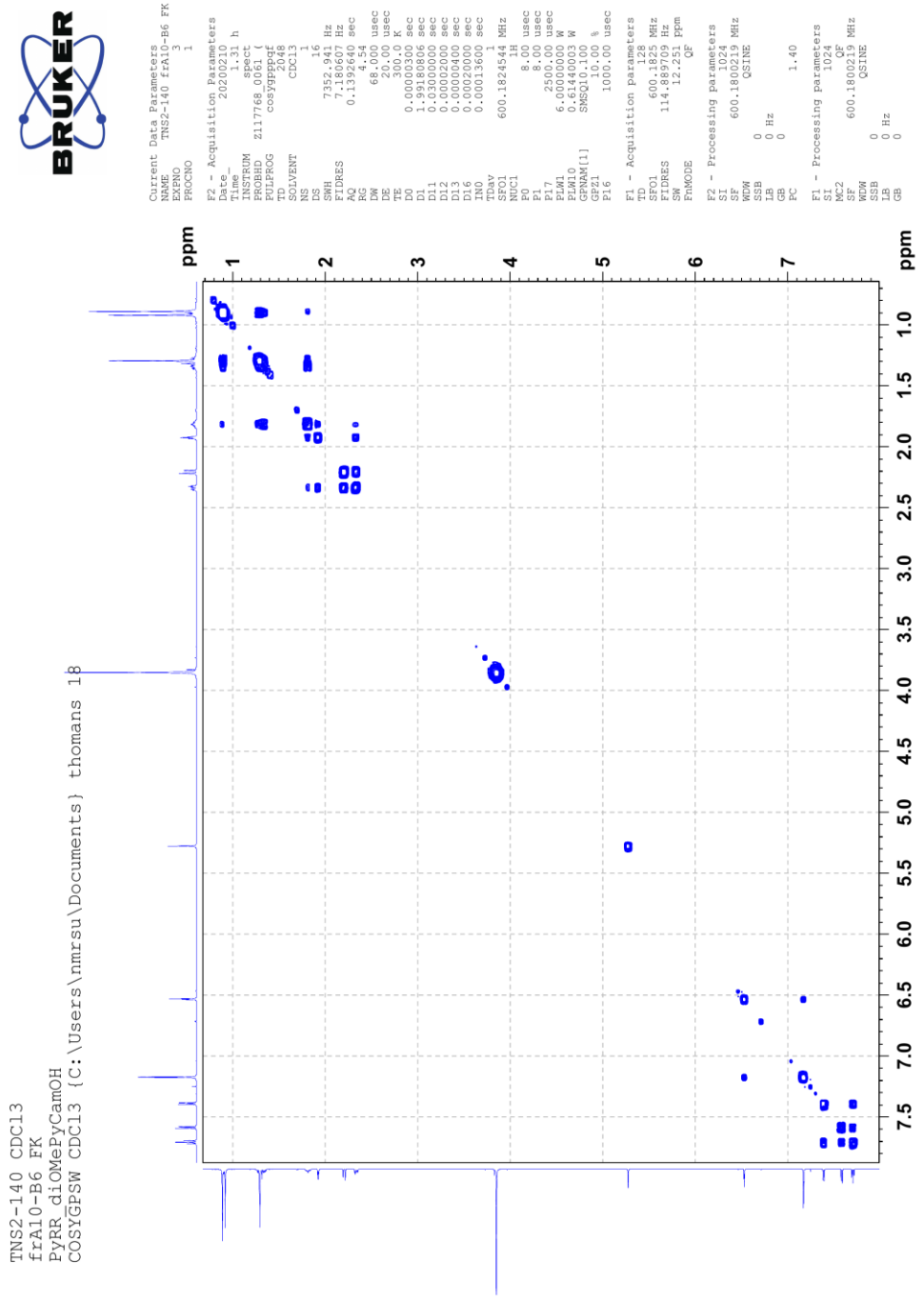

Appendix J Spectra of 2-aryl-6-alkylpyridine Alcohols, 15a-g

Appendix J.19 **HSQC NMR Spectrum of Pyridine 15e**

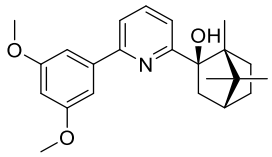

15e

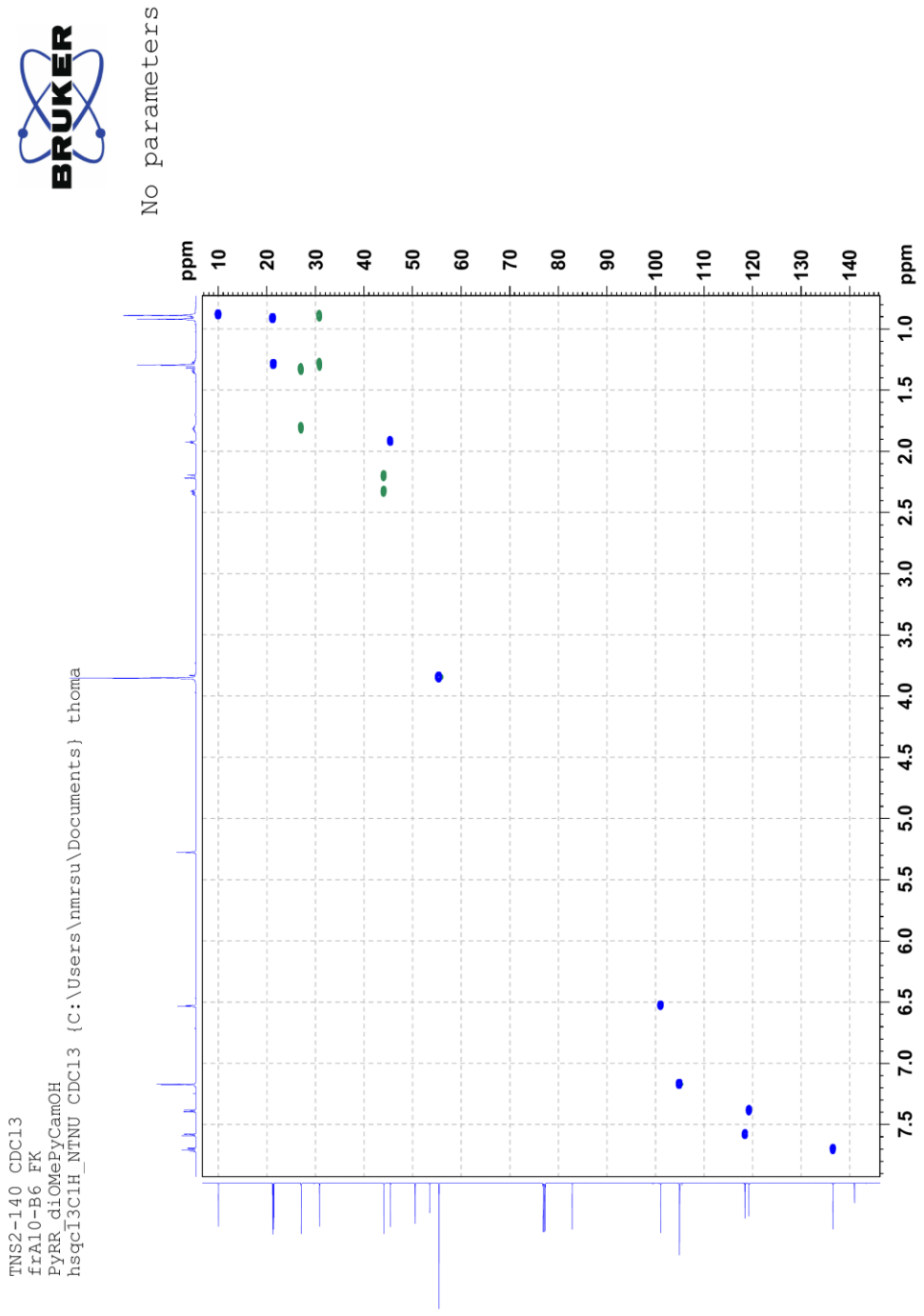

Appendix J Spectra of 2-aryl-6-alkylpyridine Alcohols, 15a-g

Appendix J.20 **^{1}H,^{13}C-HMBC NMR Spectrum of Pyridine 15e**

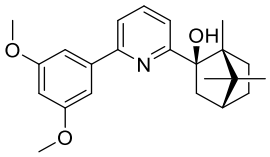

15e

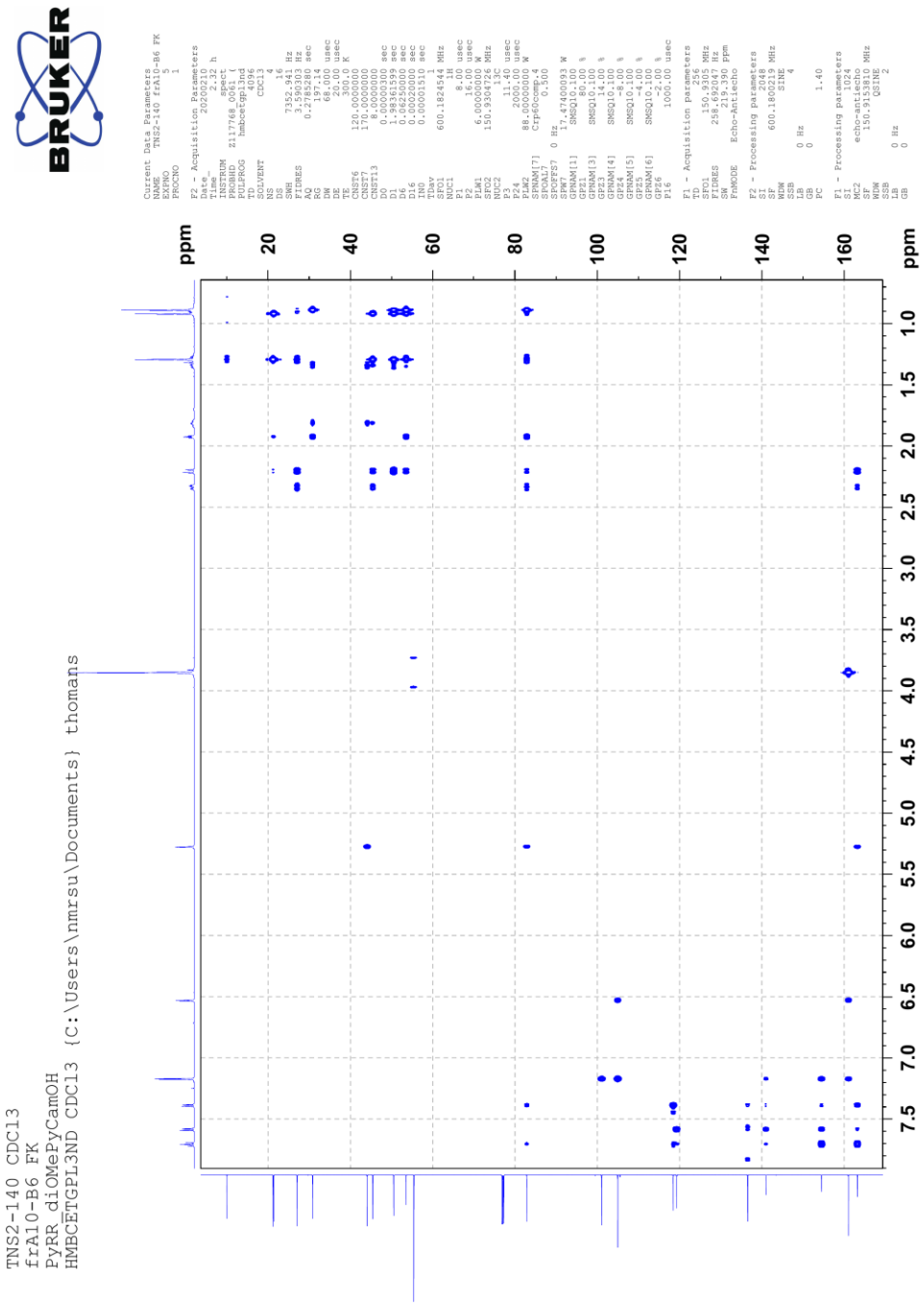

Appendix J Spectra of 2-aryl-6-alkylpyridine Alcohols, 15a-g

Appendix J.21 **$^{1}H,^{15}N$-HMBC NMR Spectrum of Pyridine 15e**

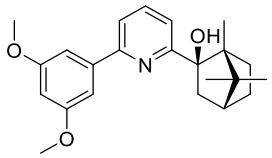

15e

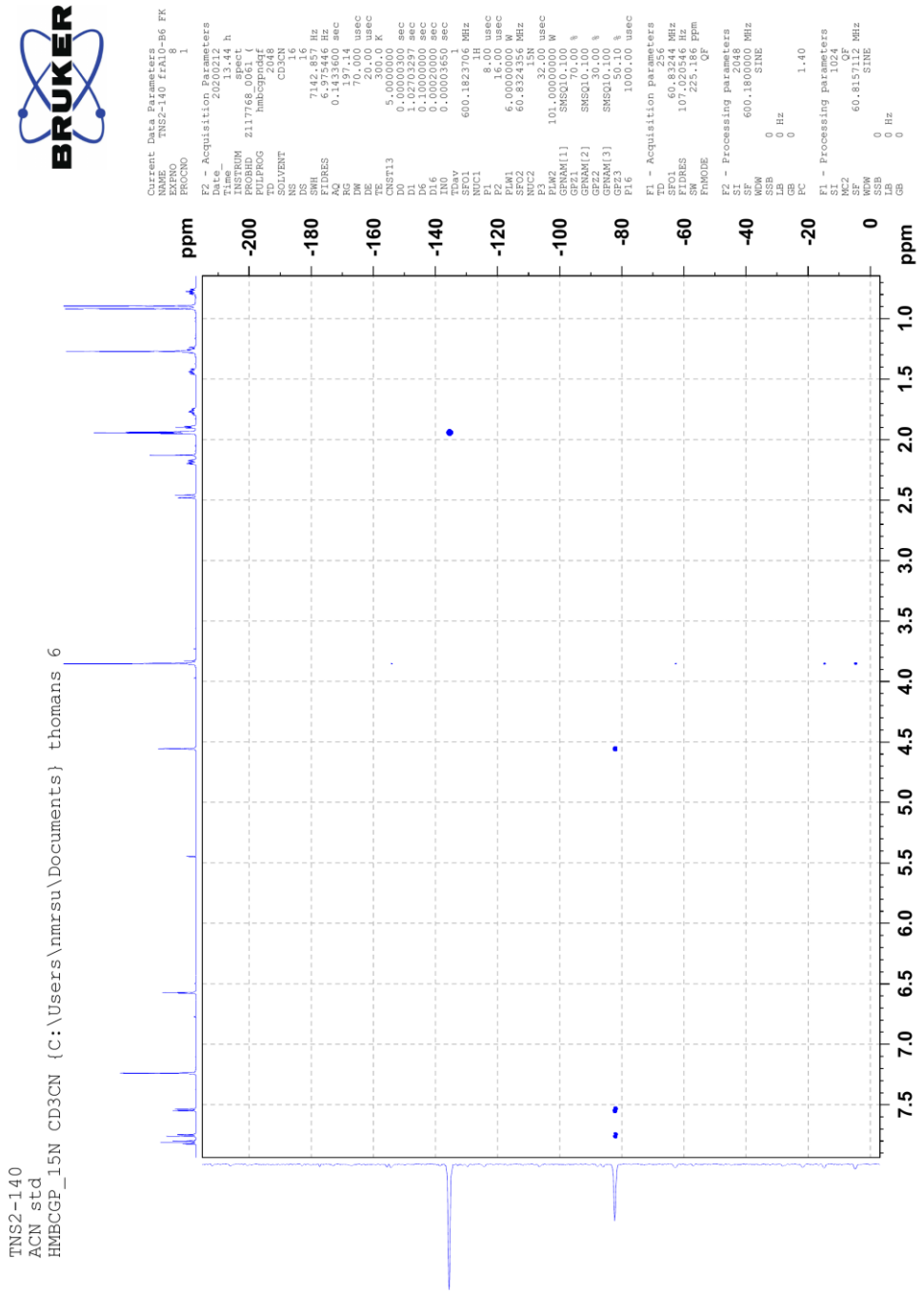

Appendix J.22 **NOESY NMR Spectrum of Pyridine 15e**

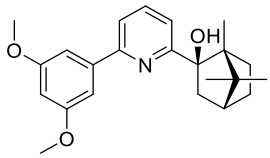

15e

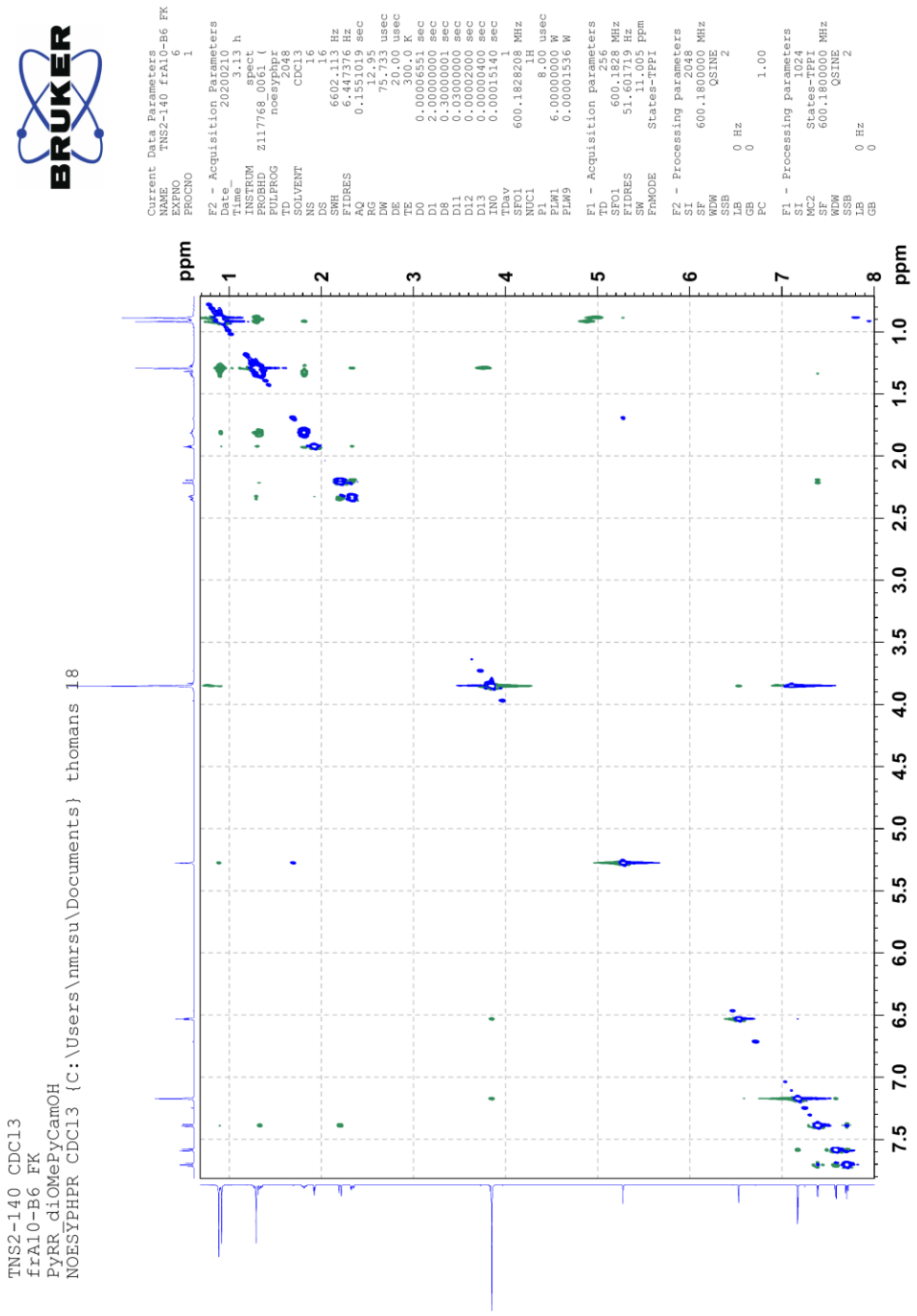

Appendix J Spectra of 2-aryl-6-alkylpyridine Alcohols, 15a-g

Appendix J.23 **HRMS Spectrum of Pyridine 15e**

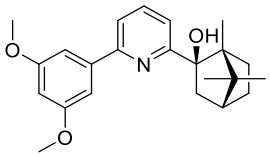

15e

Elemental Composition Report **Page 1**

Single Mass Analysis
Tolerance = 2.0 PPM / DBE: min = -5.0, max = 50.0
Element prediction: Off
Number of isotope peaks used for i-FIT = 3

Monoisotopic Mass, Even Electron Ions
308 formula(e) evaluated with 1 results within limits (all results (up to 1000) for each mass)
Elements Used:
C: 0-100 H: 0-100 N: 0-5 O: 0-10
2020_47 24 (0.482) AM2 (Ar,35000.0,0.00,0.00); Cm (19:24)
1: TOF MS ASAP+

8.16e+005

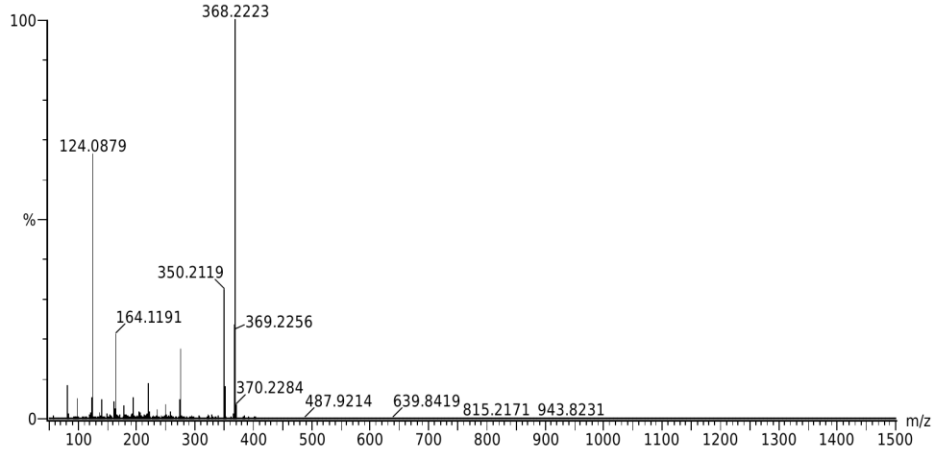

Minimum:				-5.0				
Maximum:		5.0	2.0	50.0				
Mass	Calc. Mass	mDa	PPM	DBE	i-FIT	Norm	Conf(%)	Formula
368.2223	368.2226	-0.3	-0.8	9.5	973.6	n/a	n/a	C23 H30 N O3

Appendix J Spectra of 2-aryl-6-alkylpyridine Alcohols, 15a-g

Appendix J.24 **^{1}H NMR Spectra of Pyridine 15f**

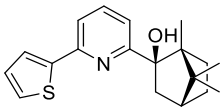

15f

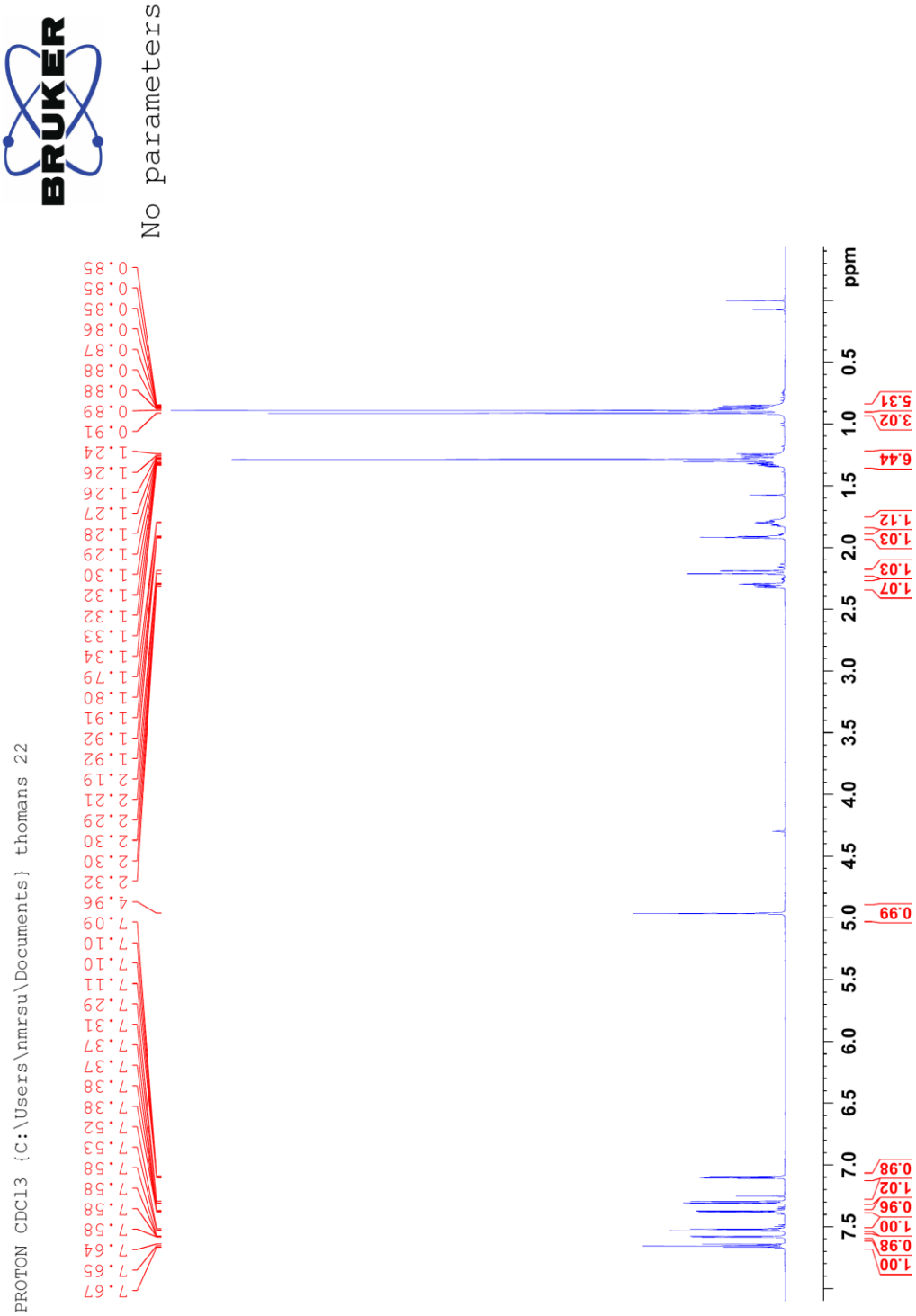

Appendix J Spectra of 2-aryl-6-alkylpyridine Alcohols, 15a-g

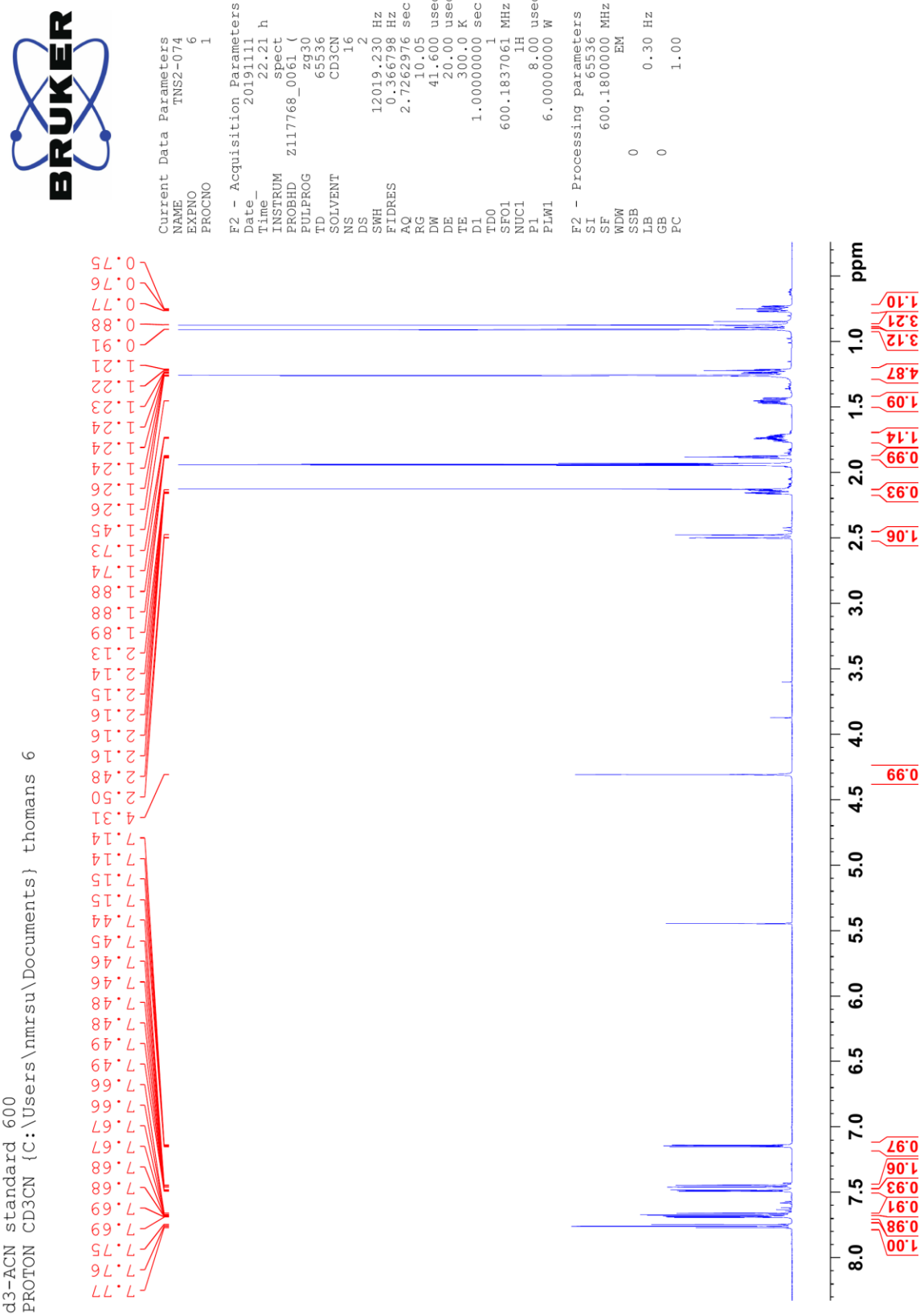

Appendix J Spectra of 2-aryl-6-alkylpyridine Alcohols, 15a-g

Appendix J.25 **^{13}C NMR Spectrum of Pyridine 15f**

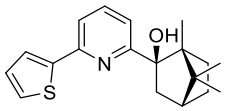

15f

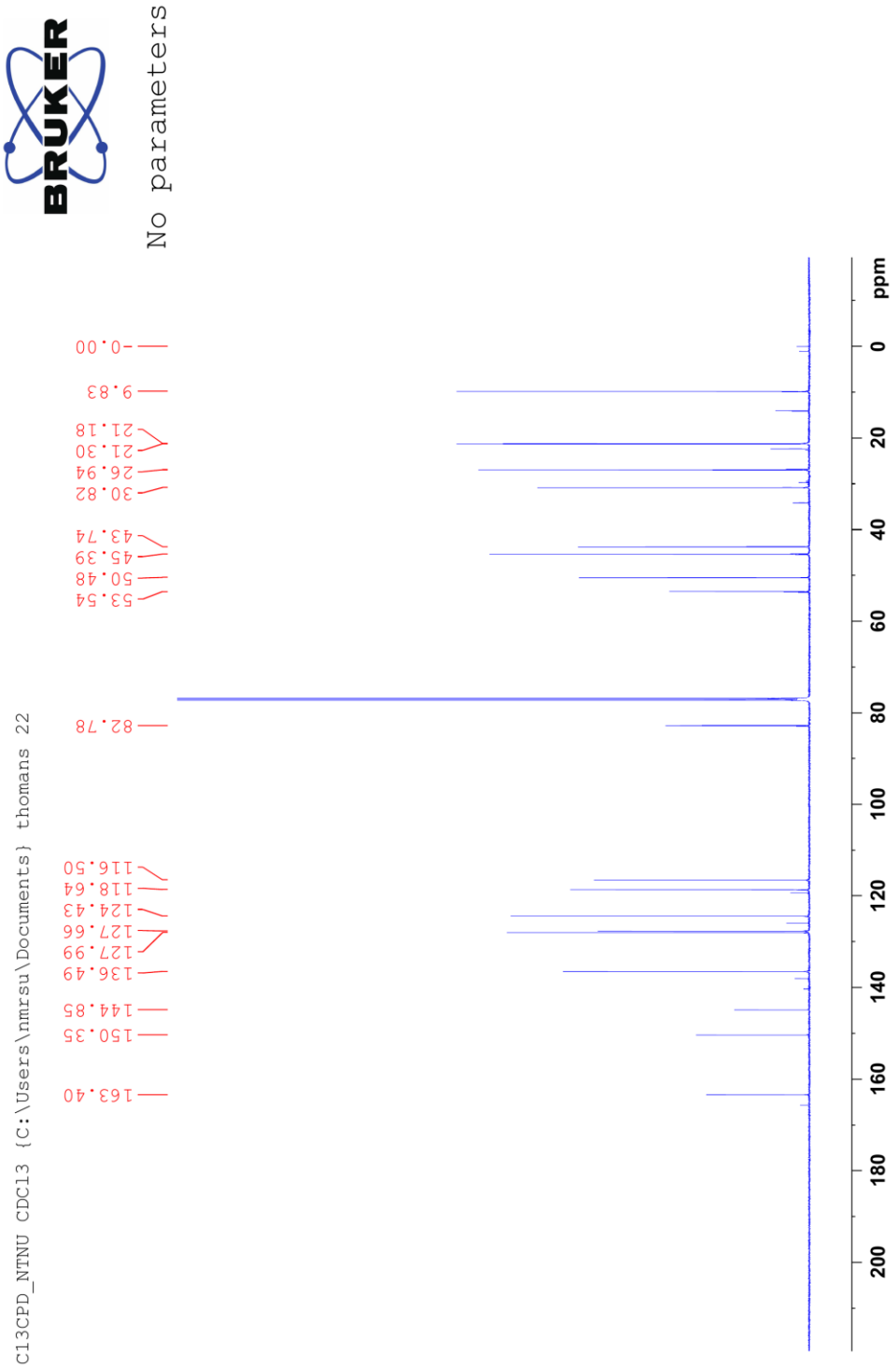

Appendix J Spectra of 2-aryl-6-alkylpyridine Alcohols, 15a-g

Appendix J.26 **COSY NMR Spectrum of Pyridine 15f**

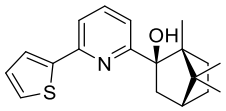

15f

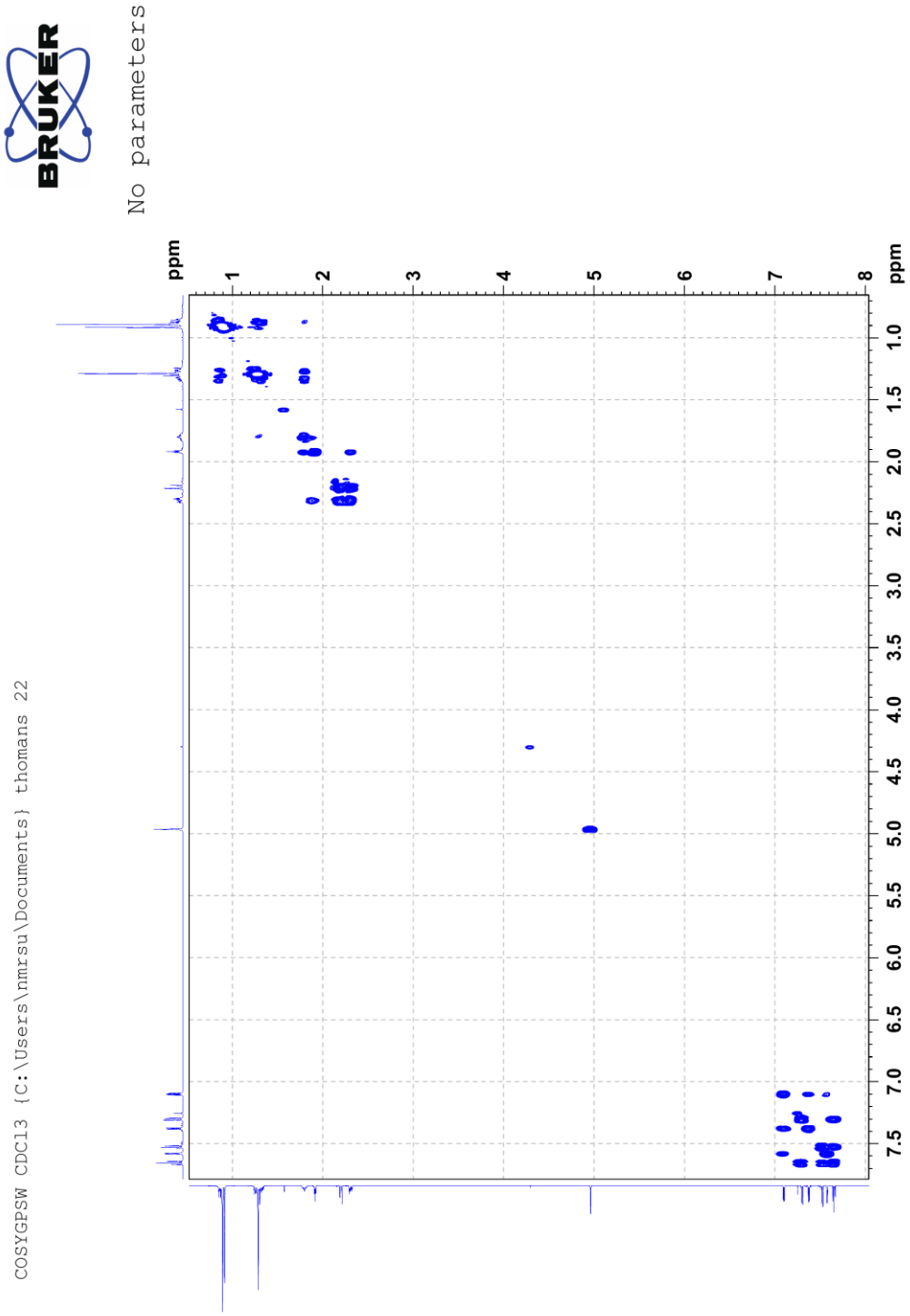

Appendix J Spectra of 2-aryl-6-alkylpyridine Alcohols, 15a-g

Appendix J.27 **HSQC NMR Spectrum of Pyridine 15f**

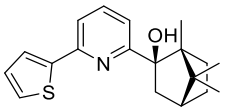

15f

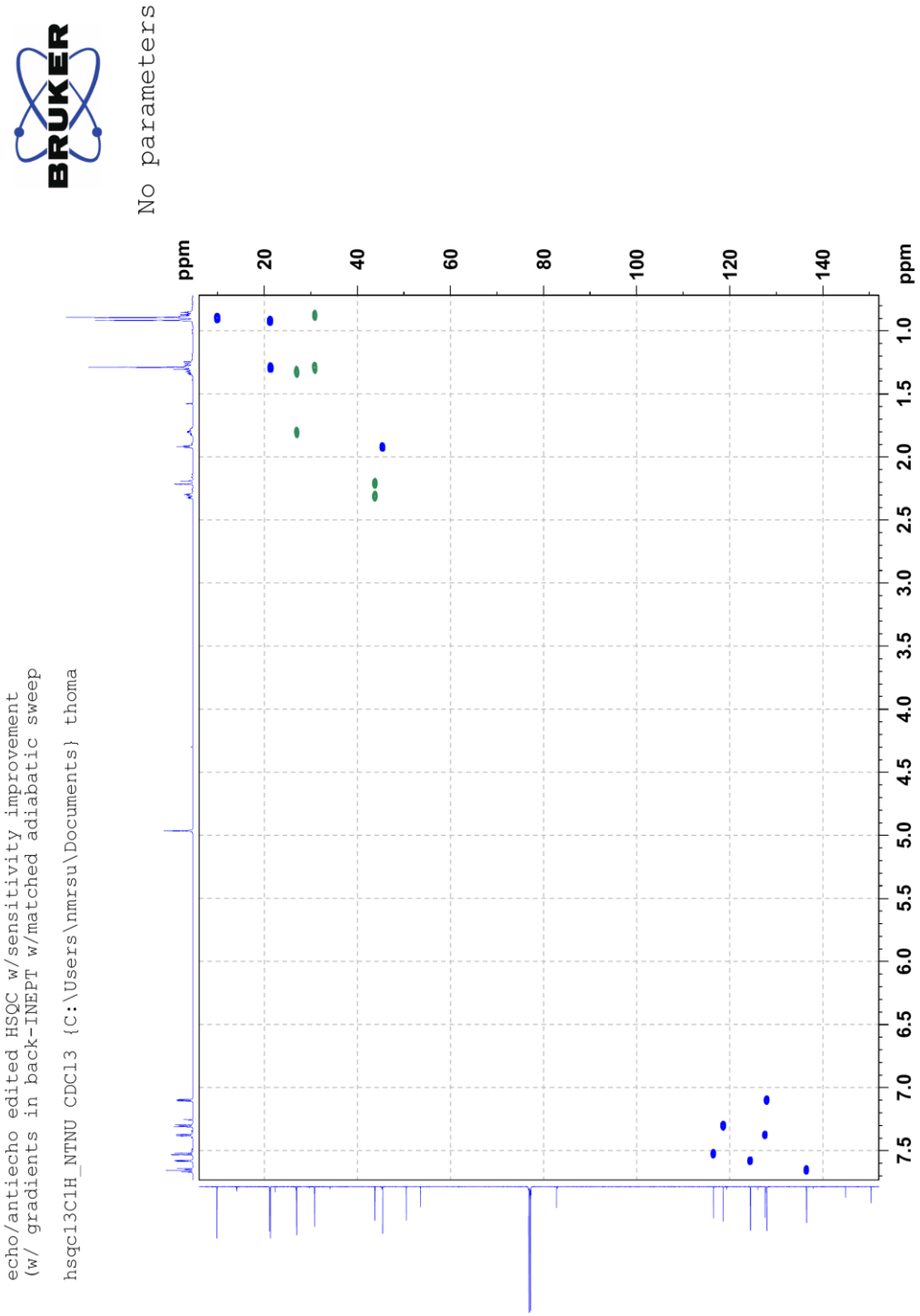

Appendix J Spectra of 2-aryl-6-alkylpyridine Alcohols, 15a-g

Appendix J.28 **$^{1}H,^{13}C$-HMBC NMR Spectrum of Pyridine 15f**

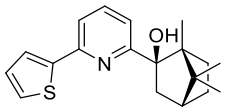

15f

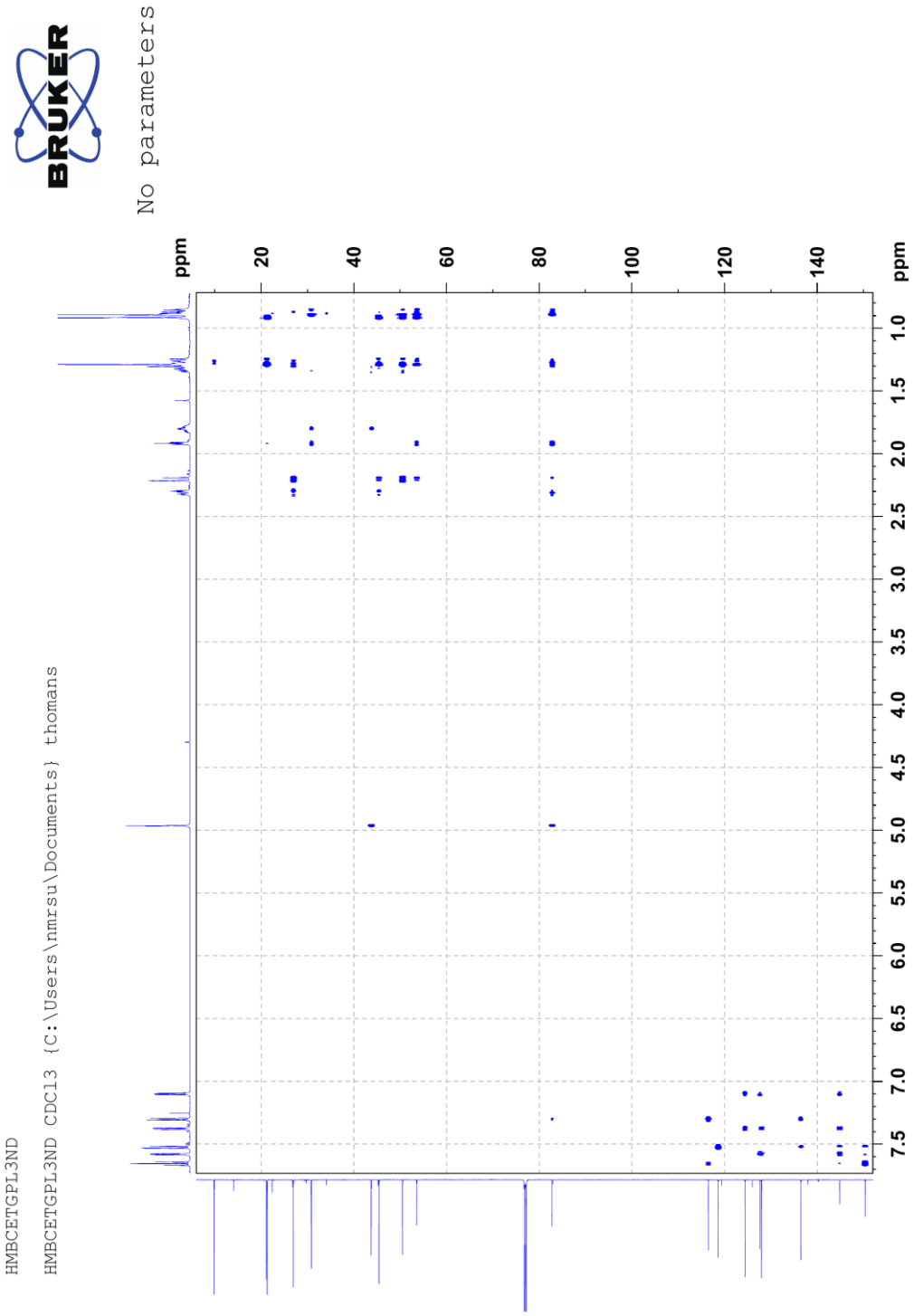

Appendix J Spectra of 2-aryl-6-alkylpyridine Alcohols, 15a-g

Appendix J.29 **HRMS Spectrum of Pyridine 15f**

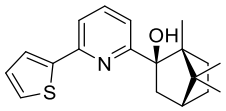

15f

Elemental Composition Report **Page 1**

Single Mass Analysis
Tolerance = 2.0 PPM / DBE: min = -50.0, max = 50.0
Element prediction: Off
Number of isotope peaks used for i-FIT = 3

Monoisotopic Mass, Even Electron Ions
3295 formula(e) evaluated with 3 results within limits (all results (up to 1000) for each mass)
Elements Used:
C: 0-100 H: 0-100 N: 0-10 O: 0-10 S: 0-3
2019-762 24 (0.482) AM2 (Ar,35000.0,0.00,0.00); Cm (24)
1: TOF MS ASAP+

6.42e+006

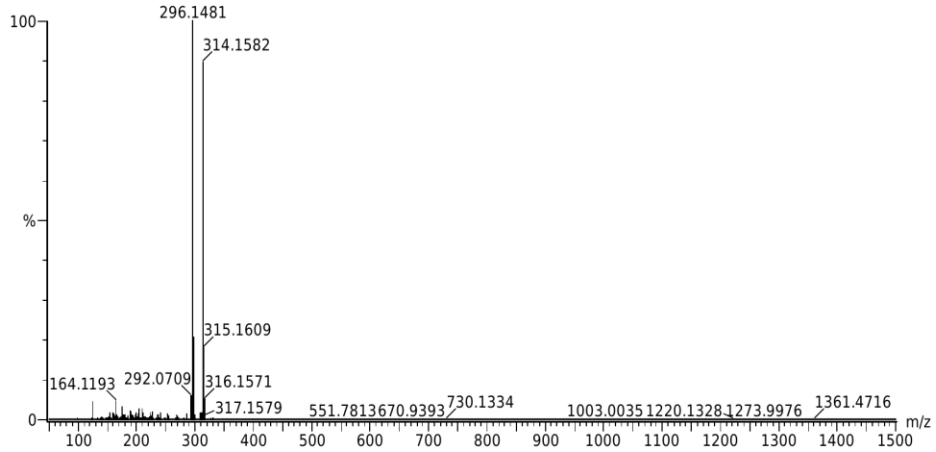

Minimum:				-50.0				
Maximum:		5.0	2.0	50.0				
Mass	Calc. Mass	mDa	PPM	DBE	i-FIT	Norm	Conf(%)	Formula
314.1582	314.1579	0.3	1.0	8.5	1487.6	0.000	100.00	C19 H24 N O S
	314.1579	0.3	1.0	-4.5	1501.9	14.330	0.00	C4 H28 N9 O S3
	314.1577	0.5	1.6	5.5	1501.4	13.812	0.00	C11 H20 N7 O4

Appendix J Spectra of 2-aryl-6-alkylpyridine Alcohols, 15a-g

Appendix J.30 **^{1}H NMR Spectra of Pyridine 15g**

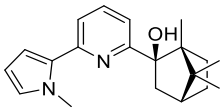

15g

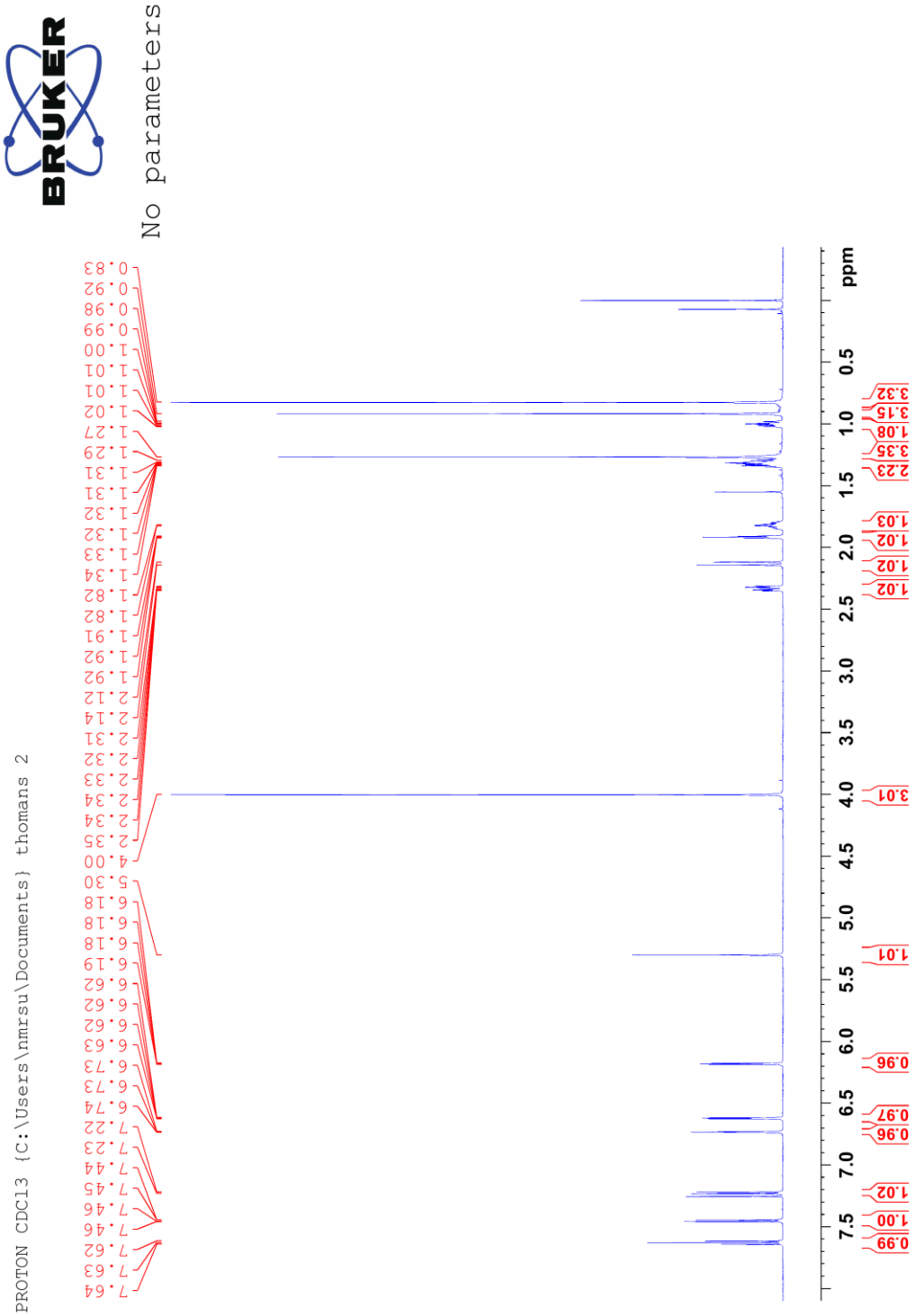

Appendix J Spectra of 2-aryl-6-alkylpyridine Alcohols, 15a-g

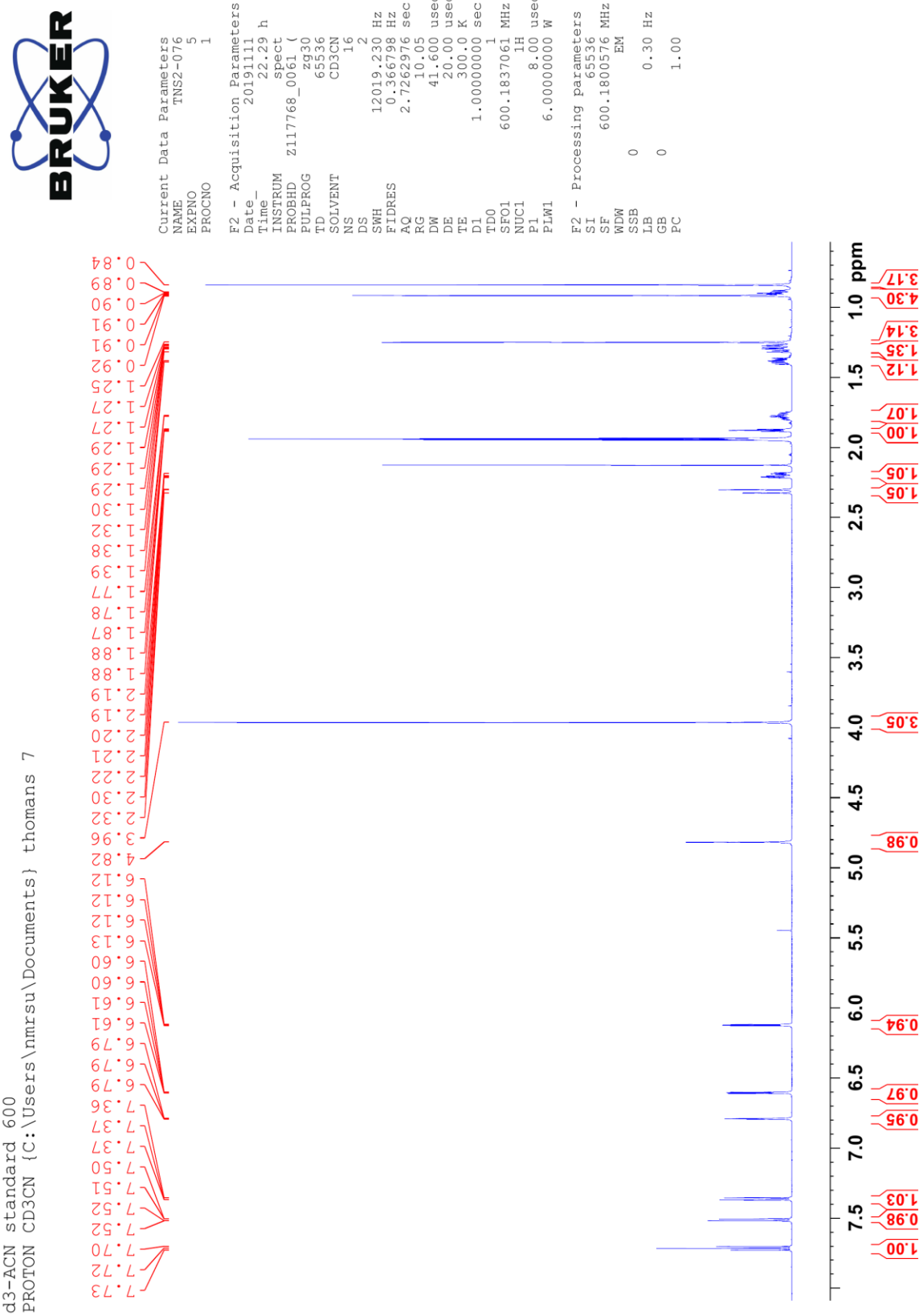

Appendix J Spectra of 2-aryl-6-alkylpyridine Alcohols, 15a-g

Appendix J.31 **^{13}C NMR Spectrum of Pyridine 15g**

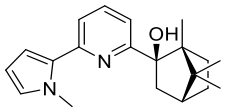

15g

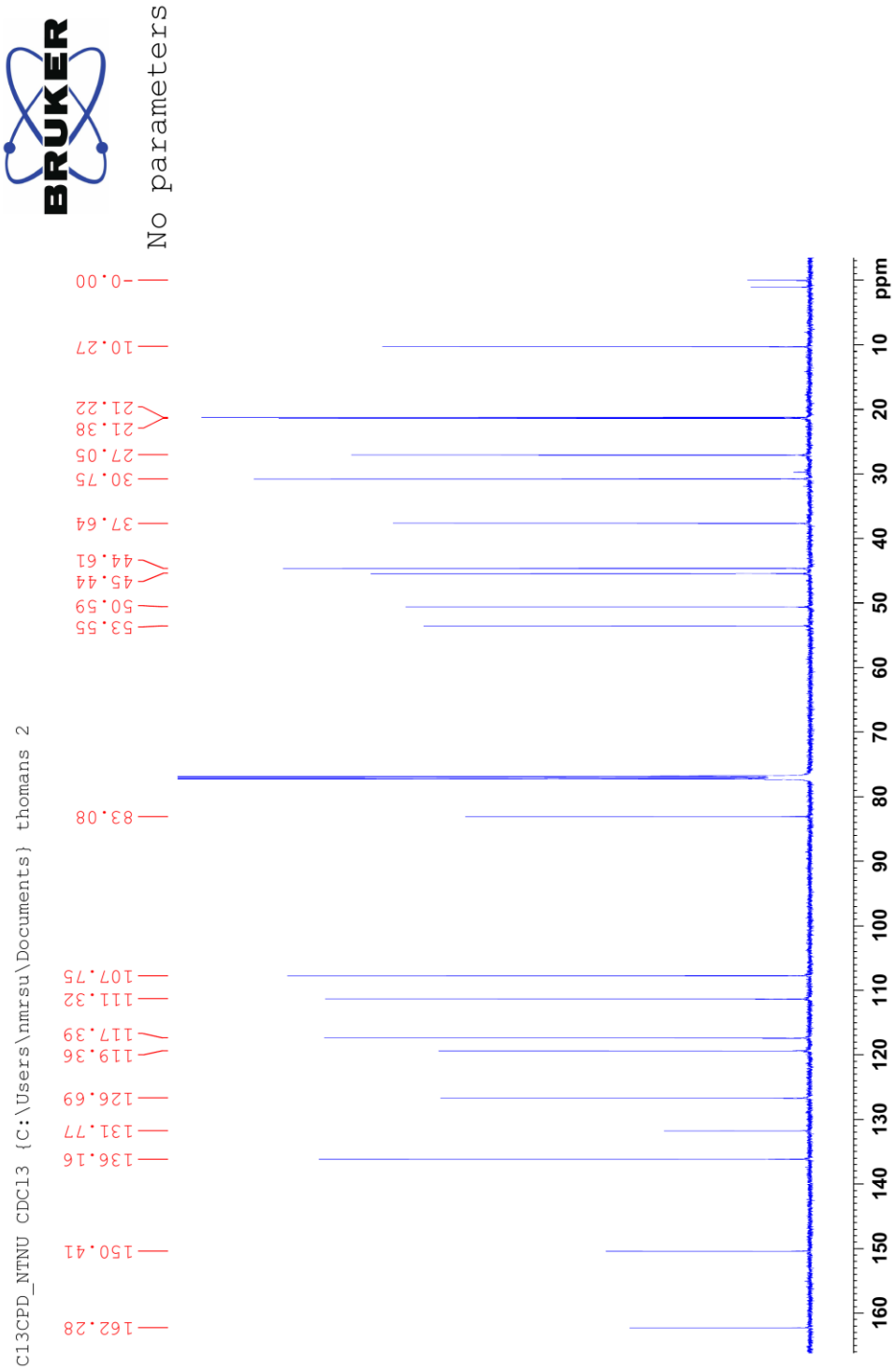

Appendix J Spectra of 2-aryl-6-alkylpyridine Alcohols, 15a-g

Appendix J.32 **COSY NMR Spectrum of Pyridine 15g**

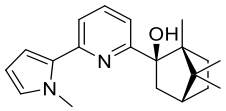

15g

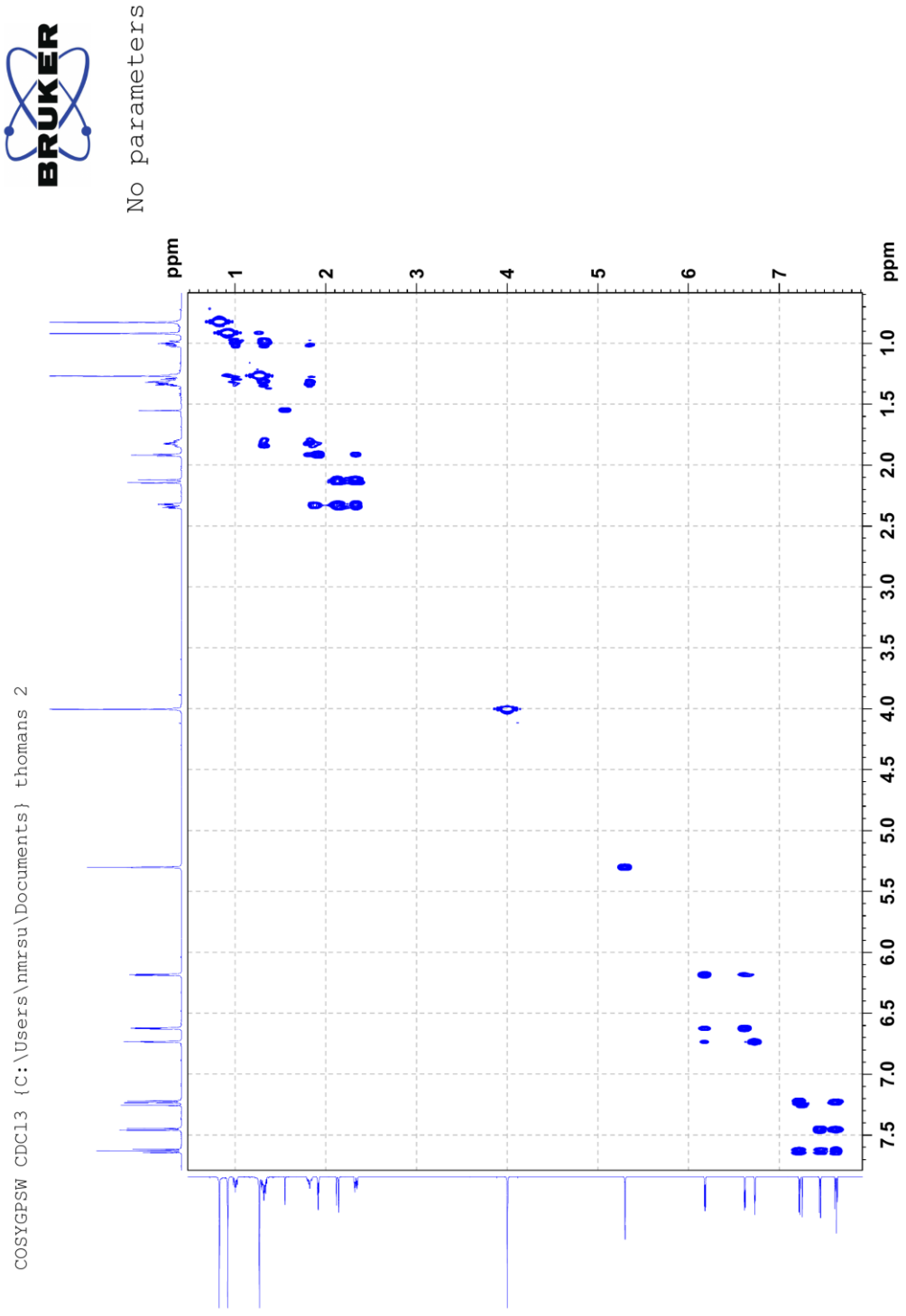

Appendix J Spectra of 2-aryl-6-alkylpyridine Alcohols, 15a-g

Appendix J.33 **HSQC NMR Spectrum of Pyridine 15g**

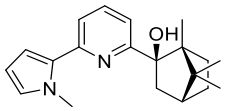

15g

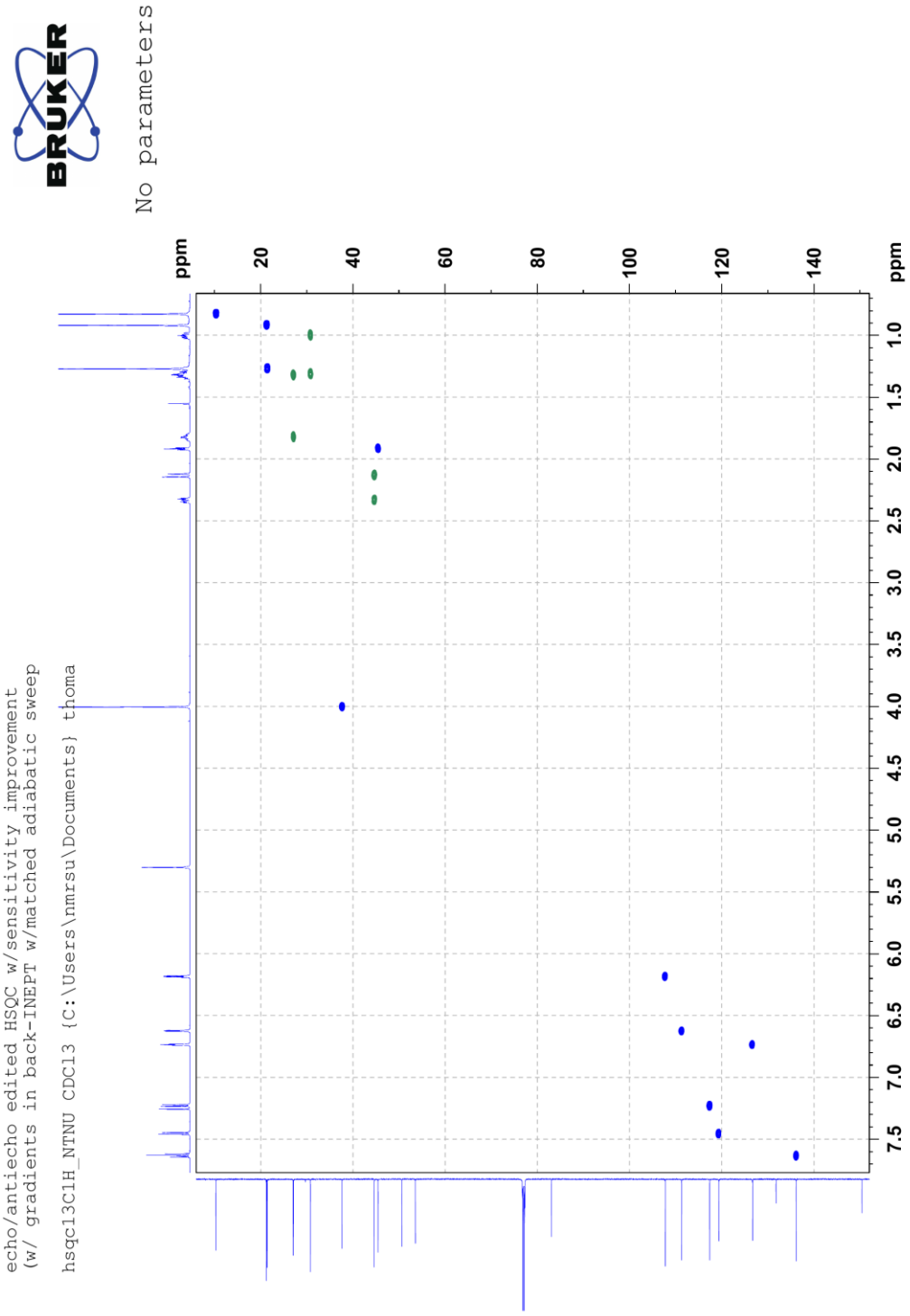

Appendix J Spectra of 2-aryl-6-alkylpyridine Alcohols, 15a-g

Appendix J.34 **$^{1}H,^{13}C$-HMBC NMR Spectrum of Pyridine 15g**

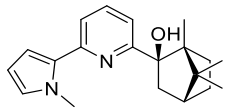

15g

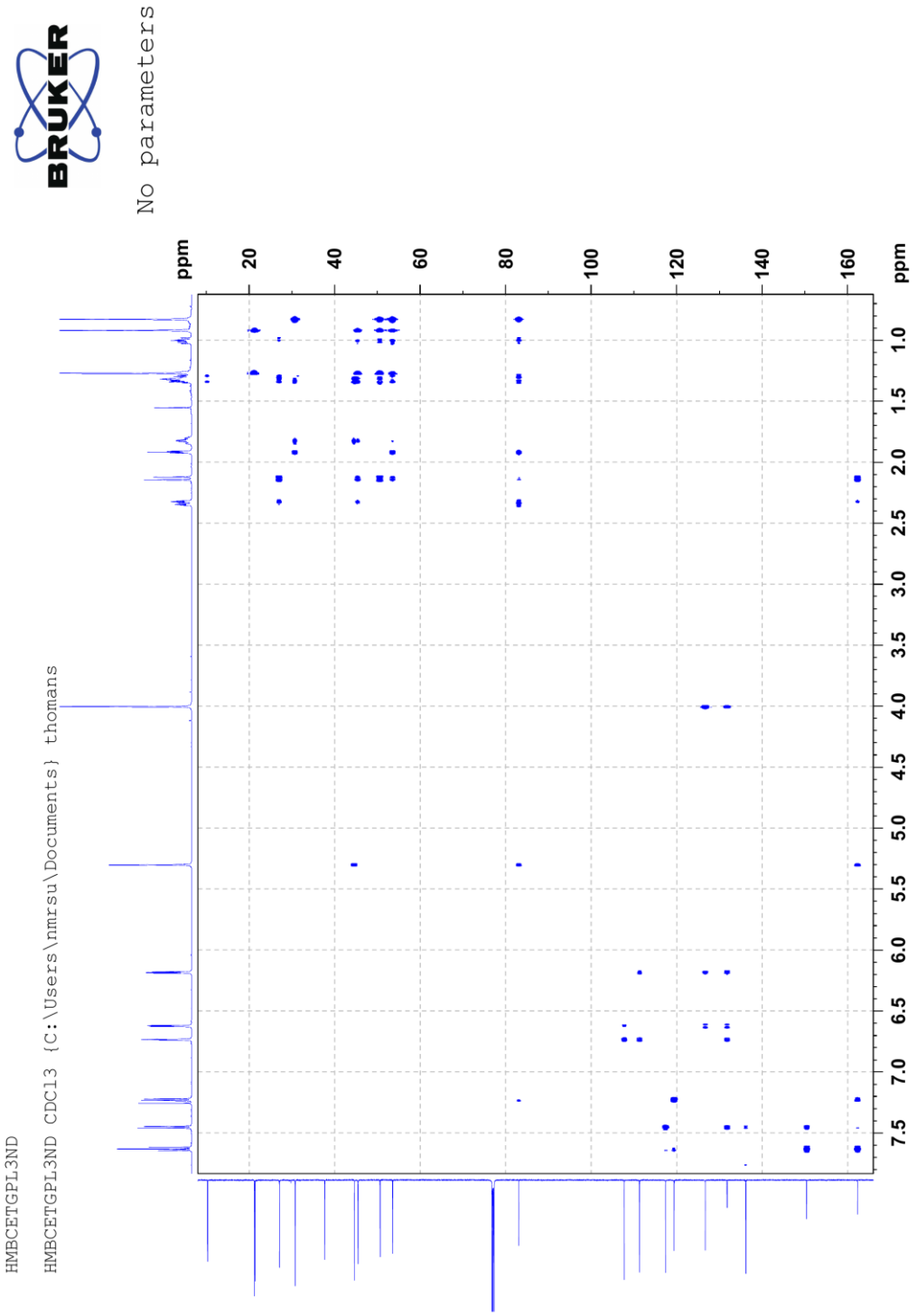

Appendix J Spectra of 2-aryl-6-alkylpyridine Alcohols, 15a-g

Appendix J.35 **HRMS Spectrum of Pyridine 15g**

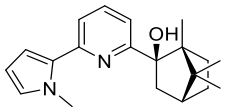

15g

Elemental Composition Report **Page 1**

Single Mass Analysis
Tolerance = 2.0 PPM / DBE: min = -50.0, max = 50.0
Element prediction: Off
Number of isotope peaks used for i-FIT = 3

Monoisotopic Mass, Even Electron Ions
2731 formula(e) evaluated with 3 results within limits (all results (up to 1000) for each mass)
Elements Used:
C: 0-100 H: 0-100 N: 0-10 O: 0-10 Si: 0-2
2019-760 16 (0.327) AM2 (Ar,35000.0,0.00,0.00); Cm (16)
1: TOF MS ASAP+

3.52e+005

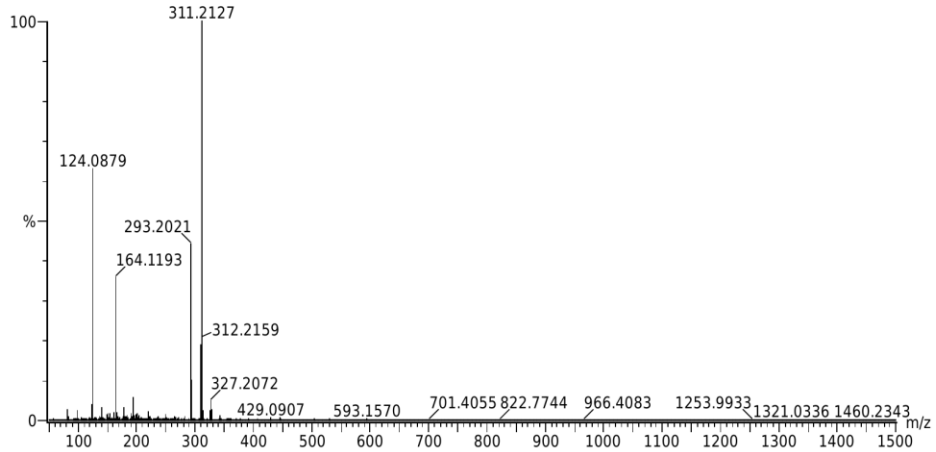

Minimum:				-50.0				
Maximum:		5.0	2.0	50.0				
Mass	Calc. Mass	mDa	PPM	DBE	i-FIT	Norm	Conf(%)	Formula
311.2127	311.2128	-0.1	-0.3	4.5	1139.4	14.789	0.00	C12 H27 N8 Si
	311.2123	0.4	1.3	8.5	1124.6	0.000	100.00	C20 H27 N2 O
	311.2133	-0.6	-1.9	-10.5	1142.8	18.202	0.00	C6 H39 O9 Si2

Appendix J Spectra of 2-aryl-6-alkylpyridine Alcohols, 15a-g

Appendix J.36 **^{1}H NMR Spectra of Pyridine 15h**

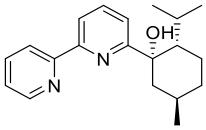

15h

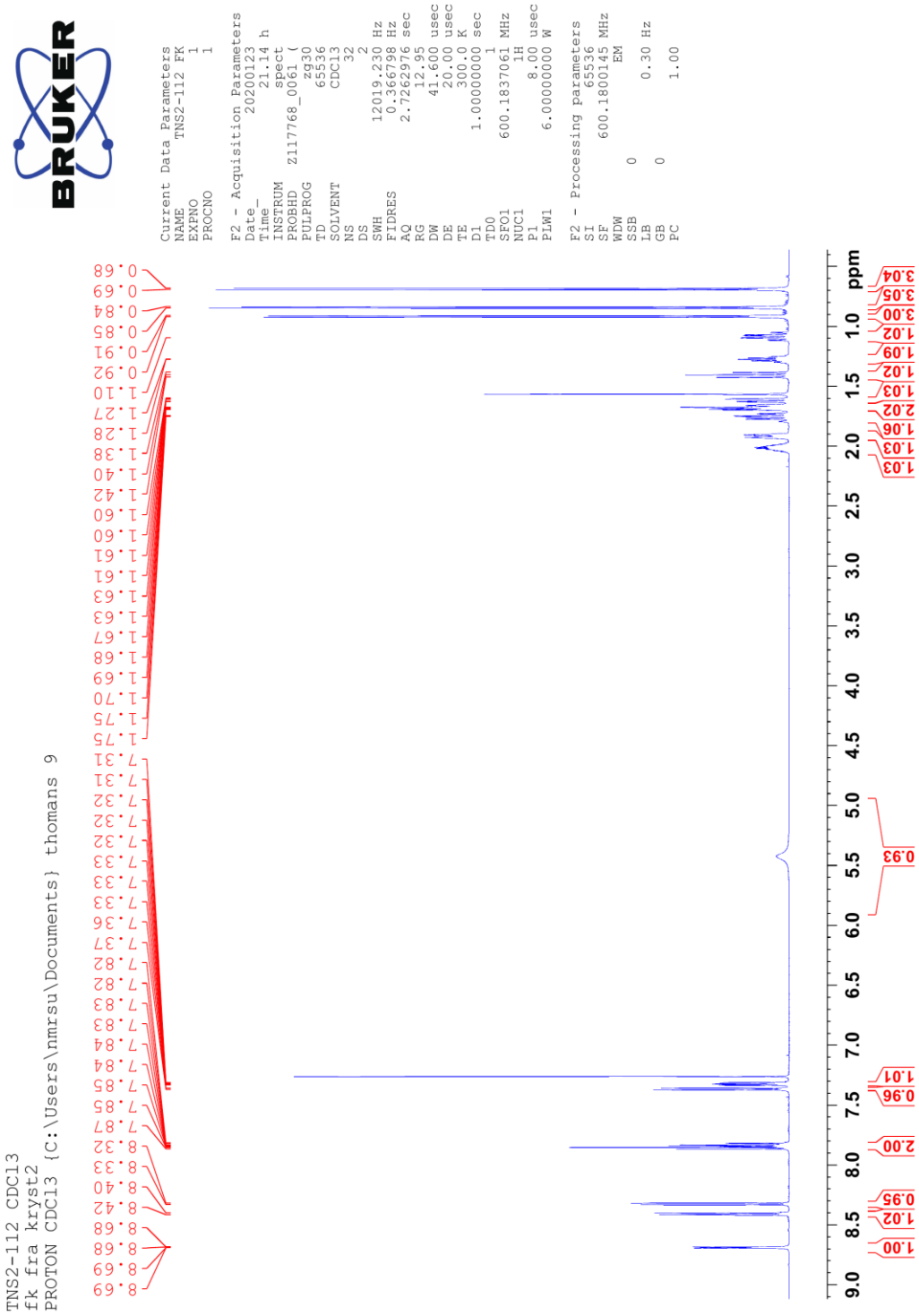

Appendix J Spectra of 2-aryl-6-alkylpyridine Alcohols, 15a-g

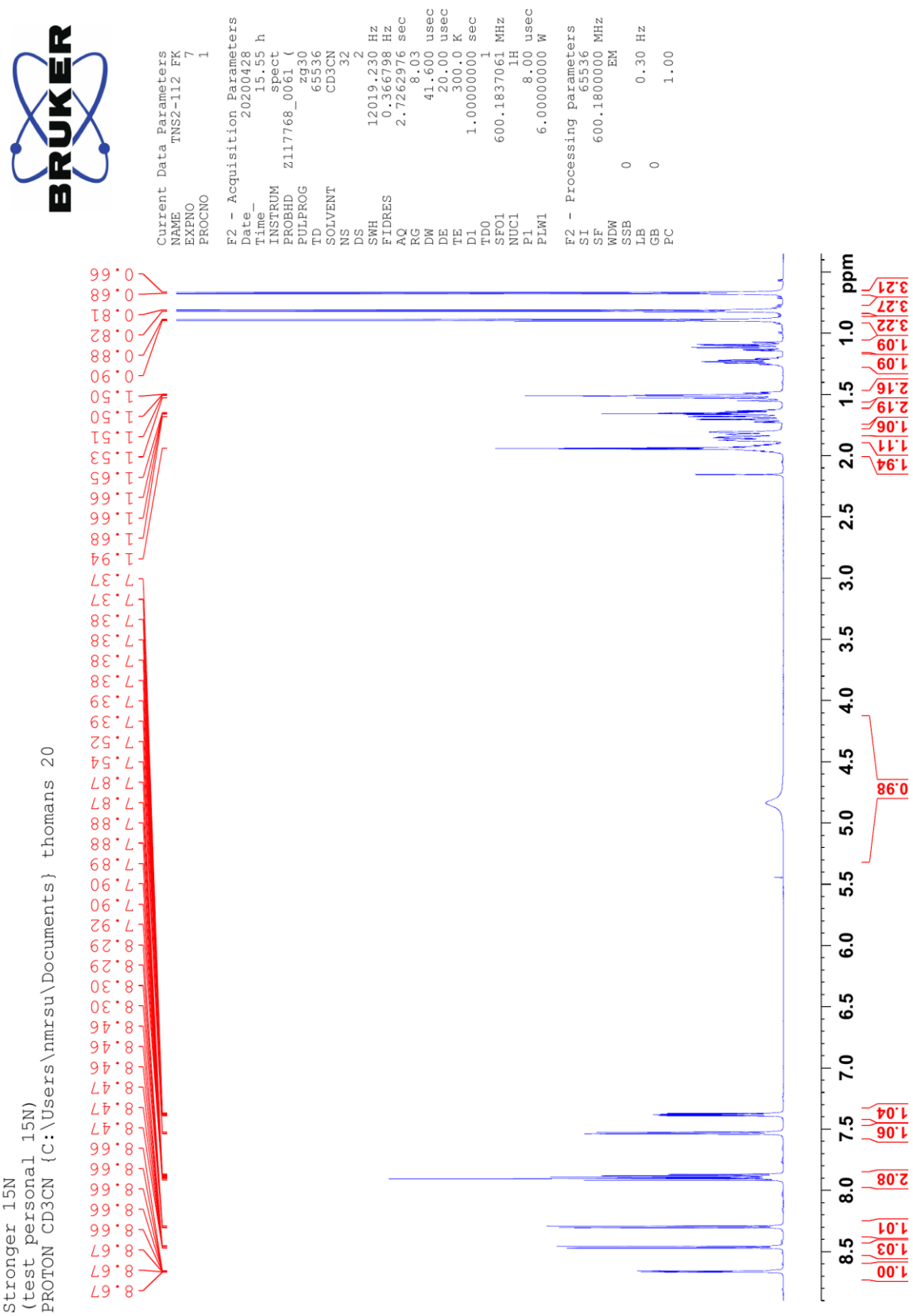

Appendix J Spectra of 2-aryl-6-alkylpyridine Alcohols, 15a-g

Appendix J.37 **$^{1}H,^{15}N$-HMBC NMR Spectrum of Pyridine 15h**

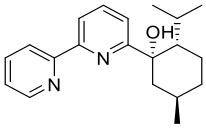

15h

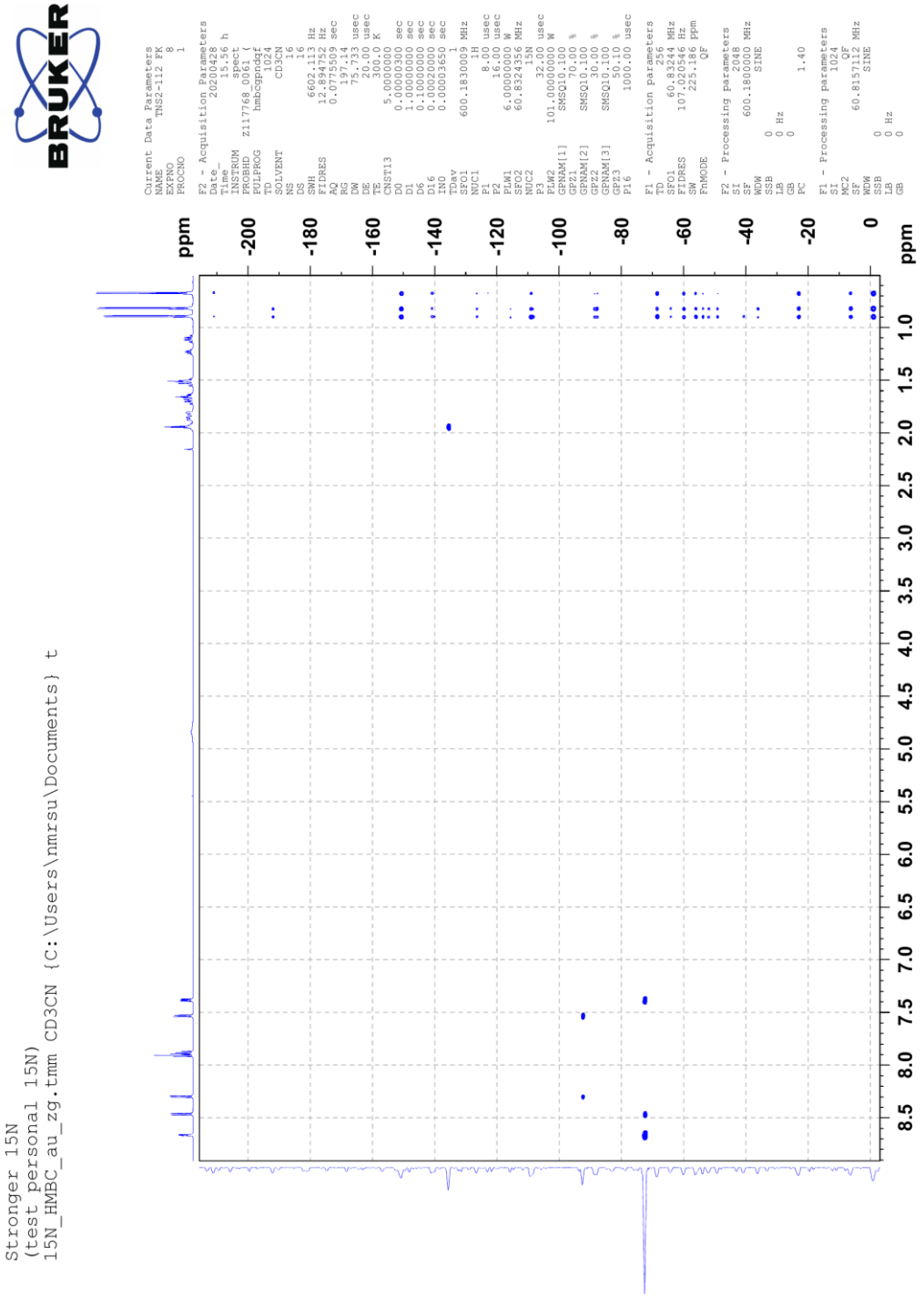

Appendix J.38 **IR Spectrum of Pyridine 15h**

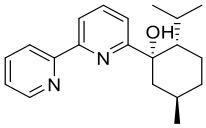

15h

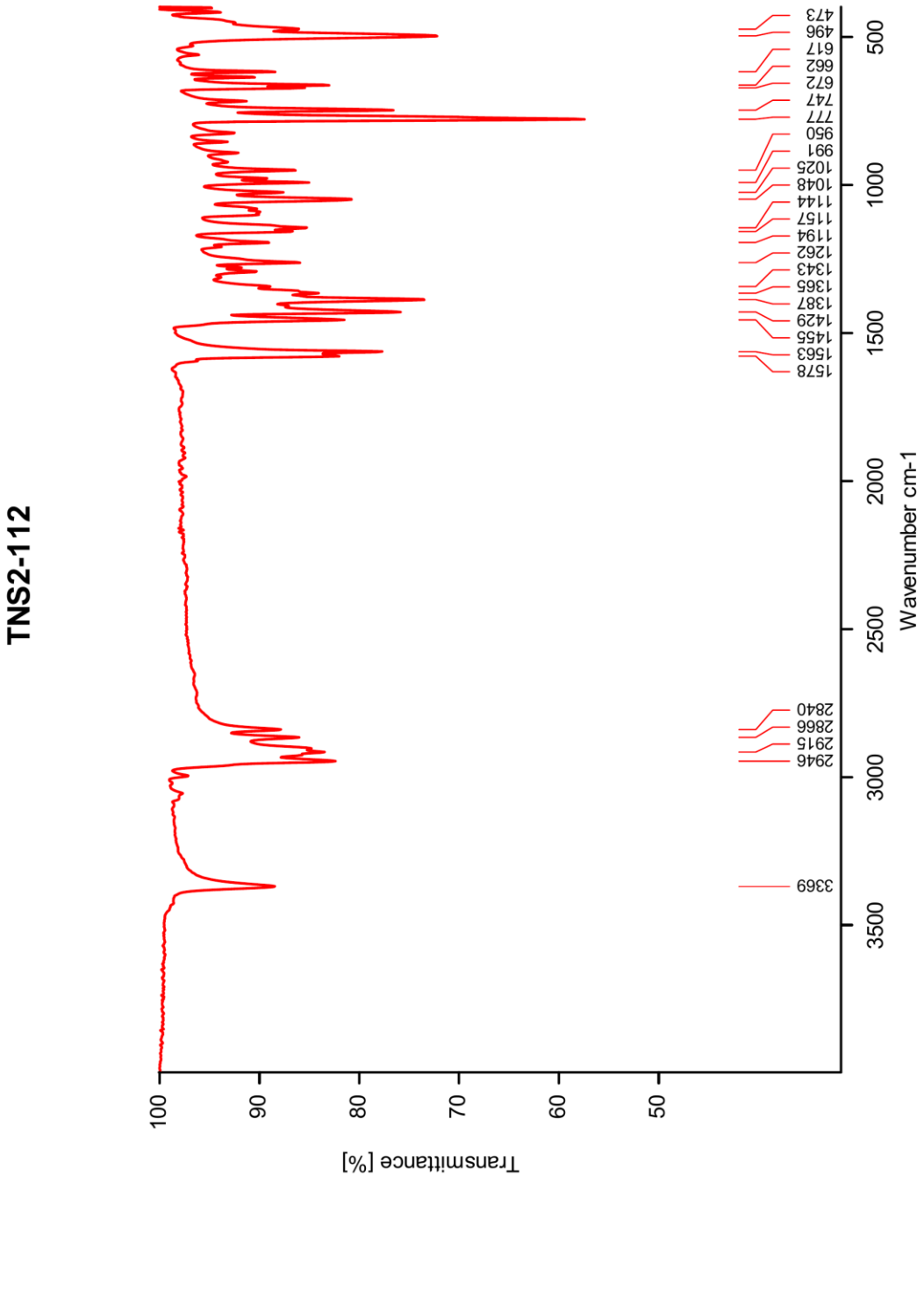

Appendix K **Spectra of 2,6-disubstituted Pyridine Methyl Ethers, 12-OMe and 15-OMe**

Appendix K.1 **^{1}H NMR Spectrum of Pyridine Methyl Ether 12b-OMe**

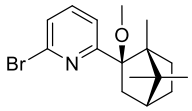

12b-OMe

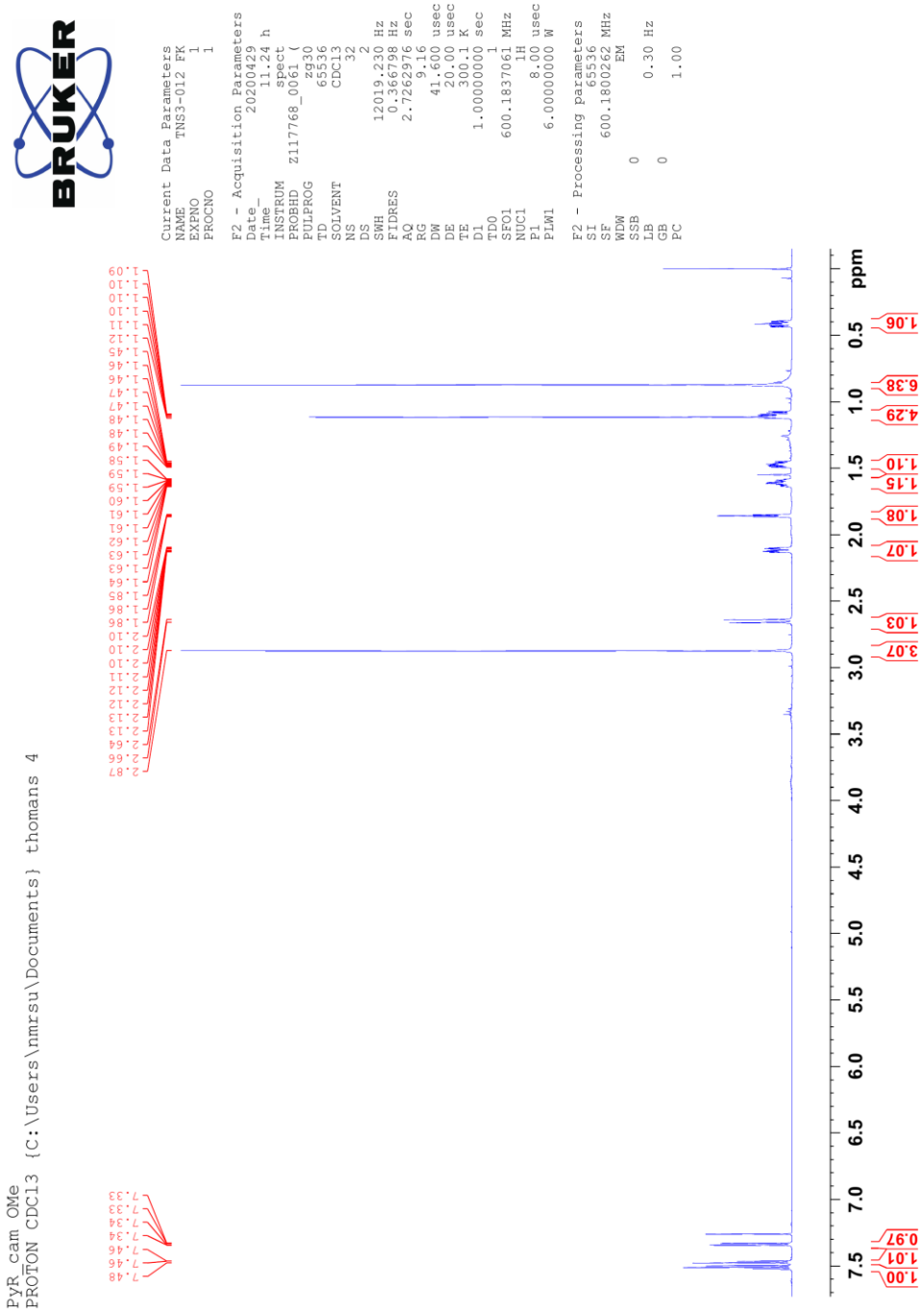

Appendix K.2 **^{13}C NMR Spectrum of Pyridine Methyl Ether 12b-OMe**

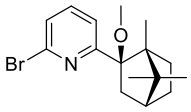

12b-OMe

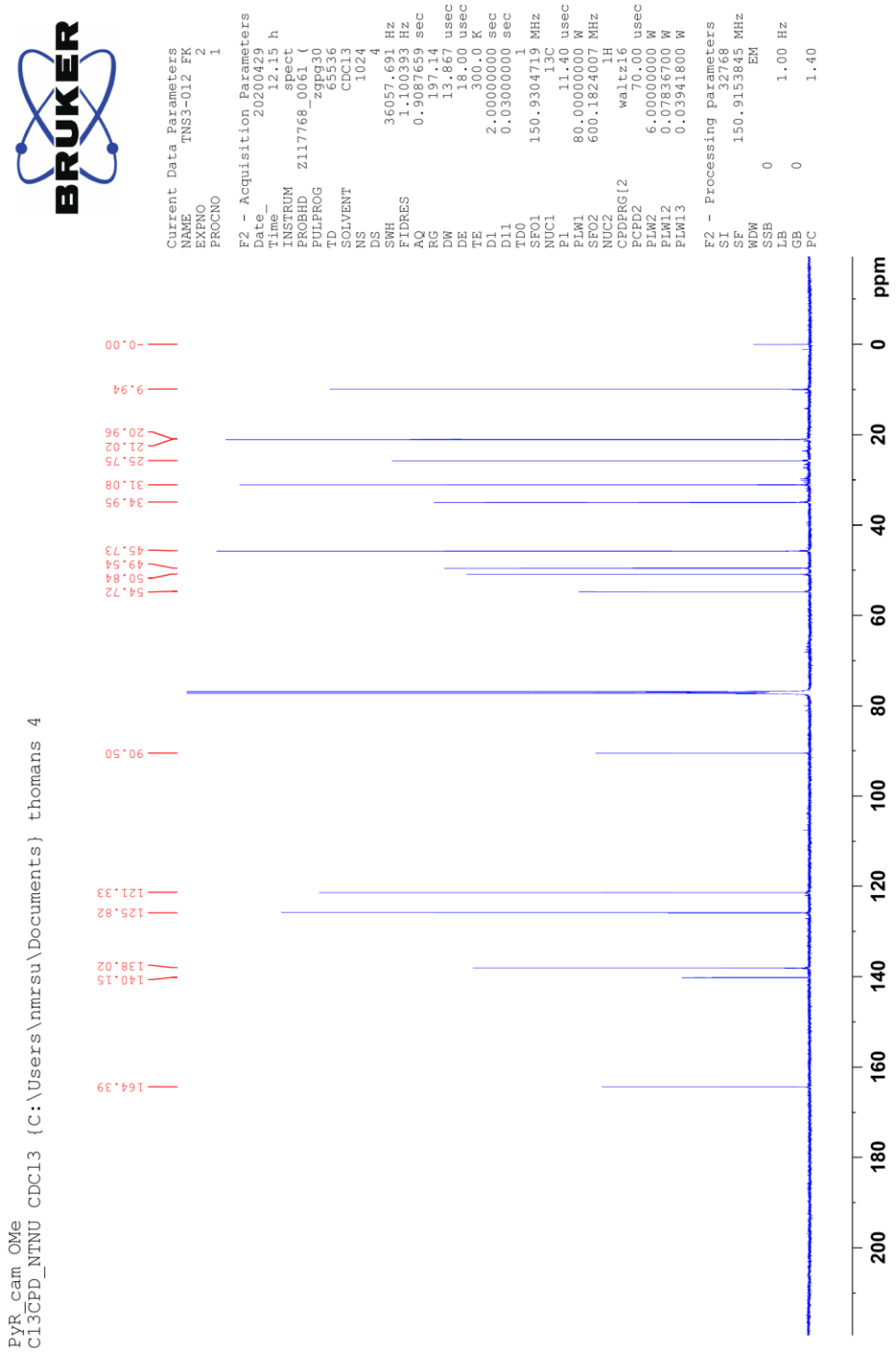

Appendix K.3 **COSY NMR Spectrum of Pyridine Methyl Ether 12b-OMe**

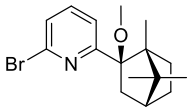

12b-OMe

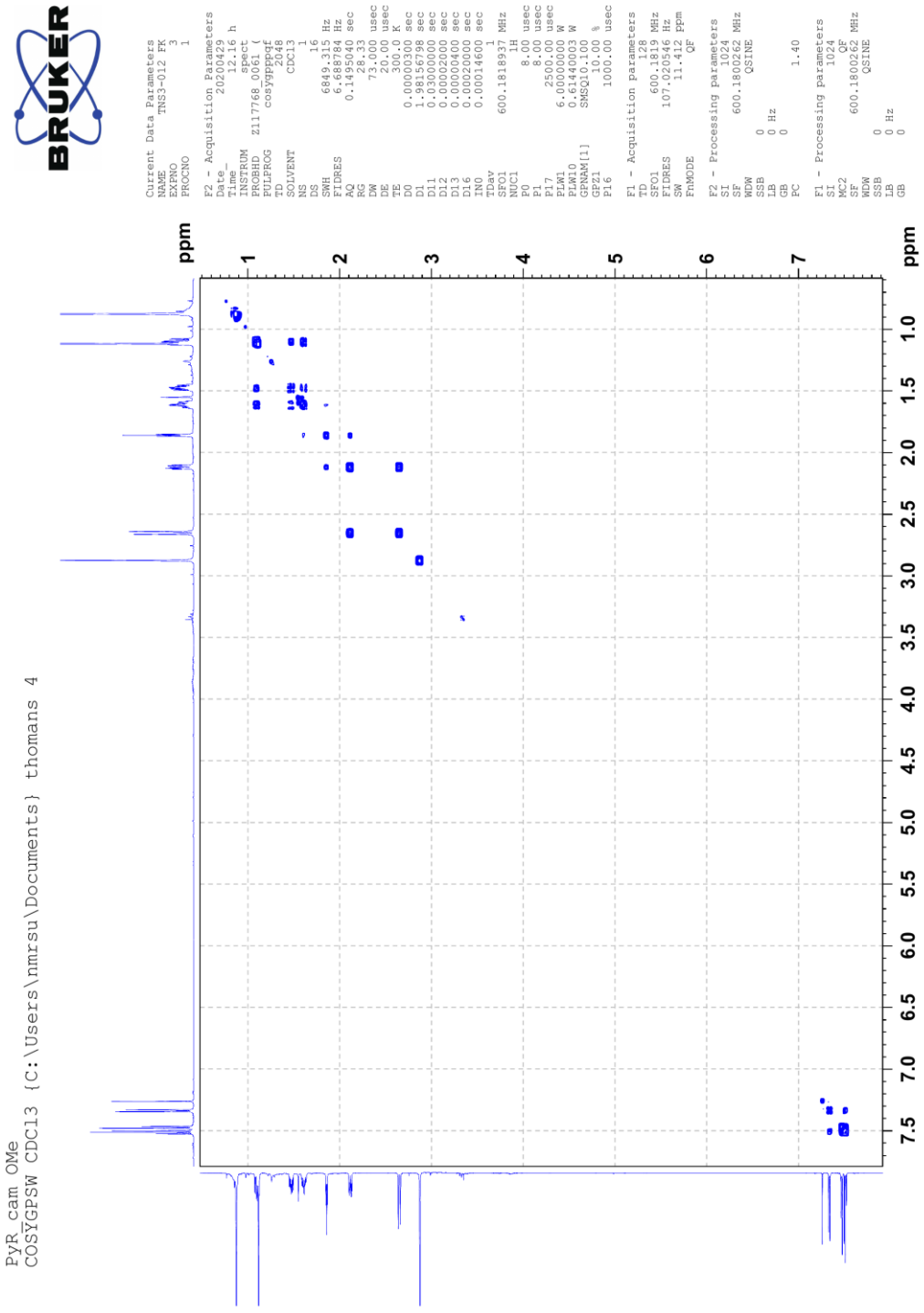

Appendix K.4 **HSQC NMR Spectrum of Pyridine Methyl Ether 12b-OMe**

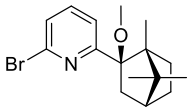

12b-OMe

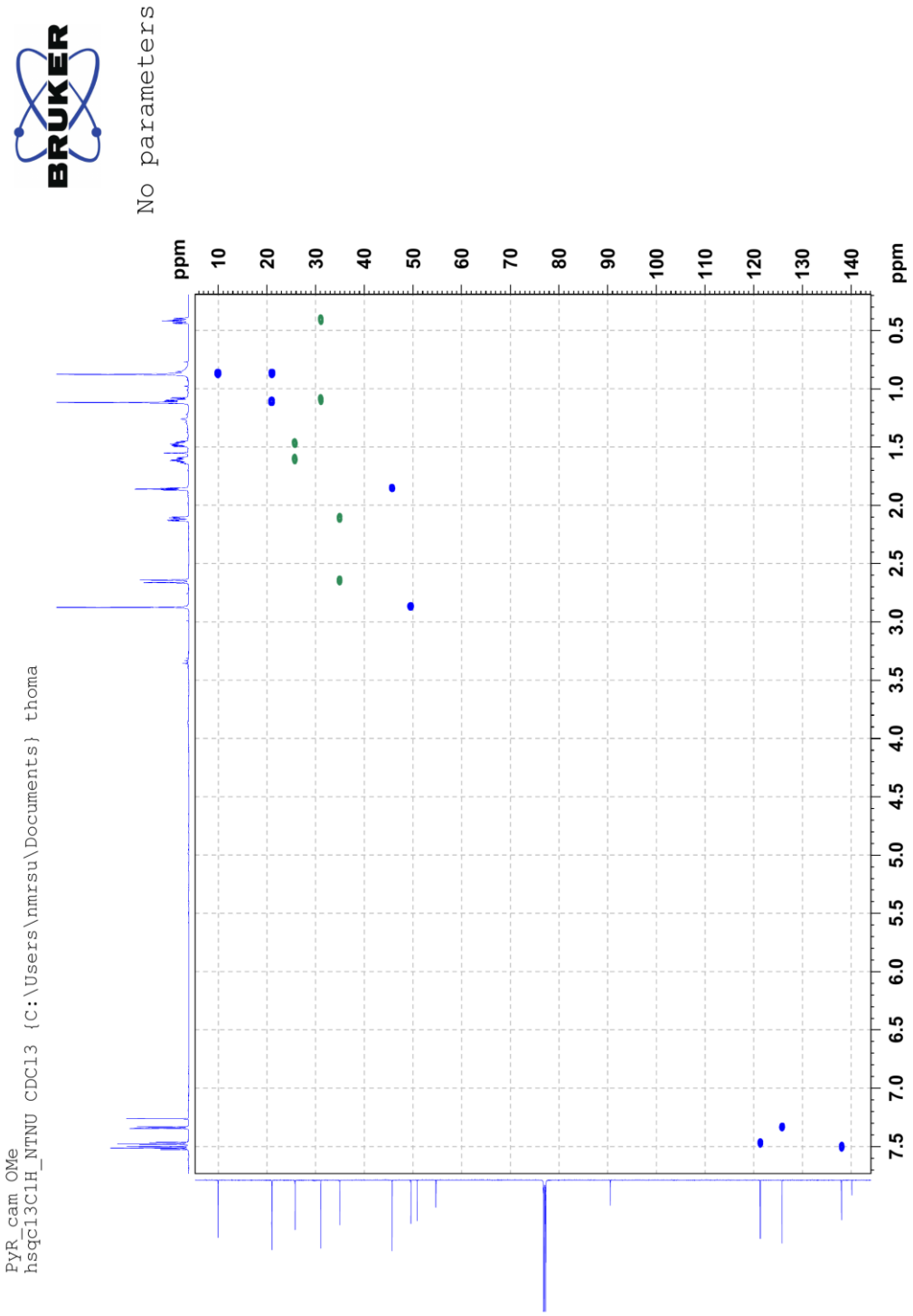

Appendix K.5 **^{1}H,^{13}C-HMBC NMR Spectrum of Pyridine Methyl Ether 12b-OMe**

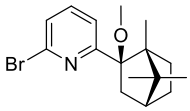

12b-OMe

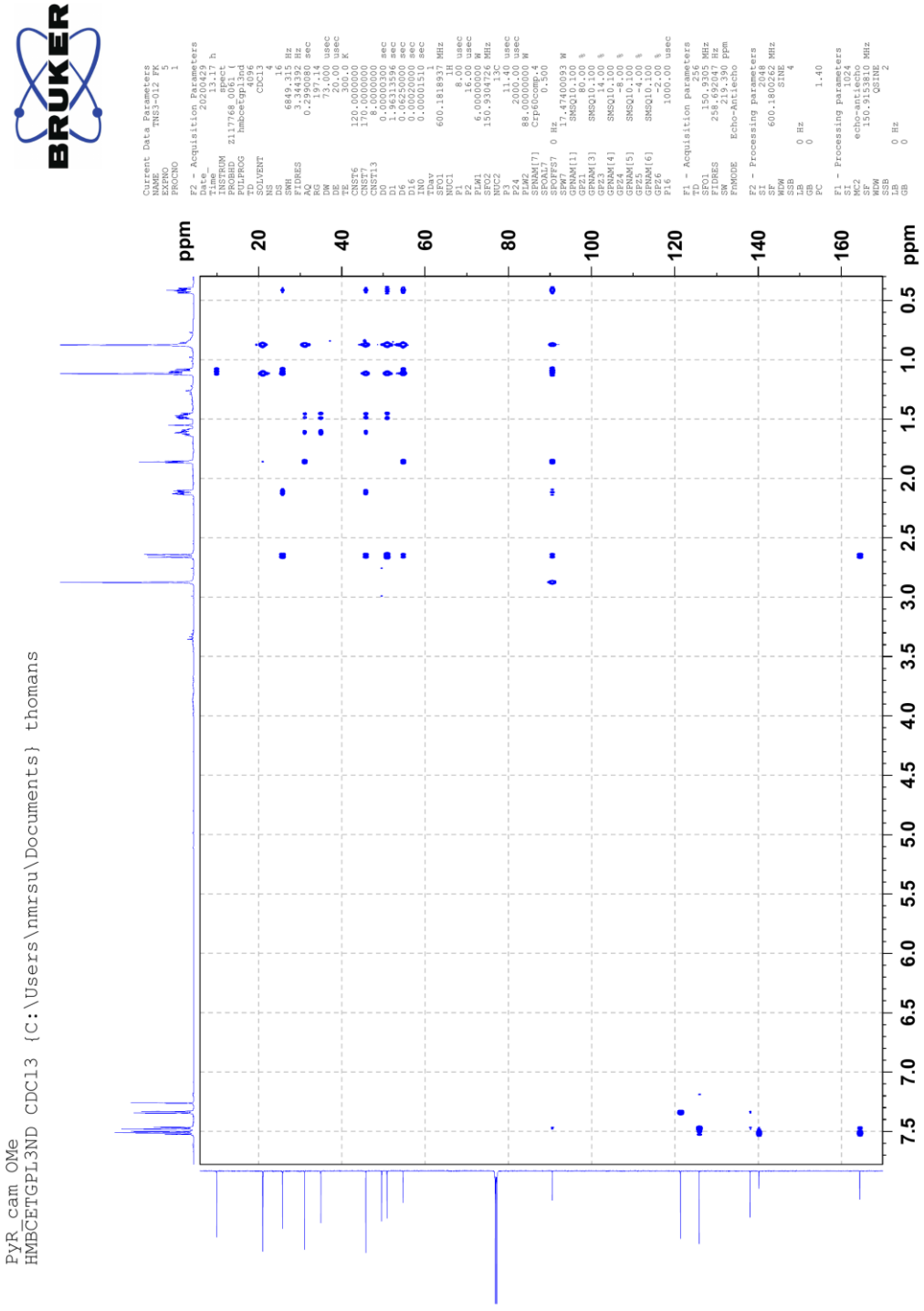

Appendix K.6 **NOESY NMR Spectrum of Pyridine Methyl Ether 12b-OMe**

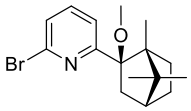

12b-OMe

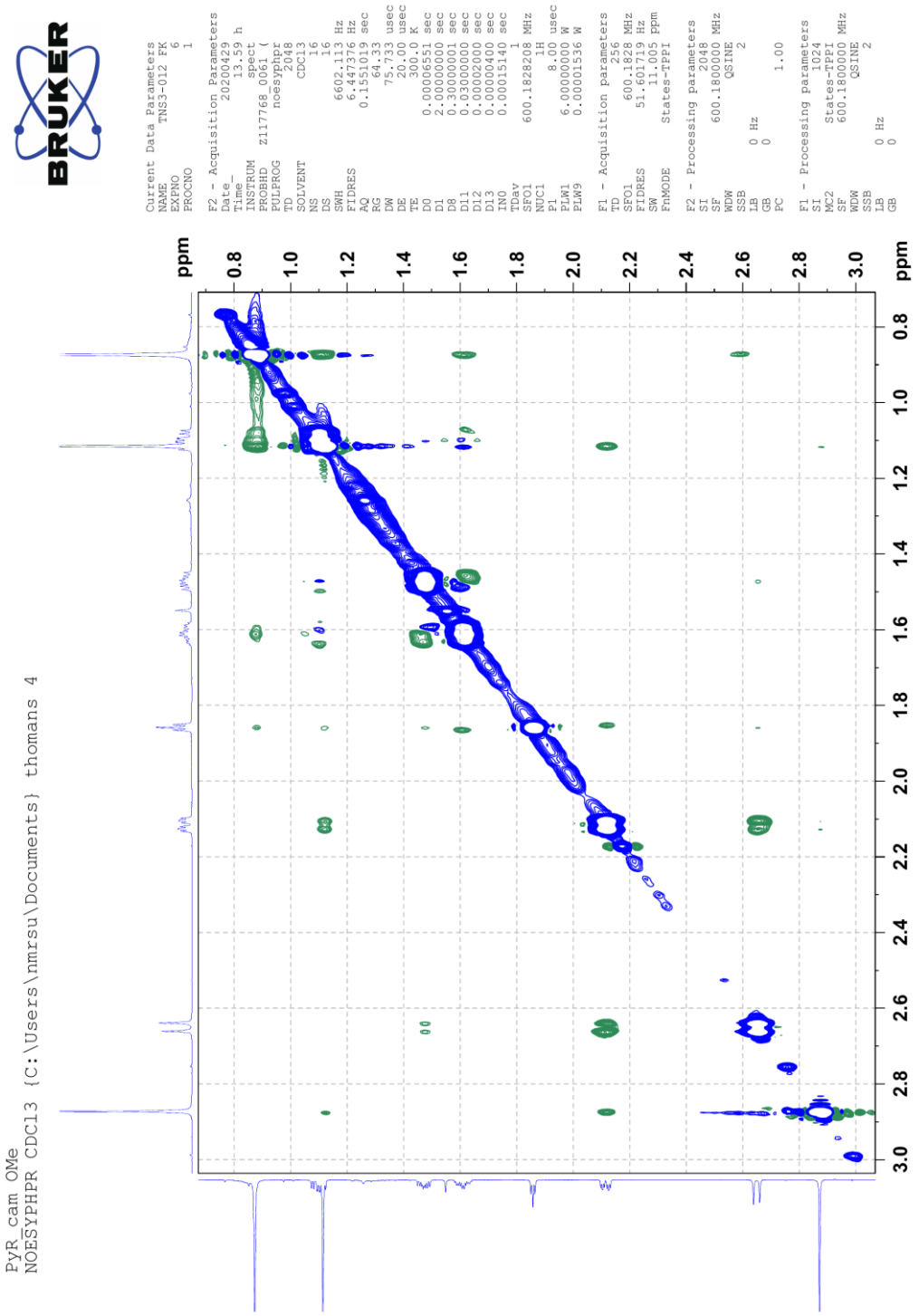

Appendix K.7 **HRMS Spectrum of Pyridine Methyl Ether 12b-OMe**

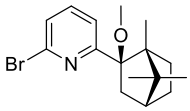

12b-OMe

Elemental Composition Report **Page 1**

Single Mass Analysis
Tolerance = 5.0 PPM / DBE: min = -5.0, max = 50.0
Element prediction: Off
Number of isotope peaks used for i-FIT = 3

Monoisotopic Mass, Even Electron Ions
346 formula(e) evaluated with 1 results within limits (all results (up to 1000) for each mass)
Elements Used:
C: 0-100 H: 0-100 N: 0-5 O: 0-5 Br: 0-2

JA_SVG_20200508_116rean 70 (1.299) AM2 (Ar,35000.0,0.00,0.00); Cm (70:74)
1: TOF MS ES+

1.05e+006

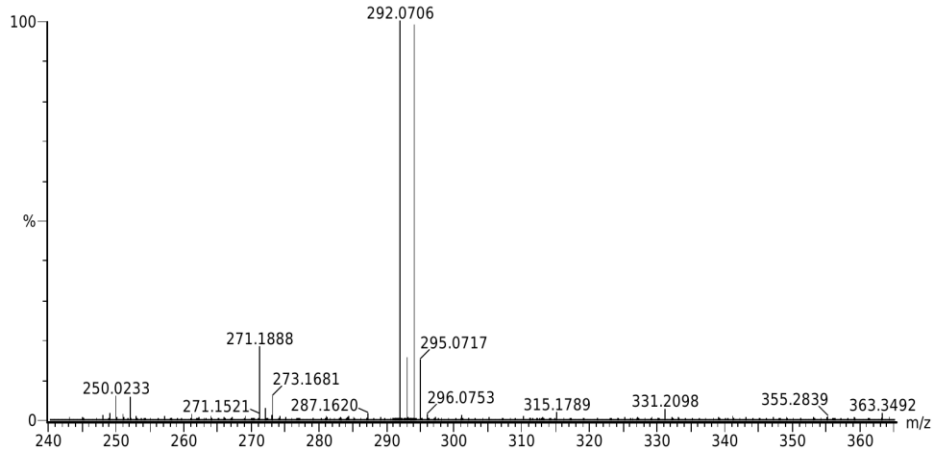

Minimum:				-5.0				
Maximum:		5.0	5.0	50.0				
Mass	Calc. Mass	mDa	PPM	DBE	i-FIT	Norm	Conf(%)	Formula
292.0706	292.0701	0.5	1.7	6.5	1356.8	n/a	n/a	C15 H19 N Br

Appendix K.8 **^{1}H NMR Spectra of Pyridine Methyl Ether 15b-OMe**

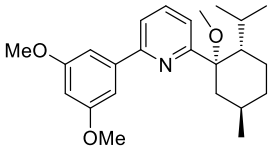

15b-OMe

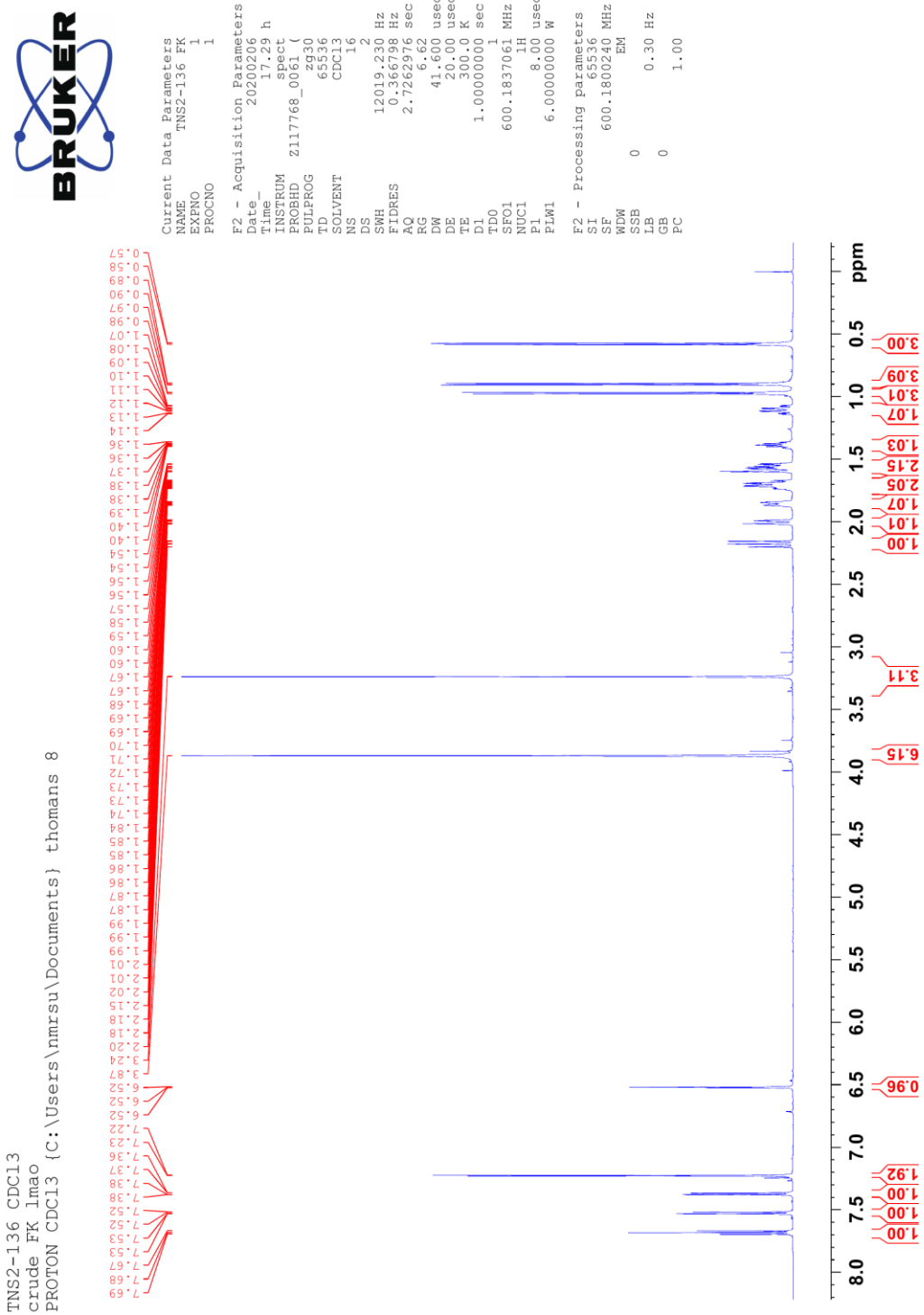

Appendix K Spectra of 2,6-disubstituted Pyridine Methyl Ethers, 12-OMe and 15-OMe

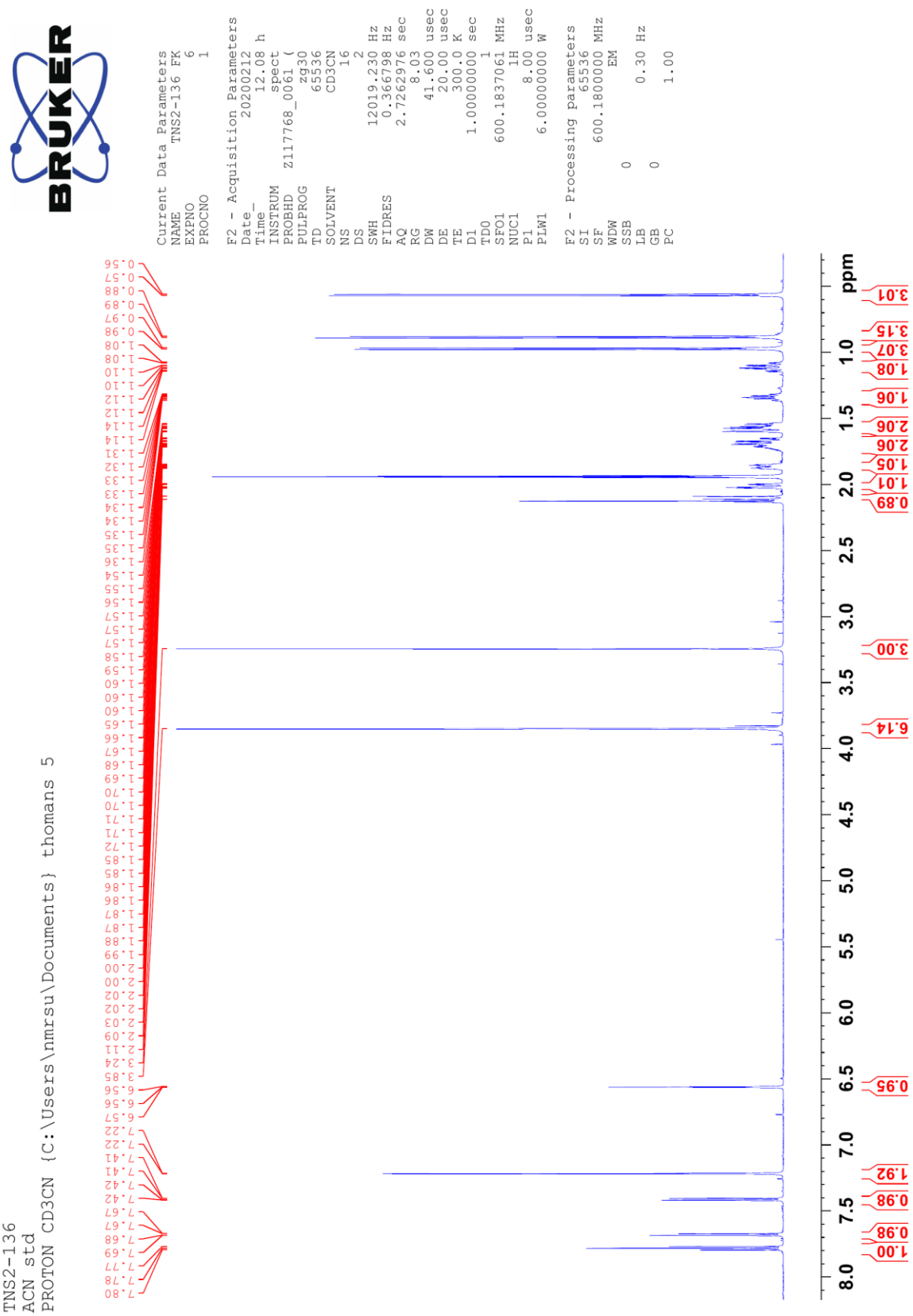

Appendix K.9 **^{13}C NMR Spectrum of Pyridine Methyl Ether 15b-OMe**

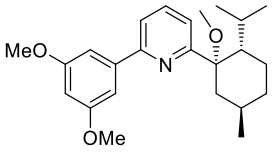

15b-OMe

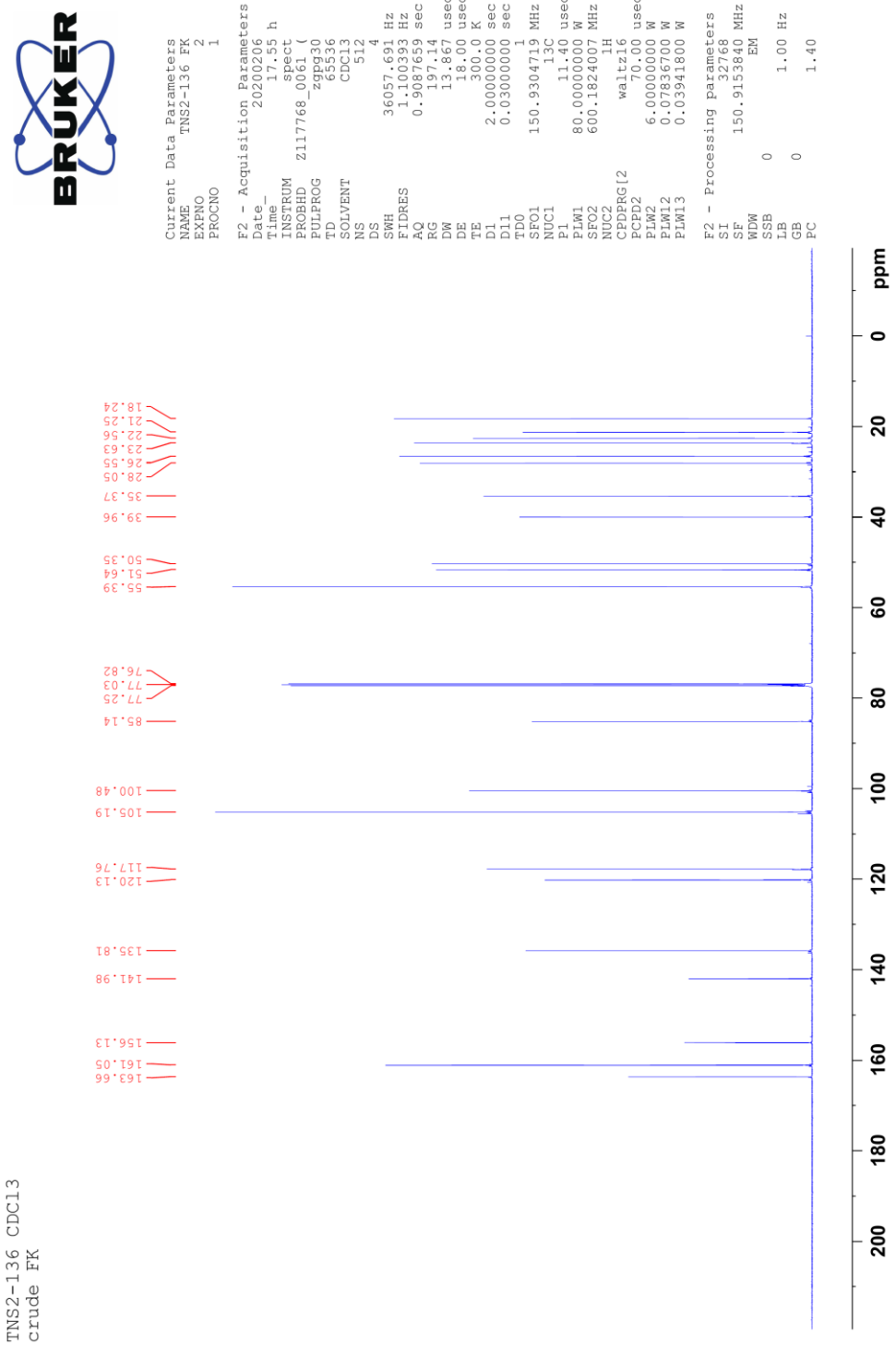

Appendix K.10 **COSY NMR Spectrum of Pyridine Methyl Ether 15b-OMe**

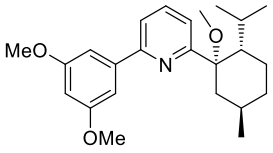

15b-OMe

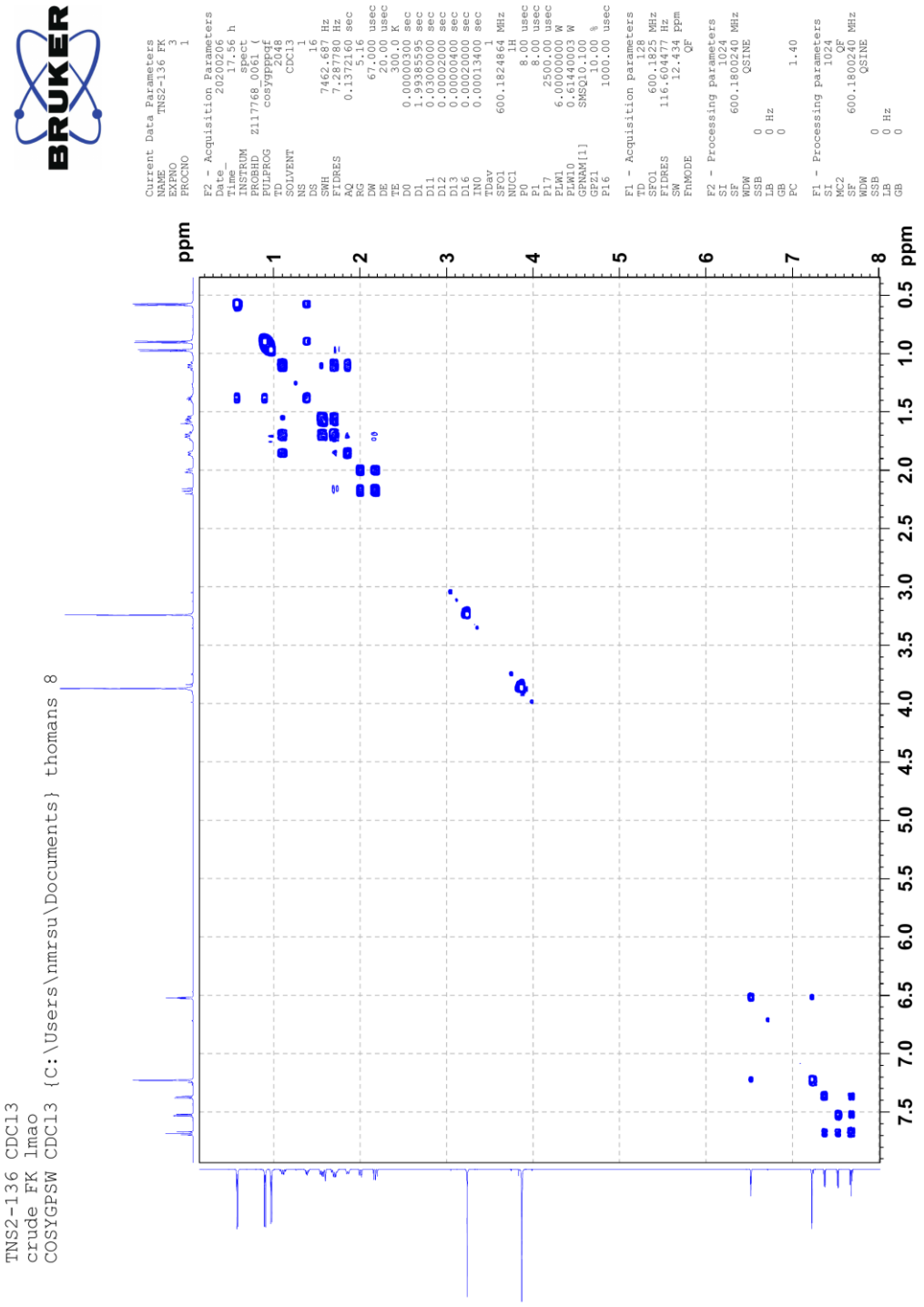

Appendix K.11 **HSQC NMR Spectrum of Pyridine Methyl Ether 15b-OMe**

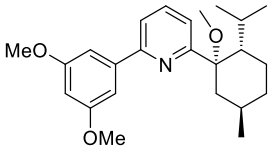

15b-OMe

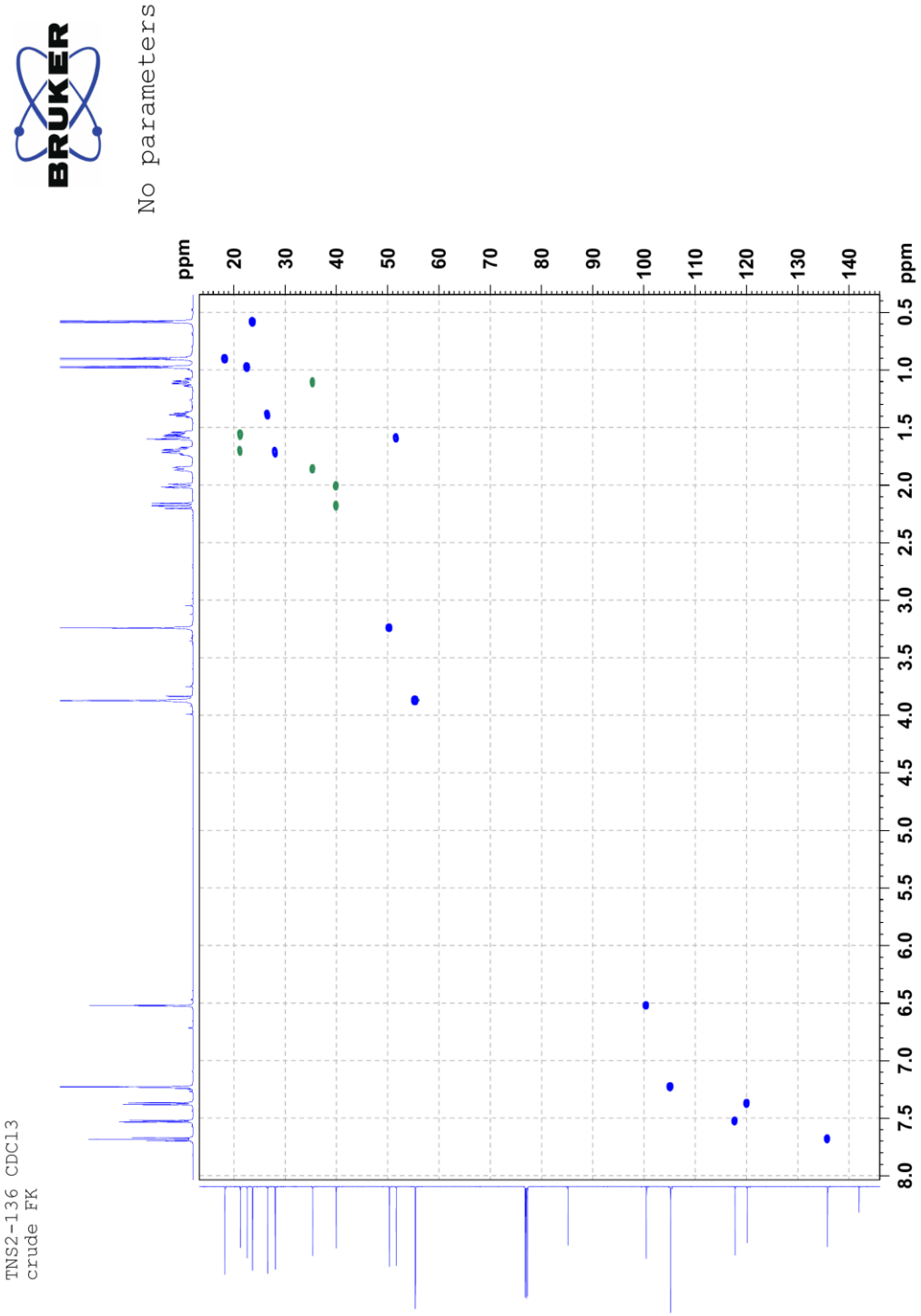

Appendix K Spectra of 2,6-disubstituted Pyridine Methyl Ethers, 12-OMe and 15-OMe

Appendix K.12 **^{1}H,^{13}C-HMBC NMR Spectrum of Pyridine Methyl Ether 15b-OMe**

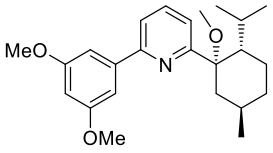

15b-OMe

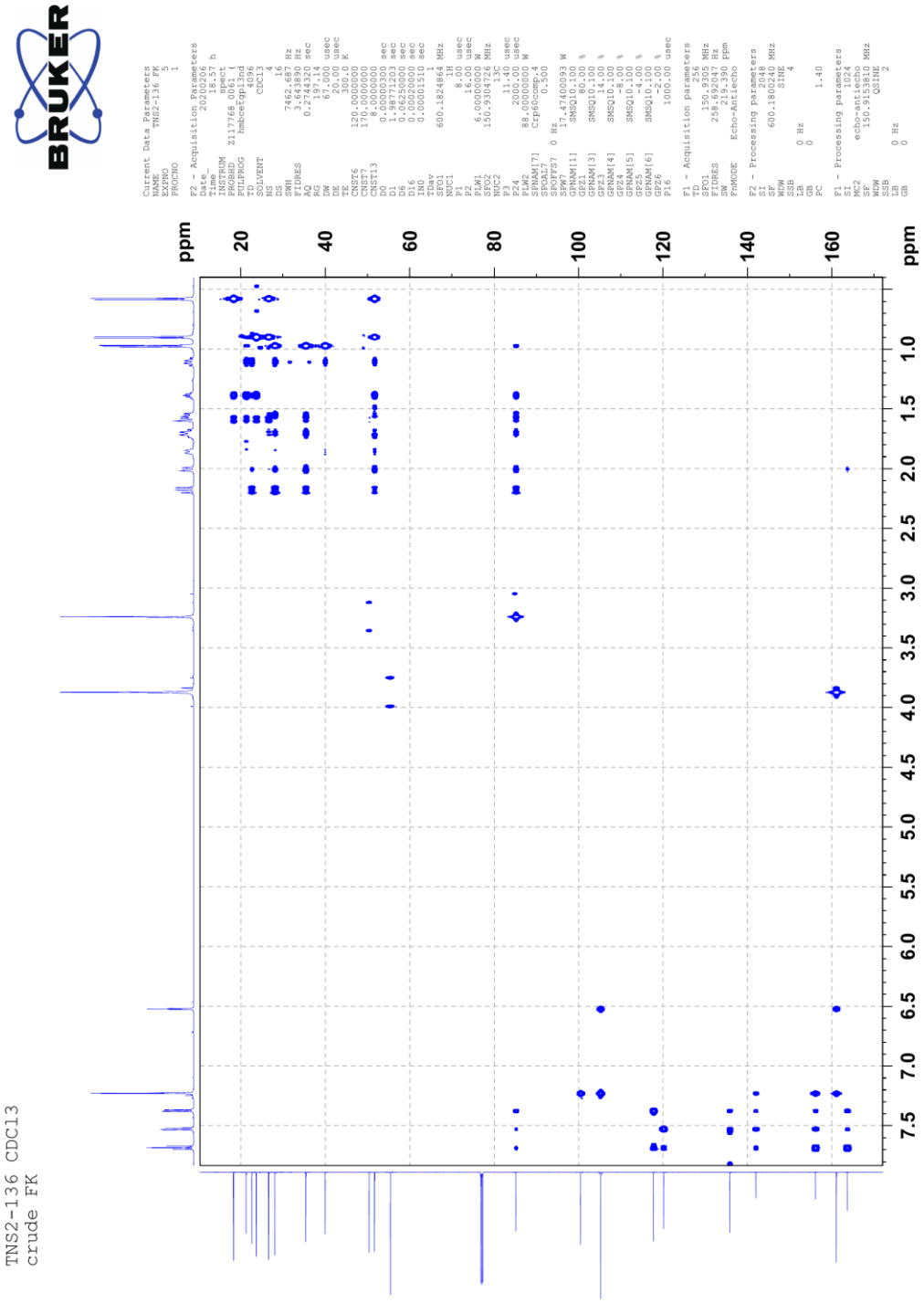

Appendix K.13 **^{1}H,^{15}N-HMBC NMR Spectrum of Pyridine Methyl Ether 15b-OMe**

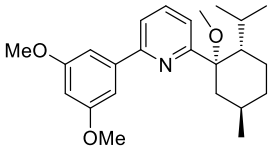

15b-OMe

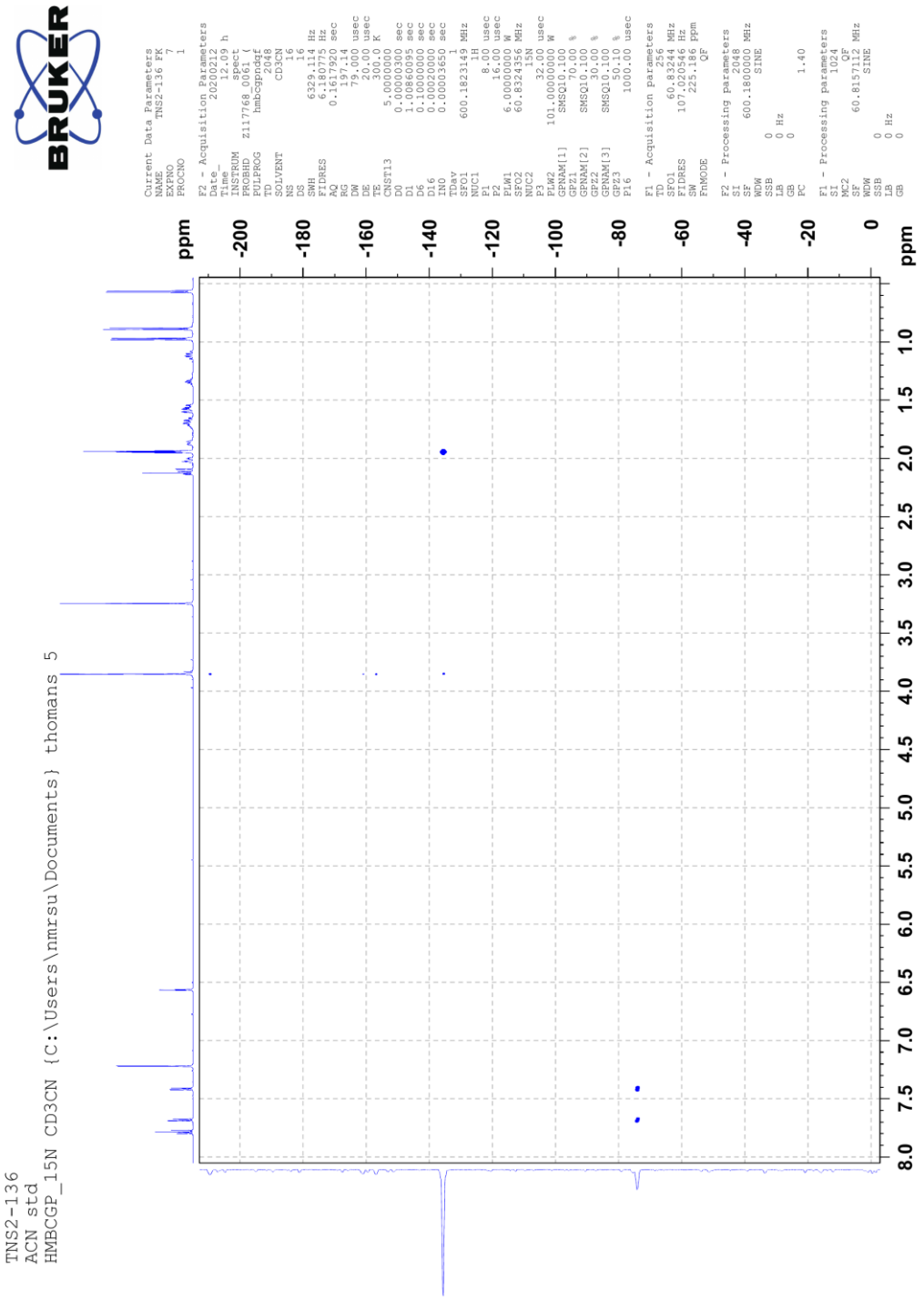

Appendix K.14 **HRMS Spectrum of Pyridine Methyl Ether 15b-OMe**

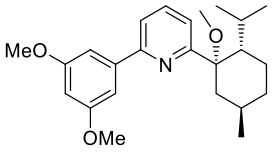

15b-OMe

Elemental Composition Report **Page 1**

Single Mass Analysis
Tolerance = 3.0 PPM / DBE: min = -5.0, max = 50.0
Element prediction: Off
Number of isotope peaks used for i-FIT = 3

Monoisotopic Mass, Even Electron Ions
323 formula(e) evaluated with 1 results within limits (all results (up to 1000) for each mass)
Elements Used:
C: 0-100 H: 0-100 N: 0-5 O: 0-10
2020_44 23 (0.465) AM2 (Ar,35000.0,0.00,0.00); Cm (23:30)
1: TOF MS ASAP+

4.13e+006

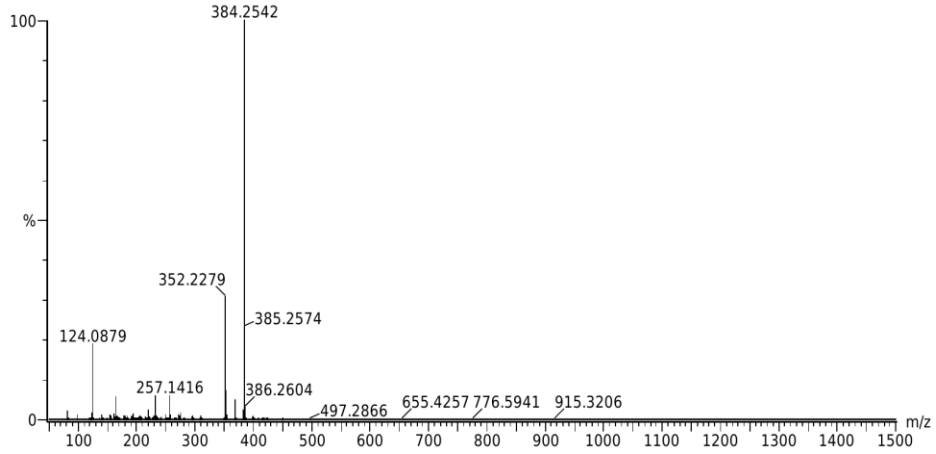

Minimum:				-5.0				
Maximum:		5.0	3.0	50.0				
Mass	Calc. Mass	mDa	PPM	DBE	i-FIT	Norm	Conf(%)	Formula
384.2542	384.2539	0.3	0.8	8.5	1141.3	n/a	n/a	C24 H34 N O3

Appendix K Spectra of 2,6-disubstituted Pyridine Methyl Ethers, 12-OMe and 15-OMe

Appendix K.15 **^{1}H NMR Spectra of Pyridine Methyl Ether 15d-OMe**

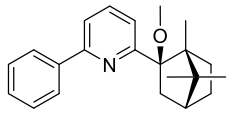

15d-OMe

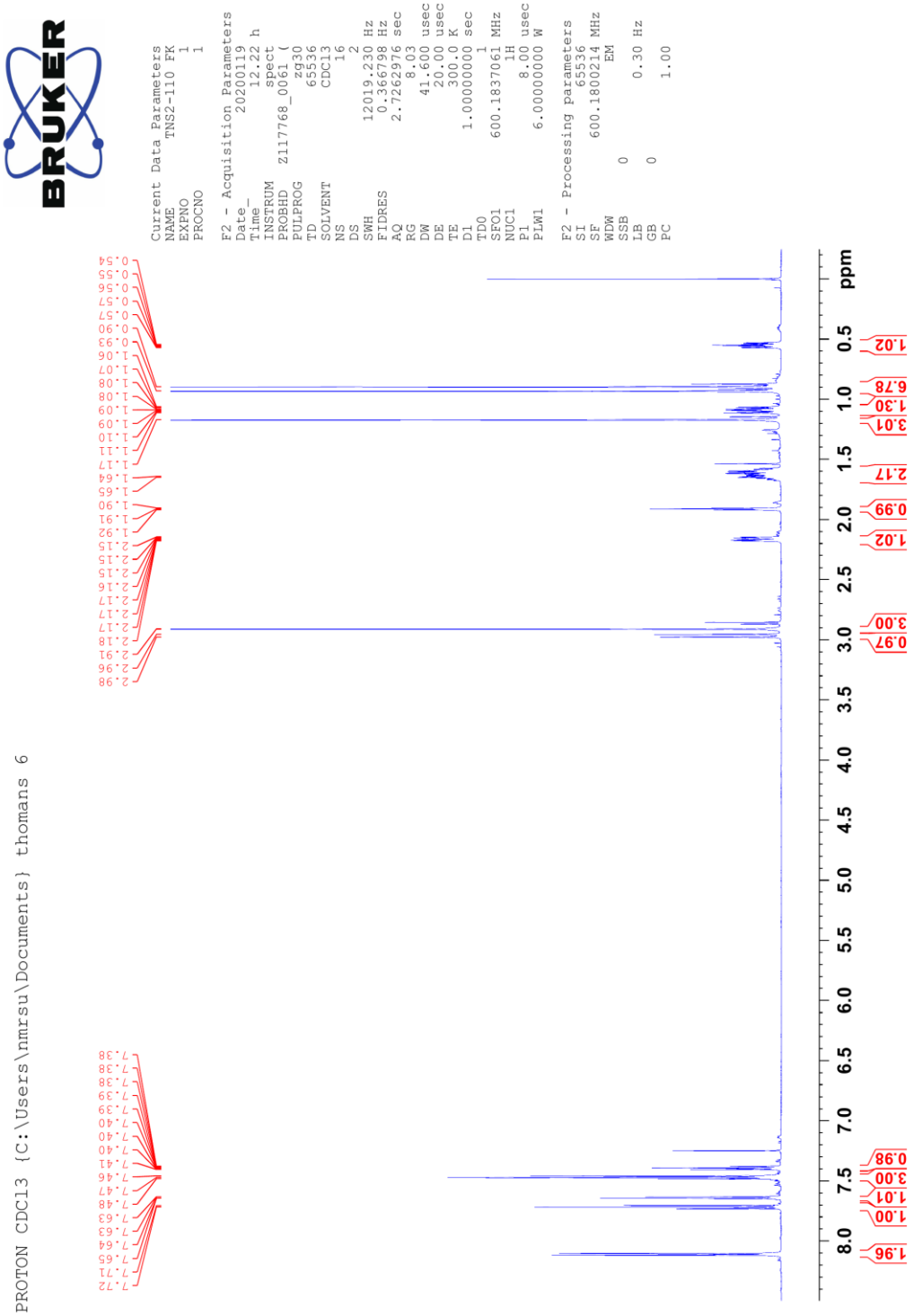

Appendix K Spectra of 2,6-disubstituted Pyridine Methyl Ethers, 12-OMe and 15-OMe

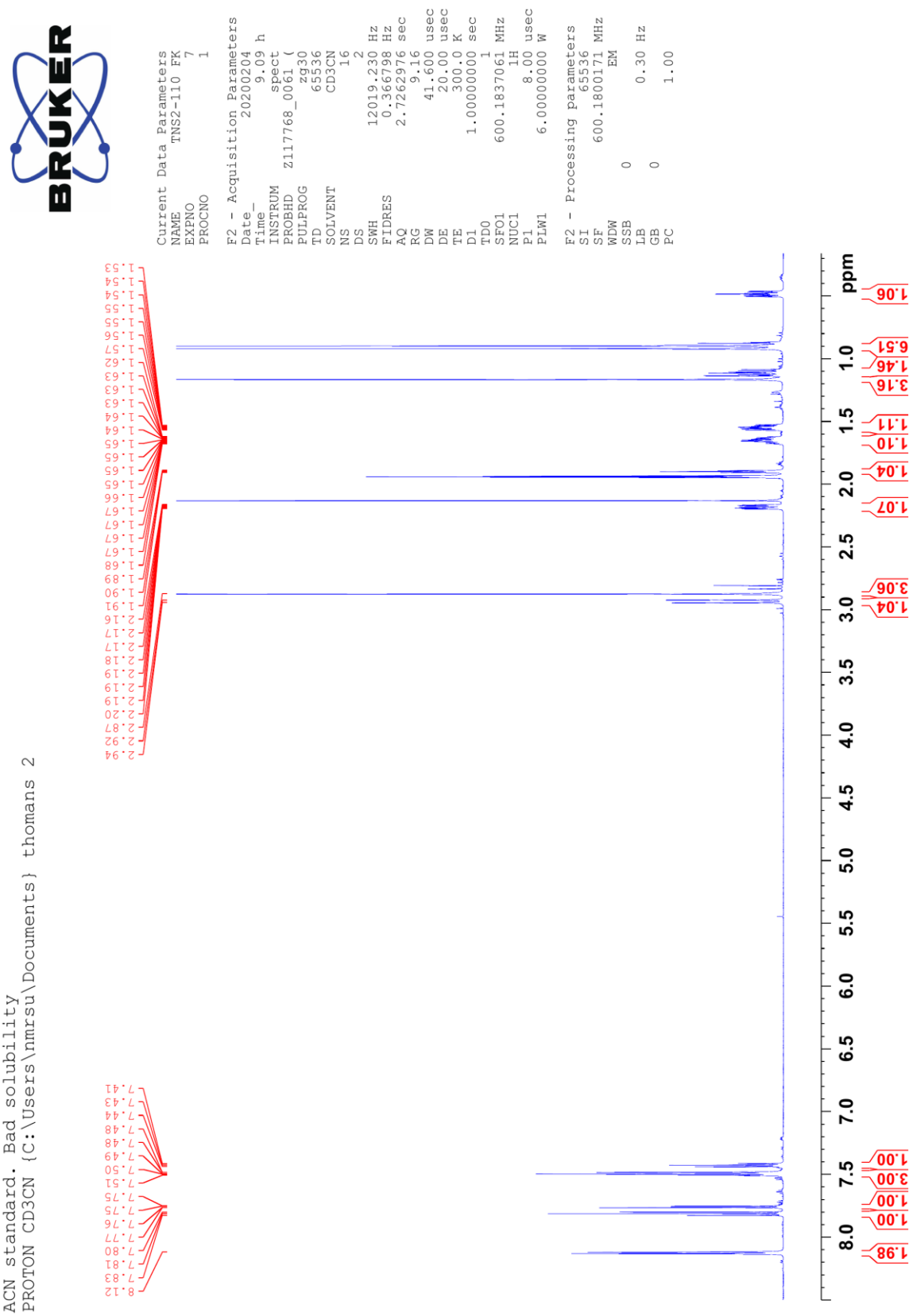

Appendix K.16 **^{13}C NMR Spectrum of Pyridine Methyl Ether 15d-OMe**

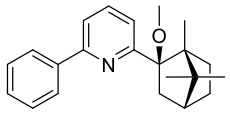

15d-OMe

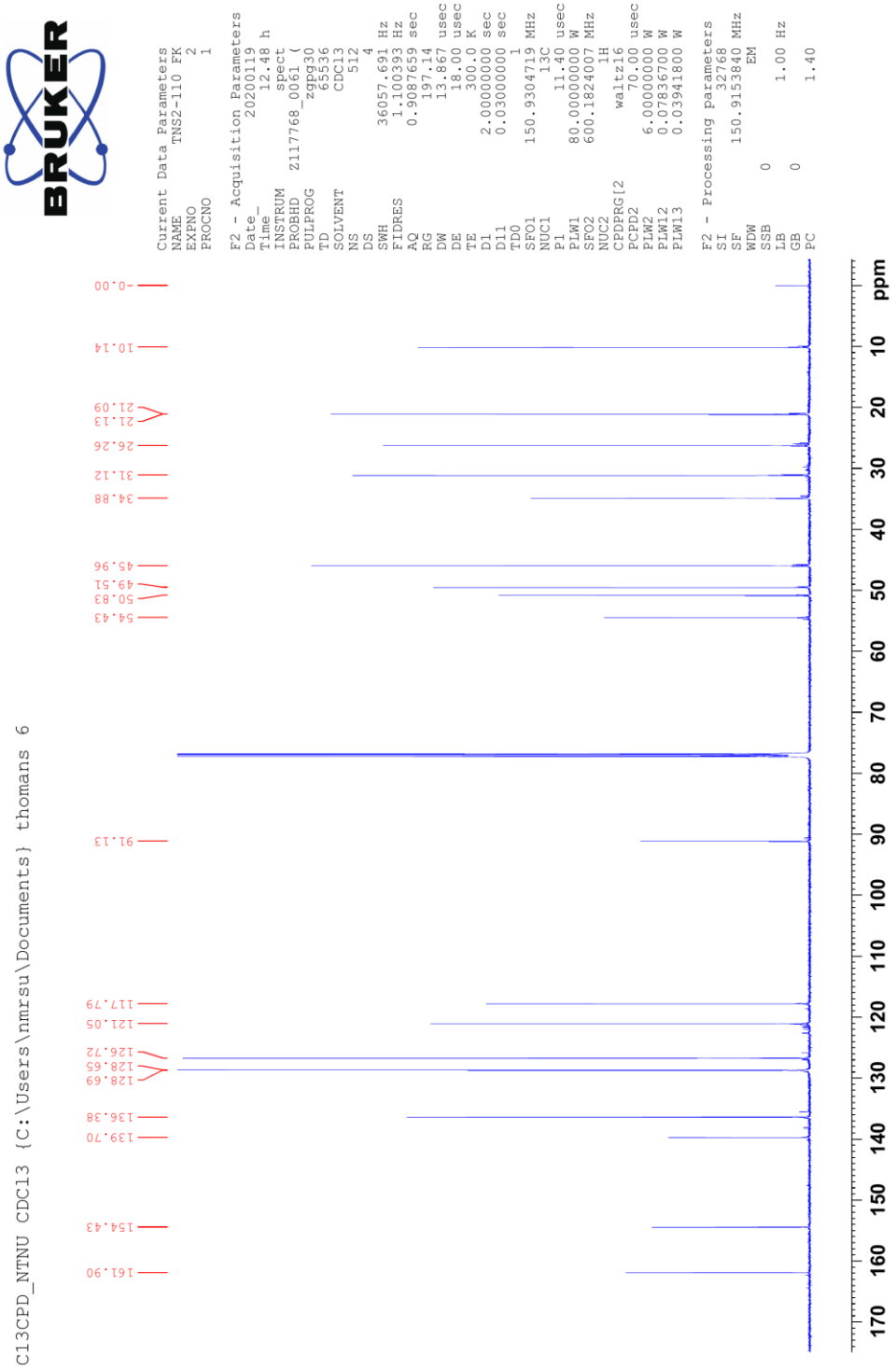

Appendix K.17 **COSY NMR Spectrum of Pyridine Methyl Ether 15d-OMe**

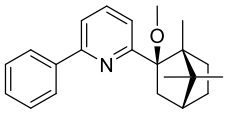

15d-OMe

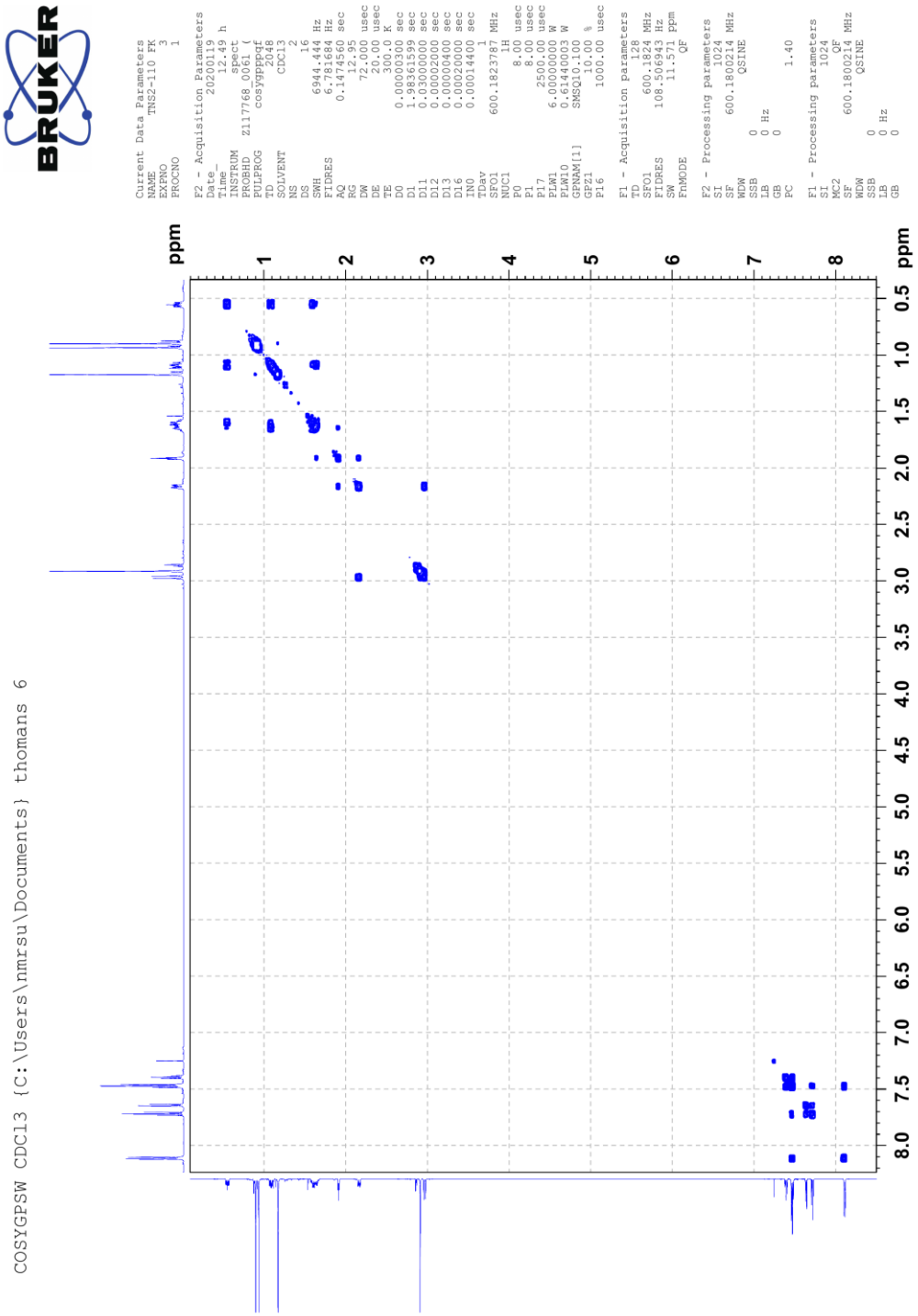

Appendix K.18 **HSQC NMR Spectrum of Pyridine Methyl Ether 15d-OMe**

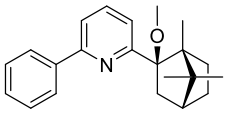

15d-OMe

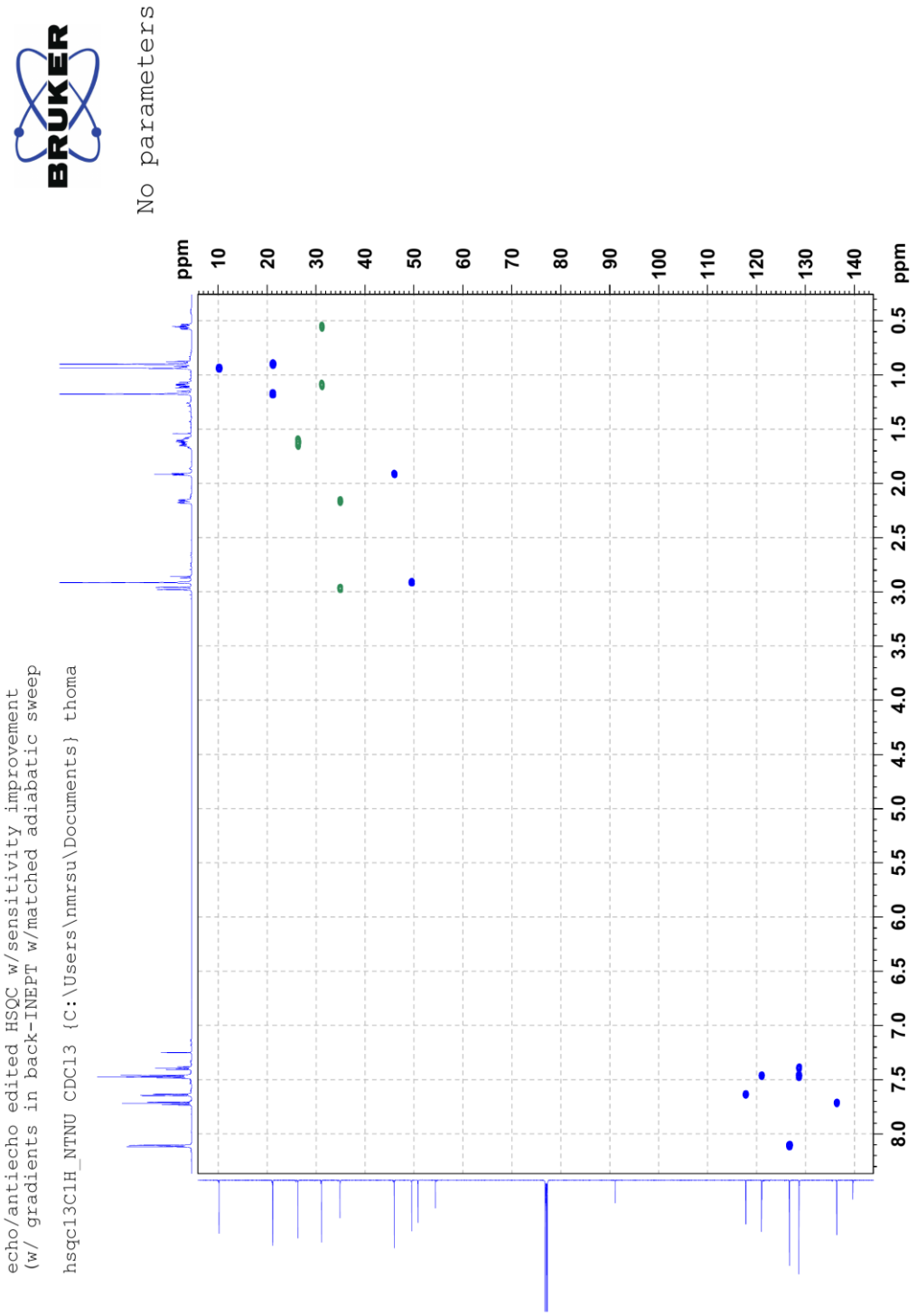

Appendix K.19 **^{1}H,^{13}C-HMBC NMR Spectrum of Pyridine Methyl Ether 15d-OMe**

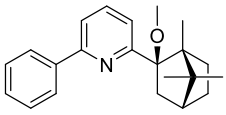

15d-OMe

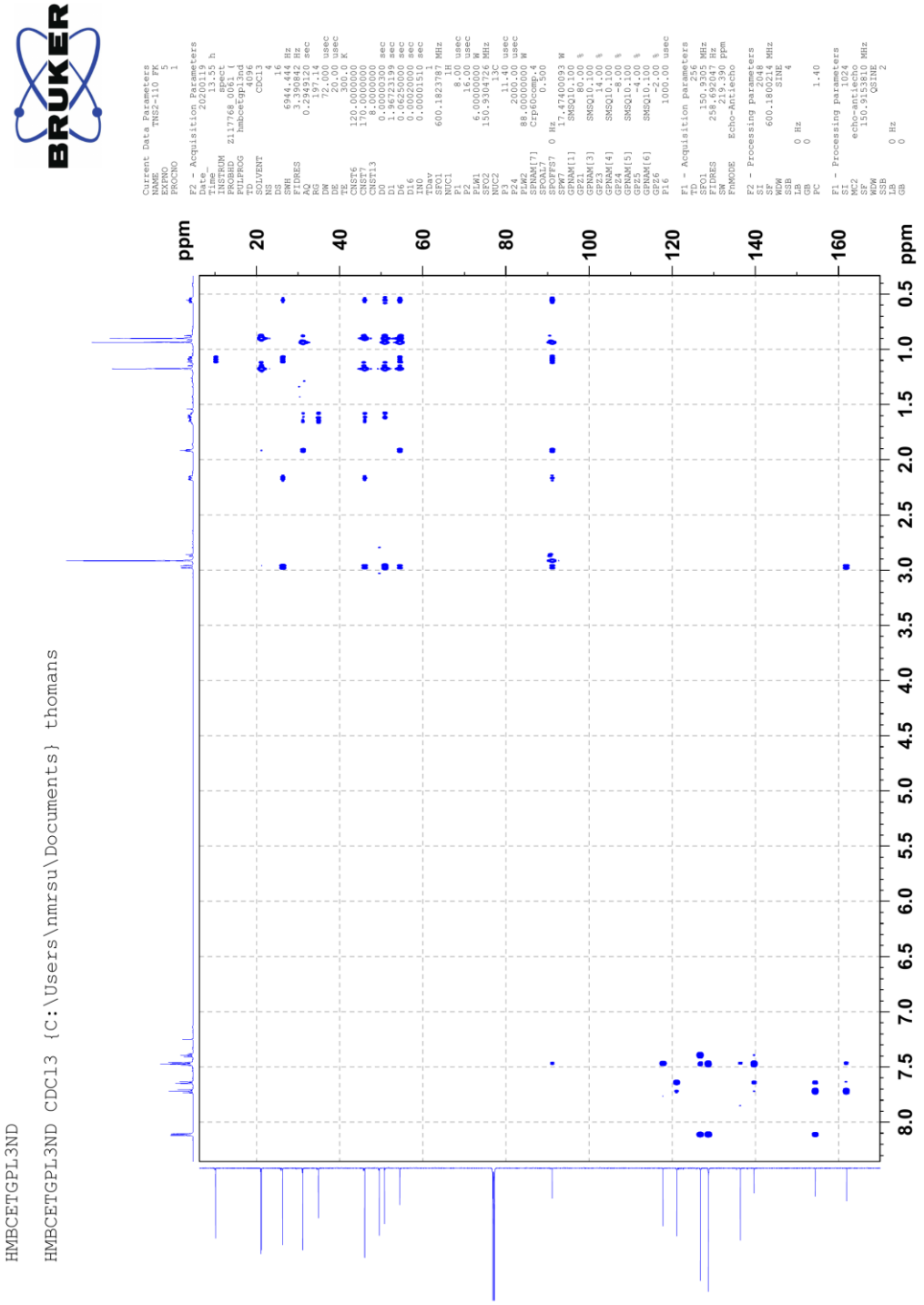

Appendix K.20 **^{1}H,^{15}N-HMBC NMR Spectrum of Pyridine Methyl Ether 15d-OMe**

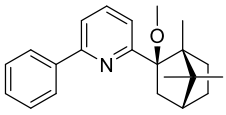

15d-OMe

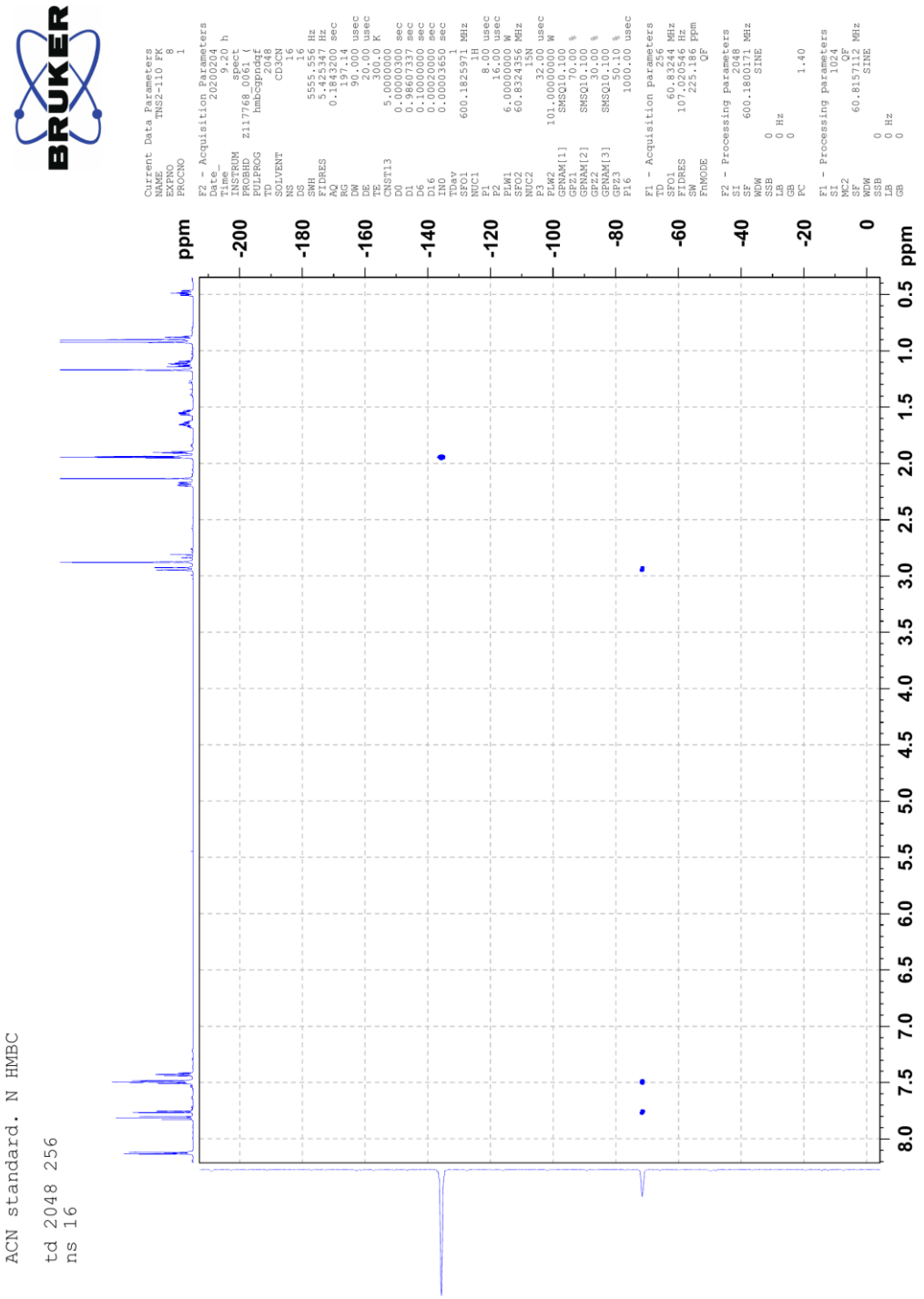

Appendix K.21 **NOESY NMR Spectrum of Pyridine Methyl Ether 15d-OMe**

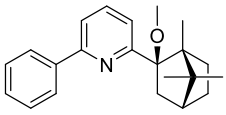

15d-OMe

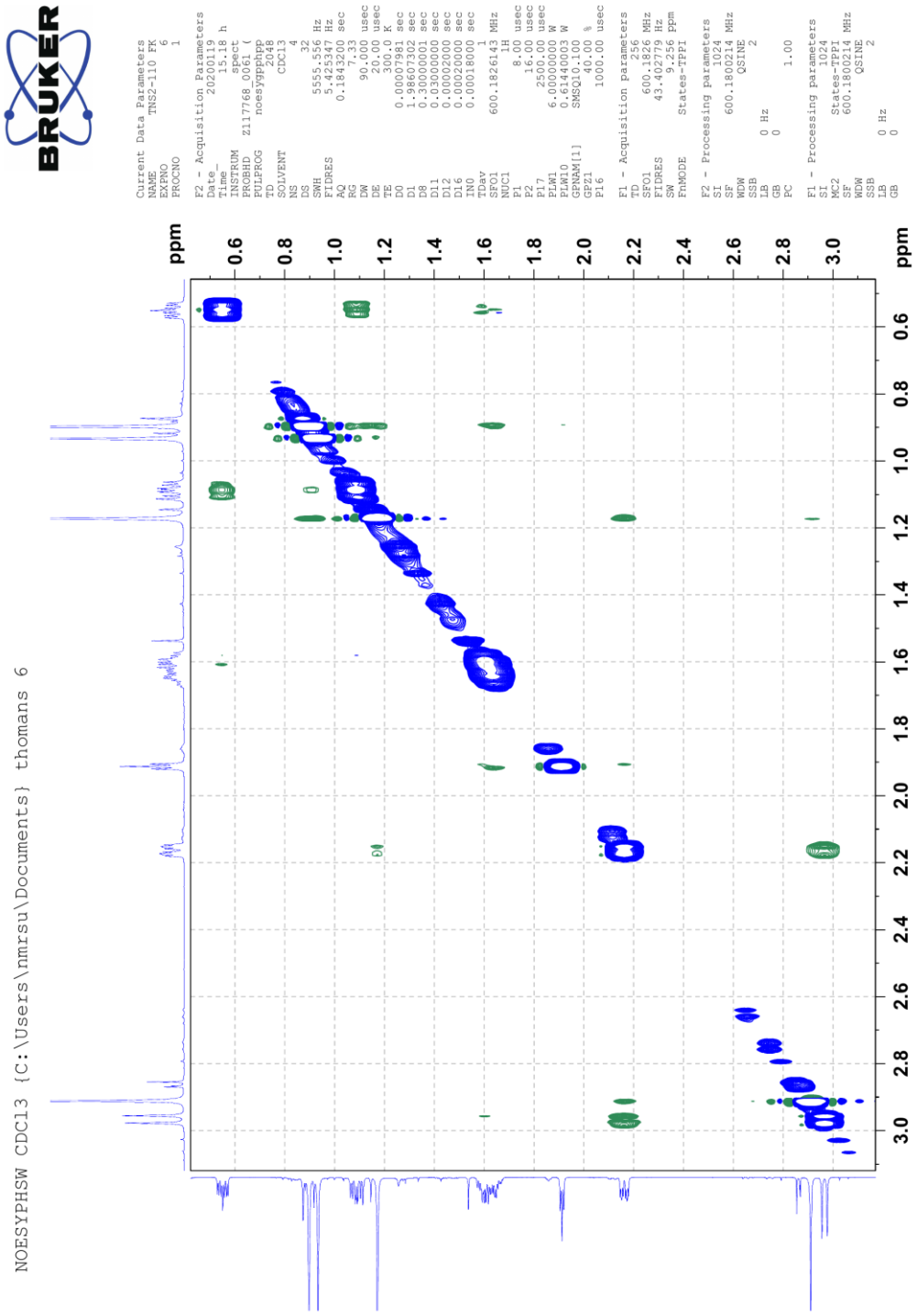

Appendix K.22 **HRMS Spectrum of Pyridine Methyl Ether 15d-OMe**

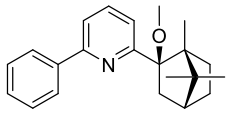

15d-OMe

Elemental Composition Report **Page 1**

Single Mass Analysis
Tolerance = 2.0 PPM / DBE: min = -5.0, max = 50.0
Element prediction: Off
Number of isotope peaks used for i-FIT = 3

Monoisotopic Mass, Even Electron Ions
2660 formula(e) evaluated with 2 results within limits (all results (up to 1000) for each mass)
Elements Used:
C: 0-100 H: 0-100 N: 0-5 O: 0-10 Si: 0-3 S: 0-2
2020_35 69 (0.657) AM2 (Ar,35000.0,0.00,0.00); Cm (67:72)
1: TOF MS ES+

3.89e+006

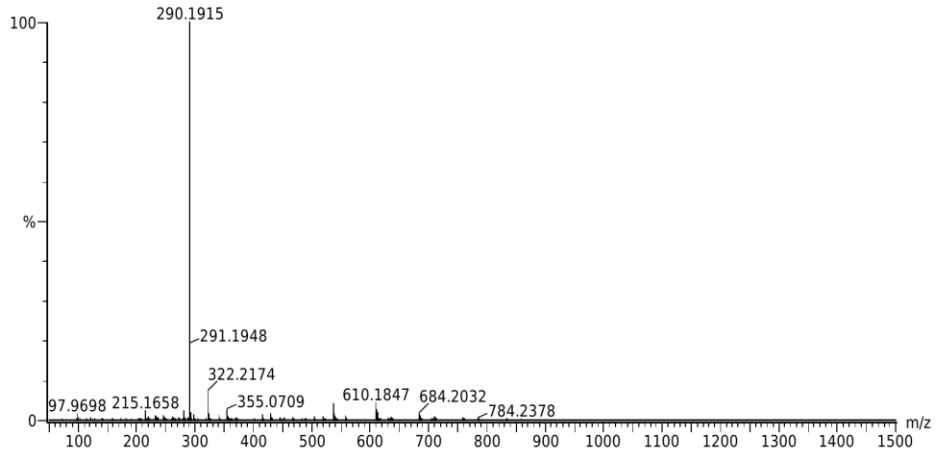

Minimum:				-5.0				
Maximum:		5.0	2.0	50.0				
Mass	Calc. Mass	mDa	PPM	DBE	i-FIT	Norm	Conf(%)	Formula
322.2174	322.2171	0.3	0.9	9.5	1032.3	0.000	100.00	C22 H28 N O
	322.2168	0.6	1.9	-0.5	1054.1	21.774	0.00	C13 H36 N3 Si2 S

Appendix K.23 **^{1}H NMR Spectra of Pyridine Methyl Ether 15e-OMe**

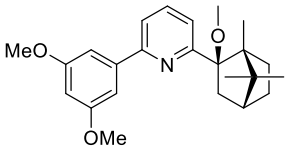

15e-OMe

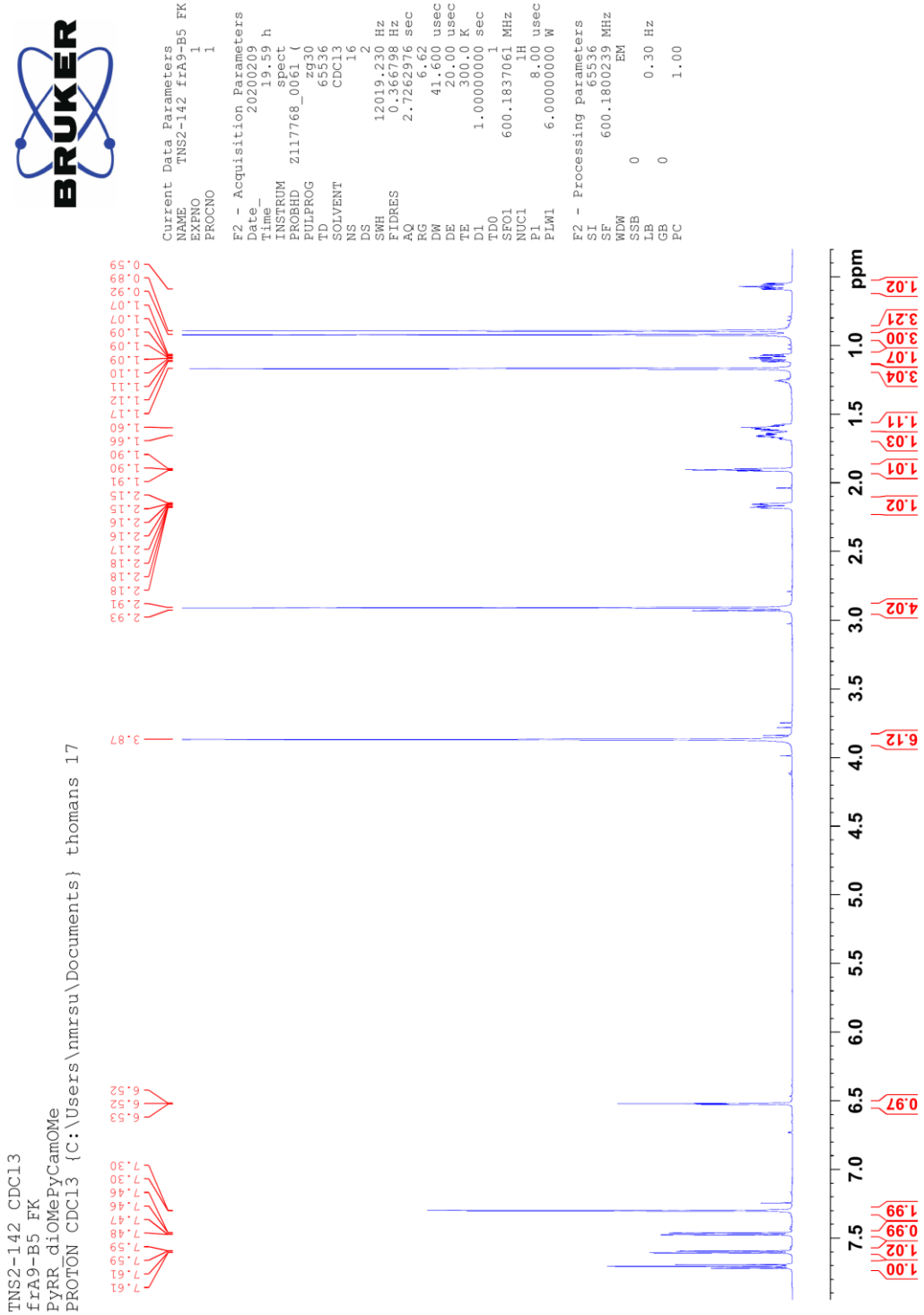

Appendix K Spectra of 2,6-disubstituted Pyridine Methyl Ethers, 12-OMe and 15-OMe

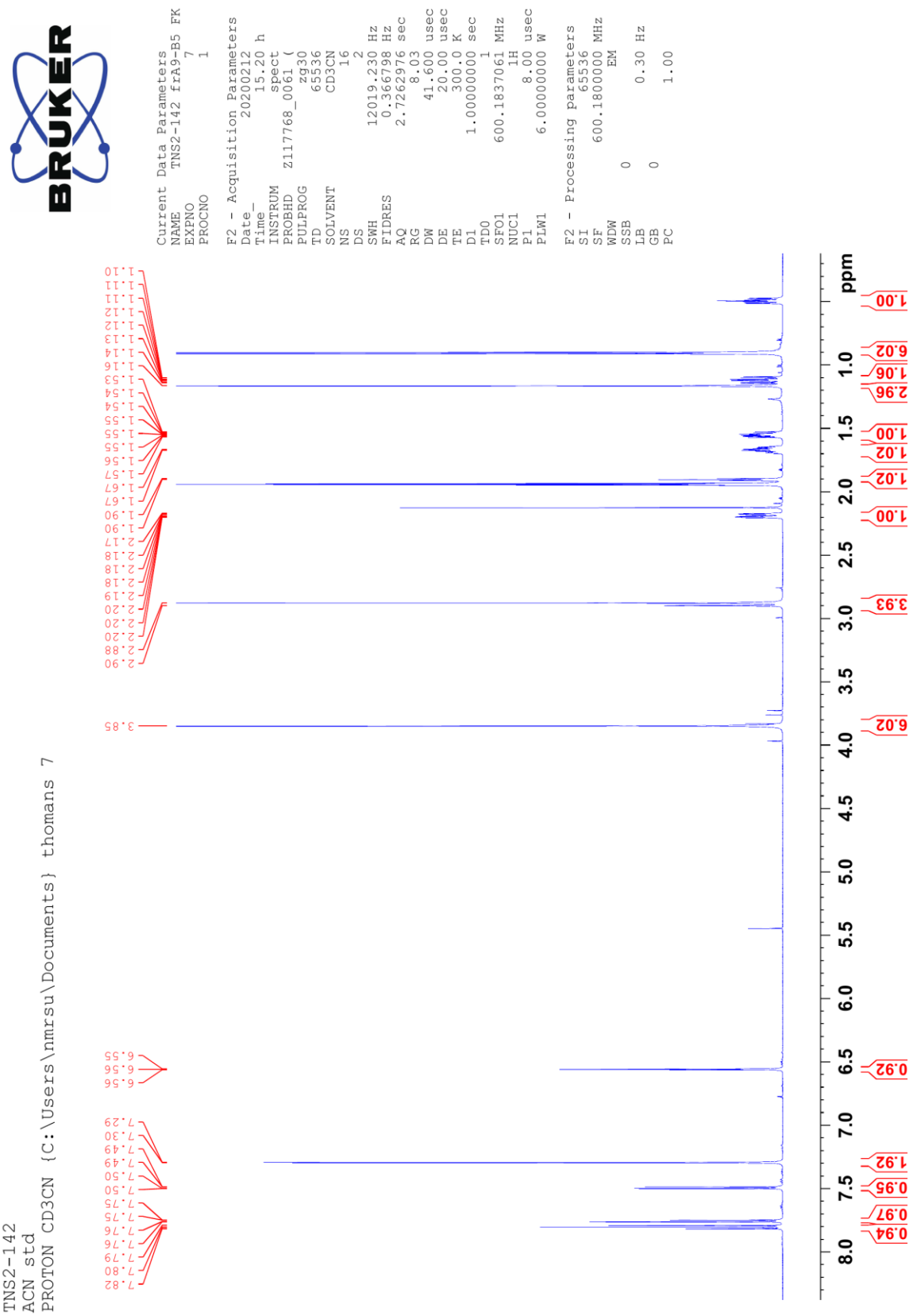

Appendix K Spectra of 2,6-disubstituted Pyridine Methyl Ethers, 12-OMe and 15-OMe

Appendix K.24 **^{13}C NMR Spectrum of Pyridine Methyl Ether 15e-OMe**

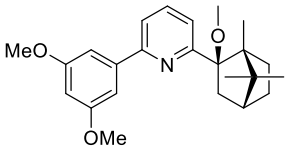

15e-OMe

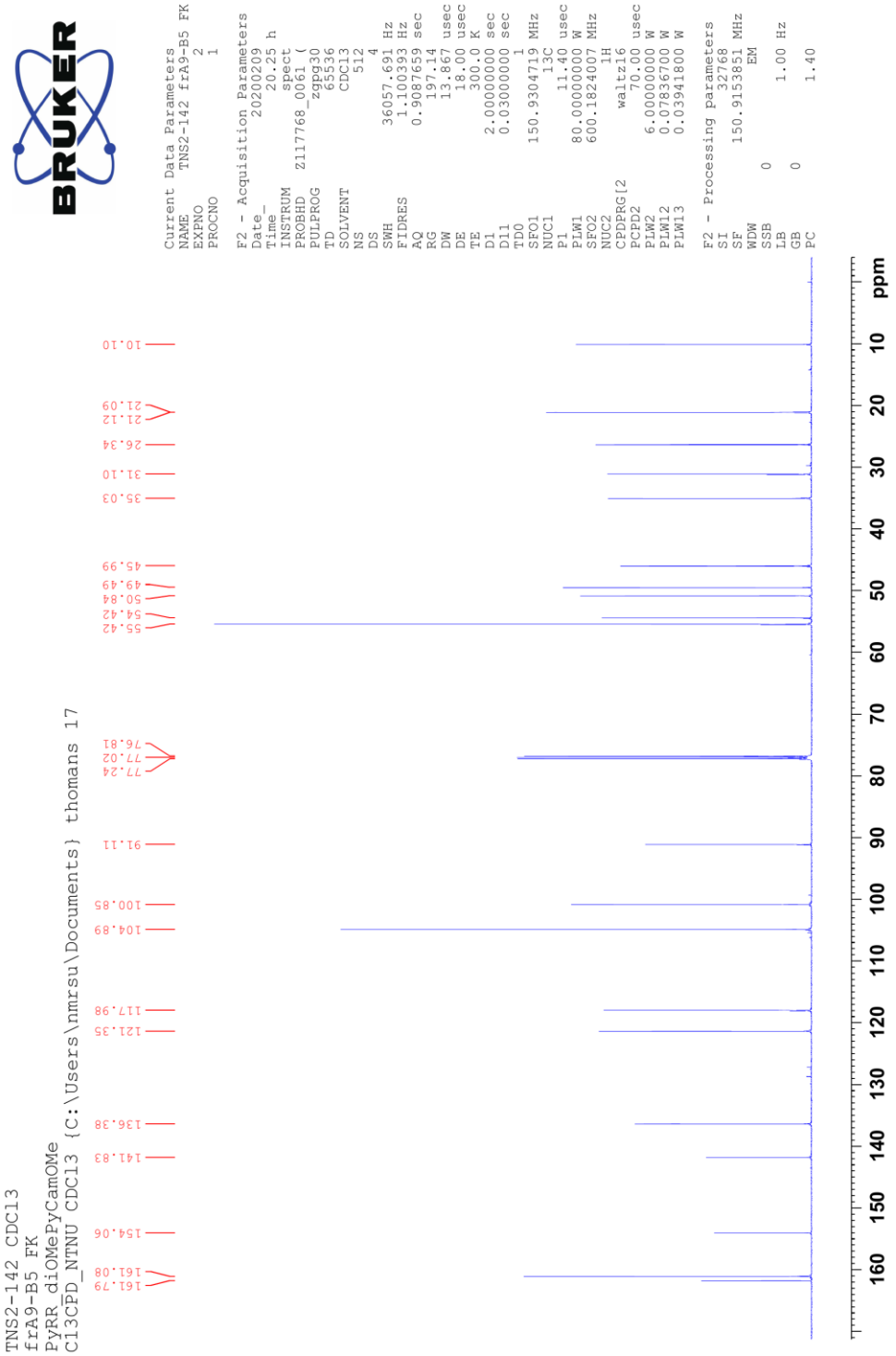

Appendix K.25 **COSY NMR Spectrum of Pyridine Methyl Ether 15e-OMe**

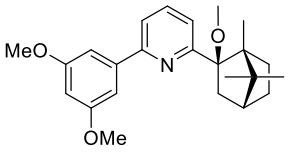

15e-OMe

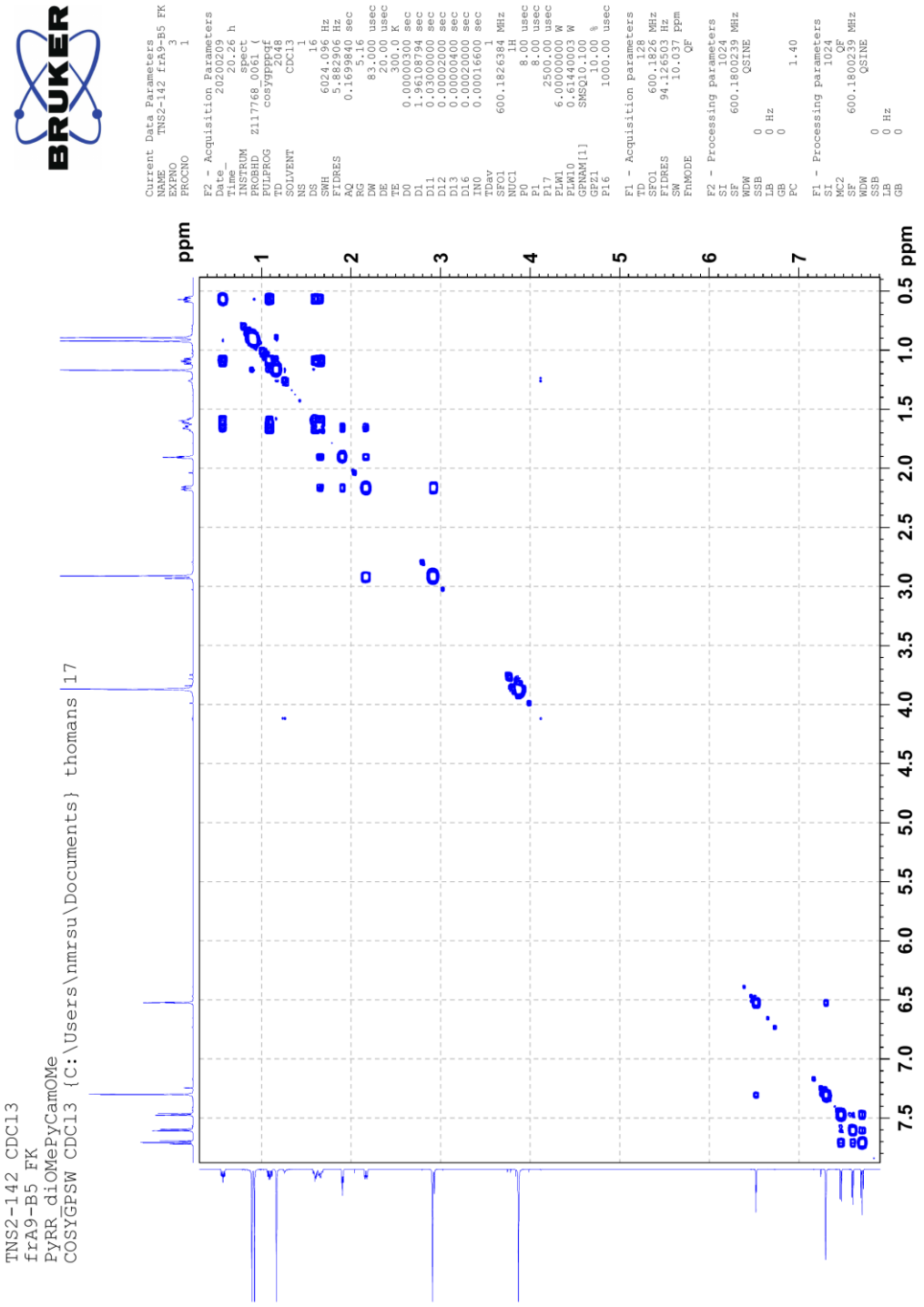

Appendix K.26 **HSQC NMR Spectrum of Pyridine Methyl Ether 15e-OMe**

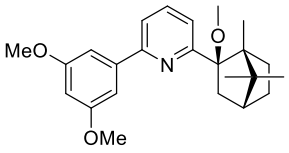

15e-OMe

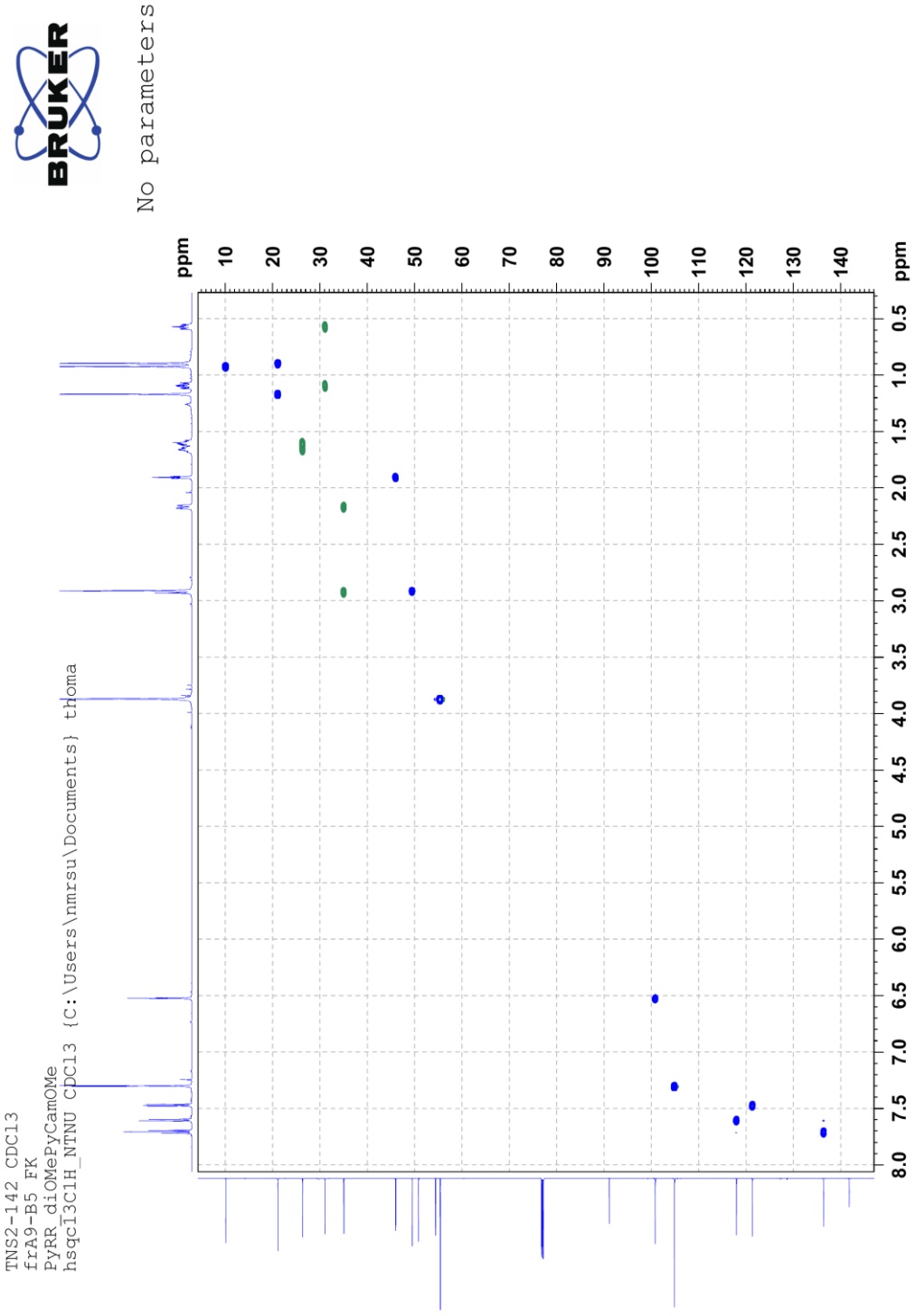

Appendix K.27 **^{1}H,^{13}C-HMBC NMR Spectrum of Pyridine Methyl Ether 15e-OMe**

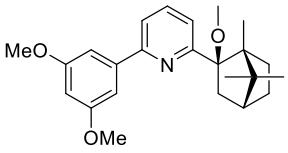

15e-OMe

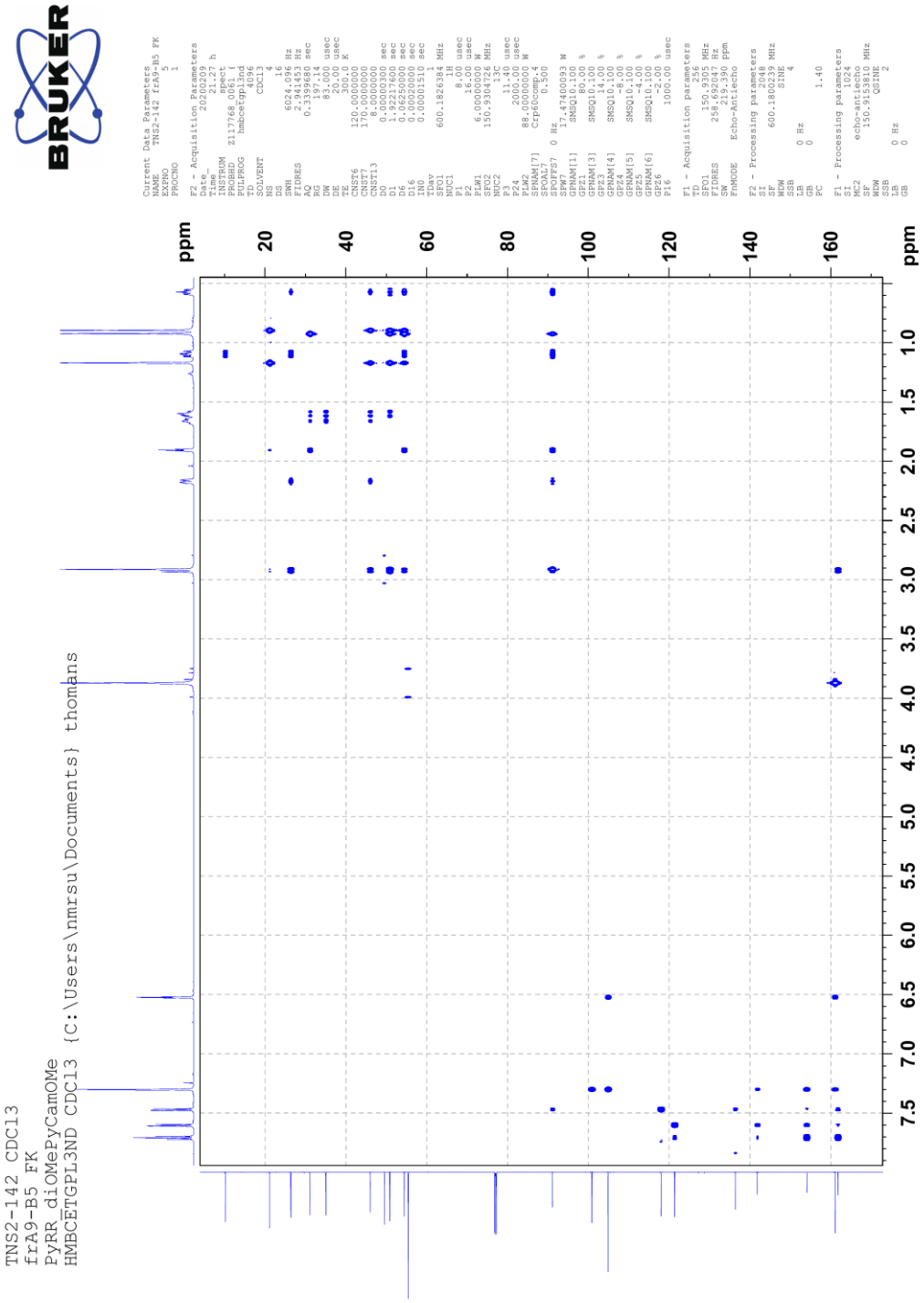

Appendix K Spectra of 2,6-disubstituted Pyridine Methyl Ethers, 12-OMe and 15-OMe

Appendix K.28 **^{1}H,^{15}N-HMBC NMR Spectrum of Pyridine Methyl Ether 15e-OMe**

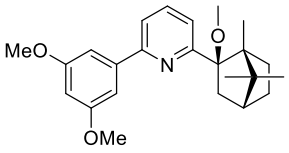

15e-OMe

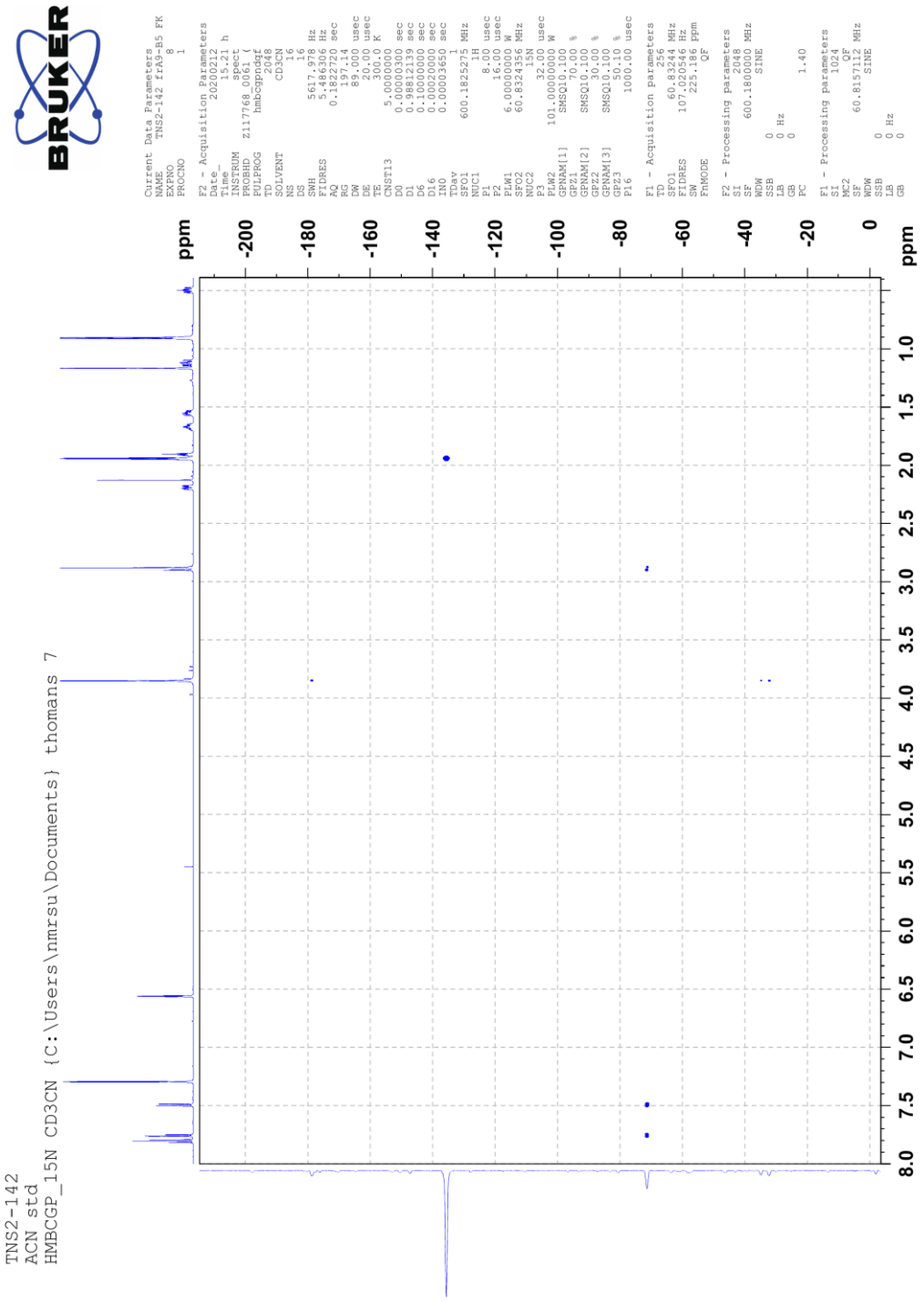

Appendix K.29 **NOESY NMR Spectrum of Pyridine Methyl Ether 15e-OMe**

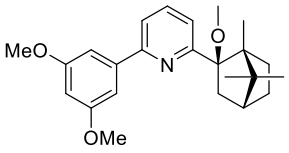

15e-OMe

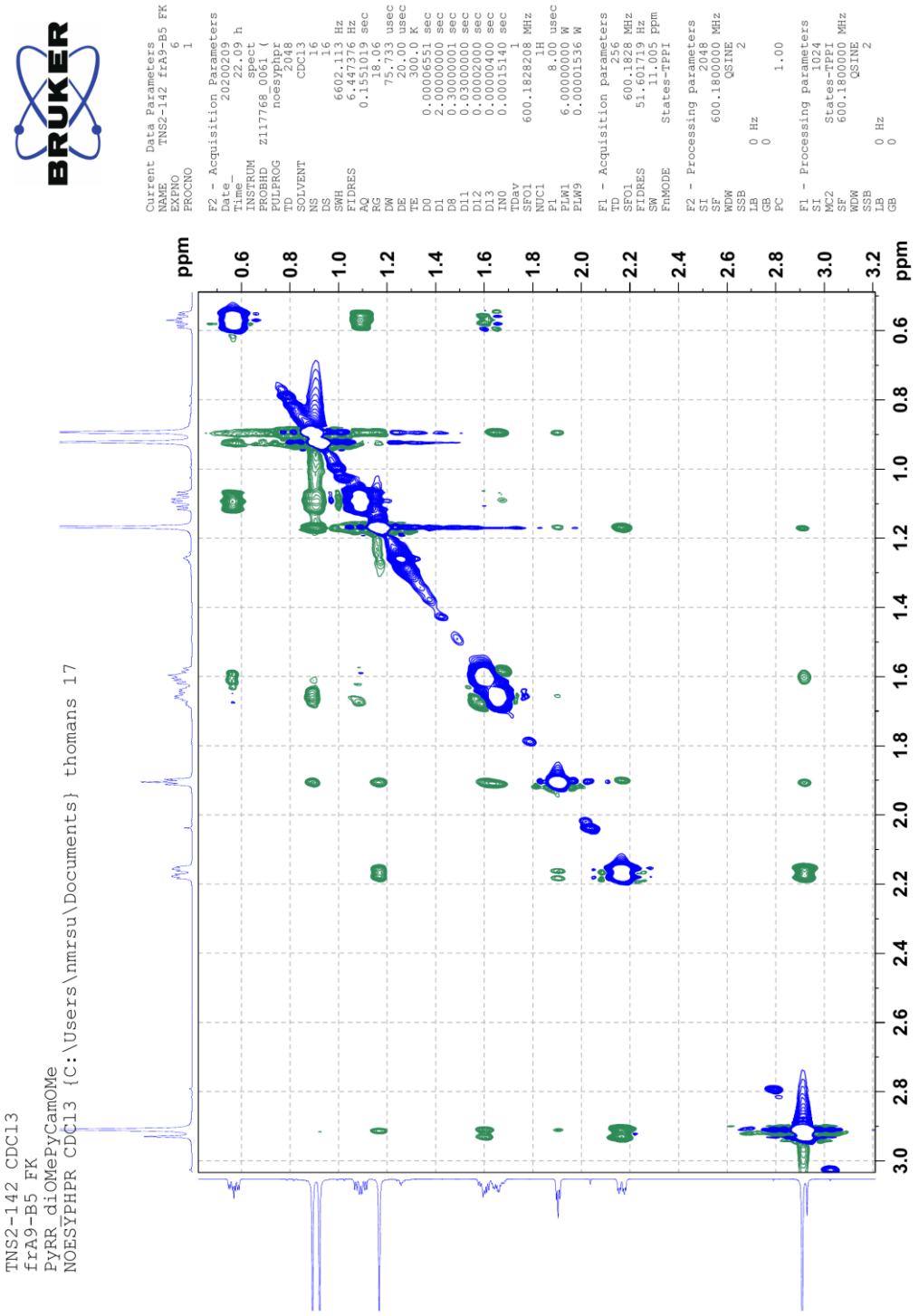

Appendix K.30 **HRMS Spectrum of Pyridine Methyl Ether 15e-OMe**

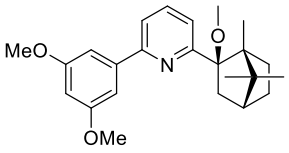

15e-OMe

Elemental Composition Report **Page 1**

Single Mass Analysis
Tolerance = 2.0 PPM / DBE: min = -5.0, max = 50.0
Element prediction: Off
Number of isotope peaks used for i-FIT = 3

Monoisotopic Mass, Even Electron Ions
319 formula(e) evaluated with 1 results within limits (all results (up to 1000) for each mass)
Elements Used:
C: 0-100 H: 0-100 N: 0-5 O: 0-10
2020_48 26 (0.536) AM2 (Ar,35000.0,0.00,0.00); Cm (26)
1: TOF MS ASAP+

3.21e+005

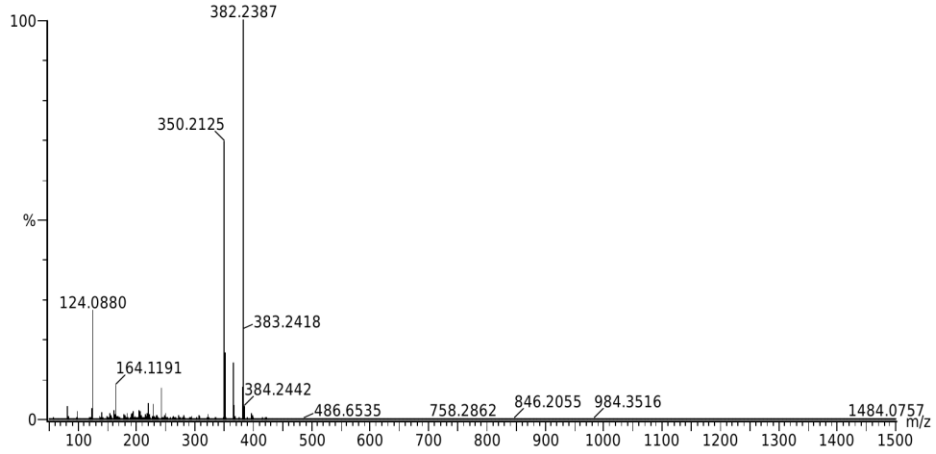

Minimum:				-5.0				
Maximum:		5.0	2.0	50.0				
Mass	Calc. Mass	mDa	PPM	DBE	i-FIT	Norm	Conf(%)	Formula
382.2387	382.2382	0.5	1.3	9.5	851.0	n/a	n/a	C24 H32 N O3

Appendix K Spectra of 2,6-disubstituted Pyridine Methyl Ethers, 12-OMe and 15-OMe

Appendix K.31 **^{1}H NMR Spectra of Pyridine Methyl Ether 15h-OMe**

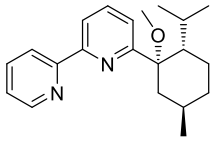

15h-OMe

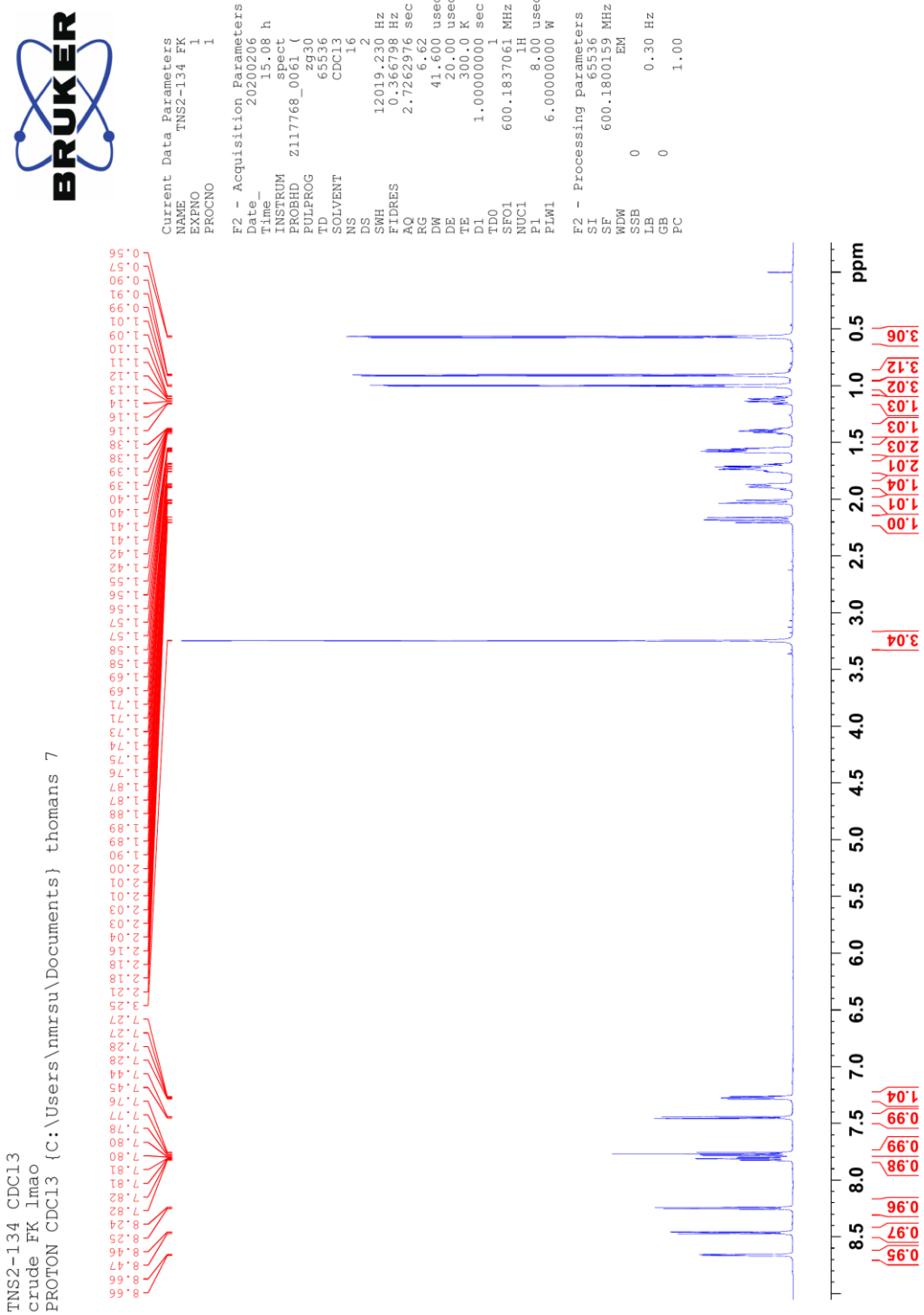

Appendix K Spectra of 2,6-disubstituted Pyridine Methyl Ethers, 12-OMe and 15-OMe

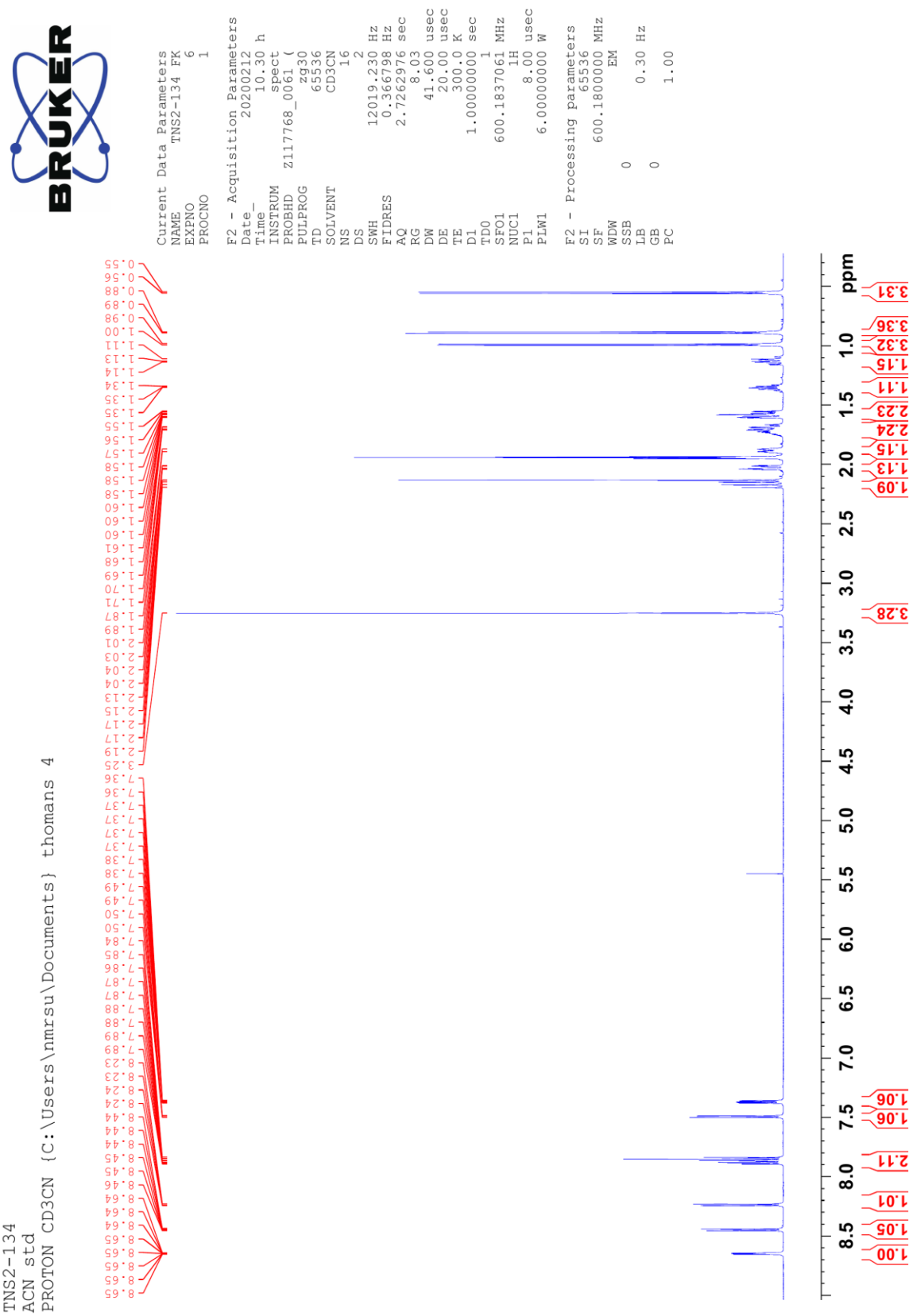

Appendix K Spectra of 2,6-disubstituted Pyridine Methyl Ethers, 12-OMe and 15-OMe

Appendix K.32 **^{13}C NMR Spectrum of Pyridine Methyl Ether 15h-OMe**

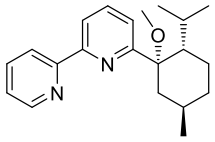

15h-OMe

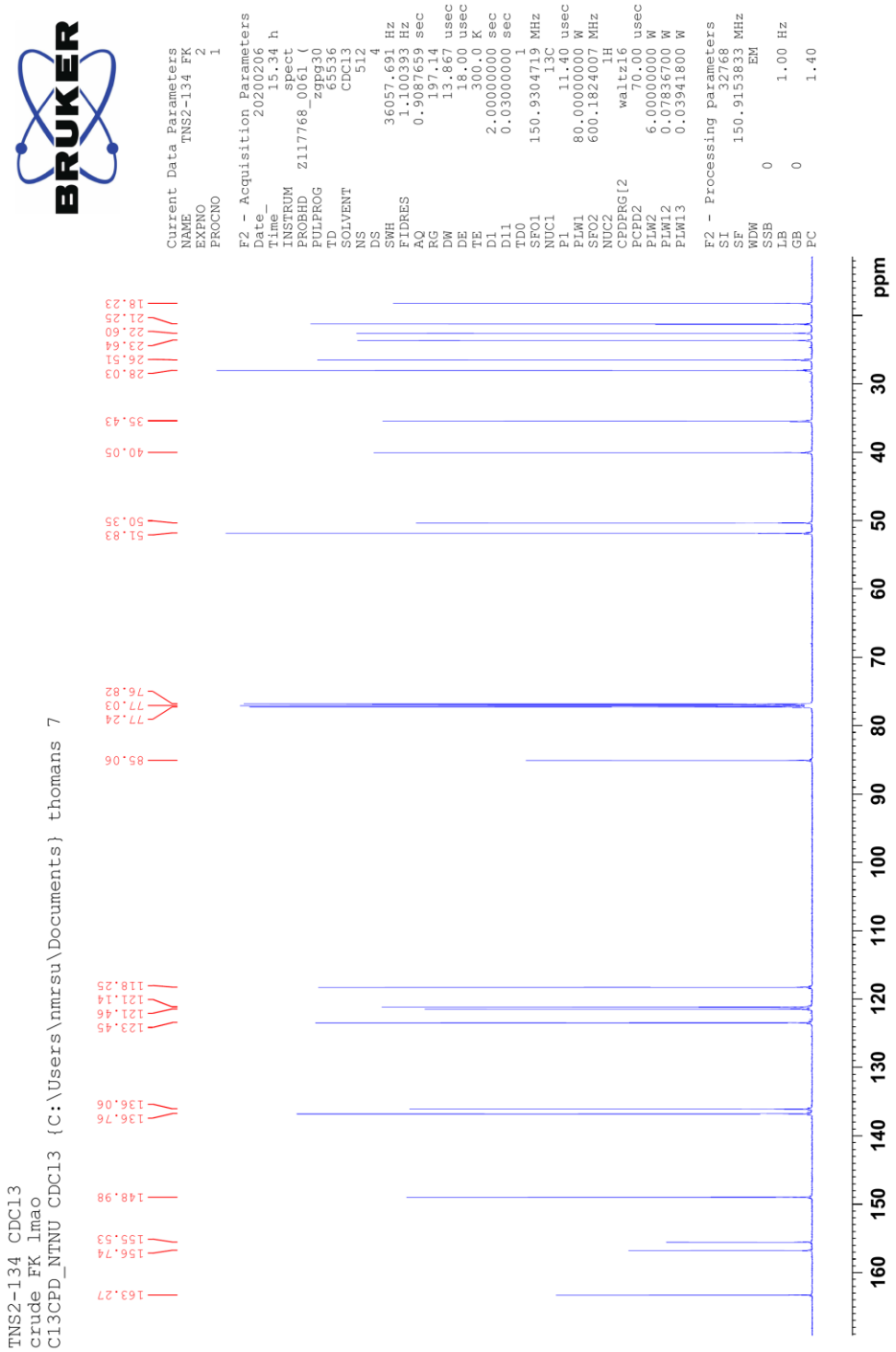

Appendix K Spectra of 2,6-disubstituted Pyridine Methyl Ethers, 12-OMe and 15-OMe

Appendix K.33 **COSY NMR Spectrum of Pyridine Methyl Ether 15h-OMe**

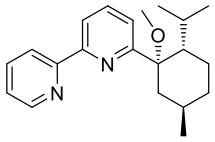

15h-OMe

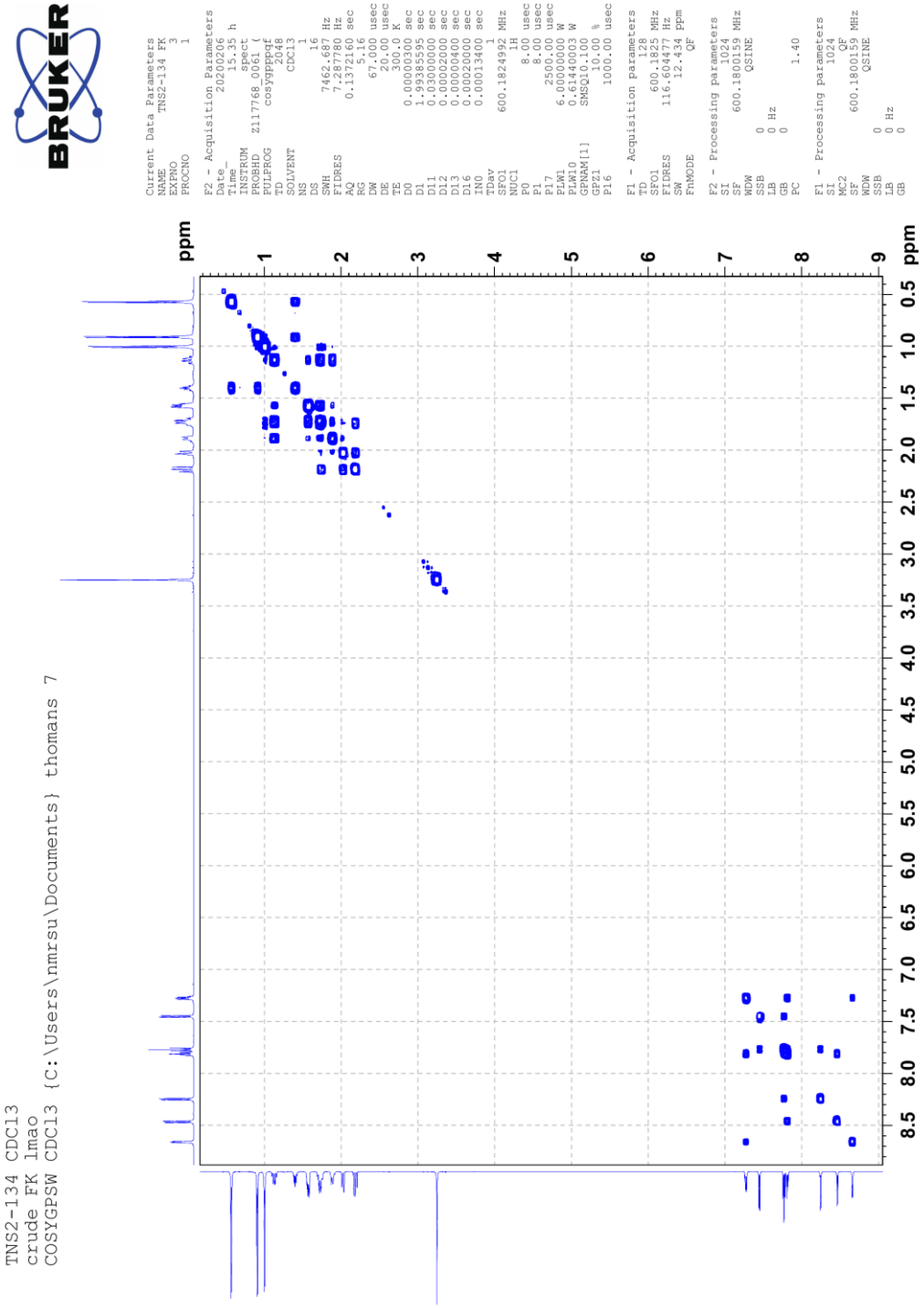

Appendix K Spectra of 2,6-disubstituted Pyridine Methyl Ethers, 12-OMe and 15-OMe

Appendix K.34 **HSQC NMR Spectrum of Pyridine Methyl Ether 15h-OMe**

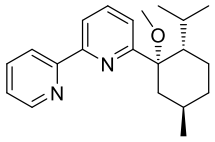

15h-OMe

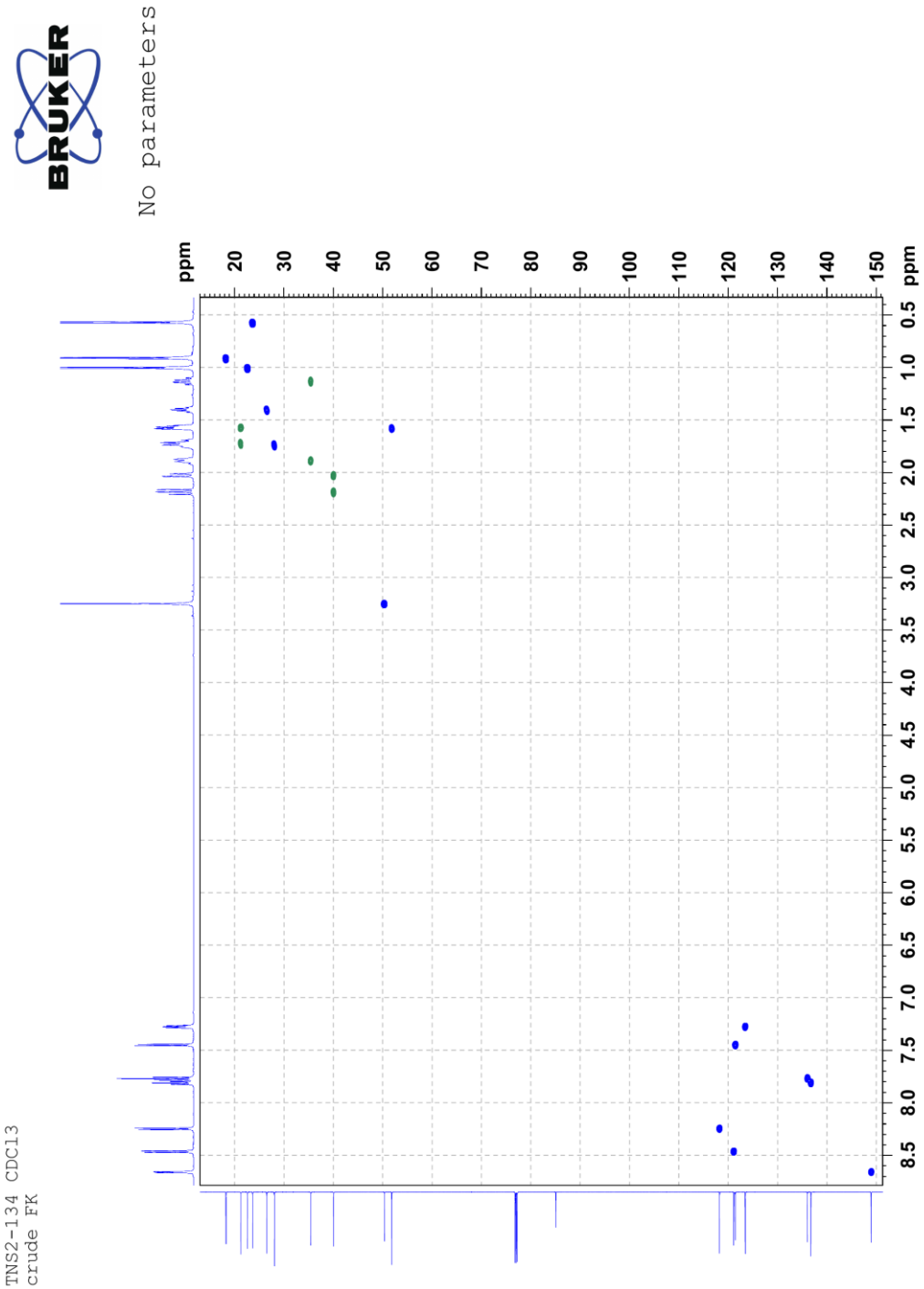

Appendix K Spectra of 2,6-disubstituted Pyridine Methyl Ethers, 12-OMe and 15-OMe

Appendix K.35 **^{1}H,^{13}C-HMBC NMR Spectrum of Pyridine Methyl Ether 15h-OMe**

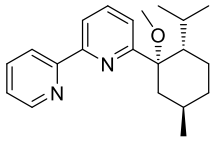

15h-OMe

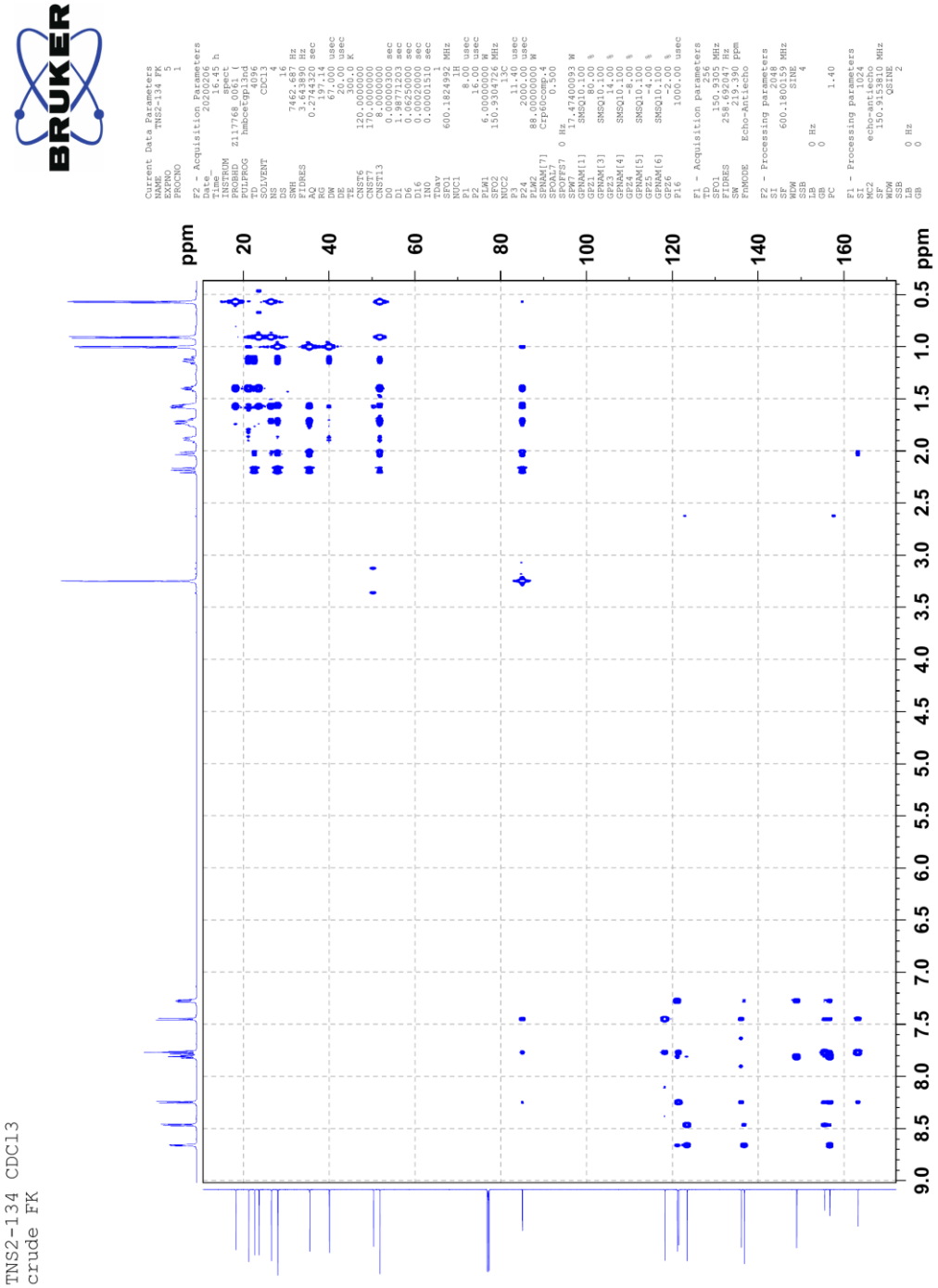

Appendix K Spectra of 2,6-disubstituted Pyridine Methyl Ethers, 12-OMe and 15-OMe

Appendix K.36 **^{1}H,^{15}N-HMBC NMR Spectrum of Pyridine Methyl Ether 15h-OMe**

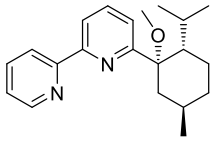

15h-OMe

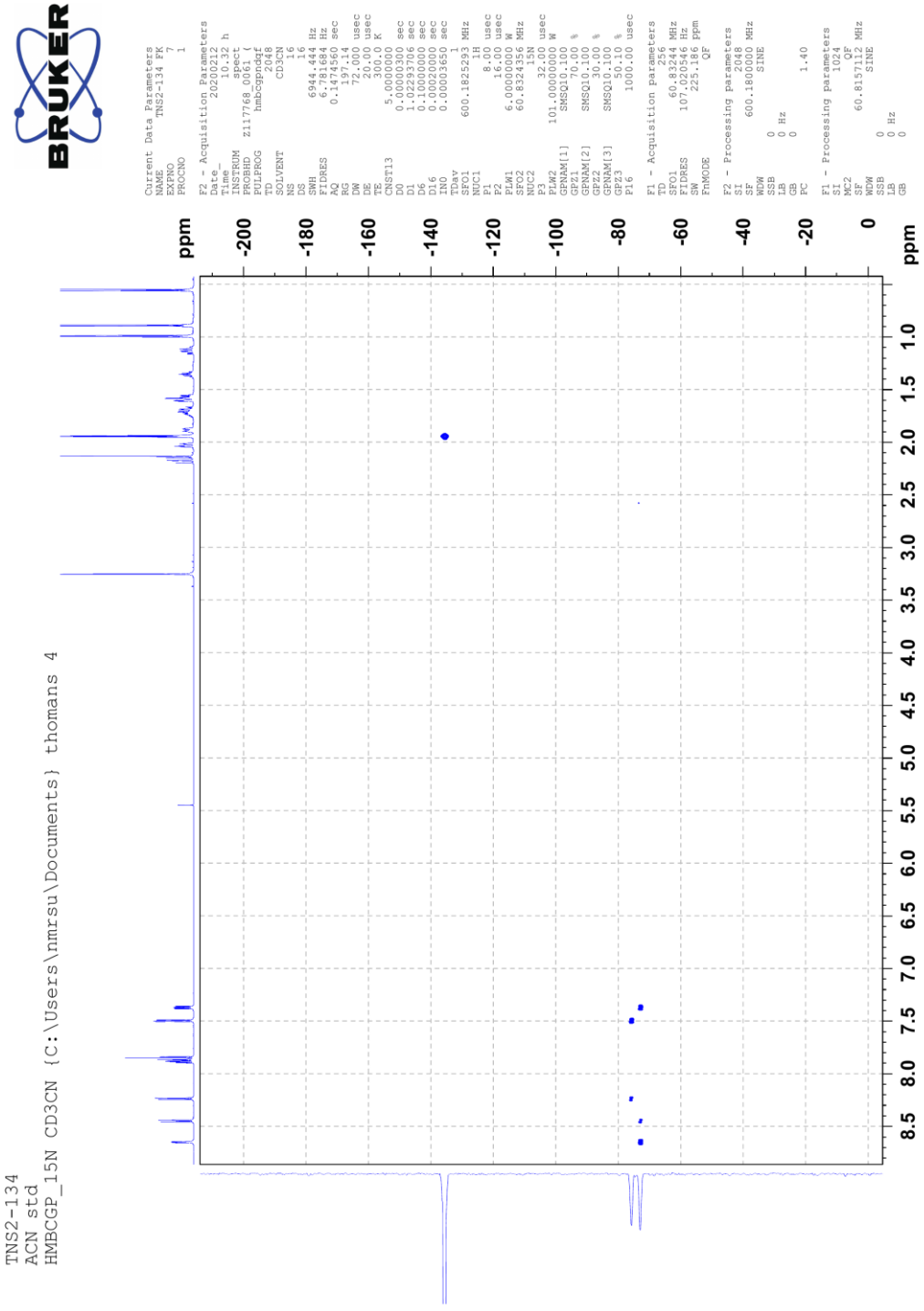

Appendix K.37 **HRMS Spectrum of Pyridine Methyl Ether 15h-OMe**

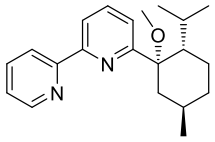

15h-OMe

Elemental Composition Report **Page 1**

Single Mass Analysis
Tolerance = 3.0 PPM / DBE: min = -5.0, max = 50.0
Element prediction: Off
Number of isotope peaks used for i-FIT = 3

Monoisotopic Mass, Even Electron Ions
2641 formula(e) evaluated with 1 results within limits (all results (up to 1000) for each mass)
Elements Used:
C: 0-100 H: 0-100 N: 0-5 O: 0-10 Si: 0-3 Cl: 0-2
2020_43 66 (1.311) AM2 (Ar,35000.0,0.00,0.00); Cm (57:71)
1: TOF MS ASAP+

2.51e+006

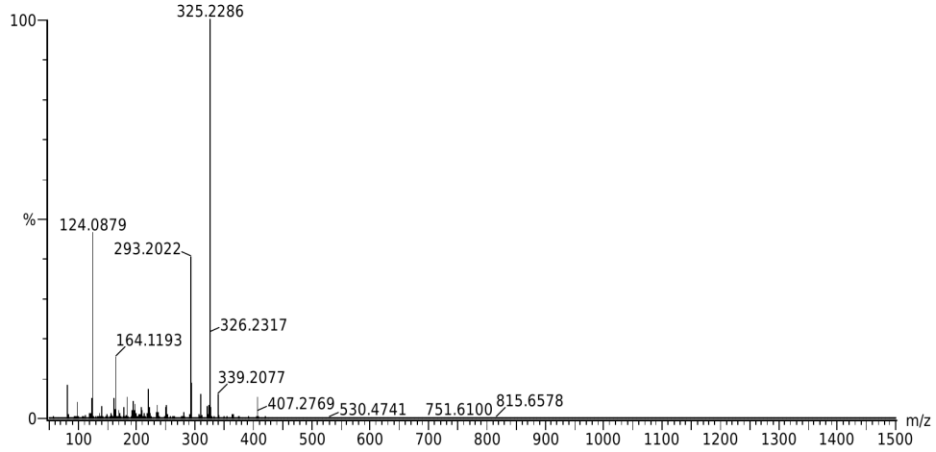

Minimum:				-5.0				
Maximum:		5.0	3.0	50.0				
Mass	Calc. Mass	mDa	PPM	DBE	i-FIT	Norm	Conf(%)	Formula
325.2286	325.2280	0.6	1.8	8.5	1265.6	n/a	n/a	C21 H29 N2 O

Appendix L **Spectra of α,β-unsaturated ketone, 19**

Appendix L.1 **^{1}H NMR Spectrum of α,β-unsaturated ketone 19**

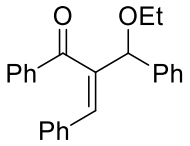

19

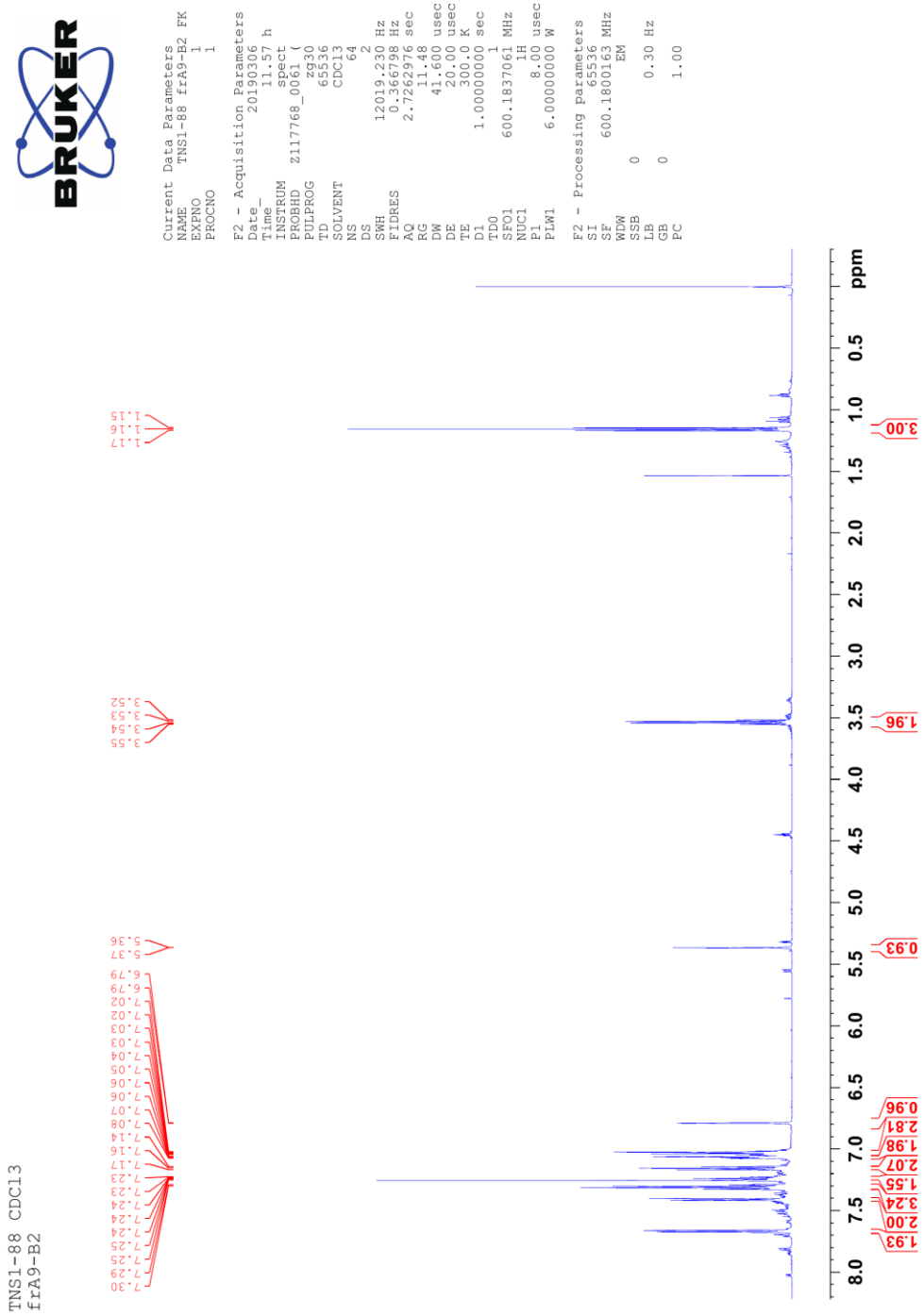

Appendix L Spectra of **α,β**-unsaturated ketone, 19

Appendix L.2 **^{13}C NMR Spectrum of α,β-unsaturated ketone 19**

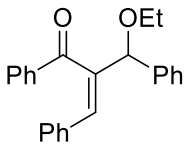

19

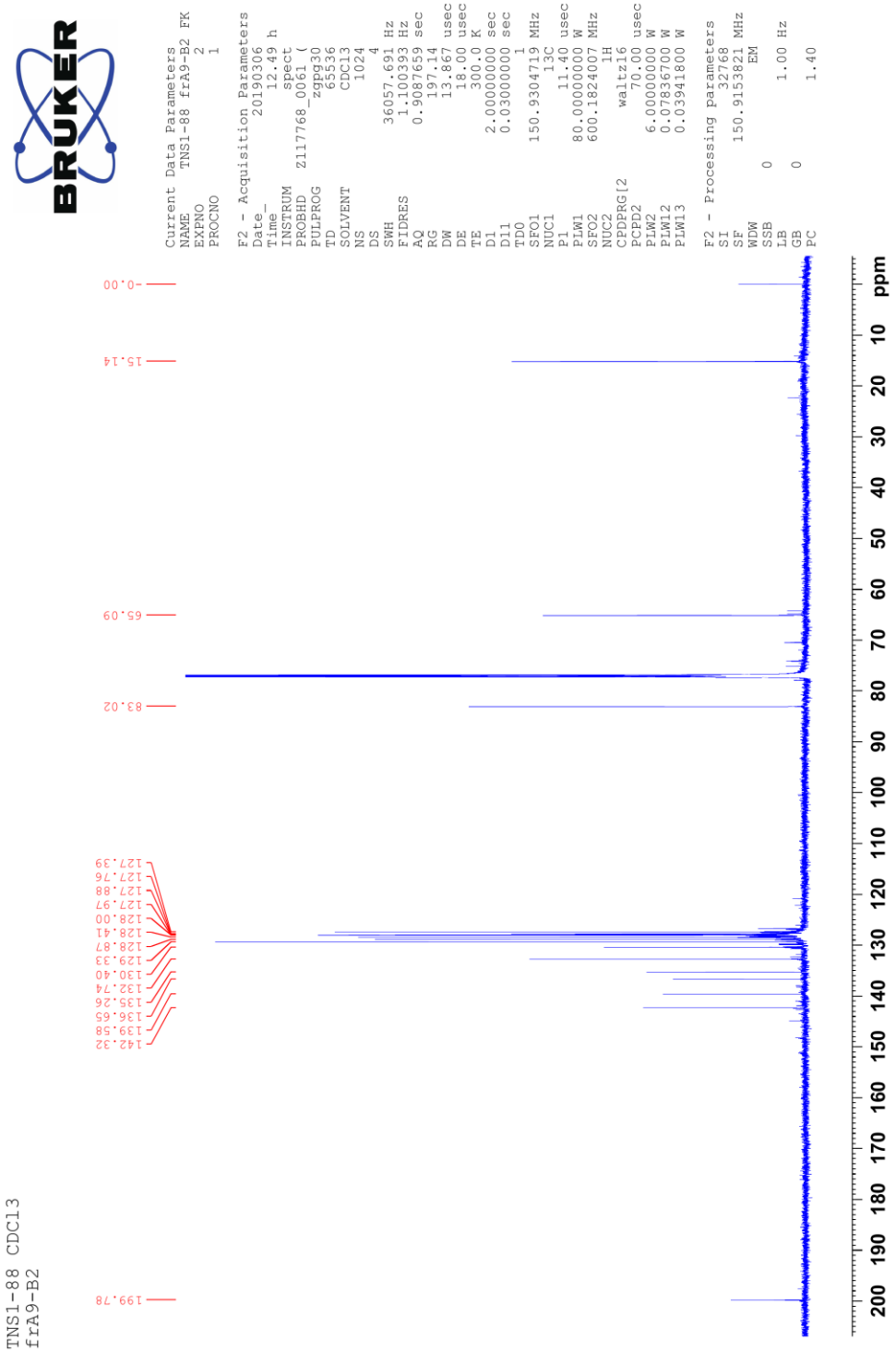

Appendix L Spectra of **α,β**-unsaturated ketone, 19

Appendix L.3 **COSY NMR Spectrum of α,β-unsaturated ketone 19**

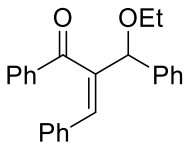

19

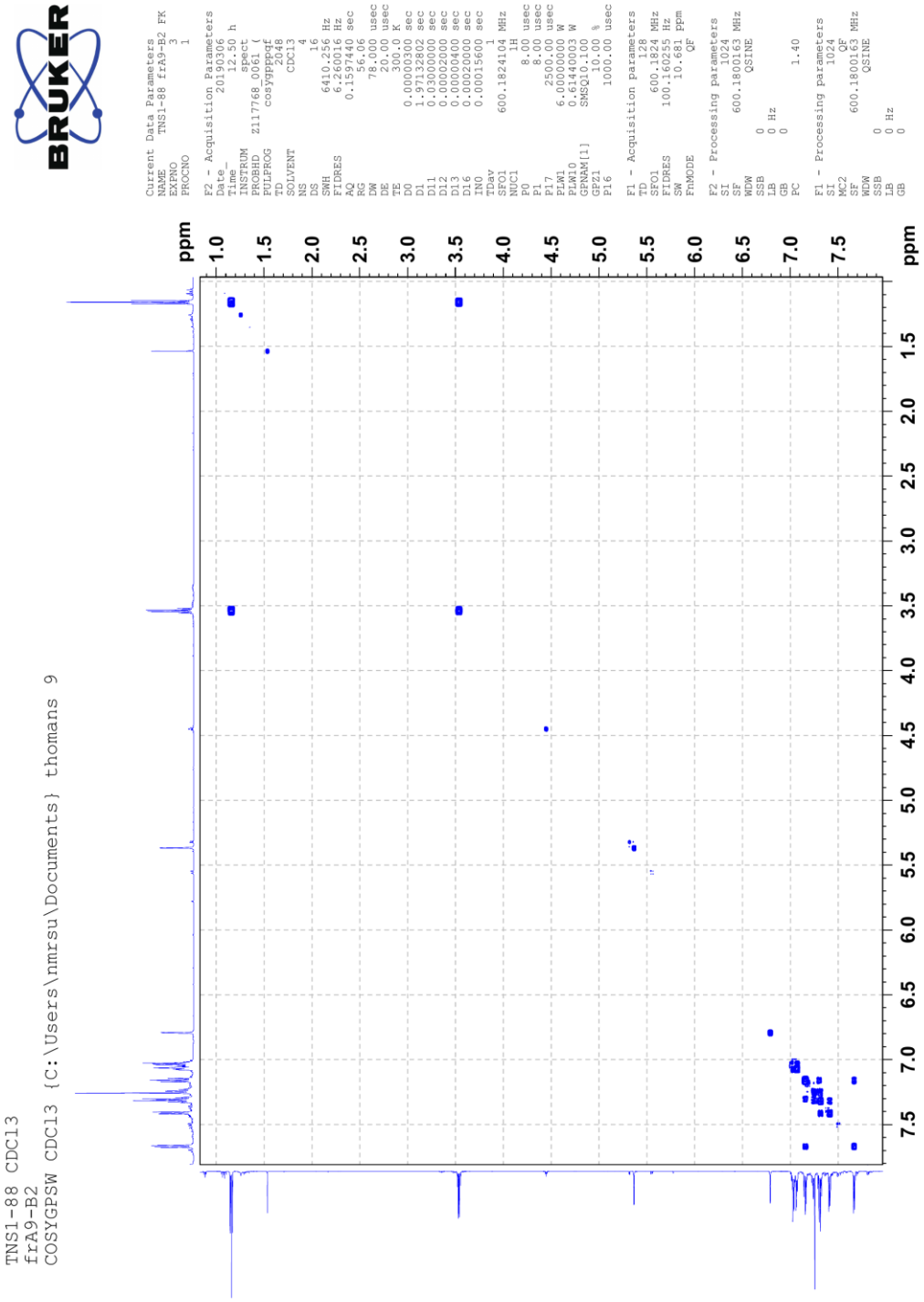

Appendix L Spectra of **α,β**-unsaturated ketone, 19

Appendix L.4 **HSQC NMR Spectrum of α,β-unsaturated ketone 19**

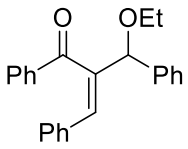

19

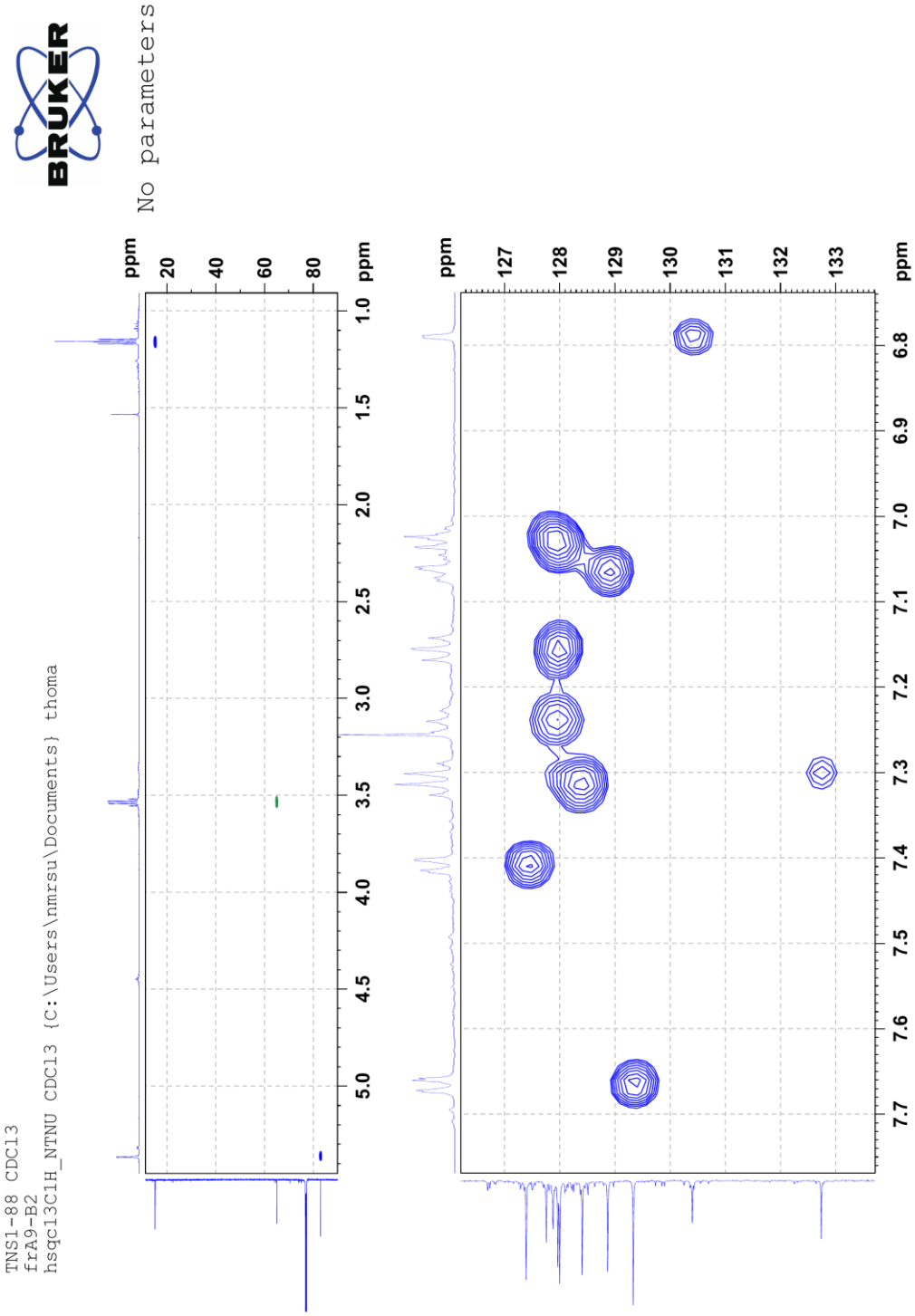

Appendix L Spectra of **α,β**-unsaturated ketone, 19

Appendix L.5 **HMBC NMR Spectrum of α,β-unsaturated ketone 19**

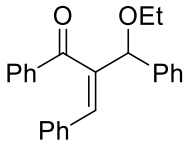

19

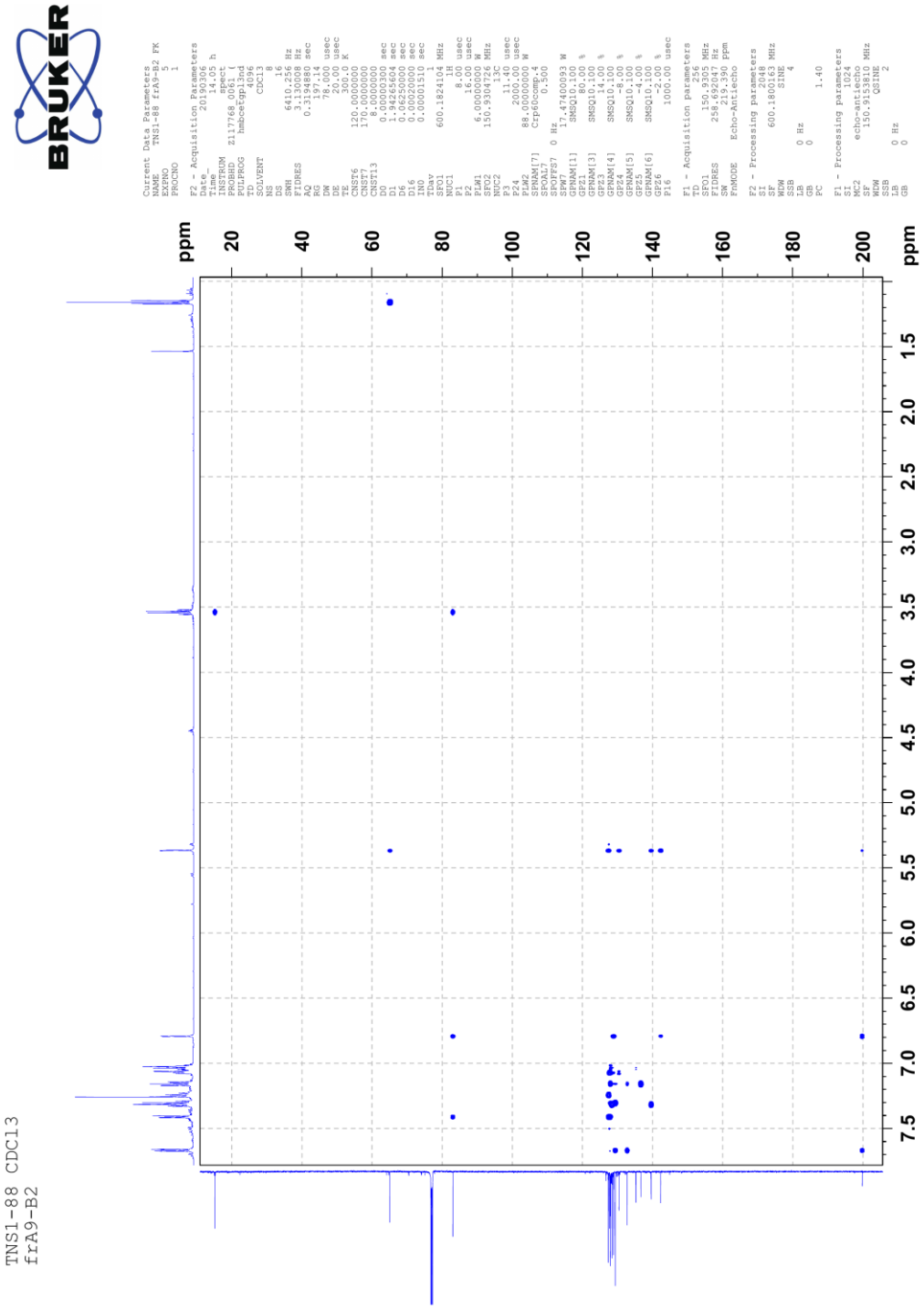

Appendix L Spectra of **α,β**-unsaturated ketone, 19

Appendix L.6 **NOESY NMR Spectrum of α,β-unsaturated ketone 19**

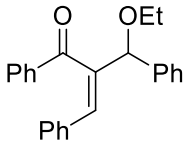

19

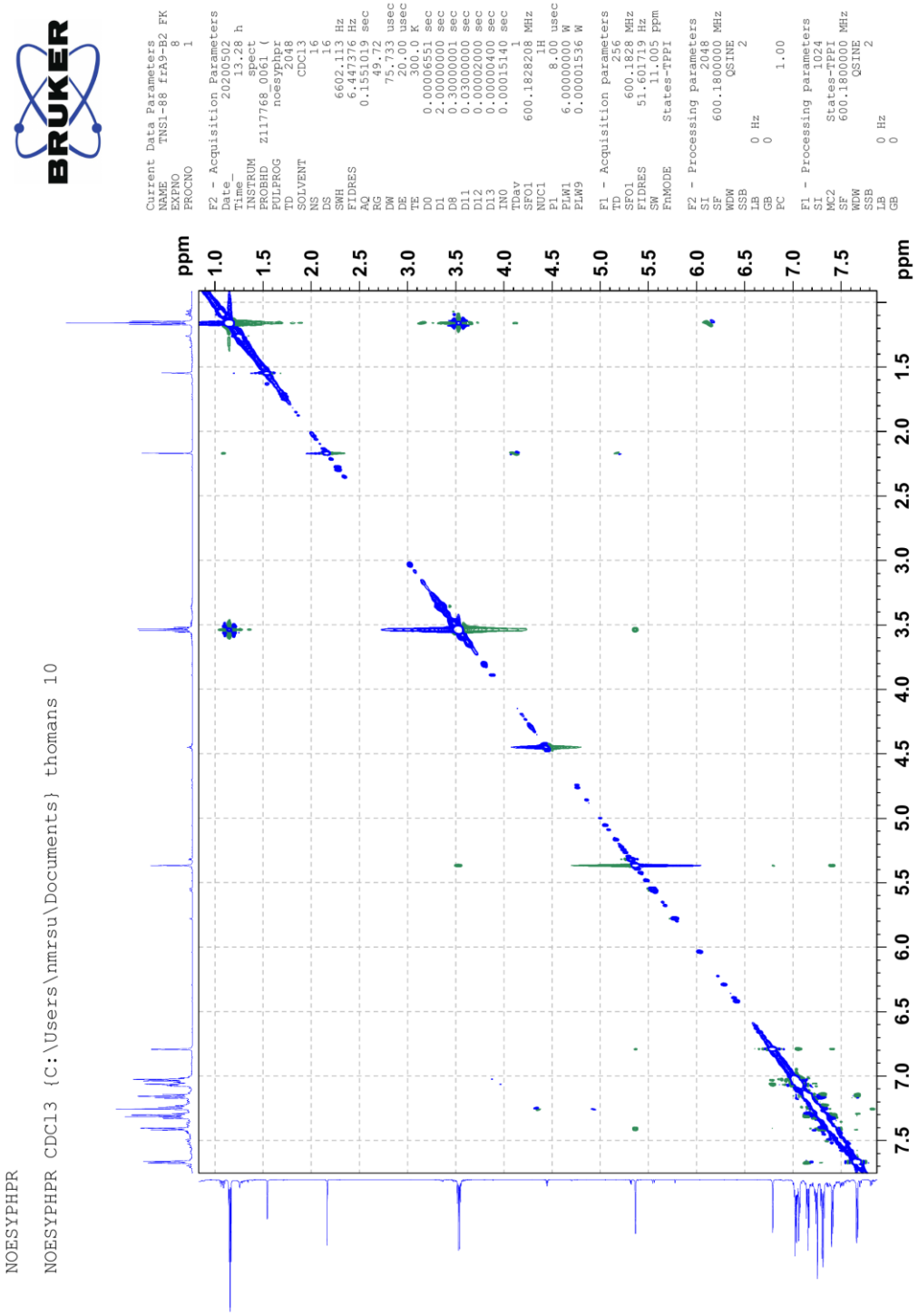

Appendix L Spectra of **α,β**-unsaturated ketone, 19

Appendix L.7 **HRMS Spectrum of α,β-unsaturated ketone 19**

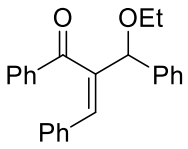

19

Elemental Composition Report **Page 1**

Single Mass Analysis
Tolerance = 5.0 PPM / DBE: min = -2.0, max = 50.0
Element prediction: Off
Number of isotope peaks used for i-FIT = 3

Monoisotopic Mass, Even Electron Ions
299 formula(e) evaluated with 2 results within limits (all results (up to 1000) for each mass)
Elements Used:
C: 0-100 H: 0-150 O: 0-10 Na: 0-1 Br: 0-3 Au: 0-3

2019-121 81 (0.768) AM2 (Ar,35000.0,0.00,0.00); Cm (79:93)
1: TOF MS ES+

1.14e+007

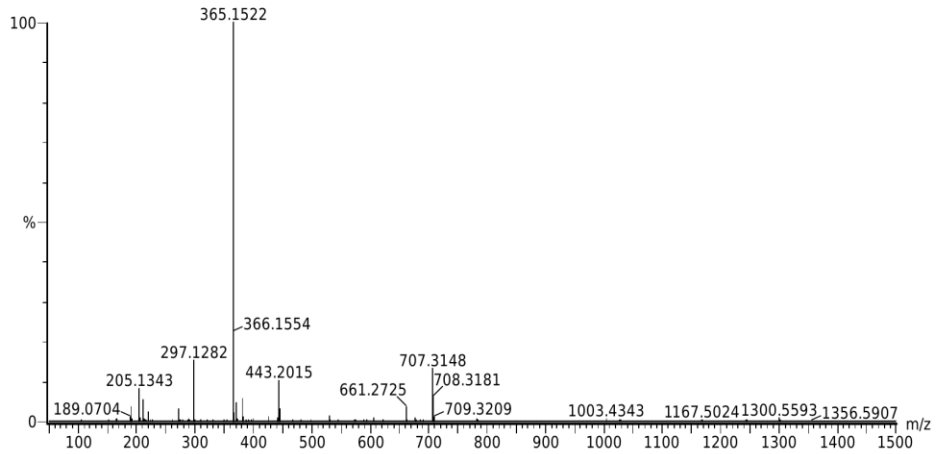

Minimum:				-2.0				
Maximum:		5.0	5.0	50.0				
Mass	Calc. Mass	mDa	PPM	DBE	i-FIT	Norm	Conf(%)	Formula
365.1522	365.1519	0.3	0.8	-1.5	1489.8	3.544	2.89	C10 H25 Na Au
	365.1517	0.5	1.4	13.5	1486.3	0.029	97.11	C24 H22 O2 Na

Appendix M Spectra of cyclopropane 20

Appendix M.1 ^{1}H NMR Spectrum of *trans*-cyclopropane 20

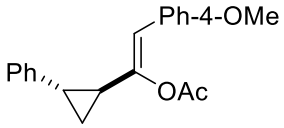

20

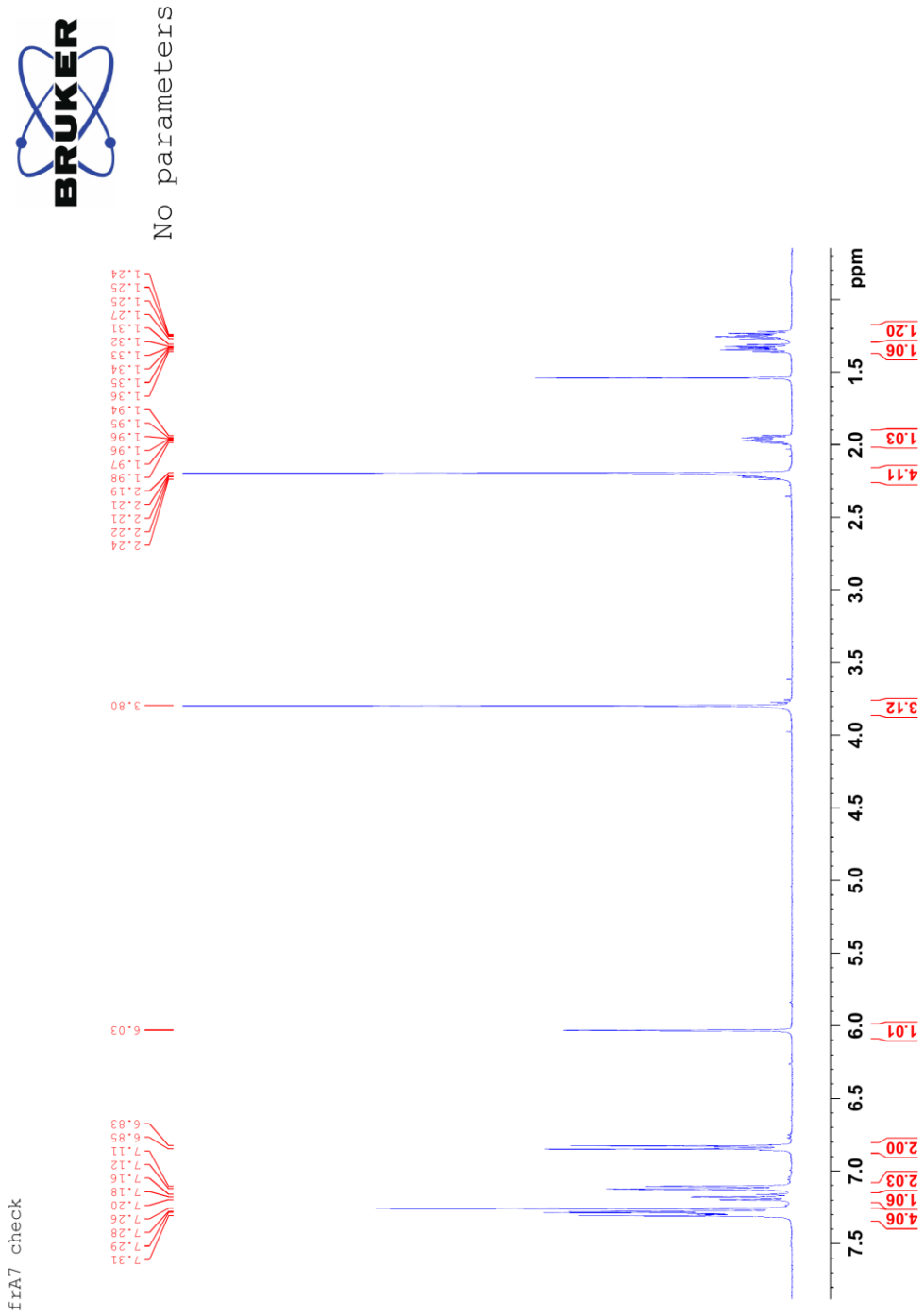

Appendix M Spectra of cyclopropane 20

Appendix M.2 **HPLC Spectrum isomer-mixture of** 20**, prepared using Au(III)-15h-NTf$_2$**

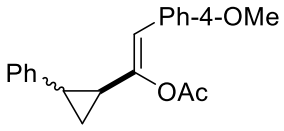

20

```
Data File C:\CHEM32\1\DATA\THOMASSOLVI\TNS3-020-000008.D
Sample Name: sample

    ========================================================================
    Acq. Operator   : Thomas Solvi
    Acq. Instrument : Instrument 1                    Location :   -
    Injection Date  : 5/4/2020 2:20:46 PM
    Acq. Method     : C:\CHEM32\1\METHODS\THOMAS NORDBØ SOLVI\TNS_CYCLOPROP.M
    Last changed    : 5/4/2020 2:18:12 PM by Thomas Solvi
    Analysis Method : C:\CHEM32\1\DATA\THOMASSOLVI\TNS3-020000000.D\DA.M (TNS_CYCLOPROP.M)
    Last changed    : 5/4/2020 3:07:18 PM by Morten Gundersen
                      (modified after loading)
    Method Info     : AD-H kolonne, iPrOH:hex 10:90, 0.8 mL/min

    Sample Info     : Heksan:iPrOH 95:5, AD-H 5 um, 0.8 mL/min
                      sample, 1 uL


    Additional Info : Peak(s) manually integrated
```

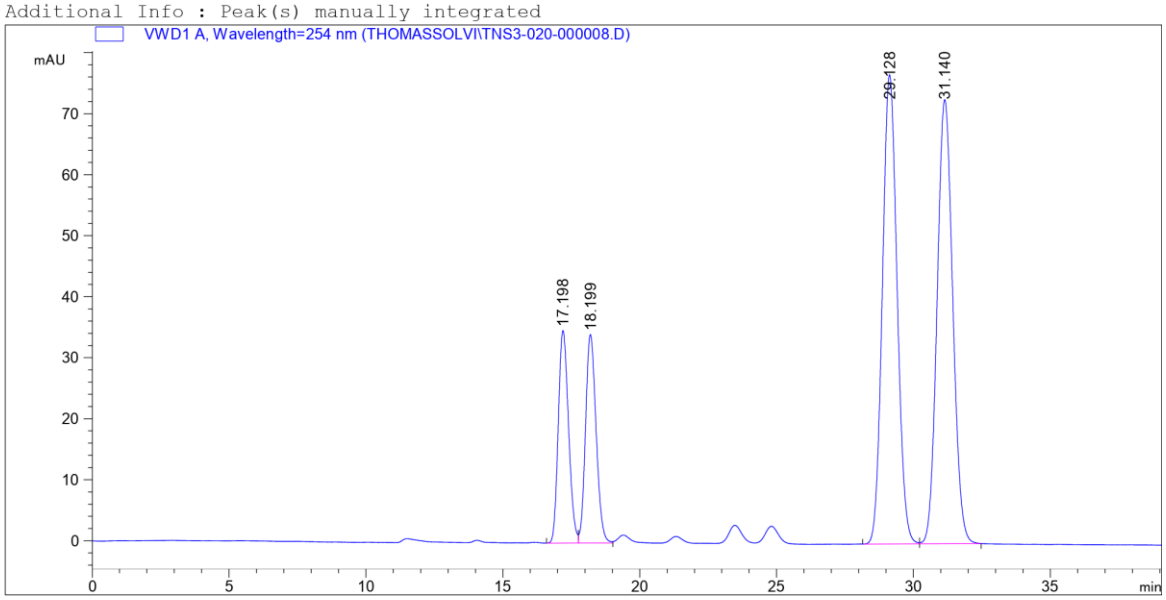


```
    ========================================================================
                               Area Percent Report
    ========================================================================

    Sorted By             :      Signal
    Multiplier:                   :      1.0000
    Dilution:                     :      1.0000
    Use Multiplier & Dilution Factor with ISTDs


    Signal 1: VWD1 A, Wavelength=254 nm

    Peak RetTime Type  Width     Area      Height     Area
      #   [min]        [min]  mAU   *s    [mAU   ]      %
    ----|-------|----|-------|----------|----------|--------|
       1  17.198 BV    0.3054  906.83063   34.84491  11.9747
       2  18.199 VV    0.3220  917.03180   34.18813  12.1094
       3  29.128 BV    0.4686 2862.45190   76.93575  37.7985
       4  31.140 VB    0.4749 2886.60278   72.81766  38.1174

Instrument 1 5/4/2020 3:07:25 PM Morten Gundersen                Page   1 of 2
```

Appendix N Spectra of Au(III)-complexes

Appendix N.1 ^{1}H NMR Spectrum of Au(III)-Box complex XIII

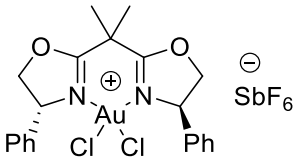

XIII

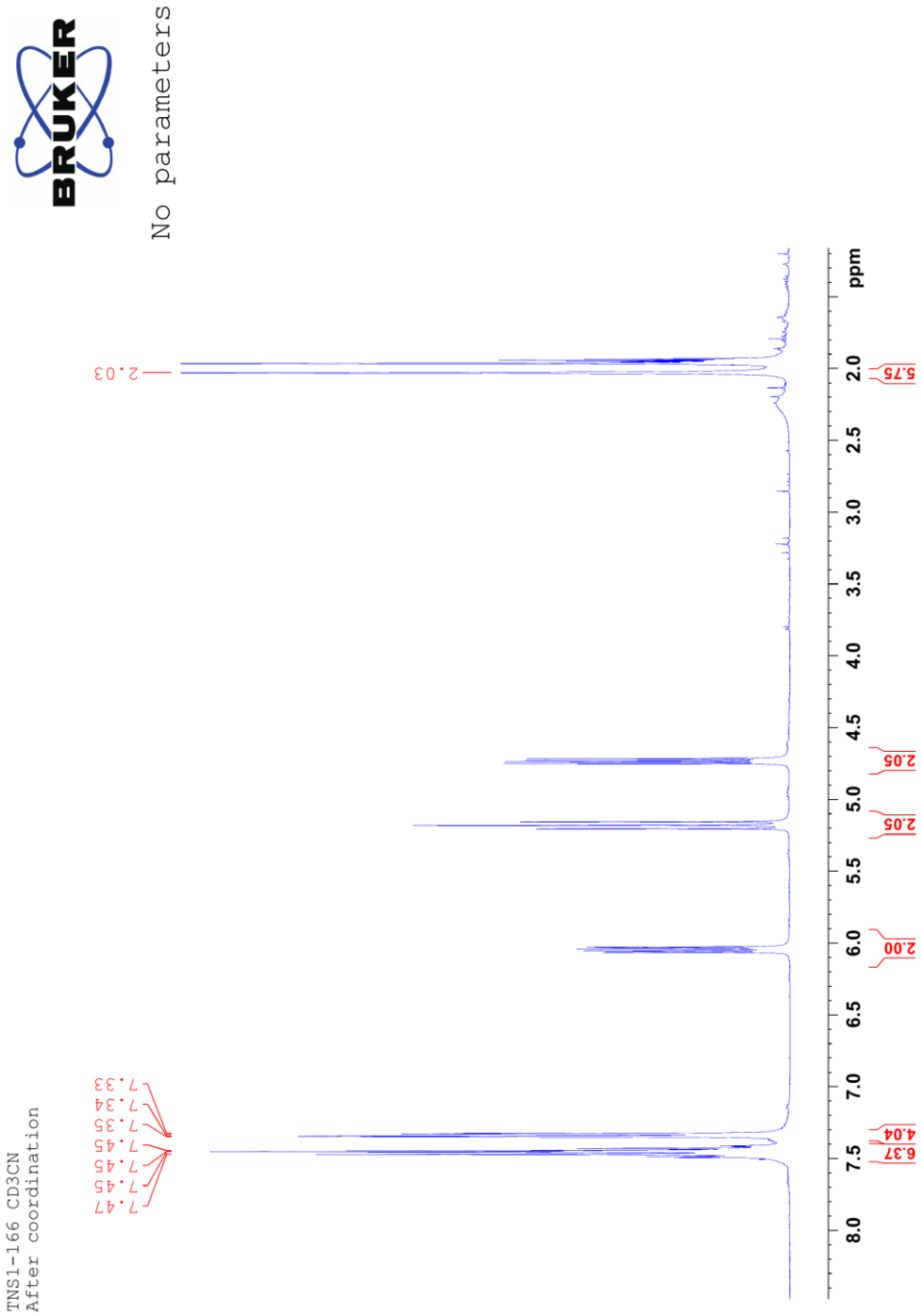

Appendix N Spectra of Au(III)-complexes

Appendix N.2 **^{1}H NMR Spectrum of Chiral Au(III)-N,N,O-tridentate Bipyridine complex Au(III)-15h-NTf$_2$**

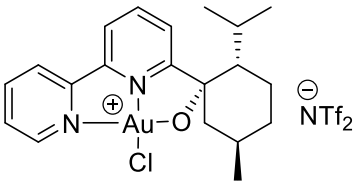

Au(III)-**15h**-NTf$_2$

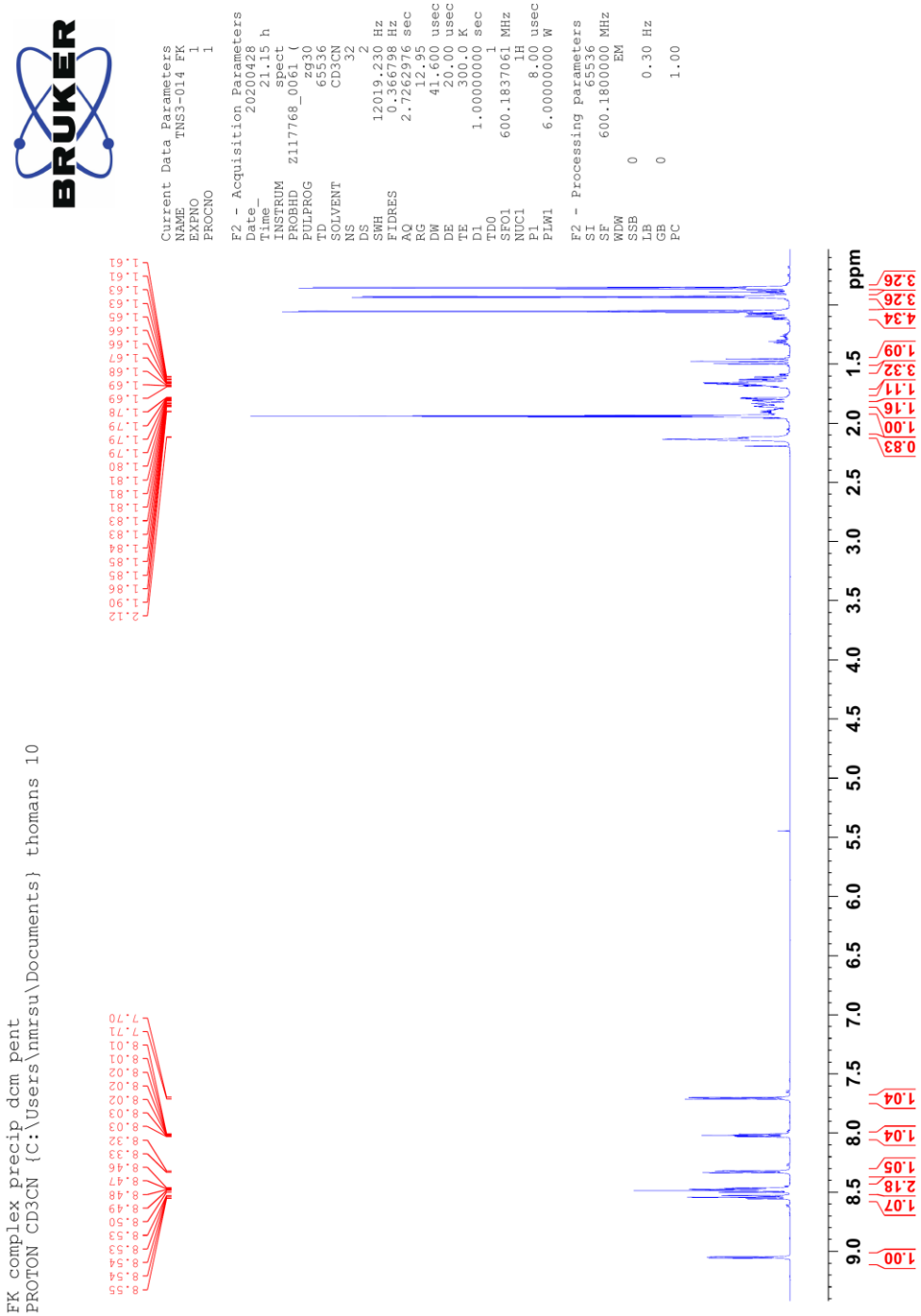

Appendix N.3 **^{13}C NMR Spectrum of Chiral Au(III)-N,N,O-tridentate Bipyridine complex Au(III)-15h-NTf$_2$**

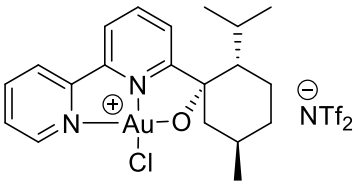

Au(III)-**15h**-NTf$_2$

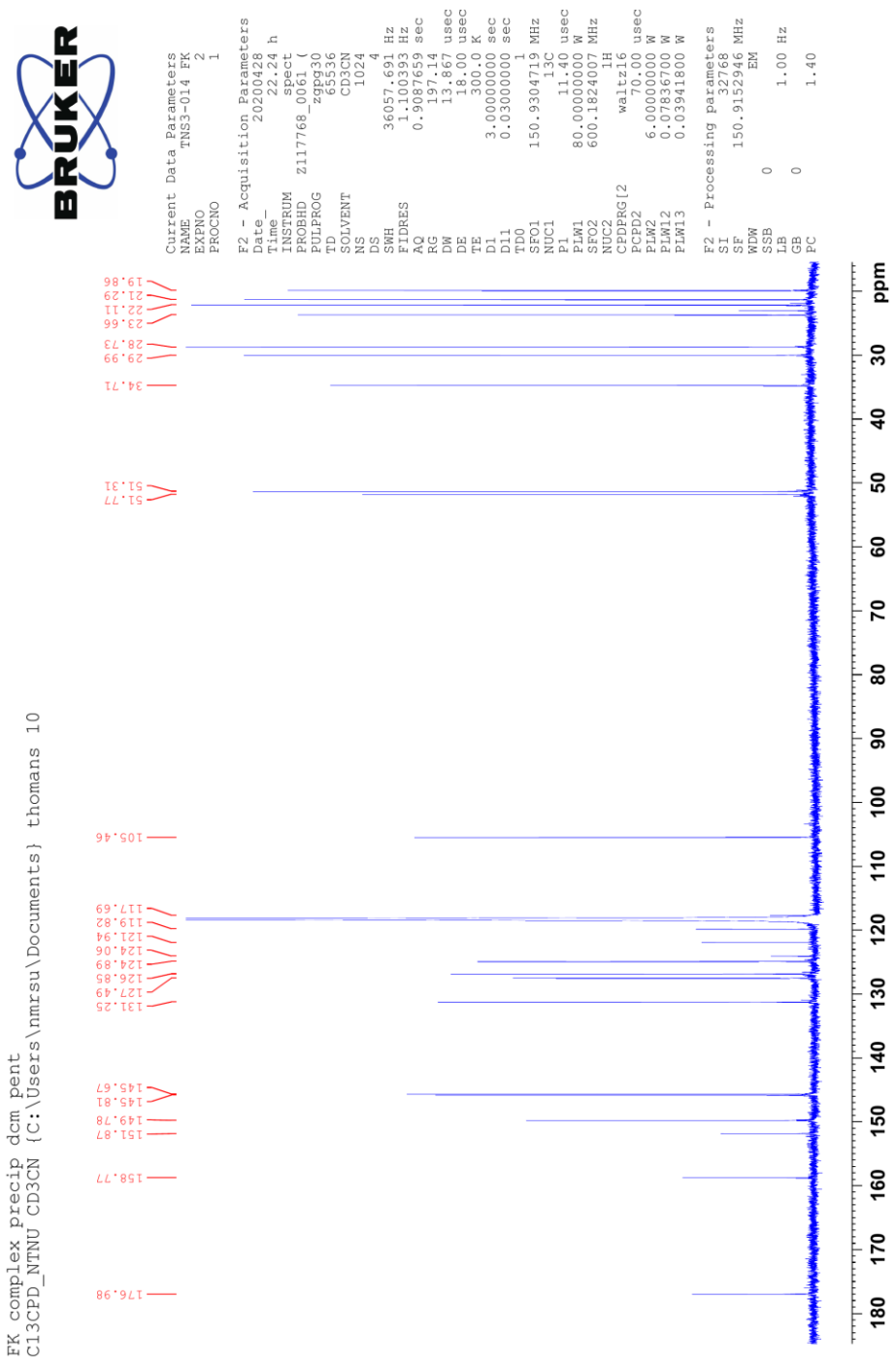

Appendix N Spectra of Au(III)-complexes

Appendix N.4 **^{19}F NMR Spectrum of Chiral Au(III)-N,N,O-tridentate Bipyridine complex Au(III)-15h-NTf$_2$**

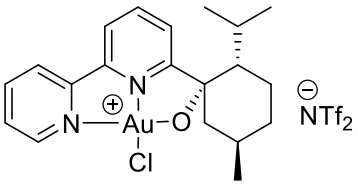

Au(III)-**15h**-NTf$_2$

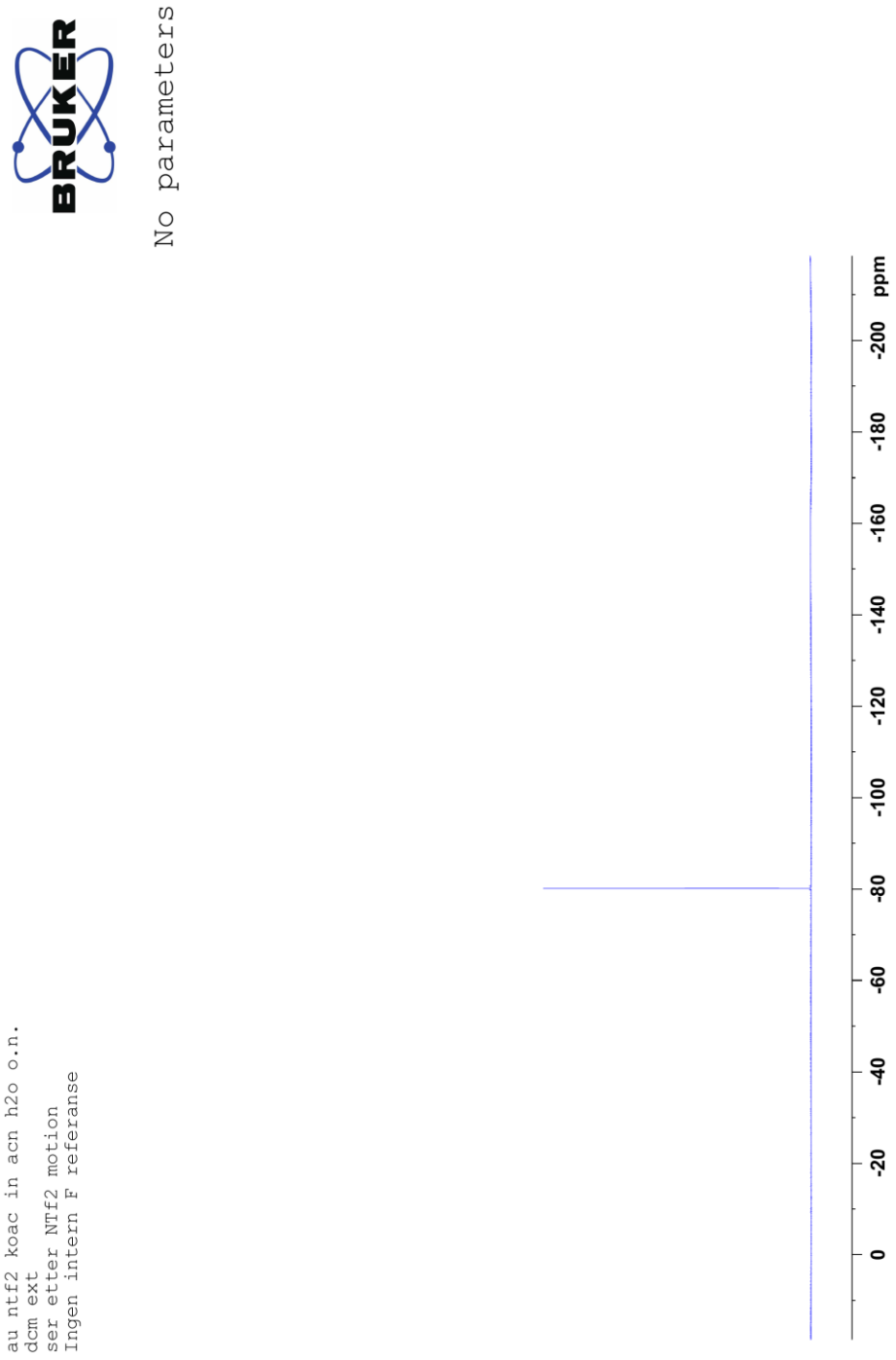

Appendix N.5 **COSY NMR Spectrum of Chiral Au(III)-N,N,O-tridentate Bipyridine complex Au(III)-15h-NTf$_2$**

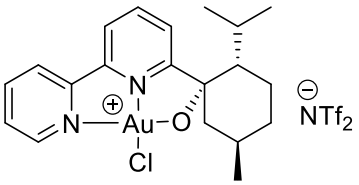

Au(III)-**15h**-NTf$_2$

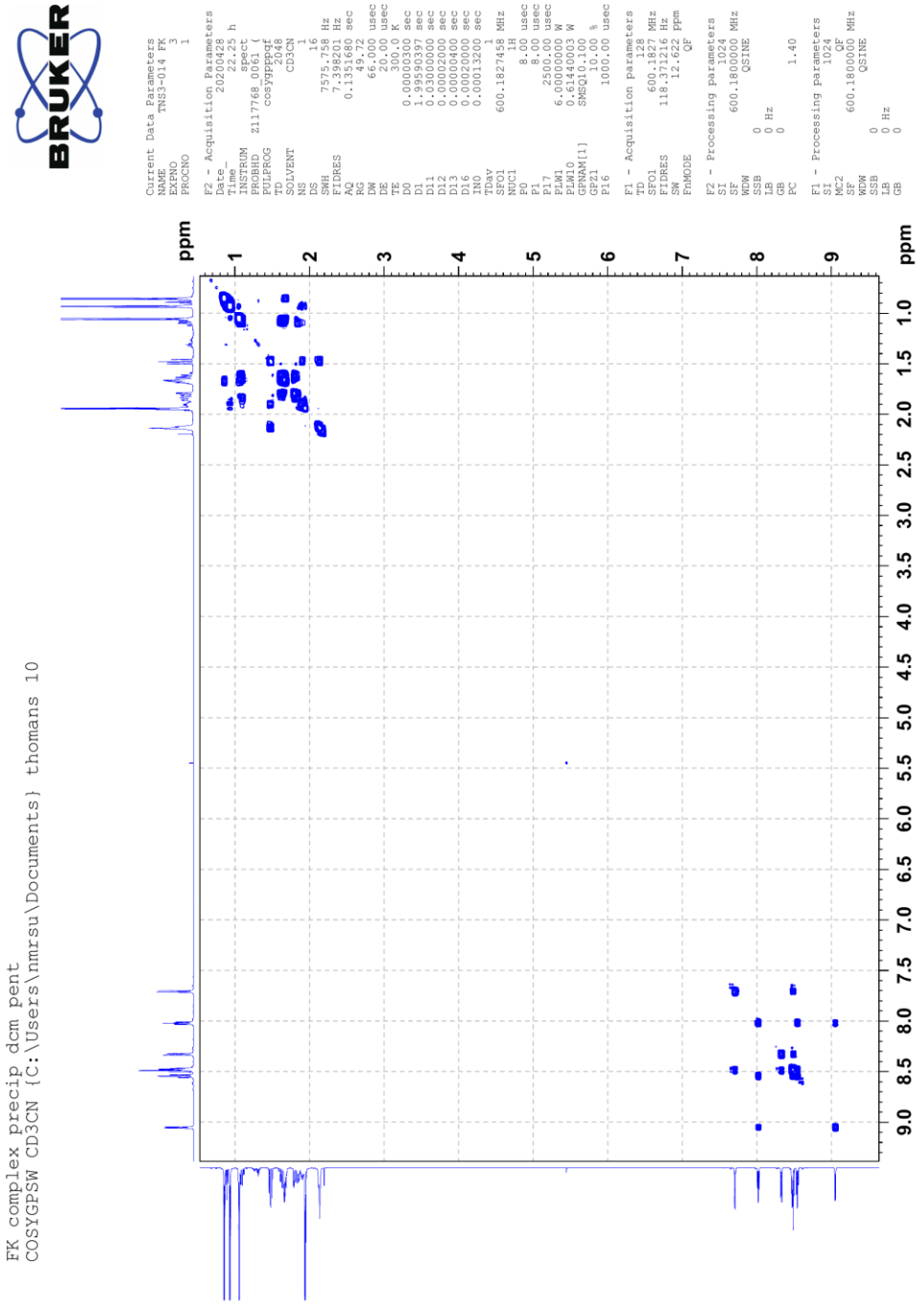

Appendix N Spectra of Au(III)-complexes

Appendix N.6 **HSQC NMR Spectrum of Chiral Au(III)-N,N,O-tridentate Bipyridine complex Au(III)-15h-NTf$_2$**

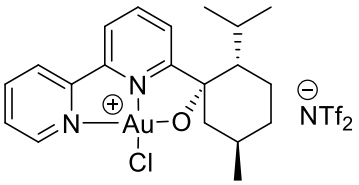

Au(III)-**15h**-NTf$_2$

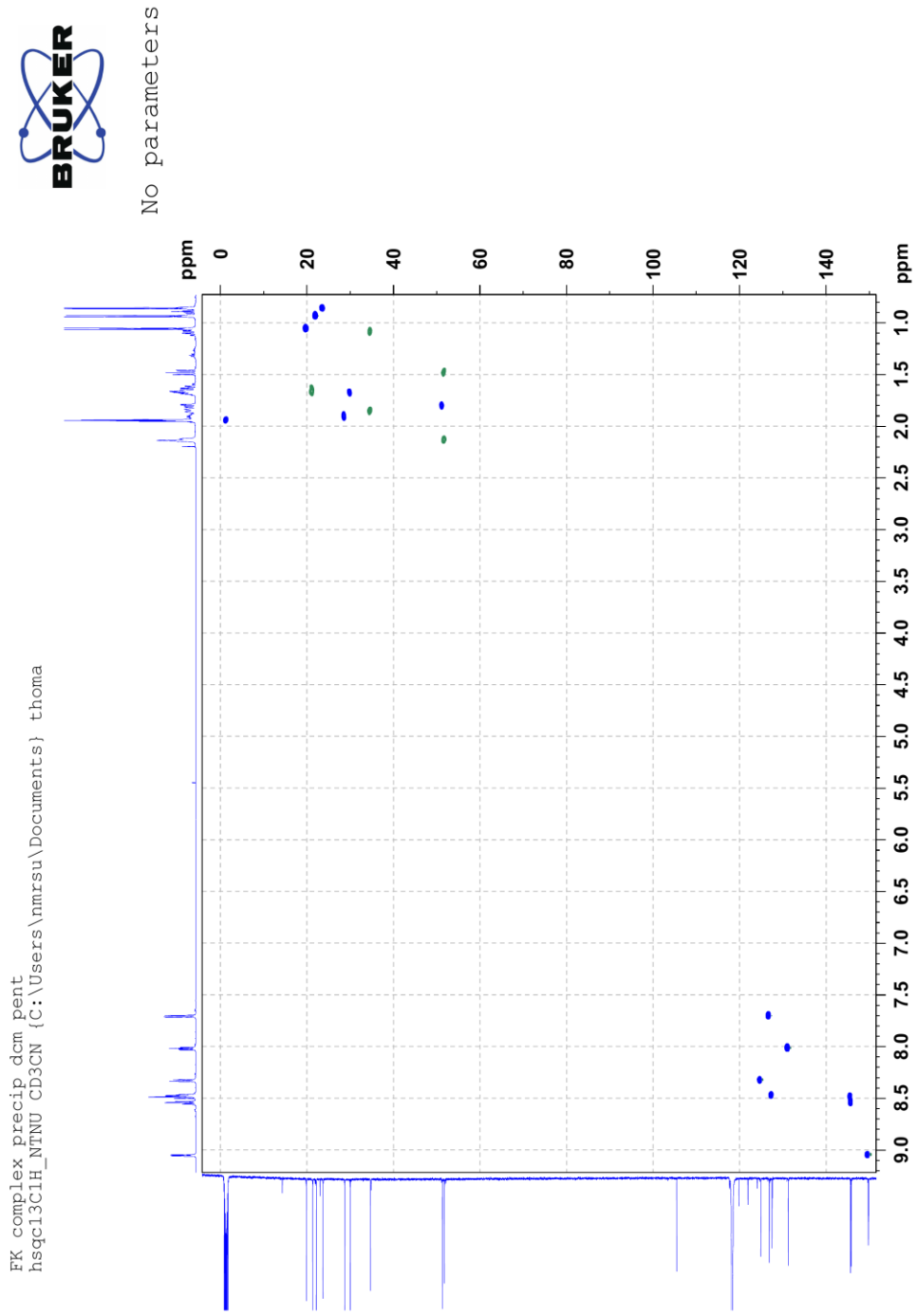

Appendix N.7 **^{1}H,^{13}C-HMBC NMR Spectrum of Chiral Au(III)-N,N,O-tridentate Bipyridine complex Au(III)-15h-NTf$_2$**

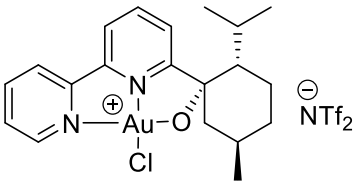

Au(III)-**15h**-NTf$_2$

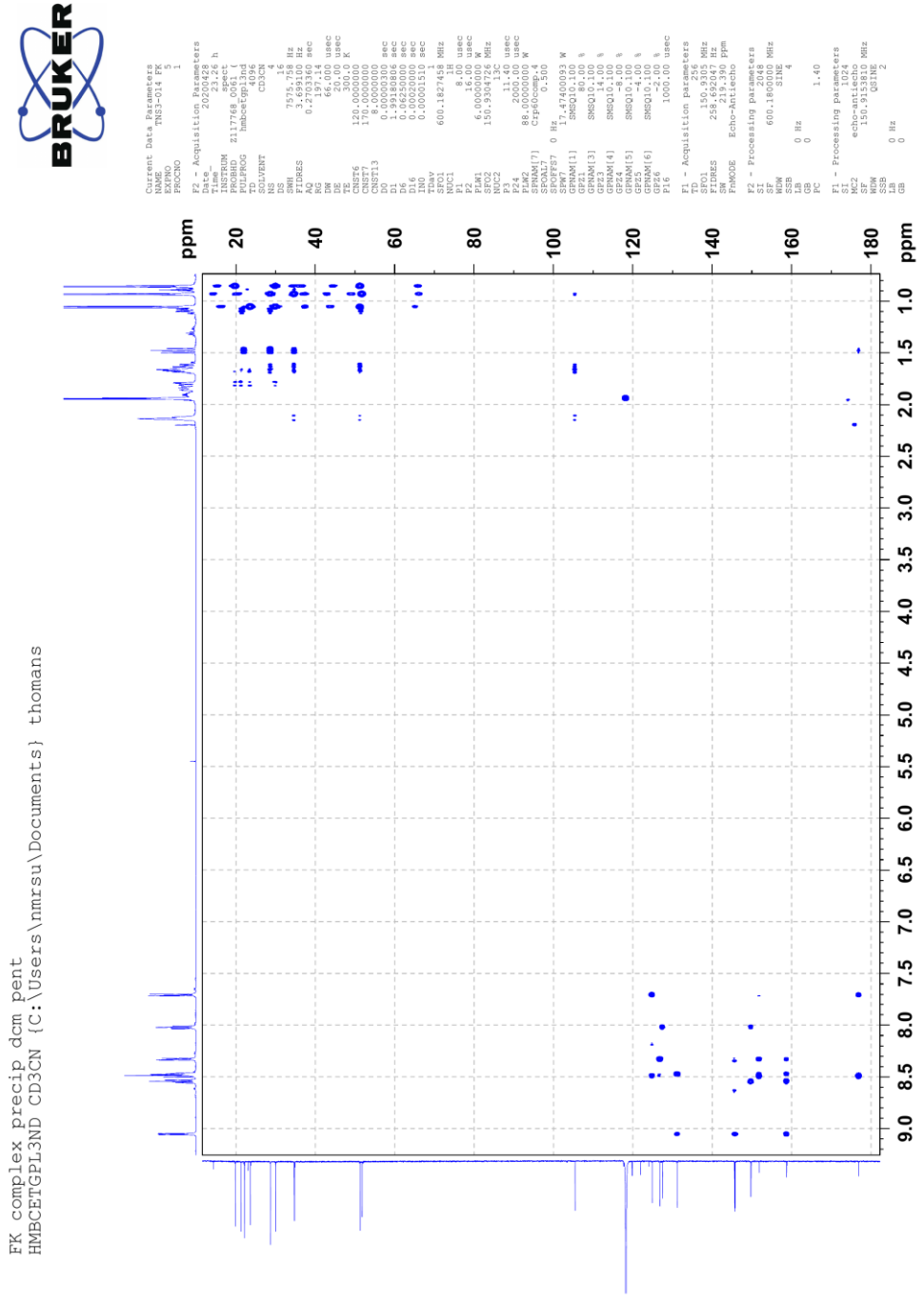

Appendix N.8 **^{1}H,^{15}N-HMBC NMR Spectrum of Chiral Au(III)-N,N,O-tridentate Bipyridine complex Au(III)-15h-NTf$_2$**

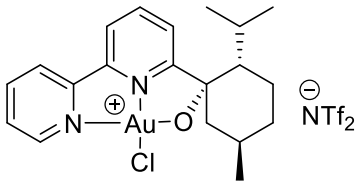

Au(III)-**15h**-NTf$_2$

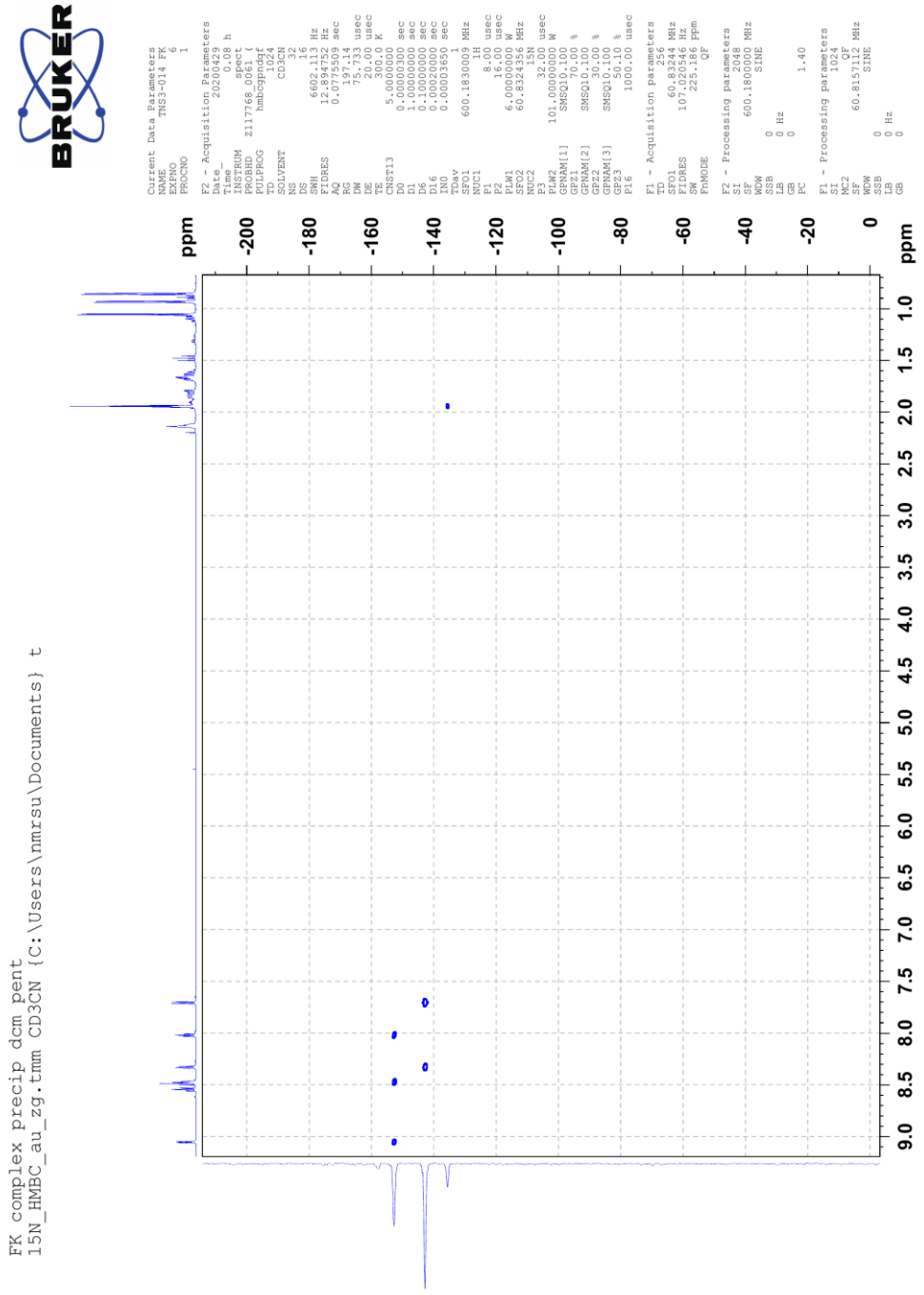

Appendix N Spectra of Au(III)-complexes

Appendix N.9 **IR Spectrum of Chiral Au(III)-N,N,O-tridentate Bipyridine complex Au(III)-15h-NTf$_2$**

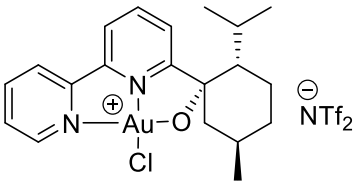

Au(III)-**15h**-NTf$_2$

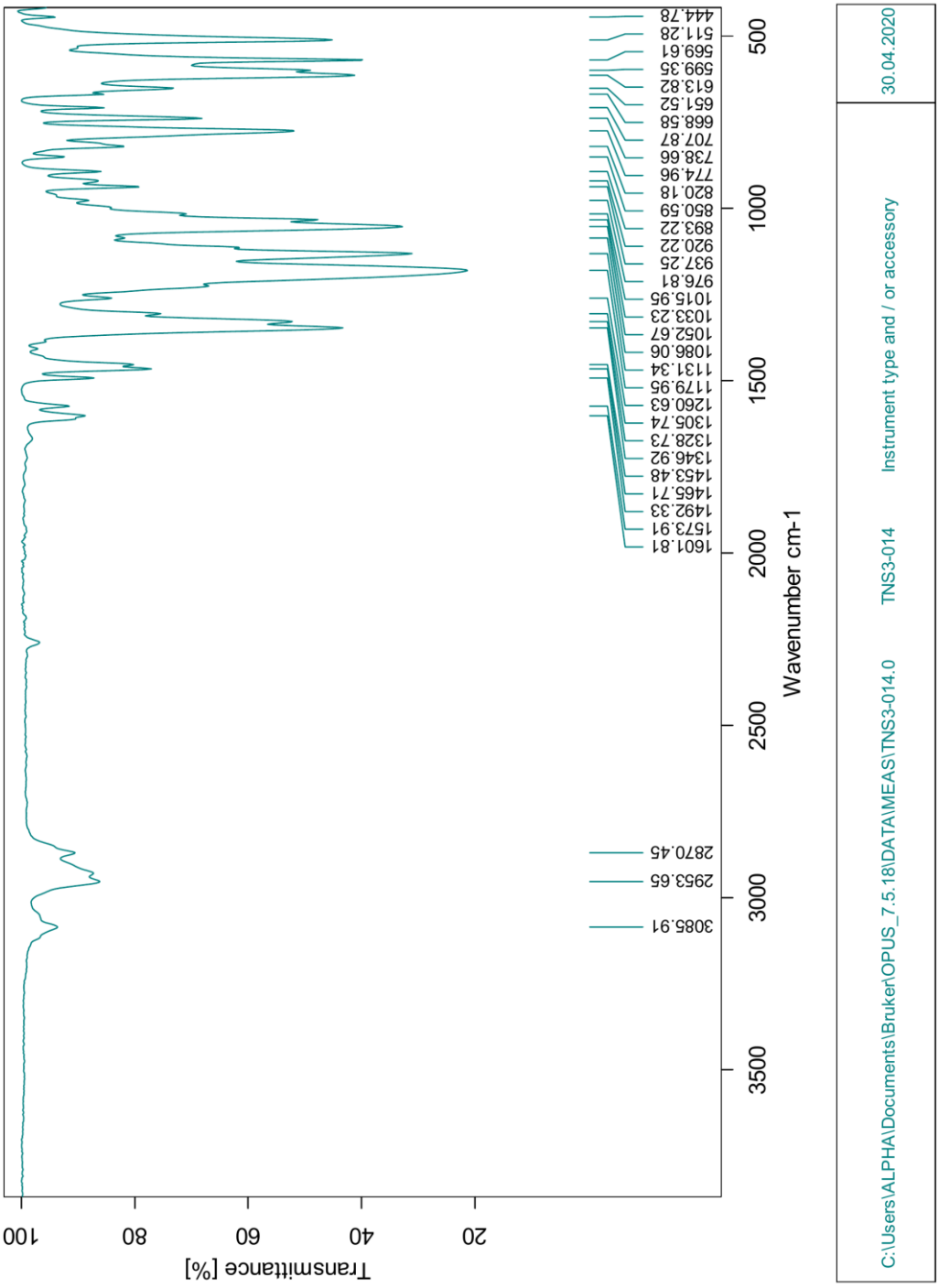

Appendix N Spectra of Au(III)-complexes

Appendix N.10 **HRMS Spectra of Chiral Au(III)-N,N,O-tridentate Bipyridine complex Au(III)-15h-NTf$_2$**

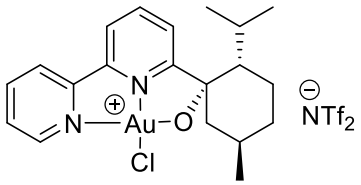

Au(III)-**15h**-NTf$_2$

Elemental Composition Report **Page 1**

Single Mass Analysis
Tolerance = 2.0 PPM / DBE: min = -5.0, max = 50.0
Element prediction: Off
Number of isotope peaks used for i-FIT = 3

Monoisotopic Mass, Even Electron Ions
10457 formula(e) evaluated with 20 results within limits (all results (up to 1000) for each mass)
Elements Used:
C: 0-100 H: 0-100 N: 0-10 O: 0-10 Na: 0-1 Cl: 0-4 Au: 0-3

2020_58 363 (3.369) AM2 (Ar,35000.0,0.00,0.00); Cm (363:371)
1: TOF MS ES+

2.87e+007

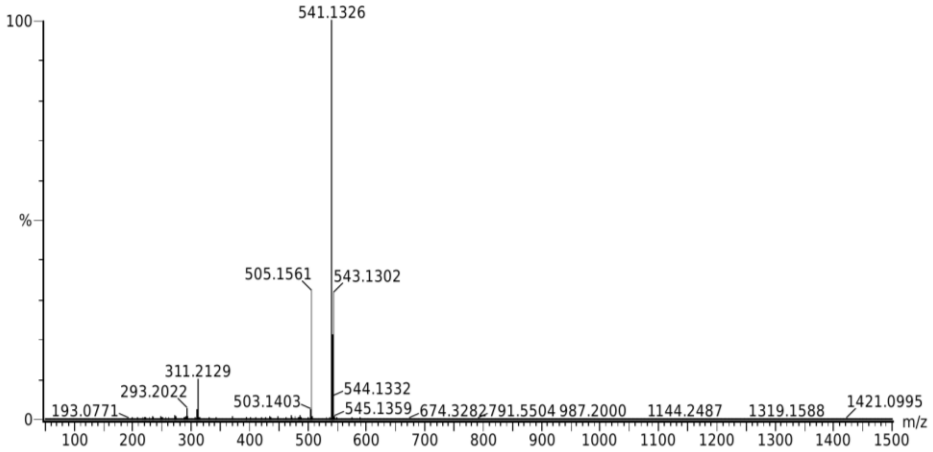

Minimum:				-5.0				
Maximum:		5.0	2.0	50.0				
Mass	Calc. Mass	mDa	PPM	DBE	i-FIT	Norm	Conf(%)	Formula
541.1326	541.1321	0.5	0.9	9.5	1124.4	0.023	97.71	C20 H25 N2 O Cl Au
	541.1327	-0.1	-0.2	13.5	1128.2	3.821	2.19	C21 H23 N8 O6 Na Cl
	541.1329	-0.3	-0.6	-1.5	1132.5	8.072	0.03	C7 H26 N8 O4 Na Cl Au
	541.1332	-0.6	-1.1	3.5	1132.8	8.362	0.02	C19 H32 N2 O10 Na Cl2
	541.1319	0.7	1.3	24.5	1133.2	8.738	0.02	C34 H22 N2 O3 Cl
	541.1329	-0.3	-0.6	7.5	1133.2	8.788	0.02	C17 H27 N8 O8 Cl2
	541.1329	-0.3	-0.6	15.5	1133.8	9.418	0.01	C28 H28 N4 O Cl3
	541.1323	0.3	0.6	7.5	1135.0	10.584	0.00	C25 H34 N2 O Na Cl4
	541.1335	-0.9	-1.7	25.5	1135.1	10.648	0.00	C37 H23 O Na Cl
	541.1323	0.3	0.6	-0.5	1135.3	10.924	0.00	C14 H33 N6 O8 Na Cl3
	541.1315	1.1	2.0	10.5	1135.7	11.300	0.00	C27 H32 O5 Cl3
	541.1337	-1.1	-2.0	4.5	1135.9	11.451	0.00	C15 H29 N10 O4 Na Cl3
	541.1317	0.9	1.7	-4.5	1136.0	11.562	0.00	C13 H35 O3 Cl3 Au

Appendix N Spectra of Au(III)-complexes

Elemental Composition Report **Page 1**

Single Mass Analysis
Tolerance = 10.0 PPM / DBE: min = -5.0, max = 50.0
Element prediction: Off
Number of isotope peaks used for i-FIT = 3

Monoisotopic Mass, Even Electron Ions
2299 formula(e) evaluated with 2 results within limits (all results (up to 1000) for each mass)
Elements Used:
C: 0-100 H: 0-100 N: 0-5 O: 0-5 F: 0-7 S: 0-2
2020_161neg2 240 (2.235) AM2 (Ar,35000.0,0.00,0.00)
1: TOF MS ES-

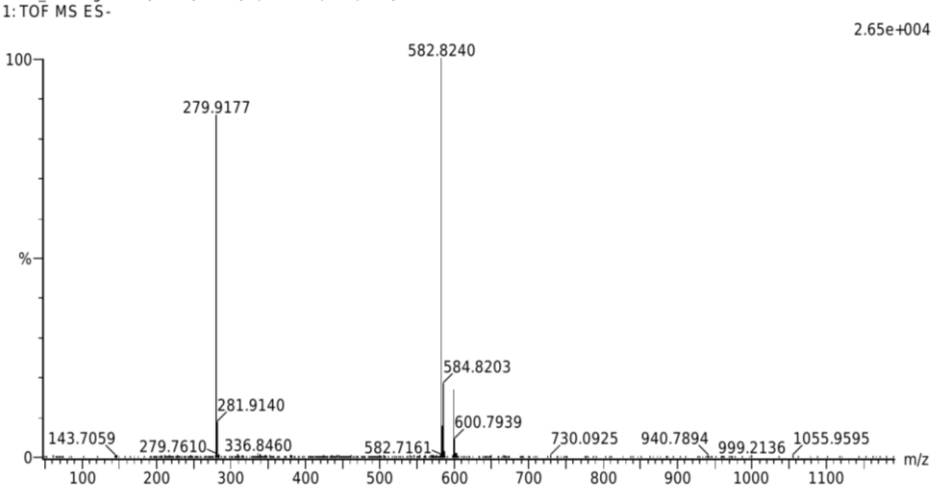

Minimum:				-5.0				
Maximum:		5.0	10.0	50.0				
Mass	Calc. Mass	mDa	PPM	DBE	i-FIT	Norm	Conf(%)	Formula
279.9177	279.9173	0.4	1.4	0.5	110.2	0.000	100.00	C2 N O4 F6 S2
	279.9186	-0.9	-3.2	7.5	123.4	13.195	0.00	C7 N O5 F2 S2

Thomas Nordbø Solvi

Studies on Au(III) complexes and reactions

NTNU
Norwegian University of
Science and Technology